

## Design Examples and Design Problems (DP)

CHAPTER 1	PAGE	DP4.3	Velocity Control System	297
Example Hybrid Fuel Vehicles	22	DP4.4	Laser Eye Surgery	297
Example Wind Power	23	DP4.5	Pulse Generating Op Amp	298
Example Embedded Computers	24	DP4.6	Hydrobot	298
Example Smart Grid Control Systems	28	DP4.7	Unmanned Underwater Vehicles	298
Example Rotating Disk Speed Control	30	DP4.8	Mobile Remote-Controlled Video Camera	299
Example Insulin Delivery Control System	31			
Example Disk Drive Read System	32	CHAPTER 5		
CDP1.1 Traction Drive Motor Control	46	Example Hubble Telescope Pointing	343	
DP1.1 Automobile Noise Control	46	Example Attitude Control of an Airplane	346	
DP1.2 Automobile Cruise Control	46	Example Disk Drive Read System	360	
DP1.3 Dairy Farm Automation	46	CDP5.1 Traction Drive Motor Control	379	
DP1.4 Welder Control	46	DP5.1 Jet Fighter Roll Angle Control	379	
DP1.5 Automobile Traction Control	46	DP5.2 Welding Arm Position Control	379	
DP1.6 Hubble Telescope Vibration	47	DP5.3 Automobile Active Suspension	379	
DP1.7 Nanorobotics in Medicine	47	DP5.4 Satellite Orientation Control	380	
DP1.8 Human Transportation Vehicle	47	DP5.5 Deburring Robot for Machined Parts	380	
CHAPTER 2		DP5.6 DC Motor Position Control	380	
Example Photovoltaic Generators	91	DP5.7 Three-Dimensional Cam	381	
Example Fluid Flow Modeling	94	DP5.8 Spray Paint Robot	381	
Example Electric Traction Motor Control	104	CHAPTER 6		
Example Mechanical Accelerometer	106	Example Tracked Vehicle Turning	404	
Example Laboratory Robot	109	Example Robot-Controlled Motorcycle	406	
Example Low-Pass Filter	111	Example Disk Drive Read System	421	
Example Disk Drive Read System	128	CDP6.1 Traction Drive Motor Control	438	
CDP2.1 Traction Drive Motor Control	155	DP6.1 Automobile Ignition Control	438	
DP2.1 Selection of Transfer Functions	155	DP6.2 Mars Guided Vehicle Control	439	
DP2.2 Television Beam Circuit	155	DP6.3 Parameter Selection	439	
DP2.3 Transfer Function Determination	155	DP6.4 Space Shuttle Rocket	439	
DP2.4 Op Amp Differentiating Circuit	155	DP6.5 Traffic Control System	439	
DP2.5 Grandfather Clock Pendulum	156	DP6.6 State Variable Feedback	439	
CHAPTER 3		DP6.7 Inner and Outer Loop Control	440	
Example Modeling the Orientation of a Space Station	193	DP6.8 PD Controller Design	440	
Example Printer Belt Drive	200	CHAPTER 7		
Example Disk Drive Read System	209	Example Wind Turbine Speed Control	497	
CDP3.1 Traction Drive Motor Control	230	Example Laser Manipulator Control	500	
DP3.1 Shock Absorber for Motorcycle	230	Example Robot Control System	502	
DP3.2 Diagonal Matrix Differential Equation	230	Example Automobile Velocity Control	505	
DP3.3 Aircraft Arresting Gear	230	Example Disk Drive Read System	516	
DP3.4 Bungee Jumping System	230	CDP7.1 Traction Drive Motor Control	543	
DP3.5 State Variable Feedback	231	DP7.1 Pitch Rate Aircraft Control	543	
CHAPTER 4		DP7.2 Helicopter Velocity Control	543	
Example English Channel Boring Machines	254	DP7.3 Mars Rover	544	
Example Mars Rover Vehicle	257	DP7.4 Remotely Controlled Welder	544	
Example Blood Pressure Control	259	DP7.5 High-Performance Jet Aircraft	545	
Example Disk Drive Read System	273	DP7.6 Control of Walking Motion	545	
CDP4.1 Traction Drive Motor Control	296	DP7.7 Mobile Robot with Vision	545	
DP4.1 Speed Control System	296	DP7.8 OP Amp Control System	545	
DP4.2 Airplane Roll Angle Control	297	DP7.9 Robot Arm Elbow Joint Actuator	546	

RICHARD C. DORF

ROBERT H. BISHOP

# MODERN CONTROL SYSTEMS

TWELFTH EDITION

DP7.10	Four-Wheel-Steered Automobile	546	DP10.7	Aircraft Roll Angle Control	828
DP7.11	Pilot Crane Control	547	DP10.8	Windmill Radiometer	828
DP7.12	Planetary Rover Vehicle	547	DP10.9	Control with Time Delay	829
DP7.13	Roll Angle Aircraft Autopilot	548	DP10.10	Loop Shaping	830
DP7.14	PD Control of a Marginally Stable Process	548	DP10.11	Polymerase Chain Reaction Control	830

## CHAPTER 8

Example Maximum Power Pointing Tracking	583
Example Engraving Machine Control	585
Example Control of a Six-Legged Robot	588
Example Disk Drive Read System	602
CDP8.1 Traction Drive Motor Control	628
DP8.1 Automobile Steering System	628
DP8.2 Autonomous Planetary Explorer-Amblor	628
DP8.3 Vial Position Control Under a Dispenser	628
DP8.4 Automatic Anesthesia Control	630
DP8.5 Black Box Control	630
DP8.6 State Variable System Design	630
DP8.7 PID Controller Design	631

## CHAPTER 9

Example PID Control of Wind Turbines	674
Example Remotely Controlled Reconnaissance Vehicle	678
Example Hot Ingot Robot Control	681
Example Disk Drive Read System	700
CDP9.1 Traction Drive Motor Control	735
DP9.1 Mobile Robot for Toxic Waste Cleanup	735
DP9.2 Control of a Flexible Arm	735
DP9.3 Blood Pressure Regulator	735
DP9.4 Robot Tennis Player	735
DP9.5 Electrohydraulic Actuator	735
DP9.6 Steel Strip-Rolling Mill	735
DP9.7 Lunar Vehicle Control	738
DP9.8 High-Speed Steel-Rolling Mill	738
DP9.9 Two-Tank Temperature Control	738
DP9.10 State Variable Feedback Control	739
DP9.11 Nuclear Reactor Control	739

## CHAPTER 10

Example Rotor Winder Control System	783
Example The X-Y Plotter	787
Example Milling Machine Control System	790
Example Disk Drive Read System	802
CDP10.1 Traction Drive Motor Control	826
DP10.1 Two Cooperating Robots	826
DP10.2 Heading Control of a Bi-Wing Aircraft	826
DP10.3 Mast Flight System	826
DP10.4 High-Speed Train Tilt Control	826
DP10.5 Tape Transport Speed Control	828
DP10.6 Automobile Engine Control	828

## CHAPTER 11

Example Automatic Test System	873
Example Diesel Electric Locomotive	876
Example Disk Drive Read System	888
CDP11.1 Traction Drive Motor Control	903
DP11.1 Levitation of a Steel Ball	903
DP11.2 Automobile Carburetor	903
DP11.3 State Variable Compensation	903
DP11.4 Helicopter Control	904
DP11.5 Manufacturing of Paper	904
DP11.6 Coupled-Drive Control	905
DP11.7 Tracking a Reference Input	905

## CHAPTER 12

Example Aircraft Autopilot	935
Example Space Telescope Control	935
Example Robust Bobbin Drive	938
Example Ultra-Precision Diamond Turning Machine	940
Example Digital Audio Tape Controller	943
Example Disk Drive Read System	958
CDP12.1 Traction Drive Motor Control	974
DP12.1 Turntable Position Control	974
DP12.2 Robust Parameter Design	974
DP12.3 Dexterous Hand Master	974
DP12.4 Microscope Control	975
DP12.5 Microscope Control	976
DP12.6 Artificial Control of Leg Articulation	976
DP12.7 Elevator Position Control	977
DP12.8 Electric Ventricular Assist Device	978
DP12.9 Space Robot Control	978
DP12.10 Solar Panel Pointing Control	979
DP12.11 Magnetically Levitated Train	979
DP12.12 Mars Guided Vehicle Control	979
DP12.13 Benchmark Mass-Spring	979

## CHAPTER 13

Example Worktable Motion Control	1009
Example Fly-by-wire Aircraft Control	1011
Example Disk Drive Read System	1023
CDP13.1 Traction Drive Motor Control	1034
DP13.1 Temperature Control System	1034
DP13.2 Disk Drive Read-Write Head-Positioning System	1034
DP13.3 Vehicle Traction Control	1034
DP13.4 Machine-Tool System	1035
DP13.5 Polymer Extruder Control	1035
DP13.6 Sampled-Data System	1035

Vice President and Editorial Director, ECS: Marcia J. Horton  
Senior Editor: Andrew Giffillan  
Associate Editor: Alice Dworkin  
Editorial Assistant: William Opaluch  
Vice President, Production: Vinessa O'Brien  
Senior Managing Editor: Scott Disanno  
Production Liaison: Jane Bonnell  
Production Editor: Maheswari PonSaravanan, TexTech International  
Senior Operations Supervisor: Alan Fischer  
Operations Specialist: Lisa McDowell  
Executive Marketing Manager: Tim Galligan  
Marketing Assistant: Mack Patterson  
Senior Art Director and Cover Designer: Kenny Beck  
Cover Images: Front: Scarlet macaw flying/Frans Lanting/Corbis; Back: Courtesy of Dr. William Kaiser and Dr. Philip Rundel of UCLA, and National Instruments  
Art Editor: Greg Dulles  
Media Editor: Daniel Sandin  
Composition/Full-Service Project Management: TexTech International

LabVIEW is a trademark of National Instruments. MATLAB is a registered trademark of The MathWorks, Inc. Company and product names mentioned herein are the trademarks or registered trademarks of their respective owners.

Copyright © 2011, 2008, 2005, 2001 by Pearson Education, Inc., Upper Saddle River, New Jersey 07458. All rights reserved. Manufactured in the United States of America. This publication is protected by Copyright and permissions should be obtained from the publisher prior to any prohibited reproduction, storage in a retrieval system, or transmission in any form or by any means, electronic, mechanical, photocopying, recording, or likewise. To obtain permission(s) to use materials from this work, please submit a written request to Pearson Higher Education, Permissions Department, 1 Lake Street, Upper Saddle River, NJ 07458.

The author and publisher of this book have used their best efforts in preparing this book. These efforts include the development, research, and testing of the theories and programs to determine their effectiveness. The author and publisher make no warranty of any kind, expressed or implied, with regard to these programs or the documentation contained in this book. The author and publisher shall not be liable in any event for incidental or consequential damages in connection with, or arising out of, the furnishing, performance, or use of these programs.

**Library of Congress Cataloging-in-Publication Data**

Dorf, Richard C.  
Modern control systems / Richard C. Dorf, Robert H. Bishop. — 12th ed.  
p. cm.  
ISBN-13: 978-0-13-602458-3  
ISBN-10: 0-13-602458-0  
1. Feedback control systems. I. Bishop, Robert H. II. Title.  
TJ216.D67 2010  
629.8'3—dc22 2010015651

Prentice Hall  
is an imprint of



www.pearsonhighered.com

10 9 8 7 6 5 4 3 2 1

ISBN-13: 978-0-13-602458-3  
ISBN-10: 0-13-602458-0

# Modern Control Systems

TWELFTH EDITION

Richard C. Dorf

University of California, Davis

Robert H. Bishop

Marquette University

Prentice Hall

Upper Saddle River Boston Columbus San Francisco New York  
Indianapolis London Toronto Sydney Singapore Tokyo Montreal  
Dubai Madrid Hong Kong Mexico City Munich Paris Amsterdam Cape Town

*Of the greater teachers—  
when they are gone,  
their students will say:  
we did it ourselves.*

*Dedicated to*  
Lynda Ferrera Bishop  
and  
Joy MacDonald Dorf  
*In grateful appreciation*



- 3.3 The State Differential Equation 166
- 3.4 Signal-Flow Graph and Block Diagram Models 171
- 3.5 Alternative Signal-Flow Graph and Block Diagram Models 182
- 3.6 The Transfer Function from the State Equation 187
- 3.7 The Time Response and the State Transition Matrix 189
- 3.8 Design Examples 193
- 3.9 Analysis of State Variable Models Using Control Design Software 206
- 3.10 Sequential Design Example: Disk Drive Read System 209
- 3.11 Summary 213
- Skills Check 214 • Exercises 217 • Problems 220 • Advanced Problems 227 • Design Problems 230 • Computer Problems 231 • Terms and Concepts 232

## CHAPTER 4 *Feedback Control System Characteristics* 234

- 4.1 Introduction 235
- 4.2 Error Signal Analysis 237
- 4.3 Sensitivity of Control Systems to Parameter Variations 239
- 4.4 Disturbance Signals in a Feedback Control System 242
- 4.5 Control of the Transient Response 247
- 4.6 Steady-State Error 250
- 4.7 The Cost of Feedback 253
- 4.8 Design Examples 254
- 4.9 Control System Characteristics Using Control Design Software 268
- 4.10 Sequential Design Example: Disk Drive Read System 273
- 4.11 Summary 277
- Skills Check 279 • Exercises 283 • Problems 287 • Advanced Problems 293 • Design Problems 296 • Computer Problems 300 • Terms and Concepts 303

## CHAPTER 5 *The Performance of Feedback Control Systems* 304

- 5.1 Introduction 305
- 5.2 Test Input Signals 305
- 5.3 Performance of Second-Order Systems 308
- 5.4 Effects of a Third Pole and a Zero on the Second-Order System Response 314
- 5.5 The  $s$ -Plane Root Location and the Transient Response 320
- 5.6 The Steady-State Error of Feedback Control Systems 322
- 5.7 Performance Indices 330
- 5.8 The Simplification of Linear Systems 339
- 5.9 Design Examples 342
- 5.10 System Performance Using Control Design Software 356
- 5.11 Sequential Design Example: Disk Drive Read System 360

- 8.7 Frequency Response Methods Using Control Design Software 596
- 8.8 Sequential Design Example: Disk Drive Read System 602
- 8.9 Summary 603
- Skills Check 608 • Exercises 613 • Problems 616 • Advanced Problems 626 • Design Problems 628 • Computer Problems 631 • Terms and Concepts 633

## CHAPTER 9 *Stability in the Frequency Domain* 634

- 9.1 Introduction 635
- 9.2 Mapping Contours in the  $s$ -Plane 636
- 9.3 The Nyquist Criterion 642
- 9.4 Relative Stability and the Nyquist Criterion 653
- 9.5 Time-Domain Performance Criteria in the Frequency Domain 661
- 9.6 System Bandwidth 668
- 9.7 The Stability of Control Systems with Time Delays 668
- 9.8 Design Examples 673
- 9.9 PID Controllers in the Frequency Domain 691
- 9.10 Stability in the Frequency Domain Using Control Design Software 692
- 9.11 Sequential Design Example: Disk Drive Read System 700
- 9.12 Summary 703
- Skills Check 711 • Exercises 715 • Problems 721 • Advanced Problems 731 • Design Problems 735 • Computer Problems 740 • Terms and Concepts 742

## CHAPTER 10 *The Design of Feedback Control Systems* 743

- 10.1 Introduction 744
- 10.2 Approaches to System Design 745
- 10.3 Cascade Compensation Networks 747
- 10.4 Phase-Lead Design Using the Bode Diagram 751
- 10.5 Phase-Lead Design Using the Root Locus 757
- 10.6 System Design Using Integration Networks 764
- 10.7 Phase-Lag Design Using the Root Locus 767
- 10.8 Phase-Lag Design Using the Bode Diagram 772
- 10.9 Design on the Bode Diagram Using Analytical Methods 776
- 10.10 Systems with a Prefilter 778
- 10.11 Design for Deadbeat Response 781
- 10.12 Design Examples 783
- 10.13 System Design Using Control Design Software 796
- 10.14 Sequential Design Example: Disk Drive Read System 802
- 10.15 Summary 804
- Skills Check 806 • Exercises 810 • Problems 814 • Advanced Problems 823 • Design Problems 826 • Computer Problems 831 • Terms and Concepts 833

# Contents

*Preface* xi

*About the Authors* xxii

## CHAPTER 1 *Introduction to Control Systems* 1

- 1.1 Introduction 2
- 1.2 Brief History of Automatic Control 5
- 1.3 Examples of Control Systems 10
- 1.4 Engineering Design 17
- 1.5 Control System Design 18
- 1.6 Mechatronic Systems 21
- 1.7 Green Engineering 25
- 1.8 The Future Evolution of Control Systems 27
- 1.9 Design Examples 28
- 1.10 Sequential Design Example: Disk Drive Read System 32
- 1.11 Summary 34
- Skills Check 35 • Exercises 37 • Problems 39 • Advanced Problems 44 • Design Problems 46 • Terms and Concepts 48

## CHAPTER 2 *Mathematical Models of Systems* 49

- 2.1 Introduction 50
- 2.2 Differential Equations of Physical Systems 50
- 2.3 Linear Approximations of Physical Systems 55
- 2.4 The Laplace Transform 58
- 2.5 The Transfer Function of Linear Systems 65
- 2.6 Block Diagram Models 79
- 2.7 Signal-Flow Graph Models 84
- 2.8 Design Examples 90
- 2.9 The Simulation of Systems Using Control Design Software 113
- 2.10 Sequential Design Example: Disk Drive Read System 128
- 2.11 Summary 130
- Skills Check 131 • Exercises 135 • Problems 141 • Advanced Problems 153 • Design Problems 155 • Computer Problems 157 • Terms and Concepts 159

## CHAPTER 3 *State Variable Models* 161

- 3.1 Introduction 162
- 3.2 The State Variables of a Dynamic System 162

- 5.12 Summary 364
- Skills Check 364 • Exercises 368 • Problems 371 • Advanced Problems 377 • Design Problems 379 • Computer Problems 382 • Terms and Concepts 384

## CHAPTER 6 *The Stability of Linear Feedback Systems* 386

- 6.1 The Concept of Stability 387
- 6.2 The Routh-Hurwitz Stability Criterion 391
- 6.3 The Relative Stability of Feedback Control Systems 399
- 6.4 The Stability of State Variable Systems 401
- 6.5 Design Examples 404
- 6.6 System Stability Using Control Design Software 413
- 6.7 Sequential Design Example: Disk Drive Read System 421
- 6.8 Summary 424
- Skills Check 425 • Exercises 428 • Problems 430 • Advanced Problems 435 • Design Problems 438 • Computer Problems 440 • Terms and Concepts 442

## CHAPTER 7 *The Root Locus Method* 443

- 7.1 Introduction 444
- 7.2 The Root Locus Concept 444
- 7.3 The Root Locus Procedure 449
- 7.4 Parameter Design by the Root Locus Method 467
- 7.5 Sensitivity and the Root Locus 473
- 7.6 PID Controllers 480
- 7.7 Negative Gain Root Locus 492
- 7.8 Design Examples 496
- 7.9 The Root Locus Using Control Design Software 510
- 7.10 Sequential Design Example: Disk Drive Read System 516
- 7.11 Summary 518
- Skills Check 522 • Exercises 526 • Problems 530 • Advanced Problems 539 • Design Problems 543 • Computer Problems 549 • Terms and Concepts 551

## CHAPTER 8 *Frequency Response Methods* 553

- 8.1 Introduction 554
- 8.2 Frequency Response Plots 556
- 8.3 Frequency Response Measurements 577
- 8.4 Performance Specifications in the Frequency Domain 579
- 8.5 Log Magnitude and Phase Diagrams 582
- 8.6 Design Examples 583

13.6	Performance of a Sampled-Data, Second-Order System	999		
13.7	Closed-Loop Systems with Digital Computer Compensation	1001		
13.8	The Root Locus of Digital Control Systems	1004		
13.9	Implementation of Digital Controllers	1008		
13.10	Design Examples	1009		
13.11	Digital Control Systems Using Control Design Software	1018		
13.12	Sequential Design Example: Disk Drive Read System	1023		
13.13	Summary	1025		
	Skills Check	1025 • Exercises	1029 • Problems	1031 •
	Advanced Problems	1033 • Design Problems	1034 • Computer	
	Problems	1036 • Terms and Concepts	1037	

## APPENDIX A MATLAB Basics 1038

References 1056

Index 1071

## WEB RESOURCES

### APPENDIX B MathScript RT Module Basics

### APPENDIX C Symbols, Units, and Conversion Factors

### APPENDIX D Laplace Transform Pairs

### APPENDIX E An Introduction to Matrix Algebra

### APPENDIX F Decibel Conversion

### APPENDIX G Complex Numbers

### APPENDIX H z-Transform Pairs Preface

### APPENDIX I Discrete-Time Evaluation of the Time Response

## CHAPTER 11 The Design of State Variable Feedback Systems 834

11.1	Introduction	835		
11.2	Controllability and Observability	835		
11.3	Full-State Feedback Control Design	841		
11.4	Observer Design	847		
11.5	Integrated Full-State Feedback and Observer	851		
11.6	Reference Inputs	857		
11.7	Optimal Control Systems	859		
11.8	Internal Model Design	869		
11.9	Design Examples	873		
11.10	State Variable Design Using Control Design Software	882		
11.11	Sequential Design Example: Disk Drive Read System	888		
11.12	Summary	890		
	Skills Check	890 • Exercises	894 • Problems	896 • Advanced
	Problems	900 • Design Problems	903 • Computer Problems	906 •
	Terms and Concepts	908		

## CHAPTER 12 Robust Control Systems 910

12.1	Introduction	911		
12.2	Robust Control Systems and System Sensitivity	912		
12.3	Analysis of Robustness	916		
12.4	Systems with Uncertain Parameters	918		
12.5	The Design of Robust Control Systems	920		
12.6	The Design of Robust PID-Controlled Systems	926		
12.7	The Robust Internal Model Control System	932		
12.8	Design Examples	935		
12.9	The Pseudo-Quantitative Feedback System	952		
12.10	Robust Control Systems Using Control Design Software	953		
12.11	Sequential Design Example: Disk Drive Read System	958		
12.12	Summary	960		
	Skills Check	961 • Exercises	965 • Problems	967 • Advanced
	Problems	971 • Design Problems	974 • Computer Problems	980 •
	Terms and Concepts	982		

## CHAPTER 13 Digital Control Systems 984

13.1	Introduction	985
13.2	Digital Computer Control System Applications	985
13.3	Sampled-Data Systems	987
13.4	The z-Transform	990
13.5	Closed-Loop Feedback Sampled-Data Systems	995

Control engineering is an exciting and a challenging field. By its very nature, control engineering is a multidisciplinary subject, and it has taken its place as a core course in the engineering curriculum. It is reasonable to expect different approaches to mastering and practicing the art of control engineering. Since the subject has a strong mathematical foundation, we might approach it from a strictly theoretical point of view, emphasizing theorems and proofs. On the other hand, since the ultimate objective is to implement controllers in real systems, we might take an ad hoc approach relying only on intuition and hands-on experience when designing feedback control systems. Our approach is to present a control engineering methodology that, while based on mathematical fundamentals, stresses physical system modeling and practical control system designs with realistic system specifications.

We believe that the most important and productive approach to learning is for each of us to rediscover and re-create anew the answers and methods of the past. Thus, the ideal is to present the student with a series of problems and questions and point to some of the answers that have been obtained over the past decades. The traditional method—to confront the student not with the problem but with the finished solution—is to deprive the student of all excitement, to shut off the creative impulse, to reduce the adventure of humankind to a dusty heap of theorems. The issue, then, is to present some of the unanswered and important problems that we continue to confront, for it may be asserted that what we have truly learned and understood, we discovered ourselves.

The purpose of this book is to present the structure of feedback control theory and to provide a sequence of exciting discoveries as we proceed through the text and problems. If this book is able to assist the student in discovering feedback control system theory and practice, it will have succeeded.

## WHAT'S NEW IN THIS EDITION

This latest edition of *Modern Control Systems* incorporates the following key updates:

- A new section in Chapter 1 on green engineering. The role of control systems in green engineering will continue to expand as global environmental challenges require ever increasing levels of automation and precision.
- New design problems in key chapters that illustrate control design to support green engineering applications, such as smart grids, environmental monitoring, wind power and solar power generation.
- A new section in each chapter entitled “Skills Check” that allows students to test their knowledge of the basic principles. Answers are provided at the end of each chapter for immediate feedback.
- A new section on the negative gain root locus.
- A new section on PID tuning methods with emphasis on manual tuning and Ziegler-Nichols tuning methods.
- Over 20% of the problems updated or newly added. With the twelfth edition we now have a total of over 1000 end-of-chapter exercises, problems, advanced problems, design problems, and computer problems. Instructors will have no difficulty finding different problems to assign semester after semester.
- Video solutions of representative homework problems are available on the companion website: [www.pearsonhighered.com/dorf](http://www.pearsonhighered.com/dorf).

## Preface

### MODERN CONTROL SYSTEMS—THE BOOK

Global issues such as climate change, clean water, sustainability, waste management, emissions reduction, and minimizing raw material and energy use have caused many engineers to re-think existing approaches to engineering design. One outcome of the evolving design strategy is to consider *green engineering*. The goal of green engineering is to design products that minimize pollution, reduce the risk to human health, and improve the environment. Applying the principles of green engineering highlights the power of feedback control systems as an enabling technology.

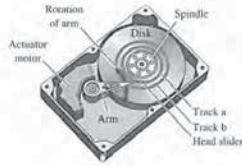
To reduce greenhouse gases and minimize pollution, it is necessary to improve both the quality and quantity of our environmental monitoring systems. One example is to use wireless measurements on mobile sensing platforms to measure the external environment. Another example is to monitor the quality of the delivered power to measure leading and lagging power, voltage variations, and waveform harmonics. Many green engineering systems and components require careful monitoring of current and voltages. For example, current transformers are used in various capacities for measuring and monitoring current within the power grid network of interconnected systems used to deliver electricity. Sensors are key components of any feedback control system because the measurements provide the required information as to the state of the system so the control system can take the appropriate action.

The role of control systems in green engineering will continue to expand as the global issues facing us require ever increasing levels of automation and precision. In the book, we present key examples from green engineering such as wind turbine control and modeling of a photovoltaic generator for feedback control to achieve maximum power delivery as the sunlight varies over time.

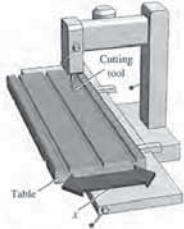
The wind and sun are important sources of renewable energy around the world. Wind energy conversion to electric power is achieved by wind energy turbines connected to electric generators. The intermittency characteristic of the wind makes smart grid development essential to bring the energy to the power grid when it is available and to provide energy from other sources when the wind dies down or is disrupted. A smart grid can be viewed as a system comprised of hardware and software that routes power more reliably and efficiently to homes, businesses, schools, and other users of power in the presence of intermittency and other disturbances. The irregular character of wind direction and power also results in the need for reliable, steady electric energy by using control systems on the wind turbines themselves. The goal of these control devices is to reduce the effects of wind intermittency and the effect of wind direction change. Energy storage systems are also critical technologies for green engineering. We seek energy storage systems that are renewable, such as fuel cells. Active control can be a key element of effective renewable energy storage systems as well.



process, sensors, and actuators. In the remaining chapters, we continue the design process, stressing the main points of the chapters.



In the same spirit as the *Sequential Design Example*, we present a design problem that we call the *Continuous Design Problem* (identified by an arrow icon in the text) to give students the opportunity to build upon a design problem from chapter to chapter. High-precision machinery places stringent demands on table slide systems. In the *Continuous Design Problem*, students apply the techniques and tools presented in each chapter to the development of a design solution that meets the specified requirements.



The computer-aided design and analysis component of the book continues to evolve and improve. The end-of-chapter computer problem set is identified by the graphical icon in the text. Also, many of the solutions to various components of the *Sequential Design Example* utilize m-files with corresponding scripts included in the figures.

A new feature of the twelfth edition is a Skills Check section at the end of each chapter. The section is noted with a check mark icon. In each Skills Check section, we provide three sets of problems to test your knowledge of the chapter material. This includes True or False, Multiple Choice, and Word Match problems. To obtain

For example, the problem set for The Root Locus Method, Chapter 7 (see page 443) includes 28 exercises, 39 problems, 14 advanced problems, 14 design problems, and 10 computer-based problems. The exercises permit the students to readily utilize the concepts and methods introduced in each chapter by solving relatively straightforward exercises before attempting the more complex problems. Answers to one-third of the exercises are provided. The problems require an extension of the concepts of the chapter to new situations. The advanced problems represent problems of increasing complexity. The design problems emphasize the design task; the computer-based problems give the student practice with problem solving using computers. In total, the book contains more than 1000 problems. The abundance of problems of increasing complexity gives students confidence in their problem-solving ability as they work their way from the exercises to the design and computer-based problems. An instructor's manual, available to all adopters of the text for course use, contains complete solutions to all end-of-chapter problems.

A set of m-files, the *Modern Control Systems Toolbox*, has been developed by the authors to supplement the text. The m-files contain the scripts from each computer-based example in the text. You may retrieve the m-files from the companion website: [www.pearsonhighered.com/dorf](http://www.pearsonhighered.com/dorf).

**Design Emphasis without Compromising Basic Principles.** The all-important topic of design of real-world, complex control systems is a major theme throughout the text. Emphasis on design for real-world applications addresses interest in design by ABET and industry.

The design process consists of seven main building blocks that we arrange into three groups:

1. Establishment of goals and variables to be controlled, and definition of specifications (metrics) against which to measure performance
2. System definition and modeling
3. Control system design and integrated system simulation and analysis

In each chapter of this book, we highlight the connection between the design process and the main topics of that chapter. The objective is to demonstrate different aspects of the design process through illustrative examples. Various aspects of the control system design process are illustrated in detail in the following examples:

- smart grids (Section 1.9, page 28)
- photovoltaic generators (Section 2.8, page 91)
- space station orientation modeling (Section 3.8, page 193)
- blood pressure control during anesthesia (Section 4.8, page 259)
- attitude control of an airplane (Section 5.9, page 346)
- robot-controlled motorcycle (Section 6.5, page 406)
- wind turbine rotor speed control (Section 7.8, page 497)
- maximum power pointing tracking (Section 8.6, page 583)
- PID control of wind turbines (Section 9.8, page 674)
- milling machine control system (Section 10.12, page 790)

## THE AUDIENCE

This text is designed for an introductory undergraduate course in control systems for engineering students. There is very little demarcation between aerospace, chemical, electrical, industrial, and mechanical engineering in control system practice; therefore, this text is written without any conscious bias toward one discipline. Thus, it is hoped that this book will be equally useful for all engineering disciplines and, perhaps, will assist in illustrating the utility of control engineering. The numerous problems and examples represent all fields, and the examples of the sociological, biological, ecological, and economic control systems are intended to provide the reader with an awareness of the general applicability of control theory to many facets of life. We believe that exposing students of one discipline to examples and problems from other disciplines will provide them with the ability to see beyond their own field of study. Many students pursue careers in engineering fields other than their own. For example, many electrical and mechanical engineers find themselves in the aerospace industry working alongside aerospace engineers. We hope this introduction to control engineering will give students a broader understanding of control system design and analysis.

In its first eleven editions, *Modern Control Systems* has been used in senior-level courses for engineering students at more than 400 colleges and universities. It also has been used in courses for engineering graduate students with no previous background in control engineering.

## THE TWELFTH EDITION

A companion website is available to students and faculty using the twelfth edition. The website contains all the m-files in the book, Laplace and z-transform tables, written materials on matrix algebra and complex numbers, symbols, units, and conversion factors, and an introduction to the LabVIEW MathScript RT Module. An icon will appear in the book margin whenever there is additional related material on the website. The companion website also includes video solutions of representative homework problems and a complete Pearson eText. The MCS website address is [www.pearsonhighered.com/dorf](http://www.pearsonhighered.com/dorf).

With the twelfth edition, we continue to evolve the design emphasis that historically has characterized *Modern Control Systems*. Using the real-world engineering problems associated with designing a controller for a disk drive read system, we present the *Sequential Design Example* (identified by an arrow icon in the text), which is considered sequentially in each chapter using the methods and concepts in that chapter. Disk drives are used in computers of all sizes and they represent an important application of control engineering. Various aspects of the design of controllers for the disk drive read system are considered in each chapter. For example, in Chapter 1 we identify the control goals, identify the variables to be controlled, write the control specifications, and establish the preliminary system configuration for the disk drive. Then, in Chapter 2, we obtain models of the

direct feedback, you can check your answers with the answer key provided at the conclusion of the end-of-chapter problems.

## PEDAGOGY

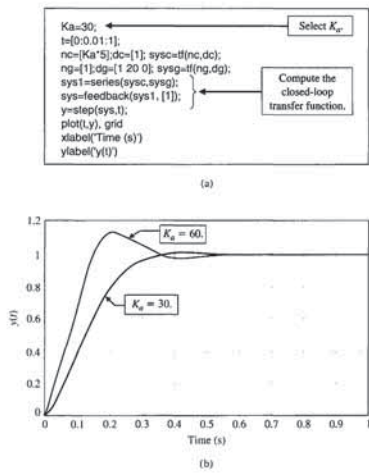
The book is organized around the concepts of control system theory as they have been developed in the frequency and time domains. An attempt has been made to make the selection of topics, as well as the systems discussed in the examples and problems, modern in the best sense. Therefore, this book includes discussions on robust control systems and system sensitivity, state variable models, controllability and observability, computer control systems, internal model control, robust PID controllers, and computer-aided design and analysis, to name a few. However, the classical topics of control theory that have proved to be so very useful in practice have been retained and expanded.

**Building Basic Principles: From Classical to Modern.** Our goal is to present a clear exposition of the basic principles of frequency- and time-domain design techniques. The classical methods of control engineering are thoroughly covered: Laplace transforms and transfer functions; root locus design; Routh-Hurwitz stability analysis; frequency response methods, including Bode, Nyquist, and Nichols; steady-state error for standard test signals; second-order system approximations; and phase and gain margin and bandwidth. In addition, coverage of the state variable method is significant. Fundamental notions of controllability and observability for state variable models are discussed. Full state feedback design with Ackermann's formula for pole placement is presented, along with a discussion on the limitations of state variable feedback. Observers are introduced as a means to provide state estimates when the complete state is not measured.

Upon this strong foundation of basic principles, the book provides many opportunities to explore topics beyond the traditional. Advances in robust control theory are introduced in Chapter 12. The implementation of digital computer control systems is discussed in Chapter 13. Each chapter (but the first) introduces the student to the notion of computer-aided design and analysis. The book concludes with an extensive references section, divided by chapter, to guide the student to further sources of information on control engineering.

**Progressive Development of Problem-Solving Skills.** Reading the chapters, attending lectures and taking notes, and working through the illustrated examples are all part of the learning process. But the real test comes at the end of the chapter with the problems. The book takes the issue of problem solving seriously. In each chapter, there are five problem types:

- Exercises
- Problems
- Advanced Problems
- Design Problems
- Computer Problems



**Learning Enhancement.** Each chapter begins with a chapter preview describing the topics the student can expect to encounter. The chapters conclude with an end-of-chapter summary, skills check, as well as terms and concepts. These sections reinforce the important concepts introduced in the chapter and serve as a reference for later use.

A second color is used to add emphasis when needed and to make the graphs and figures easier to interpret. Design Problem 4.4, page 297, asks the student to determine the value of  $K$  of the controller so that the response, denoted by  $Y(s)$ , to a step change in the position, denoted by  $R(s)$ , is satisfactory and the effect of the disturbance, denoted by  $T_d(s)$ , is minimized. The associated Figure DP4.4, p. 298, assists the student with (a) visualizing the problem and (b) taking the next step to develop the transfer function model and to complete the design.

**Chapter 5 The Performance of Feedback Control Systems.** In Chapter 5, the performance of control systems is examined. The performance of a control system is correlated with the  $s$ -plane location of the poles and zeros of the transfer function of the system.

**Chapter 6 The Stability of Linear Feedback Systems.** The stability of feedback systems is investigated in Chapter 6. The relationship of system stability to the characteristic equation of the system transfer function is studied. The Routh–Hurwitz stability criterion is introduced.

**Chapter 7 The Root Locus Method.** Chapter 7 deals with the motion of the roots of the characteristic equation in the  $s$ -plane as one or two parameters are varied. The locus of roots in the  $s$ -plane is determined by a graphical method. We also introduce the popular PID controller and the Ziegler–Nichols PID tuning method.

**Chapter 8 Frequency Response Methods.** In Chapter 8, a steady-state sinusoid input signal is utilized to examine the steady-state response of the system as the frequency of the sinusoid is varied. The development of the frequency response plot, called the Bode plot, is considered.

**Chapter 9 Stability in the Frequency Domain.** System stability utilizing frequency response methods is investigated in Chapter 9. Relative stability and the Nyquist criterion are discussed.

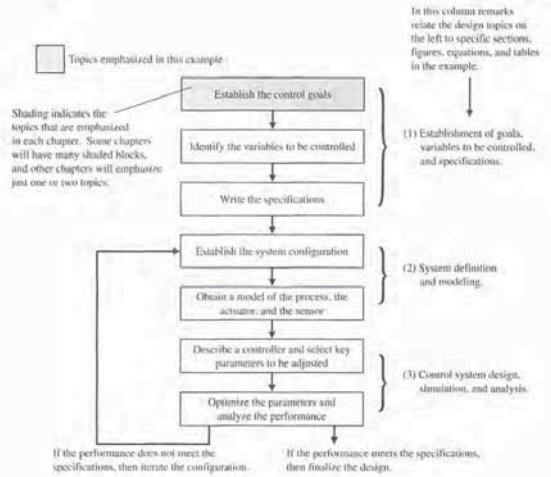
**Chapter 10 The Design of Feedback Control Systems.** Several approaches to designing and compensating a control system are described and developed in Chapter 10. Various candidates for service as compensators are presented and it is shown how they help to achieve improved performance.

**Chapter 11 The Design of State Variable Feedback Systems.** The main topic of Chapter 11 is the design of control systems using state variable models. Full-state feedback design and observer design methods based on pole placement are discussed. Tests for controllability and observability are presented, and the concept of an internal model design is discussed.

**Chapter 12 Robust Control Systems.** Chapter 12 deals with the design of highly accurate control systems in the presence of significant uncertainty. Five methods for robust design are discussed, including root locus, frequency response, ITAE methods for robust PID controllers, internal models, and pseudo-quantitative feedback.

**Chapter 13 Digital Control Systems.** Methods for describing and analyzing the performance of computer control systems are described in Chapter 13. The stability and performance of sampled-data systems are discussed.

**Appendix A MATLAB Basics**



- diesel electric locomotive control (Section 11.9, page 876)
- digital audio tape controller (Section 12.8, page 943)
- manufacturing worktable control (Section 13.10, page 1009)

Each chapter includes a section to assist students in utilizing computer-aided design and analysis concepts and in reworking many of the design examples. In Chapter 5, the Sequential Design Example: Disk Drive Read System is analyzed using computer-based methods. An m-file script that can be used to analyze the design is presented in Figure 5.47, p. 362. In general, each script is annotated with comment boxes that highlight important aspects of the script. The accompanying output of the script (generally a graph) also contains comment boxes pointing out significant elements. The scripts can also be utilized with modifications as the foundation for solving other related problems.

**Chapter 5 The Performance of Feedback Control Systems.** In Chapter 5, the performance of control systems is examined. The performance of a control system is correlated with the  $s$ -plane location of the poles and zeros of the transfer function of the system.

**Chapter 6 The Stability of Linear Feedback Systems.** The stability of feedback systems is investigated in Chapter 6. The relationship of system stability to the characteristic equation of the system transfer function is studied. The Routh–Hurwitz stability criterion is introduced.

**Chapter 7 The Root Locus Method.** Chapter 7 deals with the motion of the roots of the characteristic equation in the  $s$ -plane as one or two parameters are varied. The locus of roots in the  $s$ -plane is determined by a graphical method. We also introduce the popular PID controller and the Ziegler–Nichols PID tuning method.

**Chapter 8 Frequency Response Methods.** In Chapter 8, a steady-state sinusoid input signal is utilized to examine the steady-state response of the system as the frequency of the sinusoid is varied. The development of the frequency response plot, called the Bode plot, is considered.

**Chapter 9 Stability in the Frequency Domain.** System stability utilizing frequency response methods is investigated in Chapter 9. Relative stability and the Nyquist criterion are discussed.

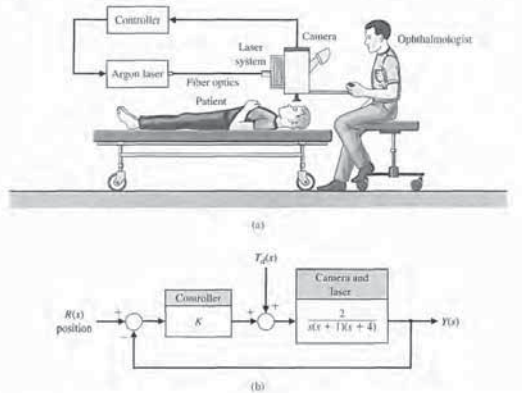
**Chapter 10 The Design of Feedback Control Systems.** Several approaches to designing and compensating a control system are described and developed in Chapter 10. Various candidates for service as compensators are presented and it is shown how they help to achieve improved performance.

**Chapter 11 The Design of State Variable Feedback Systems.** The main topic of Chapter 11 is the design of control systems using state variable models. Full-state feedback design and observer design methods based on pole placement are discussed. Tests for controllability and observability are presented, and the concept of an internal model design is discussed.

**Chapter 12 Robust Control Systems.** Chapter 12 deals with the design of highly accurate control systems in the presence of significant uncertainty. Five methods for robust design are discussed, including root locus, frequency response, ITAE methods for robust PID controllers, internal models, and pseudo-quantitative feedback.

**Chapter 13 Digital Control Systems.** Methods for describing and analyzing the performance of computer control systems are described in Chapter 13. The stability and performance of sampled-data systems are discussed.

**Appendix A MATLAB Basics**



**THE ORGANIZATION**

**Chapter 1 Introduction to Control Systems.** Chapter 1 provides an introduction to the basic history of control theory and practice. The purpose of this chapter is to describe the general approach to designing and building a control system.

**Chapter 2 Mathematical Models of Systems.** Mathematical models of physical systems in input–output or transfer function form are developed in Chapter 2. A wide range of systems (including mechanical, electrical, and fluid) are considered.

**Chapter 3 State Variable Models.** Mathematical models of systems in state variable form are developed in Chapter 3. Using matrix methods, the transient response of control systems and the performance of these systems are examined.

**Chapter 4 Feedback Control System Characteristics.** The characteristics of feedback control systems are described in Chapter 4. The advantages of feedback are discussed, and the concept of the system error signal is introduced.



**Richard C. Dorf** is a Professor of Electrical and Computer Engineering at the University of California, Davis. Known as an instructor who is highly concerned with the discipline of electrical engineering and its application to social and economic needs, Professor Dorf has written and edited several successful engineering textbooks and handbooks, including the best selling *Engineering Handbook*, second edition and the third edition of the *Electrical Engineering Handbook*. Professor Dorf is also co-author of *Technology Ventures*, a leading textbook on technology entrepreneurship. Professor Dorf is a Fellow of the IEEE and a Fellow of the ASEE. He is active in the fields of control system design and robotics. Dr. Dorf holds a patent for the PIDA controller.

**Robert H. Bishop** is the OPUS Dean of Engineering at Marquette University. Prior to coming to Marquette University, he was a Professor of Aerospace Engineering and Engineering Mechanics at The University of Texas at Austin for 20 years where he held the Joe J. King Professorship and was a Distinguished Teaching Professor. Professor Bishop started his engineering career as a member of the technical staff at the MIT Charles Stark Draper Laboratory. He authors the well-known textbook for teaching graphical programming entitled *Learning with LabVIEW* and is also the editor-in-chief of the *Mechatronics Handbook*. A talented educator, Professor Bishop has been recognized with numerous teaching awards including the coveted Lockheed Martin Tactical Aircraft Systems Award for Excellence in Engineering Teaching. He also received the John Leland Atwood Award by the American Society of Engineering Educators (ASEE) and the American Institute of Aeronautics and Astronautics (AIAA) that is given periodically to "a leader who has made lasting and significant contributions to aerospace engineering education." He is a Fellow of the AIAA, a Fellow of the American Astronautical Society (AAS), and active in ASEE and in the Institute of Electrical and Electronics Engineers (IEEE).

## ACKNOWLEDGMENTS

We wish to express our sincere appreciation to the following individuals who have assisted us with the development of this twelfth edition, as well as all previous editions: Mahmoud A. Abdallah, Central State University (OH); John N. Chiasson, University of Pittsburgh; Samy El-Sawah, California State Polytechnic University, Pomona; Peter J. Gorder, Kansas State University; Duane Hanselman, University of Maine; Ashok Iyer, University of Nevada, Las Vegas; Leslie R. Koval, University of Missouri-Rolla; L. G. Kraft, University of New Hampshire; Thomas Kurfess, Georgia Institute of Technology; Julio C. Mandojana, Mankato State University; Luigi Mariani, University of Padova; Jure Medanic, University of Illinois at Urbana-Champaign; Eduardo A. Misawa, Oklahoma State University; Medhat M. Morcos, Kansas State University; Mark Nagurka, Marquette University; D. Subbaram Naidu, Idaho State University; Ron Perez, University of Wisconsin-Milwaukee; Carla Schwartz, The MathWorks, Inc.; Murat Tanyel, Dordt College; Hal Tharp, University of Arizona; John Valasek, Texas A & M University; Paul P. Wang, Duke University; and Ravi Warrier, GMI Engineering and Management Institute.

## OPEN LINES OF COMMUNICATION

The authors would like to establish a line of communication with the users of *Modern Control Systems*. We encourage all readers to send comments and suggestions for this and future editions. By doing this, we can keep you informed of any general-interest news regarding the textbook and pass along comments of other users.

Keep in touch!

Richard C. Dorf  
Robert H. Bishop

dorf@ece.ucdavis.edu  
rbishop@marquette.edu

## 1.1 INTRODUCTION

Engineering is concerned with understanding and controlling the materials and forces of nature for the benefit of humankind. Control system engineers are concerned with understanding and controlling segments of their environment, often called **systems**, to provide useful economic products for society. The twin goals of understanding and controlling are complementary because effective systems control requires that the systems be understood and modeled. Furthermore, control engineering must often consider the control of poorly understood systems such as chemical process systems. The present challenge to control engineers is the modeling and control of modern, complex, interrelated systems such as traffic control systems, chemical processes, and robotic systems. Simultaneously, the fortunate engineer has the opportunity to control many useful and interesting industrial automation systems. Perhaps the most characteristic quality of control engineering is the opportunity to control machines and industrial and economic processes for the benefit of society.

Control engineering is based on the foundations of feedback theory and linear system analysis, and it integrates the concepts of network theory and communication theory. Therefore control engineering is not limited to any engineering discipline but is equally applicable to aeronautical, chemical, mechanical, environmental, civil, and electrical engineering. For example, a control system often includes electrical, mechanical, and chemical components. Furthermore, as the understanding of the dynamics of business, social, and political systems increases, the ability to control these systems will also increase.

A **control system** is an interconnection of components forming a system configuration that will provide a desired system response. The basis for analysis of a system is the foundation provided by linear system theory, which assumes a cause-effect relationship for the components of a system. Therefore a component or **process** to be controlled can be represented by a block, as shown in Figure 1.1. The input-output relationship represents the cause-and-effect relationship of the process, which in turn represents a processing of the input signal to provide an output signal variable, often with a power amplification. An **open-loop control system** uses a controller and an actuator to obtain the desired response, as shown in Figure 1.2. An open-loop system is a system without feedback.

An open-loop control system utilizes an actuating device to control the process directly without using feedback.

FIGURE 1.1 Process to be controlled.



FIGURE 1.2 Open-loop control system (without feedback).



## CHAPTER

# 1

# Introduction to Control Systems

1.1	Introduction	2
1.2	Brief History of Automatic Control	5
1.3	Examples of Control Systems	10
1.4	Engineering Design	17
1.5	Control System Design	18
1.6	Mechatronic Systems	21
1.7	Green Engineering	25
1.8	The Future Evolution of Control Systems	27
1.9	Design Examples	28
1.10	Sequential Design Example: Disk Drive Read System	32
1.11	Summary	34

## P R E V I E W

In this chapter, we discuss open- and closed-loop feedback control systems. A control system consists of interconnected components to achieve a desired purpose. We examine examples of control systems through the course of history. These early systems incorporated many of the same ideas of feedback that are employed in modern manufacturing processes, alternative energy, complex hybrid automobiles, and sophisticated robots. A design process is presented that encompasses the establishment of goals and variables to be controlled, definition of specifications, system definition, modeling, and analysis. The iterative nature of design allows us to handle the design gap effectively while accomplishing necessary trade-offs in complexity, performance, and cost. Finally, we introduce the Sequential Design Example: Disk Drive Read System. This example will be considered sequentially in each chapter of this book. It represents a very important and practical control system design problem while simultaneously serving as a useful learning tool.

## DESIRED OUTCOMES

Upon completion of Chapter 1, students should:

- Possess a basic understanding of control system engineering and be able to offer some illustrative examples and their relationship to key contemporary issues.
- Be able to recount a brief history of control systems and their role in society.
- Be capable of discussing the future of controls in the context of their evolutionary pathways.
- Recognize the elements of control system design and possess an appreciation of controls in the context of engineering design.



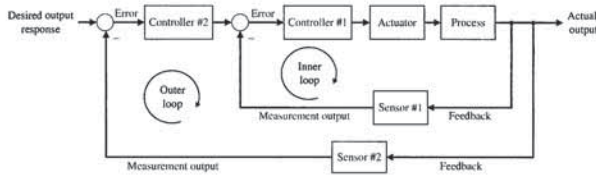


FIGURE 1.5 Multiloop feedback system with an inner loop and an outer loop.

The feedback systems in Figures 1.3 and 1.4 are single-loop feedback systems. Many feedback control systems contain more than one feedback loop. A common **multiloop feedback control system** is illustrated in Figure 1.5 with an inner loop and an outer loop. In this scenario, the inner loop has a controller and a sensor and the outer loop has a controller and sensor. Other varieties of multiloop feedback systems are considered throughout the book as they represent more practical situations found in real-world applications. However, we use the single-loop feedback system for learning about the benefits of feedback control systems since the outcomes readily extend to multiloop systems.

Due to the increasing complexity of the system under control and the interest in achieving optimum performance, the importance of control system engineering has grown in the past decade. Furthermore, as the systems become more complex, the interrelationship of many controlled variables must be considered in the control scheme. A block diagram depicting a **multivariable control system** is shown in Figure 1.6.

A common example of an open-loop control system is a microwave oven set to operate for a fixed time. An example of a closed-loop control system is a person steering an automobile (assuming his or her eyes are open) by looking at the auto's location on the road and making the appropriate adjustments.

The introduction of feedback enables us to control a desired output and can improve accuracy, but it requires attention to the issue of stability of response.

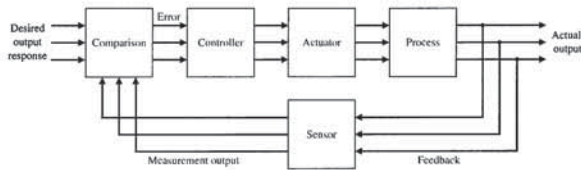


FIGURE 1.6 Multivariable control system.

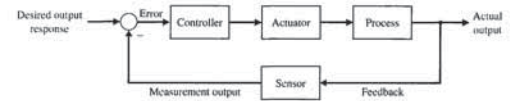


FIGURE 1.3 Closed-loop feedback control system (with feedback).

In contrast to an open-loop control system, a closed-loop control system utilizes an additional measure of the actual output to compare the actual output with the desired output response. The measure of the output is called the **feedback signal**. A simple **closed-loop feedback control system** is shown in Figure 1.3. A feedback control system is a control system that tends to maintain a prescribed relationship of one system variable to another by comparing functions of these variables and using the difference as a means of control. With an accurate sensor, the measured output is a good approximation of the actual output of the system.

A feedback control system often uses a function of a prescribed relationship between the output and reference input to control the process. Often the difference between the output of the process under control and the reference input is amplified and used to control the process so that the difference is continually reduced. In general, the difference between the desired output and the actual output is equal to the error, which is then adjusted by the controller. The output of the controller causes the actuator to modulate the process in order to reduce the error. The sequence is such, for instance, that if a ship is heading incorrectly to the right, the rudder is actuated to direct the ship to the left. The system shown in Figure 1.3 is a **negative feedback control system**, because the output is subtracted from the input and the difference is used as the input signal to the controller. The feedback concept has been the foundation for control system analysis and design.

**A closed-loop control system uses a measurement of the output and feedback of this signal to compare it with the desired output (reference or command).**

As we will discuss in Chapter 4, closed-loop control has many advantages over open-loop control including the ability to reject external **disturbances** and improve **measurement noise** attenuation. We incorporate the disturbances and measurement noise in the block diagram as external inputs, as illustrated in Figure 1.4. External disturbances and measurement noise are inevitable in real-world applications and must be addressed in practical control system designs.

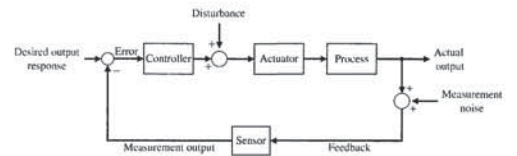


FIGURE 1.4 Closed-loop feedback system with external disturbances and measurement noise.

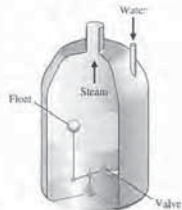


FIGURE 1.8 Water-level float regulator.

control system led to slower attenuation of the transient oscillations and even to unstable systems. It then became imperative to develop a theory of automatic control. In 1868, J. C. Maxwell formulated a mathematical theory related to control theory using a differential equation model of a governor [5]. Maxwell's study was concerned with the effect various system parameters had on the system performance. During the same period, I. A. Vyshnegradskii formulated a mathematical theory of regulators [6].

Prior to World War II, control theory and practice developed differently in the United States and western Europe than in Russia and eastern Europe. The main impetus for the use of feedback in the United States was the development of the telephone system and electronic feedback amplifiers by Bode, Nyquist, and Black at Bell Telephone Laboratories [7–10, 12].

Harold S. Black graduated from Worcester Polytechnic Institute in 1921 and joined Bell Laboratories of American Telegraph and Telephone (AT&T). In 1921, the major task confronting Bell Laboratories was the improvement of the telephone system and the design of improved signal amplifiers. Black was assigned the task of linearizing, stabilizing, and improving the amplifiers that were used in tandem to carry conversations over distances of several thousand miles.

Black reports [8]:

Then came the morning of Tuesday, August 2, 1927, when the concept of the negative feedback amplifier came to me in a flash while I was crossing the Hudson River on the Lackawanna Ferry, on my way to work. For more than 50 years I have pondered how and why the idea came, and I can't say any more today than I could that morning. All I know is that after several years of hard work on the problem, I suddenly realized that if I fed the amplifier output back to the input, in reverse phase, and kept the device from oscillating (singing, as we called it then), I would have exactly what I wanted: a means of canceling out the distortion in the output. I opened my morning newspaper and on a page of *The New York Times* I sketched a simple canonical diagram of a negative feedback amplifier plus the equations for the amplification with feedback. I signed the sketch, and 20 minutes later, when I reached the laboratory at 463 West Street, it was witnessed, understood, and signed by the late Earl C. Blessing.

I envisioned this circuit as leading to extremely linear amplifiers (40 to 50 dB of negative feedback), but an important question is: How did I know I could avoid

1.2 BRIEF HISTORY OF AUTOMATIC CONTROL

The use of feedback to control a system has a fascinating history. The first applications of feedback control appeared in the development of float regulator mechanisms in Greece in the period 300 to 100 B.C. [1, 2, 3]. The water clock of Ktesibios used a float regulator (refer to Problem P1.11). An oil lamp devised by Philon in approximately 250 B.C. used a float regulator in an oil lamp for maintaining a constant level of fuel oil. Heron of Alexandria, who lived in the first century A.D., published a book entitled *Pneumatica*, which outlined several forms of water-level mechanisms using float regulators [1].

The first feedback system to be invented in modern Europe was the temperature regulator of Cornelis Drebbel (1572–1633) of Holland [1]. Dennis Papin (1647–1712) invented the first pressure regulator for steam boilers in 1681. Papin's pressure regulator was a form of safety regulator similar to a pressure-cooker valve.

The first automatic feedback controller used in an industrial process is generally agreed to be James Watt's **flyball governor**, developed in 1769 for controlling the speed of a steam engine [1, 2]. The all-mechanical device, shown in Figure 1.7, measured the speed of the output shaft and utilized the movement of the flyball to control the steam valve and therefore the amount of steam entering the engine. As depicted in Figure 1.7, the governor shaft axis is connected via mechanical linkages and beveled gears to the output shaft of the steam engine. As the steam engine output shaft speed increases, the ball weights rise and move away from the shaft axis and through mechanical linkages the steam valve closes and the engine slows down.

The first historical feedback system, claimed by Russia, is the water-level float regulator said to have been invented by I. Polzunov in 1765 [4]. The level regulator system is shown in Figure 1.8. The float detects the water level and controls the valve that covers the water inlet in the boiler.

The next century was characterized by the development of automatic control systems through intuition and invention. Efforts to increase the accuracy of the

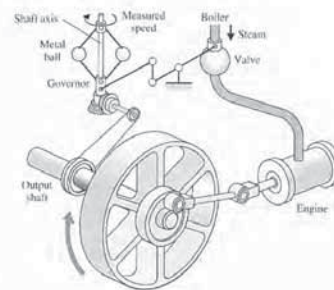


FIGURE 1.7 Watt's flyball governor.



Parkinson had a dream about an anti-aircraft gun that was successfully felling airplanes. Parkinson described the situation [13]:

After three or four shots one of the men in the crew smiled at me and beckoned me to come closer to the gun. When I drew near he pointed to the exposed end of the left trunnion. Mounted there was the control potentiometer of my level recorder!

The next morning Parkinson realized the significance of his dream:

If my potentiometer could control the pen on the recorder, something similar could, with suitable engineering, control an anti-aircraft gun.

After considerable effort, an engineering model was delivered for testing to the U.S. Army on December 1, 1941. Production models were available by early 1943, and eventually 3000 gun controllers were delivered. Input to the controller was provided by radar, and the gun was aimed by taking the data of the airplane's present position and calculating the target's future position.

Frequency-domain techniques continued to dominate the field of control following World War II with the increased use of the Laplace transform and the complex frequency plane. During the 1950s, the emphasis in control engineering theory was on the development and use of the  $s$ -plane methods and, particularly, the root locus approach. Furthermore, during the 1980s, the use of digital computers for control components became routine. The technology of these new control elements to perform accurate and rapid calculations was formerly unavailable to control engineers. There are now over 400,000 digital process control computers installed in the United States [14, 27]. These computers are employed especially for process control systems in which many variables are measured and controlled simultaneously by the computer.

With the advent of Sputnik and the space age, another new impetus was imparted to control engineering. It became necessary to design complex, highly accurate control systems for missiles and space probes. Furthermore, the necessity to minimize the weight of satellites and to control them very accurately has spawned the important field of optimal control. Due to these requirements, the time-domain methods developed by Liapunov, Minorsky, and others have been met with great interest in the last two decades. Recent theories of optimal control developed by L. S. Pontryagin in the former Soviet Union and R. Bellman in the United States, as well as recent studies of robust systems, have contributed to the interest in time-domain methods. It now is clear that control engineering must consider both the time-domain and the frequency-domain approaches simultaneously in the analysis and design of control systems.

A notable recent advance with worldwide impact is the U.S. space-based radionavigation system known as the Global Positioning System or GPS [82–85]. In the distant past, various strategies and sensors were developed to keep explorers on the oceans from getting lost, including following coastlines, using compasses to point north, and sextants to measure the angles of stars, the moon, and the sun above the horizon. The early explorers were able to estimate latitude accurately, but not longitude. It was not until the 1700s with the development of the chronometer that, when used with the sextant, the longitude could be estimated. Radio-based navigation systems began to appear in the early twentieth century and were used in World War II. With the advent of Sputnik and the space age, it became known that radio signals from satellites could be used to navigate on the ground by observing the Doppler shift of the received radio signals. Research and development culminated in the

self-oscillations over very wide frequency bands when many people doubted such circuits would be stable? My confidence stemmed from work that I had done two years earlier on certain novel oscillator circuits and three years earlier in designing the terminal circuits, including the filters, and developing the mathematics for a carrier telephone system for short toll circuits.

The frequency domain was used primarily to describe the operation of the feedback amplifiers in terms of bandwidth and other frequency variables. In contrast, the eminent mathematicians and applied mechanicians in the former Soviet Union inspired and dominated the field of control theory. Therefore, the Russian theory tended to utilize a time-domain formulation using differential equations.

The control of an industrial process (manufacturing, production, and so on) by automatic rather than manual means is often called **automation**. Automation is prevalent in the chemical, electric power, paper, automobile, and steel industries, among others. The concept of automation is central to our industrial society. Automatic machines are used to increase the production of a plant per worker in order to offset rising wages and inflationary costs. Thus industries are concerned with the productivity per worker of their plants. **Productivity** is defined as the ratio of physical output to physical input [26]. In this case, we are referring to labor productivity, which is real output per hour of work.

The transformation of the U.S. labor force in the country's brief history follows the progressive mechanization of work that attended the evolution of the agrarian republic into an industrial world power. In 1820, more than 70 percent of the labor force worked on the farm. By 1900, less than 40 percent were engaged in agriculture. Today, less than 5 percent works in agriculture [15].

In 1925, some 588,000 people—about 1.3 percent of the nation's labor force—were needed to mine 520 million tons of bituminous coal and lignite, almost all of it from underground. By 1980, production was up to 774 million tons, but the work force had been reduced to 208,000. Furthermore, only 136,000 of that number were employed in underground mining operations. The highly mechanized and highly productive surface mines, with just 72,000 workers, produced 482 million tons, or 62 percent of the total [27].

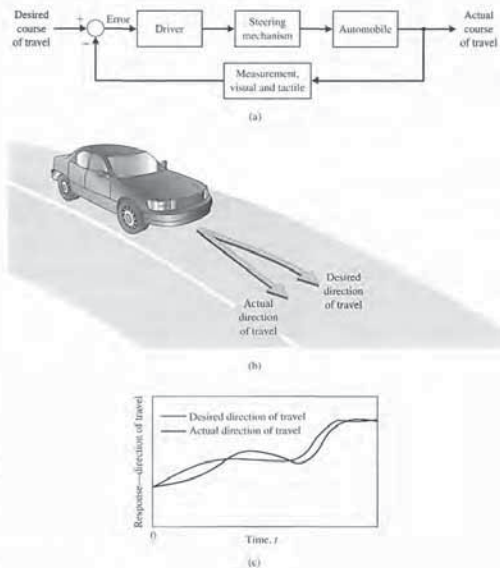
A large impetus to the theory and practice of automatic control occurred during World War II when it became necessary to design and construct automatic airplane piloting, gun-positioning systems, radar antenna control systems, and other military systems based on the feedback control approach. The complexity and expected performance of these military systems necessitated an extension of the available control techniques and fostered interest in control systems and the development of new insights and methods. Prior to 1940, for most cases, the design of control systems was an art involving a trial-and-error approach. During the 1940s, mathematical and analytical methods increased in number and utility, and control engineering became an engineering discipline in its own right [10–12].

Another example of the discovery of an engineering solution to a control system problem was the creation of a gun director by David B. Parkinson of Bell Telephone Laboratories. In the spring of 1940, Parkinson was a 29-year-old engineer intent on improving the automatic level recorder, an instrument that used strip-chart paper to plot the record of a voltage. A critical component was a small potentiometer used to control the pen of the recorder through an actuator.

### 1.3 EXAMPLES OF CONTROL SYSTEMS

Control engineering is concerned with the analysis and design of goal-oriented systems. Therefore the mechanization of goal-oriented policies has grown into a hierarchy of goal-oriented control systems. Modern control theory is concerned with systems that have self-organizing, adaptive, robust, learning, and optimum qualities.

Feedback control is a fundamental fact of modern industry and society. Driving an automobile is a pleasant task when the auto responds rapidly to the driver's commands. Many cars have power steering and brakes, which utilize hydraulic amplifiers for amplification of the force to the brakes or the steering wheel. A simple block diagram of an automobile steering control system is shown in Figure 1.9(a).



**FIGURE 1.9**  
(a) Automobile steering control system. (b) The driver uses the difference between the actual and the desired direction of travel to generate a controlled adjustment of the steering wheel. (c) Typical direction-of-travel response.

1990s with 24 navigation satellites (known as the GPS) that solved the fundamental problem that explorers faced for centuries by providing a dependable mechanism to pinpoint the current location. Freely available on a continuous worldwide basis, GPS provides very reliable location and time information anytime, day or night, anywhere in the world. Using GPS as a sensor to provide position (and velocity) information is a mainstay of active control systems for transportation systems in the air, on the ground, and on the oceans. The GPS assists relief and emergency workers to save lives, and helps us with our everyday activities including the control of power grids, banking, farming, surveying, and many other tasks.

A selected history of control system development is summarized in Table 1.1.

**Table 1.1 Selected Historical Developments of Control Systems**

1769	James Watt's steam engine and governor developed. The Watt steam engine is often used to mark the beginning of the Industrial Revolution in Great Britain. During the Industrial Revolution, great strides were made in the development of mechanization, a technology preceding automation.
1800	Eli Whitney's concept of interchangeable parts manufacturing demonstrated in the production of muskets. Whitney's development is often considered to be the beginning of mass production.
1868	J. C. Maxwell formulates a mathematical model for a governor control of a steam engine.
1913	Henry Ford's mechanized assembly machine introduced for automobile production.
1927	H. S. Black conceives of the negative feedback amplifier and H. W. Bode analyzes feedback amplifiers.
1932	H. Nyquist develops a method for analyzing the stability of systems.
1941	Creation of first anti-aircraft gun with active control.
1952	Numerical control (NC) developed at Massachusetts Institute of Technology for control of machine-tool axes.
1954	George Devol develops "programmed article transfer," considered to be the first industrial robot design.
1957	Sputnik launches the space age leading, in time, to miniaturization of computers and advances in automatic control theory.
1960	First Unimate robot introduced, based on Devol's designs. Unimate installed in 1961 for tending die-casting machines.
1970	State-variable models and optimal control developed.
1980	Robust control system design widely studied.
1983	Introduction of the personal computer (and control design software soon thereafter) brought the tools of design to the engineer's desktop.
1990	Export-oriented manufacturing companies emphasize automation.
1994	Feedback control widely used in automobiles. Reliable, robust systems demanded in manufacturing.
1995	The Global Positioning System (GPS) was operational providing positioning, navigation, and timing services worldwide.
1997	First ever autonomous rover vehicle, known as Sojourner, explores the Martian surface.
1998–2003	Advances in micro- and nanotechnology. First intelligent micromachines are developed and functioning nanomachines are created.
2007	The Orbital Express mission performed the first autonomous space rendezvous and docking.



Machines that automatically load and unload, cut, weld, or cast are used by industry to obtain accuracy, safety, economy, and productivity [14, 27, 28, 38]. The use of computers integrated with machines that perform tasks like a human worker has been foreseen by several authors. In his famous 1923 play, entitled *R.U.R.* [48], Karel Capek called artificial workers *robots*, deriving the word from the Czech noun *robota*, meaning "work."

A robot is a computer-controlled machine and involves technology closely associated with automation. Industrial robotics can be defined as a particular field of automation in which the automated machine (that is, the robot) is designed to substitute for human labor [18, 27, 33]. Thus robots possess certain humanlike characteristics. Today, the most common humanlike characteristic is a mechanical manipulator that is patterned somewhat after the human arm and wrist. Some devices even have anthropomorphic mechanisms, including what we might recognize as mechanical arms, wrists, and hands [14, 27, 28]. An example of an anthropomorphic robot is shown in Figure 1.11. We recognize that the automatic machine is well suited to some tasks, as noted in Table 1.2, and that other tasks are best carried out by humans.

Another very important application of control technology is in the control of the modern automobile [19, 20]. Control systems for suspension, steering, and engine control have been introduced. Many new autos have a four-wheel-steering system, as well as an antiskid control system.



**FIGURE 1.11**  
The Honda P3 humanoid robot. P3 walks, climbs stairs, and turns corners. Photo courtesy of American Honda Motor, Inc.

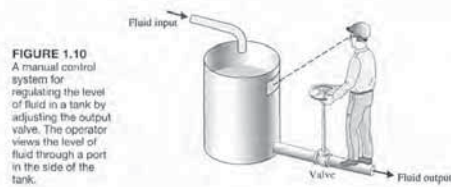
The desired course is compared with a measurement of the actual course in order to generate a measure of the error, as shown in Figure 1.9(b). This measurement is obtained by visual and tactile (body movement) feedback, as provided by the feel of the steering wheel by the hand (sensor). This feedback system is a familiar version of the steering control system in an ocean liner or the flight controls in a large airplane. A typical direction-of-travel response is shown in Figure 1.9(c).

A basic, manually controlled closed-loop system for regulating the level of fluid in a tank is shown in Figure 1.10. The input is a reference level of fluid that the operator is instructed to maintain. (This reference is memorized by the operator.) The power amplifier is the operator, and the sensor is visual. The operator compares the actual level with the desired level and opens or closes the valve (actuator), adjusting the fluid flow out, to maintain the desired level.

Other familiar control systems have the same basic elements as the system shown in Figure 1.3. A refrigerator has a temperature setting or desired temperature, a thermostat to measure the actual temperature and the error, and a compressor motor for power amplification. Other examples in the home are the oven, furnace, and water heater. In industry, there are many examples, including speed controls; process temperature and pressure controls; and position, thickness, composition, and quality controls [14, 17, 18].

In its modern usage, automation can be defined as a technology that uses programmed commands to operate a given process, combined with feedback of information to determine that the commands have been properly executed. Automation is often used for processes that were previously operated by humans. When automated, the process can operate without human assistance or interference. In fact, most automated systems are capable of performing their functions with greater accuracy and precision, and in less time, than humans are able to do. A semiautomated process is one that incorporates both humans and robots. For instance, many automobile assembly line operations require cooperation between a human operator and an intelligent robot.

Feedback control systems are used extensively in industrial applications. Thousands of industrial and laboratory robots are currently in use. Manipulators can pick up objects weighing hundreds of pounds and position them with an accuracy of one-tenth of an inch or better [28]. Automatic handling equipment for home, school, and industry is particularly useful for hazardous, repetitious, dull, or simple tasks.



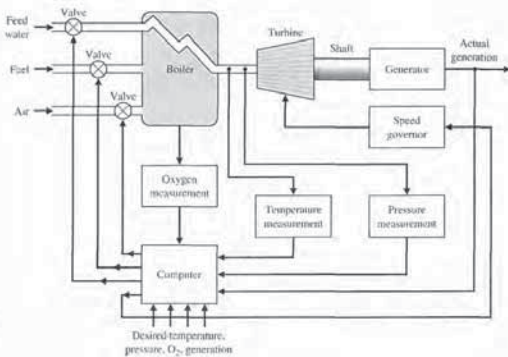
**FIGURE 1.10**  
A manual control system for regulating the level of fluid in a tank by adjusting the output valve. The operator views the level of fluid through a port in the side of the tank.

interested in energy conversion, control, and distribution. It is critical that computer control be increasingly applied to the power industry in order to improve the efficient use of energy resources. Also, the control of power plants for minimum waste emission has become increasingly important. The modern, large-capacity plants, which exceed several hundred megawatts, require automatic control systems that account for the interrelationship of the process variables and optimum power production. It is common to have 90 or more manipulated variables under coordinated control. A simplified model showing several of the important control variables of a large boiler-generator system is shown in Figure 1.13. This is an example of the importance of measuring many variables, such as pressure and oxygen, to provide information to the computer for control calculations.

The electric power industry has used the modern aspects of control engineering for significant and interesting applications. It appears that in the process industry, the factor that maintains the applications gap is the lack of instrumentation to measure all the important process variables, including the quality and composition of the product. As these instruments become available, the applications of modern control theory to industrial systems should increase measurably.

Another important industry, the metallurgical industry, has had considerable success in automatically controlling its processes. In fact, in many cases, the control theory is being fully implemented. For example, a hot-strip steel mill, which involves a \$100-million investment, is controlled for temperature, strip width, thickness, and quality.

Rapidly rising energy costs coupled with threats of energy curtailment are resulting in new efforts for efficient automatic energy management. Computer controls are used to control energy use in industry and to stabilize and connect loads evenly to gain fuel economy.



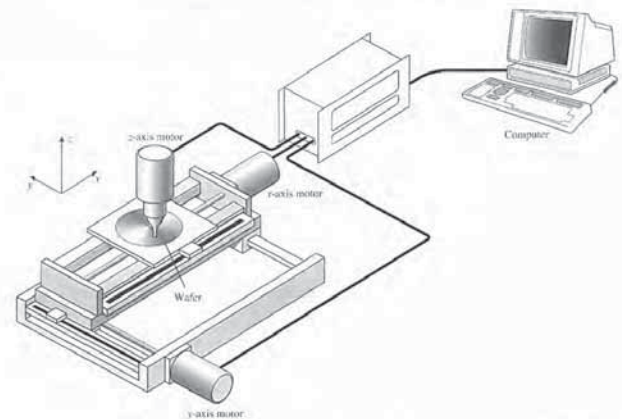
**FIGURE 1.13**  
Coordinated control system for a boiler-generator.

**Table 1.2 Task Difficulty: Human Versus Automatic Machine**

Tasks Difficult for a Machine	Tasks Difficult for a Human
Inspect seedlings in a nursery.	Inspect a system in a hot, toxic environment.
Drive a vehicle through rugged terrain.	Repetitively assemble a clock.
Identify the most expensive jewels on a tray of jewels.	Land an airliner at night, in bad weather.

A three-axis control system for inspecting individual semiconductor wafers is shown in Figure 1.12. This system uses a specific motor to drive each axis to the desired position in the *x-y-z* axis, respectively. The goal is to achieve smooth, accurate movement in each axis. This control system is an important one for the semiconductor manufacturing industry.

There has been considerable discussion recently concerning the gap between practice and theory in control engineering. However, it is natural that theory precedes the applications in many fields of control engineering. Nonetheless, it is interesting to note that in the electric power industry, the largest industry in the United States, the gap is relatively insignificant. The electric power industry is primarily



**FIGURE 1.12** A three-axis control system for inspecting individual semiconductor wafers with a highly sensitive camera.



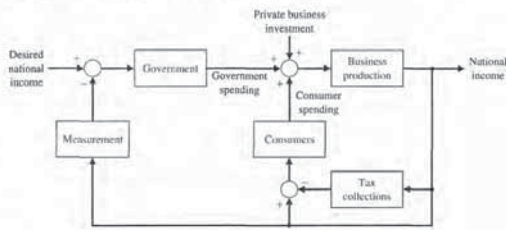


FIGURE 1.15  
A feedback control  
system model of  
the national income.

government spending. Of course, many other loops not shown also exist, since, theoretically, government spending cannot exceed the tax collected without generating a deficit, which is itself a control loop containing the Internal Revenue Service and the Congress. In a socialist country, the loop due to consumers is de-emphasized and government control is emphasized. In that case, the measurement block must be accurate and must respond rapidly; both are very difficult characteristics to realize from a bureaucratic system. This type of political or social feedback model, while usually nonrigorous, does impart information and understanding.

The ongoing area of research and development of unmanned aerial vehicles (UAVs) is full of potential for the application of control systems. An example of a UAV is shown in Figure 1.16. UAVs are unmanned but are usually controlled by ground operators. Typically they do not operate autonomously and their inability to provide the level of safety of a manned plane keeps them from flying freely in the commercial airspace. One significant challenge is to develop control systems that will avoid in-air collisions. Ultimately, the goal is to employ the UAV autonomously in such applications as aerial photography to assist in disaster mitigation, survey

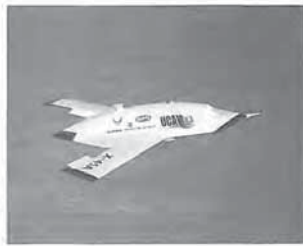
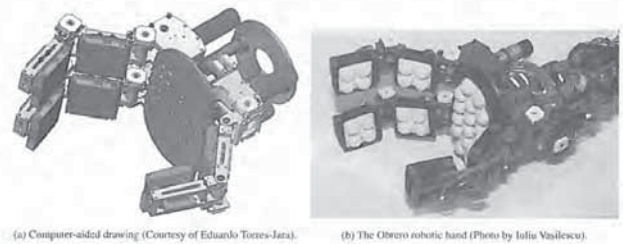


FIGURE 1.16  
An unmanned aerial  
vehicle. (Used with  
permission. Credit:  
DARPA.)

There has been considerable interest recently in applying the feedback control concepts to automatic warehousing and inventory control. Furthermore, automatic control of agricultural systems (farms) is receiving increased interest. Automatically controlled silos and tractors have been developed and tested. Automatic control of wind turbine generators, solar heating and cooling, and automobile engine performance are important modern examples [20, 21].

Also, there have been many applications of control system theory to biomedical experimentation, diagnosis, prosthetics, and biological control systems [22, 23, 48]. The control systems under consideration range from the cellular level to the central nervous system and include temperature regulation and neurological, respiratory, and cardiovascular control. Most physiological control systems are closed-loop systems. However, we find not one controller but rather control loop within control loop, forming a hierarchy of systems. The modeling of the structure of biological processes confronts the analyst with a high-order model and a complex structure. Prosthetic devices that aid the 46 million handicapped individuals in the United States are designed to provide automatically controlled aids to the disabled [22, 27, 39]. The robotic hand shown in Figure 1.14 belongs to *Obrero*, a humanoid robot developed at MIT that is capable of sensitive manipulation. The *Obrero* robot is responsive to the properties of the object it holds and does not rely on vision as the main sensor. The hand has position and force control of the fingers employing very sensitive tactile sensors and series elastic actuators in its joints.

Finally, it has become interesting and valuable to attempt to model the feedback processes prevalent in the social, economic, and political spheres. This approach is undeveloped at present but appears to have a reasonable future. Society, of course, is composed of many feedback systems and regulatory bodies, such as the Federal Reserve Board, which are controllers exerting the forces on society necessary to maintain a desired output. A simple lumped model of the national income feedback control system is shown in Figure 1.15. This type of model helps the analyst to understand the effects of government control—granted its existence—and the dynamic effects of



(a) Computer-aided drawing (Courtesy of Eduardo Torres-Jara).

(b) The Obrero robotic hand (Photo by Iulia Vasilescu).

FIGURE 1.14 The *Obrero* robot is responsive to the properties of the object it holds and does not rely on vision as the main sensor but as a complement. *Obrero* is part of the Humanoid Robotics Group at the MIT Computer Science and Artificial Intelligence Laboratory.

designed devices and products. These uncertainties are embodied in the idea of unintended consequences or **risk**. The result is that designing a system is a risk-taking activity.

Complexity, trade-off, gaps, and risk are inherent in designing new systems and devices. Although they can be minimized by considering all the effects of a given design, they are always present in the design process.

Within engineering design, there is a fundamental difference between the two major types of thinking that must take place: engineering analysis and synthesis. Attention is focused on models of the physical systems that are analyzed to provide insight and that indicate directions for improvement. On the other hand, **synthesis** is the process by which these new physical configurations are created.

Design is a process that may proceed in many directions before the desired one is found. It is a deliberate process by which a designer creates something new in response to a recognized need while recognizing realistic constraints. The design process is inherently iterative—we must start somewhere! Successful engineers learn to simplify complex systems appropriately for design and analysis purposes. A gap between the complex physical system and the design model is inevitable. Design gaps are intrinsic in the progression from the initial concept to the final product. We know intuitively that it is easier to improve an initial concept incrementally than to try to create a final design at the start. In other words, engineering design is not a linear process. It is an iterative, nonlinear, creative process.

The main approach to the most effective engineering design is parameter analysis and optimization. Parameter analysis is based on (1) identification of the key parameters, (2) generation of the system configuration, and (3) evaluation of how well the configuration meets the needs. These three steps form an iterative loop. Once the key parameters are identified and the configuration synthesized, the designer can **optimize** the parameters. Typically, the designer strives to identify a limited set of parameters to be adjusted.

## 1.5 CONTROL SYSTEM DESIGN

The design of control systems is a specific example of engineering design. The goal of control engineering design is to obtain the configuration, specifications, and identification of the key parameters of a proposed system to meet an actual need.

The control system design process is illustrated in Figure 1.17. The design process consists of seven main building blocks, which we arrange into three groups:

1. Establishment of goals and variables to be controlled, and definition of specifications (metrics) against which to measure performance
2. System definition and modeling
3. Control system design and integrated system simulation and analysis

In each chapter of this book, we will highlight the connection between the design process illustrated in Figure 1.17 and the main topics of that chapter. The objective is to demonstrate different aspects of the design process through illustrative

work to assist in construction projects, crop monitoring, and continuous weather monitoring. In a military setting, UAVs can perform intelligence, surveillance, and reconnaissance missions [74]. Smart unmanned aircraft will require significant deployment of advanced control systems throughout the airspace.

## 1.4 ENGINEERING DESIGN

**Engineering design** is the central task of the engineer. It is a complex process in which both creativity and analysis play major roles.

**Design is the process of conceiving or inventing the forms, parts, and details of a system to achieve a specified purpose.**

Design activity can be thought of as planning for the emergence of a particular product or system. Design is an innovative act whereby the engineer creatively uses knowledge and materials to specify the shape, function, and material content of a system. The design steps are (1) to determine a need arising from the values of various groups, covering the spectrum from public policy makers to the consumer; (2) to specify in detail what the solution to that need must be and to embody these values; (3) to develop and evaluate various alternative solutions to meet these specifications; and (4) to decide which one is to be designed in detail and fabricated.

An important factor in realistic design is the limitation of time. Design takes place under imposed schedules, and we eventually settle for a design that may be less than ideal but considered “good enough.” In many cases, time is the *only* competitive advantage.

A major challenge for the designer is writing the specifications for the technical product. **Specifications** are statements that explicitly state what the device or product is to be and do. The design of technical systems aims to provide appropriate design specifications and rests on four characteristics: complexity, trade-offs, design gaps, and risk.

**Complexity of design** results from the wide range of tools, issues, and knowledge to be used in the process. The large number of factors to be considered illustrates the complexity of the design specification activity, not only in assigning these factors their relative importance in a particular design, but also in giving them substance either in numerical or written form, or both.

The concept of **trade-off** involves the need to resolve conflicting design goals, all of which are desirable. The design process requires an efficient compromise between desirable but conflicting criteria.

In making a technical device, we generally find that the final product does not appear as originally visualized. For example, our image of the problem we are solving does not appear in written description and ultimately in the specifications. Such **design gaps** are intrinsic in the progression from an abstract idea to its realization.

This inability to be absolutely sure about predictions of the performance of a technological object leads to major uncertainties about the actual effects of the



As designers, we proceed to the first attempt to configure a system that will result in the desired control performance. This system configuration will normally consist of a sensor, the process under control, an actuator, and a controller, as shown in Figure 1.3. The next step consists of identifying a candidate for the actuator. This will, of course, depend on the process, but the actuation chosen must be capable of effectively adjusting the performance of the process. For example, if we wish to control the speed of a rotating flywheel, we will select a motor as the actuator. The sensor, in this case, must be capable of accurately measuring the speed. We then obtain a model for each of these elements.

Students studying controls are often given the models, frequently represented in transfer function or state variable form, with the understanding that they represent the underlying physical systems, but without further explanation. An obvious question is, where did the transfer function or state variable model come from? Within the context of a course in control systems, there is a need to address key questions surrounding modeling. To that end, in the early chapters, we will provide insight into key modeling concerns and answer fundamental questions: How is the transfer function obtained? What basic assumptions are implied in the model development? How general are the transfer functions? However, mathematical modeling of physical systems is a subject in and of itself. We cannot hope to cover the mathematical modeling in its entirety, but interested students are encouraged to seek outside references (see for example [76–80]).

The next step is the selection of a controller, which often consists of a summing amplifier that will compare the desired response and the actual response and then forward this error-measurement signal to an amplifier.

The final step in the design process is the adjustment of the parameters of the system to achieve the desired performance. If we can achieve the desired performance by adjusting the parameters, we will finalize the design and proceed to document the results. If not, we will need to establish an improved system configuration and perhaps select an enhanced actuator and sensor. Then we will repeat the design steps until we are able to meet the specifications, or until we decide the specifications are too demanding and should be relaxed.

The design process has been dramatically affected by the advent of powerful and inexpensive computers and effective control design and analysis software. For example, the Boeing 777, which incorporates the most advanced flight avionics of any U.S. commercial aircraft, was almost entirely computer-designed [56, 57]. Verification of final designs in high-fidelity computer simulations is essential. In many applications, the certification of the control system in realistic simulations represents a significant cost in terms of money and time. The Boeing 777 test pilots flew about 2400 flights in high-fidelity simulations before the first aircraft was even built.

Another notable example of computer-aided design and analysis is the McDonnell Douglas Delta Clipper experimental vehicle DC-X, which was designed, built, and flown in 24 months. Computer-aided design tools and automated code-generation contributed to an estimated 80 percent cost savings and 30 percent time savings [58].

In summary, the controller design problem is as follows: Given a model of the system to be controlled (including its sensors and actuators) and a set of design goals, find a suitable controller, or determine that none exists. As with most of engineering

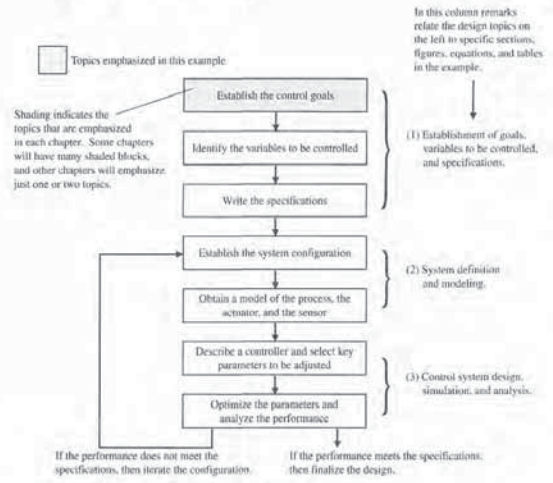


FIGURE 1.17 The control system design process.

examples, we have established the following connections between the chapters in this book and the design process block diagram:

1. Establishment of goals, control variables, and specifications: Chapters 1, 3, 4, and 13.
2. System definition and modeling: Chapters 2–4, and 11–13.
3. Control system design, simulation, and analysis: Chapters 4–13.

The first step in the design process consists of establishing the system goals. For example, we may state that our goal is to control the velocity of a motor accurately. The second step is to identify the variables that we desire to control (for example, the velocity of the motor). The third step is to write the specifications in terms of the accuracy we must attain. This required accuracy of control will then lead to the identification of a sensor to measure the controlled variable. The performance specifications will describe how the closed-loop system should perform and will include (1) good regulation against disturbances, (2) desirable responses to commands, (3) realistic actuator signals, (4) low sensitivities, and (5) robustness.

engineering, computer science, and the natural sciences. Advancements in traditional disciplines are fueling the growth of mechatronics systems by providing “enabling technologies.” A critical enabling technology was the microprocessor which has had a profound effect on the design of consumer products. We should expect continued advancements in cost-effective microprocessors and microcontrollers, novel sensors and actuators enabled by advancements in applications of microelectromechanical systems (MEMS), advanced control methodologies and real-time programming methods, networking and wireless technologies, and mature computer-aided engineering (CAE) technologies for advanced system modeling, virtual prototyping, and testing. The continued rapid development in these areas will only accelerate the pace of smart (that is, actively controlled) products.

An exciting area of future mechatronic system development in which control systems will play a significant role is the area of alternative energy production and consumption. Hybrid fuel automobiles and efficient wind power generation are two examples of systems that can benefit from mechatronic design methods. In fact, the mechatronic design philosophy can be effectively illustrated by the example of the evolution of the modern automobile [64]. Before the 1960s, the radio was the only significant electronic device in an automobile. Today, many automobiles have 30–60 microcontrollers, up to 100 electric motors, about 200 pounds of wiring, a multitude of sensors, and thousands of lines of software code. A modern automobile can no longer be classified as a strictly mechanical machine—it has been transformed into a comprehensive mechatronic system.

**EXAMPLE 1.1 Hybrid fuel vehicles**

Recent research and development has led to the next-generation **hybrid fuel automobile**, depicted in Figure 1.19. The hybrid fuel vehicle utilizes a conventional internal combustion engine in combination with a battery (or other energy storage device such as a fuel cell or flywheel) and an electric motor to provide a propulsion system capable of doubling the fuel economy over conventional automobiles. Although



FIGURE 1.19 The hybrid fuel automobile can be viewed as a mechatronic system. (Used with permission of DOE/NREL. Credit: Warren Gretz.)

design, the design of a feedback control system is an iterative and nonlinear process. A successful designer must consider the underlying physics of the plant under control, the control design strategy, the controller design architecture (that is, what type of controller will be employed), and effective controller tuning strategies. In addition, once the design is completed, the controller is often implemented in hardware, and hence issues of interfacing with hardware can appear. When taken together, these different phases of control system design make the task of designing and implementing a control system quite challenging [73].

**1.6 MECHATRONIC SYSTEMS**

A natural stage in the evolutionary process of modern engineering design is encompassed in the area known as **mechatronics** [64]. The term mechatronics was coined in Japan in the 1970s [65–67]. Mechatronics is the synergistic integration of mechanical, electrical, and computer systems and has evolved over the past 30 years, leading to a new breed of intelligent products. Feedback control is an integral aspect of modern mechatronic systems. One can understand the extent that mechatronics reaches into various disciplines by considering the components that make up mechatronics [68–71]. The key elements of mechatronics are (1) physical systems modeling, (2) sensors and actuators, (3) signals and systems, (4) computers and logic systems, and (5) software and data acquisition. Feedback control encompasses aspects of all five key elements of mechatronics, but is associated primarily with the element of signals and systems, as illustrated in Figure 1.18.

Advances in computer hardware and software technology coupled with the desire to increase the performance-to-cost ratio has revolutionized engineering design. New products are being developed at the intersection of traditional disciplines of

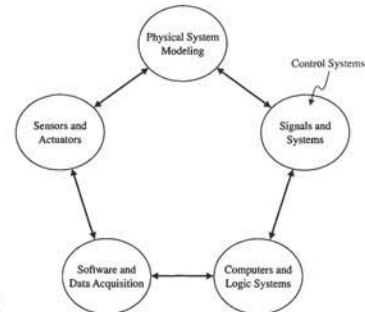


FIGURE 1.18 The key elements of mechatronics [64].



researchers have concentrated on developing technologies that work well in high wind areas (defined to be areas with a wind speed of at least 6.7 m/s at a height of 10 m). Most of the easily accessible high wind sites in the United States are now utilized, and improved technology must be developed to make lower wind areas more cost effective. New developments are required in materials and aerodynamics so that longer turbine rotors can operate efficiently in the lower winds, and in a related problem, the towers that support the turbine must be made taller without increasing the overall costs. In addition, advanced controls will be required to achieve the level of efficiency required in the wind generation drive train. ■

### EXAMPLE 1.3 Embedded computers

Many contemporary control systems are **embedded control** systems [81]. Embedded control systems employ on-board special-purpose digital computers as integral components of the feedback loop. Figure 1.21 illustrates a student-built rover constructed around the Compact RIO by National Instruments, Inc. that serves as the on-board embedded computer. In the rover design, the sensors include an optical encoder for measuring engine speed, a rate gyro and accelerometer to measure turns, and a Global Positioning System (GPS) unit to obtain position and velocity estimates of the vehicle. The actuators include two linear actuators to turn the front wheels and to brake and accelerate. The communications device permits the rover to stay in contact with the ground station.

Advances in sensors, actuators, and communication devices are leading to a new class of embedded control systems that are networked using wireless technology, thereby enabling spatially-distributed control. Embedded control system designers

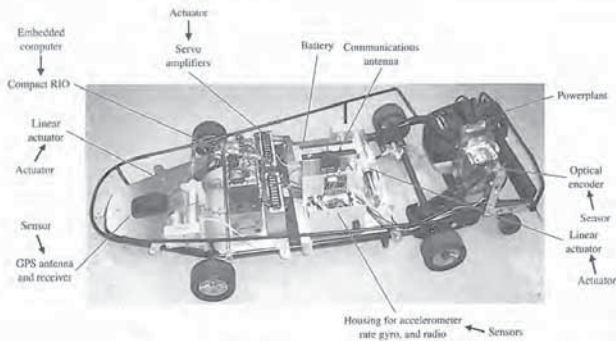


FIGURE 1.21 A rover using an embedded computer in the feedback loop. (Photo by R.H. Bishop.)

are key technology areas that enable the smart grids [87]. Green engineering applications can be classified into one of five categories [88]:

1. Environmental Monitoring
2. Energy Storage Systems
3. Power Quality Monitoring
4. Solar Energy
5. Wind Energy

As the field of green engineering matures, it is almost certain that more applications will evolve, especially as we apply the eighth principle (listed above) of green engineering to create engineering solutions beyond current or dominant technologies and improve, innovate, and invent technologies. In the subsequent chapters, we present examples from each of these areas.

There is a global effort underway to reduce greenhouse gases from all sources. To accomplish this, it is necessary to improve both the quality and quantity of our environmental monitoring systems. An example is using wireless measurements on a cabled robotic controlled mobile sensing platform moving along the forest understorey to measure key environmental parameters in a rain forest.

Energy storage systems are critical technologies for green engineering. There are many types of energy storage systems. The energy storage system we are most familiar with is the battery. Batteries are used to power most of the electronic devices in use today; some batteries are rechargeable and some are single-use throw-aways. To adhere to green engineering principles, we would favor energy storage systems that are renewable. A very important energy storage device for green engineering systems is the fuel cell.

The problems associated with power quality monitoring are varied and can include leading and lagging power, voltage variations, and waveform harmonics. Many of the green engineering systems and components require careful monitoring of current and voltages. An interesting example would be the modeling of current transformers that are used in various capacities for measuring and monitoring within the power grid network of interconnected systems used to deliver electricity.

Efficiently converting solar energy into electricity is an engineering challenge. Two technologies for generation of electricity using sunshine are solar photovoltaic and solar thermal. With photovoltaic systems the sunlight is converted directly to electricity, and with solar thermal the sun heats water to create steam that is used to power steam engines. Designing and deploying solar photovoltaic systems for solar power generation is one approach employing green engineering principles to utilize the sun's energy to power our homes, offices, and businesses.

Power derived from wind is an important source of renewable energy around the world. Wind energy conversion to electric power is achieved by wind energy turbines connected to electric generators. The intermittency characteristic of wind energy makes the smart grid development (see Example 1.4) essential to bring the energy to the power grid when it is available and to provide energy from other sources when the wind dies down or is disrupted. The irregular character of wind direction and power also results in the need for reliable, steady electric energy by using control systems on the wind turbines themselves. The goal of these control

these hybrid vehicles will never be zero-emission vehicles (since they have internal combustion engines), they can reduce the level of harmful emissions by one-third to one-half, and with future improvements, these emissions may reduce even further. As stated earlier, the modern automobile requires many advanced control systems to operate. The control systems must regulate the performance of the engine, including fuel-air mixtures, valve timing, transmissions, wheel traction control, antilock brakes, and electronically controlled suspensions, among many other functions. On the hybrid fuel vehicle, there are additional control functions that must be satisfied. Especially necessary is the control of power between the internal combustion engine and the electric motor, determining power storage needs and implementing the battery charging, and preparing the vehicle for low-emission start-ups. The overall effectiveness of the hybrid fuel vehicle depends on the combination of power units that are selected (e.g., battery versus fuel cell for power storage). Ultimately, however, the control strategy that integrates the various electrical and mechanical components into a viable transportation system strongly influences the acceptability of the hybrid fuel vehicle concept in the marketplace. ■

The second example of a mechatronic system is the advanced wind power generation system.

### EXAMPLE 1.2 Wind power

Many nations in the world today are faced with unstable energy supplies, often leading to rising fuel prices and energy shortages. Additionally, the negative effects of fossil fuel utilization on the quality of our air are well documented. Many nations have an imbalance in the supply and demand of energy, consuming more than they produce. To address this imbalance, many engineers are considering developing advanced systems to access other sources of energy, such as wind energy. In fact, wind energy is one of the fastest-growing forms of energy generation in the United States and in other locations around the world. A wind farm now in use in western Texas is illustrated in Figure 1.20.

In 2006, the installed global wind energy capacity was over 59,000 MW. In the United States, there was enough energy derived from wind to power over 2.5 million homes, according to the American Wind Energy Association. For the past 35 years,



FIGURE 1.20 Efficient wind power generation in west Texas. (Used with permission of DOE/NREL. Credit: Lower Colorado River Authority.)

must be able to understand and work with various network protocols, diverse operating systems and programming languages. While the theory of systems and controls serves as the foundation for the modern control system design, the design process is rapidly expanding into a multi-disciplinary enterprise encompassing multiple engineering areas, as well as information technology and computer science. ■

Advances in alternate energy products, such as the hybrid automobile and the generation of efficient wind power generators, provide vivid examples of mechatronics development. There are numerous other examples of intelligent systems poised to enter our everyday life, including autonomous rovers, smart home appliances (e.g., dishwashers, vacuum cleaners, and microwave ovens), wireless network-enabled devices, "human-friendly machines" [72] that perform robot-assisted surgery, and implantable sensors and actuators.

## 1.7 GREEN ENGINEERING

Global issues such as climate change, clean water, sustainability, waste management, emissions reduction, and minimizing raw material and energy use have caused many engineers to re-think existing approaches to engineering design in critical areas. One outcome of the evolving design strategy is to consider an approach that has come to be known as "green engineering." The goal of green engineering is to design products that will minimize pollution, reduce the risk to human health, and improve the environment. The basic principles of green engineering are [86]:

1. Engineer processes and products holistically, use systems analysis, and integrate environmental impact assessment tools.
2. Conserve and improve natural ecosystems while protecting human health and well-being.
3. Use life-cycle thinking in all engineering activities.
4. Ensure that all material and energy inputs and outputs are as inherently safe and benign as possible.
5. Minimize depletion of natural resources.
6. Strive to prevent waste.
7. Develop and apply engineering solutions, while being cognizant of local geography, aspirations, and cultures.
8. Create engineering solutions beyond current or dominant technologies; improve, innovate, and invent technologies to achieve sustainability.
9. Actively engage communities and stakeholders in development of engineering solutions.

Putting the principles of green engineering into practice leads us to a deeper understanding of the power of feedback control systems as an enabling technology. For example, in Section 1.9, we present a discussion on smart grids. Smart grids aim to deliver electrical power more reliably and efficiently in an environmentally friendly fashion. This in turn will potentially enable the large-scale use of renewable energy sources, such as wind and solar, that are naturally intermittent. Sensing and feedback



revolution in computer technology is causing an equally momentous social change, the expansion of information gathering and information processing as computers extend the reach of the human brain [16].

Control systems are used to achieve (1) increased productivity and (2) improved performance of a device or system. Automation is used to improve productivity and obtain high-quality products. Automation is the automatic operation or control of a process, device, or system. We use automatic control of machines and processes to produce a product reliably and with high precision [28]. With the demand for flexible, custom production, a need for flexible automation and robotics is growing [17, 25].

The theory, practice, and application of automatic control is a large, exciting, and extremely useful engineering discipline. One can readily understand the motivation for a study of modern control systems.

1.9 DESIGN EXAMPLES

In this section we present illustrative design examples. This is a pattern that we will follow in all subsequent chapters. Each chapter will contain a number of interesting examples in a special section entitled Design Examples meant to highlight the main topics of the chapter. At least one example among those presented in the Design Example section will be a more detailed problem and solution that demonstrates one or more of the steps in the design process shown in Figure 1.17. In the first example, we discuss the development of the smart grid as a concept to deliver electrical power more reliably and efficiently as part of a strategy to provide a more environmentally friendly energy delivery system. The smart grid will enable the large-scale use of renewable energy sources that depend on the natural phenomenon to generate power and which are intermittent, such as wind and solar. Providing clean energy is an engineering challenge that must necessarily include active feedback control systems, sensors, and actuators. In the second example presented here, a rotating disk speed control illustrates the concept of open-loop and closed-loop feedback control. The third example is an insulin delivery control system in which we determine the design goals, the variables to control, and a preliminary closed-loop system configuration.

EXAMPLE 1.4 Smart grid control systems

A smart grid is as much a concept as it is a physical system. In essence, the concept is to deliver power more reliably and efficiently while remaining environmentally friendly, economical, and safe [89, 90]. A smart grid can be viewed as a system comprised of hardware and software that routes power more reliably and efficiently to homes, businesses, schools, and other users of power. One view of the smart grid is illustrated schematically in Figure 1.23. Smart grids can be national or local in scope. One can even consider home smart grids (or microgrids). In fact, smart grids encompass a wide and rich field of investigation. As we will find, control systems play a key role in smart grids at all levels.

One interesting aspect of the smart grid is real-time demand side management requiring a two-way flow of information between the user and the power generation system [91]. For example, smart meters are used to measure electricity use in the home and office. These sensors transmit data to utilities and allow the utility to transmit control signals back to a home or building. These smart meters can control and turn on

devices is to reduce the effects of wind intermittency and the effect of wind direction change.

The role of control systems in green engineering will continue to expand as the global issues facing us require ever increasing levels of automation and precision.

1.8 THE FUTURE EVOLUTION OF CONTROL SYSTEMS

The continuing goal of control systems is to provide extensive flexibility and a high level of autonomy. Two system concepts are approaching this goal by different evolutionary pathways, as illustrated in Figure 1.22. Today's industrial robot is perceived as quite autonomous—once it is programmed, further intervention is not normally required. Because of sensory limitations, these robotic systems have limited flexibility in adapting to work environment changes; improving perception is the motivation of computer vision research. The control system is very adaptable, but it relies on human supervision. Advanced robotic systems are striving for task adaptability through enhanced sensory feedback. Research areas concentrating on artificial intelligence, sensor integration, computer vision, and off-line CAD/CAM programming will make systems more universal and economical. Control systems are moving toward autonomous operation as an enhancement to human control. Research in supervisory control, human-machine interface methods, and computer database management are intended to reduce operator burden and improve operator efficiency. Many research activities are common to robotics and control systems and are aimed at reducing implementation cost and expanding the realm of application. These include improved communication methods and advanced programming languages.

The easing of human labor by technology, a process that began in prehistory, is entering a new stage. The acceleration in the pace of technological innovation inaugurated by the Industrial Revolution has until recently resulted mainly in the displacement of human muscle power from the tasks of production. The current

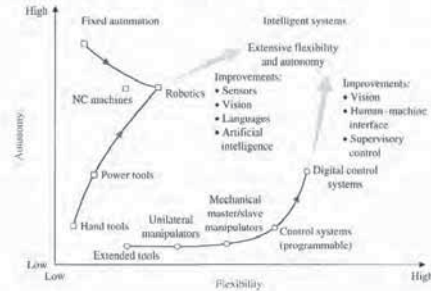


FIGURE 1.22 Future evolution of control systems and robotics.

Transmission of power is called power flow and the improved control of power will increase its security and efficiency. Transmission lines have inductive, capacitive, and resistive effects that result in dynamic impacts or disturbances. The smart grid must anticipate and respond to system disturbances rapidly. This is referred to as self-healing. In other words, a smart grid should be capable of managing significant disturbances occurring on very short time scales. To accomplish this, the self-healing process is constructed around the idea of a feedback control system where self-assessments are used to detect and analyze disturbances so that corrective action can be applied to restore the grid. This requires sensing and measurements to provide information to the control systems. One of the benefits of using smart grids is that renewable energy sources that depend on intermittent natural phenomena (such as wind and sunshine) can potentially be utilized more efficiently by allowing for load shedding when the wind dies out or clouds block the sunshine.

Feedback control systems will play an increasingly important role in the development of smart grids as we move to the target date. It may be interesting to recall the various topics discussed in this section in the context of control systems as each chapter in this textbook unfolds new methods of control system design and analysis.

EXAMPLE 1.5 Rotating disk speed control

Many modern devices employ a rotating disk held at a constant speed. For example, a CD player requires a constant speed of rotation in spite of motor wear and variation and other component changes. Our goal is to design a system for rotating disk speed control that will ensure that the actual speed of rotation is within a specified percentage of the desired speed [40, 43]. We will consider a system without feedback and a system with feedback.

To obtain disk rotation, we will select a DC motor as the actuator because it provides a speed proportional to the applied motor voltage. For the input voltage to the motor, we will select an amplifier that can provide the required power.

The open-loop system (without feedback) is shown in Figure 1.24(a). This system uses a battery source to provide a voltage that is proportional to the desired speed. This

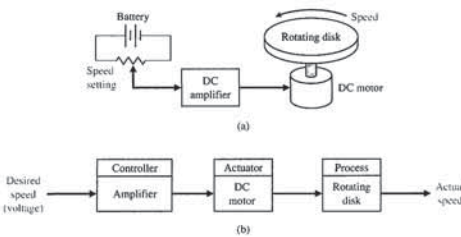


FIGURE 1.24 (a) Open-loop (without feedback) control of the speed of a rotating disk. (b) Block diagram model.

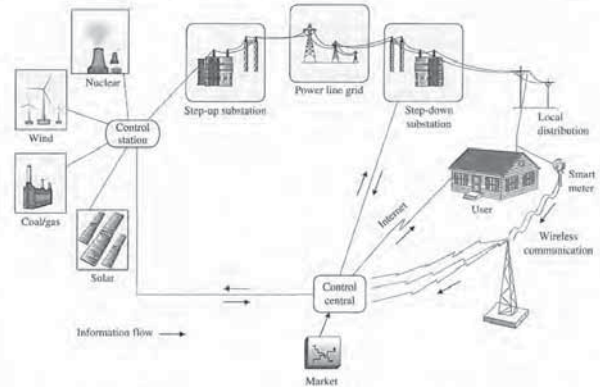


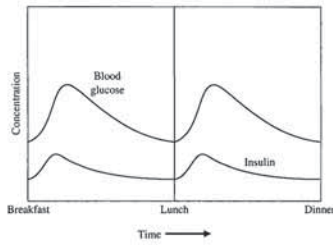
FIGURE 1.23 Smart grids are distribution networks that measure and control usage.

or off home and office appliances and devices. Smart home-energy devices enable the homeowners to control their usage and respond to price changes at peak-use times.

The five key technologies required to implement a successful modern smart grid include (i) integrated communications, (ii) sensing and measurements, (iii) advanced components, (iv) advanced control methods, and (v) improved interfaces and decision support [87]. Two of the five key technologies fall under the general category of control systems, namely (ii) sensing and measurements and (iii) advanced control methods. It is evident that control systems will play a key role in realizing the modern smart grid. The potential impact of the smart grid on delivery of power is very high. Currently, the total U.S. grid includes 16,000 power plants, about 3,300 utility companies, and 300,000 miles of power lines. A smart grid will use sensors, controllers, the Internet, and communication systems to improve the reliability and efficiency of the grid. It is estimated that deployment of smart grids could reduce emissions globally of CO<sub>2</sub> due to power systems by 14 percent by 2020 [91].

One of the elements of the smart grid are the distribution networks that measure and control usage. In a smart grid, the power generation depends on the market situation (supply/demand and cost) and the power source available (wind, coal, nuclear, geothermal, biomass, etc.). In fact, smart grid customers with solar panels or wind turbines could sell their excess energy to the grid and get paid as microgenerators [92]. In the subsequent chapters, we discuss various control problems associated with pointing solar panels to the sun and with prescribing the pitch of the wind turbine blades to manage the rotor speed thereby controlling the power output.





**FIGURE 1.26** The blood glucose and insulin levels for a healthy person.

Referring to Figure 1.26, the next step in the design process is to define the variable to be controlled. Associated with the control goal we can define the variable to be controlled to be:

**Variable to Be Controlled**  
Blood glucose concentration

In subsequent chapters, we will have the tools to quantitatively describe the control design specifications using a variety of steady-state performance specifications and transient response specifications, both in the time-domain and in the frequency domain. At this point, the control design specifications will be qualitative and imprecise. In that regard, for the problem at hand, we can state the design specification as:

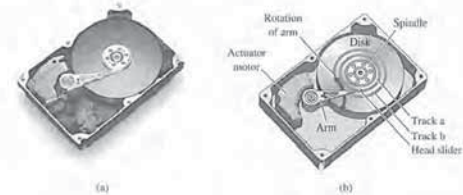
**Control Design Specifications**  
Provide a blood glucose level for the diabetic that closely approximates (tracks) the glucose level of a healthy person.

Given the design goals, variables to be controlled, and control design specifications, we can now propose a preliminary system configuration. An open-loop system would use a preprogrammed signal generator and miniature motor pump to regulate the insulin delivery rate as shown in Figure 1.27(a). The feedback control system would use a sensor to measure the actual glucose level and compare that level with the desired level, thus turning the motor pump on when it is required, as shown in Figure 1.27(b).

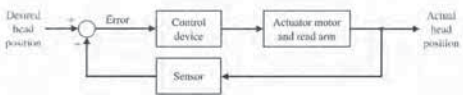
1.10 SEQUENTIAL DESIGN EXAMPLE: DISK DRIVE READ SYSTEM

This design example, identified by the arrow icon, will be considered sequentially in each chapter. We will use the design process of Figure 1.17 in each chapter to identify the steps that we are accomplishing. For example, in Chapter 1 we (1) identify the control goal, (2) identify the variables to be controlled, (3) write the initial specifications for the variables, and (4) establish the preliminary system configuration.

Information can be readily and efficiently stored on magnetic disks. Disk drives are used in notebook computers and larger computers of all sizes and are essentially all standardized as defined by ANSI standards [50, 63]. The worldwide total available market for disk drives is greater than 650 million units [51]. In the past, disk drive designers



**FIGURE 1.29** (a) A disk drive © 1999 Quantum Corporation. All rights reserved. (b) Diagram of a disk drive.

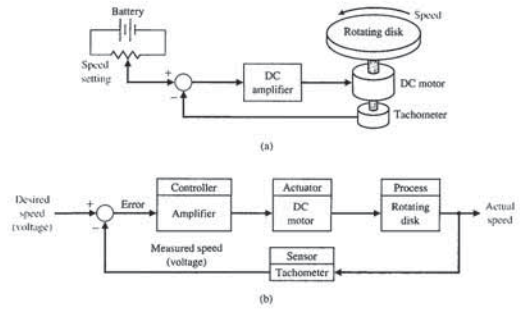


**FIGURE 1.30** Closed-loop control system for disk drive.

areas of “intelligence” under investigation include off-line error recovery, disk drive failure warnings, and storing data across multiple disk drives. Consider the basic diagram of a disk drive shown in Fig. 1.29. The goal of the disk drive reader device is to position the reader head to read the data stored on a track on the disk. The variable to accurately control is the position of the reader head (mounted on a slider device). The disk rotates at a speed between 1800 and 7200 rpm, and the head “flies” above the disk at a distance of less than 100 nm. The initial specification for the position accuracy is 1 μm. Furthermore, we plan to be able to move the head from track a to track b within 50 ms, if possible. Thus, we establish an initial system configuration as shown in Figure 1.30. This proposed closed-loop system uses a motor to actuate (move) the arm to the desired location on the disk. We will consider the design of the disk drive further in Chapter 2.

1.11 SUMMARY

In this chapter, we discussed open- and closed-loop feedback control systems. Examples of control systems through the course of history were presented to motivate and connect the subject to the past. In terms of contemporary issues, key areas of application were discussed, including humanoid robots, unmanned aerial vehicles, wind energy, hybrid automobiles, and embedded control. The central role of controls in mechatronics was discussed. Mechatronics is the synergistic integration of mechanical, electrical, and computer systems. Finally, the design process was presented in a structured form and included the following steps: the establishment of goals and variables to be controlled, definition of specifications, system definition, modeling, and analysis. The iterative nature of design allows us to handle the design gap effectively while accomplishing necessary trade-offs in complexity, performance, and cost.



**FIGURE 1.25** (a) Closed-loop control of the speed of a rotating disk. (b) Block diagram model.

voltage is amplified and applied to the motor. The block diagram of the open-loop system identifying the controller, actuator, and process is shown in Figure 1.24(b).

To obtain a feedback system, we need to select a sensor. One useful sensor is a tachometer that provides an output voltage proportional to the speed of its shaft. Thus the closed-loop feedback system takes the form shown in Fig. 1.25(a). The block diagram model of the feedback system is shown in Fig. 1.25(b). The error voltage is generated by the difference between the input voltage and the tachometer voltage.

We expect the feedback system of Figure 1.25 to be superior to the open-loop system of Figure 1.24 because the feedback system will respond to errors and act to reduce them. With precision components, we could expect to reduce the error of the feedback system to one-hundredth of the error of the open-loop system. ■

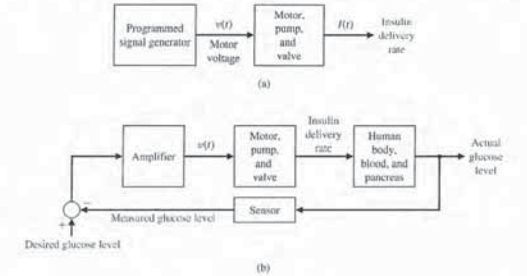
EXAMPLE 1.6 Insulin delivery control system

Control systems have been utilized in the biomedical field to create implanted automatic drug-delivery systems to patients [29–31]. Automatic systems can be used to regulate blood pressure, blood sugar level, and heart rate. A common application of control engineering is in the field of open-loop system drug delivery, in which mathematical models of the dose-effect relationship of the drugs are used. A drug-delivery system implanted in the body uses an open-loop system, since miniaturized glucose sensors are not yet available. The best solutions rely on individually programmable, pocket-sized insulin pumps that can deliver insulin according to a preset time history. More complicated systems will use closed-loop control for the measured blood glucose levels.

The blood glucose and insulin concentrations for a healthy person are shown in Figure 1.26. The system must provide the insulin from a reservoir implanted within the diabetic person. Therefore, the control goal is:

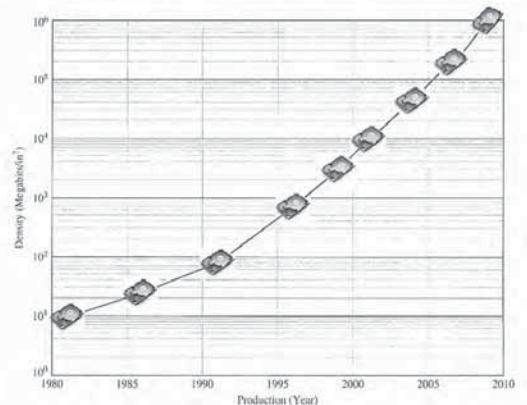
Control Goal

Design a system to regulate the blood sugar concentration of a diabetic by controlled dispensing of insulin.



**FIGURE 1.27** (a) Open-loop (without feedback) control and (b) closed-loop control of blood glucose.

have concentrated on increasing data density and data access times. Recent trends show that hard disk drive densities are increasing at about 40 percent per year [62]. Figure 1.28 shows the disk drive density trends. Designers are now considering employing disk drives to perform tasks historically delegated to central processing units (CPUs), thereby leading to improvements in the computing environment [63]. Three



**FIGURE 1.28** Disk drive data density trends (Source: IBM).

10. Complete the following sentence:  
Control engineers are concerned with understanding and controlling segments of their environments, often called \_\_\_\_\_.
- systems
  - design synthesis
  - trade-offs
  - risk
11. Early pioneers in the development of systems and control theory include:
- H. Nyquist
  - H. W. Bode
  - H. S. Black
  - All of the above
12. Complete the following sentence:  
An open-loop control system utilizes an actuating device to control a process \_\_\_\_\_.
- without using feedback
  - using feedback
  - in engineering design
  - in engineering synthesis
13. A system with more than one input variable or more than one output variable is known by what name?
- Closed-loop feedback system
  - Open-loop feedback system
  - Multivariable control system
  - Robust control system
14. Control engineering is applicable to which fields of engineering?
- Mechanical and aerospace
  - Electrical and biomedical
  - Chemical and environmental
  - All of the above
15. Closed-loop control systems should have which of the following properties:
- Good regulation against disturbances
  - Desirable responses to commands
  - Low sensitivity to changes in the plant parameters
  - All of the above
- In the following Word Match problems, match the term with the definition by writing the correct letter in the space provided.
- |                         |   |       |
|-------------------------|---|-------|
| a. Optimization         | The output signal is fed back so that it subtracts from the input signal.               | _____ |
| b. Risk                 | A system that uses a measurement of the output and compares it with the desired output. | _____ |
| c. Complexity of design | A set of prescribed performance criteria.   | _____ |
| d. System               | A measure of the output of the system used for feedback to control the system.          | _____ |
| e. Design               | A system with more than one input variable or more than one output variable.            | _____ |

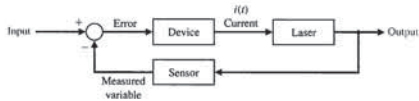


FIGURE E1.3 Partial block diagram of an optical source.

- Mechanical deformation to electrical energy
  - Chemical energy to kinetic energy
- E1.3 A precise optical signal source can control the output power level to within 1 percent [32]. A laser is controlled by an input current to yield the power output. A microprocessor controls the input current to the laser. The microprocessor compares the desired power level with a measured signal proportional to the laser power output obtained from a sensor. Complete the block diagram representing this closed-loop control system shown in Figure E1.3, identifying the output, input, and measured variables and the control device.
- E1.4 An automobile driver uses a control system to maintain the speed of the car at a prescribed level. Sketch a block diagram to illustrate this feedback system.
- E1.5 Fly-fishing is a sport that challenges the person to cast a small feathery fly using a light rod and line. The goal is to place the fly accurately and lightly on the distant surface of the stream [59]. Describe the fly-casting process and a model of this process.
- E1.6 An autofocus camera will adjust the distance of the lens from the film by using a beam of infrared or ultrasound to determine the distance to the subject [42]. Sketch a block diagram of this open-loop control system, and briefly explain its operation.
- E1.7 Because a sailboat cannot sail directly into the wind, and traveling straight downwind is usually slow, the shortest sailing distance is rarely a straight line. Thus sailboats tack upwind—the familiar zigzag course—and jibe downwind. A tactician's decision of when to tack and where to go can determine the outcome of a race. Describe the process of tacking a sailboat as the wind shifts direction. Sketch a block diagram depicting this process.
- E1.8 Modern automated highways are being implemented around the world. Consider two highway lanes merging into a single lane. Describe a feedback control system carried on the automobile trailing the lead automobile that ensures that the vehicles merge with a prescribed gap between the two vehicles.
- E1.9 Describe the block diagram of the speed control system of a motorcycle with a human driver.
- E1.10 Describe the process of human biofeedback used to regulate factors such as pain or body temperature.
- Biofeedback is a technique whereby a human can, with some success, consciously regulate pulse, reaction to pain, and body temperature.
- E1.11 Future advanced commercial aircraft will be enabled. This will allow the aircraft to take advantage of continuing improvements in computer power and network growth. Aircraft can continuously communicate their location, speed, and critical health parameters to ground controllers, and gather and transmit local meteorological data. Sketch a block diagram showing how the meteorological data from multiple aircraft can be transmitted to the ground, combined using ground-based powerful networked computers to create an accurate weather situational awareness, and then transmitted back to the aircraft for optimal routing.
- E1.12 Unmanned aerial vehicles (UAVs) are being developed to operate in the air autonomously for long periods of time (see Section 1.3). By autonomous, we mean that there is no interaction with human ground controllers. Sketch a block diagram of an autonomous UAV that is tasked for crop monitoring using aerial photography. The UAV must photograph and transmit the entire land area by flying a pre-specified trajectory as accurately as possible.
- E1.13 Consider the inverted pendulum shown in Figure E1.13. Sketch the block diagram of a feedback control.

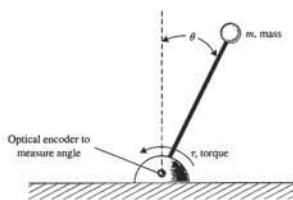


FIGURE E1.13 Inverted pendulum control.



SKILLS CHECK

In this section, we provide three sets of problems to test your knowledge: True or False, Multiple Choice, and Word Match. To obtain direct feedback, check your answers with the answer key provided at the conclusion of the end-of-chapter problems.

In the following True or False and Multiple Choice problems, circle the correct answer.

- The flyball governor is generally agreed to be the first automatic feedback controller used in an industrial process. True or False
- A closed-loop control system uses a measurement of the output and feedback of the signal to compare it with the desired input. True or False
- Engineering synthesis and engineering analysis are the same. True or False
- The block diagram in Figure 1.31 is an example of a closed-loop feedback system. True or False



FIGURE 1.31 System with control device, actuator, and process.

- A multivariable system is a system with more than one input and/or more than one output. True or False
- Early applications of feedback control include which of the following?
  - Water clock of Ktesibios
  - Watt's flyball governor
  - Drebbel's temperature regulator
  - All of the above
- Important modern applications of control systems include which of the following?
  - Fuel-efficient and safe automobiles
  - Autonomous robots
  - Automated manufacturing
  - All of the above
- Complete the following sentence:  
Control of an industrial process by automatic rather than manual means is often called \_\_\_\_\_.
  - negative feedback
  - automation
  - a design gap
  - a specification
- Complete the following sentence:  
\_\_\_\_\_ are intrinsic in the progression from an initial concept to the final product.
  - Closed-loop feedback systems
  - Flyball governors
  - Design gaps
  - Open-loop control systems

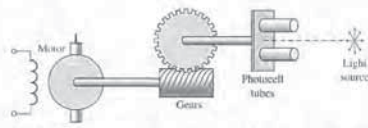
Exercises

- |  |  |       |
|--|--|-------|
| f. Closed-loop feedback control system | The result of making a judgment about how much compromise must be made between conflicting criteria.                                       | _____ |
| g. Flyball governor                    | An interconnection of elements and devices for a desired purpose.  | _____ |
| h. Specifications                      | A reprogrammable, multifunctional manipulator used for a variety of tasks.   | _____ |
| i. Synthesis                           | A gap between the complex physical system and the design model intrinsic to the progression from the initial concept to the final product. | _____ |
| j. Open-loop control system            | The intricate pattern of interwoven parts and knowledge required.  | _____ |
| k. Feedback signal                     | The ratio of physical output to physical input of an industrial process.   | _____ |
| l. Robot                               | The process of designing a technical system.   | _____ |
| m. Multivariable control system        | A system that utilizes a device to control the process without using feedback.   | _____ |
| n. Design gap                          | Uncertainties embodied in the unintended consequences of a design.   | _____ |
| o. Positive feedback                   | The process of conceiving or inventing the forms, parts, and details of a system to achieve a specified purpose.                           | _____ |
| p. Negative feedback                   | The device, plant, or system under control.  | _____ |
| q. Trade-off                           | The output signal is fed back so that it adds to the input signal.   | _____ |
| r. Productivity                        | An interconnection of components forming a system configuration that will provide a desired response.                                      | _____ |
| s. Engineering design                  | The control of a process by automatic means.   | _____ |
| t. Process                             | The adjustment of the parameters to achieve the most favorable or advantageous design.   | _____ |
| u. Control system                      | The process by which new physical configurations are created.  | _____ |
| v. Automation                          | A mechanical device for controlling the speed of a steam engine.   | _____ |

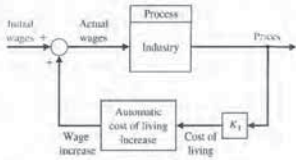
EXERCISES

- Exercises are straightforward applications of the concepts of the chapter.
- The following systems can be described by a block diagram showing the cause-effect relationship and the feedback (if present). Identify the function of each block and the desired input variable, output variable, and measured variable. Use Figure 1.3 as a model where appropriate.
- E1.1 Describe typical sensors that can measure each of the following [93]:
- Linear position
  - Velocity (or speed)
  - Nongravitational acceleration
  - Rotational position (or angle)
  - Rotational velocity
  - Temperature
  - Pressure
  - Liquid (or gas) flow rate
  - Torque
  - Force
- E1.2 Describe typical actuators that can convert the following [93]:
- Fluidic energy to mechanical energy
  - Electrical energy to mechanical energy



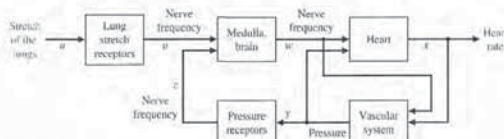


**FIGURE P1.5** A photocell is mounted in each tube. The light reaching each cell is the same in both only when the light source is exactly in the middle as shown.



**FIGURE P1.6** Positive feedback.

Figure P1.6, adds the feedback signal to the input signal, and the resulting signal is used as the input to the process. A simple model of the price-wage inflationary spiral is shown in Figure P1.6. Add additional feedback loops, such as legislative control or control of the tax rate, to stabilize the system. It is assumed that an increase in workers' salaries, after some time delay, results in an increase in prices. Under what conditions could prices be stabilized by falsifying or delaying the availability of cost-of-living data? How would a national wage and price economic guideline program affect the feedback system?

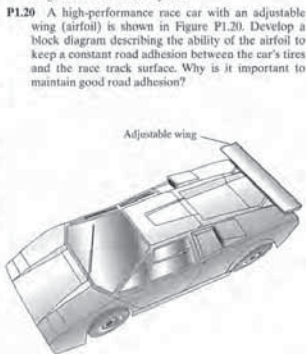


**FIGURE P1.9** Heart-rate control.

emissions significantly. Sketch a block diagram for such a system for an automobile.

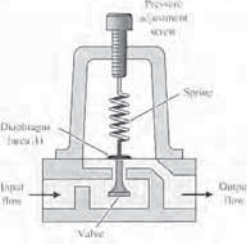
- P1.16** All humans have experienced a fever associated with an illness. A fever is related to the changing of the control input in the body's thermostat. This thermostat, within the brain, normally regulates temperature near 98°F in spite of external temperatures ranging from 0° to 100°F or more. For a fever, the input, or desired, temperature is increased. Even to many scientists, it often comes as a surprise to learn that fever does not indicate something wrong with body temperature control but rather well-contrived regulation at an elevated level of desired input. Sketch a block diagram of the temperature control system and explain how aspirin will lower a fever.
- P1.17** Baseball players use feedback to judge a fly ball and to hit a pitch [35]. Describe a method used by a batter to judge the location of a pitch so that he can have the bat in the proper position to hit the ball.
- P1.18** A cutaway view of a commonly used pressure regulator is shown in Figure P1.18. The desired pressure is set by turning a calibrated screw. This compresses the spring and sets up a force that opposes the upward motion of the diaphragm. The bottom side of the diaphragm is exposed to the water pressure that is to be controlled. Thus the motion of the diaphragm is an indication of the pressure difference between the desired and the actual pressures. It acts like a comparator. The valve is connected to the diaphragm and moves according to the pressure difference until it reaches a position in which the difference is zero. Sketch a block diagram showing the control system with the output pressure as the regulated variable.

- P1.19** Ichiro Masaki of General Motors has patented a system that automatically adjusts a car's speed to keep a safe distance from vehicles in front. Using a video camera, the system detects and stores a reference image of the car in front. It then compares this image with a stream of incoming live images as the two cars move down the highway and calculates the distance. Masaki suggests that the system could control steering as well as speed, allowing drivers to lock on to the car ahead and get a "computerized tow." Sketch a block diagram for the control system.
- P1.20** A high-performance race car with an adjustable wing (airfoil) is shown in Figure P1.20. Develop a block diagram describing the ability of the airfoil to keep a constant road adhesion between the car's tires and the race track surface. Why is it important to maintain good road adhesion?



**FIGURE P1.20** A high-performance race car with an adjustable wing.

- P1.21** The potential of employing two or more helicopters for transporting payloads that are too heavy for a single helicopter is a well-addressed issue in the civil and military rotorcraft design arenas [37]. Overall requirements can be satisfied more efficiently with a smaller aircraft by using multilift for infrequent peak demands. Hence the principal motivation for using multilift can be attributed to the promise of obtaining increased productivity without having to manufacture larger and more expensive helicopters. A specific case of a multilift arrangement where two helicopters jointly transport payloads has been named *twin lift*. Figure P1.21



**FIGURE P1.18** Pressure regulator.

system using Figure 1.3 as the model. Identify the process, sensor, actuator, and controller. The objective is to keep the pendulum in the upright position, that is to keep  $\theta = 0$ , in the presence of disturbances.

- E1.14** Describe the block diagram of a person playing a video game. Suppose that the input device is a joystick and the game is being played on a desktop computer. Use Figure 1.3 as a model of the block diagram.

**PROBLEMS**

Problems require extending the concepts of this chapter to new situations.

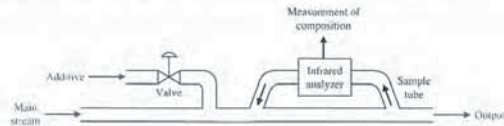
The following systems may be described by a block diagram showing the cause-effect relationship and the feedback (if present). Each block should describe its function. Use Figure 1.3 as a model where appropriate.

- P1.1** Many luxury automobiles have thermostatically controlled air-conditioning systems for the comfort of the passengers. Sketch a block diagram of an air-conditioning system where the driver sets the desired interior temperature on a dashboard panel. Identify the function of each element of the thermostatically controlled cooling system.
- P1.2** In the past, control systems used a human operator as part of a closed-loop control system. Sketch the block diagram of the valve control system shown in Figure P1.2.



**FIGURE P1.2** Fluid-flow control.

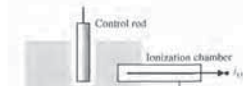
- P1.3** In a chemical process control system, it is valuable to control the chemical composition of the product. To do so, a measurement of the composition can be obtained by using an infrared stream analyzer, as shown in Figure P1.3. The valve on the additive



**FIGURE P1.3** Chemical composition control.

stream may be controlled. Complete the control feedback loop, and sketch a block diagram describing the operation of the control loop.

- P1.4** The accurate control of a nuclear reactor is important for power system generators. Assuming the number of neutrons present is proportional to the power level, an ionization chamber is used to measure the power level. The current  $i_c$  is proportional to the power level. The position of the graphite control rods moderates the power level. Complete the control system of the nuclear reactor shown in Figure P1.4 and sketch the block diagram describing the operation of the feedback control loop.



**FIGURE P1.4** Nuclear reactor control.

- P1.5** A light-seeking control system, used to track the sun, is shown in Figure P1.5. The output shaft, driven by the motor through a worm reduction gear, has a bracket attached on which are mounted two photocells. Complete the closed-loop system so that the system follows the light source.
- P1.6** Feedback systems do not always involve negative feedback. Economic inflation, which is evidenced by continually rising prices, is a **positive feedback** system. A positive feedback control system, as shown in

system is, in fact, a multivariable system, and the variables  $x, y, w, z$ , and  $u$  are vector variables. In other words, the variable  $x$  represents many heart variables  $x_1, x_2, \dots, x_n$ . Examine the model of the heart-rate control system and add or delete blocks, if necessary. Determine a control system model of one of the following physiological control systems:

1. Respiratory control system
2. Adrenaline control system
3. Human arm control system
4. Eye control system
5. Pancreas and the blood-sugar-level control system
6. Circulatory system

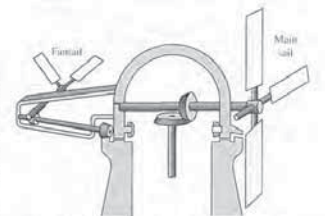
- P1.10** The role of air traffic control systems is increasing as airplane traffic increases at busy airports. Engineers are developing air traffic control systems and collision avoidance systems using the Global Positioning System (GPS) navigation satellites [34, 55]. GPS allows each aircraft to know its position in the airspace landing corridor very precisely. Sketch a block diagram depicting how an air traffic controller might use GPS for aircraft collision avoidance.

- P1.11** Automatic control of water level using a float level was used in the Middle East for a water clock [1, 11]. The water clock (Figure P1.11) was used from sometime before Christ until the 17th century. Discuss the operation of the water clock, and establish how the float provides a feedback control that maintains the accuracy of the clock. Sketch a block diagram of the feedback system.



**FIGURE P1.11** Water clock. (From Newton, Gould, and Kaiser, *Analytical Design of Linear Feedback Controls*, Wiley, New York, 1957, with permission.)

- P1.12** An automatic turning gear for windmills was invented by Meikle in about 1750 [1, 11]. The fantail gear shown in Figure P1.12 automatically turns the windmill into the wind. The fantail windmill at right angle to the main sail is used to turn the turret. The gear ratio is of the order of 3000 to 1. Discuss the operation of the windmill, and establish the feedback operation that maintains the main sails into the wind.



**FIGURE P1.12** Automatic turning gear for windmills. (From Newton, Gould, and Kaiser, *Analytical Design of Linear Feedback Controls*, Wiley, New York, 1957, with permission.)

- P1.13** A common example of a two-input control system is a home shower with separate valves for hot and cold water. The objective is to obtain (1) a desired temperature of the shower water and (2) a desired flow of water. Sketch a block diagram of the closed-loop control system.

- P1.14** Adam Smith (1723-1790) discussed the issue of free competition between the participants of an economy in his book *Wealth of Nations*. It may be said that Smith employed social feedback mechanisms to explain his theories [41]. Smith suggests that (1) the available workers as a whole compare the various possible employments and enter that one offering the greatest rewards, and (2) in any employment the rewards diminish as the number of competing workers rises. Let  $r$  = total of rewards averaged over all trades,  $c$  = total of rewards in a particular trade, and  $q$  = influx of workers into the specific trade. Sketch a feedback system to represent this system.

- P1.15** Small computers are used in automobiles to control emissions and obtain improved gas mileage. A computer-controlled fuel injection system that automatically adjusts the fuel-air mixture ratio could improve gas mileage and reduce unwanted polluting



ADVANCED PROBLEMS

Advanced problems represent problems of increasing complexity.

**AP1.1** The development of robotic microsurgery devices will have major implications on delicate eye and brain surgical procedures. The microsurgery devices employ feedback control to reduce the effects of the surgeon's muscle tremors. Precision movements by an articulated robotic arm can greatly help a surgeon by providing a carefully controlled hand. One such device is shown in Figure AP1.1. The microsurgical



FIGURE AP1.1 Microsurgery robotic manipulator. (Photo courtesy of NASA.)

devices have been evaluated in clinical procedures and are now being commercialized. Sketch a block diagram of the surgical process with a microsurgical device in the loop being operated by a surgeon. Assume that the position of the end-effector on the microsurgical device can be measured and is available for feedback.

**AP1.2** Advanced wind energy systems are being installed in many locations throughout the world as a way for nations to deal with rising fuel prices and energy shortages, and to reduce the negative effects of fossil fuel utilization on the quality of the air (refer to Example 1.2 in Section 1.6). The modern windmill can be viewed as a mechatronic system. Consider Figure 1.18, which illustrates the key elements of mechatronic systems. Using Figure 1.18 as a guide, think about how an advanced wind energy system would be designed as a mechatronic system. List the various components of the wind energy system and associate each component with one of the five elements of a mechatronic system: physical system modeling, signals and systems, computers and logic systems, software and data acquisition, and sensors and actuators.

**AP1.3** Many modern luxury automobiles have an autopark option. This feature will parallel park an automobile without driver intervention. Figure AP1.3 illustrates the parallel parking scenario. Using Figure 1.3 as a model, sketch a block diagram of the automated parallel parking feedback control system. In your own words, describe the control problem and the challenges facing the designers of the control system.

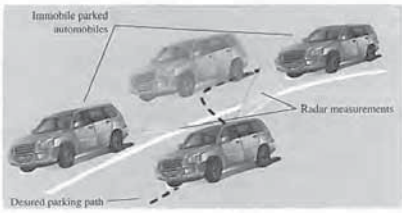


FIGURE AP1.3 Automated parallel parking of an automobile.

Problems

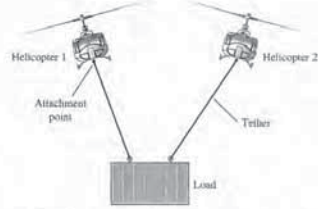


FIGURE P1.21 Two helicopters used to lift and move a large load.

shows a typical "two-point pendant" (twin lift configuration) in the lateral/vertical plane.

Develop the block diagram describing the pilots' action, the position of each helicopter, and the position of the load.

**P1.22** Engineers want to design a control system that will allow a building or other structure to react to the force of an earthquake much as a human would. The structure would yield to the force, but only so much, before developing strength to push back [47]. Develop a block diagram of a control system to reduce the effect of an earthquake force.

**P1.23** Engineers at the Science University of Tokyo are developing a robot with a humanlike face [52]. The robot can display facial expressions, so that it can work cooperatively with human workers. Sketch a block diagram for a facial expression control system of your own design.

**P1.24** An innovation for an intermittent automobile windshield wiper is the concept of adjusting its wiping cycle according to the intensity of the rain [54]. Sketch a block diagram of the wiper control system.

**P1.25** In the past 40 years, over 20,000 metric tons of hardware have been placed in Earth's orbit. During the same time span, over 15,000 metric tons of hardware returned to Earth. The objects remaining in Earth's orbit range in size from large operational spacecraft to tiny flecks of paint. There are about 150,000 objects in Earth's orbit 1 cm or larger in size. About 10,000 of the space objects are currently tracked from groundstations on the Earth. Space traffic control

[61] is becoming an important issue, especially for commercial satellite companies that plan to "fly" their satellites through orbit altitudes where other satellites are operating, and through areas where high concentrations of space debris may exist. Sketch a block diagram of a space traffic control system that commercial companies might use to keep their satellites safe from collisions while operating in space.

**P1.26** NASA is developing a compact rover designed to transmit data from the surface of an asteroid back to Earth, as illustrated in Figure P1.26. The rover will use a camera to take panoramic shots of the asteroid surface. The rover can position itself so that the camera can be pointed straight down at the surface or straight up at the sky. Sketch a block diagram illustrating how the micro-rover can be positioned to point the camera in the desired direction. Assume that the pointing commands are relayed from the Earth to the micro-rover and that the position of the camera is measured and relayed back to Earth.



FIGURE P1.26 Micro-rover designed to explore an asteroid. (Photo courtesy of NASA.)

**P1.27** A direct methanol fuel cell is an electrochemical device that converts a methanol-water solution to electricity [75]. Like rechargeable batteries, fuel cells directly convert chemicals to energy; they are very often compared to batteries, specifically rechargeable batteries. However, one significant difference between rechargeable batteries and direct methanol fuel cells is that, by adding more methanol-water solution, the fuel cells recharge instantly. Sketch a block diagram of the direct methanol fuel cell recharging system that uses feedback (refer to Figure 1.3) to continuously monitor and recharge the fuel cell.

over 800 m with more than 160 stories. There are 57 elevators servicing this tallest free-standing structure in the world. Traveling at up to 10 m/s, the elevators have the world's longest travel distance from lowest to highest stop. Describe a closed-loop feedback control system that guides an elevator of a high-rise building to a desired floor while maintaining a reasonable transit time [95]. Remember that high accelerations will make the passengers uncomfortable.

**AP1.6** Control systems are aiding humans in maintaining their homes. The robotic vacuum cleaner depicted in Figure AP1.6 is an example of a mechatronic system under active control that relies on infrared sensors and microchip technology to navigate around furniture. Describe a closed-loop feedback control system that guides the robotic vacuum cleaner to avoid collisions with obstacles [96].



FIGURE AP1.6 A robotic vacuum cleaner communicates with the base station as it maneuvers around the room. (Photo courtesy of Alamy Images.)

DESIGN PROBLEMS

Design problems emphasize the design task. Continuous design problems (CDP) build upon a design problem from chapter to chapter.

**CDP1.1** Increasingly stringent requirements of modern, high-precision machinery are placing increasing demands on slide systems [53]. The typical goal is to accurately control the desired path of the table shown in Figure CDP1.1. Sketch a block diagram model of a feedback system to achieve the desired goal. The table can move in the  $x$  direction as shown.

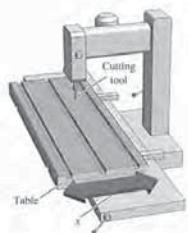


FIGURE CDP1.1 Machine tool with table.

**DP1.1** The road and vehicle noise that invade an automobile's cabin hastens occupant fatigue [60]. Design the block diagram of an "antinoise" feedback system that will reduce the effect of unwanted noise. Indicate the device within each block.

**DP1.2** Many cars are fitted with cruise control that, at the press of a button, automatically maintains a set speed. In this way, the driver can cruise at a speed limit or economic speed without continually checking the speedometer. Design a feedback-control in block diagram form for a cruise control system.

**DP1.3** As part of the automation of a dairy farm, the automation of cow milking is under study [36]. Design a milking machine that can milk cows four or five times a day at the cow's demand. Sketch a block diagram and indicate the devices in each block.

**DP1.4** A large, braced robot arm for welding large structures is shown in Figure DP1.4. Sketch the block diagram of a closed-loop feedback control system for accurately controlling the location of the weld tip.

**DP1.5** Vehicle traction control, which includes antiskid braking and antislip acceleration, can enhance vehicle performance and handling. The objective of this control is to maximize tire traction by preventing locked brakes as well as tire spinning during acceleration. Wheel slip, the difference between the vehicle speed and the wheel speed, is chosen as the controlled variable because of its strong influence on the tractive force between the tire and the road [19]. The adhesion coefficient between the wheel and the road reaches a

Advanced Problems

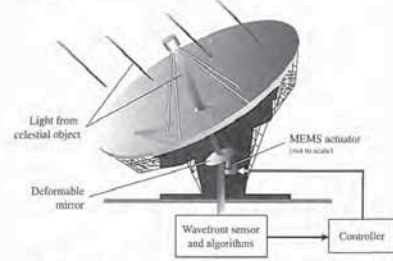


FIGURE AP1.4 Extremely large optical telescope with deformable mirrors for atmosphere compensation.

**AP1.4** Adaptive optics has applications to a wide variety of key control problems, including imaging of the human retina and large-scale, ground-based astronomical observations [98]. In both cases, the approach is to use a wavefront sensor to measure distortions in the incoming light and to actively control and compensate to the errors induced by the distortions. Consider the case of an extremely large ground-based optical telescope, possibly an optical telescope up to 100 meters in diameter. The telescope components include deformable mirrors actuated by micro-electro-mechanical (MEMS) devices and sensors to measure the distortion of the incoming light as it passes through the turbulent and uncertain atmosphere of Earth.

There is at least one major technological barrier to constructing a 100-m optical telescope. The numerical computations associated with the control and compensation of the extremely large optical telescope can be on the order of  $10^{19}$  calculations each 1.5 ms. To date, this computational power is unachievable. If we assume that the computational capability will ultimately be available, then one can consider the design of a feedback control system that uses the available computational power. We can consider many control issues associated with the large-scale optical telescope. Some of the controls problems that might be considered include controlling the pointing of the main dish, controlling the individual deformable mirrors, and attenuating the deformation of the dish due to changes in outside temperature.

Employing Figure 1.3 as a model for the block diagram, describe a closed-loop feedback control system to

control one of the deformable mirrors to compensate for the distortions in the incoming light. Figure AP1.4 shows a diagram of the telescope with a single deformable mirror. Suppose that the mirror has an associated MEMS actuator that can be used to vary the orientation. Also, assume that the wavefront sensor and associated algorithms provide the desired configuration of the deformable mirror to the feedback control system.

**AP1.5** The Burj Dubai is the tallest building in the world [94]. The building, shown in Figure AP1.5, stands at



FIGURE AP1.5 The world's tallest building in Dubai. (Photo courtesy of Alamy Images.)





## ANSWERS TO SKILLS CHECK

True or False: (1) True; (2) True; (3) False; (4) False; (5) True  
 Multiple Choice: (6) d; (7) d; (8) b; (9) c; (10) a;  
 (11) d; (12) a; (13) c; (14) d; (15) d

Word Match (in order, top to bottom): p, f, h, k, m,  
 q, d, l, n, c, r, s, j, b, e, t, o, u, v, a, i, g

## TERMS AND CONCEPTS

**Automation** The control of a process by automatic means.  
**Closed-loop feedback control system** A system that uses a measurement of the output and compares it with the desired output to control the process.  
**Complexity of design** The intricate pattern of interwoven parts and knowledge required.  
**Control system** An interconnection of components forming a system configuration that will provide a desired response.  
**Design** The process of conceiving or inventing the forms, parts, and details of a system to achieve a specified purpose.  
**Design gap** A gap between the complex physical system and the design model intrinsic to the progression from the initial concept to the final product.  
**Disturbance** An unwanted input signal that affects the output signal.  
**Embedded control** Feedback control system that employs on-board special-purpose digital computers as integral components of the feedback loop.  
**Engineering design** The process of designing a technical system.  
**Feedback signal** A measure of the output of the system used for feedback to control the system.  
**Flyball governor** A mechanical device for controlling the speed of a steam engine.  
**Hybrid fuel automobile** An automobile that uses a conventional internal combustion engine in combination with an energy storage device to provide a propulsion system.  
**Measurement noise** An unwanted input signal that affects the measured output signal.  
**Mechanics** The synergistic integration of mechanical, electrical, and computer systems.

**Multiloop feedback control system** A feedback control system with more than one feedback control loop.  
**Multivariable control system** A system with more than one input variable or more than one output variable.  
**Negative feedback** An output signal fed back so that it subtracts from the input signal.  
**Open-loop control system** A system that uses a device to control the process without using feedback. Thus the output has no effect upon the signal to the process.  
**Optimization** The adjustment of the parameters to achieve the most favorable or advantageous design.  
**Plant** See Process.  
**Positive feedback** An output signal fed back so that it adds to the input signal.  
**Process** The device, plant, or system under control.  
**Productivity** The ratio of physical output to physical input of an industrial process.  
**Risk** Uncertainties embodied in the unintended consequences of a design.  
**Robot** Programmable computers integrated with a manipulator. A reprogrammable, multifunctional manipulator used for a variety of tasks.  
**Specifications** Statements that explicitly state what the device or product is to be and to do. A set of prescribed performance criteria.  
**Synthesis** The process by which new physical configurations are created. The combining of separate elements or devices to form a coherent whole.  
**System** An interconnection of elements and devices for a desired purpose.  
**Trade-off** The result of making a judgment about how to compromise between conflicting criteria.

## Design Problems

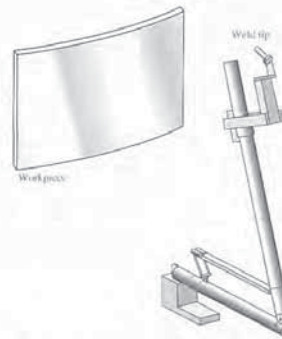


FIGURE DP1.4 Robot welder.

maximum at a low slip. Develop a block diagram model of one wheel of a traction control system.

**DP1.6** The Hubble space telescope was repaired and modified in space on several occasions [44, 46, 49]. One challenging problem with controlling the Hubble is damping the jitter that vibrates the spacecraft each time it passes into or out of the Earth's shadow. The worst vibration has a period of about 20 seconds, or a frequency of 0.05 hertz. Design a feedback system that will reduce the vibrations of the Hubble space telescope.

**DP1.7** A challenging application of control design is the use of nanorobots in medicine. Nanorobots will require onboard computing capability, and very tiny sensors and actuators. Fortunately, advances in bio-molecular computing, bio-sensors, and actuators are promising to enable medical nanorobots to emerge within the next decade [98]. Many interesting medical applications will benefit from nanorobotics. For example, one use might be to use the robotic devices to precisely deliver anti-HIV drugs or to combat cancer by targeted delivering of chemotherapy.

At the present time, we cannot construct practical nanorobots, but we can consider the control design process that would enable the eventual development and installation of these tiny devices in the medical field. Consider the problem of designing a nanorobot



FIGURE DP1.7 An artist illustration of a nanorobot interacting with human blood cells.

to deliver a cancer drug to a specific location within the human body. The target site might be the location of a tumor, for example. Using the control design process illustrated in Figure 1.15, suggest one or more control goals that might guide the design process. Recommend the variables that should be controlled and provide a list of reasonable specifications for those variables.

**DP1.8** Consider the human transportation vehicle (HTV) depicted in Figure DP1.8. The self-balancing HTV is actively controlled to allow safe and easy transportation of a single person [97]. Using Figure 1.3 as a model for the block diagram, describe a closed-loop feedback control system to assist the rider of the HTV in balancing and maneuvering the vehicle.



FIGURE DP1.8 Personal transportation vehicle. (Photo courtesy of newscom.com.)

## 2.1 INTRODUCTION

To understand and control complex systems, one must obtain quantitative **mathematical models** of these systems. It is necessary therefore to analyze the relationships between the system variables and to obtain a mathematical model. Because the systems under consideration are dynamic in nature, the descriptive equations are usually **differential equations**. Furthermore, if these equations can be **linearized**, then the **Laplace transform** can be used to simplify the method of solution. In practice, the complexity of systems and our ignorance of all the relevant factors necessitate the introduction of **assumptions** concerning the system operation. Therefore we will often find it useful to consider the physical system, express any necessary assumptions, and linearize the system. Then, by using the physical laws describing the linear equivalent system, we can obtain a set of linear differential equations. Finally, using mathematical tools, such as the Laplace transform, we obtain a solution describing the operation of the system. In summary, the approach to dynamic system modeling can be listed as follows:

1. Define the system and its components.
2. Formulate the mathematical model and fundamental necessary assumptions based on basic principles.
3. Obtain the differential equations representing the mathematical model.
4. Solve the equations for the desired output variables.
5. Examine the solutions and the assumptions.
6. If necessary, reanalyze or redesign the system.

## 2.2 DIFFERENTIAL EQUATIONS OF PHYSICAL SYSTEMS

The differential equations describing the dynamic performance of a physical system are obtained by utilizing the physical laws of the process [1–3]. This approach applies equally well to mechanical [1], electrical [3], fluid, and thermodynamic systems [4]. Consider the torsional spring-mass system in Figure 2.1 with applied torque  $T_a(t)$ . Assume the torsional spring element is massless. Suppose we want to measure the torque  $T_s(t)$  transmitted to the mass  $m$ . Since the spring is massless, the sum of the torques acting on the spring itself must be zero, or

$$T_a(t) - T_s(t) = 0,$$

which implies that  $T_s(t) = T_a(t)$ . We see immediately that the external torque  $T_a(t)$  applied at the end of the spring is transmitted *through* the torsional spring. Because of this, we refer to the torque as a **through-variable**. In a similar manner, the angular rate difference associated with the torsional spring element is

$$\omega(t) = \omega_s(t) - \omega_m(t).$$

## CHAPTER

## 2

## Mathematical Models of Systems

2.1	Introduction	50
2.2	Differential Equations of Physical Systems	50
2.3	Linear Approximations of Physical Systems	55
2.4	The Laplace Transform	58
2.5	The Transfer Function of Linear Systems	65
2.6	Block Diagram Models	79
2.7	Signal-Flow Graph Models	84
2.8	Design Examples	90
2.9	The Simulation of Systems Using Control Design Software	113
2.10	Sequential Design Example: Disk Drive Read System	128
2.11	Summary	130

## PREVIEW

Mathematical models of physical systems are key elements in the design and analysis of control systems. The dynamic behavior is generally described by ordinary differential equations. We will consider a wide range of systems, including mechanical, hydraulic, and electrical. Since most physical systems are nonlinear, we will discuss linearization approximations, which allow us to use Laplace transform methods. We will then proceed to obtain the input-output relationship for components and subsystems in the form of transfer functions. The transfer function blocks can be organized into block diagrams or signal-flow graphs to graphically depict the interconnections. Block diagrams (and signal-flow graphs) are very convenient and natural tools for designing and analyzing complicated control systems. We conclude the chapter by developing transfer function models for the various components of the Sequential Design Example: Disk Drive Read System.

## DESIRED OUTCOMES

Upon completion of Chapter 2, students should:

- Recognize that differential equations can describe the dynamic behavior of physical systems.
- Be able to utilize linearization approximations through the use of Taylor series expansions.
- Understand the application of Laplace transforms and their role in obtaining transfer functions.
- Be aware of block diagrams (and signal-flow graphs) and their role in analyzing control systems.
- Understand the important role of modeling in the control system design process.



linear, dynamic elements is given in Table 2.2 [5]. The equations in Table 2.2 are idealized descriptions and only approximate the actual conditions (for example, when a linear, lumped approximation is used for a distributed element).

Table 2.2 Summary of Governing Differential Equations for Ideal Elements

Type of Element	Physical Element	Governing Equation	Energy $E$ or Power $\mathcal{P}$	Symbol
Inductive storage	Electrical inductance	$v_{21} = L \frac{di}{dt}$	$E = \frac{1}{2} L i^2$	$v_2 \text{ --- } L \text{ --- } i \text{ --- } v_1$
	Translational spring	$v_{21} = \frac{1}{k} \frac{dF}{dt}$	$E = \frac{1}{2} \frac{F^2}{k}$	$v_2 \text{ --- } k \text{ --- } F \text{ --- } v_1$
	Rotational spring	$\omega_{21} = \frac{1}{k} \frac{dT}{dt}$	$E = \frac{1}{2} \frac{T^2}{k}$	$\omega_2 \text{ --- } k \text{ --- } T \text{ --- } \omega_1$
	Fluid inertia	$P_{21} = I \frac{dQ}{dt}$	$E = \frac{1}{2} I Q^2$	$P_2 \text{ --- } I \text{ --- } Q \text{ --- } P_1$
Capacitive storage	Electrical capacitance	$i = C \frac{dv_{21}}{dt}$	$E = \frac{1}{2} C v_{21}^2$	$v_2 \text{ --- } C \text{ --- } v_1$
	Translational mass	$F = M \frac{dv_2}{dt}$	$E = \frac{1}{2} M v_2^2$	$F \text{ --- } M \text{ --- } v_2 = \text{constant}$
	Rotational mass	$T = J \frac{d\omega_2}{dt}$	$E = \frac{1}{2} J \omega_2^2$	$T \text{ --- } J \text{ --- } \omega_2 = \text{constant}$
	Fluid capacitance	$Q = C_f \frac{dP_{21}}{dt}$	$E = \frac{1}{2} C_f P_{21}^2$	$Q \text{ --- } C_f \text{ --- } P_1$
	Thermal capacitance	$q = C_t \frac{dT_2}{dt}$	$E = C_t T_2$	$q \text{ --- } C_t \text{ --- } T_1 = \text{constant}$
Energy dissipators	Electrical resistance	$i = \frac{1}{R} v_{21}$	$\mathcal{P} = \frac{1}{R} v_{21}^2$	$v_2 \text{ --- } R \text{ --- } i \text{ --- } v_1$
	Translational damper	$F = b v_{21}$	$\mathcal{P} = b v_{21}^2$	$F \text{ --- } b \text{ --- } v_1$
	Rotational damper	$T = b \omega_{21}$	$\mathcal{P} = b \omega_{21}^2$	$T \text{ --- } b \text{ --- } \omega_1$
	Fluid resistance	$Q = \frac{1}{R_f} P_{21}$	$\mathcal{P} = \frac{1}{R_f} P_{21}^2$	$P_2 \text{ --- } R_f \text{ --- } Q \text{ --- } P_1$
	Thermal resistance	$q = \frac{1}{R_t} T_{21}$	$\mathcal{P} = \frac{1}{R_t} T_{21}^2$	$T_2 \text{ --- } R_t \text{ --- } q \text{ --- } T_1$

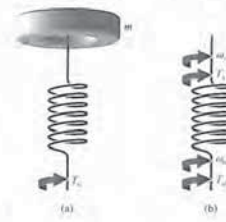


FIGURE 2.1 (a) Torsional spring-mass system. (b) Spring element.

This, the angular rate difference is measured across the torsional spring element and is referred to as an **across-variable**. These same types of arguments can be made for most common physical variables (such as force, current, volume, flow rate, etc.). A more complete discussion on through- and across-variables can be found in [26, 27]. A summary of the through- and across-variables of dynamic systems is given in Table 2.1 [5]. Information concerning the International System (SI) of units associated with the various variables discussed in this section can be found at the MCS website.<sup>1</sup> For example, variables that measure temperature are degrees Kelvin in SI units, and variables that measure length are meters. Important conversions between SI and English units are also given at the MCS website. A summary of the describing equations for lumped,

Table 2.1 Summary of Through- and Across-Variables for Physical Systems

System	Variable Through Element	Integrated Through-Variable	Variable Across Element	Integrated Across-Variable
Electrical	Current, $i$	Charge, $q$	Voltage difference, $v_{21}$	Flux linkage, $\lambda_{21}$
Mechanical translational	Force, $F$	Translational momentum, $P$	Velocity difference, $v_{21}$	Displacement difference, $y_{21}$
Mechanical rotational	Torque, $T$	Angular momentum, $h$	Angular velocity difference, $\omega_{21}$	Angular displacement difference, $\theta_{21}$
Fluid	Fluid volumetric rate of flow, $Q$	Volume, $V$	Pressure difference, $P_{21}$	Pressure momentum, $\gamma_{21}$
Thermal	Heat flow rate, $q$	Heat energy, $H$	Temperature difference, $T_{21}$	

The companion website is found at [www.pearsonhighered.com/dorf](http://www.pearsonhighered.com/dorf).

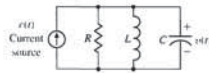


FIGURE 2.3 RLC circuit.

Alternatively, one may describe the electrical RLC circuit of Figure 2.3 by utilizing Kirchhoff's current law. Then we obtain the following integrodifferential equation:

$$\frac{v(t)}{R} + C \frac{dv(t)}{dt} + \frac{1}{L} \int_0^t v(t) dt = r(t). \quad (2.2)$$

The solution of the differential equation describing the process may be obtained by classical methods such as the use of integrating factors and the method of undetermined coefficients [1]. For example, when the mass is initially displaced a distance  $y(0) = y_0$  and released, the dynamic response of the system can be represented by an equation of the form

$$y(t) = K_1 e^{-\beta_1 t} \sin(\beta_2 t + \theta_1). \quad (2.3)$$

A similar solution is obtained for the voltage of the RLC circuit when the circuit is subjected to a constant current  $r(t) = I$ . Then the voltage is

$$v(t) = K_2 e^{-\beta_1 t} \cos(\beta_2 t + \theta_2). \quad (2.4)$$

A voltage curve typical of an RLC circuit is shown in Figure 2.4.

To reveal further the close similarity between the differential equations for the mechanical and electrical systems, we shall rewrite Equation (2.1) in terms of velocity:

$$v(t) = \frac{dy(t)}{dt}.$$

Then we have

$$M \frac{dv(t)}{dt} + bv(t) + k \int_0^t v(t) dt = r(t). \quad (2.5)$$

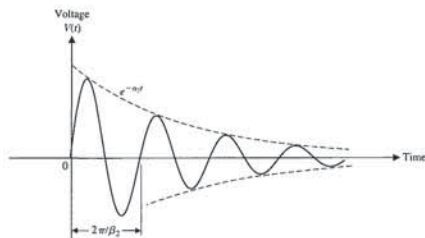


FIGURE 2.4 Typical voltage response for an RLC circuit.

Nomenclature

- **Through-variable:**  $F$  = force,  $T$  = torque,  $i$  = current,  $Q$  = fluid volumetric flow rate,  $q$  = heat flow rate.
- **Across-variable:**  $v$  = translational velocity,  $\omega$  = angular velocity,  $v$  = voltage,  $P$  = pressure,  $T$  = temperature.
- **Inductive storage:**  $L$  = inductance,  $1/k$  = reciprocal translational or rotational stiffness,  $I$  = fluid inertia.
- **Capacitive storage:**  $C$  = capacitance,  $M$  = mass,  $J$  = moment of inertia,  $C_f$  = fluid capacitance,  $C_t$  = thermal capacitance.
- **Energy dissipators:**  $R$  = resistance,  $b$  = viscous friction,  $R_f$  = fluid resistance,  $R_t$  = thermal resistance.

The symbol  $v$  is used for both voltage in electrical circuits and velocity in translational mechanical systems and is distinguished within the context of each differential equation. For mechanical systems, one uses Newton's laws; for electrical systems, Kirchhoff's voltage laws. For example, the simple spring-mass-damper mechanical system shown in Figure 2.2(a) is described by Newton's second law of motion. (This system could represent, for example, an automobile shock absorber.) The free-body diagram of the mass  $M$  is shown in Figure 2.2(b). In this spring-mass-damper example, we model the wall friction as a **viscous damper**, that is, the friction force is linearly proportional to the velocity of the mass. In reality the friction force may behave in a more complicated fashion. For example, the wall friction may behave as a **Coulomb damper**. Coulomb friction, also known as dry friction, is a nonlinear function of the mass velocity and possesses a discontinuity around zero velocity. For a well-lubricated, sliding surface, the viscous friction is appropriate and will be used here and in subsequent spring-mass-damper examples. Summing the forces acting on  $M$  and utilizing Newton's second law yields

$$M \frac{d^2 y(t)}{dt^2} + b \frac{dy(t)}{dt} + ky(t) = r(t), \quad (2.1)$$

where  $k$  is the spring constant of the ideal spring and  $b$  is the friction constant. Equation (2.1) is a second-order linear constant-coefficient differential equation.

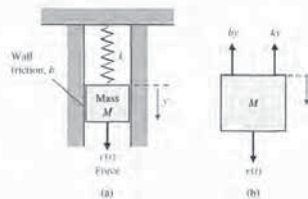


FIGURE 2.2 (a) Spring-mass-damper system. (b) Free-body diagram.



second system may be considered linear about an operating point  $x_0, y_0$  for small changes  $\Delta x$  and  $\Delta y$ . When  $x = x_0 + \Delta x$  and  $y = y_0 + \Delta y$ , we have

$$y = mx + b$$

or

$$y_0 + \Delta y = mx_0 + m \Delta x + b.$$

Therefore,  $\Delta y = m \Delta x$ , which satisfies the necessary conditions.

The linearity of many mechanical and electrical elements can be assumed over a reasonably large range of the variables [7]. This is not usually the case for thermal and fluid elements, which are more frequently nonlinear in character. Fortunately, however, one can often linearize nonlinear elements assuming small-signal conditions. This is the normal approach used to obtain a linear equivalent circuit for electronic circuits and transistors. Consider a general element with an excitation (through-) variable  $x(t)$  and a response (across-) variable  $y(t)$ . Several examples of dynamic system variables are given in Table 2.1. The relationship of the two variables is written as

$$y(t) = g(x(t)), \quad (2.6)$$

where  $g(x(t))$  indicates  $y(t)$  is a function of  $x(t)$ . The normal operating point is designated by  $x_0$ . Because the curve (function) is continuous over the range of interest, a Taylor series expansion about the operating point may be utilized [7]. Then we have

$$y = g(x) = g(x_0) + \left. \frac{dg}{dx} \right|_{x=x_0} (x - x_0) + \frac{d^2g}{dx^2} \Big|_{x=x_0} \frac{(x - x_0)^2}{2!} + \dots \quad (2.7)$$

The slope at the operating point,

$$\left. \frac{dg}{dx} \right|_{x=x_0}$$

is a good approximation to the curve over a small range of  $(x - x_0)$ , the deviation from the operating point. Then, as a reasonable approximation, Equation (2.7) becomes

$$y = g(x_0) + \left. \frac{dg}{dx} \right|_{x=x_0} (x - x_0) = y_0 + m(x - x_0), \quad (2.8)$$

where  $m$  is the slope at the operating point. Finally, Equation (2.8) can be rewritten as the linear equation

$$(y - y_0) = m(x - x_0)$$

or

$$\Delta y = m \Delta x. \quad (2.9)$$

Consider the case of a mass,  $M$ , sitting on a nonlinear spring, as shown in Figure 2.5(a). The normal operating point is the equilibrium position that occurs when the spring force balances the gravitational force  $Mg$ , where  $g$  is the gravitational constant. Thus, we obtain  $f_0 = Mg$ , as shown. For the nonlinear spring with  $f = y^2$ , the equilibrium position is  $y_0 = (Mg)^{1/2}$ . The linear model for small deviation is

$$\Delta f = m \Delta y.$$

One immediately notes the equivalence of Equations (2.5) and (2.2) where velocity  $v(t)$  and voltage  $v(t)$  are equivalent variables, usually called **analogous variables**, and the systems are analogous systems. Therefore the solution for velocity is similar to Equation (2.4), and the response for an underdamped system is shown in Figure 2.4. The concept of analogous systems is a very useful and powerful technique for system modeling. The voltage-velocity analogy, often called the force-current analogy, is a natural one because it relates the analogous through- and across-variables of the electrical and mechanical systems. Another analogy that relates the velocity and current variables is often used and is called the force-voltage analogy [21, 23].

Analogous systems with similar solutions exist for electrical, mechanical, thermal, and fluid systems. The existence of analogous systems and solutions provides the analyst with the ability to extend the solution of one system to all analogous systems with the same describing differential equations. Therefore what one learns about the analysis and design of electrical systems is immediately extended to an understanding of fluid, thermal, and mechanical systems.

2.3 LINEAR APPROXIMATIONS OF PHYSICAL SYSTEMS

A great majority of physical systems are linear within some range of the variables. In general, systems ultimately become nonlinear as the variables are increased without limit. For example, the spring-mass-damper system of Figure 2.2 is linear and described by Equation (2.1) as long as the mass is subjected to small deflections  $y(t)$ . However, if  $y(t)$  were continually increased, eventually the spring would be overextended and break. Therefore the question of linearity and the range of applicability must be considered for each system.

A system is defined as linear in terms of the system excitation and response. In the case of the electrical network, the excitation is the input current  $i(t)$  and the response is the voltage  $v(t)$ . In general, a **necessary condition** for a linear system can be determined in terms of an excitation  $x(t)$  and a response  $y(t)$ . When the system at rest is subjected to an excitation  $x_1(t)$ , it provides a response  $y_1(t)$ . Furthermore, when the system is subjected to an excitation  $x_2(t)$ , it provides a corresponding response  $y_2(t)$ . For a linear system, it is necessary that the excitation  $x_1(t) + x_2(t)$  result in a response  $y_1(t) + y_2(t)$ . This is usually called the **principle of superposition**.

Furthermore, the magnitude scale factor must be preserved in a **linear system**. Again, consider a system with an input  $x(t)$  that results in an output  $y(t)$ . Then the response of a linear system to a constant multiple  $\beta$  of an input  $x$  must be equal to the response to the input multiplied by the same constant so that the output is equal to  $\beta y$ . This is called the property of **homogeneity**.

**A linear system satisfies the properties of superposition and homogeneity.**

A system characterized by the relation  $y = x^2$  is not linear, because the superposition property is not satisfied. A system represented by the relation  $y = mx + b$  is not linear, because it does not satisfy the homogeneity property. However, this

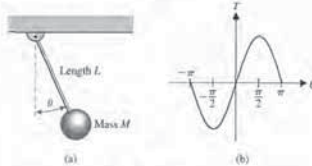


FIGURE 2.6 Pendulum oscillator.

where  $T_0 = 0$ . Then, we have

$$T = MgL(\cos 0^\circ)(\theta - 0^\circ) = MgL\theta. \quad (2.13)$$

This approximation is reasonably accurate for  $-\pi/4 \leq \theta \leq \pi/4$ . For example, the response of the linear model for the swing through  $\pm 30^\circ$  is within 5% of the actual nonlinear pendulum response. ■

2.4 THE LAPLACE TRANSFORM

The ability to obtain linear approximations of physical systems allows the analyst to consider the use of the **Laplace transformation**. The Laplace transform method substitutes relatively easily solved algebraic equations for the more difficult differential equations [1, 3]. The time-response solution is obtained by the following operations:

1. Obtain the linearized differential equations.
2. Obtain the Laplace transformation of the differential equations.
3. Solve the resulting algebraic equation for the transform of the variable of interest.

The Laplace transform exists for linear differential equations for which the transformation integral converges. Therefore, for  $f(t)$  to be transformable, it is sufficient that

$$\int_0^\infty |f(t)|e^{-\sigma_1 t} dt < \infty,$$

for some real, positive  $\sigma_1$  [1]. The  $0^-$  indicates that the integral should include any discontinuity, such as a delta function at  $t = 0$ . If the magnitude of  $f(t)$  is  $|f(t)| < Me^{\alpha t}$  for all positive  $t$ , the integral will converge for  $\sigma_1 > \alpha$ . The region of convergence is therefore given by  $\infty > \sigma_1 > \alpha$ , and  $\sigma_1$  is known as the abscissa of absolute convergence. Signals that are physically realizable always have a Laplace transform. The Laplace transformation for a function of time,  $f(t)$ , is

$$F(s) = \int_0^\infty f(t)e^{-st} dt = \mathcal{L}\{f(t)\}. \quad (2.14)$$

The **inverse Laplace transform** is written as

$$f(t) = \frac{1}{2\pi j} \int_{\sigma - j\infty}^{\sigma + j\infty} F(s)e^{st} ds. \quad (2.15)$$

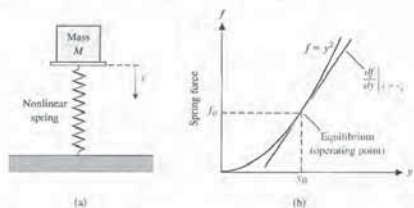


FIGURE 2.5 (a) A mass sitting on a nonlinear spring. (b) The spring force versus  $y$ .

where

$$m = \left. \frac{df}{dy} \right|_{y=y_0}$$

as shown in Figure 2.5(b). Thus,  $m = 2y_0$ . A **linear approximation** is as accurate as the assumption of small signals is applicable to the specific problem.

If the dependent variable  $y$  depends upon several excitation variables,  $x_1, x_2, \dots, x_n$ , then the functional relationship is written as

$$y = g(x_1, x_2, \dots, x_n). \quad (2.10)$$

The Taylor series expansion about the operating point  $x_{1_0}, x_{2_0}, \dots, x_{n_0}$  is useful for a linear approximation to the nonlinear function. When the higher-order terms are neglected, the linear approximation is written as

$$y = g(x_{1_0}, x_{2_0}, \dots, x_{n_0}) + \left. \frac{\partial g}{\partial x_1} \right|_{x=x_0} (x_1 - x_{1_0}) + \left. \frac{\partial g}{\partial x_2} \right|_{x=x_0} (x_2 - x_{2_0}) + \dots + \left. \frac{\partial g}{\partial x_n} \right|_{x=x_0} (x_n - x_{n_0}), \quad (2.11)$$

where  $x_0$  is the operating point. Example 2.1 will clearly illustrate the utility of this method.

EXAMPLE 2.1 Pendulum oscillator model

Consider the pendulum oscillator shown in Figure 2.6(a). The torque on the mass is

$$T = MgL \sin \theta, \quad (2.12)$$

where  $g$  is the gravity constant. The equilibrium condition for the mass is  $\theta_0 = 0^\circ$ . The nonlinear relation between  $T$  and  $\theta$  is shown graphically in Figure 2.6(b). The first derivative evaluated at equilibrium provides the linear approximation, which is

$$T - T_0 = MgL \left. \frac{\partial \sin \theta}{\partial \theta} \right|_{\theta=\theta_0} (\theta - \theta_0).$$



Alternatively, the Laplace variable  $s$  can be considered to be the differential operator so that

$$s = \frac{d}{dt} \tag{2.16}$$

Then we also have the integral operator

$$\frac{1}{s} = \int_0^t dt. \tag{2.17}$$

The inverse Laplace transformation is usually obtained by using the Heaviside partial fraction expansion. This approach is particularly useful for systems analysis and design because the effect of each characteristic root or eigenvalue can be clearly observed.

To illustrate the usefulness of the Laplace transformation and the steps involved in the system analysis, reconsider the spring-mass-damper system described by Equation (2.1), which is

$$M \frac{d^2y}{dt^2} + b \frac{dy}{dt} + ky = r(t). \tag{2.18}$$

We wish to obtain the response,  $y$ , as a function of time. The Laplace transform of Equation (2.18) is

$$M(s^2Y(s) - sy(0^-) - \frac{dy}{dt}(0^-)) + b(sY(s) - y(0^-)) + kY(s) = R(s). \tag{2.19}$$

When

$$r(t) = 0, \text{ and } y(0^-) = y_0, \text{ and } \left. \frac{dy}{dt} \right|_{t=0^-} = 0,$$

we have

$$Ms^2Y(s) - Msy_0 + bsY(s) - by_0 + kY(s) = 0. \tag{2.20}$$

Solving for  $Y(s)$ , we obtain

$$Y(s) = \frac{(Ms + b)y_0}{Ms^2 + bs + k} = \frac{p(s)}{q(s)}. \tag{2.21}$$

The denominator polynomial  $q(s)$ , when set equal to zero, is called the **characteristic equation** because the roots of this equation determine the character of the time response. The roots of this characteristic equation are also called the **poles** of the system. The roots of the numerator polynomial  $p(s)$  are called the **zeros** of the system; for example,  $s = -b/M$  is a zero of Equation (2.21). Poles and zeros are critical frequencies. At the poles, the function  $Y(s)$  becomes infinite, whereas at the zeros, the function becomes zero. The complex frequency **s-plane** plot of the poles and zeros graphically portrays the character of the natural transient response of the system.

For a specific case, consider the system when  $k/M = 2$  and  $b/M = 3$ . Then Equation (2.21) becomes

$$Y(s) = \frac{(s + 3)y_0}{(s + 1)(s + 2)}. \tag{2.22}$$

The inverse Laplace transform of Equation (2.22) is then

$$y(t) = \mathcal{L}^{-1} \left\{ \frac{2}{s + 1} \right\} + \mathcal{L}^{-1} \left\{ \frac{-1}{s + 2} \right\}. \tag{2.26}$$

Using Table 2.3, we find that

$$y(t) = 2e^{-t} - 1e^{-2t}. \tag{2.27}$$

Finally, it is usually desired to determine the **steady-state** or **final value** of the response of  $y(t)$ . For example, the final or steady-state rest position of the spring-mass-damper system may be calculated. The **final value theorem** states that

$$\lim_{t \rightarrow \infty} y(t) = \lim_{s \rightarrow 0} sY(s), \tag{2.28}$$

where a simple pole of  $Y(s)$  at the origin is permitted, but poles on the imaginary axis and in the right half-plane and repeated poles at the origin are excluded. Therefore, for the specific case of the spring-mass-damper, we find that

$$\lim_{t \rightarrow \infty} y(t) = \lim_{s \rightarrow 0} sY(s) = 0. \tag{2.29}$$

Hence the final position for the mass is the normal equilibrium position  $y = 0$ .

Reconsider the spring-mass-damper system. The equation for  $Y(s)$  may be written as

$$Y(s) = \frac{(s + b/M)y_0}{s^2 + (b/M)s + k/M} = \frac{(s + 2\xi\omega_n)y_0}{s^2 + 2\xi\omega_n s + \omega_n^2}, \tag{2.30}$$

where  $\xi$  is the dimensionless **damping ratio**, and  $\omega_n$  is the **natural frequency** of the system. The roots of the characteristic equation are

$$s_1, s_2 = -\xi\omega_n \pm \omega_n\sqrt{\xi^2 - 1}, \tag{2.31}$$

where, in this case,  $\omega_n = \sqrt{k/M}$  and  $\xi = b/(2\sqrt{kM})$ . When  $\xi > 1$ , the roots are real and the system is **overdamped**; when  $\xi < 1$ , the roots are complex and the system is **underdamped**. When  $\xi = 1$ , the roots are repeated and real, and the condition is called **critical damping**.

When  $\xi < 1$ , the response is underdamped, and

$$s_{1,2} = -\xi\omega_n \pm j\omega_n\sqrt{1 - \xi^2}. \tag{2.32}$$

The s-plane plot of the poles and zeros of  $Y(s)$  is shown in Figure 2.9, where  $\theta = \cos^{-1}\xi$ . As  $\xi$  varies with  $\omega_n$  constant, the complex conjugate roots follow a circular

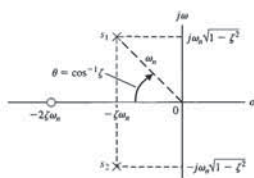


FIGURE 2.9 An s-plane plot of the poles and zeros of  $Y(s)$ .



The transformation integrals have been employed to derive tables of Laplace transforms that are used for the great majority of problems. A table of important Laplace transform pairs is given in Table 2.3, and a more complete list of Laplace transform pairs can be found at the MCS website.

Table 2.3 Important Laplace Transform Pairs

$f(t)$	$F(s)$
Step function, $u(t)$	$\frac{1}{s}$
$e^{-at}$	$\frac{1}{s+a}$
$\sin \omega t$	$\frac{\omega}{s^2 + \omega^2}$
$\cos \omega t$	$\frac{s}{s^2 + \omega^2}$
$t^n$	$\frac{n!}{s^{n+1}}$
$f^{(k)}(t) = \frac{d^k f(t)}{dt^k}$	$s^k F(s) - s^{k-1}f(0^-) - s^{k-2}f'(0^-) - \dots - f^{(k-1)}(0^-)$
$\int_{-\infty}^t f(t) dt$	$\frac{F(s)}{s} + \frac{1}{s} \int_{-\infty}^0 f(t) dt$
Impulse function $\delta(t)$	1
$e^{-at} \sin \omega t$	$\frac{\omega}{(s+a)^2 + \omega^2}$
$e^{-at} \cos \omega t$	$\frac{s+a}{(s+a)^2 + \omega^2}$
$\frac{1}{\omega} [(\alpha - a)^2 + \omega^2]^{1/2} e^{-\alpha t} \sin(\omega t + \phi)$	$\frac{s + \alpha}{(s + a)^2 + \omega^2}$
$\phi = \tan^{-1} \frac{\omega}{\alpha - a}$	
$\frac{\omega_n}{\sqrt{1 - \xi^2}} e^{-\xi\omega_n t} \sin \omega_n \sqrt{1 - \xi^2} t + \phi$	$\frac{\omega_n^2}{s^2 + 2\xi\omega_n s + \omega_n^2}$
$\frac{1}{\alpha^2 + \omega^2} + \frac{1}{\omega\sqrt{\alpha^2 + \omega^2}} e^{-\alpha t} \sin(\omega t - \phi)$	$\frac{1}{s[(s + \alpha)^2 + \omega^2]}$
$\phi = \tan^{-1} \frac{\omega}{-\alpha}$	
$1 - \frac{1}{\sqrt{1 - \xi^2}} e^{-\xi\omega_n t} \sin(\omega_n \sqrt{1 - \xi^2} t + \phi)$	$\frac{\omega_n^2}{s(s^2 + 2\xi\omega_n s + \omega_n^2)}$
$\phi = \cos^{-1} \xi, \xi < 1$	
$\frac{\alpha}{\alpha^2 + \omega^2} + \frac{1}{\omega} [(\alpha - a)^2 + \omega^2]^{1/2} e^{-\alpha t} \sin(\omega t + \phi)$	$\frac{s + \alpha}{s[(s + \alpha)^2 + \omega^2]}$
$\phi = \tan^{-1} \frac{\omega}{\alpha - a} - \tan^{-1} \frac{\omega}{-a}$	

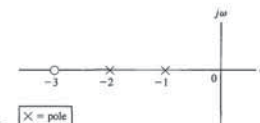


FIGURE 2.7 An s-plane pole and zero plot.

The poles and zeros of  $Y(s)$  are shown on the s-plane in Figure 2.7.

Expanding Equation (2.22) in a partial fraction expansion, we obtain

$$Y(s) = \frac{k_1}{s + 1} + \frac{k_2}{s + 2} \tag{2.23}$$

where  $k_1$  and  $k_2$  are the coefficients of the expansion. The coefficients  $k_i$  are called **residues** and are evaluated by multiplying through by the denominator factor of Equation (2.22) corresponding to  $k_i$  and setting  $s$  equal to the root. Evaluating  $k_1$  when  $y_0 = 1$ , we have

$$k_1 = \left. \frac{(s - s_1)p(s)}{q(s)} \right|_{s=s_1} = \left. \frac{(s + 1)(s + 3)}{(s + 1)(s + 2)} \right|_{s=-1} = 2$$

and  $k_2 = -1$ . Alternatively, the residues of  $Y(s)$  at the respective poles may be evaluated graphically on the s-plane plot, since Equation (2.24) may be written as

$$k_1 = \frac{s + 3}{s + 2} \Big|_{s=s_1=-1} = \frac{s_1 + 3}{s_1 + 2} = 2$$

The graphical representation of Equation (2.25) is shown in Figure 2.8. The graphical method of evaluating the residues is particularly valuable when the order of the characteristic equation is high and several poles are complex conjugate pairs.

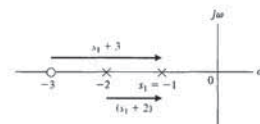


FIGURE 2.8 Graphical evaluation of the residues.



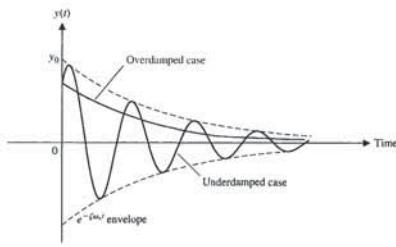


FIGURE 2.12 Response of the spring-mass-damper system.

where  $\theta = \cos^{-1} \zeta$ . Therefore,

$$k_2 = \frac{y_0}{2\sqrt{1-\zeta^2}} e^{j(\pi/2-\theta)}. \quad (2.36)$$

Finally, letting  $\beta = \sqrt{1-\zeta^2}$ , we find that

$$\begin{aligned} y(t) &= k_1 e^{s_1 t} + k_2 e^{s_2 t} \\ &= \frac{y_0}{2\sqrt{1-\zeta^2}} (e^{j(\theta-\pi/2)t} e^{-\zeta\omega_n t} e^{j\omega_n \beta t} + e^{j(\pi/2-\theta)t} e^{-\zeta\omega_n t} e^{-j\omega_n \beta t}) \\ &= \frac{y_0}{\sqrt{1-\zeta^2}} e^{-\zeta\omega_n t} \sin(\omega_n \sqrt{1-\zeta^2} t + \theta). \end{aligned} \quad (2.37)$$

The solution, Equation (2.37), can also be obtained using item 11 of Table 2.3. The transient responses of the overdamped ( $\zeta > 1$ ) and underdamped ( $\zeta < 1$ ) cases are shown in Figure 2.12. The transient response that occurs when  $\zeta < 1$  exhibits an oscillation in which the amplitude decreases with time, and it is called a **damped oscillation**.

The relationship between the  $s$ -plane location of the poles and zeros and the form of the transient response can be interpreted from the  $s$ -plane pole-zero plots. For example, as seen in Equation (2.37), adjusting the value of  $\zeta\omega_n$  varies the  $e^{-\zeta\omega_n t}$  envelope, hence the response  $y(t)$  shown in Figure 2.12. The larger the value of  $\zeta\omega_n$ , the faster the damping of the response,  $y(t)$ . In Figure 2.9, we see that the location of the complex pole  $s_1$  is given by  $s_1 = -\zeta\omega_n + j\omega_n\sqrt{1-\zeta^2}$ . So, making  $\zeta\omega_n$  larger moves the pole further to the left in the  $s$ -plane. Thus, the connection between the location of the pole in the  $s$ -plane and the step response is apparent—moving the pole  $s_1$  farther in the left half-plane leads to a faster damping of the transient step response. Of course, most control systems will have more than one complex pair of poles, so the transient response will be the result of the contributions of all the poles. In fact, the magnitude of the response of each pole, represented by the residue, can be visualized by examining the graphical residues on the  $s$ -plane. We will discuss the connection between the

Therefore, solving Equation (2.40) for  $I(s)$  and substituting in Equation (2.41), we have

$$V_2(s) = \frac{(1/Cs)V_1(s)}{R + 1/Cs}$$

Then the transfer function is obtained as the ratio  $V_2(s)/V_1(s)$ , which is

$$G(s) = \frac{V_2(s)}{V_1(s)} = \frac{1}{RCs + 1} = \frac{1}{\tau s + 1} = \frac{1/\tau}{s + 1/\tau}. \quad (2.42)$$

where  $\tau = RC$ , the **time constant** of the network. The single pole of  $G(s)$  is  $s = -1/\tau$ . Equation (2.42) could be immediately obtained if one observes that the circuit is a voltage divider, where

$$\frac{V_2(s)}{V_1(s)} = \frac{Z_2(s)}{Z_1(s) + Z_2(s)}, \quad (2.43)$$

and  $Z_1(s) = R$ ,  $Z_2 = 1/Cs$ .

A multiloop electrical circuit or an analogous multiple-mass mechanical system results in a set of simultaneous equations in the Laplace variable. It is usually more convenient to solve the simultaneous equations by using matrices and determinants [1, 3, 15]. An introduction to matrices and determinants can be found on the MCS website.

Let us consider the long-term behavior of a system and determine the response to certain inputs that remain after the transients fade away. Consider the dynamic system represented by the differential equation

$$\frac{d^n y}{dt^n} + q_{n-1} \frac{d^{n-1} y}{dt^{n-1}} + \dots + q_0 y = p_{n-1} \frac{d^{n-1} r}{dt^{n-1}} + p_{n-2} \frac{d^{n-2} r}{dt^{n-2}} + \dots + p_0 r, \quad (2.44)$$

where  $y(t)$  is the response, and  $r(t)$  is the input or forcing function. If the initial conditions are all zero, then the transfer function is the coefficient of  $R(s)$  in

$$Y(s) = G(s)R(s) = \frac{p(s)}{q(s)} R(s) = \frac{p_{n-1}s^{n-1} + p_{n-2}s^{n-2} + \dots + p_0}{s^n + q_{n-1}s^{n-1} + \dots + q_0} R(s). \quad (2.45)$$

The output response consists of a natural response (determined by the initial conditions) plus a forced response determined by the input. We now have

$$Y(s) = \frac{m(s)}{q(s)} + \frac{p(s)}{q(s)} R(s),$$

where  $q(s) = 0$  is the characteristic equation. If the input has the rational form

$$R(s) = \frac{n(s)}{d(s)}$$

then

$$Y(s) = \frac{m(s)}{q(s)} + \frac{p(s)}{q(s)} \frac{n(s)}{d(s)} = Y_1(s) + Y_2(s) + Y_3(s), \quad (2.46)$$

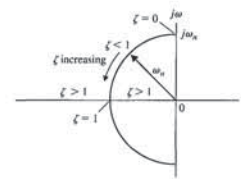


FIGURE 2.10 The locus of roots as  $\zeta$  varies with  $\omega_n$  constant.

locus, as shown in Figure 2.10. The transient response is increasingly oscillatory as the roots approach the imaginary axis when  $\zeta$  approaches zero.

The inverse Laplace transform can be evaluated using the graphical residue evaluation. The partial fraction expansion of Equation (2.30) is

$$Y(s) = \frac{k_1}{s-s_1} + \frac{k_2}{s-s_2}. \quad (2.33)$$

Since  $s_2$  is the complex conjugate of  $s_1$ , the residue  $k_2$  is the complex conjugate of  $k_1$  so that we obtain

$$Y(s) = \frac{k_1}{s-s_1} + \frac{k_1^*}{s-s_1^*},$$

where the asterisk indicates the conjugate relation. The residue  $k_1$  is evaluated from Figure 2.11 as

$$k_1 = \frac{y_0(s_1 + 2\zeta\omega_n)}{s_1 - s_1^*} = \frac{y_0 M_1 e^{j\theta}}{M_2 e^{j\pi/2}}, \quad (2.34)$$



where  $M_1$  is the magnitude of  $s_1 + 2\zeta\omega_n$ , and  $M_2$  is the magnitude of  $s_1 - s_1^*$ . (A review of complex numbers can be found on the MCS website.) In this case, we obtain

$$k_1 = \frac{y_0(\omega_n e^{j\theta})}{2\omega_n \sqrt{1-\zeta^2} e^{j\pi/2}} = \frac{y_0}{2\sqrt{1-\zeta^2} e^{j(\pi/2-\theta)}}, \quad (2.35)$$

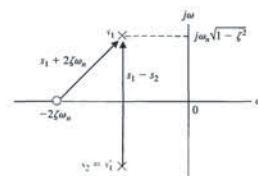


FIGURE 2.11 Evaluation of the residue  $k_1$ .

pole and zero locations and the transient and steady-state response more in subsequent chapters. We will find that the Laplace transformation and the  $s$ -plane approach are very useful techniques for system analysis and design where emphasis is placed on the transient and steady-state performance. In fact, because the study of control systems is concerned primarily with the transient and steady-state performance of dynamic systems, we have real cause to appreciate the value of the Laplace transform techniques.

## 2.5 THE TRANSFER FUNCTION OF LINEAR SYSTEMS

The **transfer function** of a linear system is defined as the ratio of the Laplace transform of the output variable to the Laplace transform of the input variable, with all initial conditions assumed to be zero. The transfer function of a system (or element) represents the relationship describing the dynamics of the system under consideration.

A transfer function may be defined only for a linear, stationary (constant parameter) system. A nonstationary system, often called a time-varying system, has one or more time-varying parameters, and the Laplace transformation may not be utilized. Furthermore, a transfer function is an input-output description of the behavior of a system. Thus, the transfer function description does not include any information concerning the internal structure of the system and its behavior.

The transfer function of the spring-mass-damper system is obtained from the original Equation (2.19), rewritten with zero initial conditions as follows:

$$Ms^2 Y(s) + bsY(s) + kY(s) = R(s). \quad (2.38)$$

Then the transfer function is

$$\frac{\text{Output}}{\text{Input}} = G(s) = \frac{Y(s)}{R(s)} = \frac{1}{Ms^2 + bs + k}. \quad (2.39)$$

The transfer function of the  $RC$  network shown in Figure 2.13 is obtained by writing the Kirchhoff voltage equation, yielding

$$V_1(s) = \left( R + \frac{1}{Cs} \right) I(s), \quad (2.40)$$

expressed in terms of transform variables. We shall frequently refer to variables and their transforms interchangeably. The transform variable will be distinguishable by the use of an uppercase letter or the argument ( $s$ ).

The output voltage is

$$V_2(s) = I(s) \left( \frac{1}{Cs} \right). \quad (2.41)$$

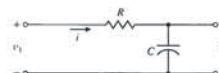


FIGURE 2.13 An  $RC$  network.



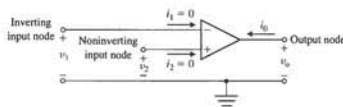


FIGURE 2.14 The ideal op-amp.

The operating conditions for the ideal op-amp are (1)  $i_1 = 0$  and  $i_2 = 0$ , thus implying that the input impedance is infinite, and (2)  $v_2 - v_1 = 0$  (or  $v_1 = v_2$ ). The input-output relationship for an ideal op-amp is

$$v_0 = K(v_2 - v_1) = -K(v_1 - v_2),$$

where the gain  $K$  approaches infinity. In our analysis, we will assume that the linear op-amps are operating with high gain and under idealized conditions.

Consider the inverting amplifier shown in Figure 2.15. Under ideal conditions, we have  $i_1 = 0$ , so that writing the node equation at  $v_1$  yields

$$\frac{v_1 - v_{in}}{R_1} + \frac{v_1 - v_0}{R_2} = 0.$$

Since  $v_2 = v_1$  (under ideal conditions) and  $v_2 = 0$  (see Figure 2.15 and compare it with Figure 2.14), it follows that  $v_1 = 0$ . Therefore,

$$-\frac{v_{in}}{R_1} - \frac{v_0}{R_2} = 0,$$

and rearranging terms, we obtain

$$\frac{v_0}{v_{in}} = -\frac{R_2}{R_1}.$$

We see that when  $R_2 = R_1$ , the ideal op-amp circuit inverts the sign of the input, that is,  $v_0 = -v_{in}$  when  $R_2 = R_1$ . ■

**EXAMPLE 2.4 Transfer function of a system**

Consider the mechanical system shown in Figure 2.16 and its electrical circuit analog shown in Figure 2.17. The electrical circuit analog is a force-current analog as outlined in Table 2.1. The velocities  $v_1(t)$  and  $v_2(t)$  of the mechanical system are directly

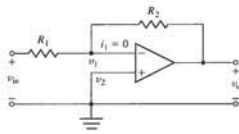


FIGURE 2.15 An inverting amplifier operating with ideal conditions.

Assuming that the velocity of  $M_1$  is the output variable, we solve for  $V_1(s)$  by matrix inversion or Cramer's rule to obtain [1,3]

$$V_1(s) = \frac{(M_2s + b_1 + k/s)R(s)}{(M_1s + b_1 + b_2)(M_2s + b_1 + k/s) - b_1^2} \quad (2.50)$$

Then the transfer function of the mechanical (or electrical) system is

$$G(s) = \frac{V_1(s)}{R(s)} = \frac{(M_2s + b_1 + k/s)}{(M_1s + b_1 + b_2)(M_2s + b_1 + k/s) - b_1^2} \\ = \frac{(M_2s^2 + b_1s + k)}{(M_1s + b_1 + b_2)(M_2s^2 + b_1s + k) - b_1^2s} \quad (2.51)$$

If the transfer function in terms of the position  $x_1(t)$  is desired, then we have

$$\frac{X_1(s)}{R(s)} = \frac{V_1(s)}{sR(s)} = \frac{G(s)}{s} \quad (2.52) \blacksquare$$

As an example, let us obtain the transfer function of an important electrical control component, the **DC motor** [8]. A DC motor is used to move loads and is called an **actuator**.

**An actuator is a device that provides the motive power to the process.**

**EXAMPLE 2.5 Transfer function of the DC motor**

The DC motor is a power actuator device that delivers energy to a load, as shown in Figure 2.18(a); a sketch of a DC motor is shown in Figure 2.18(b). The DC motor converts direct current (DC) electrical energy into rotational mechanical energy. A major fraction of the torque generated in the rotor (armature) of the motor is available to drive an external load. Because of features such as high torque, speed controllability over a wide range, portability, well-behaved speed-torque characteristics, and adaptability to various types of control methods, DC motors are widely used in numerous control applications, including robotic manipulators, tape transport mechanisms, disk drives, machine tools, and servovalve actuators.

The transfer function of the DC motor will be developed for a linear approximation to an actual motor, and second-order effects, such as hysteresis and the voltage drop across the brushes, will be neglected. The input voltage may be applied to the field or armature terminals. The air-gap flux  $\phi$  of the motor is proportional to the field current, provided the field is unsaturated, so that

$$\phi = K_f i_f \quad (2.53)$$

The torque developed by the motor is assumed to be related linearly to  $\phi$  and the armature current as follows:

$$T_m = K_t \phi i_a(t) = K_t K_f i_f(t) i_a(t). \quad (2.54)$$

where  $Y_1(s)$  is the partial fraction expansion of the natural response,  $Y_2(s)$  is the partial fraction expansion of the terms involving factors of  $q(s)$ , and  $Y_3(s)$  is the partial fraction expansion of terms involving factors of  $d(s)$ .

Taking the inverse Laplace transform yields

$$y(t) = y_1(t) + y_2(t) + y_3(t).$$

The transient response consists of  $y_1(t) + y_2(t)$ , and the steady-state response is  $y_3(t)$ .

**EXAMPLE 2.2 Solution of a differential equation**

Consider a system represented by the differential equation

$$\frac{d^2y}{dt^2} + 4\frac{dy}{dt} + 3y = 2r(t),$$

where the initial conditions are  $y(0) = 1$ ,  $\frac{dy}{dt}(0) = 0$ , and  $r(t) = 1, t \geq 0$ .

The Laplace transform yields

$$[s^2Y(s) - sy(0)] + 4[sY(s) - y(0)] + 3Y(s) = 2R(s).$$

Since  $R(s) = 1/s$  and  $y(0) = 1$ , we obtain

$$Y(s) = \frac{s + 4}{s^2 + 4s + 3} + \frac{2}{s(s^2 + 4s + 3)},$$

where  $q(s) = s^2 + 4s + 3 = (s + 1)(s + 3) = 0$  is the characteristic equation, and  $d(s) = s$ . Then the partial fraction expansion yields

$$Y(s) = \left[ \frac{3/2}{s + 1} + \frac{-1/2}{s + 3} \right] + \left[ \frac{-1}{s + 1} + \frac{1/3}{s + 3} \right] + \frac{2/3}{s} = Y_1(s) + Y_2(s) + Y_3(s).$$

Hence, the response is

$$y(t) = \left[ \frac{3}{2}e^{-t} - \frac{1}{2}e^{-3t} \right] + \left[ -1e^{-t} + \frac{1}{3}e^{-3t} \right] + \frac{2}{3},$$

and the steady-state response is

$$\lim_{t \rightarrow \infty} y(t) = \frac{2}{3} \blacksquare$$

**EXAMPLE 2.3 Transfer function of an op-amp circuit**

The operational amplifier (op-amp) belongs to an important class of analog integrated circuits commonly used as building blocks in the implementation of control systems and in many other important applications. Op-amps are active elements (that is, they have external power sources) with a high gain when operating in their linear regions. A model of an ideal op-amp is shown in Figure 2.14.

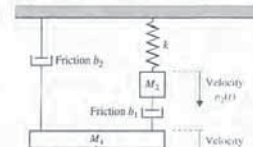


FIGURE 2.16 Two-mass mechanical system.

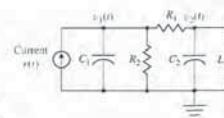


FIGURE 2.17 Two-node electric circuit analog.  $C_1 = M_1$ ,  $C_2 = M_2$ ,  $L = 1/k$ ,  $R_1 = 1/b_1$ ,  $R_2 = 1/b_2$ .

analogous to the node voltages  $v_1(t)$  and  $v_2(t)$  of the electrical circuit. The simultaneous equations, assuming that the initial conditions are zero, are

$$M_1sV_1(s) + (b_1 + b_2)V_1(s) - b_1V_2(s) = R(s), \quad (2.47)$$

and

$$M_2sV_2(s) + b_1(V_2(s) - V_1(s)) + k\frac{V_2(s)}{s} = 0. \quad (2.48)$$

These equations are obtained using the force equations for the mechanical system of Figure 2.16. Rearranging Equations (2.47) and (2.48), we obtain

$$(M_1s + (b_1 + b_2))V_1(s) + (-b_1)V_2(s) = R(s),$$

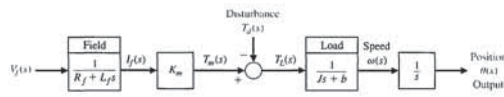
$$(-b_1)V_1(s) + \left( M_2s + b_1 + \frac{k}{s} \right) V_2(s) = 0,$$

or, in matrix form,

$$\begin{bmatrix} M_1s + b_1 + b_2 & -b_1 \\ -b_1 & M_2s + b_1 + \frac{k}{s} \end{bmatrix} \begin{bmatrix} V_1(s) \\ V_2(s) \end{bmatrix} = \begin{bmatrix} R(s) \\ 0 \end{bmatrix} \quad (2.49)$$



FIGURE 2.19 Block diagram model of field-controlled DC motor.



Therefore, the transfer function of the motor-load combination, with  $T_d(s) = 0$ , is

$$\frac{\theta(s)}{V_f(s)} = \frac{K_m}{s(Js + b)(L_f s + R_f)} = \frac{K_m(JL_f)}{s(s + b/J)(s + R_f/L_f)} \quad (2.62)$$

The block diagram model of the field-controlled DC motor is shown in Figure 2.19. Alternatively, the transfer function may be written in terms of the time constants of the motor as

$$\frac{\theta(s)}{V_f(s)} = G(s) = \frac{K_m(bR_f)}{s(\tau_f s + 1)(\tau_L s + 1)} \quad (2.63)$$

where  $\tau_f = L_f/R_f$  and  $\tau_L = J/b$ . Typically, one finds that  $\tau_L > \tau_f$  and often the field time constant may be neglected.

The armature-controlled DC motor uses the armature current  $i_a$  as the control variable. The stator field can be established by a field coil and current or a permanent magnet. When a constant field current is established in a field coil, the motor torque is

$$T_m(s) = (K_f K_f I_f) I_a(s) = K_m I_a(s) \quad (2.64)$$

When a permanent magnet is used, we have

$$T_m(s) = K_m I_a(s),$$

where  $K_m$  is a function of the permeability of the magnetic material.

The armature current is related to the input voltage applied to the armature by

$$V_a(s) = (R_a + L_a s) I_a(s) + V_b(s), \quad (2.65)$$

where  $V_b(s)$  is the back electromotive-force voltage proportional to the motor speed. Therefore, we have

$$V_b(s) = K_b \omega(s), \quad (2.66)$$

where  $\omega(s) = s\theta(s)$  is the transform of the angular speed and the armature current is

$$I_a(s) = \frac{V_a(s) - K_b \omega(s)}{R_a + L_a s}. \quad (2.67)$$

Equations (2.58) and (2.59) represent the load torque, so that

$$T_L(s) = Js^2\theta(s) + bs\theta(s) = T_m(s) - T_d(s). \quad (2.68)$$

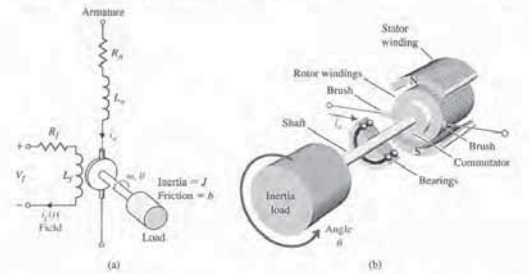


FIGURE 2.18 A DC motor (a) electrical diagram and (b) sketch.

It is clear from Equation (2.54) that, to have a linear system, one current must be maintained constant while the other current becomes the input current. First, we shall consider the field current controlled motor, which provides a substantial power amplification. Then we have, in Laplace transform notation,

$$T_m(s) = (K_f K_f I_f) I_a(s) = K_m I_a(s), \quad (2.55)$$

where  $I_f = I_a$  is a constant armature current, and  $K_m$  is defined as the motor constant. The field current is related to the field voltage as

$$V_f(s) = (R_f + L_f s) I_f(s). \quad (2.56)$$

The motor torque  $T_m(s)$  is equal to the torque delivered to the load. This relation may be expressed as

$$T_m(s) = T_L(s) + T_d(s), \quad (2.57)$$

where  $T_L(s)$  is the load torque and  $T_d(s)$  is the disturbance torque, which is often negligible. However, the disturbance torque often must be considered in systems subjected to external forces such as antenna wind-gust forces. The load torque for rotating inertia, as shown in Figure 2.18, is written as

$$T_L(s) = Js^2\theta(s) + bs\theta(s). \quad (2.58)$$

Rearranging Equations (2.55)–(2.57), we have

$$T_L(s) = T_m(s) - T_d(s), \quad (2.59)$$

$$T_m(s) = K_m I_a(s), \quad (2.60)$$

$$I_f(s) = \frac{V_f(s)}{R_f + L_f s}. \quad (2.61)$$

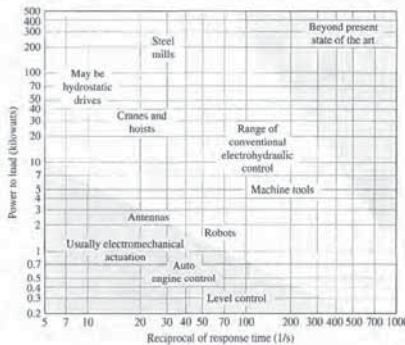


FIGURE 2.21 Range of control response time and power to load for electromechanical and electrohydraulic devices.

EXAMPLE 2.6 Transfer function of a hydraulic actuator

A useful actuator for the linear positioning of a mass is the hydraulic actuator shown in Table 2.5, item 9 [9, 10]. The hydraulic actuator is capable of providing a large power amplification. It will be assumed that the hydraulic fluid is available from a constant pressure source and that the compressibility of the fluid is negligible. A downward input displacement  $x$  moves the control valve; thus, fluid passes into the upper part of the cylinder, and the piston is forced downward. A small, low-power displacement of  $x(t)$  causes a larger, high-power displacement,  $y(t)$ . The volumetric fluid flow rate  $Q$  is related to the input displacement  $x(t)$  and the differential pressure across the piston as  $Q = g(x, P)$ . Using the Taylor series linearization as in Equation (2.11), we have

$$Q = \left( \frac{\partial g}{\partial x} \right)_{x_0, P_0} x + \left( \frac{\partial g}{\partial P} \right)_{x_0, P_0} P = k_x x - k_P P, \quad (2.71)$$

where  $g = g(x, P)$  and  $(x_0, P_0)$  is the operating point. The force developed by the actuator piston is equal to the area of the piston,  $A$ , multiplied by the pressure,  $P$ . This force is applied to the mass, so we have

$$AP = M \frac{d^2 y}{dt^2} + b \frac{dy}{dt}. \quad (2.72)$$

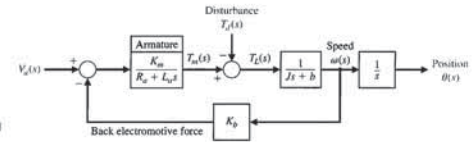


FIGURE 2.20 Armature-controlled DC motor.

The relations for the armature-controlled DC motor are shown schematically in Figure 2.20. Using Equations (2.64), (2.67), and (2.68) or the block diagram, and letting  $T_d(s) = 0$ , we solve to obtain the transfer function

$$G(s) = \frac{\theta(s)}{V_a(s)} = \frac{K_m}{s[(R_a + L_a s)(Js + b) + K_b K_m]} = \frac{K_m}{s(s^2 + 2\zeta\omega_n s + \omega_n^2)} \quad (2.69)$$

However, for many DC motors, the time constant of the armature,  $\tau_a = L_a/R_a$ , is negligible; therefore,

$$G(s) = \frac{\theta(s)}{V_a(s)} = \frac{K_m}{s[R_a(Js + b) + K_b K_m]} = \frac{K_m/(R_a b + K_b K_m)}{s(\tau_1 s + 1)}, \quad (2.70)$$

where the equivalent time constant  $\tau_1 = R_a J/(R_a b + K_b K_m)$ .

Note that  $K_m$  is equal to  $K_b$ . This equality may be shown by considering the steady-state motor operation and the power balance when the rotor resistance is neglected. The power input to the rotor is  $(K_b \omega) I_a$ , and the power delivered to the shaft is  $T \omega$ . In the steady-state condition, the power input is equal to the power delivered to the shaft so that  $(K_b \omega) I_a = T \omega$ ; since  $T = K_m I_a$  (Equation 2.64), we find that  $K_b = K_m$ .

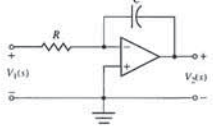
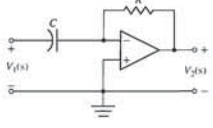
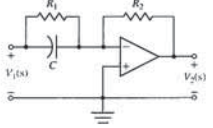
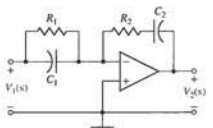
Electric motors are used for moving loads when a rapid response is not required and for relatively low power requirements. Typical constants for a fractional horsepower motor are provided in Table 2.4. Actuators that operate as a result of hydraulic pressure are used for large loads. Figure 2.21 shows the usual ranges of use for electromechanical drives as contrasted to electrohydraulic drives. Typical applications are also shown on the figure. ■

Table 2.4 Typical Constants for a Fractional Horsepower DC Motor

Motor constant $K_m$	$50 \times 10^{-3} \text{ N} \cdot \text{m}/\text{A}$
Rotor inertia $J_a$	$1 \times 10^{-3} \text{ N} \cdot \text{m} \cdot \text{s}^2/\text{rad}$
Field time constant $\tau_f$	1 ms
Rotor time constant $\tau$	100 ms
Maximum output power	$1/4 \text{ hp}$ , 187 W



**Table 2.5 Transfer Functions of Dynamic Elements and Networks**

Element or System	G(s)
1. Integrating circuit, filter	
	$\frac{V_2(s)}{V_1(s)} = -\frac{1}{RCs}$
2. Differentiating circuit	
	$\frac{V_2(s)}{V_1(s)} = -RCs$
3. Differentiating circuit	
	$\frac{V_2(s)}{V_1(s)} = -\frac{R_2(R_1Cs + 1)}{R_1}$
4. Integrating filter	
	$\frac{V_2(s)}{V_1(s)} = -\frac{(R_1C_1s + 1)(R_2C_2s + 1)}{R_1C_2s}$

(continued)

Thus, substituting Equation (2.71) into Equation (2.72), we obtain

$$\frac{A}{k_p}(k_p x - Q) = M \frac{d^2 y}{dt^2} + b \frac{dy}{dt} \quad (2.73)$$

Furthermore, the volumetric fluid flow is related to the piston movement as

$$Q = A \frac{dy}{dt} \quad (2.74)$$

Then, substituting Equation (2.74) into Equation (2.73) and rearranging, we have

$$\frac{Ak_p}{k_p} x = M \frac{d^2 y}{dt^2} + \left(b + \frac{A^2}{k_p}\right) \frac{dy}{dt} \quad (2.75)$$

Therefore, using the Laplace transformation, we have the transfer function

$$\frac{Y(s)}{X(s)} = \frac{K}{s(Ms + B)} \quad (2.76)$$

where

$$K = \frac{Ak_p}{k_p} \quad \text{and} \quad B = b + \frac{A^2}{k_p}$$

Note that the transfer function of the hydraulic actuator is similar to that of the electric motor. For an actuator operating at high pressure levels and requiring a rapid response of the load, we must account for the effect of the compressibility of the fluid [4, 5].

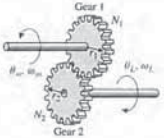
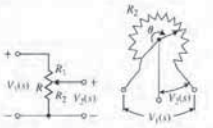
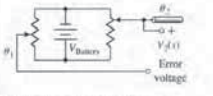
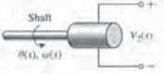



Symbols, units, and conversion factors associated with many of the variables in Table 2.5 are located at the MCS website. The symbols and units for each variable can be found in tables with corresponding conversions between SI and English units. ■

The transfer function concept and approach is very important because it provides the analyst and designer with a useful mathematical model of the system elements. We shall find the transfer function to be a continually valuable aid in the attempt to model dynamic systems. The approach is particularly useful because the s-plane poles and zeros of the transfer function represent the transient response of the system. The transfer functions of several dynamic elements are given in Table 2.5.

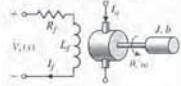
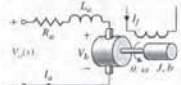

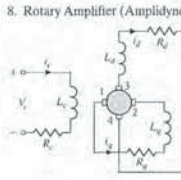
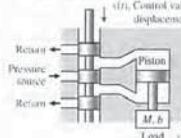
In many situations in engineering, the transmission of rotary motion from one shaft to another is a fundamental requirement. For example, the output power of an automobile engine is transferred to the driving wheels by means of the gearbox and differential. The gearbox allows the driver to select different gear ratios depending on the traffic situation, whereas the differential has a fixed ratio. The speed of the engine in this case is not constant, since it is under the control of the driver. Another example is a set of gears that transfer the power at the shaft of an electric motor to the shaft of a rotating antenna. Examples of mechanical converters are gears, chain drives, and belt drives. A commonly used electric converter is the electric transformer. An example of a device that converts rotational motion to linear motion is the rack-and-pinion gear shown in Table 2.5, item 17.

**Table 2.5 Continued**

Element or System	G(s)
10. Gear train, rotational transformer	
	$\text{Gear ratio} = n = \frac{N_1}{N_2}$ $N_2 \theta_L = N_1 \theta_m, \quad \theta_L = n \theta_m$ $\omega_L = n \omega_m$
11. Potentiometer, voltage control	
	$\frac{V_2(s)}{V_1(s)} = \frac{R_2}{R} = \frac{R_2}{R_1 + R_2}$ $\frac{R_2}{R} = \frac{\theta}{\theta_{max}}$
12. Potentiometer, error detector bridge	
	$V_2(s) = k_1(\theta_1(s) - \theta_2(s))$ $V_1(s) = k_2 \theta_{error}(s)$ $k_s = \frac{V_{battery}}{\theta_{max}}$
13. Tachometer, velocity sensor	
	$V_2(s) = K_t \omega(s) = K_t s \theta(s)$ $K_t = \text{constant}$
14. DC amplifier	
	$\frac{V_2(s)}{V_1(s)} = \frac{k_g}{s\tau + 1}$ $R_o = \text{output resistance}$ $C_o = \text{output capacitance}$ $\tau = R_o C_o, \tau \ll 1s$ <p>and is often negligible for controller amplifier</p>

(continued)

**Table 2.5 Continued**

Element or System	G(s)
5. DC motor, field-controlled, rotational actuator	
	$\frac{\theta(s)}{V_f(s)} = \frac{K_m}{s(Is + b)(L_f s + R_f)}$
6. DC motor, armature-controlled, rotational actuator	
	$\frac{\theta(s)}{V_a(s)} = \frac{K_m}{s[(R_a + L_a s)(Is + b) + K_s K_m]}$
7. AC motor, two-phase control field, rotational actuator	
	$\frac{\theta(s)}{V_c(s)} = \frac{K_m}{s(\tau s + 1)}$ $\tau = J/(b - m)$ <p>m = slope of linearized torque-speed curve (normally negative)</p>
8. Rotary Amplifier (Amplidyne)	
	$\frac{V_o(s)}{V_i(s)} = \frac{K/(R_s R_o)}{(s\tau_c + 1)(s\tau_o + 1)}$ $\tau_c = L_s/R_s, \quad \tau_o = L_o/R_o$ <p>for the unloaded case, <math>i_d = 0, \tau_c = \tau_o</math>, <math>0.05s &lt; \tau_c &lt; 0.5s</math></p> $V_o, V_{i1} = V_i$
9. Hydraulic actuator	
	$\frac{Y(s)}{X(s)} = \frac{K}{s(Ms + B)}$ $K = \frac{Ak_p}{k_p}, \quad B = \left(b + \frac{A^2}{k_p}\right)$ $k_s = \frac{\partial g}{\partial x} \Big _{x_0}, \quad k_p = \frac{\partial g}{\partial P} \Big _{P_0}$ $g = g(x, P) = \text{flow}$ $A = \text{area of piston}$

(continued)



FIGURE 2.22 Block diagram of a DC motor.

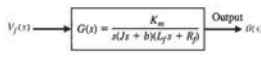
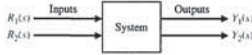


FIGURE 2.23 General block representation of two-input, two-output system.



the input and output variables. Therefore, one can correctly assume that the transfer function is an important relation for control engineering.

The importance of this cause-and-effect relationship is evidenced by the facility to represent the relationship of system variables by diagrammatic means. The **block diagram** representation of the system relationships is prevalent in control system engineering. Block diagrams consist of unidirectional, operational blocks that represent the transfer function of the variables of interest. A block diagram of a field-controlled DC motor and load is shown in Figure 2.22. The relationship between the displacement  $\theta(s)$  and the input voltage  $V_f(s)$  is clearly portrayed by the block diagram.

To represent a system with several variables under control, an interconnection of blocks is utilized. For example, the system shown in Figure 2.23 has two input variables and two output variables [6]. Using transfer function relations, we can write the simultaneous equations for the output variables as

$$Y_1(s) = G_{11}(s)R_1(s) + G_{12}(s)R_2(s), \quad (2.77)$$

and

$$Y_2(s) = G_{21}(s)R_1(s) + G_{22}(s)R_2(s), \quad (2.78)$$

where  $G_{ij}(s)$  is the transfer function relating the  $i$ th output variable to the  $j$ th input variable. The block diagram representing this set of equations is shown in Figure 2.24. In general, for  $J$  inputs and  $I$  outputs, we write the simultaneous equation in matrix form as

$$\begin{bmatrix} Y_1(s) \\ Y_2(s) \\ \vdots \\ Y_I(s) \end{bmatrix} = \begin{bmatrix} G_{11}(s) & \cdots & G_{1J}(s) \\ G_{21}(s) & \cdots & G_{2J}(s) \\ \vdots & \vdots & \vdots \\ G_{I1}(s) & \cdots & G_{IJ}(s) \end{bmatrix} \begin{bmatrix} R_1(s) \\ R_2(s) \\ \vdots \\ R_J(s) \end{bmatrix} \quad (2.79)$$

or simply

$$\mathbf{Y} = \mathbf{GR}. \quad (2.80)$$

FIGURE 2.24 Block diagram of interconnected system.

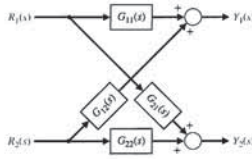
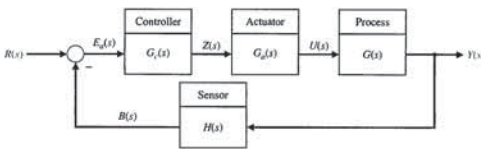


FIGURE 2.25 Negative feedback control system.



When two blocks are connected in cascade, as in Table 2.6, item 1, we assume that

$$X_3(s) = G_2(s)G_1(s)X_1(s)$$

holds true. This assumes that when the first block is connected to the second block, the effect of loading of the first block is negligible. Loading and interaction between interconnected components or systems may occur. If the loading of interconnected devices does occur, the engineer must account for this change in the transfer function and use the corrected transfer function in subsequent calculations.

Block diagram transformations and reduction techniques are derived by considering the algebra of the diagram variables. For example, consider the block diagram shown in Figure 2.25. This negative feedback control system is described by the equation for the actuating signal, which is

$$E_e(s) = R(s) - B(s) = R(s) - H(s)Y(s). \quad (2.81)$$

Because the output is related to the actuating signal by  $G(s)$ , we have

$$Y(s) = G(s)U(s) = G(s)G_a(s)Z(s) = G(s)G_a(s)G_c(s)E_e(s); \quad (2.82)$$

thus,

$$Y(s) = G(s)G_a(s)G_c(s)[R(s) - H(s)Y(s)]. \quad (2.83)$$

Combining the  $Y(s)$  terms, we obtain

$$Y(s)[1 + G(s)G_a(s)G_c(s)H(s)] = G(s)G_a(s)G_c(s)R(s). \quad (2.84)$$

Therefore, the transfer function relating the output  $Y(s)$  to the input  $R(s)$  is

$$\frac{Y(s)}{R(s)} = \frac{G(s)G_a(s)G_c(s)}{1 + G(s)G_a(s)G_c(s)H(s)}. \quad (2.85)$$

This **closed-loop transfer function** is particularly important because it represents many of the existing practical control systems.

The reduction of the block diagram shown in Figure 2.25 to a single block representation is one example of several useful techniques. These diagram transformations are given in Table 2.6. All the transformations in Table 2.6 can be derived by simple algebraic manipulation of the equations representing the blocks. System analysis by the method of block diagram reduction affords a better understanding of the contribution of each component element than possible by the manipulation of

Table 2.5 Continued

Element or System	$G(s)$
15. Accelerometer, acceleration sensor	$x_o(t) = y(t) - x_{in}(t),$ $\frac{X_o(s)}{X_{in}(s)} = \frac{-s^2}{s^2 + (b/M)s + k/M}$ <p>For low-frequency oscillations, where <math>\omega &lt; \omega_n</math>,</p> $\frac{X_o(j\omega)}{X_{in}(j\omega)} = \frac{\omega^2}{k/M}$
16. Thermal heating system	$\frac{\bar{T}(s)}{q(s)} = \frac{1}{C_p s + (QS + 1/R_i)}$ <p>where <math>\bar{T} = \bar{T}_o - \bar{T}_e =</math> temperature difference due to thermal process  <math>C_p =</math> thermal capacitance  <math>Q =</math> fluid flow rate = constant  <math>S =</math> specific heat of water  <math>R_i =</math> thermal resistance of insulation  <math>q(s) =</math> transform of rate of heat flow of heating element</p>
17. Rack and pinion	$x = r\theta$ <p>converts radial motion to linear motion</p>

2.6 BLOCK DIAGRAM MODELS

The dynamic systems that comprise automatic control systems are represented mathematically by a set of simultaneous differential equations. As we have noted in the previous sections, the Laplace transformation reduces the problem to the solution of a set of linear algebraic equations. Since control systems are concerned with the control of specific variables, the controlled variables must relate to the controlling variables. This relationship is typically represented by the transfer function of the subsystem relating

Here the  $\mathbf{Y}$  and  $\mathbf{R}$  matrices are column matrices containing the  $I$  output and the  $J$  input variables, respectively, and  $\mathbf{G}$  is an  $I$  by  $J$  transfer function matrix. The matrix representation of the interrelationship of many variables is particularly valuable for complex multi-variable control systems. An introduction to matrix algebra is provided on the MCS website for those unfamiliar with matrix algebra or who would find a review helpful [21].

The block diagram representation of a given system often can be reduced to a simplified block diagram with fewer blocks than the original diagram. Since the transfer functions represent linear systems, the multiplication is commutative. Thus, in Table 2.6, item 1, we have

$$X_3(s) = G_2(s)X_2(s) = G_1(s)G_2(s)X_1(s).$$

Table 2.6 Block Diagram Transformations

Transformation	Original Diagram	Equivalent Diagram
1. Combining blocks in cascade		
2. Moving a summing point behind a block		
3. Moving a pickoff point ahead of a block		
4. Moving a pickoff point behind a block		
5. Moving a summing point ahead of a block		
6. Eliminating a feedback loop		



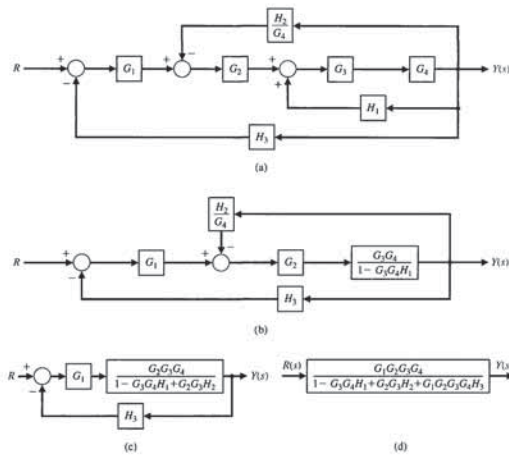


FIGURE 2.27 Block diagram reduction of the system of Figure 2.26.

2.7 SIGNAL-FLOW GRAPH MODELS

Block diagrams are adequate for the representation of the interrelationships of controlled and input variables. However, for a system with reasonably complex interrelationships, the block diagram reduction procedure is cumbersome and often quite difficult to complete. An alternative method for determining the relationship between system variables has been developed by Mason and is based on a representation of the system by line segments [4, 25]. The advantage of the line path method, called the signal-flow graph method, is the availability of a flow graph gain formula, which provides the relation between system variables without requiring any reduction procedure or manipulation of the flow graph.

The transition from a block diagram representation to a directed line segment representation is easy to accomplish by reconsidering the systems of the previous section. A **signal-flow graph** is a diagram consisting of nodes that are connected by several directed branches and is a graphical representation of a set of linear relations. Signal-flow graphs are particularly useful for feedback control systems because feedback theory is primarily concerned with the flow and processing of signals in systems. The basic element of a signal-flow graph is a unidirectional path segment called a **branch**, which relates the dependency of an input and an output variable in

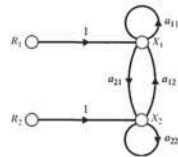


FIGURE 2.30 Signal-flow graph of two algebraic equations.

and

$$x_2 = \frac{(1 - a_{11})r_2 + a_{21}r_1}{(1 - a_{11})(1 - a_{22}) - a_{12}a_{21}} = \frac{1 - a_{11}}{\Delta} r_2 + \frac{a_{21}}{\Delta} r_1 \quad (2.94)$$

The denominator of the solution is the determinant  $\Delta$  of the set of equations and is rewritten as

$$\Delta = (1 - a_{11})(1 - a_{22}) - a_{12}a_{21} = 1 - a_{11} - a_{22} + a_{11}a_{22} - a_{12}a_{21} \quad (2.95)$$

In this case, the denominator is equal to 1 minus each self-loop  $a_{11}$ ,  $a_{22}$ , and  $a_{12}a_{21}$ , plus the product of the two nontouching loops  $a_{11}$  and  $a_{22}$ . The loops  $a_{22}$  and  $a_{21}a_{12}$  are touching, as are  $a_{11}$  and  $a_{21}a_{12}$ .

The numerator for  $x_1$  with the input  $r_1$  is 1 times  $1 - a_{22}$ , which is the value of  $\Delta$  excluding terms that touch the path 1 from  $r_1$  to  $x_1$ . Therefore the numerator from  $r_2$  to  $x_1$  is simply  $a_{21}$  because the path through  $a_{12}$  touches all the loops. The numerator for  $x_2$  is symmetrical to that of  $x_1$ .

In general, the linear dependence  $T_{ij}$  between the independent variable  $x_i$  (often called the input variable) and a dependent variable  $x_j$  is given by Mason's signal-flow gain formula [11, 12],

$$T_{ij} = \frac{\sum_k P_{ijk} \Delta_{ijk}}{\Delta} \quad (2.96)$$

$P_{ijk}$  = gain of  $k$ th path from variable  $x_i$  to variable  $x_j$ ,

$\Delta$  = determinant of the graph,

$\Delta_{ijk}$  = cofactor of the path  $P_{ijk}$ ,

and the summation is taken over all possible  $k$  paths from  $x_i$  to  $x_j$ . The path gain or transmittance  $P_{ijk}$  is defined as the product of the gains of the branches of the path, traversed in the direction of the arrows with no node encountered more than once. The cofactor  $\Delta_{ijk}$  is the determinant with the loops touching the  $k$ th path removed. The determinant  $\Delta$  is

$$\Delta = 1 - \sum_{n=1}^N L_n + \sum_{\substack{n,m \\ \text{nontouching}}} L_n L_m - \sum_{\substack{n,m,p \\ \text{nontouching}}} L_n L_m L_p + \dots \quad (2.97)$$

where  $L_q$  equals the value of the  $q$ th loop transmittance. Therefore the rule for evaluating  $\Delta$  in terms of loops  $L_1, L_2, L_3, \dots, L_N$  is

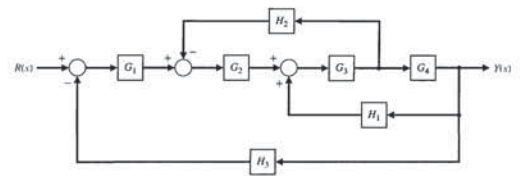


FIGURE 2.26 Multiple-loop feedback control system.

equations. The utility of the block diagram transformations will be illustrated by an example using block diagram reduction.

EXAMPLE 2.7 Block diagram reduction

The block diagram of a multiple-loop feedback control system is shown in Figure 2.26. It is interesting to note that the feedback signal  $H_3(s)Y(s)$  is a positive feedback signal, and the loop  $G_3(s)G_4(s)H_1(s)$  is a **positive feedback loop**. The block diagram reduction procedure is based on the use of Table 2.6, transformation 6, which eliminates feedback loops. Therefore the other transformations are used to transform the diagram to a form ready for eliminating feedback loops. First, to eliminate the loop  $G_2G_4H_1$ , we move  $H_2$  behind block  $G_4$  by using transformation 4, and obtain Figure 2.27(a). Eliminating the loop  $G_2G_4H_1$  by using transformation 6, we obtain Figure 2.27(b). Then, eliminating the inner loop containing  $H_2/G_4$ , we obtain Figure 2.27(c). Finally, by reducing the loop containing  $H_3$ , we obtain the closed-loop system transfer function as shown in Figure 2.27(d). It is worthwhile to examine the form of the numerator and denominator of this closed-loop transfer function. We note that the numerator is composed of the cascade transfer function of the feed-forward elements connecting the input  $R(s)$  and the output  $Y(s)$ . The denominator is composed of 1 minus the sum of each loop transfer function. The loop  $G_2G_4H_1$  has a plus sign in the sum to be subtracted because it is a positive feedback loop, whereas the loops  $G_1G_2G_3G_4H_3$  and  $G_2G_3H_2$  are negative feedback loops. To illustrate this point, the denominator can be rewritten as

$$q(s) = 1 - (+G_2G_4H_1 - G_2G_3H_2 - G_1G_2G_3G_4H_3) \quad (2.86)$$

This form of the numerator and denominator is quite close to the general form for multiple-loop feedback systems, as we shall find in the following section. ■

The block diagram representation of feedback control systems is a valuable and widely used approach. The block diagram provides the analyst with a graphical representation of the interrelationships of controlled and input variables. Furthermore, the designer can readily visualize the possibilities for adding blocks to the existing system block diagram to alter and improve the system performance. The transition from the block diagram method to a method utilizing a line path representation instead of a block representation is readily accomplished and is presented in the following section.

FIGURE 2.28 Signal-flow graph of the DC motor.

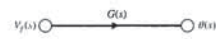
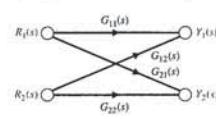


FIGURE 2.29 Signal-flow graph of interconnected system.



a manner equivalent to a block of a block diagram. Therefore, the branch relating the output  $\theta(s)$  of a DC motor to the field voltage  $V_f(s)$  is similar to the block diagram of Figure 2.22 and is shown in Figure 2.28. The input and output points or junctions are called **nodes**. Similarly, the signal-flow graph representing Equations (2.77) and (2.78), as well as Figure 2.24, is shown in Figure 2.29. The relation between each variable is written next to the directional arrow. All branches leaving a node will pass the nodal signal to the output node of each branch (unidirectionally). The summation of all signals entering a node is equal to the node variable. A **path** is a branch or a continuous sequence of branches that can be traversed from one signal (node) to another signal (node). A **loop** is a closed path that originates and terminates on the same node, with no node being met twice along the path. Two loops are said to be **nontouching** if they do not have a common node. Two touching loops share one or more common nodes. Therefore, considering Figure 2.29 again, we obtain

$$Y_1(s) = G_{11}(s)R_1(s) + G_{12}(s)R_2(s) \quad (2.87)$$

and

$$Y_2(s) = G_{21}(s)R_1(s) + G_{22}(s)R_2(s) \quad (2.88)$$

The flow graph is simply a pictorial method of writing a system of algebraic equations that indicates the interdependencies of the variables. As another example, consider the following set of simultaneous algebraic equations:

$$a_{11}x_1 + a_{12}x_2 + r_1 = x_1 \quad (2.89)$$

$$a_{21}x_1 + a_{22}x_2 + r_2 = x_2 \quad (2.90)$$

The two input variables are  $r_1$  and  $r_2$ , and the output variables are  $x_1$  and  $x_2$ . A signal-flow graph representing Equations (2.89) and (2.90) is shown in Figure 2.30. Equations (2.89) and (2.90) may be rewritten as

$$x_1(1 - a_{11}) + x_2(-a_{12}) = r_1 \quad (2.91)$$

and

$$x_1(-a_{21}) + x_2(1 - a_{22}) = r_2 \quad (2.92)$$

The simultaneous solution of Equations (2.91) and (2.92) using Cramer's rule results in the solutions

$$x_1 = \frac{(1 - a_{22})r_1 + a_{12}r_2}{(1 - a_{11})(1 - a_{22}) - a_{12}a_{21}} = \frac{1 - a_{22}}{\Delta} r_1 + \frac{a_{12}}{\Delta} r_2 \quad (2.93)$$

There are four self-loops:

$$L_1 = G_2H_2, \quad L_2 = H_3G_3, \quad L_3 = G_6H_6, \quad \text{and} \quad L_4 = G_7H_7.$$

Loops  $L_1$  and  $L_2$  do not touch  $L_3$  and  $L_4$ . Therefore, the determinant is

$$\Delta = 1 - (L_1 + L_2 + L_3 + L_4) + (L_1L_3 + L_1L_4 + L_2L_3 + L_2L_4). \quad (2.99)$$

The cofactor of the determinant along path 1 is evaluated by removing the loops that touch path 1 from  $\Delta$ . Hence, we have

$$L_1 = L_2 = 0 \quad \text{and} \quad \Delta_1 = 1 - (L_3 + L_4).$$

Similarly, the cofactor for path 2 is

$$\Delta_2 = 1 - (L_1 + L_2).$$

Therefore, the transfer function of the system is

$$\begin{aligned} \frac{Y(s)}{R(s)} = T(s) &= \frac{P_1\Delta_1 + P_2\Delta_2}{\Delta} \quad (2.100) \\ &= \frac{G_1G_2G_3G_4(1 - L_3 - L_4) + G_5G_6G_7G_8(1 - L_1 - L_2)}{1 - L_1 - L_2 - L_3 - L_4 + L_1L_3 + L_1L_4 + L_2L_3 + L_2L_4}. \end{aligned}$$

A similar analysis can be accomplished using block diagram reduction techniques. The block diagram shown in Figure 2.31(b) has four inner feedback loops within the overall block diagram. The block diagram reduction is simplified by first reducing the four inner feedback loops and then placing the resulting systems in series. Along the top path, the transfer function is

$$\begin{aligned} Y_1(s) &= G_1(s) \left[ \frac{G_2(s)}{1 - G_2(s)H_2(s)} \right] \left[ \frac{G_3(s)}{1 - G_3(s)H_3(s)} \right] G_4(s)R(s) \\ &= \left[ \frac{G_1(s)G_2(s)G_3(s)G_4(s)}{(1 - G_2(s)H_2(s))(1 - G_3(s)H_3(s))} \right] R(s). \end{aligned}$$

Similarly across the bottom path, the transfer function is

$$\begin{aligned} Y_2(s) &= G_5(s) \left[ \frac{G_6(s)}{1 - G_6(s)H_6(s)} \right] \left[ \frac{G_7(s)}{1 - G_7(s)H_7(s)} \right] G_8(s)R(s) \\ &= \left[ \frac{G_5(s)G_6(s)G_7(s)G_8(s)}{(1 - G_6(s)H_6(s))(1 - G_7(s)H_7(s))} \right] R(s). \end{aligned}$$

The total transfer function is then given by

$$\begin{aligned} Y(s) = Y_1(s) + Y_2(s) &= \left[ \frac{G_1(s)G_2(s)G_3(s)G_4(s)}{(1 - G_2(s)H_2(s))(1 - G_3(s)H_3(s))} \right. \\ &\quad \left. + \frac{G_5(s)G_6(s)G_7(s)G_8(s)}{(1 - G_6(s)H_6(s))(1 - G_7(s)H_7(s))} \right] R(s). \quad \blacksquare \end{aligned}$$

$\Delta = 1 -$  (sum of all different loop gains)

- + (sum of the gain products of all combinations of two nontouching loops)
- (sum of the gain products of all combinations of three nontouching loops)
- + ...

The gain formula is often used to relate the output variable  $Y(s)$  to the input variable  $R(s)$  and is given in somewhat simplified form as

$$T = \frac{\sum_k P_k \Delta_k}{\Delta} \quad (2.98)$$

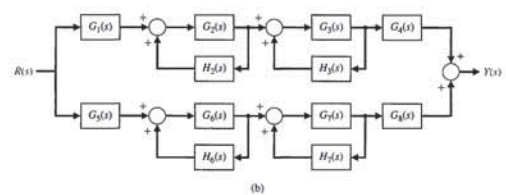
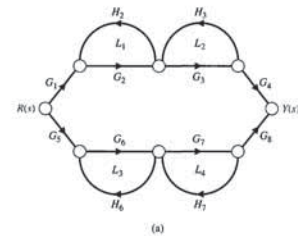
where  $T(s) = Y(s)/R(s)$ .

Several examples will illustrate the utility and ease of this method. Although the gain Equation (2.96) appears to be formidable, one must remember that it represents a summation process, not a complicated solution process.

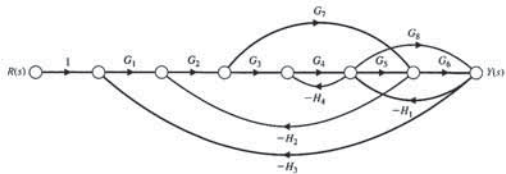
**EXAMPLE 2.8 Transfer function of an interacting system**

A two-path signal-flow graph is shown in Figure 2.31(a) and the corresponding block diagram is shown in Figure 2.31(b). An example of a control system with multiple signal paths is a multilegged robot. The paths connecting the input  $R(s)$  and output  $Y(s)$  are

$$P_1 = G_1G_2G_3G_4 \quad (\text{path 1}) \quad \text{and} \quad P_2 = G_5G_6G_7G_8 \quad (\text{path 2}).$$



**FIGURE 2.31** Two-path interacting system. (a) Signal-flow graph. (b) Block diagram.



**FIGURE 2.33** Multiple-loop system.

**EXAMPLE 2.11 Transfer function of a complex system**

Finally, we shall consider a reasonably complex system that would be difficult to reduce by block diagram techniques. A system with several feedback loops and feedforward paths is shown in Figure 2.33. The forward paths are

$$P_1 = G_1G_2G_3G_4G_5G_6, \quad P_2 = G_1G_2G_7G_8, \quad \text{and} \quad P_3 = G_1G_2G_9G_4G_6.$$

The feedback loops are

$$\begin{aligned} L_1 &= -G_2G_3G_4G_5H_2, & L_2 &= -G_2G_6H_1, & L_3 &= -G_8H_1, & L_4 &= -G_7H_2G_2, \\ L_5 &= -G_4H_6, & L_6 &= -G_1G_2G_7G_4G_5G_6H_3, & L_7 &= -G_1G_2G_9G_4H_3, & & \\ L_8 &= -G_7G_2G_9G_4G_5H_3. & & & & & & \end{aligned}$$

Loop  $L_5$  does not touch loop  $L_4$  or loop  $L_7$ , and loop  $L_3$  does not touch loop  $L_4$ ; but all other loops touch. Therefore, the determinant is

$$\Delta = 1 - (L_1 + L_2 + L_3 + L_4 + L_5 + L_6 + L_7 + L_8) + (L_5L_7 + L_5L_4 + L_3L_4). \quad (2.103)$$

The cofactors are

$$\Delta_1 = \Delta_3 = 1 \quad \text{and} \quad \Delta_2 = 1 - L_5 = 1 + G_4H_6.$$

Finally, the transfer function is

$$T(s) = \frac{Y(s)}{R(s)} = \frac{P_1 + P_2\Delta_2 + P_3}{\Delta} \quad (2.104) \quad \blacksquare$$

Signal-flow graphs and Mason's signal-flow gain formula may be used profitably for the analysis of feedback control systems, electronic amplifier circuits, statistical systems, and mechanical systems, among many other examples.

**2.8 DESIGN EXAMPLES**

In this section, we present six illustrative design examples. The first example describes modeling of a photovoltaic generator in a manner amenable to feedback control to achieve maximum power delivery as the sunlight varies over time. Using feedback control to improve the efficiency of producing electricity using solar energy in areas

**EXAMPLE 2.9 Armature-controlled motor**

The block diagram of the armature-controlled DC motor is shown in Figure 2.20. This diagram was obtained from Equations (2.64)–(2.68). The signal-flow diagram can be obtained either from Equations (2.64)–(2.68) or from the block diagram and is shown in Figure 2.32. Using Mason's signal-flow gain formula, let us obtain the transfer function for  $\theta(s)/V_a(s)$  with  $T_d(s) = 0$ . The forward path is  $P_1(s)$ , which touches the one loop,  $L_1(s)$ , where

$$P_1(s) = \frac{1}{s}G_1(s)G_2(s) \quad \text{and} \quad L_1(s) = -K_fG_1(s)G_2(s).$$

Therefore, the transfer function is

$$T(s) = \frac{P_1(s)}{1 - L_1(s)} = \frac{(1/s)G_1(s)G_2(s)}{1 + K_fG_1(s)G_2(s)} = \frac{K_m}{s[(R_a + L_a s)(Js + b) + K_f K_m]}$$

which is exactly the same as that derived earlier (Equation 2.69).  $\blacksquare$

The signal-flow graph gain formula provides a reasonably straightforward approach for the evaluation of complicated systems. To compare the method with block diagram reduction, which is really not much more difficult, let us reconsider the complex system of Example 2.7.

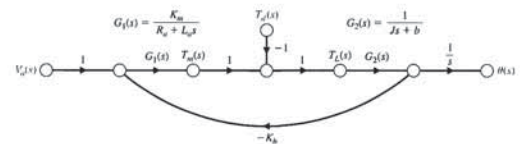
**EXAMPLE 2.10 Transfer function of a multiple-loop system**

A multiple-loop feedback system is shown in Figure 2.26 in block diagram form. There is no need to redraw the diagram in signal-flow graph form, and so we shall proceed as usual by using Mason's signal-flow gain formula, Equation (2.98). There is one forward path  $P_1 = G_1G_2G_3G_4$ . The feedback loops are

$$L_1 = -G_2G_3H_2, \quad L_2 = G_3G_4H_1, \quad \text{and} \quad L_3 = -G_1G_2G_3G_4H_3. \quad (2.101)$$

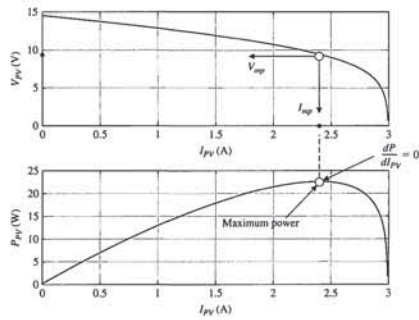
All the loops have common nodes and therefore are all touching. Furthermore, the path  $P_1$  touches all the loops, so  $\Delta_1 = 1$ . Thus, the closed-loop transfer function is

$$\begin{aligned} T(s) = \frac{Y(s)}{R(s)} &= \frac{P_1\Delta_1}{1 - L_1 - L_2 - L_3} \\ &= \frac{G_1G_2G_3G_4}{1 + G_2G_3H_2 - G_3G_4H_1 + G_1G_2G_3G_4H_3} \quad (2.102) \quad \blacksquare \end{aligned}$$



**FIGURE 2.32** The signal-flow graph of the armature-controlled DC motor.





**FIGURE 2.35** Voltage versus current and power versus current for an example photovoltaic generator at a specific insolation level.

The insolation level is a measure of the amount of incident solar radiation on the solar cells.

Suppose that we have a single silicon solar panel ( $M = 1$ ) with 10 series cells ( $N = 10$ ) and the parameters given by  $1/\lambda = 0.05 \text{ V}$ ,  $R_s = 0.025 \Omega$ ,  $I_{PH} = 3 \text{ A}$ , and  $I_0 = 0.001 \text{ A}$ . The voltage versus current relationship in Equation (2.105) and the power versus voltage are shown in Figure 2.35 for one particular insolation level where  $I_{PH} = 3 \text{ A}$ . In Figure 2.35, we see that when  $dP/dI_{PV} = 0$  we are at the maximum power level with an associated  $V_{PV} = V_{ref}$  and  $I_{PV} = I_{ref}$ , the values of voltage and current at the maximum power, respectively. As the sunlight varies, the insolation level,  $I_{PH}$ , varies resulting in different power curves.

The goal of the power point tracking is to seek the voltage and current condition that maximizes the power output as conditions vary. This is accomplished by varying the reference voltage as a function of the insolation level. The reference voltage is the voltage at the maximum power point as shown in Figure 2.36. The feedback control system should track the reference voltage in a rapid and accurate fashion.

Figure 2.37 illustrates a simplified block diagram of the controlled system. The main components are a power circuit (e.g., a phase control IC and a thyristor bridge), photovoltaic generator, and current transducer. The plant including the power circuit, photovoltaic generator, and current transducer is modeled as a second-order transfer function given by

$$G(s) = \frac{K}{s(s + p)}, \quad (2.106)$$

where  $K$  and  $p$  depend on the photovoltaic generator and associated electronics [35]. The controller,  $G_c(s)$ , in Figure 2.37 is designed such that as the insolation level varies (that is, as  $I_{PH}$  varies), the voltage output will approach the reference input voltage,  $V_{ref}$ , which has been set to the voltage associated with the maximum

of abundant sunlight is a valuable contribution to green engineering (discussed in Chapter 1). In the second example, we present a detailed look at modeling of the fluid level in a reservoir. The modeling is presented in a very detailed manner to emphasize the effort required to obtain a linear model in the form of a transfer function. The design process depicted in Figure 1.17 is highlighted in this example. The remaining four examples include an electric traction motor model development, a look at a mechanical accelerometer aboard a rocket sled, an overview of a laboratory robot and the associated hardware specifications, and the design of a low-pass filter.

**EXAMPLE 2.12 Photovoltaic generators**

Photovoltaic cells were developed at Bell Laboratories in 1954. Solar cells are one example of photovoltaic cells and convert solar light to electricity. Other types of photovoltaic cells can detect radiation and measure light intensity. The use of solar cells to produce energy supports the principles of green engineering by minimizing pollution. Solar panels minimize the depletion of natural resources and are effective in areas where sunlight is abundant. Photovoltaic generators are systems that provide electricity using an assortment of photovoltaic modules comprised of interconnected solar cells. Photovoltaic generators can be used to recharge batteries, they can be directly connected to an electrical grid, or they can drive electric motors without a battery [34–42].

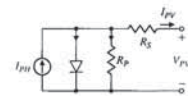
The power output of a solar cell varies with available solar light, temperature, and external loads. To increase the overall efficiency of the photovoltaic generator, feedback control strategies can be employed to seek to maximize the power output. This is known as maximum power point tracking (MPPT) [34–36]. There are certain values of current and voltage associated with the solar cells corresponding to the maximum power output. The MPPT uses closed-loop feedback control to seek the optimal point to allow the power converter circuit to extract the maximum power from the photovoltaic generator system. We will discuss the control design in later chapters, but here we focus on the modeling of the system.

The solar cell can be modeled as an equivalent circuit shown in Figure 2.34 composed of a current generator,  $I_{PH}$ , a light sensitive diode, a resistance series,  $R_s$ , and a shunt resistance,  $R_p$  [34, 36–38].

The output voltage,  $V_{PV}$ , is given by

$$V_{PV} = \frac{N}{\lambda} \ln \left( \frac{I_{PH} - I_{PV} + MI_0}{MI_0} \right) - \frac{N}{M} R_s I_{PV}, \quad (2.105)$$

where the photovoltaic generator is comprised of  $M$  parallel strings with  $N$  series cells per string,  $I_0$  is the reverse saturation current of the diode,  $I_{PH}$  represents the insolation level, and  $\lambda$  is a known constant that depends on the cell material [34–36].



**FIGURE 2.34** Equivalent circuit of the photovoltaic generator.

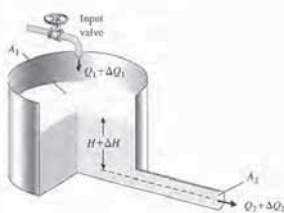
**EXAMPLE 2.13 Fluid flow modeling**

A fluid flow system is shown in Figure 2.38. The reservoir (or tank) contains water that evacuates through an output port. Water is fed to the reservoir through a pipe controlled by an input valve. The variables of interest are the fluid velocity  $V$  (m/s), fluid height in the reservoir  $H$  (m), and pressure  $p$  (N/m<sup>2</sup>). The pressure is defined as the force per unit area exerted by the fluid on a surface immersed (and at rest with respect to) the fluid. Fluid pressure acts normal to the surface. For further reading on fluid flow modeling, see [28–30].

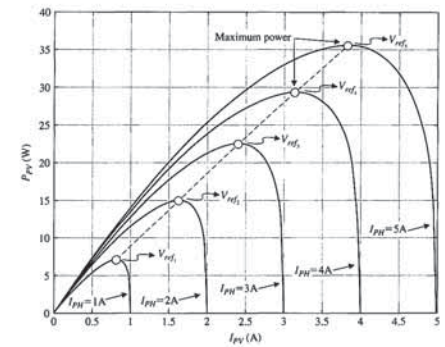
The elements of the control system design process emphasized in this example are shown in Figure 2.39. The strategy is to establish the system configuration and then obtain the appropriate mathematical models describing the fluid flow reservoir from an input–output perspective.

The general equations of motion and energy describing fluid flow are quite complicated. The governing equations are coupled nonlinear partial differential equations. We must make some selective assumptions that reduce the complexity of the mathematical model. Although the control engineer is not required to be a fluid dynamicist, and a deep understanding of fluid dynamics is not necessarily acquired during the control system design process, it makes good engineering sense to gain at least a rudimentary understanding of the important simplifying assumptions. For a more complete discussion of fluid motion, see [31–33].

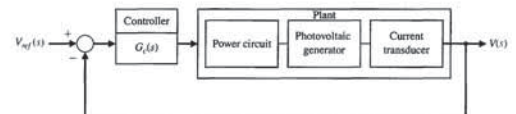
To obtain a realistic, yet tractable, mathematical model for the fluid flow reservoir, we first make several key assumptions. We assume that the water in the tank is incompressible and that the flow is inviscid, irrotational and steady. An incompressible fluid has a constant density  $\rho$  (kg/m<sup>3</sup>). In fact, all fluids are compressible to some extent. The compressibility factor,  $k$ , is a measure of the compressibility of a fluid. A smaller value of  $k$  indicates less compressibility. Air (which is a compressible fluid) has a compressibility factor of  $k_{air} = 0.98 \text{ m}^2/\text{N}$ , while water has a compressibility factor of  $k_{H_2O} = 4.9 \times 10^{-10} \text{ m}^2/\text{N} = 50 \times 10^{-6} \text{ atm}^{-1}$ . In other words, a given volume of water decreases by 50 one-millionths of the original volume for each atmosphere (atm) increase in pressure. Thus the assumption that the water is incompressible is valid for our application.



**FIGURE 2.38** The fluid flow reservoir configuration.



**FIGURE 2.36** Maximum power point for varying values of  $I_{PH}$  specifies  $V_{ref}$ .



**FIGURE 2.37** Block diagram of feedback control system for maximum power transfer with parameters  $K$  and  $p$ .

power point resulting in maximum power transfer. If, for example, the controller is the proportional plus integral controller

$$G_c(s) = K_p + \frac{K_I}{s},$$

the closed-loop transfer function is

$$T(s) = \frac{K(K_p s + K_I)}{s^3 + p s^2 + K K_p s + K K_I} \quad (2.107)$$

We can select the controller gains in Equation (2.107) to place the poles of  $T(s)$  in the desired locations (see Chapters 4 and 5) to meet the desired performance specifications.

the reservoir and output pipe. We can neglect viscosity in our model development. We say our fluid is inviscid.

If each fluid element at each point in the flow has no net angular velocity about that point, the flow is termed irrotational. Imagine a small paddle wheel immersed in the fluid (say in the output port). If the paddle wheel translates without rotating, the flow is irrotational. We will assume the water in the tank is irrotational. For an inviscid fluid, an initially irrotational flow remains irrotational.

The water flow in the tank and output port can be either steady or unsteady. The flow is steady if the velocity at each point is constant in time. This does not necessarily imply that the velocity is the same at every point but rather that at any given point the velocity does not change with time. Steady-state conditions can be achieved at low fluid speeds. We will assume steady flow conditions. If the output port area is too large, then the flow through the reservoir may not be slow enough to establish the steady-state condition that we are assuming exists and our model will not accurately predict the fluid flow motion.

To obtain a mathematical model of the flow within the reservoir, we employ basic principles of science and engineering, such as the principle of conservation of mass. The mass of water in the tank at any given time is

$$m = \rho A_1 H, \quad (2.108)$$

where  $A_1$  is the area of the tank,  $\rho$  is the water density, and  $H$  is the height of the water in the reservoir. The constants for the reservoir system are given in Table 2.7.

In the following formulas, a subscript 1 denotes quantities at the input, and a subscript 2 refers to quantities at the output. Taking the time derivative of  $m$  in Equation (2.108) yields

$$\dot{m} = \rho A_1 \dot{H},$$

where we have used the fact that our fluid is incompressible (that is,  $\dot{\rho} = 0$ ) and that the area of the tank,  $A_1$ , does not change with time. The change in mass in the reservoir is equal to the mass that enters the tank minus the mass that leaves the tank, or

$$\dot{m} = \rho A_1 \dot{H} = Q_1 - \rho A_2 v_2, \quad (2.109)$$

where  $Q_1$  is the steady-state input mass flow rate,  $v_2$  is the exit velocity, and  $A_2$  is the output port area. The exit velocity,  $v_2$ , is a function of the water height. From Bernoulli's equation [39] we have

$$\frac{1}{2} \rho v_1^2 + P_1 + \rho g H = \frac{1}{2} \rho v_2^2 + P_2,$$

where  $v_1$  is the water velocity at the mouth of the reservoir, and  $P_1$  and  $P_2$  are the atmospheric pressures at the input and output, respectively. But  $P_1$  and  $P_2$  are equal to

**Table 2.7 Water Tank Physical Constants**

$\rho$ (kg/m <sup>3</sup> )	$g$ (m/s <sup>2</sup> )	$A_1$ (m <sup>2</sup> )	$A_2$ (m <sup>2</sup> )	$H^*$ (m)	$Q^*$ (kg/s)
1000	9.8	$\pi/4$	$\pi/400$	1	34.77

where  $\Delta H$  and  $\Delta Q_1$  are small deviations from the equilibrium (steady-state) values. The Taylor series expansion about the equilibrium conditions is given by

$$\dot{H} = f(H, Q_1) = f(H^*, Q^*) + \left. \frac{\partial f}{\partial H} \right|_{H^*, Q^*} (H - H^*) \quad (2.116)$$

$$+ \left. \frac{\partial f}{\partial Q_1} \right|_{H^*, Q^*} (Q_1 - Q^*) + \dots,$$

where

$$\left. \frac{\partial f}{\partial H} \right|_{H^*, Q^*} = \left. \frac{\partial(k_1 \sqrt{H} + k_2 Q_1)}{\partial H} \right|_{H^*, Q^*} = \frac{1}{2} \frac{k_1}{\sqrt{H^*}},$$

and

$$\left. \frac{\partial f}{\partial Q_1} \right|_{H^*, Q^*} = \left. \frac{\partial(k_1 \sqrt{H} + k_2 Q_1)}{\partial Q_1} \right|_{H^*, Q^*} = k_2.$$

Using Equation (2.114), we have

$$\sqrt{H^*} = \frac{Q^*}{\rho \sqrt{2gA_2}},$$

so that

$$\left. \frac{\partial f}{\partial H} \right|_{H^*, Q^*} = \frac{A_2^2 g \rho}{A_1 Q^*}$$

It follows from Equation (2.115) that

$$\dot{H} = \Delta \dot{H},$$

since  $H^*$  is constant. Also, the term  $f(H^*, Q^*)$  is identically zero, by definition of the equilibrium condition. Neglecting the higher order terms in the Taylor series expansion yields

$$\Delta \dot{H} = -\frac{A_2^2 g \rho}{A_1 Q^*} \Delta H + \frac{1}{\rho A_1} \Delta Q_1. \quad (2.117)$$

Equation (2.117) is a linear model describing the deviation in water level  $\Delta H$  from the steady-state due to a deviation from the nominal input mass flow rate  $\Delta Q_1$ .

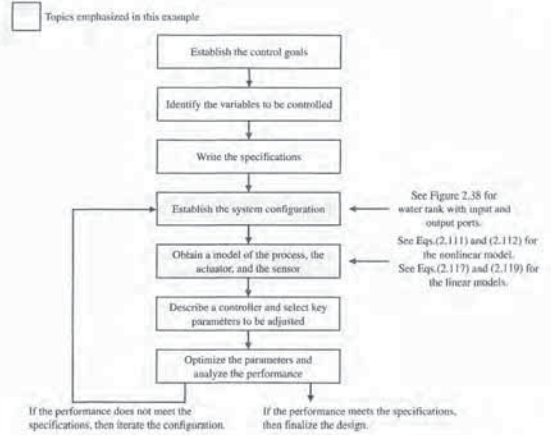
Similarly, for the output variable  $Q_2$  we have

$$Q_2 = Q_2^* + \Delta Q_2 = h(H, Q_1) \quad (2.118)$$

$$\approx h(H^*, Q^*) + \left. \frac{\partial h}{\partial H} \right|_{H^*, Q^*} \Delta H + \left. \frac{\partial h}{\partial Q_1} \right|_{H^*, Q^*} \Delta Q_1,$$

where  $\Delta Q_2$  is a small deviation in the output mass flow rate and

$$\left. \frac{\partial h}{\partial H} \right|_{H^*, Q^*} = \frac{g \rho^2 A_2^2}{Q^*},$$



**FIGURE 2.39** Elements of the control system design process emphasized in the fluid flow reservoir example.

Consider a fluid in motion. Suppose that initially the flow velocities are different for adjacent layers of fluid. Then an exchange of molecules between the two layers tends to equalize the velocities in the layers. This is internal friction, and the exchange of momentum is known as viscosity. Solids are more viscous than fluids, and fluids are more viscous than gases. A measure of viscosity is the coefficient of viscosity  $\mu$  (N s/m<sup>2</sup>). A larger coefficient of viscosity implies higher viscosity. The coefficient of viscosity (under standard conditions, 20°C) for air is

$$\mu_{\text{air}} = 0.178 \times 10^{-4} \text{ N s/m}^2,$$

and for water we have

$$\mu_{\text{H}_2\text{O}} = 1.054 \times 10^{-3} \text{ N s/m}^2.$$

So water is about 60 times more viscous than air. Viscosity depends primarily on temperature, not pressure. For comparison, water at 0°C is about 2 times more viscous than water at 20°C. With fluids of low viscosity, such as air and water, the effects of friction are important only in the boundary layer, a thin layer adjacent to the wall of

atmospheric pressure, and  $A_2$  is sufficiently small ( $A_2 = A_1/100$ ), so the water flows out slowly and the velocity  $v_1$  is negligible. Thus Bernoulli's equation reduces to

$$v_2 = \sqrt{2gH}. \quad (2.110)$$

Substituting Equation (2.110) into Equation (2.109) and solving for  $\dot{H}$  yields

$$\dot{H} = -\left[ \frac{A_2 \sqrt{2g}}{A_1} \right] \sqrt{H} + \frac{1}{\rho A_1} Q_1. \quad (2.111)$$

Using Equation (2.110), we obtain the exit mass flow rate

$$Q_2 = \rho A_2 v_2 = (\rho \sqrt{2gA_2}) \sqrt{H}. \quad (2.112)$$

To keep the equations manageable, define

$$k_1 := \frac{A_2 \sqrt{2g}}{A_1},$$

$$k_2 := \frac{1}{\rho A_1},$$

$$k_3 := \rho \sqrt{2gA_2}.$$

Then, it follows that

$$\begin{aligned} \dot{H} &= k_1 \sqrt{H} + k_2 Q_1, \\ Q_2 &= k_3 \sqrt{H}. \end{aligned} \quad (2.113)$$

Equation (2.113) represents our model of the water tank system, where the input is  $Q_1$  and the output is  $Q_2$ . Equation (2.113) is a nonlinear, first-order, ordinary differential equation model. The nonlinearity comes from the  $H^{1/2}$  term. The model in Equation (2.113) has the functional form

$$\begin{aligned} \dot{H} &= f(H, Q_1), \\ Q_2 &= h(H, Q_1), \end{aligned}$$

where

$$f(H, Q_1) = k_1 \sqrt{H} + k_2 Q_1 \quad \text{and} \quad h(H, Q_1) = k_3 \sqrt{H}.$$

A set of linearized equations describing the height of the water in the reservoir is obtained using Taylor series expansions about an equilibrium flow condition. When the tank system is in equilibrium, we have  $\dot{H} = 0$ . We can define  $Q^*$  and  $H^*$  as the equilibrium input mass flow rate and water level, respectively. The relationship between  $Q^*$  and  $H^*$  is given by

$$Q^* = \frac{k_1}{k_2} \sqrt{H^*} = \rho \sqrt{2gA_2} \sqrt{H^*}. \quad (2.114)$$

This condition occurs when just enough water enters the tank in  $A_1$  to make up for the amount leaving through  $A_2$ . We can write the water level and input mass flow rate as

$$\begin{aligned} H &= H^* + \Delta H, \\ Q_1 &= Q^* + \Delta Q_1, \end{aligned} \quad (2.115)$$



The partial fraction expansion yields

$$\Delta Q_2(s) = \frac{-q_0}{s + \Omega} + \frac{q_0}{s}.$$

Taking the inverse Laplace transform yields

$$\Delta Q_2(t) = -q_0 e^{-\Omega t} + q_0.$$

Note that  $\Omega > 0$  (see Equation (2.120)), so the term  $e^{-\Omega t}$  approaches zero as  $t$  approaches  $\infty$ . Therefore, the steady-state output due to the step input of magnitude  $q_0$  is

$$\Delta Q_{2s} = q_0.$$

We see that in the steady state, the deviation of the output mass flow rate from the equilibrium value is equal to the deviation of the input mass flow rate from the equilibrium value. By examining the variable  $\Omega$  in Equation (2.120), we find that the larger the output port opening  $A_2$ , the faster the system reaches steady state. In other words, as  $\Omega$  gets larger, the exponential term  $e^{-\Omega t}$  vanishes more quickly, and steady state is reached faster.

Similarly for the water level we have

$$\Delta H(s) = \frac{-q_0 k_2}{\Omega} \left( \frac{1}{s + \Omega} - \frac{1}{s} \right).$$

Taking the inverse Laplace transform yields

$$\Delta H(t) = \frac{-q_0 k_2}{\Omega} (e^{-\Omega t} - 1).$$

The steady-state change in water level due to the step input of magnitude  $q_0$  is

$$\Delta H_{ss} = \frac{q_0 k_2}{\Omega}.$$

Consider the sinusoidal input

$$\Delta Q_1(t) = q_0 \sin \omega t,$$

which has Laplace transform

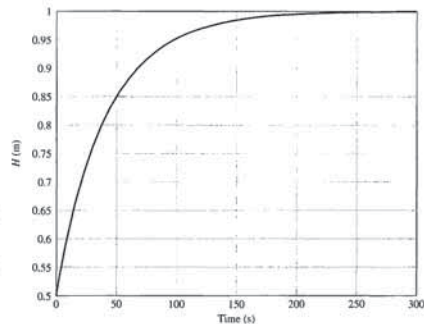
$$\Delta Q_1(s) = \frac{q_0 \omega}{s^2 + \omega^2}.$$

Suppose the system has zero initial conditions, that is,  $\Delta Q_2(0) = 0$ . Then from Equation (2.122) we have

$$\Delta Q_2(s) = \frac{q_0 \omega \Omega}{(s + \Omega)(s^2 + \omega^2)}.$$

Expanding in a partial fraction expansion and taking the inverse Laplace transform yields

$$\Delta Q_2(t) = q_0 \Omega \omega \left( \frac{e^{-\Omega t}}{\Omega^2 + \omega^2} + \frac{\sin(\omega t - \phi)}{\omega(\Omega^2 + \omega^2)^{1/2}} \right).$$



**FIGURE 2.40**  
The tank water level time history obtained by integrating the nonlinear equations of motion in Equation (2.125) with  $H(0) = 0.5$  m and  $Q_1(t) = Q^* = 34.77$  kg/s.

With  $H(0) = 0.5$  m and  $Q_1(t) = 34.77$  kg/s, we can numerically integrate the nonlinear model given by Equation (2.125) to obtain the time history of  $H(t)$  and  $Q_2(t)$ . The response of the system is shown in Figure 2.40. As expected from Equation (2.114), the system steady-state water level is  $H^* = 1$  m when  $Q^* = 34.77$  kg/m<sup>3</sup>.

It takes about 250 seconds to reach steady-state. Suppose that the system is at steady state and we want to evaluate the response to a step change in the input mass flow rate. Consider

$$\Delta Q_1(t) = 1 \text{ kg/s}.$$

Then we can use the transfer function model to obtain the unit step response. The step response is shown in Figure 2.41 for both the linear and nonlinear models. Using the linear model, we find that the steady-state change in water level is  $\Delta H = 5.75$  cm. Using the nonlinear model, we find that the steady-state change in water level is  $\Delta H = 5.84$  cm. So we see a small difference in the results obtained from the linear model and the more accurate nonlinear model.

As the final step, we consider the system response to a sinusoidal change in the input flow rate. Let

$$\Delta Q_1(s) = \frac{q_0 \omega}{s^2 + \omega^2},$$

where  $\omega = 0.05$  rad/s and  $q_0 = 1$ . The total water input flow rate is

$$Q_1(t) = Q^* + \Delta Q_1(t),$$

where  $Q^* = 34.77$  kg/s. The output flow rate is shown in Figure 2.42.

and

$$\frac{\partial h}{\partial Q_1} \Big|_{Q_1=Q^*} = 0.$$

Therefore, the linearized equation for the output variable  $Q_2$  is

$$\Delta Q_2 = \frac{g \rho^2 A_2^2}{Q^*} \Delta H. \quad (2.119)$$

For control system design and analysis, it is convenient to obtain the input-output relationship in the form of a transfer function. The tool to accomplish this is the Laplace transform, discussed in Section 2.4. Taking the time-derivative of Equation (2.119) and substituting into Equation (2.117) yields the input-output relationship

$$\Delta \dot{Q}_2 + \frac{A_2^2 g \rho}{A_1 Q^*} \Delta Q_2 = \frac{A_2^2 g \rho}{A_1 Q^*} \Delta Q_1.$$

If we define

$$\Omega := \frac{A_2^2 g \rho}{A_1 Q^*}, \quad (2.120)$$

then we have

$$\Delta \dot{Q}_2 + \Omega \Delta Q_2 = \Omega \Delta Q_1. \quad (2.121)$$

Taking the Laplace transform (with zero initial conditions) yields the transfer function

$$\Delta Q_2(s) / \Delta Q_1(s) = \frac{\Omega}{s + \Omega}. \quad (2.122)$$

Equation (2.122) describes the relationship between the change in the output mass flow rate  $\Delta Q_2(s)$  due to a change in the input mass flow rate  $\Delta Q_1(s)$ . We can also obtain a transfer function relationship between the change in the input mass flow rate and the change in the water level in the tank,  $\Delta H(s)$ . Taking the Laplace transform (with zero initial conditions) of Eq. (2.117) yields

$$\Delta H(s) / \Delta Q_1(s) = \frac{k_2}{s + \Omega}. \quad (2.123)$$

Given the linear time-invariant model of the water tank system in Equation (2.121), we can obtain solutions for step and sinusoidal inputs. Remember that our input  $\Delta Q_1(s)$  is actually a change in the input mass flow rate from the steady-state value  $Q^*$ .

Consider the step input

$$\Delta Q_1(s) = q_0 / s,$$

where  $q_0$  is the magnitude of the step input, and the initial condition is  $\Delta Q_2(0) = 0$ . Then we can use the transfer function form given in Eq. (2.122) to obtain

$$\Delta Q_2(s) = \frac{q_0 \Omega}{s(s + \Omega)}.$$

where  $\phi = \tan^{-1}(\omega/\Omega)$ . So, as  $t \rightarrow \infty$ , we have

$$\Delta Q_2(t) \rightarrow \frac{q_0 \Omega}{\sqrt{\Omega^2 + \omega^2}} \sin(\omega t - \phi).$$

The maximum change in output flow rate is

$$|\Delta Q_2(t)|_{\max} = \frac{q_0 \Omega}{\sqrt{\Omega^2 + \omega^2}}. \quad (2.124)$$

The above analytic analysis of the linear system model to step and sinusoidal inputs is a valuable way to gain insight into the system response to test signals. Analytic analysis is limited, however, in the sense that a more complete representation can be obtained with carefully constructed numerical investigations using computer simulations of both the linear and nonlinear mathematical models. A computer simulation uses a model and the actual conditions of the system being modeled, as well as actual input commands to which the system will be subjected.

Various levels of simulation fidelity (that is, accuracy) are available to the control engineer. In the early stages of the design process, highly interactive design software packages are effective. At this stage, computer speed is not as important as the time it takes to obtain an initial valid solution and to iterate and fine tune that solution. Good graphics output capability is crucial. The analysis simulations are generally low fidelity in the sense that many of the simplifications (such as linearization) made in the design process are retained in the simulation.

As the design matures usually it is necessary to conduct numerical experiments in a more realistic simulation environment. At this point in the design process, the computer processing speed becomes more important, since long simulation times necessarily reduce the number of computer experiments that can be obtained and correspondingly raise costs. Usually these high-fidelity simulations are programmed in FORTRAN, C, C++, Matlab, LabVIEW or similar languages.

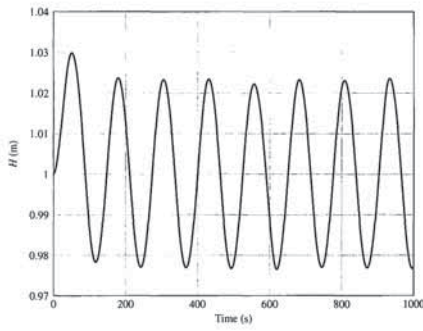
Assuming that a model and the simulation are reliably accurate, computer simulation has the following advantages [13]:

1. System performance can be observed under all conceivable conditions.
2. Results of field-system performance can be extrapolated with a simulation model for prediction purposes.
3. Decisions concerning future systems presently in a conceptual stage can be examined.
4. Trials of systems under test can be accomplished in a much-reduced period of time.
5. Simulation results can be obtained at lower cost than real experimentation.
6. Study of hypothetical situations can be achieved even when the hypothetical situation would be unrealizable at present.
7. Computer modeling and simulation is often the only feasible or safe technique to analyze and evaluate a system.

The nonlinear model describing the water level flow rate is as follows (using the constants given in Table 2.7):

$$\dot{H} = -0.0443 \sqrt{H} + 1.2732 \times 10^{-3} Q_1, \quad (2.125)$$

$$Q_2 = 34.77 \sqrt{H}.$$



**FIGURE 2.43** The water level response to a sinusoidal variation in the input flow.

Thus in the steady-state (see Figure 2.42) we expect that the output flow rate will oscillate at a frequency of  $\omega = 0.05$  rad/s, with a maximum value of

$$Q_{2,max} = Q^* + |\Delta Q_2(t)|_{max} = 35.18 \text{ kg/s. } \blacksquare$$

**EXAMPLE 2.14 Electric traction motor control**

A majority of modern trains and local transit vehicles utilize electric traction motors. The electric motor drive for a railway vehicle is shown in block diagram form in Figure 2.44(a), incorporating the necessary control of the velocity of the vehicle. The goal of the design is to obtain a system model and the closed-loop transfer function of the system,  $\omega(s)/\omega_d(s)$ , select appropriate resistors  $R_1, R_2, R_3,$  and  $R_4$ , and then predict the system response.

The first step is to describe the transfer function of each block. We propose the use of a tachometer to generate a voltage proportional to velocity and to connect that voltage,  $v_1$ , to one input of a difference amplifier, as shown in Figure 2.44(b). The power amplifier is nonlinear and can be approximately represented by  $v_2 = 2e^{3v_1} = g(v_1)$ , an exponential function with a normal operating point,  $v_{10} = 1.5$  V. Using the technique in Section 2.3, we then obtain a linear model:

$$\Delta v_2 = \left. \frac{dg(v_1)}{dv_1} \right|_{v_{10}} \Delta v_1 = 2[3 \exp(3v_{10})] \Delta v_1 = 2(270) \Delta v_1 = 540 \Delta v_1. \quad (2.126)$$

Then, discarding the delta notation and using the Laplace transform, we find that

$$V_2(s) = 540V_1(s).$$

**Table 2.8 Parameters of a Large DC Motor**

$K_m = 10$	$J = 2$
$R_a = 1$	$b = 0.5$
$L_a = 1$	$K_t = 0.1$

When the system is in balance,  $v_1 = 0$ , and when  $K_t = 0.1$ , we have

$$\frac{1 + R_2/R_1}{1 + R_3/R_4} = \frac{R_2}{R_1} K_t = 1.$$

This relation can be achieved when

$$R_2/R_1 = 10 \text{ and } R_3/R_4 = 10.$$

The parameters of the motor and load are given in Table 2.8. The overall system is shown in Figure 2.44(b). Reducing the block diagram in Figure 2.44(c) or the signal-flow graph in Figure 2.44(d) yields the transfer function

$$\begin{aligned} \frac{\omega(s)}{\omega_d(s)} &= \frac{540G_1(s)G_2(s)}{1 + 0.1G_1G_2 + 540G_1G_2} = \frac{540G_1G_2}{1 + 540.1G_1G_2} \\ &= \frac{5400}{(s + 1)(2s + 0.5) + 5401} = \frac{5400}{2s^2 + 2.5s + 5401.5} \\ &= \frac{2700}{s^2 + 1.25s + 2700.75} \end{aligned} \quad (2.129)$$

Since the characteristic equation is second order, we note that  $\omega_n = 52$  and  $\zeta = 0.012$ , and we expect the response of the system to be highly oscillatory (underdamped). ■

**EXAMPLE 2.15 Mechanical accelerometer**

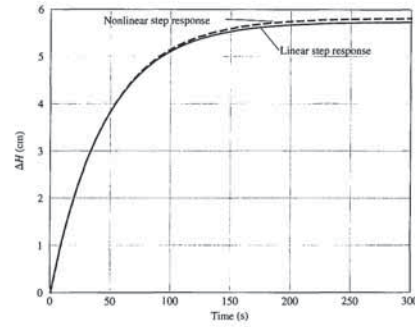
A mechanical accelerometer is used to measure the acceleration of a rocket test sled, as shown in Figure 2.45. The test sled maneuvers above a guide rail a small distance  $\delta$ . The accelerometer provides a measurement of the acceleration  $a(t)$  of the sled, since the position  $y$  of the mass  $M$ , with respect to the accelerometer case, is proportional to the acceleration of the case (and the sled). The goal is to design an accelerometer with an appropriate dynamic responsiveness. We wish to design an accelerometer with an acceptable time for the desired measurement characteristic,  $y(t) = qa(t)$ , to be attained ( $q$  is a constant).

The sum of the forces acting on the mass is

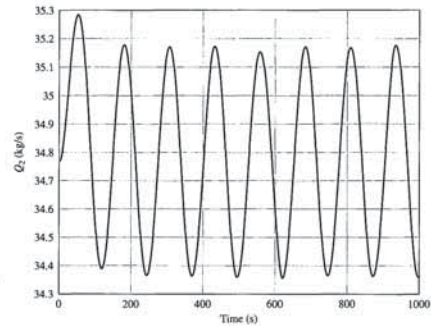
$$-b \frac{dy}{dt} - ky = M \frac{d^2y}{dt^2} (y + x)$$

or

$$M \frac{d^2y}{dt^2} + b \frac{dy}{dt} + ky = -M \frac{d^2x}{dt^2}. \quad (2.130)$$



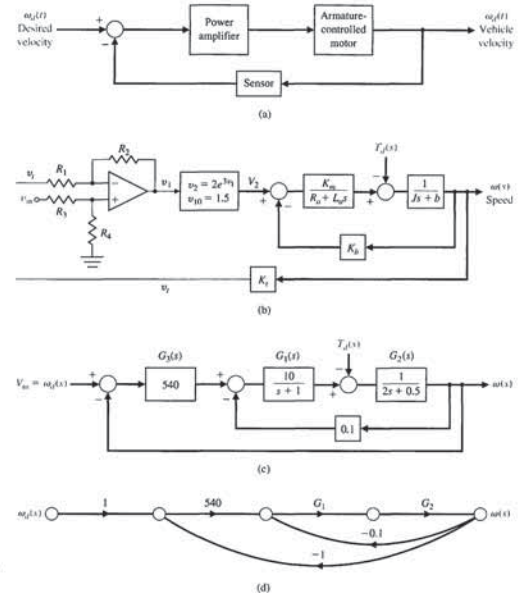
**FIGURE 2.41** The response showing the linear versus nonlinear response to a step input.



**FIGURE 2.42** The output flow rate response to a sinusoidal variation in the input flow.

The response of the water level is shown in Figure 2.43. The water level is sinusoidal, with an average value of  $H_{av} = H^* = 1$  m. As shown in Equation (2.124), the output flow rate is sinusoidal in the steady-state, with

$$|\Delta Q_2(t)|_{max} = \frac{q_0 \Omega}{\sqrt{\Omega^2 + \omega^2}} = 0.4 \text{ kg/s.}$$



**FIGURE 2.44** Speed control of an electric traction motor.

Also, for the differential amplifier, we have

$$v_1 = \frac{1 + R_2/R_1}{1 + R_3/R_4} v_{in} - \frac{R_2}{R_1} v_2. \quad (2.127)$$

We wish to obtain an input control that sets  $\omega_d(t) = v_{in}$ , where the units of  $\omega_d$  are rad/s and the units of  $v_{in}$  are volts. Then, when  $v_{in} = 10$  V, the steady-state speed is  $\omega = 10$  rad/s. We note that  $v_1 = K_t \omega_d$  in steady state, and we expect, in balance, the steady-state output to be

$$v_1 = \frac{1 + R_2/R_1}{1 + R_3/R_4} v_{in} - \frac{R_2}{R_1} K_t v_{in}. \quad (2.128)$$



We select the coefficients where  $b/M = 3$ ,  $k/M = 2$ ,  $F(t)/M_s = Q(t)$ , and we consider the initial conditions  $y(0) = -1$  and  $\dot{y}(0) = 2$ . We then obtain the Laplace transform equation, when the force, and thus  $Q(t)$ , is a step function, as follows:

$$(s^2Y(s) - sy(0) - \dot{y}(0)) + 3(sY(s) - y(0)) + 2Y(s) = -Q(s). \quad (2.132)$$

Since  $Q(s) = P/s$ , where  $P$  is the magnitude of the step function, we obtain

$$(s^2Y(s) + s - 2) + 3(sY(s) + 1) + 2Y(s) = -\frac{P}{s},$$

or

$$(s^2 + 3s + 2)Y(s) = \frac{-(s^2 + s + P)}{s}. \quad (2.133)$$

Thus the output transform is

$$Y(s) = \frac{-(s^2 + s + P)}{s(s^2 + 3s + 2)} = \frac{-(s^2 + s + P)}{s(s + 1)(s + 2)}. \quad (2.134)$$

Expanding in partial fraction form yields

$$Y(s) = \frac{k_1}{s} + \frac{k_2}{s + 1} + \frac{k_3}{s + 2}. \quad (2.135)$$

We then have

$$k_1 = \left. \frac{-(s^2 + s + P)}{(s + 1)(s + 2)} \right|_{s=0} = -\frac{P}{2}. \quad (2.136)$$

Similarly,  $k_2 = +P$  and  $k_3 = \frac{-P - 2}{2}$ . Thus,

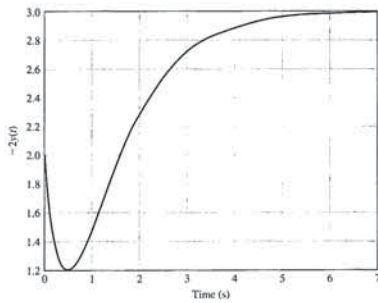


FIGURE 2.46 Accelerometer response.

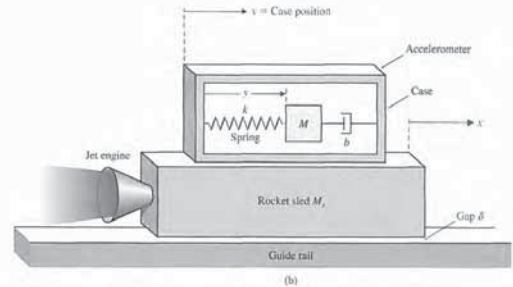


FIGURE 2.45 (a) This rocket-propelled sled set a world land speed record for a rail vehicle at 6,453 mph (J.S. Air Force photo by 2nd Lt. Heather Newcomb). (b) A schematic of an accelerometer mounted on the rocket sled.

Since

$$M_s \frac{d^2x}{dt^2} = F(t),$$

is the engine force, we have

$$M\ddot{y} + b\dot{y} + ky = -\frac{M}{M_s}F(t),$$

or

$$\ddot{y} + \frac{b}{M}\dot{y} + \frac{k}{M}y = -\frac{F(t)}{M_s}. \quad (2.131)$$



FIGURE 2.47 Laboratory robot used for sample preparation. The robot manipulates small objects, such as test tubes, and probes in and out of tight places at relatively high speeds [15]. (Photo courtesy of Beckman Coulter, Inc.)

Table 2.9 ORCA Robot Arm Hardware Specifications

Arm	Articulated, Rail-Mounted	Teach Pendant	Joy Stick with Emergency Stop
Degrees of Freedom	6	Cycle time	4 s (move 1 inch up, 12 inch across, 1 inch down, and back)
Reach	+54 cm	Maximum speed	75 cm/s
Height	78 cm	Dwell time	50 ms typical (for moves within a motion)
Rail	1 and 2 m	Payload	0.5 kg continuous, 2.5 kg transient (with restrictions)
Weight	8.0 kg	Vertical deflection	<1.5 mm at continuous payload
Precision	±0.25 mm	Cross-sectional	1 m <sup>2</sup>
Finger travel (gripper)	40 mm	work envelope	
Gripper rotation	±77 revolutions		

The physical and performance specifications of the ORCA system are shown in Table 2.9. The design for the ORCA laboratory robot progressed to the selection of the component parts required to obtain the total system. The exploded view of the robot is shown in Figure 2.48. This device uses six DC motors, gears, belt drives, and a rail and carriage. The specifications are challenging and require the designer to model the system components and their interconnections accurately. ■

$$Y(s) = \frac{-P}{2s} + \frac{P}{s + 1} + \frac{-P - 2}{2(s + 2)}. \quad (2.137)$$

Therefore, the output measurement is

$$y(t) = \frac{1}{2}[-P + 2Pe^{-t} - (P + 2)e^{-2t}], \quad t \geq 0.$$

A plot of  $y(t)$  is shown in Figure 2.46 for  $P = 3$ . We can see that  $y(t)$  is proportional to the magnitude of the force after 5 seconds. Thus in steady state, after 5 seconds, the response  $y(t)$  is proportional to the acceleration, as desired. If this period is excessively long, we must increase the spring constant,  $k$ , and the friction,  $b$ , while reducing the mass,  $M$ . If we are able to select the components so that  $b/M = 12$  and  $k/M = 32$ , the accelerometer will attain the proportional response in 1 second. (It is left to the reader to show this.) ■

EXAMPLE 2.16 Design of a laboratory robot

In this example, we endeavor to show the physical design of a laboratory device and demonstrate its complex design. We will also exhibit the many components commonly used in a control system.

A robot for laboratory use is shown in Figure 2.47. A laboratory robot's work volume must allow the robot to reach the entire bench area and access existing analytical instruments. There must also be sufficient area for a stockroom of supplies for unattended operation.

The laboratory robot can be involved in three types of tasks during an analytical experiment. The first is sample introduction, wherein the robot is trained to accept a number of different sample trays, racks, and containers and to introduce them into the system. The second set of tasks involves the robot transporting the samples between individual dedicated automated stations for chemical preparation and instrumental analysis. Samples must be scheduled and moved between these stations as necessary to complete the analysis. In the third set of tasks for the robot, flexible automation provides new capability to the analytical laboratory. The robot must be programmed to emulate the human operator or work with various devices. All of these types of operations are required for an effective laboratory robot.

The ORCA laboratory robot is an anthropomorphic arm, mounted on a rail, designed as the optimum configuration for the analytical laboratory [14]. The rail can be located at the front or back of a workbench, or placed in the middle of a table when access to both sides of the rail is required. Simple software commands permit moving the arm from one side of the rail to the other while maintaining the wrist position (to transfer open containers) or locking the wrist angle (to transfer objects in virtually any orientation). The rectilinear geometry, in contrast to the cylindrical geometry used by many robots, permits more accessories to be placed within the robot workspace and provides an excellent match to the laboratory bench. Movement of all joints is coordinated through software, which simplifies the use of the robot by representing the robot positions and movements in the more familiar Cartesian coordinate space.

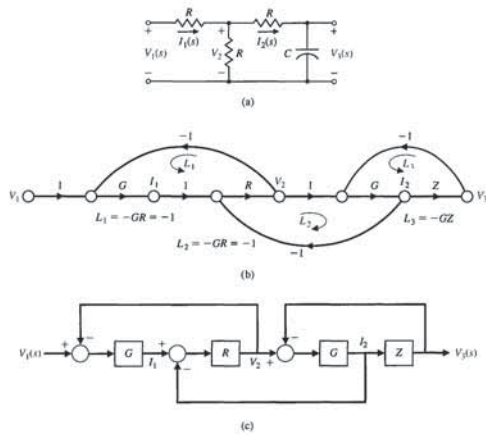


FIGURE 2.49 (a) Ladder network, (b) its signal-flow graph, and (c) its block diagram.

where  $G = 1/R$ ,  $Z(s) = 1/Cs$ , and  $I_1(s) = I_1$  (we omit the  $(s)$ ). The signal-flow graph constructed for the four equations is shown in Figure 2.49(b), and the corresponding block diagram is shown in Figure 2.49(c). The three loops are  $L_1 = -GR = -1$ ,  $L_2 = -GR = -1$ , and  $L_3 = -GZ$ . All loops touch the forward path. Loops  $L_1$  and  $L_3$  are nontouching. Therefore, the transfer function is

$$T(s) = \frac{V_2}{V_1} = \frac{P_1}{1 - (L_1 + L_2 + L_3) + L_1L_2} = \frac{GZ}{3 + 2GZ} = \frac{1}{3RCs + 2} = s + 2/(3RC)$$

If one prefers to utilize block diagram reduction techniques, one can start at the output with

$$V_3(s) = ZI_2(s).$$

But the block diagram shows that

$$I_2(s) = G(V_2(s) - V_3(s)).$$

Therefore,

$$V_3(s) = ZGV_2(s) - ZGV_3(s)$$

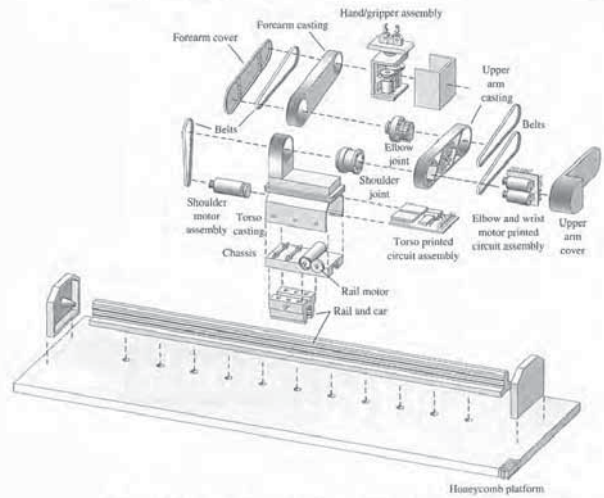


FIGURE 2.48 Exploded view of the ORCA robot showing the components [15]. (Courtesy of Beckman Coulter, Inc.)

EXAMPLE 2.17 Design of a low-pass filter

Our goal is to design a first-order low-pass filter that passes signals at a frequency below 106.1 Hz and attenuates signals with a frequency above 106.1 Hz. In addition, the DC gain should be  $1/2$ .

A ladder network with one energy storage element, as shown in Figure 2.49(a), will act as a first-order low-pass network. Note that the DC gain will be equal to  $1/2$  (open-circuit the capacitor). The current and voltage equations are

$$\begin{aligned} I_1 &= (V_1 - V_2)G, \\ I_2 &= (V_2 - V_3)G, \\ V_2 &= (I_1 - I_2)R, \\ V_3 &= I_2Z, \end{aligned}$$

so

$$V_2(s) = \frac{1 + ZG}{ZG} V_3(s).$$

We will use this relationship between  $V_3(s)$  and  $V_2(s)$  in the subsequent development. Continuing with the block diagram reduction, we have

$$V_3(s) = -ZGV_3(s) + ZGR(I_1(s) - I_2(s)),$$

but from the block diagram, we see that

$$I_1 = G(V_1(s) - V_2(s)), \quad I_2 = \frac{V_3(s)}{Z}.$$

Therefore,

$$V_3(s) = -ZGV_3(s) + ZG^2R(V_1(s) - V_2(s)) - GRV_3(s).$$

Substituting for  $V_2(s)$  yields

$$V_3(s) = \frac{(GR)(GZ)}{1 + 2GR + GZ + (GR)(GZ)} V_1(s).$$

But we know that  $GR = 1$ ; hence, we obtain

$$V_3(s) = \frac{GZ}{3 + 2GZ} V_1(s).$$

Note that the DC gain is  $1/2$ , as expected. The pole is desired at  $p = 2\pi(106.1) = 666.7 = 2000/3$ . Therefore, we require  $RC = 0.001$ . Select  $R = 1 \text{ k}\Omega$  and  $C = 1 \mu\text{F}$ . Hence, we achieve the filter

$$T(s) = \frac{333.3}{(s + 666.7)} \blacksquare$$

2.9 THE SIMULATION OF SYSTEMS USING CONTROL DESIGN SOFTWARE

Application of the many classical and modern control system design and analysis tools is based on mathematical models. Most popular control design software packages can be used with systems given in the form of transfer function descriptions. In this book, we will focus on m-file scripts containing commands and functions to analyze and design control systems. Various commercial control system packages are available for student use. The m-files described here are compatible with the MATLAB<sup>1</sup> Control System Toolbox and the LabVIEW MathScript RT Module.<sup>2</sup>

<sup>1</sup>See Appendix A for an introduction to MATLAB.

<sup>2</sup>See Appendix B for an introduction to LabVIEW MathScript RT Module.

We begin this section by analyzing a typical spring-mass-damper mathematical model of a mechanical system. Using an m-file script, we will develop an interactive analysis capability to analyze the effects of natural frequency and damping on the unforced response of the mass displacement. This analysis will use the fact that we have an analytic solution that describes the unforced time response of the mass displacement.

Later, we will discuss transfer functions and block diagrams. In particular, we are interested in manipulating polynomials, computing poles and zeros of transfer functions, computing closed-loop transfer functions, computing block diagram reductions, and computing the response of a system to a unit step input. The section concludes with the electric traction motor control design of Example 2.14.

The functions covered in this section are roots, poly, conv, polyval, if, pzmap, pole, zero, series, parallel, feedback, minreal, and step.

**Spring-Mass-Damper System.** A spring-mass-damper mechanical system is shown in Figure 2.2. The motion of the mass, denoted by  $y(t)$ , is described by the differential equation

$$M\ddot{y}(t) + b\dot{y}(t) + ky(t) = r(t).$$

The unforced dynamic response  $y(t)$  of the spring-mass-damper mechanical system is

$$y(t) = \frac{y(0)}{\sqrt{1 - \zeta^2}} e^{-\zeta\omega_n t} \sin(\omega_n \sqrt{1 - \zeta^2} t + \theta),$$

where  $\omega_n = \sqrt{k/M}$ ,  $\zeta = b/(2\sqrt{kM})$ , and  $\theta = \cos^{-1} \zeta$ . The initial displacement is  $y(0)$ . The transient system response is underdamped when  $\zeta < 1$ , overdamped when  $\zeta > 1$ , and critically damped when  $\zeta = 1$ . We can visualize the unforced time response of the mass displacement following an initial displacement of  $y(0)$ . Consider the underdamped case:

$$\square y(0) = 0.15 \text{ m}, \quad \omega_n = \sqrt{2} \frac{\text{rad}}{\text{sec}}, \quad \zeta = \frac{1}{2\sqrt{2}} \left( \frac{k}{M} = 2, \frac{b}{M} = 1 \right).$$

The commands to generate the plot of the unforced response are shown in Figure 2.50. In the setup, the variables  $y(0)$ ,  $\omega_n$ ,  $t$ , and  $\zeta$  are input at the command level. Then the script `unforced.m` is executed to generate the desired plots. This creates an interactive analysis capability to analyze the effects of natural frequency and damping on the unforced response of the mass displacement. One can investigate the effects of the natural frequency and the damping on the time response by simply entering new values of  $\omega_n$  and  $\zeta$  at the command prompt and running the script `unforced.m` again. The time-response plot is shown in Figure 2.51. Notice that the script automatically labels the plot with the values of the damping coefficient and natural frequency. This avoids confusion when making many interactive simulations. Using scripts is an important aspect of developing an effective interactive design and analysis capability.

For the spring-mass-damper problem, the unforced solution to the differential equation was readily available. In general, when simulating closed-loop feedback



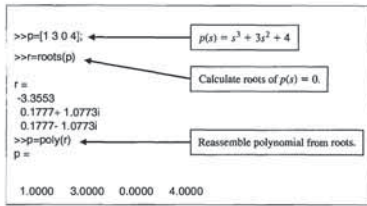


FIGURE 2.52 Entering the polynomial  $p(s) = s^3 + 3s^2 + 4$  and calculating its roots.

Polynomials are represented by row vectors containing the polynomial coefficients in order of descending degree. For example, the polynomial

$$p(s) = s^3 + 3s^2 + 4$$

is entered as shown in Figure 2.52. Notice that even though the coefficient of the  $s$  term is zero, it is included in the input definition of  $p(s)$ .

If  $p$  is a row vector containing the coefficients of  $p(s)$  in descending degree, then  $\text{roots}(p)$  is a column vector containing the roots of the polynomial. Conversely, if  $r$  is a column vector containing the roots of the polynomial, then  $\text{poly}(r)$  is a row vector with the polynomial coefficients in descending degree. We can compute the roots of the polynomial  $p(s) = s^3 + 3s^2 + 4$  with the roots function as shown in Figure 2.52. In this figure, we show how to reassemble the polynomial with the `poly` function.

Multiplication of polynomials is accomplished with the `conv` function. Suppose we want to expand the polynomial

$$n(s) = (3s^2 + 2s + 1)(s + 4).$$

The associated commands using the `conv` function are shown in Figure 2.53. Thus, the expanded polynomial is

$$n(s) = 3s^3 + 14s^2 + 9s + 4.$$

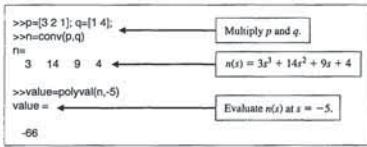


FIGURE 2.53 Using `conv` and `polyval` to multiply and evaluate the polynomials  $(3s^2 + 2s + 1)(s + 4)$ .

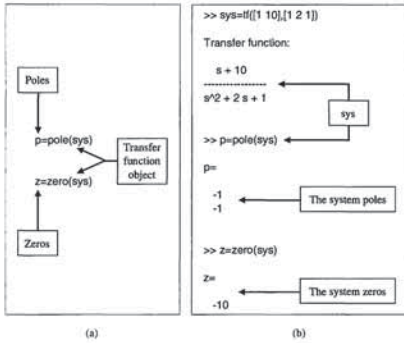


FIGURE 2.55 (a) The pole and zero locations of a linear system. (b) Using the pole and zero functions to compute the pole and zero locations of a linear system.

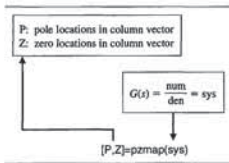


FIGURE 2.56 The `pzmap` function.

EXAMPLE 2.18 Transfer functions

Consider the transfer functions

$$G(s) = \frac{6s^2 + 1}{s^3 + 3s^2 + 3s + 1} \quad \text{and} \quad H(s) = \frac{(s + 1)(s + 2)}{(s + 2)(s - 2)(s + 3)}$$

Using an m-file script, we can compute the poles and zeros of  $G(s)$ , the characteristic equation of  $H(s)$ , and divide  $G(s)$  by  $H(s)$ . We can also obtain a plot of the pole-zero map of  $G(s)/H(s)$  in the complex plane.

The pole-zero map of the transfer function  $G(s)/H(s)$  is shown in Figure 2.57, and the associated commands are shown in Figure 2.58. The pole-zero map shows clearly the five zero locations, but it appears that there are only two poles. This

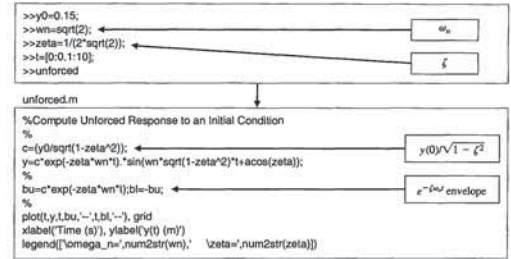


FIGURE 2.50 Script to analyze the spring-mass-damper unforced response.

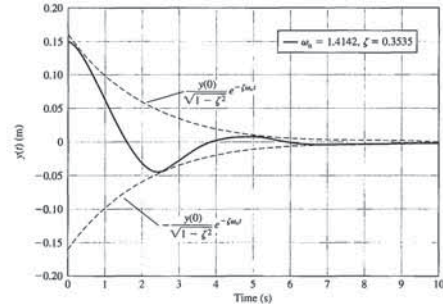


FIGURE 2.51 Spring-mass-damper unforced response.

control systems subject to a variety of inputs and initial conditions, it is difficult to obtain the solution analytically. In these cases, we can compute the solutions numerically and to display the solution graphically.

Most systems considered in this book can be described by transfer functions. Since the transfer function is a ratio of polynomials, we begin by investigating how to manipulate polynomials, remembering that working with transfer functions means that both a numerator polynomial and a denominator polynomial must be specified.

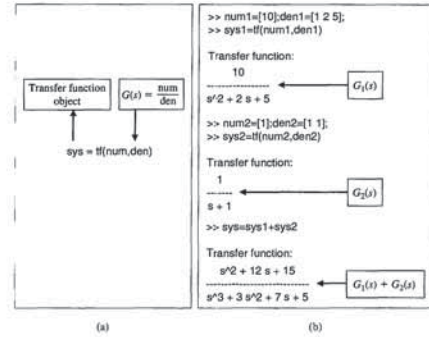


FIGURE 2.54 (a) The `tf` function. (b) Using the `tf` function to create transfer function objects and adding them using the "+" operator.

The function `polyval` is used to evaluate the value of a polynomial at the given value of the variable. The polynomial  $n(s)$  has the value  $n(-5) = -66$ , as shown in Figure 2.53.

Linear, time-invariant system models can be treated as *objects*, allowing one to manipulate the system models as single entities. In the case of transfer functions, one creates the system models using the `tf` function; for state variable models one employs the `ss` function (see Chapter 3). The use of `tf` is illustrated in Figure 2.54(a). For example, if one has two system models

$$G_1(s) = \frac{10}{s^2 + 2s + 5} \quad \text{and} \quad G_2(s) = \frac{1}{s + 1}$$

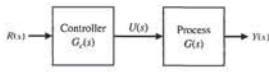
one can add them using the "+" operator to obtain

$$G(s) = G_1(s) + G_2(s) = \frac{s^2 + 12s + 15}{s^3 + 3s^2 + 7s + 5}$$

The corresponding commands are shown in Figure 2.54(b) where `sys1` represents  $G_1(s)$  and `sys2` represents  $G_2(s)$ . Computing the poles and zeros associated with a transfer function is accomplished by operating on the system model object with the `pole` and `zero` functions, respectively, as illustrated in Figure 2.55.

In the next example, we will obtain a plot of the pole-zero locations in the complex plane. This will be accomplished using the `pzmap` function, shown in Figure 2.56. On the pole-zero map, zeros are denoted by an "o" and poles are denoted by an "x". If the `pzmap` function is invoked without left-hand arguments, the plot is generated automatically.

FIGURE 2.59 Open-loop control system (without feedback).



**Block Diagram Models.** Suppose we have developed mathematical models in the form of transfer functions for a process, represented by  $G(s)$ , and a controller, represented by  $G_c(s)$ , and possibly many other system components such as sensors and actuators. Our objective is to interconnect these components to form a control system.

A simple open-loop control system can be obtained by interconnecting a process and a controller in series as illustrated in Figure 2.59. We can compute the transfer function from  $R(s)$  to  $Y(s)$ , as follows.

**EXAMPLE 2.19 Series connection**

Let the process represented by the transfer function  $G(s)$  be

$$G(s) = \frac{1}{500s^2}$$

and let the controller represented by the transfer function  $G_c(s)$  be

$$G_c(s) = \frac{s+1}{s+2}$$

We can use the series function to cascade two transfer functions  $G_1(s)$  and  $G_2(s)$ , as shown in Figure 2.60.

The transfer function  $G_c(s)G(s)$  is computed using the series function as shown in Figure 2.61. The resulting transfer function is

$$G_c(s)G(s) = \frac{s+1}{500s^2 + 1000s^2} = \text{sys},$$

where **sys** is the transfer function name in the m-file script. ■

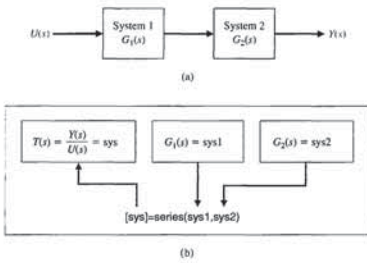


FIGURE 2.60 (a) Block diagram. (b) The series function.

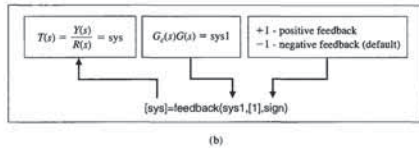
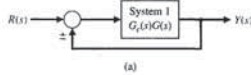


FIGURE 2.64 (a) Block diagram. (b) The feedback function with unity feedback.

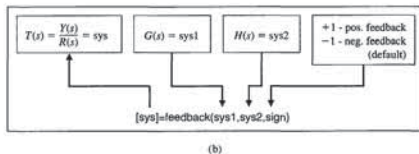
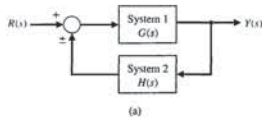


FIGURE 2.65 (a) Block diagram. (b) The feedback function.

We can utilize the feedback function to aid in the block diagram reduction process to compute closed-loop transfer functions for single- and multiple-loop control systems.

It is often the case that the closed-loop control system has unity feedback, as illustrated in Figure 2.63. We can use the feedback function to compute the closed-loop transfer function by setting  $H(s) = 1$ . The use of the feedback function for unity feedback is depicted in Figure 2.64.

The feedback function is shown in Figure 2.65 with the associated system configuration, which includes  $H(s)$  in the feedback path. If the input “sign” is omitted, then negative feedback is assumed.

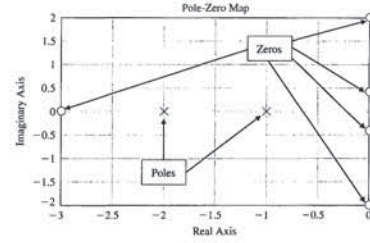
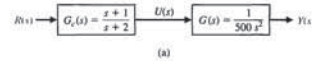


FIGURE 2.57 Pole-zero map for  $G(s)/H(s)$ .

```
>>numg=[6 0 1]; deng=[1 3 3];sysg=tf(numg,deng);
>>z=zero(sysg)
Z =
 0 + 0.4082i
 0 - 0.4082i
>>p=pole(sysg)
p =
-1.0000
-1.0000 + 0.0000i
-1.0000 - 0.0000i
>>n1=[1 1]; n2=[1 2]; d1=[1 2]; d2=[1 2]; d3=[1 3];
>>numh=conv(n1,n2); denh=conv(d1,conv(d2,d3));
>>sysh=tf(numh,denh)
Transfer function:
      s^2 + 3 s + 2
    s^3 + 3 s^2 + 4 s + 12
>>sys=sysg/sysh
Transfer function:
 6 s^5 + 18 s^4 + 25 s^3 + 75 s^2 + 4 s + 12
 5 s^5 + 6 s^4 + 14 s^3 + 16 s^2 + 9 s + 2
>>pzmap(sys)
```

FIGURE 2.58 Transfer function example for  $G(s)$  and  $H(s)$ .

cannot be the case, since we know that for physical systems the number of poles must be greater than or equal to the number of zeros. Using the roots function, we can ascertain that there are in fact four poles at  $s = -1$ . Hence, multiple poles or multiple zeros at the same location cannot be discerned on the pole-zero map. ■



```
>>numg=[1]; deng=[500 0 0]; sysg=tf(numg,deng);
>>numh=[1 1]; denh=[1 2]; sysh=tf(numh,denh);
>>sys=series(sysg,syssh);
>>sys
Transfer function:
      s + 1
    500 s^3 + 1000 s^2
      Gc(s)G(s)
```

FIGURE 2.61 Application of the series function.

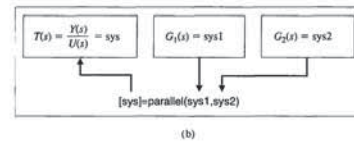
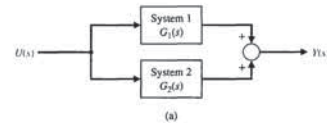


FIGURE 2.62 (a) Block diagram. (b) The parallel function.

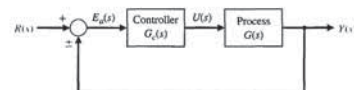


FIGURE 2.63 A basic control system with unity feedback.

Block diagrams quite often have transfer functions in parallel. In such cases, the function parallel can be quite useful. The parallel function is described in Figure 2.62.

We can introduce a feedback signal into the control system by closing the loop with **unity feedback**, as shown in Figure 2.63. The signal  $E_e(s)$  is an **error signal**; the signal  $R(s)$  is a **reference input**. In this control system, the controller is in the forward path, and the closed-loop transfer function is

$$T(s) = \frac{G_c(s)G(s)}{1 \mp G_c(s)G(s)}$$



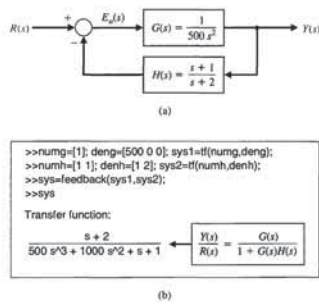


FIGURE 2.66 Application of the feedback function: (a) block diagram, (b) m-file script.

the feedback function. The command sequence is shown in Figure 2.68(b). The closed-loop transfer function is

$$T(s) = \frac{s + 2}{500s^3 + 1000s^2 + s + 1} = \text{sys.}$$

The functions series, parallel, and feedback can be used as aids in block diagram manipulations for multiple-loop block diagrams.

EXAMPLE 2.22 Multiloop reduction

A multiloop feedback system is shown in Figure 2.26. Our objective is to compute the closed-loop transfer function

$$T(s) = \frac{Y(s)}{R(s)}$$

when

$$G_1(s) = \frac{1}{s + 10}, \quad G_2(s) = \frac{1}{s + 1},$$

$$G_3(s) = \frac{s^2 + 1}{s^2 + 4s + 4}, \quad G_4(s) = \frac{s + 1}{s + 6},$$

and

$$H_1(s) = \frac{s + 1}{s + 2}, \quad H_2(s) = 2, \quad \text{and} \quad H_3(s) = 1.$$

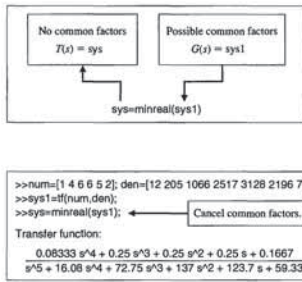


FIGURE 2.70 The mirreal function.

FIGURE 2.71 Application of the mirreal function.

EXAMPLE 2.23 Electric traction motor control

Finally, let us reconsider the electric traction motor system from Example 2.14. The block diagram is shown in Figure 2.44(c). The objective is to compute the closed-loop transfer function and investigate the response of  $\omega(s)$  to a commanded  $\omega_d(s)$ . The first step, as shown in Figure 2.72, is to compute the closed-loop transfer function  $\omega(s)/\omega_d(s) = T(s)$ . The closed-loop characteristic equation is second order with  $\omega_n = 52$  and  $\zeta = 0.012$ . Since the damping is low, we expect the response to be highly oscillatory. We can investigate the response  $\omega(t)$  to a reference input,  $\omega_d(t)$ , by utilizing the step function. The step function, shown in Figure 2.73, calculates the unit step response of a linear system. The step function is very important, since control system performance specifications are often given in terms of the unit step response.

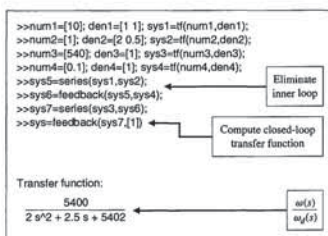


FIGURE 2.72 Electric traction motor block reduction.

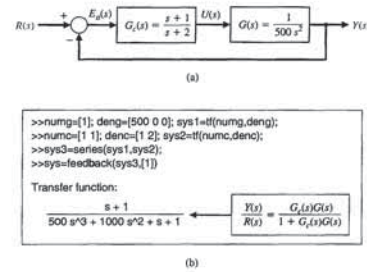
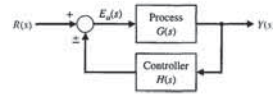


FIGURE 2.66 (a) Block diagram, (b) Application of the feedback function.

FIGURE 2.67 A basic control system with the controller in the feedback loop.



EXAMPLE 2.20 The feedback function with unity feedback

Let the process,  $G(s)$ , and the controller,  $G_c(s)$ , be as in Figure 2.66(a). To apply the feedback function, we first use the series function to compute  $G_c(s)G(s)$ , followed by the feedback function to close the loop. The command sequence is shown in Figure 2.66(b). The closed-loop transfer function, as shown in Figure 2.66(b), is

$$T(s) = \frac{G_c(s)G(s)}{1 + G_c(s)G(s)} = \frac{s + 1}{500s^3 + 1000s^2 + s + 1} = \text{sys.}$$

Another basic feedback control configuration is shown in Figure 2.67. In this case, the controller is located in the feedback path. The closed-loop transfer function is

$$T(s) = \frac{G(s)}{1 \mp G(s)H(s)}$$

EXAMPLE 2.21 The feedback function

Let the process,  $G(s)$ , and the controller,  $H(s)$ , be as in Figure 2.68(a). To compute the closed-loop transfer function with the controller in the feedback loop, we use

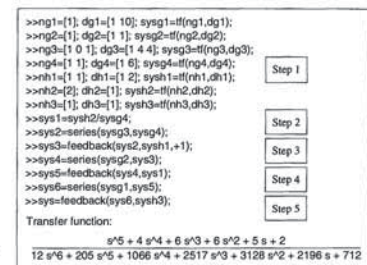


FIGURE 2.69 Multiple-loop block reduction.

For this example, a five-step procedure is followed:

- Step 1. Input the system transfer functions.
- Step 2. Move  $H_2$  behind  $G_4$ .
- Step 3. Eliminate the  $G_2G_4H_1$  loop.
- Step 4. Eliminate the loop containing  $H_2$ .
- Step 5. Eliminate the remaining loop and calculate  $T(s)$ .

The five steps are utilized in Figure 2.69, and the corresponding block diagram reduction is shown in Figure 2.27. The result of executing the commands is

$$\text{sys} = \frac{s^5 + 4s^4 + 6s^3 + 6s^2 + 5s + 2}{12s^6 + 205s^5 + 1066s^4 + 2517s^3 + 3128s^2 + 2196s + 712}$$

We must be careful in calling this the closed-loop transfer function. The transfer function is defined as the input-output relationship after pole-zero cancellations. If we compute the poles and zeros of  $T(s)$ , we find that the numerator and denominator polynomials have  $(s + 1)$  as a common factor. This must be canceled before we can claim we have the closed-loop transfer function. To assist us in the pole-zero cancellation, we will use the mirreal function. The mirreal function, shown in Figure 2.70, removes common pole-zero factors of a transfer function. The final step in the block reduction process is to cancel out the common factors, as shown in Figure 2.71. After the application of the mirreal function, we find that the order of the denominator polynomial has been reduced from six to five, implying one pole-zero cancellation. ■

2.10 SEQUENTIAL DESIGN EXAMPLE: DISK DRIVE READ SYSTEM



In Section 1.10, we developed an initial goal for the disk drive system; to position the reader head accurately at the desired track and to move from one track to another within 10 ms, if possible. We need to identify the plant, the sensor, and the controller. We will obtain a model of the plant  $G(s)$  and the sensor. The disk drive reader uses a permanent magnet DC motor to rotate the reader arm (see Figure 1.29). The DC motor is called a voice coil motor in the disk drive industry. The read head is mounted on a slider device, which is connected to the arm as shown in Figure 2.75. A flexure (spring metal) is used to enable the head to float above the disk at a gap of less than 100 nm. The thin-film head reads the magnetic flux and provides a signal to an amplifier. The error signal of Figure 2.76(a) is provided by reading the error from a prerecorded index track. Assuming an accurate read head, the sensor has a transfer function  $H(s) = 1$ , as shown in Figure 2.76(b). The model of the permanent magnet DC motor and a linear amplifier is shown in Figure 2.76(b). As a good approximation, we use the model of the armature-controlled DC motor as shown earlier in

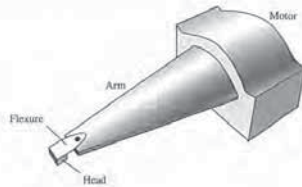


FIGURE 2.75 Head mount for reader, showing flexure.

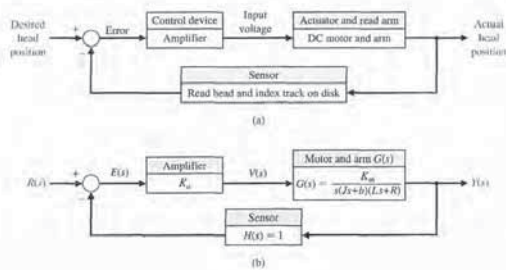


FIGURE 2.76 Block diagram model of disk drive read system.

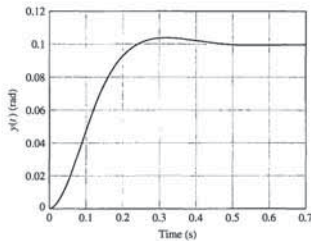


FIGURE 2.78 The system response of the system shown in Figure 2.77 for  $R(s) = \frac{0.1}{s}$ .

Using the approximate second-order model for  $G(s)$ , we obtain

$$\frac{Y(s)}{R(s)} = \frac{5K_a}{s^2 + 20s + 5K_a}$$

When  $K_a = 40$ , we have

$$Y(s) = \frac{200}{s^2 + 20s + 200} R(s).$$

We obtain the step response for  $R(s) = \frac{0.1}{s}$  rad, as shown in Figure 2.78.

2.11 SUMMARY

In this chapter, we have been concerned with quantitative mathematical models of control components and systems. The differential equations describing the dynamic performance of physical systems were utilized to construct a mathematical model. The physical systems under consideration included mechanical, electrical, fluid, and thermodynamic systems. A linear approximation using a Taylor series expansion about the operating point was utilized to obtain a small-signal linear approximation for nonlinear control components. Then, with the approximation of a linear system, one may utilize the Laplace transformation and its related input-output relationship given by the transfer function. The transfer function approach to linear systems allows the analyst to determine the response of the system to various input signals in terms of the location of the poles and zeros of the transfer function. Using transfer function notations, block diagram models of systems of interconnected components were developed. The block relationships were obtained. Additionally, an alternative use of transfer function models in signal-flow graph form was investigated. Mason's signal-flow gain formula was investigated and was found to be useful for obtaining the relationship between system variables in a complex feedback system. The advantage of the signal-flow graph method was the availability of Mason's signal-flow gain formula, which provides the relationship between system variables without requiring any reduction or manipulation of the flow

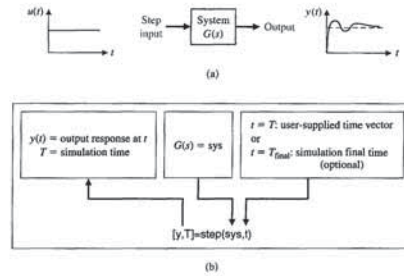


FIGURE 2.73 The step function.

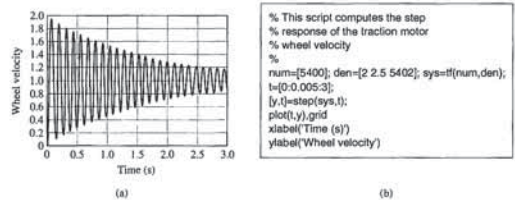


FIGURE 2.74 (a) Traction motor wheel velocity step response. (b) m-file script.

If the only objective is to plot the output,  $y(t)$ , we can use the step function without left-hand arguments and obtain the plot automatically with axis labels. If we need  $y(t)$  for any purpose other than plotting, we must use the step function with left-hand arguments, followed by the plot function to plot  $y(t)$ . We define  $t$  as a row vector containing the times at which we wish the value of the output variable  $y(t)$ . We can also select  $t = t_{final}$ , which results in a step response from  $t = 0$  to  $t = t_{final}$  and the number of intermediate points are selected automatically.

The step response of the electric traction motor is shown in Figure 2.74. As expected, the wheel velocity response, given by  $y(t)$ , is highly oscillatory. Note that the output is  $y(t) = \omega(t)$ .

Table 2.10 Typical Parameters for Disk Drive Reader

Parameter	Symbol	Typical Value
Inertia of arm and read head	$J$	1 N m s <sup>2</sup> /rad
Friction	$b$	20 N m s/rad
Amplifier	$K_a$	10–1000
Armature resistance	$R$	1 $\Omega$
Motor constant	$K_m$	5 N m/A
Armature inductance	$L$	1 mH

Figure 2.20 with  $K_b = 0$ . The model shown in Figure 2.76(b) assumes that the flexure is entirely rigid and does not significantly flex. In Chapter 4, we will consider the model when the flexure cannot be assumed to be completely rigid.

Typical parameters for the disk drive system are given in Table 2.10. Thus, we have

$$G(s) = \frac{K_m}{s(Js + b)(Ls + R)} = \frac{5000}{s(s + 20)(s + 1000)} \quad (2.138)$$

We can also write

$$G(s) = \frac{K_m/(bR)}{s(\tau_L s + 1)(\tau s + 1)} \quad (2.139)$$

where  $\tau_L = J/b = 50$  ms and  $\tau = L/R = 1$  ms. Since  $\tau \ll \tau_L$ , we often neglect  $\tau$ . Then, we would have

$$G(s) \approx \frac{K_m/(bR)}{s(\tau_L s + 1)} = \frac{0.25}{s(0.05s + 1)}$$

or

$$G(s) = \frac{5}{s(s + 20)}$$

The block diagram of the closed-loop system is shown in Figure 2.77. Using the block diagram transformation of Table 2.6, we have

$$\frac{Y(s)}{R(s)} = \frac{K_a G(s)}{1 + K_a G(s)} \quad (2.140)$$

FIGURE 2.77 Block diagram of closed-loop system.





7. Consider the system in Figure 2.79 with

$$G_c(s) = 20, \quad H(s) = 1, \quad \text{and} \quad G(s) = \frac{s + 4}{s^2 - 12s - 65}$$

When all initial conditions are zero, the input  $R(s)$  is an impulse, the disturbance  $T_d(s) = 0$ , and the noise  $N(s) = 0$ , the output  $y(t)$  is

- a.  $y(t) = 10e^{-2t} + 10e^{-5t}$
- b.  $y(t) = e^{-2t} + 10e^{-5t}$
- c.  $y(t) = 10e^{-2t} - 10e^{-5t}$
- d.  $y(t) = 20e^{-2t} + 5e^{-5t}$

8. Consider a system represented by the block diagram in Figure 2.80.

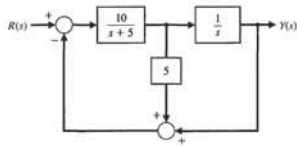


FIGURE 2.80 Block diagram with an internal loop.

The closed-loop transfer function  $T(s) = Y(s)/R(s)$  is

- a.  $T(s) = \frac{50}{s^2 + 55s + 50}$
- b.  $T(s) = \frac{10}{s^2 + 55s + 10}$
- c.  $T(s) = \frac{10}{s^2 + 50s + 55}$
- d. None of the above

Consider the block diagram in Figure 2.79 for Problems 9 through 11 where

$$G_c(s) = 4, \quad H(s) = 1, \quad \text{and} \quad G(s) = \frac{5}{s^2 + 10s + 5}$$

9. The closed-loop transfer function  $T(s) = Y(s)/R(s)$  is:

- a.  $T(s) = \frac{50}{s^2 + 5s + 50}$
- b.  $T(s) = \frac{20}{s^2 + 10s + 25}$
- c.  $T(s) = \frac{50}{s^2 + 5s + 56}$
- d.  $T(s) = \frac{20}{s^2 + 10s - 15}$

14. Consider the closed-loop system in Figure 2.79 with

$$G_c(s) = 15, \quad H(s) = 1, \quad \text{and} \quad G(s) = \frac{1000}{s^2 + 50s^2 + 4500s + 1000}$$

Compute the closed-loop transfer function and the closed-loop zeros and poles.

- a.  $T(s) = \frac{15000}{s^3 + 50s^2 + 4500s + 16000}, s_1 = -3.70, s_{2,3} = -23.15 \pm 61.59j$
- b.  $T(s) = \frac{15000}{50s^2 + 4500s + 16000}, s_1 = -3.70, s_2 = -86.29$
- c.  $T(s) = \frac{1}{s^3 + 50s^2 + 4500s + 16000}, s_1 = -3.70, s_{2,3} = -23.2 \pm 63.2j$
- d.  $T(s) = \frac{15000}{s^3 + 50s^2 + 4500s + 16000}, s_1 = -3.70, s_2 = -23.2, s_3 = -63.2$

15. Consider the feedback system in Figure 2.79 with

$$G_c(s) = \frac{K(s + 0.3)}{s}, \quad H(s) = 2s, \quad \text{and} \quad G(s) = \frac{1}{(s - 2)(s^2 + 10s + 45)}$$

Assuming  $R(s) = 0$  and  $N(s) = 0$ , the closed-loop transfer function from the disturbance  $T_d(s)$  to the output  $Y(s)$  is:

- a.  $\frac{Y(s)}{T_d(s)} = \frac{1}{s^3 + 8s^2 + (2K + 25)s + (0.6K - 90)}$
- b.  $\frac{Y(s)}{T_d(s)} = \frac{100}{s^3 + 8s^2 + (2K + 25)s + (0.6K - 90)}$
- c.  $\frac{Y(s)}{T_d(s)} = \frac{1}{8s^2 + (2K + 25)s + (0.6K - 90)}$
- d.  $\frac{Y(s)}{T_d(s)} = \frac{K(s + 0.3)}{s^4 + 8s^3 + (2K + 25)s^2 + (0.6K - 90)s}$

In the following Word Match problems, match the term with the definition by writing the correct letter in the space provided.

- |                            |  |       |
|----------------------------|--|-------|
| a. Actuator                | An oscillation in which the amplitude decreases with time.   | _____ |
| b. Block diagrams          | A system that satisfies the properties of superposition and homogeneity.                                       | _____ |
| c. Characteristic equation | The case where damping is on the boundary between underdamped and overdamped.                                  | _____ |
| d. Critical damping        | A transformation of a function $f(t)$ from the time domain into the complex frequency domain yielding $F(s)$ . | _____ |
| e. Damped oscillation      | The device that provides the motive power to the process.  | _____ |
| f. Damping ratio           | A measure of damping. A dimensionless number for the second-order characteristic equation.                     | _____ |
| g. DC motor                | The relation formed by equating to zero the denominator of a transfer function.                                | _____ |

graph. Thus, in Chapter 2, we have obtained a useful mathematical model for feedback control systems by developing the concept of a transfer function of a linear system and the relationship among system variables using block diagram and signal-flow graph models. We considered the utility of the computer simulation of linear and nonlinear systems to determine the response of a system for several conditions of the system parameters and the environment. Finally, we continued the development of the Disk Drive Read System by obtaining a model in transfer function form of the motor and arm.



SKILLS CHECK

In this section, we provide three sets of problems to test your knowledge: True or False, Multiple Choice, and Word Match. To obtain direct feedback, check your answers with the answer key provided at the conclusion of the end-of-chapter problems. Use the block diagram in Figure 2.79 as specified in the various problem statements.

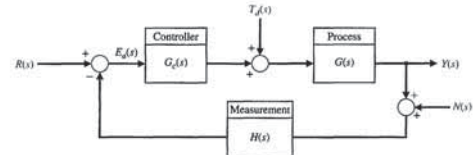


FIGURE 2.79 Block diagram for the Skills Check.

In the following True or False and Multiple Choice problems, circle the correct answer.

- 1. Very few physical systems are linear within some range of the variables. True or False
- 2. The  $s$ -plane plot of the poles and zeros graphically portrays the character of the natural response of a system. True or False
- 3. The roots of the characteristic equation are the zeros of the closed-loop system. True or False
- 4. A linear system satisfies the properties of superposition and homogeneity. True or False
- 5. The transfer function is the ratio of the Laplace transform of the output variable to the Laplace transform of the input variable, with all initial conditions equal to zero. True or False
- 6. Consider the system in Figure 2.79 where

$$G_c(s) = 10, \quad H(s) = 1, \quad \text{and} \quad G(s) = \frac{s + 50}{s^2 + 60s + 500}$$

If the input  $R(s)$  is a unit step input,  $T_d(s) = 0$ , and  $N(s) = 0$ , the final value of the output  $Y(s)$  is:

- a.  $y_{ss} = \lim_{t \rightarrow \infty} y(t) = 100$
- b.  $y_{ss} = \lim_{t \rightarrow \infty} y(t) = 1$
- c.  $y_{ss} = \lim_{t \rightarrow \infty} y(t) = 50$
- d. None of the above

10. The closed-loop unit step response is:

- a.  $y(t) = \frac{20}{25} + \frac{20}{25}e^{-5t} - t^2e^{-5t}$
- b.  $y(t) = 1 + 20te^{-5t}$
- c.  $y(t) = \frac{20}{25} - \frac{20}{25}e^{-5t} - 4te^{-5t}$
- d.  $y(t) = 1 - 2e^{-5t} - 4te^{-5t}$

11. The final value of  $y(t)$  is:

- a.  $y_{ss} = \lim_{t \rightarrow \infty} y(t) = 0.8$
- b.  $y_{ss} = \lim_{t \rightarrow \infty} y(t) = 1.0$
- c.  $y_{ss} = \lim_{t \rightarrow \infty} y(t) = 2.0$
- d.  $y_{ss} = \lim_{t \rightarrow \infty} y(t) = 1.25$

12. Consider the differential equation

$$\ddot{y} + 2\dot{y} + y = u$$

where  $y(0) = \dot{y}(0) = 0$  and  $u(t)$  is a unit step. The poles of this system are:

- a.  $s_1 = -1, s_2 = -1$
- b.  $s_1 = 1j, s_2 = -1j$
- c.  $s_1 = -1, s_2 = -2$
- d. None of the above

13. A cart of mass  $m = 1000$  kg is attached to a truck using a spring of stiffness  $k = 20,000$  N/m and a damper of constant  $b = 200$  Ns/m, as shown in Figure 2.81. The truck moves at a constant acceleration of  $a = 0.7$  m/s<sup>2</sup>.

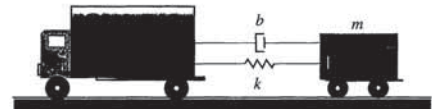


FIGURE 2.81 Truck pulling a cart of mass  $m$ .

The transfer function between the speed of the truck and the speed of the cart is:

- a.  $T(s) = \frac{50}{5s^2 + s + 100}$
- b.  $T(s) = \frac{20 + s}{s^2 + 10s + 25}$
- c.  $T(s) = \frac{100 + s}{5s^2 + s + 100}$
- d. None of the above

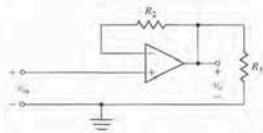


FIGURE E2.5 A noninverting amplifier using an op-amp.

E2.6 A nonlinear device is represented by the function  $y = f(x) = e^x$ ,

where the operating point for the input  $x$  is  $x_0 = 1$ . Determine a linear approximation valid near the operating point.

Answer:  $y = ex$

E2.7 A lamp's intensity stays constant when monitored by an optotransistor-controlled feedback loop. When the voltage drops, the lamp's output also drops, and optotransistor  $Q_1$  draws less current. As a result, a power transistor conducts more heavily and charges a capacitor more rapidly [24]. The capacitor voltage controls the lamp voltage directly. A block diagram of the system is shown in Figure E2.7 where  $I(s)$  is the lamp intensity, and  $R(s)$  is the command or desired level of light.

E2.8 A control engineer, N. Minorsky, designed an innovative ship steering system in the 1930s for the U.S. Navy. The system is represented by the block diagram shown in Figure E2.8 where  $Y(s)$  is the ship's course,  $R(s)$  is the desired course, and  $A(s)$  is the rudder angle [16]. Find the transfer function  $Y(s)/R(s)$ .

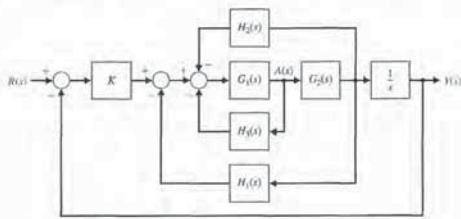


FIGURE E2.8 Ship steering system.

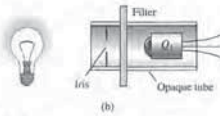
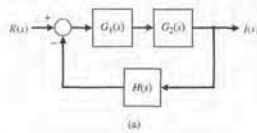
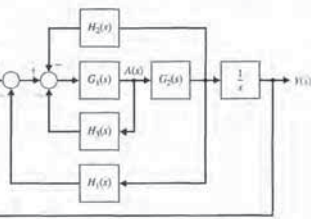


FIGURE E2.7 Lamp controller.

Answer:  $\frac{Y(s)}{R(s)} = \frac{KG_1(s)G_2(s)/s}{1 + G_1(s)H_1(s) + G_1(s)G_2(s)[H_2(s) + H_3(s)] + KG_1(s)G_2(s)/s}$

E2.9 A four-wheel antilock automobile braking system uses electronic feedback to control automatically the brake force on each wheel [15]. A block diagram model of a brake control system is shown in Figure E2.9, where  $F_f(s)$  and  $F_r(s)$  are the braking force of the front and rear wheels, respectively, and  $R(s)$  is the desired automobile response on an icy road. Find  $F_f(s)/R(s)$ .



E2.13 Consider the feedback system in Figure E2.13. Compute the transfer functions  $Y(s)/T_d(s)$  and  $Y(s)/N(s)$ .

E2.14 Find the transfer function  $\frac{Y_1(s)}{R_2(s)}$  for the multivariable system in Figure E2.14.

E2.15 Obtain the differential equations for the circuit in Figure E2.15 in terms of  $i_1$  and  $i_2$ .

E2.16 The position control system for a spacecraft platform is governed by the following equations:

$$\frac{d^2 p}{dt^2} + 2 \frac{dp}{dt} + 4p = \theta$$

$$v_1 = r - p$$

$$\frac{d\theta}{dt} = 0.6v_2$$

$$v_2 = 7v_1$$

The variables involved are as follows:

- $r(t)$  = desired platform position
- $p(t)$  = actual platform position
- $v_1(t)$  = amplifier input voltage
- $v_2(t)$  = amplifier output voltage
- $\theta(t)$  = motor shaft position

Sketch a signal-flow diagram or a block diagram of the system, identifying the component parts and determine the system transfer function  $P(s)/R(s)$ .

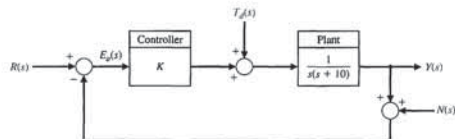


FIGURE E2.13 Feedback system with measurement noise,  $N(s)$ , and plant disturbances,  $T_d(s)$ .

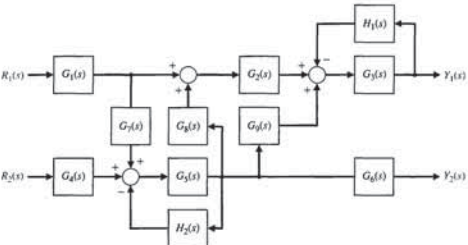


FIGURE E2.14 Multivariable system.

- h. Laplace transform Unidirectional, operational blocks that represent the transfer functions of the elements of the system.
- i. Linear approximation A rule that enables the user to obtain a transfer function by tracing paths and loops within a system.
- j. Linear system An electric actuator that uses an input voltage as a control variable.
- k. Mason loop rule The ratio of the Laplace transform of the output variable to the Laplace transform of the input variable.
- l. Mathematical models Descriptions of the behavior of a system using mathematics.
- m. Signal-flow graph A model of a system that is used to investigate the behavior of a system by utilizing actual input signals.
- n. Simulation A diagram that consists of nodes connected by several directed branches and that is a graphical representation of a set of linear relations.
- o. Transfer function An approximate model that results in a linear relationship between the output and the input of the device.

EXERCISES

Exercises are straightforward applications of the concepts of the chapter.

E2.1 A unity, negative feedback system has a nonlinear function  $y = f(x) = x^2$ , as shown in Figure E2.1. For an input  $x$  in the range of 0 to 4, calculate and plot the open-loop and closed-loop output versus input and show that the feedback system results in a more linear relationship.

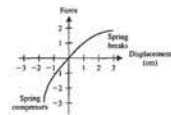


FIGURE E2.3 Spring behavior.

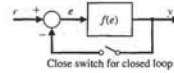


FIGURE E2.1 Open and closed loop.

E2.2 A thermistor has a response to temperature represented by

$$R = R_0 e^{-0.17T}$$

where  $R_0 = 10,000 \Omega$ ,  $R$  = resistance, and  $T$  = temperature in degrees Celsius. Find the linear model for the thermistor operating at  $T = 20^\circ\text{C}$  and for a small range of variation of temperature.

Answer:  $\Delta R = -135\Delta T$

E2.3 The force versus displacement for a spring is shown in Figure E2.3 for the spring-mass-damper system of Figure 2.1. Graphically find the spring constant for the equilibrium point of  $y = 0.5$  cm and a range of operation of  $\pm 1.5$  cm.

E2.4 A laser printer uses a laser beam to print copy rapidly for a computer. The laser is positioned by a control input  $r(t)$ , so that we have

$$Y(s) = \frac{4(s + 50)}{s^2 + 30s + 200} R(s)$$

The input  $r(t)$  represents the desired position of the laser beam.

(a) If  $r(t)$  is a unit step input, find the output  $y(t)$ .

(b) What is the final value of  $y(t)$ ?

Answer: (a)  $y(t) = 1 + 0.6e^{-20t} - 1.6e^{-10t}$ , (b)  $y_\infty = 1$

E2.5 A noninverting amplifier uses an op-amp as shown in Figure E2.5. Assume an ideal op-amp model and determine  $v_o/v_a$ .

Answer:  $\frac{v_o}{v_a} = 1 + \frac{R_2}{R_1}$

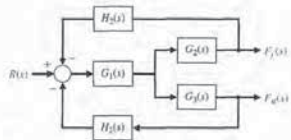


FIGURE E2.9 Brake control system.

E2.10 One of the most potentially beneficial applications of an automotive control system is the active control of the suspension system. One feedback control system uses a shock absorber consisting of a cylinder filled with a compressible fluid that provides both spring and damping forces [17]. The cylinder has a plunger activated by a gear motor, a displacement-measuring sensor, and a piston. Spring force is generated by piston displacement, which compresses the fluid. During piston displacement, the pressure imbalance across the piston is used to control damping. The plunger varies the internal volume of the cylinder. This feedback system is shown in Figure E2.10. Develop a linear model for this device using a block diagram model.

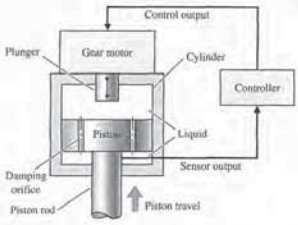


FIGURE E2.10 Shock absorber.

E2.11 A spring exhibits a force-versus-displacement characteristic as shown in Figure E2.11. For small deviations from the operating point  $x_0$ , find the spring constant when  $x_0$  is (a)  $-1.4$ , (b)  $0$ , (c)  $3.5$ .

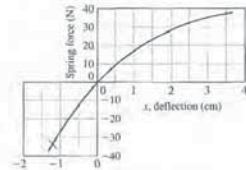


FIGURE E2.11 Spring characteristic.

E2.12 Off-road vehicles experience many disturbance inputs as they traverse over rough roads. An active suspension system can be controlled by a sensor that looks "ahead" at the road conditions. An example of a simple suspension system that can accommodate the bumps is shown in Figure E2.12. Find the appropriate

gain  $K_1$  so that the vehicle does not bounce when the desired deflection is  $R(s) = 0$  and the disturbance is  $T_d(s)$ .

Answer:  $K_1 K_2 = 1$

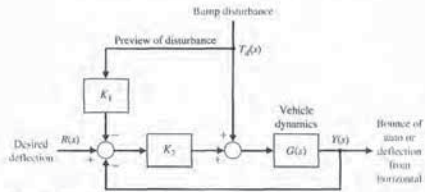


FIGURE E2.12 Active suspension system.



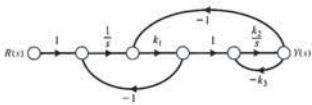


FIGURE E2.23 Control system with three feedback loops.

E2.24 The block diagram of a system is shown in Figure E2.24. Determine the transfer function  $T(s) = Y(s)/R(s)$ .

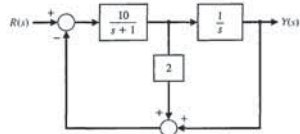


FIGURE E2.24 Multiloop feedback system.

E2.25 An amplifier may have a region of deadband as shown in Figure E2.25. Use an approximation that uses a cubic equation  $y = ax^3$  in the approximately linear region. Select  $a$  and determine a linear approximation for the amplifier when the operating point is  $x = 0.6$ .

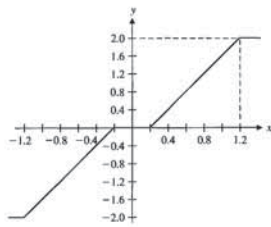


FIGURE E2.25 An amplifier with a deadband region.

E2.26 Determine the transfer function  $X_2(s)/F(s)$  for the system shown in Figure E2.26. Both masses slide on a frictionless surface, and  $k = 1$  N/m.

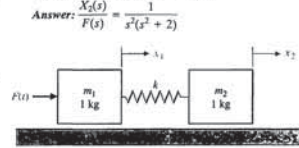


FIGURE E2.26 Two connected masses on a frictionless surface.

E2.27 Find the transfer function  $Y(s)/T_d(s)$  for the system shown in Figure E2.27.

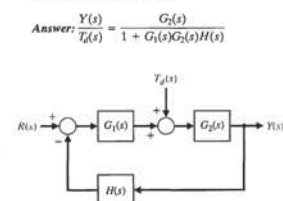


FIGURE E2.27 System with disturbance.

Answer:  $X_2(s)/F(s) = \frac{1}{s^2(s^2 + 2)}$

Answer:  $\frac{Y(s)}{T_d(s)} = \frac{G_2(s)}{1 + G_1(s)G_2(s)H(s)}$

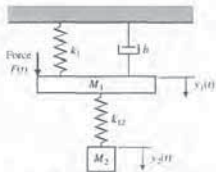


FIGURE P2.2 Vibration absorber.

P2.3 A coupled spring-mass system is shown in Figure P2.3. The masses and springs are assumed to be equal. Obtain the differential equations describing the system.

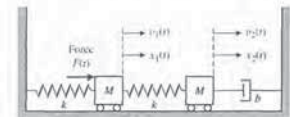


FIGURE P2.3 Two-mass system.

P2.4 A nonlinear amplifier can be described by the following characteristic:

$$v_o(t) = \begin{cases} v_m^2 & v_m \geq 0 \\ -v_m^2 & v_m < 0 \end{cases}$$

The amplifier will be operated over a range of  $\pm 0.5$  volts around the operating point for  $v_m$ . Describe the amplifier by a linear approximation (a) when the operating point is  $v_m = 0$  and (b) when the operating point is  $v_m = 1$  volt. Obtain a sketch of the nonlinear function and the approximation for each case.

P2.5 Fluid flowing through an orifice can be represented by the nonlinear equation

$$Q = K(P_1 - P_2)^{1/2}$$

where the variables are shown in Figure P2.5 and  $K$  is a constant [2]. (a) Determine a linear approximation



FIGURE P2.5 Flow through an orifice.

for the fluid-flow equation. (b) What happens to the approximation obtained in part (a) if the operating point is  $P_1 = P_2 = 0$ ?

P2.6 Using the Laplace transformation, obtain the current  $i_2(s)$  of Problem P2.1. Assume that all the initial currents are zero, the initial voltage across capacitor  $C_1$  is zero,  $v(t)$  is zero, and the initial voltage across  $C_2$  is 10 volts.

P2.7 Obtain the transfer function of the differentiating circuit shown in Figure P2.7.

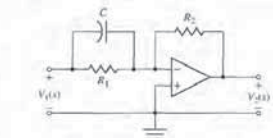


FIGURE P2.7 A differentiating circuit.

P2.8 A bridged-T network is often used in AC control systems as a filter network [8]. The circuit of one bridged-T network is shown in Figure P2.8. Show that the transfer function of the network is

$$\frac{V_o(s)}{V_i(s)} = \frac{1 + 2R_1C_1s + R_1R_2C_1^2s^2}{1 + (2R_1 + R_2)C_1s + R_1R_2C_1^2s^2}$$

Sketch the pole-zero diagram when  $R_1 = 0.5$ ,  $R_2 = 1$ , and  $C = 0.5$ .

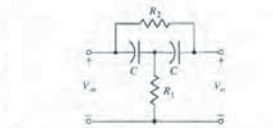


FIGURE P2.8 Bridged-T network.

P2.9 Determine the transfer function  $X_2(s)/F(s)$  for the coupled spring-mass system of Problem P2.3. Sketch the  $s$ -plane pole-zero diagram for low damping when  $M = 1$ ,  $b/k = 1$ , and

$$\zeta = \frac{1}{2} \frac{b}{\sqrt{kM}} = 0.1.$$

P2.10 Determine the transfer function  $Y(s)/F(s)$  for the vibration absorber system of Problem P2.2. Determine

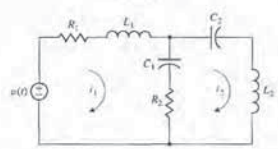


FIGURE E2.15 Electric circuit.

E2.17 A spring develops a force  $f$  represented by the relation

$$f = kx^2,$$

where  $x$  is the displacement of the spring. Determine a linear model for the spring when  $x_0 = \frac{1}{2}$ .

E2.18 The output  $y$  and input  $x$  of a device are related by

$$y = x + 1.4x^3.$$

(a) Find the values of the output for steady-state operation at the two operating points  $x_0 = 1$  and  $x_0 = 2$ . (b) Obtain a linearized model for both operating points and compare them.

E2.19 The transfer function of a system is

$$\frac{Y(s)}{R(s)} = \frac{15(s+1)}{s^2 + 9s + 14}$$

Determine  $y(t)$  when  $r(t)$  is a unit step input. Answer:  $y(t) = 1.07 + 1.5e^{-2t} - 2.57e^{-7t}$ ,  $t \geq 0$

E2.20 Determine the transfer function  $V_o(s)/V_i(s)$  of the operational amplifier circuit shown in Figure E2.20. Assume an ideal operational amplifier. Determine the transfer function when  $R_1 = R_2 = 100$  k $\Omega$ ,  $C_1 = 10$   $\mu$ F, and  $C_2 = 5$   $\mu$ F.

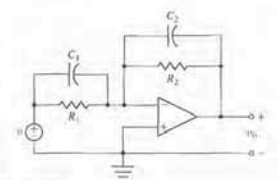


FIGURE E2.20 Op-amp circuit.

E2.21 A high-precision positioning slide is shown in Figure E2.21. Determine the transfer function  $X_p(s)/X_d(s)$  when the drive shaft friction is  $b_d = 0.7$ , the drive shaft spring constant is  $k_d = 2$ ,  $m_c = 1$ , and the sliding friction is  $b_s = 0.8$ .

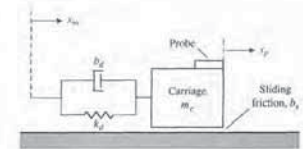


FIGURE E2.21 Precision slide.

E2.22 The rotational velocity  $\omega$  of the satellite shown in Figure E2.22 is adjusted by changing the length of the beam  $L$ . The transfer function between  $\omega(s)$  and the incremental change in beam length  $\Delta L(s)$  is

$$\frac{\omega(s)}{\Delta L(s)} = \frac{2(s+4)}{(s+5)(s+1)^2}$$

The beam length change is  $\Delta L(s) = 1/s$ . Determine the response of the rotation  $\omega(t)$ .

Answer:  $\omega(t) = 1.6 + 0.025e^{-5t} - 1.625e^{-t} - 1.5t e^{-t}$

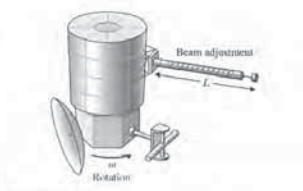


FIGURE E2.22 Satellite with adjustable rotational velocity.

E2.23 Determine the closed-loop transfer function  $T(s) = Y(s)/R(s)$  for the system of Figure E2.23.

E2.28 Determine the transfer function  $V_o(s)/V_i(s)$  for the op-amp circuit shown in Figure E2.28 [1]. Let  $R_1 = 167$  k $\Omega$ ,  $R_2 = 240$  k $\Omega$ ,  $R_3 = 1$  k $\Omega$ ,  $R_4 = 100$  k $\Omega$ , and  $C = 1$   $\mu$ F. Assume an ideal op-amp.

E2.29 A system is shown in Fig. E2.29(a).

(a) Determine  $G(s)$  and  $H(s)$  of the block diagram shown in Figure E2.29(b) that are equivalent to those of the block diagram of Figure E2.29(a).

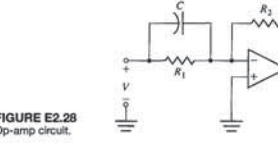


FIGURE E2.28 Op-amp circuit.

(b) Determine  $Y(s)/R(s)$  for Figure E2.29(b).

E2.30 A system is shown in Figure E2.30.

(a) Find the closed-loop transfer function  $Y(s)/R(s)$  when  $G(s) = \frac{10}{s^2 + 2s + 10}$ .

(b) Determine  $Y(s)$  when the input  $R(s)$  is a unit step. (c) Compute  $y(t)$ .

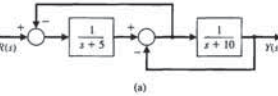


FIGURE E2.29 Block diagram equivalence.

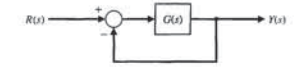


FIGURE E2.30 Unity feedback control system.

E2.31 Determine the partial fraction expansion for  $V(s)$  and compute the inverse Laplace transform. The transfer function  $V(s)$  is given by:

$$V(s) = \frac{400}{s^2 + 8s + 400}$$

PROBLEMS

Problems require an extension of the concepts of the chapter to new situations.

P2.1 An electric circuit is shown in Figure P2.1. Obtain a set of simultaneous integrodifferential equations representing the network.

P2.2 A dynamic vibration absorber is shown in Figure P2.2. This system is representative of many situations involving the vibration of machines containing unbalanced components. The parameters  $M_2$  and  $k_2$  may be chosen so that the main mass  $M_1$  does not vibrate in the steady state when  $F(t) = a \sin(\omega_0 t)$ . Obtain the differential equations describing the system.

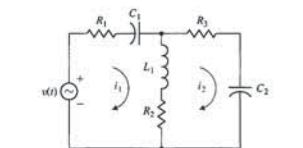


FIGURE P2.1 Electric circuit.

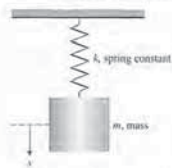


FIGURE P2.15 Suspended spring-mass system.

P2.16 Obtain a signal-flow graph to represent the following set of algebraic equations where  $x_1$  and  $x_2$  are to be considered the dependent variables and 6 and 11 are the inputs:

$$x_1 + 1.5x_2 = 6, \quad 2x_1 + 4x_2 = 11.$$

Determine the value of each dependent variable by using the gain formula. After solving for  $x_1$  by Mason's signal-flow gain formula, verify the solution by using Cramer's rule.

P2.17 A mechanical system is shown in Figure P2.17, which is subjected to a known displacement  $x_1(t)$  with respect to the reference. (a) Determine the two independent equations of motion. (b) Obtain the equations of motion in terms of the Laplace transform, assuming that the initial conditions are zero. (c) Sketch a signal-flow graph representing the system of equations. (d)

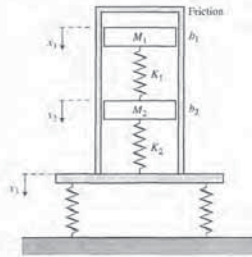


FIGURE P2.17 Mechanical system.

Obtain the relationship  $T_{12}(s)$  between  $X_1(s)$  and  $X_2(s)$  by using Mason's signal-flow gain formula. Compare the work necessary to obtain  $T_{12}(s)$  by matrix methods to that using Mason's signal-flow gain formula.

P2.18 An L-C ladder network is shown in Figure P2.18. One may write the equations describing the network as follows:

$$I_1 = (V_1 - V_2)Y_1, \quad V_2 = (I_1 - I_2)Z_2, \\ I_2 = (V_2 - V_3)Y_2, \quad V_3 = I_2 Z_3.$$

Construct a flow graph from the equations and determine the transfer function  $V_3(s)/V_1(s)$ .

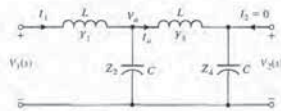


FIGURE P2.18 L-C ladder network.

P2.19 A voltage follower (buffer amplifier) is shown in Figure P2.19. Show that  $T = v_0/v_{in} = 1$ . Assume an ideal op-amp.

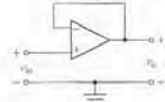


FIGURE P2.19 A buffer amplifier.

P2.20 The source follower amplifier provides lower output impedance and essentially unity gain. The circuit diagram is shown in Figure P2.20(a), and the small-signal model is shown in Figure P2.20(b). This circuit uses an FET and provides a gain of approximately unity. Assume that  $R_2 \gg R_1$  for biasing purposes and that  $R_2 \gg R_1$ . (a) Solve for the amplifier gain. (b) Solve for the gain when  $\beta_{m0} = 2000 \mu\text{A/V}$  and  $R_1 = 10 \text{ k}\Omega$  where  $R_1 = R_1 + R_2$ . (c) Sketch a block diagram that represents the circuit equations.

P2.21 A hydraulic servomechanism with mechanical feedback is shown in Figure P2.21 [18]. The power piston has an area equal to  $A$ . When the valve is moved a small amount  $\Delta z$ , the oil will flow through to the cylinder at a rate  $p \cdot \Delta z$ , where  $p$  is the port coefficient. The

necessary parameters  $M_2$  and  $k_{12}$  so that the mass  $M_2$  does not vibrate in the steady state when  $F(t) = a \sin(\omega_0 t)$ .

P2.11 For electromechanical systems that require large power amplification, rotary amplifiers are often used

[8.19]. An amplidyne is a power amplifying rotary amplifier. An amplidyne and a servomotor are shown in Figure P2.11. Obtain the transfer function  $\theta(s)/V_f(s)$ , and draw the block diagram of the system. Assume  $v_d = k_1 i_d$  and  $v_a = k_2 i_a$ .

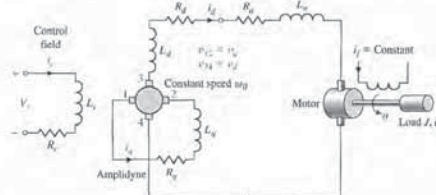


FIGURE P2.11 Amplidyne and armature-controlled motor.

P2.12 For the open-loop control system described by the block diagram shown in Figure P2.12, determine the value of  $K$  such that  $y(t) \rightarrow 1$  as  $t \rightarrow \infty$  when  $r(t)$  is a unit step input. Assume zero initial conditions.

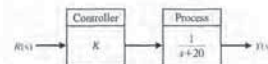


FIGURE P2.12 Open-loop control system.

P2.13 An electromechanical open-loop control system is shown in Figure P2.13. The generator, driven at a constant speed, provides the field voltage for the motor. The motor has an inertia  $J_m$  and bearing friction  $b_m$ . Obtain

the transfer function  $\theta_2(s)/V_f(s)$  and draw a block diagram of the system. The generator voltage  $v_g$  can be assumed to be proportional to the field current  $i_f$ .

P2.14 A rotating load is connected to a field-controlled DC electric motor through a gear system. The motor is assumed to be linear. A test results in the output load reaching a speed of 1 rad/s within 0.5 s when a constant 80 V is applied to the motor terminals. The output steady-state speed is 2.4 rad/s. Determine the transfer function  $\theta(s)/V_f(s)$  of the motor, in rad/V. The inductance of the field may be assumed to be negligible (see Figure 2.18). Also, note that the application of 80 V to the motor terminals is a step input of 80 V in magnitude.

P2.15 Consider the spring-mass system depicted in Figure P2.15. Determine a differential equation to describe the motion of the mass  $m$ . Obtain the system response  $x(t)$  with the initial conditions  $x(0) = x_0$  and  $\dot{x}(0) = 0$ .

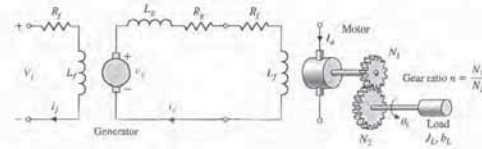


FIGURE P2.13 Motor and generator.

neglects the bias resistors and the shunt capacitors. A block diagram representing the circuit is shown in Figure P2.24(b). This block diagram neglects the effect of  $R_{be}$ , which is usually an accurate approximation, and assumes that  $R_1 + R_2 \gg R_1$ . (a) Determine the voltage gain  $v_o/v_{in}$ . (b) Determine the current gain  $i_o/i_{in}$ . (c) Determine the input impedance  $v_{in}/i_{in}$ .

P2.25 H. S. Black is noted for developing a negative feedback amplifier in 1927. Often overlooked is the fact that three years earlier he had invented a circuit de-

sign technique known as feedforward correction [19]. Recent experiments have shown that this technique offers the potential for yielding excellent amplifier stabilization. Black's amplifier is shown in Figure P2.25(a) in the form recorded in 1924. The block diagram is shown in Figure P2.25(b). Determine the transfer function between the output  $Y(s)$  and the input  $R(s)$  and between the output and the disturbance  $T_d(s)$ .  $G(s)$  is used to denote the amplifier represented by  $\mu$  in Figure P2.25(a).

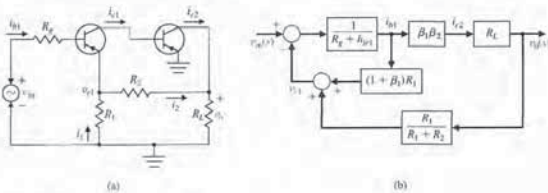


FIGURE P2.24 Feedback amplifier.

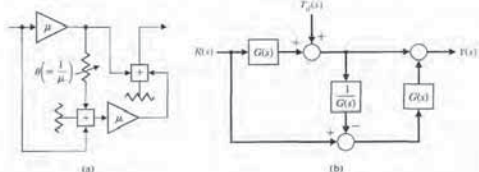


FIGURE P2.25 H. S. Black's amplifier.

P2.26 A robot includes significant flexibility in the arm members with a heavy load in the gripper [6, 20]. A two-mass model of the robot is shown in Figure. P2.26. Find the transfer function  $Y(s)/F(s)$ .

P2.27 Magnetic levitation trains provide a high-speed, very low friction alternative to steel wheels on steel rails. The train floats on an air gap as shown in Figure P2.27 [25]. The levitation force  $F_L$  is controlled by the coil current  $i$  in the levitation coils and may be approximated by

$$F_L = k \frac{i^2}{z^2}$$

where  $z$  is the air gap. This force is opposed by the downward force  $F = mg$ . Determine the linearized

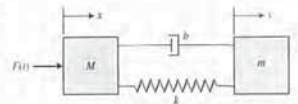


FIGURE P2.26 The spring-mass-damper model of a robot arm.

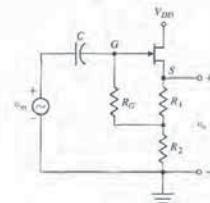


FIGURE P2.20 The source follower or common drain amplifier using an FET.

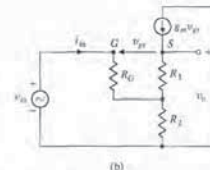
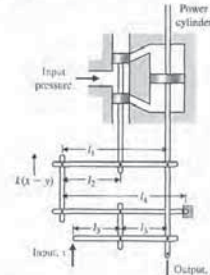


FIGURE P2.21 Hydraulic servomechanism.



input oil pressure is assumed to be constant. From the geometry, we find that  $\Delta z = k \frac{L^2 - L^2}{L^2} (x - y) - \frac{L}{L} y$ .

(a) Determine the closed-loop signal-flow graph or block diagram for this mechanical system. (b) Obtain the closed-loop transfer function  $Y(s)/X(s)$ .

P2.22 Figure P2.22 shows two pendulums suspended from frictionless pivots and connected at their midpoints by a spring [1]. Assume that each pendulum can be represented by a mass  $M$  at the end of a massless bar of length  $L$ . Also assume that the displacement is small and linear approximations can be used for  $\sin \theta$  and  $\cos \theta$ . The spring located in the middle of the bars is unstretched when  $\theta_1 = \theta_2$ . The input force is represented by  $f(t)$ , which influences the left-hand bar only. (a) Obtain the equations of motion, and sketch a block diagram for them. (b) Determine the transfer function  $T(s) = \theta_2(s)/F(s)$ . (c) Sketch the location of the poles and zeros of  $T(s)$  on the  $s$ -plane.

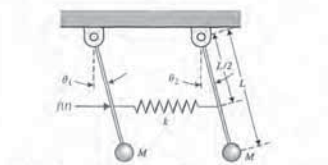


FIGURE P2.22 The bars are each of length  $L$  and the spring is located at  $L/2$ .

P2.23 The small-signal circuit equivalent to a common-emitter transistor amplifier is shown in Figure P2.23. The transistor amplifier includes a feedback resistor  $R_f$ . Determine the input-output ratio  $v_o/v_{in}$ .

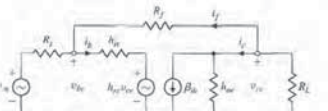


FIGURE P2.23 CE amplifier.

P2.24 A two-transistor series voltage feedback amplifier is shown in Figure P2.24(a). This AC equivalent circuit

FIGURE P2.21 Hydraulic servomechanism.



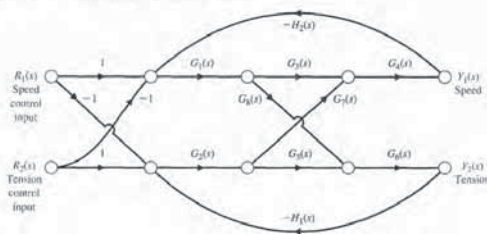


FIGURE P2.32 A model of the coupled motor drives.

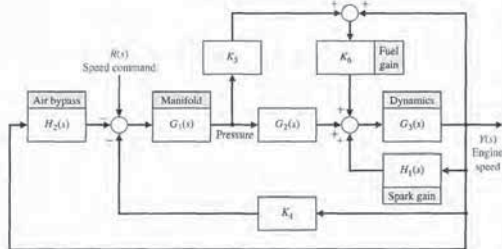


FIGURE P2.33 Idle speed control system.

P2.33 Find the transfer function for  $Y(s)/R(s)$  for the idle speed control system for a fuel-injected engine as shown in Figure P2.33.

P2.34 The suspension system for one wheel of an old-fashioned pickup truck is illustrated in Figure P2.34. The mass of the vehicle is  $m_1$  and the mass of the wheel is  $m_2$ . The suspension spring has a spring constant  $k_1$  and the tire has a spring constant  $k_2$ . The damping constant of the shock absorber is  $b$ . Obtain the transfer function  $Y(s)/X(s)$ , which represents the vehicle response to bumps in the road.

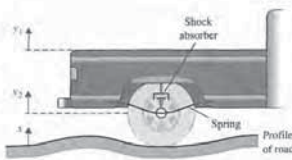


FIGURE P2.34 Pickup truck suspension. so that the closed-loop response to a step input is critically damped with two equal roots at  $s = -10$ . (d) Plot the critically damped response for a unit step

P2.35 A feedback control system has the structure shown in Figure P2.35. Determine the closed-loop transfer function  $Y(s)/R(s)$  (a) by block diagram manipulation and (b) by using a signal-flow graph and Mason's signal-flow gain formula. (c) Select the gains  $K_1$  and  $K_2$

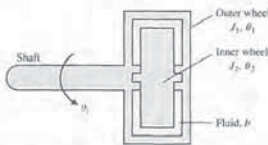


FIGURE P2.40 Cutaway view of damping device.

Figure P2.40. When vibration becomes excessive, the relative motion of the two wheels creates damping. When the device is rotating without vibration, there is no relative motion and no damping occurs. Find  $\theta_1(s)$  and  $\theta_2(s)$ . Assume that the shaft has a spring constant  $K$  and that  $b$  is the damping constant of the fluid. The load torque is  $T$ .

P2.41 The lateral control of a rocket with a gimballed engine is shown in Figure P2.41. The lateral deviation from the desired trajectory is  $h$  and the forward rocket speed is  $V$ . The control torque of the engine is  $T_e$  and the disturbance torque is  $T_d$ . Derive the describing equations of a linear model of the system, and draw the block diagram with the appropriate transfer functions.

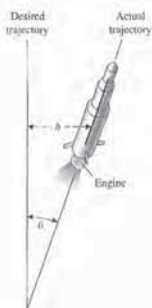


FIGURE P2.41 Rocket with gimballed engine.

P2.42 In many applications, such as reading product codes in supermarkets and in printing and manufacturing, an optical scanner is utilized to read codes as

shown in Figure P2.42. As the mirror rotates, a friction force is developed that is proportional to its angular speed. The friction constant is equal to 0.06 N s/rad, and the moment of inertia is equal to 0.1 kg m<sup>2</sup>. The output variable is the velocity  $\omega(t)$ . (a) Obtain the differential equation for the motor. (b) Find the response of the system when the input motor torque is a unit step and the initial velocity at  $t = 0$  is equal to 0.7.

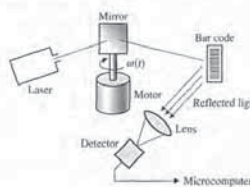


FIGURE P2.42 Optical scanner.

P2.43 An ideal set of gears is shown in Table 2.5, item 10. Neglect the inertia and friction of the gears and assume that the work done by one gear is equal to that of the other. Derive the relationships given in item 10 of Table 2.5. Also, determine the relationship between the torques  $T_m$  and  $T_L$ .

P2.44 An ideal set of gears is connected to a solid cylinder load as shown in Figure P2.44. The inertia of the motor shaft and gear  $G_2$  is  $J_m$ . Determine (a) the inertia of the load  $J_L$  and (b) the torque  $T$  at the motor shaft. Assume the friction at the load is  $b_L$  and the friction at the motor shaft is  $b_m$ . Also assume the density of the load disk is  $\rho$  and the gear ratio is  $n$ . Hint: The torque at the motor shaft is given by  $T = T_1 + T_m$ .

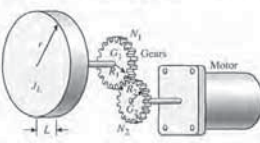


FIGURE P2.44 Motor, gears, and load.

P2.45 To exploit the strength advantage of robot manipulators and the intellectual advantage of humans, a class of manipulators called **extenders** has been examined

relationship between the air gap  $z$  and the controlling current near the equilibrium condition.

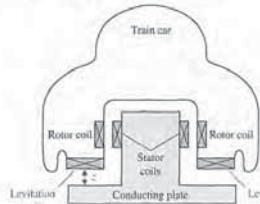


FIGURE P2.27 Cutaway view of train.

P2.28 A multiple-loop model of an urban ecological system might include the following variables: number of people in the city ( $P$ ), modernization ( $M$ ), migration into the city ( $C$ ), sanitation facilities ( $S$ ), number of diseases ( $D$ ), bacteria/area ( $B$ ), and amount of garbage/area ( $G$ ), where the symbol for the variable is given in parentheses. The following causal loops are hypothesized:

1.  $P \rightarrow G \rightarrow B \rightarrow D \rightarrow P$
2.  $P \rightarrow M \rightarrow C \rightarrow P$
3.  $P \rightarrow M \rightarrow S \rightarrow D \rightarrow P$
4.  $P \rightarrow M \rightarrow S \rightarrow B \rightarrow D \rightarrow P$

Sketch a signal-flow graph for these causal relationships, using appropriate gain symbols. Indicate whether you believe each gain transmission is positive or negative. For example, the causal link  $S$  to  $D$  is negative because improved sanitation facilities lead to reduced bacteria/area. Which of the four loops are positive feedback loops and which are negative feedback loops?

P2.29 We desire to balance a rolling ball on a tilting beam as shown in Figure P2.29. We will assume the motor

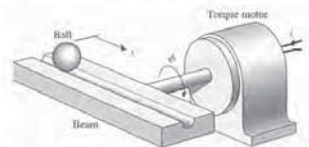


FIGURE P2.29 Tilt beam and ball.

input current  $i$  controls the torque with negligible friction. Assume the beam may be balanced near the horizontal ( $\phi = 0$ ); therefore, we have a small deviation of  $\phi$ . Find the transfer function  $X(s)/I(s)$ , and draw a block diagram illustrating the transfer function showing  $\phi(s)$ ,  $X(s)$ , and  $I(s)$ .

P2.30 The measurement or sensor element in a feedback system is important to the accuracy of the system [6]. The dynamic response of the sensor is important. Most sensor elements possess a transfer function

$$H(s) = \frac{k}{\tau s + 1}$$

Suppose that a position-sensing photo detector has  $\tau = 4 \mu\text{s}$  and  $0.999 < k < 1.001$ . Obtain the step response of the system, and find the  $k$  resulting in the fastest response—that is, the fastest time to reach 98% of the final value.

P2.31 An interacting control system with two inputs and two outputs is shown in Figure P2.31. Solve for  $Y_1(s)/R_1(s)$  and  $Y_2(s)/R_1(s)$  when  $R_2 = 0$ .

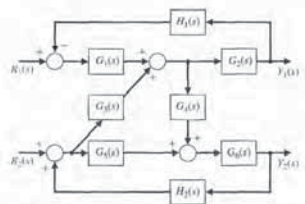


FIGURE P2.31 Interacting System.

P2.32 A system consists of two electric motors that are coupled by a continuous flexible belt. The belt also passes over a swinging arm that is instrumented to allow measurement of the belt speed and tension. The basic control problem is to regulate the belt speed and tension by varying the motor torques.

An example of a practical system similar to that shown occurs in textile fiber manufacturing processes when yarn is wound from one spool to another at high speed. Between the two spools, the yarn is processed in a way that may require the yarn speed and tension to be controlled within defined limits. A model of the system is shown in Figure P2.32. Find  $Y_2(s)/R_1(s)$ . Determine a relationship for the system that will make  $Y_2$  independent of  $R_1$ .

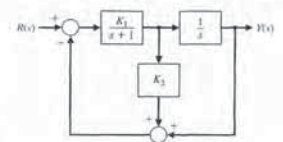


FIGURE P2.35 Multiloop feedback system.

input. What is the time required for the step response to reach 90% of its final value?

P2.36 A system is represented by Figure P2.36. (a) Determine the partial fraction expansion and  $y(t)$  for a ramp input,  $r(t) = t, t \geq 0$ . (b) Obtain a plot of  $r(t)$  for part (a), and find  $y(t)$  for  $t = 1.0$  s. (c) Determine the impulse response of the system  $y(t)$  for  $t \geq 0$ . (d) Obtain a plot of  $y(t)$  for part (c) and find  $y(t)$  for  $t = 1.0$  s.

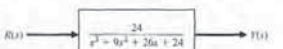


FIGURE P2.36 A third-order system.

P2.37 A two-mass system is shown in Figure P2.37 with an input force  $u(t)$ . When  $m_1 = m_2 = 1$  and  $K_1 = K_2 = 1$ , find the set of differential equations describing the system.

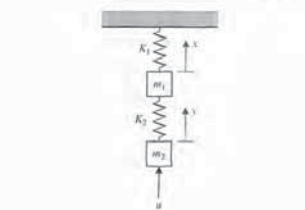


FIGURE P2.37 Two-mass system.

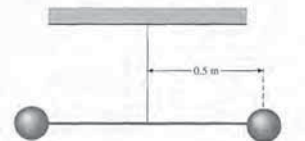


FIGURE P2.38 Winding oscillator.

viscous friction coefficient for the sphere in air is  $2 \times 10^{-4} \text{ N m s/rad}$ . The sphere has a mass of 1 kg.

P2.39 For the circuit in Figure P2.39, determine the transform of the output voltage  $v_0(s)$ . Assume that the circuit is in steady state when  $t < 0$ . Assume that the switch moves instantaneously from contact 1 to contact 2 at  $t = 0$ .

P2.40 A damping device is used to reduce the undesired vibrations of machines. A viscous fluid, such as a heavy oil, is placed between the wheels as shown in

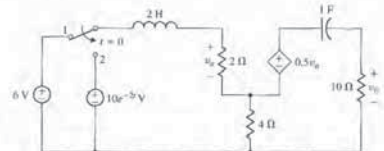
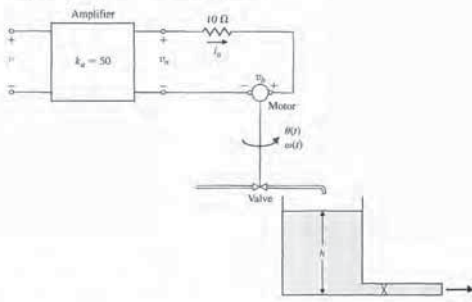
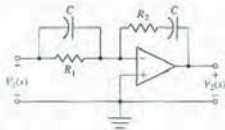


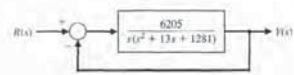
FIGURE P2.39 Model of an electronic circuit.



**FIGURE P2.47** Open-loop control system for the water level of a tank.



**FIGURE P2.46** Lead-lag filter.

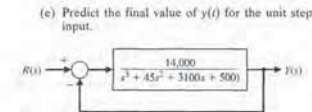


**FIGURE P2.49** Unity feedback control system.

(d) Plot  $y(t)$  and discuss the effect of the real and complex poles of  $T(s)$ . Do the complex poles or the real poles dominate the response?

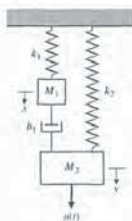
**P2.50** A closed-loop control system is shown in Figure P2.50.

- (a) Determine the transfer function  $T(s) = Y(s)/R(s)$ .
- (b) Determine the poles and zeros of  $T(s)$ .
- (c) Use a unit step input,  $R(s) = 1/s$ , and obtain the partial fraction expansion for  $Y(s)$  and the value of the residues.
- (d) Plot  $y(t)$  and discuss the effect of the real and complex poles of  $T(s)$ . Do the complex poles or the real poles dominate the response?

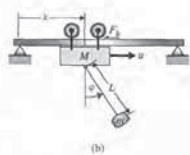


**FIGURE P2.50** Third-order feedback system.

**P2.51** Consider the two-mass system in Figure P2.51. Find the set of differential equations describing the system.

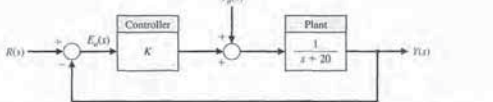


**FIGURE P2.51** Two-mass system with two springs and one damper.



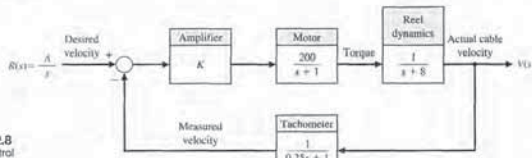
**FIGURE AP2.6** (a) Hanging crane supporting the Space Shuttle Atlantis (Image Credit: NASA/Jack Plafie) and (b) schematic representation of the hanging crane structure.

**FIGURE AP2.7** Unity feedback control system with controller  $G_c(s) = K$ .



Determine a relationship between the gain  $K$  and the minimum time it takes the impulse disturbance response of the system to reach  $y(t) \leq 0.1$ . Assume that  $K > 0$ . For what value of  $K$  does the disturbance response first reach at  $y(t) = 0.1$  at  $t = 0.057$ ?

**AP2.8** Consider the cable reel control system given in Figure AP2.8. Find the value of  $A$  and  $K$  such that the percent overshoot is  $P.O. \leq 10\%$  and a desired velocity of 50 m/s in the steady state is achieved. Compute the closed-loop response  $y(t)$  analytically and confirm that the steady-state response and  $P.O.$  meet the specifications.



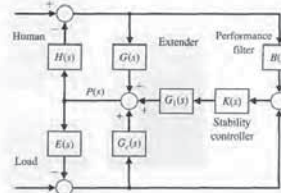
**FIGURE AP2.8** Cable reel control system.

**AP2.9** Consider the inverting operational amplifier in Figure AP2.9. Find the transfer function  $V_o(s)/V_i(s)$ . Show that the transfer function can be expressed as

$$G(s) = \frac{V_o(s)}{V_i(s)} = K_p + \frac{K_I}{s} + K_D s,$$

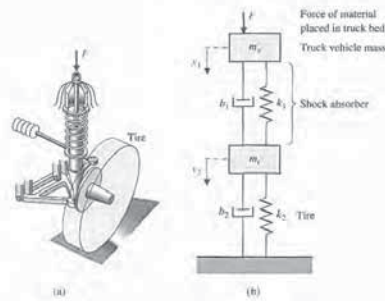
where the gains  $K_p, K_I,$  and  $K_D$  are functions of  $C_1, C_2, R_1,$  and  $R_2$ . This circuit is a proportional-integral-derivative (PID) controller (more on PID controllers in Chapter 7).

[22] The extender is defined as an active manipulator worn by a human to augment the human's strength. The human provides an input  $U(s)$ , as shown in Figure P2.45. The endpoint of the extender is  $P(s)$ . Determine the output  $P(s)$  for both  $U(s)$  and  $F(s)$  in the form  $P(s) = T_1(s)U(s) + T_2(s)F(s)$ .



**FIGURE P2.45** Model of extender.

**P2.46** A load added to a truck results in a force  $F$  on the support spring, and the tire flexes as shown in Figure P2.46(a). The model for the tire movement is shown in Figure P2.46(b). Determine the transfer function  $X_1(s)/F(s)$ .



**FIGURE P2.46** Truck support model.

**P2.47** The water level  $h(t)$  in a tank is controlled by an open-loop system, as shown in Figure P2.47. A DC motor controlled by an armature current  $i_a$  turns a shaft, opening a valve. The inductance of the DC motor is negligible, that is,  $L_m = 0$ . Also, the rotational friction of the motor shaft and valve is negligible, that is,  $b = 0$ . The height of the water in the tank is

$$h(t) = \int [1.6\theta(t) - h(t)] dt,$$

the motor constant is  $K_m = 10$ , and the inertia of the motor shaft and valve is  $J = 6 \times 10^{-3} \text{ kg m}^2$ . Determine (a) the differential equation for  $h(t)$  and  $v(t)$  and (b) the transfer function  $H(s)/V(s)$ .

**P2.48** The circuit shown in Figure P2.48 is called a lead-lag filter.

- (a) Find the transfer function  $V_2(s)/V_1(s)$ . Assume an ideal op-amp.
- (b) Determine  $V_2(s)/V_1(s)$  when  $R_1 = 100 \text{ k}\Omega$ ,  $R_2 = 200 \text{ k}\Omega$ ,  $C_1 = 1 \mu\text{F}$ , and  $C_2 = 0.1 \mu\text{F}$ .
- (c) Determine the partial fraction expansion for  $V_2(s)/V_1(s)$ .

**P2.49** A closed-loop control system is shown in Figure P2.49.

- (a) Determine the transfer function  $T(s) = Y(s)/R(s)$ .
- (b) Determine the poles and zeros of  $T(s)$ .
- (c) Use a unit step input,  $R(s) = 1/s$ , and obtain the partial fraction expansion for  $Y(s)$  and the value of the residues.

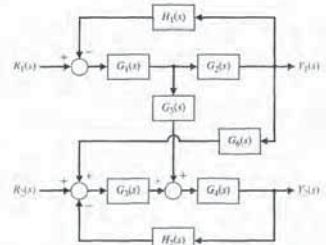
**ADVANCED PROBLEMS**

**AP2.1** An armature-controlled DC motor is driving a load. The input voltage is 5 V. The speed at  $t = 2$  seconds is 30 rad/s, and the steady speed is 70 rad/s when  $t \rightarrow \infty$ . Determine the transfer function  $\omega(s)/V(s)$ .

**AP2.2** A system has a block diagram as shown in Figure AP2.2. Determine the transfer function

$$T(s) = \frac{Y(s)}{R_1(s)}$$

It is desired to decouple  $Y_2(s)$  from  $R_1(s)$  by obtaining  $T(s) = 0$ . Select  $G_3(s)$  in terms of the other  $G_i(s)$  to achieve decoupling.



**FIGURE AP2.2** Interacting control system.

**AP2.3** Consider the feedback control system in Figure AP2.3. Define the tracking error as

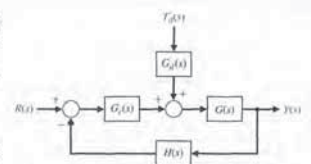
$$E(s) = R(s) - Y(s).$$

- (a) Determine a suitable  $H(s)$  such that the tracking error is zero for any input  $R(s)$  in the absence of a disturbance input (that is, when  $T_d(s) = 0$ ).
- (b) Using  $H(s)$  determined in part (a), determine the response  $Y(s)$  for a disturbance  $T_d(s)$  when the input  $R(s) = 0$ .
- (c) Is it possible to obtain  $Y(s) = 0$  for an arbitrary disturbance  $T_d(s)$  when  $G_2(s) \neq 0$ ? Explain your answer.

**AP2.4** Consider a thermal heating system given by

$$\frac{\mathcal{T}(s)}{q(s)} = \frac{1}{C_s s + (QS + 1/R_s)}$$

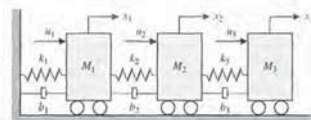
where the output  $\mathcal{T}(s)$  is the temperature difference due to the thermal process, the input  $q(s)$  is the rate of



**FIGURE AP2.3** Feedback system with a disturbance input.

heat flow of the heating element. The system parameters are  $C_s, Q, S,$  and  $R_s$ . The thermal heating system is illustrated in Table 2.5. (a) Determine the response of the system to a unit step  $q(s) = 1/s$ . (b) As  $t \rightarrow \infty$ , what value does the step response determined in part (a) approach? This is known as the steady-state response. (c) Describe how you would select the system parameters  $C_s, Q, S,$  and  $R_s$  to increase the speed of response of the system to a step input.

**AP2.5** For the three-cart system illustrated in Figure AP2.5, obtain the equations of motion. The system has three inputs  $u_1, u_2,$  and  $u_3$  and three outputs  $x_1, x_2,$  and  $x_3$ . Obtain three second-order ordinary differential equations with constant coefficients. If possible, write the equations of motion in matrix form.



**FIGURE AP2.5** Three-cart system with three inputs and three outputs.

**AP2.6** Consider the hanging crane structure in Figure AP2.6. Write the equations of motion describing the motion of the cart and the payload. The mass of the cart is  $M$ , the mass of the payload is  $m$ , the massless rigid connector has length  $L$ , and the friction is modeled as  $F_f = -b\dot{x}$  where  $x$  is the distance traveled by the cart.

**AP2.7** Consider the unity feedback system described in the block diagram in Figure AP2.7. Compute analytically the response of the system to an impulse disturbance.



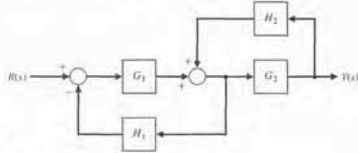


FIGURE DP2.1 Selection of transfer functions.

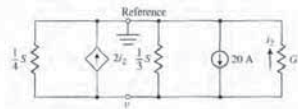


FIGURE DP2.2 Television beam circuit.

DP2.5 Consider the clock shown in Figure DP2.5. The pendulum rod of length  $L$  supports a pendulum disk. Assume that the pendulum rod is a massless rigid thin rod and the pendulum disk has mass  $m$ . Design the length of the pendulum,  $L$ , so that the period of motion is 2 seconds. Note that with a period of 2 seconds each "tick" and each "tock" of the clock represents 1 second, as desired. Assume small angles,  $\varphi$ , in the

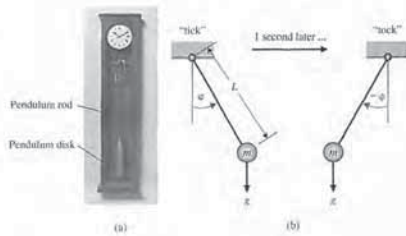


FIGURE DP2.5 (a) Typical clock (photo courtesy of SuperStock) and (b) schematic representation of the pendulum.

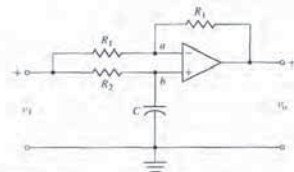


FIGURE DP2.4 Operational amplifier circuit.

analysis so that  $\sin \varphi \approx \varphi$ . Can you explain why most grandfather clocks are about 1.5 m or taller?

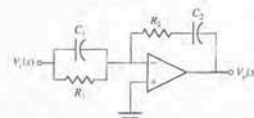


FIGURE AP2.9 An inverting operational amplifier circuit representing a PID controller.

DESIGN PROBLEMS

CDP2.1 We want to accurately position a table for a machine as shown in Figure CDP2.1. A traction-drive motor with a capstan roller possesses several desirable characteristics compared to the more popular ball screw. The traction drive exhibits low friction and no backlash. However, it is susceptible to disturbances. Develop a model of the traction drive shown in Figure CDP2.1(a) for the parameters given in Table CDP2.1. The drive uses a DC armature-controlled motor with a capstan roller attached to the shaft. The drive bar moves the linear slide-table. The slide uses an air bearing, so its friction is negligible. We are considering the open-loop model. Figure CDP2.1(b), and its transfer function in this problem. Feedback will be introduced later.

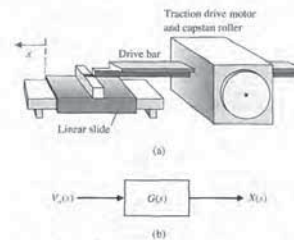


FIGURE CDP2.1 (a) Traction drive, capstan roller, and linear slide. (b) The block diagram model.

Table CDP2.1 Typical Parameters for the Armature-Controlled DC Motor and the Capstan and Slide

$M_f$	Mass of slide	5.693 kg
$M_b$	Mass of drive bar	6.96 kg
$J_m$	Inertia of roller, shaft, motor and tachometer	$10.91 \cdot 10^{-3} \text{ kg m}^2$
$r$	Roller radius	$31.75 \cdot 10^{-3} \text{ m}$
$b_m$	Motor damping	$0.268 \text{ N m/rad}$
$K_{tm}$	Torque constant	$0.8379 \text{ N m/amp}$
$K_b$	Back emf constant	$0.838 \text{ V s/rad}$
$R_m$	Motor resistance	1.36 $\Omega$
$L_m$	Motor inductance	3.6 mH

the closed-loop transfer function  $Y(s)/R(s)$  is exactly equal to 1.

DP2.2 The television beam circuit of a television is represented by the model in Figure DP2.2. Select the unknown conductance  $G$  so that the voltage  $v$  is 24 V. Each conductance is given in siemens (S).

DP2.3 An input  $r(t) = t, t \geq 0$ , is applied to a black box with a transfer function  $G(s)$ . The resulting output response, when the initial conditions are zero, is

$$y(t) = e^{-t} - \frac{1}{4}e^{-2t} - \frac{3}{4} + \frac{1}{2}t, t \geq 0.$$

Determine  $G(s)$  for this system.

DP2.4 An operational amplifier circuit that can serve as a filter circuit is shown in Figure DP2.4. Determine the transfer function of the circuit, assuming an ideal op-amp. Find  $u_0(t)$  when the input is  $v_0(t) = A t, t \geq 0$ .

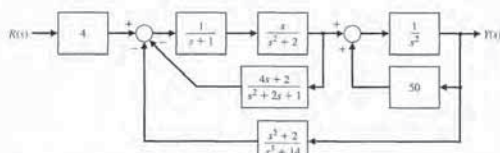


FIGURE CP2.6 A multiple-loop feedback control system block diagram.

- (b) Generate a pole-zero map of the closed-loop transfer function in graphical form using the pzmap function.
  - (c) Determine explicitly the poles and zeros of the closed-loop transfer function using the pole and zero functions and correlate the results with the pole-zero map in part (b).
- CP2.7 For the simple pendulum shown in Figure CP2.7, the nonlinear equation of motion is given by

$$\ddot{\theta}(t) + \frac{g}{L} \sin \theta = 0,$$

where  $L = 0.5 \text{ m}$ ,  $m = 1 \text{ kg}$ , and  $g = 9.8 \text{ m/s}^2$ . When the nonlinear equation is linearized about the equilibrium point  $\theta = 0$ , we obtain the linear time-invariant model,

$$\ddot{\theta} + \frac{g}{L} \theta = 0.$$

Create an m-file to plot both the nonlinear and the linear response of the simple pendulum when the initial angle of the pendulum is  $\theta(0) = 30^\circ$  and explain any differences.

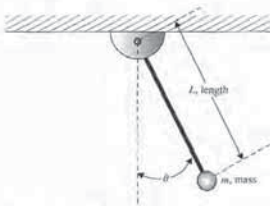


FIGURE CP2.7 Simple pendulum.

CP2.8 A system has a transfer function

$$\frac{X(s)}{R(s)} = \frac{(20/z)(s+z)}{s^2+3s+20}$$

Plot the response of the system when  $R(s)$  is a unit step for the parameter  $z = 5, 10$ , and  $15$ .

CP2.9 Consider the feedback control system in Figure CP2.9, where

$$G(s) = \frac{s+1}{s+2} \quad \text{and} \quad H(s) = \frac{1}{s+1}$$

- (a) Using an m-file, determine the closed-loop transfer function.
- (b) Obtain the pole-zero map using the pzmap function. Where are the closed-loop system poles and zeros?
- (c) Are there any pole-zero cancellations? If so, use the minreal function to cancel common poles and zeros in the closed-loop transfer function.
- (d) Why is it important to cancel common poles and zeros in the transfer function?

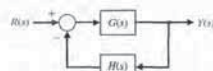


FIGURE CP2.9 Control system with nonunity feedback.

CP2.10 Consider the block diagram in Figure CP2.10. Create an m-file to complete the following tasks:

- (a) Compute the step response of the closed-loop system (that is,  $R(s) = 1/s$  and  $T_d(s) = 0$ ) and plot the steady-state value of the output  $Y(s)$  as a function of the controller gain  $0 < K \leq 10$ .
- (b) Compute the disturbance step response of the closed-loop system (that is,  $R(s) = 0$  and

COMPUTER PROBLEMS

CP2.1 Consider the two polynomials:

$$p(x) = x^2 + 7x + 10$$

and

$$q(x) = x + 2.$$

Compute the following

- (a)  $p(s)q(s)$
- (b) poles and zeros of  $G(s) = \frac{q(s)}{p(s)}$
- (c)  $p(-1)$

CP2.2 Consider the feedback system depicted in Figure CP2.2.

- (a) Compute the closed-loop transfer function using the series and feedback functions.
- (b) Obtain the closed-loop system unit step response with the step function, and verify that final value of the output is 25.

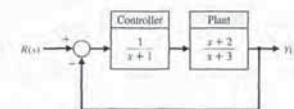


FIGURE CP2.2 A negative feedback control system.

CP2.3 Consider the differential equation

$$\ddot{y} + 4\dot{y} + 3y = u,$$

where  $y(0) = \dot{y}(0) = 0$  and  $u(t)$  is a unit step. Determine the solution  $y(t)$  analytically and verify by computing the analytic solution and the step response with the step function.

CP2.4 Consider the mechanical system depicted in Figure CP2.4. The input is given by  $f(t)$ , and the output is  $y(t)$ . Determine the transfer function from  $f(t)$  to  $y(t)$  and, using an m-file, plot the system response to a

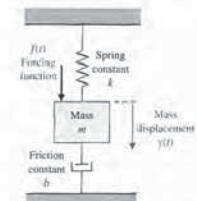


FIGURE CP2.4 A mechanical spring-mass-damper system.

unit step input. Let  $m = 10$ ,  $k = 1$ , and  $b = 0.5$ . Show that the peak amplitude of the output is about 1.8.

CP2.5 A satellite single-axis attitude control system can be represented by the block diagram in Figure CP2.5. The variables  $k$ ,  $a$ , and  $b$  are controller parameters, and  $J$  is the spacecraft moment of inertia. Suppose the nominal moment of inertia is  $J = 10.8 \text{ ER}$  (slug ft<sup>2</sup>), and the controller parameters are  $k = 10.8 \text{ ER}$ ,  $a = 1$ , and  $b = 8$ .

- (a) Develop an m-file script to compute the closed-loop transfer function  $T(s) = \theta(s)/\theta_d(s)$ .
- (b) Compute and plot the step response to a  $10^\circ$  step input.
- (c) The exact moment of inertia is generally unknown and may change slowly with time. Compare the step response performance of the spacecraft when  $J$  is reduced by 20% and 50%. Use the controller parameters  $k = 10.8 \text{ ER}$ ,  $a = 1$ , and  $b = 8$  and a  $10^\circ$  step input. Discuss your results.

CP2.6 Consider the block diagram in Figure CP2.6.

- (a) Use an m-file to reduce the block diagram in Figure CP2.6, and compute the closed-loop transfer function.

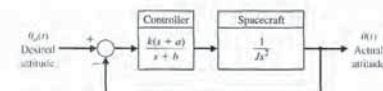


FIGURE CP2.5 A spacecraft single-axis attitude control block diagram.



**Homogeneity** The property of a linear system in which the system response,  $y(t)$ , to an input  $u(t)$  leads to the response  $\beta y(t)$  when the input is  $\beta u(t)$ .

**Inverse Laplace transform** A transformation of a function  $F(s)$  from the complex frequency domain into the time domain yielding  $f(t)$ .

**Laplace transform** A transformation of a function  $f(t)$  from the time domain into the complex frequency domain yielding  $F(s)$ .

**Linear approximation** An approximate model that results in a linear relationship between the output and the input of the device.

**Linear system** A system that satisfies the properties of superposition and homogeneity.

**Linearized** Made linear or placed in a linear form. Taylor series approximations are commonly employed to obtain linear models of physical systems.

**Loop** A closed path that originates and terminates on the same node of a signal-flow graph with no node being met twice along the path.

**Mass loop rule** A rule that enables the user to obtain a transfer function by tracing paths and loops within a system.

**Mathematical models** Descriptions of the behavior of a system using mathematics.

**Natural frequency** The frequency of natural oscillation that would occur for two complex poles if the damping were equal to zero.

**Necessary condition** A condition or statement that must be satisfied to achieve a desired effect or result. For example, for a linear system it is necessary that the input  $u_1(t) + u_2(t)$  results in the response  $y_1(t) + y_2(t)$ , where the input  $u_1(t)$  results in the response  $y_1(t)$  and the input  $u_2(t)$  results in the response  $y_2(t)$ .

**Node** The input and output points or junctions in a signal-flow graph.

**Nontouching** Two loops in a signal-flow graph that do not have a common node.

**Overdamped** The case where the damping ratio is  $\zeta > 1$ .

**Path** A branch or a continuous sequence of branches that can be traversed from one signal (node) to another signal (node) in a signal-flow graph.

**Poles** The roots of the denominator polynomial (i.e., the roots of the characteristic equation) of the transfer function.

**Positive feedback loop** Feedback loop wherein the output signal is fed back so that it adds to the input signal.

**Principle of superposition** The law that states that if two inputs are scaled and summed and routed through a linear, time-invariant system, then the output will be identical to the sum of outputs due to the individual scaled inputs when routed through the same system.

**Reference input** The input to a control system often representing the desired output, denoted by  $R(s)$ .

**Residues** The constants  $k_i$  associated with the partial fraction expansion of the output  $Y(s)$ , when the output is written in a residue-pole format.

**Signal-flow graph** A diagram that consists of nodes connected by several directed branches and that is a graphical representation of a set of linear relations.

**Simulation** A model of a system that is used to investigate the behavior of a system by utilizing actual input signals.

**Steady state** The value that the output achieves after all the transient constituents of the response have faded. Also referred to as the final value.

**s-plane** The complex plane where, given the complex number  $s = \sigma + j\omega$ , the  $x$ -axis (or horizontal axis) is the  $\sigma$ -axis, and the  $y$ -axis (or vertical axis) is the  $j\omega$ -axis.

**Taylor series** A power series defined by  $g(x) = \sum_{m=0}^{\infty} \frac{g^{(m)}(x_0)}{m!} (x - x_0)^m$ . For  $m < \infty$ , the series is an approximation which is used to linearize functions and system models.

**Through-variable** A variable that has the same value at both ends of an element.

**Time constant** The time interval necessary for a system to change from one state to another by a specified percentage. For a first order system, the time constant is the time it takes the output to manifest a 63.2% change due to a step input.

**Transfer function** The ratio of the Laplace transform of the output variable to the Laplace transform of the input variable.

**Underdamped** The case where the damping ratio is  $\zeta < 1$ .

**Unity feedback** A feedback control system wherein the gain of the feedback loop is one.

**Viscous damper** A type of mechanical damper where the model of the friction force is linearly proportional to the velocity of the mass.

**Zeros** The roots of the numerator polynomial of the transfer function.

3.1 INTRODUCTION

In the preceding chapter, we developed and studied several useful approaches to the analysis and design of feedback systems. The Laplace transform was used to transform the differential equations representing the system to an algebraic equation expressed in terms of the complex variable  $s$ . Using this algebraic equation, we were able to obtain a transfer function representation of the input-output relationship.

The ready availability of digital computers makes it practical to consider the time-domain formulation of the equations representing control systems. The time-domain techniques can be used for nonlinear, time-varying, and multivariable systems.

**A time-varying control system is a system in which one or more of the parameters of the system may vary as a function of time.**

For example, the mass of a missile varies as a function of time as the fuel is expended during flight. A multivariable system, as discussed in Section 2.6, is a system with several input and output signals.

The solution of a time-domain formulation of a control system problem is facilitated by the availability and ease of use of digital computers. Therefore we are interested in reconsidering the time-domain description of dynamic systems as they are represented by the system differential equation. The **time domain** is the mathematical domain that incorporates the response and description of a system in terms of time,  $t$ .

The time-domain representation of control systems is an essential basis for modern control theory and system optimization. In Chapter 11, we will have an opportunity to design an optimum control system by utilizing time-domain methods. In this chapter, we develop the time-domain representation of control systems and illustrate several methods for the solution of the system time response.

3.2 THE STATE VARIABLES OF A DYNAMIC SYSTEM

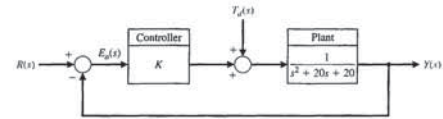
The time-domain analysis and design of control systems uses the concept of the state of a system [1-3, 5].

**The state of a system is a set of variables whose values, together with the input signals and the equations describing the dynamics, will provide the future state and output of the system.**

For a dynamic system, the state of a system is described in terms of a set of **state variables**  $[x_1(t), x_2(t), \dots, x_n(t)]$ . The state variables are those variables that determine the future behavior of a system when the present state of the system and the excitation signals are known. Consider the system shown in Figure 3.1, where  $y_1(t)$

$T_d(s) = 1/s$  and co-plot the steady-state value of the output  $Y(s)$  as a function of the controller gain  $0 < K \leq 10$  on the same plot as in (a) above.

(c) Determine the value of  $K$  such that the steady-state value of the output is equal for both the input response and the disturbance response.



**FIGURE CP2.10** Block diagram of a unity feedback system with a reference input  $R(s)$  and a disturbance input  $T_d(s)$ .



**ANSWERS TO SKILLS CHECK**

True or False: (1) False; (2) True; (3) False; (4) True; (5) True  
 Word Match (in order, top to bottom): e, j, d, h, a, f, c, b, k, g, o, l, n, m, i  
 Multiple Choice: (6) b; (7) a; (8) b; (9) b; (10) c; (11) a; (12) a; (13) c; (14) a; (15) a

**TERMS AND CONCEPTS**

**Across-Variable** A variable determined by measuring the difference of the values at the two ends of an element.

**Actuator** The device that causes the process to provide the output. The device that provides the motive power to the process.

**Analogous variables** Variables associated with electrical, mechanical, thermal, and fluid systems possessing similar solutions providing the analyst with the ability to extend the solution of one system to all analogous systems with the same describing differential equations.

**Assumptions** Statements that reflect situations and conditions that are taken for granted and without proof. In control systems, assumptions are often employed to simplify the physical dynamical models of systems under consideration to make the control design problem more tractable.

**Block diagrams** Unidirectional, operational blocks that represent the transfer functions of the elements of the system.

**Branch** A unidirectional path segment in a signal-flow graph that relates the dependency of an input and an output variable.

**Characteristic equation** The relation formed by equating to zero the denominator of a transfer function.

**Close-loop transfer function** A ratio of the output signal to the input signal for an interconnection of systems when all the feedback or feedforward loops have been closed or otherwise accounted for. Generally obtained by block diagram or signal-flow graph reduction.

**Coulomb damper** A type of mechanical damper where the model of the friction force is a nonlinear function of the mass velocity and possesses a discontinuity around zero velocity. Also known as dry friction.

**Critical damping** The case where damping is on the boundary between underdamped and overdamped.

**Damped oscillation** An oscillation in which the amplitude decreases with time.

**Damping ratio** A measure of damping. A dimensionless number for the second-order characteristic equation.

**DC motor** An electric actuator that uses an input voltage as a control variable.

**Differential equation** An equation including differentials of a function.

**Error signal** The difference between the desired output  $R(s)$  and the actual output  $Y(s)$ ; therefore  $E_e(s) = R(s) - Y(s)$ .

**Final value** The value that the output achieves after all the transient constituents of the response have faded. Also referred to as the steady-state value.

**Final value theorem** The theorem that states that  $\lim_{t \rightarrow \infty} y(t) = \lim_{s \rightarrow 0} sY(s)$ , where  $Y(s)$  is the Laplace transform of  $y(t)$ .

CHAPTER

3

State Variable Models

3.1 Introduction 162  
 3.2 The State Variables of a Dynamic System 162  
 3.3 The State Differential Equation 166  
 3.4 Signal-Flow Graph and Block Diagram Models 171  
 3.5 Alternative Signal-Flow Graph and Block Diagram Models 182  
 3.6 The Transfer Function from the State Equation 187  
 3.7 The Time Response and the State Transition Matrix 189  
 3.8 Design Examples 193  
 3.9 Analysis of State Variable Models Using Control Design Software 206  
 3.10 Sequential Design Example: Disk Drive Read System 209  
 3.11 Summary 213

P R E V I E W

In this chapter, we consider system modeling using time-domain methods. As before, we will consider physical systems described by an  $n$ th-order ordinary differential equation. Utilizing a (nonunique) set of variables, known as state variables, we can obtain a set of first-order differential equations. We group these first-order equations using a compact matrix notation in a model known as the state variable model. The time-domain state variable model lends itself readily to computer solution and analysis. The relationship between signal-flow graph models and state variable models will be investigated. Several interesting physical systems, including a space station and a printer belt drive, are presented and analyzed. The chapter concludes with the development of a state variable model for the Sequential Design Example: Disk Drive Read System.

DESIRED OUTCOMES

Upon completion of Chapter 3, students should:

- Understand state variables, state differential equations, and output equations.
- Recognize that state variable models can describe the dynamic behavior of physical systems and can be represented by block diagrams and signal flow graphs.
- Know how to obtain the transfer function model from a state variable model, and vice versa.
- Be aware of solution methods for state variable models and the role of the state transition matrix in obtaining the time responses.
- Understand the important role of state variable modeling in control system design.





FIGURE 3.3 A spring-mass-damper system.

To write Equation (3.1) in terms of the state variables, we substitute the state variables as already defined and obtain

$$M \frac{dx_2}{dt} + bx_2 + kx_1 = u(t). \quad (3.2)$$

Therefore, we can write the equations that describe the behavior of the spring-mass-damper system as the set of two first-order differential equations

$$\frac{dx_1}{dt} = x_2 \quad (3.3)$$

and

$$\frac{dx_2}{dt} = -\frac{b}{M}x_2 - \frac{k}{M}x_1 + \frac{1}{M}u. \quad (3.4)$$

This set of differential equations describes the behavior of the state of the system in terms of the rate of change of each state variable.

As another example of the state variable characterization of a system, consider the *RLC* circuit shown in Figure 3.4. The state of this system can be described by a set of state variables  $(x_1, x_2)$ , where  $x_1$  is the capacitor voltage  $v_c(t)$  and  $x_2$  is the inductor current  $i_L(t)$ . This choice of state variables is intuitively satisfactory because the stored energy of the network can be described in terms of these variables as

$$\mathcal{E} = \frac{1}{2}Li_L^2 + \frac{1}{2}Cv_c^2. \quad (3.5)$$

Therefore  $x_1(t_0)$  and  $x_2(t_0)$  provide the total initial energy of the network and the state of the system at  $t = t_0$ . For a passive *RLC* network, the number of state variables required is equal to the number of independent energy-storage elements. Utilizing Kirchhoff's current law at the junction, we obtain a first-order differential equation by describing the rate of change of capacitor voltage as

$$i_c = C \frac{dv_c}{dt} = +u(t) - i_L. \quad (3.6)$$

Kirchhoff's voltage law for the right-hand loop provides the equation describing the rate of change of inductor current as

$$L \frac{di_L}{dt} = -Ri_L + v_c. \quad (3.7)$$

The output of this system is represented by the linear algebraic equation

$$v_o = Ri_L(t).$$

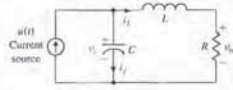


FIGURE 3.4 An *RLC* circuit.

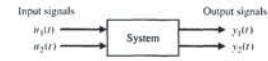


FIGURE 3.1 System block diagram.

and  $y_2(t)$  are the output signals and  $u_1(t)$  and  $u_2(t)$  are the input signals. A set of state variables  $(x_1, x_2, \dots, x_n)$  for the system shown in the figure is a set such that knowledge of the initial values of the state variables  $[x_1(t_0), x_2(t_0), \dots, x_n(t_0)]$  at the initial time  $t_0$ , and of the input signals  $u_1(t)$  and  $u_2(t)$  for  $t \geq t_0$ , suffices to determine the future values of the outputs and state variables [2].

**The state variables describe the present configuration of a system and can be used to determine the future response, given the excitation inputs and the equations describing the dynamics.**

The general form of a dynamic system is shown in Figure 3.2. A simple example of a state variable is the state of an on-off light switch. The switch can be in either the on or the off position, and thus the state of the switch can assume one of two possible values. Thus, if we know the present state (position) of the switch at  $t_0$  and if an input is applied, we are able to determine the future value of the state of the element.

The concept of a set of state variables that represent a dynamic system can be illustrated in terms of the spring-mass-damper system shown in Figure 3.3. The number of state variables chosen to represent this system should be as small as possible in order to avoid redundant state variables. A set of state variables sufficient to describe this system includes the position and the velocity of the mass. Therefore, we will define a set of state variables as  $(x_1, x_2)$ , where

$$x_1(t) = y(t) \quad \text{and} \quad x_2(t) = \frac{dy(t)}{dt}.$$

The differential equation describes the behavior of the system and is usually written as

$$M \frac{d^2y}{dt^2} + b \frac{dy}{dt} + ky = u(t). \quad (3.1)$$

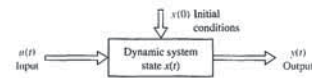


FIGURE 3.2 Dynamic system.

3.3 THE STATE DIFFERENTIAL EQUATION

The response of a system is described by the set of first-order differential equations written in terms of the state variables  $(x_1, x_2, \dots, x_n)$  and the inputs  $(u_1, u_2, \dots, u_m)$ . These first-order differential equations can be written in general form as

$$\begin{aligned} \dot{x}_1 &= a_{11}x_1 + a_{12}x_2 + \dots + a_{1n}x_n + b_{11}u_1 + \dots + b_{1m}u_m, \\ \dot{x}_2 &= a_{21}x_1 + a_{22}x_2 + \dots + a_{2n}x_n + b_{21}u_1 + \dots + b_{2m}u_m, \\ &\vdots \\ \dot{x}_n &= a_{n1}x_1 + a_{n2}x_2 + \dots + a_{nn}x_n + b_{n1}u_1 + \dots + b_{nm}u_m, \end{aligned} \quad (3.13)$$

where  $\dot{x} = dx/dt$ . Thus, this set of simultaneous differential equations can be written in matrix form as follows [2, 5]:

$$\frac{d}{dt} \begin{bmatrix} x_1 \\ x_2 \\ \vdots \\ x_n \end{bmatrix} = \begin{bmatrix} a_{11} & a_{12} & \dots & a_{1n} \\ a_{21} & a_{22} & \dots & a_{2n} \\ \vdots & \vdots & \dots & \vdots \\ a_{n1} & a_{n2} & \dots & a_{nn} \end{bmatrix} \begin{bmatrix} x_1 \\ x_2 \\ \vdots \\ x_n \end{bmatrix} + \begin{bmatrix} b_{11} & \dots & b_{1m} \\ b_{21} & \dots & b_{2m} \\ \vdots & \dots & \vdots \\ b_{n1} & \dots & b_{nm} \end{bmatrix} \begin{bmatrix} u_1 \\ \vdots \\ u_m \end{bmatrix}. \quad (3.14)$$

The column matrix consisting of the state variables is called the **state vector** and is written as

$$\mathbf{x} = \begin{bmatrix} x_1 \\ x_2 \\ \vdots \\ x_n \end{bmatrix}, \quad (3.15)$$

where the boldface indicates a vector. The vector of input signals is defined as  $\mathbf{u}$ . Then the system can be represented by the compact notation of the **state differential equation** as

$$\dot{\mathbf{x}} = \mathbf{Ax} + \mathbf{Bu}. \quad (3.16)$$

The differential equation (3.16) is also commonly called the state equation.

The matrix  $\mathbf{A}$  is an  $n \times n$  square matrix, and  $\mathbf{B}$  is an  $n \times m$  matrix.<sup>1</sup> The state differential equation relates the rate of change of the state of the system to the state of the system and the input signals. In general, the outputs of a linear system can be related to the state variables and the input signals by the **output equation**

$$\mathbf{y} = \mathbf{Cx} + \mathbf{Du}. \quad (3.17)$$

<sup>1</sup>Boldfaced lowercase letters denote vector quantities and boldfaced uppercase letters denote matrices. For an introduction to matrices and elementary matrix operations, refer to the MCS website and references [1] and [2].

We can rewrite Equations (3.6) and (3.7) as a set of two first-order differential equations in terms of the state variables  $x_1$  and  $x_2$  as follows:

$$\frac{dx_1}{dt} = -\frac{1}{C}x_2 + \frac{1}{C}u(t), \quad (3.8)$$

and

$$\frac{dx_2}{dt} = +\frac{1}{L}x_1 - \frac{R}{L}x_2. \quad (3.9)$$

The output signal is then

$$y(t) = v_o(t) = Rx_2. \quad (3.10)$$

Utilizing Equations (3.8) and (3.9) and the initial conditions of the network represented by  $[x_1(t_0), x_2(t_0)]$ , we can determine the system's future behavior and its output.

The state variables that describe a system are not a unique set, and several alternative sets of state variables can be chosen. For example, for a second-order system, such as the spring-mass-damper or *RLC* circuit, the state variables may be any two independent linear combinations of  $x_1(t)$  and  $x_2(t)$ . For the *RLC* circuit, we might choose the set of state variables as the two voltages,  $v_c(t)$  and  $v_L(t)$ , where  $v_L$  is the voltage drop across the inductor. Then the new state variables,  $x_1^*$  and  $x_2^*$ , are related to the old state variables,  $x_1$  and  $x_2$ , as

$$x_1^* = v_c = x_1, \quad (3.11)$$

and

$$x_2^* = v_L = v_c - Ri_L = x_1 - Rx_2. \quad (3.12)$$

Equation (3.12) represents the relation between the inductor voltage and the former state variables  $v_c$  and  $i_L$ . In a typical system, there are several choices of a set of state variables that specify the energy stored in a system and therefore adequately describe the dynamics of the system. It is usual to choose a set of state variables that can be readily measured.

An alternative approach to developing a model of a device is the use of the bond graph. Bond graphs can be used for electrical, mechanical, hydraulic, and thermal devices or systems as well as for combinations of various types of elements. Bond graphs produce a set of equations in the state variable form [7].

The state variables of a system characterize the dynamic behavior of a system. The engineer's interest is primarily in physical systems, where the variables are voltages, currents, velocities, positions, pressures, temperatures, and similar physical variables. However, the concept of system state is not limited to the analysis of physical systems and is particularly useful in analyzing biological, social, and economic systems. For these systems, the concept of state is extended beyond the concept of the current configuration of a physical system to the broader viewpoint of variables that will be capable of describing the future behavior of the system.

which converges for all finite  $t$  and any  $\mathbf{A}$  [2]. Then the solution of the state differential equation is found to be

$$\mathbf{x}(t) = \exp(\mathbf{A}t)\mathbf{x}(0) + \int_0^t \exp[\mathbf{A}(t - \tau)]\mathbf{B}\mathbf{u}(\tau) d\tau. \quad (3.24)$$

Equation (3.24) may be verified by taking the Laplace transform of Equation (3.16) and rearranging to obtain

$$\mathbf{X}(s) = [s\mathbf{I} - \mathbf{A}]^{-1}\mathbf{x}(0) + [s\mathbf{I} - \mathbf{A}]^{-1}\mathbf{B}\mathbf{U}(s), \quad (3.25)$$

where we note that  $[s\mathbf{I} - \mathbf{A}]^{-1} = \Phi(s)$  is the Laplace transform of  $\Phi(t) = \exp(\mathbf{A}t)$ . Taking the inverse Laplace transform of Equation (3.25) and noting that the second term on the right-hand side involves the product  $\Phi(s)\mathbf{B}\mathbf{U}(s)$ , we obtain Equation (3.24). The matrix exponential function describes the unforced response of the system and is called the **fundamental** or **state transition matrix**  $\Phi(t)$ . Thus, Equation (3.24) can be written as

$$\mathbf{x}(t) = \Phi(t)\mathbf{x}(0) + \int_0^t \Phi(t - \tau)\mathbf{B}\mathbf{u}(\tau) d\tau. \quad (3.26)$$

The solution to the unforced system (that is, when  $\mathbf{u} = 0$ ) is simply

$$\begin{bmatrix} x_1(t) \\ x_2(t) \\ \vdots \\ x_n(t) \end{bmatrix} = \begin{bmatrix} \phi_{11}(t) & \cdots & \phi_{1n}(t) \\ \phi_{21}(t) & \cdots & \phi_{2n}(t) \\ \vdots & \ddots & \vdots \\ \phi_{n1}(t) & \cdots & \phi_{nn}(t) \end{bmatrix} \begin{bmatrix} x_1(0) \\ x_2(0) \\ \vdots \\ x_n(0) \end{bmatrix}, \quad (3.27)$$

We note therefore that to determine the state transition matrix, all initial conditions are set to 0 except for one state variable, and the output of each state variable is evaluated. That is, the term  $\phi_{ij}(t)$  is the response of the  $i$ th state variable due to an initial condition on the  $j$ th state variable when there are zero initial conditions on all the other variables. We shall use this relationship between the initial conditions and the state variables to evaluate the coefficients of the transition matrix in a later section. However, first we shall develop several suitable signal-flow state models of systems and investigate the stability of the systems by utilizing these flow graphs.

**EXAMPLE 3.1 Two rolling carts**

Consider the system shown in Figure 3.5. The variables of interest are noted on the figure and defined as:  $M_1, M_2$  = mass of carts,  $p, q$  = position of carts,  $u$  = external force acting on system,  $k_1, k_2$  = spring constants, and  $b_1, b_2$  = damping coefficients. The free-body diagram of mass  $M_1$  is shown in Figure 3.6(b), where  $\dot{p}, \dot{q}$  = velocity of  $M_1$  and  $M_2$ , respectively. We assume that the carts have negligible rolling friction. We consider any existing rolling friction to be lumped into the damping coefficients,  $b_1$  and  $b_2$ .

where we use the relationship for  $\ddot{p}$  given in Equation (3.28) and the relationship for  $\ddot{q}$  given in Equation (3.29). But  $\dot{p} = x_3$  and  $\dot{q} = x_4$ , so Equation (3.32) can be written as

$$\dot{x}_3 = -\frac{k_1}{M_1}x_1 + \frac{k_1}{M_1}x_2 - \frac{b_1}{M_1}x_3 + \frac{b_1}{M_1}x_4 + \frac{1}{M_1}u \quad (3.34)$$

and Equation (3.33) as

$$\dot{x}_4 = \frac{k_1}{M_2}x_1 - \frac{k_1 + k_2}{M_2}x_2 + \frac{b_1}{M_2}x_3 - \frac{b_1 + b_2}{M_2}x_4. \quad (3.35)$$

In matrix form, Equations (3.30), (3.31), (3.34), and (3.35) can be written as

$$\dot{\mathbf{x}} = \mathbf{A}\mathbf{x} + \mathbf{B}u$$

where

$$\mathbf{x} = \begin{pmatrix} x_1 \\ x_2 \\ x_3 \\ x_4 \end{pmatrix} = \begin{pmatrix} p \\ q \\ \dot{p} \\ \dot{q} \end{pmatrix},$$

$$\mathbf{A} = \begin{bmatrix} 0 & 0 & 1 & 0 \\ 0 & 0 & 0 & 1 \\ -\frac{k_1}{M_1} & \frac{k_1}{M_1} & -\frac{b_1}{M_1} & \frac{b_1}{M_1} \\ \frac{k_1}{M_2} & -\frac{k_1 + k_2}{M_2} & \frac{b_1}{M_2} & -\frac{b_1 + b_2}{M_2} \end{bmatrix}, \text{ and } \mathbf{B} = \begin{bmatrix} 0 \\ 0 \\ \frac{1}{M_1} \\ 0 \end{bmatrix}.$$

and  $u$  is the external force acting on the system (see Figure 3.6). If we choose  $p$  as the output, then

$$y = [1 \ 0 \ 0 \ 0]\mathbf{x} = \mathbf{C}\mathbf{x}.$$

Suppose that the two rolling carts have the following parameter values:  $k_1 = 150$  N/m;  $k_2 = 700$  N/m;  $b_1 = 15$  N s/m;  $b_2 = 30$  N s/m;  $M_1 = 5$  kg; and  $M_2 = 20$  kg. The

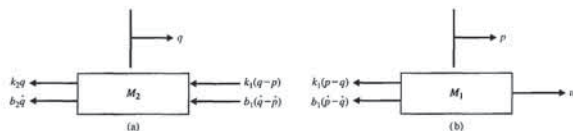


FIGURE 3.6 Free-body diagrams of the two rolling carts. (a) Cart 2; (b) Cart 1.

where  $\mathbf{y}$  is the set of output signals expressed in column vector form. The **state-space representation** (or state-variable representation) comprises the state differential equation and the output equation.

We use Equations (3.8) and (3.9) to obtain the state variable differential equation for the *RLC* of Figure 3.4 as

$$\dot{\mathbf{x}} = \begin{bmatrix} 0 & -\frac{1}{C} \\ \frac{1}{L} & -\frac{R}{L} \end{bmatrix} \mathbf{x} + \begin{bmatrix} \frac{1}{C} \\ 0 \end{bmatrix} u(t) \quad (3.18)$$

and the output as

$$y = [0 \ R]\mathbf{x}. \quad (3.19)$$

When  $R = 3$ ,  $L = 1$ , and  $C = 1/2$ , we have

$$\dot{\mathbf{x}} = \begin{bmatrix} 0 & -2 \\ 1 & -3 \end{bmatrix} \mathbf{x} + \begin{bmatrix} 2 \\ 0 \end{bmatrix} u$$

and

$$y = [0 \ 3]\mathbf{x}.$$

The solution of the state differential equation (Equation 3.16) can be obtained in a manner similar to the method for solving a first-order differential equation. Consider the first-order differential equation

$$\dot{x} = ax + bu, \quad (3.20)$$

where  $x(t)$  and  $u(t)$  are scalar functions of time. We expect an exponential solution of the form  $e^{at}$ . Taking the Laplace transform of Equation (3.20), we have

$$sX(s) - x(0) = aX(s) + bU(s);$$

therefore,

$$X(s) = \frac{x(0)}{s - a} + \frac{b}{s - a}U(s). \quad (3.21)$$

The inverse Laplace transform of Equation (3.21) can be shown to be

$$x(t) = e^{at}x(0) + \int_0^t e^{a(t-\tau)}bu(\tau) d\tau. \quad (3.22)$$

We expect the solution of the general state differential equation to be similar to Equation (3.22) and to be of exponential form. The **matrix exponential function** is defined as

$$e^{\mathbf{A}t} = \exp(\mathbf{A}t) = \mathbf{I} + \mathbf{A}t + \frac{\mathbf{A}^2 t^2}{2!} + \cdots + \frac{\mathbf{A}^k t^k}{k!} + \cdots, \quad (3.23)$$

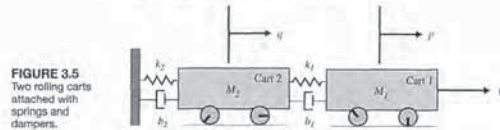


FIGURE 3.5 Two rolling carts attached with springs and dampers.

Now, given the free-body diagram with forces and directions appropriately applied, we use Newton's second law (sum of the forces equals mass of the object multiplied by its acceleration) to obtain the equations of motion—one equation for each mass. For mass  $M_1$  we have

$$M_1\ddot{p} = u + f_x + f_d = u - k_1(p - q) - b_1(\dot{p} - \dot{q}),$$

or

$$M_1\ddot{p} + b_1\dot{p} + k_1p = u + k_1q + b_1\dot{q}, \quad (3.28)$$

where

$$\ddot{p}, \dot{q} = \text{acceleration of } M_1 \text{ and } M_2, \text{ respectively.}$$

Similarly, for mass  $M_2$  we have

$$M_2\ddot{q} = k_1(p - q) + b_1(\dot{p} - \dot{q}) - k_2q - b_2\dot{q},$$

or

$$M_2\ddot{q} + (k_1 + k_2)q + (b_1 + b_2)\dot{q} = k_1p + b_1\dot{p}. \quad (3.29)$$

We now have a model given by the two second-order ordinary differential equations in Equations (3.28) and (3.29). We can start developing a state-space model by defining

$$\begin{aligned} x_1 &= p, \\ x_2 &= \dot{q}. \end{aligned}$$

We could have alternatively defined  $x_1 = q$  and  $x_2 = \dot{p}$ . The state-space model is not unique. Denoting the derivatives of  $x_1$  and  $x_2$  as  $x_3$  and  $x_4$ , respectively, it follows that

$$x_3 = \dot{x}_1 = \dot{p}, \quad (3.30)$$

$$x_4 = \dot{x}_2 = \dot{q}. \quad (3.31)$$

Taking the derivative of  $x_3$  and  $x_4$  yields, respectively,

$$\dot{x}_3 = \ddot{p} = \frac{b_1}{M_1}\dot{p} - \frac{k_1}{M_1}p + \frac{1}{M_1}u + \frac{k_1}{M_1}q + \frac{b_1}{M_1}\dot{q}, \quad (3.32)$$

$$\dot{x}_4 = \ddot{q} = \frac{k_1 + k_2}{M_2}q - \frac{b_1 + b_2}{M_2}\dot{q} + \frac{k_1}{M_2}p + \frac{b_1}{M_2}\dot{p}. \quad (3.33)$$



where  $\alpha$ ,  $\beta$ , and  $\gamma$  are functions of the circuit parameters  $R$ ,  $L$ , and  $C$ , respectively. The values of  $\alpha$ ,  $\beta$ , and  $\gamma$  can be determined from the differential equations that describe the circuit. For the  $RLC$  circuit (see Equations 3.8 and 3.9), we have

$$\dot{x}_1 = -\frac{1}{C}x_2 + \frac{1}{C}u(t), \quad (3.37)$$

$$\dot{x}_2 = \frac{1}{L}x_1 - \frac{R}{L}x_2, \quad (3.38)$$

and

$$v_o = Rx_2. \quad (3.39)$$

The flow graph representing these simultaneous equations is shown in Figure 3.8(a), where  $1/s$  indicates an integration. The corresponding block diagram model is shown in Figure 3.8(b). The transfer function is found to be

$$\frac{V_o(s)}{U(s)} = \frac{+R/(LCs^2)}{1 + R/(Ls) + 1/(LCs^2)} = \frac{+R/(LC)}{s^2 + (R/L)s + 1/(LC)}. \quad (3.40)$$

Unfortunately many electric circuits, electromechanical systems, and other control systems are not as simple as the  $RLC$  circuit of Figure 3.4, and it is often a difficult task to determine a set of first-order differential equations describing the system. Therefore, it is often simpler to derive the transfer function of the system by the techniques of Chapter 2 and then derive the state model from the transfer function.

The signal-flow graph state model and the block diagram model can be readily derived from the transfer function of a system. However, as we noted in Section 3.3,

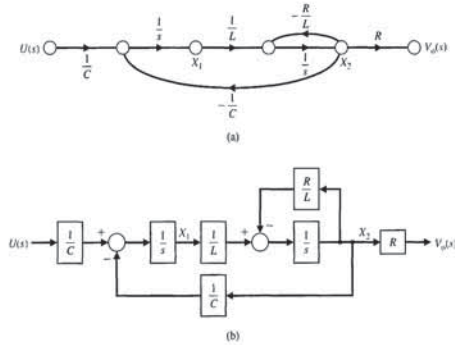


FIGURE 3.8  $RLC$  network. (a) Signal-flow graph. (b) Block diagram.

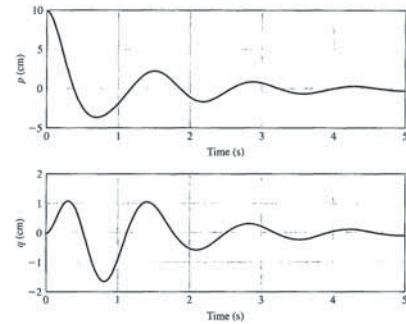


FIGURE 3.7 Initial condition response of the two cart system.

response of the two rolling cart system is shown in Figure 3.7 when the initial conditions are  $p(0) = 10$  cm,  $q(0) = 0$ , and  $\dot{p}(0) = \dot{q}(0) = 0$  and there is no input driving force, that is,  $u(t) = 0$ .

3.4 SIGNAL-FLOW GRAPH AND BLOCK DIAGRAM MODELS

The state of a system describes that system's dynamic behavior where the dynamics of the system are represented by a set of first-order differential equations. Alternatively, the dynamics of the system can be represented by a state differential equation as in Equation (3.16). In either case, it is useful to develop a graphical model of the system and use this model to relate the state variable concept to the familiar transfer function representation. The graphical model can be represented via signal-flow graphs or block diagrams.

As we have learned in previous chapters, a system can be meaningfully described by an input-output relationship, the transfer function  $G(s)$ . For example, if we are interested in the relation between the output voltage and the input voltage of the network of Figure 3.4, we can obtain the transfer function

$$G(s) = \frac{V_o(s)}{U(s)}$$

The transfer function for the  $RLC$  network of Figure 3.4 is of the form

$$G(s) = \frac{V_o(s)}{U(s)} = \frac{\alpha}{s^2 + \beta s + \gamma}. \quad (3.36)$$

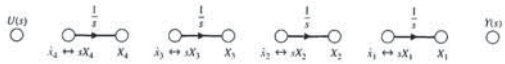


FIGURE 3.9 Flow graph nodes and integrators for fourth-order system.

represent the transfer function by the flow graph of Figure 3.10. Examining this figure, we note that all the loops are touching and that the transfer function of this flow graph is indeed Equation (3.45). The reader can readily verify this by noting that the forward-path factor of the flow graph is  $b_0/s^4$  and the denominator is equal to 1 minus the sum of the loop gains.

We can also consider the block diagram model of Equation (3.45). Rearranging the terms in Equation (3.45) and taking the inverse Laplace transform yields the differential equation model

$$\frac{d^4(y/b_0)}{dt^4} + a_3 \frac{d^3(y/b_0)}{dt^3} + a_2 \frac{d^2(y/b_0)}{dt^2} + a_1 \frac{d(y/b_0)}{dt} + a_0(y/b_0) = u.$$

Define the four state variables as follows:

$$\begin{aligned} x_1 &= y/b_0 \\ x_2 &= \dot{x}_1 = \dot{y}/b_0 \\ x_3 &= \dot{x}_2 = \ddot{y}/b_0 \\ x_4 &= \dot{x}_3 = \dddot{y}/b_0 \end{aligned}$$

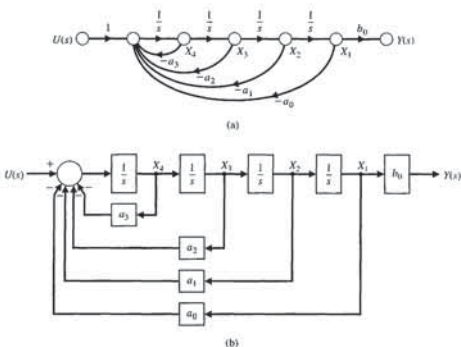


FIGURE 3.10 Model for  $G(s)$  of Equation (3.45). (a) Signal-flow graph. (b) Block diagram.

there is more than one alternative set of state variables, and therefore there is more than one possible form for the signal-flow graph and block diagram models. There are several key **canonical forms** of the state-variable representation, such as the phase variable canonical form, that we will investigate in this chapter. In general, we can represent a transfer function as

$$G(s) = \frac{Y(s)}{U(s)} = \frac{b_m s^m + b_{m-1} s^{m-1} + \dots + b_1 s + b_0}{s^n + a_{n-1} s^{n-1} + \dots + a_1 s + a_0} \quad (3.41)$$

where  $n \geq m$ , and all the  $a$  and  $b$  coefficients are real numbers. If we multiply the numerator and denominator by  $s^{-n}$ , we obtain

$$G(s) = \frac{b_m s^{-(n-m)} + b_{m-1} s^{-(n-m+1)} + \dots + b_1 s^{-(n-1)} + b_0 s^{-n}}{1 + a_{n-1} s^{-1} + \dots + a_1 s^{-(n-1)} + a_0 s^{-n}}. \quad (3.42)$$

Our familiarity with Mason's signal-flow gain formula allows us to recognize the familiar feedback factors in the denominator and the forward-path factors in the numerator. Mason's signal-flow gain formula was discussed in Section 2.7 and is written as

$$G(s) = \frac{Y(s)}{U(s)} = \frac{\sum_k P_k \Delta_k}{\Delta}. \quad (3.43)$$

When all the feedback loops are touching and all the forward paths touch the feedback loops, Equation (3.43) reduces to

$$G(s) = \frac{\sum_k P_k}{1 - \sum_{q=1}^N L_q} = \frac{\text{Sum of the forward-path factors}}{1 - \text{sum of the feedback loop factors}}. \quad (3.44)$$

There are several flow graphs that could represent the transfer function. Two flow graph configurations based on Mason's signal-flow gain formula are of particular interest, and we will consider these in greater detail. In the next section, we will consider two additional configurations: the physical state variable model and the diagonal (or Jordan canonical) form model.

To illustrate the derivation of the signal-flow graph state model, let us initially consider the fourth-order transfer function

$$\begin{aligned} G(s) &= \frac{Y(s)}{U(s)} = \frac{b_0}{s^4 + a_3 s^3 + a_2 s^2 + a_1 s + a_0} \\ &= \frac{b_0 s^{-4}}{1 + a_3 s^{-1} + a_2 s^{-2} + a_1 s^{-3} + a_0 s^{-4}} \end{aligned} \quad (3.45)$$

First we note that the system is fourth order, and hence we identify four state variables ( $x_1, x_2, x_3, x_4$ ). Recalling Mason's signal-flow gain formula, we note that the denominator can be considered to be 1 minus the sum of the loop gains. Furthermore, the numerator of the transfer function is equal to the forward-path factor of the flow graph. The flow graph must include a minimum number of integrators equal to the order of the system. Therefore, we use four integrators to represent this system. The necessary flow graph nodes and the four integrators are shown in Figure 3.9. Considering the simplest series interconnection of integrators, we can

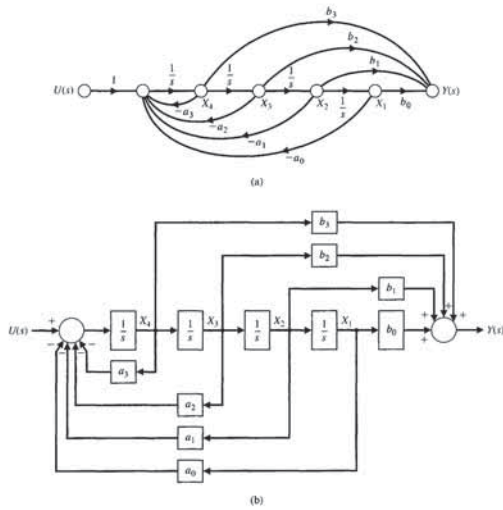


FIGURE 3.11 Model for  $G(s)$  of Equation (3.46) in the phase variable format. (a) Signal-flow graph. (b) Block diagram.

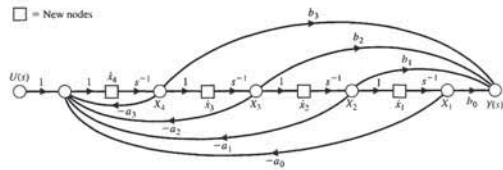


FIGURE 3.12 Flow graph of Figure 3.11 with nodes inserted.

In matrix form, we can represent the system in Equation (3.46) as

$$\dot{\mathbf{x}} = \mathbf{Ax} + \mathbf{Bu}, \quad (3.49)$$

or

$$\frac{d}{dt} \begin{bmatrix} x_1 \\ x_2 \\ x_3 \\ x_4 \end{bmatrix} = \begin{bmatrix} 0 & 1 & 0 & 0 \\ 0 & 0 & 1 & 0 \\ 0 & 0 & 0 & 1 \\ -a_0 & -a_1 & -a_2 & -a_3 \end{bmatrix} \begin{bmatrix} x_1 \\ x_2 \\ x_3 \\ x_4 \end{bmatrix} + \begin{bmatrix} 0 \\ 0 \\ 0 \\ 1 \end{bmatrix} u(t). \quad (3.50)$$

The output is then

$$y(t) = \mathbf{Cx} = [b_0 \quad b_1 \quad b_2 \quad b_3] \begin{bmatrix} x_1 \\ x_2 \\ x_3 \\ x_4 \end{bmatrix}. \quad (3.51)$$

The graphical structures of Figure 3.11 are not unique representations of Equation (3.46); another equally useful structure can be obtained. A flow graph that represents Equation (3.46) equally well is shown in Figure 3.13(a). In this case, the forward-path factors are obtained by feeding forward the signal  $U(s)$ . We will call this model the **input feedforward canonical form**.

Then the output signal  $y(t)$  is equal to the first state variable  $x_1(t)$ . This flow graph structure has the forward-path factors  $b_0/s^4, b_1/s^3, b_2/s^2, b_3/s$ , and all the forward paths touch the feedback loops. Therefore, the resulting transfer function is indeed equal to Equation (3.46).

Associated with the input feedforward format, we have the set of first-order differential equations

$$\begin{aligned} \dot{x}_1 &= -a_3x_1 + x_2 + b_3u, & \dot{x}_2 &= -a_2x_1 + x_3 + b_2u, \\ \dot{x}_3 &= -a_1x_1 + x_4 + b_1u, & \dot{x}_4 &= -a_0x_1 + b_0u. \end{aligned} \quad (3.52)$$

Thus, in matrix form, we have

$$\frac{d\mathbf{x}}{dt} = \begin{bmatrix} -a_3 & 1 & 0 & 0 \\ -a_2 & 0 & 1 & 0 \\ -a_1 & 0 & 0 & 1 \\ -a_0 & 0 & 0 & 0 \end{bmatrix} \mathbf{x} + \begin{bmatrix} b_3 \\ b_2 \\ b_1 \\ b_0 \end{bmatrix} u(t) \quad (3.53)$$

and

$$y(t) = [1 \quad 0 \quad 0 \quad 0]\mathbf{x} + [0]u(t).$$

Although the input feedforward canonical form of Figure 3.13 represents the same transfer function as the phase variable canonical form of Figure 3.11, the state variables of each graph are not equal. Furthermore we recognize that the initial conditions of the system can be represented by the initial conditions of the integrators,  $x_1(0), x_2(0), \dots, x_n(0)$ . Let us consider a control system and determine the state differential equation by utilizing the two forms of flow graph state models.

Then it follows that the fourth-order differential equation can be written equivalently as four first-order differential equations, namely,

$$\begin{aligned} \dot{x}_1 &= x_2, \\ \dot{x}_2 &= x_3, \\ \dot{x}_3 &= x_4, \end{aligned}$$

and

$$\dot{x}_4 = -a_0x_1 - a_1x_2 - a_2x_3 - a_3x_4 + u;$$

and the corresponding output equation is

$$y = b_0x_1.$$

The block diagram model can be readily obtained from the four first-order differential equations as illustrated in Figure 3.10(b).

Now consider the fourth-order transfer function when the numerator is a polynomial in  $s$ , so that we have

$$\begin{aligned} G(s) &= \frac{b_3s^3 + b_2s^2 + b_1s + b_0}{s^4 + a_3s^3 + a_2s^2 + a_1s + a_0} \\ &= \frac{b_3s^{-1} + b_2s^{-2} + b_1s^{-3} + b_0s^{-4}}{1 + a_3s^{-1} + a_2s^{-2} + a_1s^{-3} + a_0s^{-4}}. \end{aligned} \quad (3.46)$$

The numerator terms represent forward-path factors in Mason's signal-flow gain formula. The forward paths will touch all the loops, and a suitable signal-flow graph realization of Equation (3.46) is shown in Figure 3.11(a). The forward-path factors are  $b_0/s, b_1/s^2, b_2/s^3, b_3/s^4$  as required to provide the numerator of the transfer function. Recall that Mason's signal-flow gain formula indicates that the numerator of the transfer function is simply the sum of the forward-path factors. This general form of a signal-flow graph can represent the general transfer function of Equation (3.46) by utilizing  $n$  feedback loops involving the  $a_m$  coefficients and  $m$  forward-path factors involving the  $b_m$  coefficients. The general form of the flow graph state model and the block diagram model shown in Figure 3.11 is called the **phase variable canonical form**.

The state variables are identified in Figure 3.11 as the output of each energy storage element, that is, the output of each integrator. To obtain the set of first-order differential equations representing the state model of Equation (3.46), we will introduce a new set of flow graph nodes immediately preceding each integrator of Figure 3.11(a) [5, 6]. The nodes are placed before each integrator, and therefore they represent the derivative of the output of each integrator. The signal-flow graph, including the added nodes, is shown in Figure 3.12. Using the flow graph of this figure, we are able to obtain the following set of first-order differential equations describing the state of the model:

$$\begin{aligned} \dot{x}_1 &= x_2, & \dot{x}_2 &= x_3, & \dot{x}_3 &= x_4, \\ \dot{x}_4 &= -a_0x_1 - a_1x_2 - a_2x_3 - a_3x_4 + u. \end{aligned} \quad (3.47)$$

In this equation,  $x_1, x_2, \dots, x_n$  are the  $n$  phase variables.

The block diagram model can also be constructed directly from Equation (3.46). Define the intermediate variable  $Z(s)$  and rewrite Equation (3.46) as

$$G(s) = \frac{Y(s)}{U(s)} = \frac{b_3s^3 + b_2s^2 + b_1s + b_0}{s^4 + a_3s^3 + a_2s^2 + a_1s + a_0} \frac{Z(s)}{Z(s)}.$$

Notice that, by multiplying by  $Z(s)/Z(s)$ , we do not change the transfer function,  $G(s)$ . Equating the numerator and denominator polynomials yields

$$Y(s) = [b_3s^3 + b_2s^2 + b_1s + b_0]Z(s)$$

and

$$U(s) = [s^4 + a_3s^3 + a_2s^2 + a_1s + a_0]Z(s).$$

Taking the inverse Laplace transform of both equations yields the differential equations

$$y = b_3 \frac{d^3z}{dt^3} + b_2 \frac{d^2z}{dt^2} + b_1 \frac{dz}{dt} + b_0z$$

and

$$u = \frac{d^4z}{dt^4} + a_3 \frac{d^3z}{dt^3} + a_2 \frac{d^2z}{dt^2} + a_1 \frac{dz}{dt} + a_0z.$$

Define the four state variables as follows:

$$\begin{aligned} x_1 &= z \\ x_2 &= \dot{x}_1 = \dot{z} \\ x_3 &= \dot{x}_2 = \ddot{z} \\ x_4 &= \dot{x}_3 = \dddot{z}. \end{aligned}$$

Then the differential equation can be written equivalently as

$$\begin{aligned} \dot{x}_1 &= x_2, \\ \dot{x}_2 &= x_3, \\ \dot{x}_3 &= x_4, \end{aligned}$$

and

$$\dot{x}_4 = -a_0x_1 - a_1x_2 - a_2x_3 - a_3x_4 + u,$$

and the corresponding output equation is

$$y = b_0x_1 + b_1x_2 + b_2x_3 + b_3x_4.$$

The block diagram model can be readily obtained from the four first-order differential equations and the output equation as illustrated in Figure 3.11(b).

Furthermore, the output is simply

$$y(t) = b_0x_1 + b_1x_2 + b_2x_3 + b_3x_4. \quad (3.48)$$



Multiplying the numerator and denominator by  $s^{-3}$ , we have

$$T(s) = \frac{Y(s)}{U(s)} = \frac{2s^{-1} + 8s^{-2} + 6s^{-3}}{1 + 8s^{-1} + 16s^{-2} + 6s^{-3}} \quad (3.54)$$

The first model is the phase variable state model using the feedforward of the state variables to provide the output signal. The signal-flow graph and block diagram are shown in Figures 3.15(a) and (b), respectively. The state differential equation is

$$\dot{\mathbf{x}} = \begin{bmatrix} 0 & 1 & 0 \\ 0 & 0 & 1 \\ -6 & -16 & -8 \end{bmatrix} \mathbf{x} + \begin{bmatrix} 0 \\ 0 \\ 1 \end{bmatrix} u(t), \quad (3.55)$$

and the output is

$$y(t) = [6 \quad 8 \quad 2] \begin{bmatrix} x_1 \\ x_2 \\ x_3 \end{bmatrix} \quad (3.56)$$

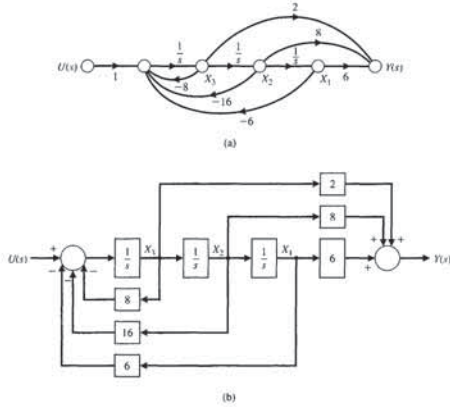


FIGURE 3.15 (a) Phase variable flow graph state model for  $T(s)$ . (b) Block diagram for the phase variable canonical form.

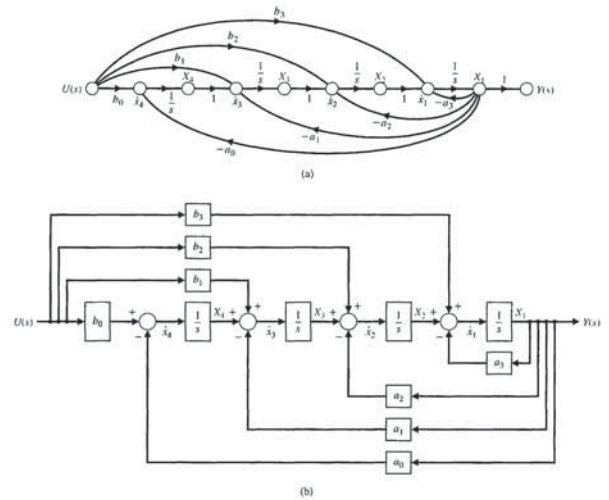


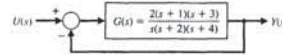
FIGURE 3.13 (a) Alternative flow graph state model for Equation (3.46). This model is called the input feedforward canonical form. (b) Block diagram of the input feedforward canonical form.

EXAMPLE 3.2 Two state variable models

A single-loop control system is shown in Figure 3.14. The closed-loop transfer function of the system is

$$T(s) = \frac{Y(s)}{U(s)} = \frac{2s^2 + 8s + 6}{s^3 + 8s^2 + 16s + 6}$$

FIGURE 3.14 Single-loop control system.



$$\frac{d^m y}{dt^m} + a_{m-1} \frac{d^{m-1} y}{dt^{m-1}} + \dots + a_0 y(t) = \frac{d^m u}{dt^m} + b_{m-1} \frac{d^{m-1} u}{dt^{m-1}} + \dots + b_0 u(t). \quad (3.58)$$

Accordingly, we can obtain the  $n$  first-order equations for the  $n$ th-order differential equation by utilizing the phase variable model or the input feedforward model of this section.

3.5 ALTERNATIVE SIGNAL-FLOW GRAPH AND BLOCK DIAGRAM MODELS

Often the control system designer studies an actual control system block diagram that represents physical devices and variables. An example of a model of a DC motor with shaft velocity as the output is shown in Figure 3.17 [9]. We wish to select the physical variables as the state variables. Thus, we select:  $x_1 = y(t)$ , the velocity output;  $x_2 = i(t)$ , the field current; and the third state variable,  $x_3$ , is selected to be  $x_3 = \frac{1}{s} i(t) = \frac{1}{s^2} u(t)$ , where  $u(t)$  is the field voltage. We may draw the models for these physical variables, as shown in Figure 3.18. Note that the state variables  $x_1$ ,  $x_2$ , and  $x_3$  are identified on the models. We will denote this format as the physical state variable model. This model is particularly useful when we can measure the physical state variables. Note that the model of each block is separately determined. For example, note that the transfer

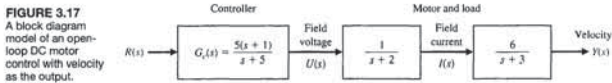


FIGURE 3.17 A block diagram model of an open-loop DC motor control with velocity as the output.

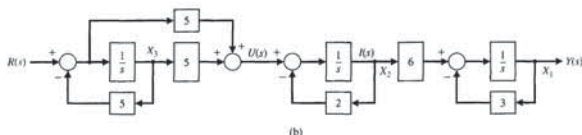
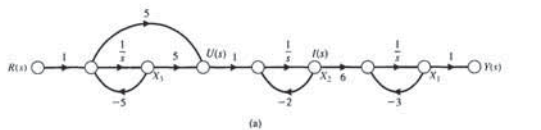


FIGURE 3.18 (a) The physical state variable signal-flow graph for the block diagram of Figure 3.17. (b) Physical state block diagram.

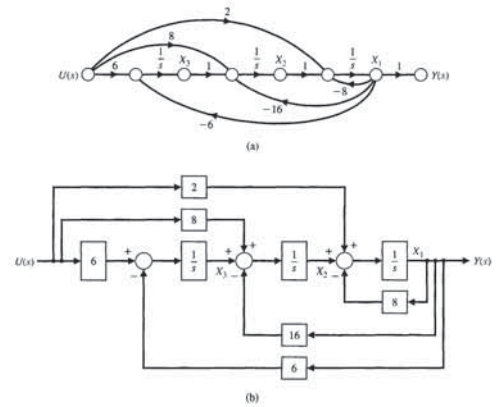


FIGURE 3.16 (a) Alternative flow graph state model for  $T(s)$  using the input feedforward canonical form. (b) Block diagram model.

The second model uses the feedforward of the input variable, as shown in Figure 3.16. The vector differential equation for the input feedforward model is

$$\dot{\mathbf{x}} = \begin{bmatrix} -8 & 1 & 0 \\ -16 & 0 & 1 \\ -6 & 0 & 0 \end{bmatrix} \mathbf{x} + \begin{bmatrix} 2 \\ 8 \\ 6 \end{bmatrix} u(t), \quad (3.57)$$

and the output is  $y(t) = x_1(t)$ .

We note that it was not necessary to factor the numerator or denominator polynomial to obtain the state differential equations for the phase variable model or the input feedforward model. Avoiding the factoring of polynomials permits us to avoid the tedious effort involved. Both models require three integrators because the system is third order. However, it is important to emphasize that the state variables of the state model of Figure 3.15 are not identical to the state variables of the state model of Figure 3.16. Of course, one set of state variables is related to the other set of state variables by an appropriate linear transformation of variables. A linear matrix transformation is represented by  $\mathbf{z} = \mathbf{M}\mathbf{x}$ , which transforms the  $\mathbf{x}$ -vector into the  $\mathbf{z}$ -vector by means of the  $\mathbf{M}$  matrix (see Appendix E on the MCS website). Finally, we note that the transfer function of Equation (3.41) represents a single-output linear constant coefficient system; thus, the transfer function can represent an  $n$ th-order differential equation

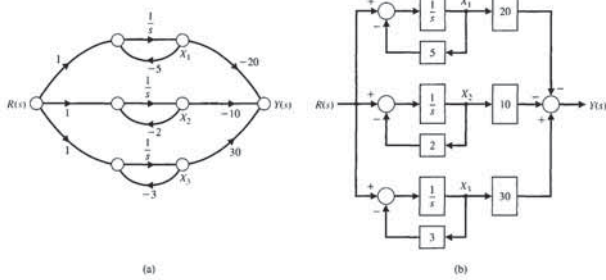


FIGURE 3.19 (a) The decoupled state variable flow graph model for the system shown in block diagram form in Figure 3.17. (b) The decoupled state variable block diagram model.

EXAMPLE 3.3 Spread of an epidemic disease

The spread of an epidemic disease can be described by a set of differential equations. The population under study is made up of three groups,  $x_1$ ,  $x_2$ , and  $x_3$ , such that the group  $x_1$  is susceptible to the epidemic disease, group  $x_2$  is infected with the disease, and group  $x_3$  has been removed from the initial population. The removal of  $x_3$  will be due to immunization, death, or isolation from  $x_1$ . The feedback system can be represented by the following equations:

$$\begin{aligned} \frac{dx_1}{dt} &= -\alpha x_1 - \beta x_2 + u_1(t), \\ \frac{dx_2}{dt} &= \beta x_1 - \gamma x_2 + u_2(t), \\ \frac{dx_3}{dt} &= \alpha x_1 + \gamma x_2. \end{aligned}$$

The rate at which new susceptibles are added to the population is equal to  $u_1(t)$ , and the rate at which new infectives are added to the population is equal to  $u_2(t)$ . For a closed population, we have  $u_1(t) = u_2(t) = 0$ . It is interesting to note that these equations could equally well represent the spread of information or a new idea through a population.

The physical state variables for this system are  $x_1$ ,  $x_2$ , and  $x_3$ . The model that represents this set of differential equations is shown in Figure 3.20. The vector differential equation is equal to

$$\frac{d}{dt} \begin{bmatrix} x_1 \\ x_2 \\ x_3 \end{bmatrix} = \begin{bmatrix} -\alpha & -\beta & 0 \\ \beta & -\gamma & 0 \\ \alpha & \gamma & 0 \end{bmatrix} \begin{bmatrix} x_1 \\ x_2 \\ x_3 \end{bmatrix} + \begin{bmatrix} 1 & 0 \\ 0 & 1 \\ 0 & 0 \end{bmatrix} \begin{bmatrix} u_1(t) \\ u_2(t) \end{bmatrix}. \quad (3.63)$$

EXAMPLE 3.4 Inverted pendulum control

The problem of balancing a broomstick on a person's hand is illustrated in Figure 3.21. The only equilibrium condition is  $\theta(t) = 0$  and  $d\theta/dt = 0$ . The problem of balancing a broomstick on one's hand is not unlike the problem of controlling the attitude of a missile during the initial stages of launch. This problem is the classic and intriguing problem of the inverted pendulum mounted on a cart, as shown in Figure 3.22. The cart must be moved so that mass  $m$  is always in an upright position. The state variables must be expressed in terms of the angular rotation  $\theta(t)$  and the position of the cart  $y(t)$ . The differential equations describing the motion of the system can be obtained by writing the sum of the forces in the horizontal direction and the sum of the moments about the pivot point [2, 3, 10, 23]. We will assume that  $M \gg m$  and the angle of rotation  $\theta$  is small so that the equations are linear. The sum of the forces in the horizontal direction is

$$M\ddot{y} + m\ddot{\theta} - u(t) = 0, \quad (3.66)$$

where  $u(t)$  equals the force on the cart, and  $l$  is the distance from the mass  $m$  to the pivot point. The sum of the torques about the pivot point is

$$m\ddot{y} + ml\ddot{\theta} - mlg\theta = 0. \quad (3.67)$$

The state variables for the two second-order equations are chosen as  $(x_1, x_2, x_3, x_4) = (y, \dot{y}, \theta, \dot{\theta})$ . Then Equations (3.66) and (3.67) are written in terms of the state variables as

$$M\dot{x}_2 + ml\dot{x}_4 - u(t) = 0 \quad (3.68)$$

FIGURE 3.21 An inverted pendulum balanced on a person's hand by moving the hand to reduce  $\theta(t)$ . Assume, for ease, that the pendulum rotates in the  $x$ - $y$  plane.

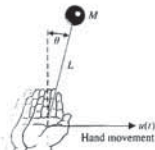
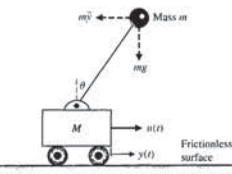


FIGURE 3.22 A cart and an inverted pendulum. The pendulum is constrained to pivot in the vertical plane.



function for the controller is

$$\frac{U(s)}{R(s)} = G_c(s) = \frac{5(s+1)}{s+5} = \frac{5+5s^{-1}}{1+5s^{-1}},$$

and the flow graph between  $R(s)$  and  $U(s)$  represents  $G_c(s)$ .

The state variable differential equation is directly obtained from Figure 3.18 as

$$\dot{\mathbf{x}} = \begin{bmatrix} -3 & 6 & 0 \\ 0 & -2 & -20 \\ 0 & 0 & -5 \end{bmatrix} \mathbf{x} + \begin{bmatrix} 0 \\ 5 \\ 1 \end{bmatrix} r(t) \quad (3.59)$$

and

$$\mathbf{y} = [1 \ 0 \ 0] \mathbf{x}. \quad (3.60)$$

A second form of the model we need to consider is the decoupled response modes. The overall input-output transfer function of the block diagram system shown in Figure 3.17 is

$$\frac{Y(s)}{R(s)} = T(s) = \frac{30(s+1)}{(s+5)(s+2)(s+3)} = \frac{q(s)}{(s-s_1)(s-s_2)(s-s_3)}$$

and the transient response has three modes dictated by  $s_1$ ,  $s_2$ , and  $s_3$ . These modes are indicated by the partial fraction expansion as

$$\frac{Y(s)}{R(s)} = T(s) = \frac{k_1}{s+5} + \frac{k_2}{s+2} + \frac{k_3}{s+3} \quad (3.61)$$

Using the procedure described in Chapter 2, we find that  $k_1 = -20$ ,  $k_2 = -10$ , and  $k_3 = 30$ . The decoupled state variable model representing Equation (3.61) is shown in Figure 3.19. The state variable matrix differential equation is

$$\dot{\mathbf{x}} = \begin{bmatrix} -5 & 0 & 0 \\ 0 & -2 & 0 \\ 0 & 0 & -3 \end{bmatrix} \mathbf{x} + \begin{bmatrix} 1 \\ 1 \\ 1 \end{bmatrix} r(t)$$

and

$$\mathbf{y}(t) = [-20 \ -10 \ 30] \mathbf{x}. \quad (3.62)$$

Note that we chose  $x_1$  as the state variable associated with  $s_1 = -5$ ,  $x_2$  associated with  $s_2 = -2$ , and  $x_3$  associated with  $s_3 = -3$ , as indicated in Figure 3.19. This choice of state variables is arbitrary; for example,  $x_1$  could be chosen as associated with the factor  $s+2$ .

The decoupled form of the state differential matrix equation displays the distinct model poles  $-s_1, -s_2, \dots, -s_m$ , and this format is often called the **diagonal canonical form**. A system can always be written in diagonal form if it possesses distinct poles; otherwise, it can only be written in a block diagonal form, known as the **Jordan canonical form** [24].

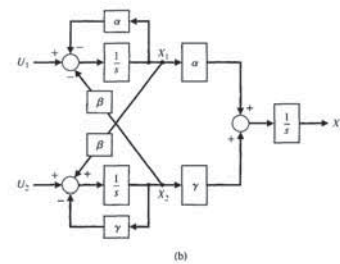
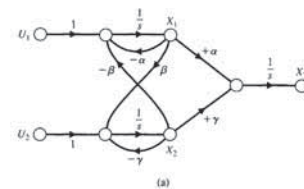


FIGURE 3.20 Model for the spread of an epidemic disease. (a) Signal-flow graph. (b) Block diagram model.

By examining Equation (3.63) and the models depicted in Figure 3.20, we find that the state variable  $x_3$  is dependent on  $x_1$  and  $x_2$  and does not affect the variables  $x_1$  and  $x_2$ .

Let us consider a closed population, so that  $u_1(t) = u_2(t) = 0$ . The equilibrium point in the state space for this system is obtained by setting  $dx/dt = 0$ . The equilibrium point in the state space is the point at which the system settles in the equilibrium, or rest, condition. Examining Equation (3.63), we find that the equilibrium point for this system is  $x_1 = x_2 = 0$ . Thus, to determine whether the epidemic disease is eliminated from the population, we must obtain the characteristic equation of the system. From the signal-flow graph shown in Figure 3.20, we obtain the flow graph determinant

$$\Delta(s) = 1 - (-\alpha s^{-1} - \gamma s^{-1} - \beta^2 s^{-2}) + (\alpha\gamma s^{-2}), \quad (3.64)$$

where there are three loops, two of which are nontouching. Thus, the characteristic equation is

$$q(s) = s^2 \Delta(s) = s^2 + (\alpha + \gamma)s + (\alpha\gamma + \beta^2) = 0. \quad (3.65)$$

The roots of this characteristic equation will lie in the left-hand  $s$ -plane when  $\alpha + \gamma > 0$  and  $\alpha\gamma + \beta^2 > 0$ . When roots are in the left-hand plane, we expect the unforced response to decay to zero as  $t \rightarrow \infty$ . ■



Since  $[s\mathbf{I} - \mathbf{A}]^{-1} = \Phi(s)$ , we have

$$\mathbf{X}(s) = \Phi(s)\mathbf{B}U(s).$$

Substituting  $\mathbf{X}(s)$  into Equation (3.77), we obtain

$$Y(s) = [\mathbf{C}\Phi(s)\mathbf{B} + \mathbf{D}]U(s). \quad (3.78)$$

Therefore, the transfer function  $G(s) = Y(s)/U(s)$  is

$$G(s) = \mathbf{C}\Phi(s)\mathbf{B} + \mathbf{D} \quad (3.79)$$

#### EXAMPLE 3.5 Transfer function of an RLC circuit

Let us determine the transfer function  $G(s) = Y(s)/U(s)$  for the RLC circuit of Figure 3.4 as described by the differential equations (see Equations 3.18 and 3.19):

$$\dot{\mathbf{x}} = \begin{bmatrix} 0 & -\frac{1}{C} \\ \frac{1}{L} & -\frac{R}{L} \end{bmatrix} \mathbf{x} + \begin{bmatrix} \frac{1}{C} \\ 0 \end{bmatrix} u$$

$$y = [0 \quad R]\mathbf{x}.$$

Then we have

$$[s\mathbf{I} - \mathbf{A}] = \begin{bmatrix} s & \frac{1}{C} \\ -\frac{1}{L} & s + \frac{R}{L} \end{bmatrix}.$$

Therefore, we obtain

$$\Phi(s) = [s\mathbf{I} - \mathbf{A}]^{-1} = \frac{1}{\Delta(s)} \begin{bmatrix} (s + \frac{R}{L}) & -\frac{1}{C} \\ \frac{1}{L} & s \end{bmatrix},$$

where

$$\Delta(s) = s^2 + \frac{R}{L}s + \frac{1}{LC}.$$

Then the transfer function is

$$G(s) = [0 \quad R] \begin{bmatrix} \frac{s + \frac{R}{L}}{\Delta(s)} & -\frac{1}{C\Delta(s)} \\ \frac{1}{L\Delta(s)} & \frac{s}{\Delta(s)} \end{bmatrix} \begin{bmatrix} \frac{1}{C} \\ 0 \end{bmatrix}$$

simply the inverse transform of  $\Phi(s)$ ; that is,

$$\Phi(t) = \mathcal{L}^{-1}\{\Phi(s)\}. \quad (3.83)$$

The relationship between a state variable  $X_i(s)$  and the initial conditions  $\mathbf{x}(0)$  is obtained by using Mason's signal-flow gain formula. Thus, for a second-order system, we would have

$$X_1(s) = \phi_{11}(s)x_1(0) + \phi_{12}(s)x_2(0),$$

$$X_2(s) = \phi_{21}(s)x_1(0) + \phi_{22}(s)x_2(0), \quad (3.84)$$

and the relation between  $X_i(s)$  as an output and  $x_1(0)$  as an input can be evaluated by Mason's signal-flow gain formula. All the elements of the state transition matrix,  $\phi_{ij}(s)$ , can be obtained by evaluating the individual relationships between  $X_i(s)$  and  $x_j(0)$  from the state model flow graph. An example will illustrate this approach to determining the transition matrix.

#### EXAMPLE 3.6 Evaluation of the state transition matrix

We will consider the RLC network of Figure 3.4. We seek to evaluate  $\Phi(s)$  by (1) determining the matrix inversion  $\Phi(s) = [s\mathbf{I} - \mathbf{A}]^{-1}$  and (2) using the signal-flow diagram and Mason's signal-flow gain formula.

First, we determine  $\Phi(s)$  by evaluating  $\Phi(s) = [s\mathbf{I} - \mathbf{A}]^{-1}$ . We note from Equation (3.18) that

$$\mathbf{A} = \begin{bmatrix} 0 & -2 \\ 1 & -3 \end{bmatrix}.$$

Then

$$[s\mathbf{I} - \mathbf{A}] = \begin{bmatrix} s & 2 \\ -1 & s + 3 \end{bmatrix}. \quad (3.85)$$

The inverse matrix is

$$\Phi(s) = [s\mathbf{I} - \mathbf{A}]^{-1} = \frac{1}{\Delta(s)} \begin{bmatrix} s + 3 & -2 \\ 1 & s \end{bmatrix}, \quad (3.86)$$

where  $\Delta(s) = s(s + 3) + 2 = s^2 + 3s + 2 = (s + 1)(s + 2)$ .

The signal-flow graph state model of the RLC network of Figure 3.4 is shown in Figure 3.8. This RLC network, which was discussed in Sections 3.3 and 3.4, can be represented by the state variables  $x_1 = v_c$  and  $x_2 = i_L$ . The initial conditions,  $x_1(0)$  and  $x_2(0)$ , represent the initial capacitor voltage and inductor current, respectively. The flow graph, including the initial conditions of each state variable, is shown in Figure 3.23. The initial conditions appear as the initial value of the state variable at the output of each integrator.

To obtain  $\Phi(s)$ , we set  $U(s) = 0$ . When  $R = 3$ ,  $L = 1$ , and  $C = 1/2$ , we obtain the signal-flow graph shown in Figure 3.24, where the output and input nodes are deleted because they are not involved in the evaluation of  $\Phi(s)$ . Then, using Mason's

and

$$\dot{x}_2 + \dot{i}x_4 - gx_3 = 0. \quad (3.69)$$

To obtain the necessary first-order differential equations, we solve for  $\dot{i}x_4$  in Equation (3.69) and substitute into Equation (3.68) to obtain

$$M\dot{x}_2 + mgx_3 = u(t), \quad (3.70)$$

since  $M \gg m$ . Substituting  $\dot{x}_2$  from Equation (3.68) into Equation (3.69), we have

$$M\dot{i}x_4 - Mgx_3 + u(t) = 0. \quad (3.71)$$

Therefore, the four first-order differential equations can be written as

$$\dot{x}_1 = x_2, \quad \dot{x}_2 = -\frac{mg}{M}x_3 + \frac{1}{M}u(t),$$

$$\dot{x}_3 = x_4, \quad \text{and} \quad \dot{x}_4 = \frac{g}{l}x_3 - \frac{1}{Ml}u(t). \quad (3.72)$$

Thus, the system matrices are

$$\mathbf{A} = \begin{bmatrix} 0 & 1 & 0 & 0 \\ 0 & 0 & -mg/M & 0 \\ 0 & 0 & 0 & 1 \\ 0 & 0 & g/l & 0 \end{bmatrix}, \quad \mathbf{B} = \begin{bmatrix} 0 \\ 1/M \\ 0 \\ -1/(Ml) \end{bmatrix}. \quad (3.73) \blacksquare$$

### 3.6 THE TRANSFER FUNCTION FROM THE STATE EQUATION

Given a transfer function  $G(s)$ , we can obtain the state variable equations using the signal-flow graph model. Now we turn to the matter of determining the transfer function  $G(s)$  of a single-input, single-output (SISO) system. Recalling Equations (3.16) and (3.17), we have

$$\dot{\mathbf{x}} = \mathbf{A}\mathbf{x} + \mathbf{B}u \quad (3.74)$$

and

$$y = \mathbf{C}\mathbf{x} + \mathbf{D}u \quad (3.75)$$

where  $y$  is the single output and  $u$  is the single input. The Laplace transforms of Equations (3.74) and (3.75) are

$$s\mathbf{X}(s) = \mathbf{A}\mathbf{X}(s) + \mathbf{B}U(s) \quad (3.76)$$

and

$$Y(s) = \mathbf{C}\mathbf{X}(s) + \mathbf{D}U(s) \quad (3.77)$$

where  $\mathbf{B}$  is an  $n \times 1$  matrix, since  $u$  is a single input. Note that we do not include initial conditions, since we seek the transfer function. Rearranging Equation (3.76), we obtain

$$(s\mathbf{I} - \mathbf{A})\mathbf{X}(s) = \mathbf{B}U(s).$$

$$= \frac{R/(LC)}{\Delta(s)} = \frac{R/(LC)}{s^2 + \frac{R}{L}s + \frac{1}{LC}},$$

which agrees with the result Equation (3.40) obtained from the flow graph model using Mason's signal-flow gain formula.  $\blacksquare$

### 3.7 THE TIME RESPONSE AND THE STATE TRANSITION MATRIX

It is often desirable to obtain the time response of the state variables of a control system and thus examine the performance of the system. The transient response of a system can be readily obtained by evaluating the solution to the state vector differential equation. In Section 3.3, we found that the solution for the state differential equation (3.26) was

$$\mathbf{x}(t) = \Phi(t)\mathbf{x}(0) + \int_0^t \Phi(t - \tau)\mathbf{B}u(\tau) d\tau. \quad (3.80)$$

Clearly, if the initial conditions  $\mathbf{x}(0)$ , the input  $u(\tau)$ , and the state transition matrix  $\Phi(t)$  are known, the time response of  $\mathbf{x}(t)$  can be numerically evaluated. Thus the problem focuses on the evaluation of  $\Phi(t)$ , the state transition matrix that represents the response of the system. Fortunately, the state transition matrix can be readily evaluated by using the signal-flow graph techniques with which we are already familiar.

Before proceeding to the evaluation of the state transition matrix using signal-flow graphs, we should note that several other methods exist for evaluating the transition matrix, such as the evaluation of the exponential series

$$\Phi(t) = \exp(\mathbf{A}t) = \sum_{k=0}^{\infty} \frac{\mathbf{A}^k t^k}{k!} \quad (3.81)$$

in a truncated form [2, 8]. Several efficient methods exist for the evaluation of  $\Phi(t)$  by means of a computer algorithm [21].

In Equation (3.25), we found that  $\Phi(s) = [s\mathbf{I} - \mathbf{A}]^{-1}$ . Therefore, if  $\Phi(s)$  is obtained by completing the matrix inversion, we can obtain  $\Phi(t)$  by noting that  $\Phi(t) = \mathcal{L}^{-1}\{\Phi(s)\}$ . The matrix inversion process is generally unwieldy for higher-order systems.

The usefulness of the signal-flow graph state model for obtaining the state transition matrix becomes clear upon consideration of the Laplace transformation version of Equation (3.80) when the input is zero. Taking the Laplace transformation of Equation (3.80) when  $u(\tau) = 0$ , we have

$$\mathbf{X}(s) = \Phi(s)\mathbf{x}(0). \quad (3.82)$$

Therefore, we can evaluate the Laplace transform of the transition matrix from the signal-flow graph by determining the relation between a state variable  $X_i(s)$  and the state initial conditions  $[x_1(0), x_2(0), \dots, x_n(0)]$ . Then the state transition matrix is

$$\phi_{22}(s) = \frac{1(1/s)}{1 + 3s^{-1} + 2s^{-2}} = \frac{s}{s^2 + 3s + 2} \quad (3.91)$$

Therefore, the state transition matrix in Laplace transformation form is

$$\Phi(s) = \begin{bmatrix} (s + 3)/(s^2 + 3s + 2) & -2/(s^2 + 3s + 2) \\ 1/(s^2 + 3s + 2) & s/(s^2 + 3s + 2) \end{bmatrix} \quad (3.92)$$

The factors of the characteristic equation are  $(s + 1)$  and  $(s + 2)$ , so that

$$(s + 1)(s + 2) = s^2 + 3s + 2.$$

Then the state transition matrix is

$$\Phi(t) = \mathcal{F}^{-1}\{\Phi(s)\} = \begin{bmatrix} (2e^{-t} - e^{-2t}) & (-2e^{-t} + 2e^{-2t}) \\ (e^{-t} - e^{-2t}) & (-e^{-t} + 2e^{-2t}) \end{bmatrix} \quad (3.93)$$

The evaluation of the time response of the RLC network to various initial conditions and input signals can now be evaluated by using Equation (3.80). For example, when  $x_1(0) = x_2(0) = 1$  and  $u(t) = 0$ , we have

$$\begin{bmatrix} x_1(t) \\ x_2(t) \end{bmatrix} = \Phi(t) \begin{bmatrix} 1 \\ 1 \end{bmatrix} = \begin{bmatrix} e^{-2t} \\ e^{-2t} \end{bmatrix} \quad (3.94)$$

The response of the system for these initial conditions is shown in Figure 3.25. The trajectory of the state vector  $[x_1(t), x_2(t)]$  on the  $(x_1, x_2)$ -plane is shown in Figure 3.26.

The evaluation of the time response is facilitated by the determination of the state transition matrix. Although this approach is limited to linear systems, it is a powerful method and utilizes the familiar signal-flow graph to evaluate the transition matrix. ■

FIGURE 3.25 Time response of the state variables of the RLC network for  $x_1(0) = x_2(0) = 1$ .

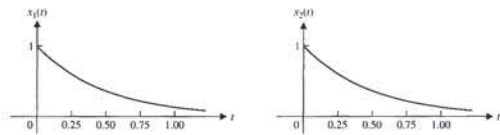
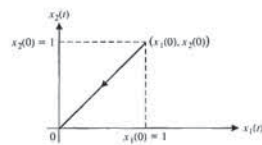


FIGURE 3.26 Trajectory of the state vector in the  $(x_1, x_2)$ -plane.



scientific instruments pointing up will see deep space, as desired. To achieve earth-pointing attitude, the spacecraft needs an attitude hold control system capable of applying the necessary torques. The torques are the inputs to the system, in this case, the space station. The attitude is the output of the system. The International Space Station employs control moment gyros and reaction control jets as actuators to control the attitude. The control moment gyros are momentum exchangers and are preferable to reaction control jets because they do not expend fuel. They are actuators that consist of a constant-rate flywheel mounted on a set of gimbals. The flywheel orientation is varied by rotating the gimbals, resulting in a change in direction of the flywheel angular momentum. In accord with the basic principle of conservation of angular momentum, changes in control moment gyro momentum must be transferred to the space station, thereby producing a reaction torque. The reaction torque can be employed to control the space station attitude. However, there is a maximum limit of control that can be provided by the control moment gyro. When that maximum is attained, the device is said to have reached saturation. So, while control moment gyros do not expend fuel, they can provide only a limited amount of control. In practice, it is possible to control the attitude of the space station while simultaneously desaturating the control moment gyros.

Several methods for desaturating the control moment gyros are available, but using existing natural environmental torques is the preferred method because it minimizes the use of the reaction control jets. A clever idea is to use gravity gradient torques (which occur naturally and come free of charge) to continuously desaturate the momentum exchange devices. Due to the variation of the earth's gravitational field over the International Space Station, the total moment generated by the gravitational forces about the spacecraft's center of mass is nonzero. This nonzero moment is called the gravity gradient torque. A change in attitude changes the gravity gradient torque acting on the vehicle. Thus, combining attitude control and momentum management becomes a matter of compromise.

The elements of the design process emphasized in this example are illustrated in Figure 3.28. We can begin the modeling process by defining the attitude of the space station using the three angles,  $\theta_2$  (the pitch angle),  $\theta_3$  (the yaw angle), and  $\theta_1$  (the roll angle). These three angles represent the attitude of the space station relative to the desired earth-pointing attitude. When  $\theta_1 = \theta_2 = \theta_3 = 0$ , the space station is oriented in the desired direction. The goal is to keep the space station oriented in the desired attitude while minimizing the amount of momentum exchange required by the control moment gyros (keeping in mind that we want to avoid saturation). The control goal can be stated as

**Control Goal**

Minimize the roll, yaw, and pitch angles in the presence of persistent external disturbances while simultaneously minimizing the control moment gyro momentum. The time rate of change of the angular momentum of a body about its center of mass is equal to the sum of the external torques acting on that body. Thus the attitude dynamics of a spacecraft are driven by externally acting torques. The main external torque acting on the space station is due to gravity. Since we treat the earth as a point mass, the gravity gradient torque [30] acting on the spacecraft is given by

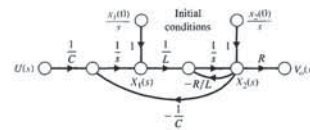


FIGURE 3.23 Flow graph of the RLC network.

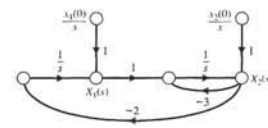


FIGURE 3.24 Flow graph of the RLC network with  $U(s) = 0$ .

signal-flow gain formula, we obtain  $X_1(s)$  in terms of  $x_1(0)$  as

$$X_1(s) = \frac{1 \cdot \Delta_1(s) \cdot [x_1(0)/s]}{\Delta(s)} \quad (3.87)$$

where  $\Delta(s)$  is the graph determinant, and  $\Delta_1(s)$  is the path cofactor. The graph determinant is

$$\Delta(s) = 1 + 3s^{-1} + 2s^{-2}.$$

The path cofactor is  $\Delta_1 = 1 + 3s^{-1}$  because the path between  $x_1(0)$  and  $X_1(s)$  does not touch the loop with the factor  $-3s^{-1}$ . Therefore, the first element of the transition matrix is

$$\phi_{11}(s) = \frac{(1 + 3s^{-1})(1/s)}{1 + 3s^{-1} + 2s^{-2}} = \frac{s + 3}{s^2 + 3s + 2} \quad (3.88)$$

The element  $\phi_{12}(s)$  is obtained by evaluating the relationship between  $X_1(s)$  and  $x_2(0)$  as

$$X_1(s) = \frac{(-2s^{-1})(x_2(0)/s)}{1 + 3s^{-1} + 2s^{-2}}.$$

Therefore, we obtain

$$\phi_{12}(s) = \frac{-2}{s^2 + 3s + 2} \quad (3.89)$$

Similarly, for  $\phi_{21}(s)$  we have

$$\phi_{21}(s) = \frac{(s^{-1})(1/s)}{1 + 3s^{-1} + 2s^{-2}} = \frac{1}{s^2 + 3s + 2} \quad (3.90)$$

Finally, for  $\phi_{22}(s)$ , we obtain

3.8 DESIGN EXAMPLES

In this section we present two illustrative design examples. In the first example, we present a detailed look at modeling a large space vehicle (such as a space station) using a state variable model. The state variable model is then used to take a look at the stability of the orientation of the spacecraft in a low earth orbit. The design process depicted in Figure 1.15 is highlighted in this example. The second example is a printer belt drive modeling exercise. The relationship between the state variable model and the block diagram discussed in Chapter 2 is illustrated and, using block diagram reduction methods, the transfer function equivalent of the state variable model is obtained.

**EXAMPLE 3.7 Modeling the orientation of a space station**

The International Space Station, shown in Figure 3.27, is a good example of a multi-purpose spacecraft that can operate in many different configurations. An important step in the control system design process is to develop a mathematical model of the spacecraft motion. In general, this model describes the translation and attitude motion of the spacecraft under the influence of external forces and torques, and controller and actuator forces and torques. The resulting spacecraft dynamic model is a set of highly coupled, nonlinear ordinary differential equations. Our objective is to simplify the model while retaining important system characteristics. This is not a trivial task, but an important, and often neglected component of control engineering. In this example, the rotational motion is considered. The translational motion, while critically important to orbit maintenance, can be decoupled from the rotational motion.

Many spacecraft (such as the International Space Station) will maintain an earth-pointing attitude. This means that cameras and other scientific instruments pointing down will be able to sense the earth, as depicted in Figure 3.27. Conversely,



FIGURE 3.27 The International Space Station moments after the Space Shuttle undocked from the Station. (Courtesy of NASA.)



attitude motion. The aerodynamic torque acting on the space station is generated by the atmospheric drag force that acts through the center of pressure. In general, the center of pressure and the center of mass do not coincide, so aerodynamic torques develop. In low earth orbit, the aerodynamic torque is a sinusoidal function that tends to oscillate around a small bias. The oscillation in the torque is primarily a result of the earth's diurnal atmospheric bulge. Due to heating, the atmosphere closest to the sun extends further into space than the atmosphere on the side of the earth away from the sun. As the space station travels around the earth (once every 90 minutes or so), it moves through varying air densities, thus causing a cyclic aerodynamic torque. Also, the space station solar panels rotate as they track the sun. This results in another cyclic component of aerodynamic torque. The aerodynamic torque is generally much smaller than the gravity gradient torque. Therefore, for design purposes we can ignore the atmospheric drag torque and view it as a disturbance torque. We would like the controller to minimize the effects of the aerodynamic disturbance on the spacecraft attitude.

Torques caused by the gravitation of other planetary bodies, magnetic fields, solar radiation and wind, and other less significant phenomena are much smaller than the earth's gravity-induced torque and aerodynamic torque. We ignore these torques in the dynamic model and view them as disturbances.

Finally, we need to discuss the control moment gyros themselves. First, we will lump all the control moment gyros together and view them as a single source of torque. We represent the total control moment gyro momentum with the variable  $\mathbf{h}$ . We need to know and understand the dynamics in the design phase to manage the angular momentum. But since the time constants associated with these dynamics are much shorter than for attitude dynamics, we can ignore the dynamics and assume that the control moment gyros can produce precisely and without a time delay the torque demanded by the control system.

Based on the above discussion, a simplified nonlinear model that we can use as the basis for the control design is

$$\dot{\Theta} = \mathbf{R}\Omega + \mathbf{n}, \tag{3.96}$$

$$\mathbf{I}\dot{\Omega} = -\Omega \times \mathbf{I}\Omega + 3n^2\mathbf{c} \times \mathbf{Ic} - \mathbf{u}, \tag{3.97}$$

$$\dot{\mathbf{h}} = -\Omega \times \mathbf{h} + \mathbf{u}, \tag{3.98}$$

where

$$\mathbf{R}(\Theta) = \frac{1}{\cos \theta_3} \begin{bmatrix} \cos \theta_3 & -\cos \theta_1 \sin \theta_3 & \sin \theta_1 \sin \theta_3 \\ 0 & \cos \theta_1 & -\sin \theta_1 \\ \cos \theta_3 & 0 & \cos \theta_1 \cos \theta_3 \end{bmatrix}$$

$$\mathbf{n} = \begin{bmatrix} 0 \\ n \\ 0 \end{bmatrix}, \quad \Omega = \begin{bmatrix} \omega_1 \\ \omega_2 \\ \omega_3 \end{bmatrix}, \quad \Theta = \begin{bmatrix} \theta_1 \\ \theta_2 \\ \theta_3 \end{bmatrix}, \quad \mathbf{u} = \begin{bmatrix} u_1 \\ u_2 \\ u_3 \end{bmatrix}$$

where  $\mathbf{u}$  is the control moment gyro input torque,  $\Omega$  is the angular velocity,  $\mathbf{I}$  is the moment of inertia matrix, and  $\mathbf{n}$  is the orbital angular velocity. Two good references that describe the fundamentals of spacecraft dynamic modeling are [26] and [27]. There have been many papers dealing with space station control and momentum

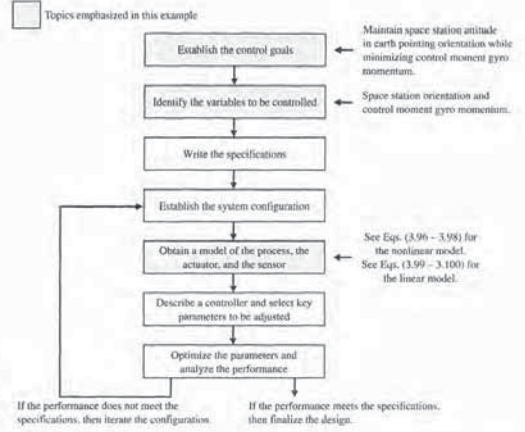


FIGURE 3.28 Elements of the control system design process emphasized in the spacecraft control example.

$$\mathbf{Ic} = 3n^2\mathbf{c} \times \mathbf{Ic}, \tag{3.95}$$

where  $n$  is the orbital angular velocity ( $n = 0.0011$  rad/s for the space station), and  $\mathbf{c}$  is

$$\mathbf{c} = \begin{bmatrix} -\sin \theta_2 \cos \theta_3 \\ \sin \theta_1 \cos \theta_2 + \cos \theta_1 \sin \theta_2 \sin \theta_3 \\ \cos \theta_1 \cos \theta_2 - \sin \theta_1 \sin \theta_2 \sin \theta_3 \end{bmatrix}$$

The notation ' $\times$ ' denotes vector cross-product. Matrix  $\mathbf{I}$  is the spacecraft inertia matrix and is a function of the space station configuration. It also follows from Equation (3.95) that the gravity gradient torques are a function of the attitude  $\theta_1$ ,  $\theta_2$ , and  $\theta_3$ . We want to maintain a prescribed attitude (that is earth-pointing  $\theta_1 = \theta_2 = \theta_3 = 0$ ), but sometimes we must deviate from that attitude so that we can generate gravity gradient torques to assist in the control moment gyro momentum management. Therein lies the conflict; as engineers we often are required to develop control systems to manage conflicting goals.

Now we examine the effect of the aerodynamic torque acting on the space station. Even at the high altitude of the space station, the aerodynamic torque does affect the

The subscript 2 refers to the pitch axis terms, the subscript 1 is for the roll axis terms, and 3 is for the yaw axis terms. The linearized equations for the roll/yaw axes are

$$\begin{bmatrix} \dot{\theta}_1 \\ \dot{\theta}_3 \\ \dot{\omega}_1 \\ \dot{\omega}_3 \\ \dot{h}_1 \\ \dot{h}_3 \end{bmatrix} = \begin{bmatrix} 0 & n & 1 & 0 & 0 & 0 \\ -n & 0 & 0 & 1 & 0 & 0 \\ -3n^2\Delta_1 & 0 & 0 & -n\Delta_1 & 0 & 0 \\ 0 & 0 & -n\Delta_3 & 0 & 0 & 0 \\ 0 & 0 & 0 & 0 & n & 0 \\ 0 & 0 & 0 & 0 & -n & 0 \end{bmatrix} \begin{bmatrix} \theta_1 \\ \theta_3 \\ \omega_1 \\ \omega_3 \\ h_1 \\ h_3 \end{bmatrix} + \begin{bmatrix} 0 & 0 \\ 0 & 0 \\ -\frac{1}{I_1} & 0 \\ 0 & -\frac{1}{I_3} \\ 1 & 0 \\ 0 & 1 \end{bmatrix} \begin{bmatrix} u_1 \\ u_3 \end{bmatrix}, \tag{3.100}$$

where

$$\Delta_1 := \frac{I_2 - I_3}{I_1} \quad \text{and} \quad \Delta_3 := \frac{I_1 - I_2}{I_3}$$

Consider the analysis of the pitch axis. Define the state-vector as

$$\mathbf{x}(t) := \begin{bmatrix} \theta_2(t) \\ \omega_2(t) \\ h_2(t) \end{bmatrix}$$

and the output as

$$y(t) = \theta_2(t) = [1 \ 0 \ 0]\mathbf{x}(t).$$

Here we are considering the spacecraft attitude,  $\theta_2(t)$ , as the output of interest. We can just as easily consider both the angular velocity  $\omega_2$  and the control moment gyro momentum,  $h_2$ , as outputs. The state variable model is

$$\dot{\mathbf{x}} = \mathbf{A}\mathbf{x} + \mathbf{B}u, \tag{3.101}$$

$$y = \mathbf{C}\mathbf{x} + \mathbf{D}u,$$

where

$$\mathbf{A} = \begin{bmatrix} 0 & 1 & 0 \\ 3n^2\Delta_2 & 0 & 0 \\ 0 & 0 & 0 \end{bmatrix}, \quad \mathbf{B} = \begin{bmatrix} 0 \\ -\frac{1}{I_2} \\ 1 \end{bmatrix},$$

$$\mathbf{C} = [1 \ 0 \ 0], \quad \mathbf{D} = [0],$$

and where  $n$  is the control moment gyro torque in the pitch axis. The solution to the state differential equation, given in Equation (3.101), is

$$\mathbf{x}(t) = \Phi(t)\mathbf{x}(0) + \int_0^t \Phi(t - \tau)\mathbf{B}u(\tau) d\tau,$$

management. One of the first to present the nonlinear model in Equations (3.96–3.98) is Wie et al. [28]. Other related information about the model and the control problem in general appears in [29–33]. Articles related to advanced control topics on the space station can be found in [34–40]. Researchers are developing nonlinear control laws based on the nonlinear model in Equations (3.96)–(3.98). Several good articles on this topic appear in [41–50].

Equation (3.96) represents the kinematics—the relationship between the Euler angles, denoted by  $\Theta$ , and the angular velocity vector,  $\Omega$ . Equation (3.97) represents the space station attitude dynamics. The terms on the right side represent the sum of the external torques acting on the spacecraft. The first torque is due to inertia cross-coupling. The second term represents the gravity gradient torque, and the last term is the torque applied to the spacecraft from the actuators. The disturbance torques (due to such factors as the atmosphere) are not included in the model used in the design. Equation (3.98) represents the control moment gyro total momentum.

The conventional approach to spacecraft momentum management design is to develop a linear model, representing the spacecraft attitude and control moment gyro momentum by linearizing the nonlinear model. This linearization is accomplished by a standard Taylor series approximation. Linear control design methods can then be readily applied. For linearization purposes we assume that the spacecraft has zero products of inertia (that is, the inertia matrix is diagonal) and the aerodynamic disturbances are negligible. The equilibrium state that we linearize about is

$$\Theta = \mathbf{0},$$

$$\Omega = \begin{bmatrix} 0 \\ -n \\ 0 \end{bmatrix}$$

$$\mathbf{h} = \mathbf{0},$$

and where we assume that

$$\mathbf{I} = \begin{bmatrix} I_1 & 0 & 0 \\ 0 & I_2 & 0 \\ 0 & 0 & I_3 \end{bmatrix}$$

In reality, the inertia matrix,  $\mathbf{I}$ , is not a diagonal matrix. Neglecting the off-diagonal terms is consistent with the linearization approximations and is a common assumption. Applying the Taylor series approximations yields the linear model, which as it turns out decouples the pitch axis from the roll/yaw axis.

The linearized equations for the pitch axis are

$$\begin{bmatrix} \dot{\theta}_2 \\ \dot{\omega}_2 \\ \dot{h}_2 \end{bmatrix} = \begin{bmatrix} 0 & 1 & 0 \\ 3n^2\Delta_2 & 0 & 0 \\ 0 & 0 & 0 \end{bmatrix} \begin{bmatrix} \theta_2 \\ \omega_2 \\ h_2 \end{bmatrix} + \begin{bmatrix} 0 \\ -\frac{1}{I_2} \\ 1 \end{bmatrix} u_2, \tag{3.99}$$

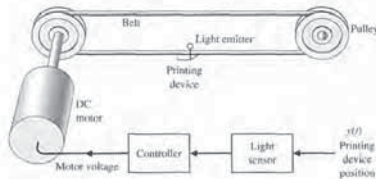
where

$$\Delta_2 := \frac{I_3 - I_1}{I_2}$$

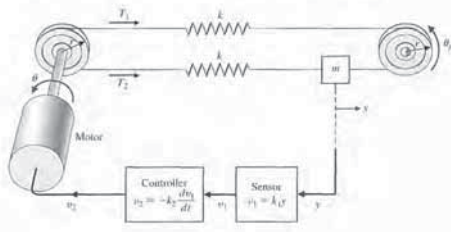
**EXAMPLE 3.8 Printer belt drive modeling**

A commonly used low-cost printer for a computer uses a belt drive to move the printing device laterally across the printed page [11]. The printing device may be a laser printer, a print ball, or thermal printhead. An example of a belt drive printer with a DC motor actuator is shown in Figure 3.29. In this model, a light sensor is used to measure the position of the printing device, and the belt tension adjusts the spring flexibility of the belt. The goal of the design is to determine the effect of the belt spring constant  $k$  and select appropriate parameters for the motor, the belt pulley, and the controller. To achieve the analysis, we will determine a model of the belt-drive system and select many of its parameters. Using this model, we will obtain the signal-flow graph model and select the state variables. We then will determine an appropriate transfer function for the system and select its other parameters, except for the spring constant. Finally, we will examine the effect of varying the spring constant within a realistic range.

We propose the model of the belt-drive system shown in Figure 3.30. This model assumes that the spring constant of the belt is  $k$ , the radius of the pulley is  $r$ , the angular rotation of the motor shaft is  $\theta$ , and the angular rotation of the right-hand pulley is  $\theta_p$ . The mass of the printing device is  $m$ , and its position is  $y(t)$ . A light sensor is used to measure  $y$ , and the output of the sensor is a voltage  $v_1$ , where  $v_1 = k_1 y$ . The controller



**FIGURE 3.29** Printer belt-drive system.



**FIGURE 3.30** Printer belt-drive model.

when we select the third state variable as  $x_3 = d\theta/dt$ . We now require a differential equation describing the motor rotation. When  $L = 0$ , we have the field current  $i = v_2/R$  and the motor torque  $T_m = K_m i$ . Therefore,

$$T_m = \frac{K_m}{R} v_2,$$

and the motor torque provides the torque to drive the belts plus the disturbance or undesired load torque, so that

$$T_m = T + T_d.$$

The torque  $T$  drives the shaft to the pulley, so that

$$T = J \frac{d^2\theta}{dt^2} + b \frac{d\theta}{dt} + r(T_1 - T_2).$$

Therefore,

$$\frac{dx_3}{dt} = \frac{d^2\theta}{dt^2}.$$

Hence,

$$\frac{dx_3}{dt} = \frac{T_m - T_d}{J} - \frac{b}{J} x_3 - \frac{2kr}{J} x_1,$$

where

$$T_m = \frac{K_m}{R} v_2, \text{ and } v_2 = -k_1 k_2 \frac{dy}{dt} = -k_1 k_2 x_2.$$

Thus, we obtain

$$\frac{dx_3}{dt} = -\frac{K_m k_1 k_2}{JR} x_2 - \frac{b}{J} x_3 - \frac{2kr}{J} x_1 - \frac{T_d}{J}. \quad (3.106)$$

Equations (3.104)–(3.106) are the three first-order differential equations required to describe this system. The matrix differential equation is

$$\dot{\mathbf{x}} = \begin{bmatrix} 0 & -1 & r \\ \frac{2k}{m} & 0 & 0 \\ -\frac{2kr}{J} & -\frac{K_m k_1 k_2}{JR} & -\frac{b}{J} \end{bmatrix} \mathbf{x} + \begin{bmatrix} 0 \\ 0 \\ -\frac{1}{J} \end{bmatrix} T_d. \quad (3.107)$$

where

$$\Phi(t) = \exp(\mathbf{A}t) = \mathcal{L}^{-1}\{(\mathbf{sI} - \mathbf{A})^{-1}\} = \begin{bmatrix} \frac{1}{2}(e^{\sqrt{3n^2\Delta_2}t} + e^{-\sqrt{3n^2\Delta_2}t}) & \frac{1}{2\sqrt{3n^2\Delta_2}}(e^{\sqrt{3n^2\Delta_2}t} - e^{-\sqrt{3n^2\Delta_2}t}) & 0 \\ \frac{\sqrt{3n^2\Delta_2}}{2}(e^{\sqrt{3n^2\Delta_2}t} - e^{-\sqrt{3n^2\Delta_2}t}) & \frac{1}{2}(e^{\sqrt{3n^2\Delta_2}t} + e^{-\sqrt{3n^2\Delta_2}t}) & 0 \\ 0 & 0 & 1 \end{bmatrix}.$$

We can see that if  $\Delta_2 > 0$ , then some elements of the state transition matrix have terms of the form  $e^{at}$ , where  $a > 0$ . As we shall see (in Chapter 6) this indicates that our system is unstable. Also, if we are interested in the output,  $y(t) = \theta_e(t)$ , we have

$$y(t) = \mathbf{C}\mathbf{x}(t).$$

With  $\mathbf{x}(t)$  given by

$$\mathbf{x}(t) = \Phi(t)\mathbf{x}(0) + \int_0^t \Phi(t - \tau)\mathbf{B}u(\tau)d\tau,$$

it follows that

$$y(t) = \mathbf{C}\Phi(t)\mathbf{x}(0) + \int_0^t \mathbf{C}\Phi(t - \tau)\mathbf{B}u(\tau)d\tau.$$

The transfer function relating the output  $Y(s)$  to the input  $U(s)$  is

$$G(s) = \frac{Y(s)}{U(s)} = \mathbf{C}(\mathbf{sI} - \mathbf{A})^{-1}\mathbf{B} = \frac{1}{I_2(s^2 - 3n^2\Delta_2)}.$$

The characteristic equation is

$$s^2 - 3n^2\Delta_2 = (s + \sqrt{3n^2\Delta_2})(s - \sqrt{3n^2\Delta_2}) = 0.$$

If  $\Delta_2 > 0$  (that is, if  $I_3 > I_1$ ), then we have two real poles—one in the left half-plane and the other in the right half-plane. For spacecraft with  $I_3 > I_1$ , we can say that an earth-pointing attitude is an unstable orientation. This means that active control is necessary.

Conversely, when  $\Delta_2 < 0$  (that is, when  $I_1 > I_3$ ), the characteristic equation has two imaginary roots at

$$s = \pm j\sqrt{3n^2|\Delta_2|}.$$

This type of spacecraft is marginally stable. In the absence of any control moment gyro torques, the spacecraft will oscillate around the earth-pointing orientation for any small initial deviation from the desired attitude. ■

provides an output voltage  $v_2$ , where  $v_2$  is a function of  $v_1$ . The voltage  $v_2$  is connected to the field of the motor. Let us assume that we can use the linear relationship

$$v_2 = -\left[ k_2 \frac{dv_1}{dt} + k_3 v_1 \right],$$

and elect to use  $k_2 = 0.1$  and  $k_3 = 0$  (velocity feedback).

The inertia of the motor and pulley is  $J = J_{\text{motor}} + J_{\text{pulley}}$ . We plan to use a moderate-DC motor. Selecting a typical 1/8-hp DC motor, we find that  $J = 0.01 \text{ kg m}^2$ , the field inductance is negligible, the field resistance is  $R = 2 \Omega$ , the motor constant is  $K_m = 2 \text{ N m/A}$ , and the motor and pulley friction is  $b = 0.25 \text{ N ms/rad}$ . The radius of the pulley is  $r = 0.15 \text{ m}$ . The system parameters are summarized in Table 3.1.

We now proceed to write the equations of the motion for the system; note that  $y = r\theta_p$ . Then the tension from equilibrium  $T_1$  is

$$T_1 = k(r\theta - r\theta_p) = k(r\theta - y).$$

The tension from equilibrium  $T_2$  is

$$T_2 = k(y - r\theta).$$

The net tension at the mass  $m$  is

$$T_1 - T_2 = m \frac{d^2 y}{dt^2} \quad (3.102)$$

and

$$T_1 - T_2 = k(r\theta - y) - k(y - r\theta) = 2k(r\theta - y) = 2kx_1, \quad (3.103)$$

where the first state variable is  $x_1 = r\theta - y$ . Let the second state variable be  $x_2 = dy/dt$ , and use Equations (3.102) and (3.103) to obtain

$$\frac{dx_2}{dt} = \frac{2k}{m} x_1. \quad (3.104)$$

The first derivative of  $x_1$  is

$$\frac{dx_1}{dt} = r \frac{d\theta}{dt} - \frac{dy}{dt} = rx_3 - x_2 \quad (3.105)$$

**Table 3.1 Parameters of Printing Device**

Mass	$m = 0.2 \text{ kg}$
Light sensor	$k_1 = 1 \text{ V/m}$
Radius	$r = 0.15 \text{ m}$
Motor	
Inductance	$L \approx 0$
Friction	$b = 0.25 \text{ N ms/rad}$
Resistance	$R = 2 \Omega$
Constant	$K_m = 2 \text{ N m/A}$
Inertia	$J = J_{\text{motor}} + J_{\text{pulley}}; J = 0.01 \text{ kg m}^2$



We therefore have

$$\frac{X_1(s)}{T_d(s)} = \frac{-\left(\frac{r}{J}\right)s}{s^3 + \left(\frac{b}{J}\right)s^2 + \left(\frac{2k}{m} + \frac{2kr^2}{J}\right)s + \left(\frac{2kb}{Jm} + \frac{2kK_m k_1 k_2 r}{JmR}\right)}$$

We can also determine the closed-loop transfer function using block diagram reduction methods, as illustrated in Figure 3.32. Remember, there is no unique path to follow in reducing the block diagram; however, there is only one correct solution in the end. The original block diagram is shown in Figure 3.31(b). The result of the first step is shown in Figure 3.32(a), where the upper feedback loop has been reduced to a single transfer

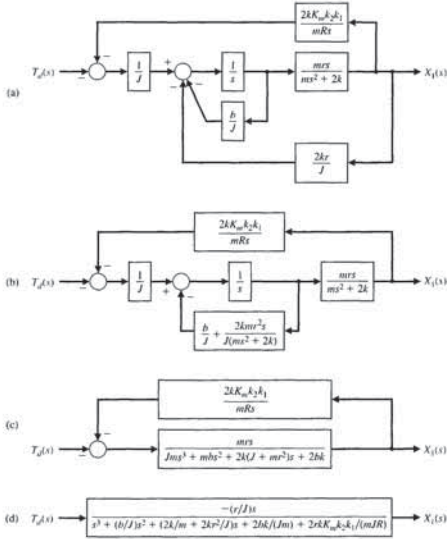


FIGURE 3.32 Printer belt drive block diagram reduction.

The actual response of  $x_1$  is shown in Figure 3.33. This system will reduce the effect of the unwanted disturbance to a relatively small magnitude. Thus we have achieved our design objective. ■

3.9 ANALYSIS OF STATE VARIABLE MODELS USING CONTROL DESIGN SOFTWARE

The time-domain method utilizes a state-space representation of the system model, given by

$$\dot{\mathbf{x}} = \mathbf{A}\mathbf{x} + \mathbf{B}u \quad \text{and} \quad y = \mathbf{C}\mathbf{x} + \mathbf{D}u. \quad (3.114)$$

The vector  $\mathbf{x}$  is the state of the system,  $\mathbf{A}$  is the constant  $n \times n$  system matrix,  $\mathbf{B}$  is the constant  $n \times m$  input matrix,  $\mathbf{C}$  is the constant  $p \times n$  output matrix, and  $\mathbf{D}$  is a constant  $p \times m$  matrix. The number of inputs,  $m$ , and the number of outputs,  $p$ , are taken to be one, since we are considering only single-input, single-output (SISO) problems. Therefore  $y$  and  $u$  are not bold (matrix) variables.

The main elements of the state-space representation in Equation (3.114) are the state vector  $\mathbf{x}$  and the constant matrices  $(\mathbf{A}, \mathbf{B}, \mathbf{C}, \mathbf{D})$ . Two new functions covered in this section are `ss` and `lsim`. We also consider the use of the `expm` function to calculate the state transition matrix.

Given a transfer function, we can obtain an equivalent state-space representation and vice versa. The function `tf` can be used to convert a state-space representation to a transfer function representation; the function `ss` can be used to convert a transfer function representation to a state-space representation. These functions are shown in Figure 3.34, where `sys_tf` represents a transfer function model and `sys_ss` is a state-space representation.

For instance, consider the third-order system

$$T(s) = \frac{Y(s)}{R(s)} = \frac{2s^2 + 8s + 6}{s^3 + 8s^2 + 16s + 6} \quad (3.115)$$

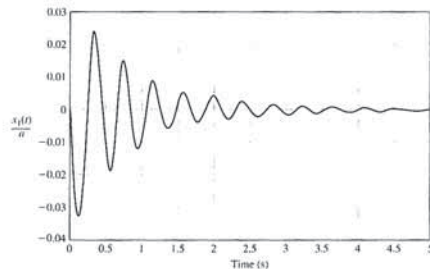


FIGURE 3.33 Response of  $x_1(t)$  to a step disturbance; peak value = 0.025.

The signal-flow graph and block diagram models representing the matrix differential equation are shown in Figure 3.31, where we include the identification of the node for the disturbance torque  $T_d$ .

We can use the flow graph to determine the transfer function  $X_1(s)/T_d(s)$ . The goal is to reduce the effect of the disturbance  $T_d$ , and the transfer function will show us how to accomplish this goal. Using Mason's signal-flow gain formula, we obtain

$$\frac{X_1(s)}{T_d(s)} = \frac{-\frac{r}{J}s^{-2}}{1 - (L_1 + L_2 + L_3 + L_4) + L_1L_2}$$

where

$$L_1 = \frac{-b}{J}s^{-1}, \quad L_2 = \frac{-2k}{m}s^{-2}, \quad L_3 = \frac{-2kr^2s^{-2}}{J}, \quad \text{and} \quad L_4 = \frac{-2kK_m k_1 k_2 r s^{-3}}{mJR}$$

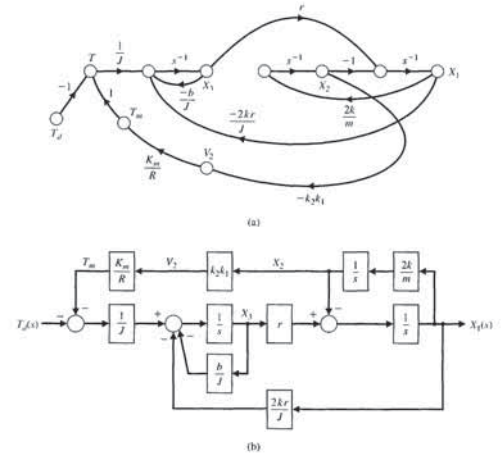


FIGURE 3.31 Printer belt drive. (a) Signal-flow graph. (b) Block diagram model.

The second step illustrated in Figure 3.32(b) then reduces the two lower feedback loops to a single transfer function. In the third step shown in Figure 3.32(c), the lower feedback loop is closed and then the remaining transfer functions in series in the lower loop are combined. The final step closed-loop transfer function is shown in Figure 3.32(d). Substituting the parameter values summarized in Table 3.1, we obtain

$$\frac{X_1(s)}{T_d(s)} = \frac{-15s}{s^3 + 25s^2 + 14.5ks + 1000k(0.25 + 0.15k_2)} \quad (3.108)$$

We wish to select the spring constant  $k$  and the gain  $k_2$  so that the state variable  $x_1$  will quickly decline to a low value when a disturbance occurs. For test purposes, consider a step disturbance  $T_d(s) = a/s$ . Recalling that  $x_1 = r\theta - y$ , we thus seek a small magnitude for  $x_1$  so that  $y$  is nearly equal to the desired  $r\theta$ . If we have a perfectly stiff belt with  $k \rightarrow \infty$ , then  $y = r\theta$  exactly. With a step disturbance,  $T_d(s) = a/s$ , we have

$$X_1(s) = \frac{-15a}{s^3 + 25s^2 + 14.5ks + 1000k(0.25 + 0.15k_2)} \quad (3.109)$$

The final value theorem gives

$$\lim_{t \rightarrow \infty} x_1(t) = \lim_{s \rightarrow 0} sX_1(s) = 0, \quad (3.110)$$

and thus the steady-state value of  $x_1(t)$  is zero. We need to use a realistic value for  $k$  in the range  $1 \leq k \leq 40$ . For an average value of  $k = 20$  and  $k_2 = 0.1$ , we have

$$X_1(s) = \frac{-15a}{s^3 + 25s^2 + 290s + 5300} = \frac{-15a}{(s + 22.56)(s^2 + 2.44s + 234.93)} \quad (3.111)$$

The characteristic equation has one real root and two complex roots. The partial fraction expansion yields

$$\frac{X_1(s)}{a} = \frac{A}{s + 22.56} + \frac{Bs + C}{(s + 1.22)^2 + (15.28)^2}, \quad (3.112)$$

where we find  $A = -0.0218$ ,  $B = 0.0218$ , and  $C = -0.4381$ . Clearly with these small residues, the response to the unit disturbance is relatively small. Because  $A$  and  $B$  are small compared to  $C$ , we may approximate  $X_1(s)$  as

$$\frac{X_1(s)}{a} \approx \frac{-0.4381}{(s + 1.22)^2 + (15.28)^2}$$

Using Table 2.3, we obtain

$$\frac{x_1(t)}{a} \approx -0.0287e^{-1.22t} \sin 15.28t. \quad (3.113)$$

The state-space representation of the transfer function in Equation (3.115) is depicted in Figure 3.36.

The state variable representation is not unique. For example, another equally valid state variable representation is given by

$$A = \begin{bmatrix} -8 & -2 & -0.75 \\ 8 & 0 & 0 \\ 0 & 1 & 0 \end{bmatrix}, B = \begin{bmatrix} 0.125 \\ 0 \\ 0 \end{bmatrix}, C = [16 \ 8 \ 6], D = [0].$$

It is possible that when using the ss function, the state variable representation provided by your control design software will be different from the above two examples depending on the specific software and version.

The time response of the system in Equation (3.114) is given by the solution to the vector integral equation

$$x(t) = \exp(At)x(0) + \int_0^t \exp[A(t - \tau)]Bu(\tau) d\tau. \quad (3.116)$$

The matrix exponential function in Equation (3.116) is the state transition matrix,  $\Phi(t)$ , where (Equation 3.23)

$$\Phi(t) = \exp(At).$$

We can use the function expm to compute the transition matrix for a given time, as illustrated in Figure 3.37. The expm(A) function computes the matrix exponential. In contrast, the exp(A) function calculates  $e^{a_{ij}}$  for each of the elements  $a_{ij} \in A$ .

For example, let us consider the RLC network of Figure 3.4 described by the state-space representation of Equation (3.18) with

$$A = \begin{bmatrix} 0 & -2 \\ 1 & -3 \end{bmatrix}, B = \begin{bmatrix} 2 \\ 0 \end{bmatrix}, C = [1 \ 0], \text{ and } D = 0.$$

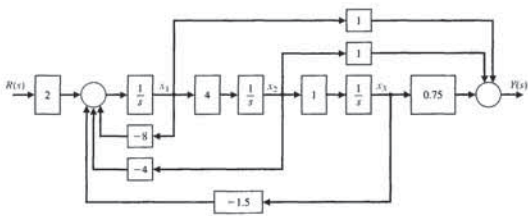


FIGURE 3.36 Block diagram with  $x_1$  defined as the leftmost state variable.

We can obtain a state-space representation using the ss function, as shown in Figure 3.35. A state-space representation of Equation (3.115) is given by Equation (3.114), where

$$A = \begin{bmatrix} -8 & -4 & -1.5 \\ 4 & 0 & 0 \\ 0 & 1 & 0 \end{bmatrix}, B = \begin{bmatrix} 2 \\ 0 \\ 0 \end{bmatrix}, C = [1 \ 1 \ 0.75], \text{ and } D = [0].$$

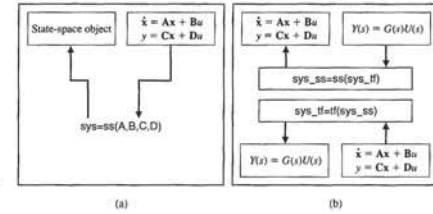


FIGURE 3.34 (a) The ss function. (b) Linear system model conversion.

```
>>convert
a =
    x1    x2    x3
x1    -8    -4   -1.5
x2     4     0     0
x3     0     1     0

b =
    u1
x1     2
x2     0
x3     0

c =
    x1    x2    x3
y1     1     1    0.75

d =
    u1
y1     0

convert.m
% Convert G(s) = (2s^2+8s+6)/(s^3+8s^2+16s+6)
% to a state-space representation
%
num=[2 8 6]; den=[1 8 16 6]; sys_tf=tf(num,den);
sys_ss=ss(sys_tf);
```

FIGURE 3.35 Conversion of Equation (3.115) to a state-space representation. (a) m-file script. (b) Output printout.

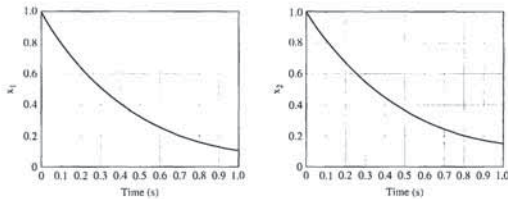


FIGURE 3.39 Computing the time response for nonzero initial conditions and zero input using lsim.

```
A=[0 -2; 1 -3]; B=[2; 0]; C=[1 0]; D=[0];
sys=ss(A,B,C,D);
x0=[1 1]; % Initial conditions
t=[0:0.01:1]; % Zero input
u=0*t;
[y,T,x]=lsim(sys,u,t,x0);
subplot(121), plot(T,x(:,1));
xlabel('Time (s)'), ylabel('x_1');
subplot(122), plot(T,x(:,2));
xlabel('Time (s)'), ylabel('x_2');
```

will develop a state variable model of the disk drive system that will include the effect of the flexure mount.

Consider again the head mount shown in Figure 2.71. Since we want a light-weight arm and flexure for rapid movement, we must consider the effect of the flexure, which is a very thin mount made of spring steel. Again, we wish to accurately control the position of the head  $y(t)$  as shown in Figure 3.40(a). We will attempt to derive a model for the system shown in Figure 3.40(a). Here we identify the motor mass as  $M_1$  and the head mount mass as  $M_2$ . The flexure spring is represented by the spring constant  $k$ . The force  $u(t)$  to drive the mass  $M_1$  is generated by the DC motor. If the spring is absolutely rigid (nonspringy), then we obtain the simplified model shown in Figure 3.40(b). Typical parameters for the two-mass system are given in Table 3.2.

Let us obtain the transfer function model of the simplified system of Figure 3.40(b). Note that  $M = M_1 + M_2 = 20.5 \text{ g} = 0.0205 \text{ kg}$ . Then we have

$$M \frac{d^2y}{dt^2} + b_1 \frac{dy}{dt} = u(t). \quad (3.117)$$

Therefore, the transfer function model is

$$\frac{Y(s)}{U(s)} = \frac{1}{s(Ms + b_1)}$$

```
>>A=[0 -2; 1 -3]; dt=0.2; Phi=expm(A*dt)

Phi =
    0.9671    -0.2968
    0.1484     0.5219
```

FIGURE 3.37 Computing the state transition matrix for a given time,  $\Delta t = dt$ .

The initial conditions are  $x_1(0) = x_2(0) = 1$  and the input  $u(t) = 0$ . At  $t = 0.2$ , the state transition matrix is as given in Figure 3.37. The state at  $t = 0.2$  is predicted by the state transition methods to be

$$\begin{bmatrix} x_1 \\ x_2 \end{bmatrix}_{t=0.2} = \begin{bmatrix} 0.9671 & -0.2968 \\ 0.1484 & 0.5219 \end{bmatrix} \begin{bmatrix} x_1 \\ x_2 \end{bmatrix}_{t=0} = \begin{bmatrix} 0.6703 \\ 0.6703 \end{bmatrix}$$

The time response of the system of Equation (3.115) can also be obtained by using the lsim function. The lsim function can accept as input nonzero initial conditions as well as an input function, as shown in Figure 3.38. Using the lsim function, we can calculate the response for the RLC network as shown in Figure 3.39.

The state at  $t = 0.2$  is predicted with the lsim function to be  $x_1(0.2) = x_2(0.2) = 0.6703$ . If we can compare the results obtained by the lsim function and by multiplying the initial condition state vector by the state transition matrix, we find identical results.

3.10 SEQUENTIAL DESIGN EXAMPLE: DISK DRIVE READ SYSTEM



Advanced disks have as many as 5000 tracks per cm. These tracks are typically  $1 \mu\text{m}$  wide. Thus, there are stringent requirements on the accuracy of the reader head position and of the movement from one track to another. In this chapter, we

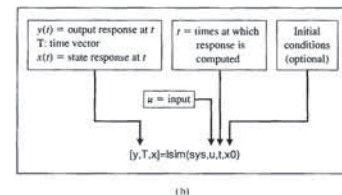
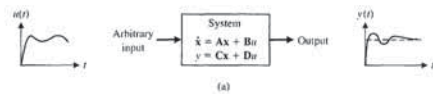


FIGURE 3.38 The lsim function for calculating the output and state response.



$$\text{Mass } M_2: M_2 \frac{d^2 y}{dt^2} + b_2 \frac{dy}{dt} + k(y - q) = 0.$$

To develop the state variable model, we choose the state variables as  $x_1 = q$  and  $x_2 = \dot{y}$ . Then we have

$$x_3 = \frac{dq}{dt} \quad \text{and} \quad x_4 = \frac{dy}{dt}.$$

Then, in matrix form,

$$\dot{\mathbf{x}} = \mathbf{A}\mathbf{x} + \mathbf{B}u,$$

and we have

$$\mathbf{x} = \begin{bmatrix} q \\ y \\ \dot{q} \\ \dot{y} \end{bmatrix}, \quad \mathbf{B} = \begin{bmatrix} 0 \\ 0 \\ 1/M_1 \\ 0 \end{bmatrix},$$

and

$$\mathbf{A} = \begin{bmatrix} 0 & 0 & 1 & 0 \\ 0 & 0 & 0 & 1 \\ -k/M_1 & k/M_1 & -b_1/M_1 & 0 \\ k/M_2 & -k/M_2 & 0 & -b_2/M_2 \end{bmatrix}, \quad (3.119)$$

Note that the output is  $\dot{y}(t) = x_4$ . Also, for  $L = 0$  or negligible inductance, then  $u(t) = K_m v(t)$ . For the typical parameters and for  $k = 10$ , we have

$$\mathbf{B} = \begin{bmatrix} 0 \\ 0 \\ 50 \\ 0 \end{bmatrix}$$

and

$$\mathbf{A} = \begin{bmatrix} 0 & 0 & 1 & 0 \\ 0 & 0 & 0 & 1 \\ -500 & +500 & -20.5 & 0 \\ +20000 & -20000 & 0 & -8.2 \end{bmatrix}.$$

The response of  $\dot{y}$  for  $u(t) = 1, t > 0$  is shown in Figure 3.42. This response is quite oscillatory, and it is clear that we want a very rigid flexure with  $k > 100$ .

Table 3.2 Typical Parameters of the Two-Mass Model

Parameter	Symbol	Value
Motor mass	$M_1$	20 g = 0.02 kg
Flexure spring	$k$	$10 \leq k \leq \infty$
Head mounting mass	$M_2$	0.5 g = 0.0005 kg
Head position	$x_2(t)$	variable in mm
Friction at mass 1	$b_1$	$410 \times 10^{-3}$ N/(m/s)
Field resistance	$R$	1 $\Omega$
Field inductance	$L$	1 mH
Motor constant	$K_m$	0.1025 N m/A
Friction at mass 2	$b_2$	$4.1 \times 10^{-3}$ N/(m/s)

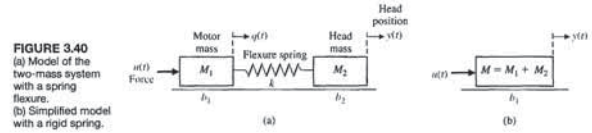


FIGURE 3.40 (a) Model of the two-mass system with a spring flexure. (b) Simplified model with a rigid spring.

For the parameters of Table 3.2, we obtain

$$\frac{Y(s)}{U(s)} = \frac{1}{s(0.0205s + 0.410)} = \frac{48.78}{s(s + 20)}.$$

The transfer function model of the head reader, including the effect of the motor coil, is shown in Figure 3.41. When  $R = 1 \Omega$ ,  $L = 1$  mH, and  $K_m = 0.1025$ , we obtain

$$G(s) = \frac{Y(s)}{V(s)} = \frac{5000}{s(s + 20)(s + 1000)}, \quad (3.118)$$

which is exactly the same model we obtained in Chapter 2.

Now let us obtain the state variable model of the two-mass system shown in Figure 3.40(a). Write the differential equations as

$$\text{Mass } M_1: M_1 \frac{d^2 q}{dt^2} + b_1 \frac{dq}{dt} + k(q - y) = u(t)$$

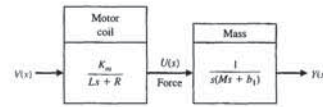


FIGURE 3.41 Transfer function model of head reader device with a rigid spring.



SKILLS CHECK

In this section, we provide three sets of problems to test your knowledge: True or False, Multiple Choice, and Word Match. To obtain direct feedback, check your answers with the answer key provided at the conclusion of the end-of-chapter problems.

- The state variables of a system comprise a set of variables that describe the future response of the system, when given the present state, all future excitation inputs, and the mathematical model describing the dynamics. True or False
- The matrix exponential function describes the unforced response of the system and is called the state transition matrix. True or False
- The outputs of a linear system can be related to the state variables and the input signals by the state differential equation. True or False
- A time-invariant control system is a system for which one or more of the parameters of the system may vary as a function of time. True or False
- A state variable representation of a system can always be written in diagonal form. True or False
- Consider a system with the mathematical model given by the differential equation: True or False

$$5 \frac{d^3 y}{dt^3} + 10 \frac{d^2 y}{dt^2} + 5 \frac{dy}{dt} + 2y = u(t).$$

A state variable representation of the system is:

$$\mathbf{a. } \dot{\mathbf{x}} = \begin{bmatrix} -2 & -1 & -0.4 \\ 1 & 0 & 0 \\ 0 & 1 & 0 \end{bmatrix} \mathbf{x} + \begin{bmatrix} 1 \\ 0 \\ 0 \end{bmatrix} u$$

$$y = [0 \ 0 \ 0.2] \mathbf{x}$$

$$\mathbf{b. } \dot{\mathbf{x}} = \begin{bmatrix} -5 & -1 & -0.7 \\ 1 & 0 & 0 \\ 0 & 1 & 0 \end{bmatrix} \mathbf{x} + \begin{bmatrix} -1 \\ 0 \\ 0 \end{bmatrix} u$$

$$y = [0 \ 0 \ 0.2] \mathbf{x}$$

$$\mathbf{c. } \dot{\mathbf{x}} = \begin{bmatrix} -2 & -1 \\ 1 & 0 \end{bmatrix} \mathbf{x} + \begin{bmatrix} 1 \\ 0 \end{bmatrix} u$$

$$y = [1 \ 0] \mathbf{x}$$

$$\mathbf{d. } \dot{\mathbf{x}} = \begin{bmatrix} -2 & -1 & -0.4 \\ 1 & 0 & 0 \\ 0 & 1 & 0 \end{bmatrix} \mathbf{x} + \begin{bmatrix} 1 \\ 0 \\ 0 \end{bmatrix} u$$

$$y = [1 \ 0 \ 0.2] \mathbf{x}$$

For Problems 7 and 8, consider the system represented by

$$\dot{\mathbf{x}} = \mathbf{A}\mathbf{x} + \mathbf{B}u,$$

where

$$\mathbf{A} = \begin{bmatrix} 0 & 5 \\ 0 & 0 \end{bmatrix} \quad \text{and} \quad \mathbf{B} = \begin{bmatrix} 1 \\ 0 \end{bmatrix}.$$

- The associated state-transition matrix is:

$$\mathbf{a. } \Phi(t,0) = [5t]$$

$$\mathbf{b. } \Phi(t,0) = \begin{bmatrix} 1 & 5t \\ 0 & 1 \end{bmatrix}$$

```
% Model Parameters
k=10;
M1=0.02; M2=0.0005;
b1=410e-03; b2=4.1e-03;
L=0.001; R=1;
% State Space Model
A=[0 0 1 0 0 0 1; -k/M1 -b1/M1 0; k/M2 -k/M2 0 -b2/M2];
B=[0;0;1/M1;0]; C=[0 0 0 1]; D=[0]; sys=ss(A,B,C,D);
% Simulated Step Response
y=step(sys,1); plot(t,y); grid
xlabel('Time (s)'); ylabel('y dot (m/s)')
```

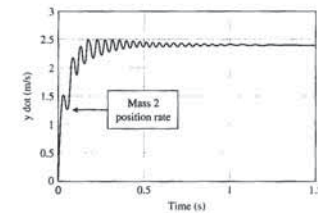


FIGURE 3.42 Response of  $\dot{y}$  for a step input for the two-mass model with  $k = 10$ .

3.11 SUMMARY

In this chapter, we have considered the description and analysis of systems in the time domain. The concept of the state of a system and the definition of the state variables of a system were discussed. The selection of a set of state variables of a system was examined, and the nonuniqueness of the state variables was noted. The state differential equation and the solution for  $\mathbf{x}(t)$  were discussed. Alternative signal-flow graph and block diagram model structures were considered for representing the transfer function (or differential equation) of a system. Using Mason's signal-flow gain formula, we noted the ease of obtaining the flow graph model. The state differential equation representing the flow graph and block diagram models was also examined. The time response of a linear system and its associated transition matrix was discussed, and the utility of Mason's signal-flow gain formula for obtaining the transition matrix was illustrated. A detailed analysis of a space station model development was presented for a realistic scenario where the attitude control is accomplished in conjunction with minimizing the actuator control. The relationship between modeling with state variable forms and control system design was established. The use of control design software to convert a transfer function to state variable form and calculate the state transition matrix was discussed and illustrated. The chapter concluded with the development of a state variable model for the Sequential Design Example: Disk Drive Read System.

Consider the block diagram in Figure 3.43 for Problems 12 through 14:

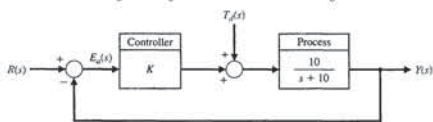


FIGURE 3.43 Block diagram for the Skills Check.

12. The effect of the input  $R(s)$  and the disturbance  $T_d(s)$  on the output  $Y(s)$  can be considered independently of each other because:
  - a. This is a linear system, therefore we can apply the principle of superposition.
  - b. The input  $R(s)$  does not influence the disturbance  $T_d(s)$ .
  - c. The disturbance  $T_d(s)$  occurs at high frequency, while the input  $R(s)$  occurs at low frequency.
  - d. The system is causal.
13. The state-space representation of the closed-loop system from  $R(s)$  to  $Y(s)$  is:
  - a.  $\dot{x} = -10x + 10Kr$   
 $y = x$
  - b.  $\dot{x} = -(10 + 10K)x + r$   
 $y = 10x$
  - c.  $\dot{x} = -(10 + 10K)x + 10Kr$   
 $y = x$
  - d. None of the above
14. The steady-state error  $E(s) = Y(s) - R(s)$  due to a unit step disturbance  $T_d(s) = 1/s$  is:
  - a.  $e_{ss} = \lim_{t \rightarrow \infty} e(t) = \infty$
  - b.  $e_{ss} = \lim_{t \rightarrow \infty} e(t) = 1$
  - c.  $e_{ss} = \lim_{t \rightarrow \infty} e(t) = \frac{1}{K+1}$
  - d.  $e_{ss} = \lim_{t \rightarrow \infty} e(t) = K+1$
15. A system is represented by the transfer function
 
$$\frac{Y(s)}{R(s)} = T(s) = \frac{5(s+10)}{s^3 + 10s^2 + 20s + 50}$$

A state variable representation is:

  - a.  $\dot{x} = \begin{bmatrix} -10 & -20 & -50 \\ 1 & 0 & 0 \\ 0 & 1 & 0 \end{bmatrix} x + \begin{bmatrix} 1 \\ 1 \\ 0 \end{bmatrix} u$   
 $y = [0 \ 5 \ 50]x$
  - b.  $\dot{x} = \begin{bmatrix} -10 & -20 & -50 \\ 1 & 0 & 0 \\ 0 & 1 & 0 \end{bmatrix} x + \begin{bmatrix} 1 \\ 0 \\ 0 \end{bmatrix} u$   
 $y = [1 \ 0 \ 50]x$

E3.6 A system is represented by Equation (3.16), where

$$A = \begin{bmatrix} 0 & 1 \\ 0 & 0 \end{bmatrix}$$

(a) Find the matrix  $\Phi(t)$ . (b) For the initial conditions  $x_1(0) = x_2(0) = 1$ , find  $x(t)$ .

Answer: (b)  $x_1 = 1 + t$ ,  $x_2 = t$ ,  $t \geq 0$

E3.7 Consider the spring and mass shown in Figure 3.3 where  $M = 1$  kg,  $k = 100$  N/m, and  $b = 20$  Ns/m. (a) Find the state vector differential equation. (b) Find the roots of the characteristic equation for this system.

Answer: (a)  $\dot{x} = \begin{bmatrix} 0 & 1 \\ -100 & -20 \end{bmatrix} x + \begin{bmatrix} 0 \\ 1 \end{bmatrix} u$

(b)  $s = -10, -10$

E3.8 The manual, low-altitude hovering task above a moving landing deck of a small ship is very demanding, particularly in adverse weather and sea conditions. The hovering condition is represented by the matrix

$$A = \begin{bmatrix} 0 & 1 & 0 \\ 0 & 0 & 1 \\ 0 & -6 & -3 \end{bmatrix}$$

Find the roots of the characteristic equation.

E3.9 A multi-loop block diagram is shown in Figure E3.9. The state variables are denoted by  $x_1$  and  $x_2$ . (a) Determine a state variable representation of the closed-loop system where the output is denoted by  $y(t)$  and the input is  $r(t)$ . (b) Determine the characteristic equation.

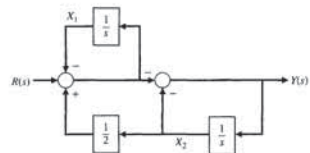


FIGURE E3.9 Multi-loop feedback control system.

E3.10 A hovering vehicle control system is represented by two state variables, and [13]

$$A = \begin{bmatrix} 0 & 6 \\ -1 & -5 \end{bmatrix}$$

(a) Find the roots of the characteristic equation. (b) Find the state transition matrix  $\Phi(t)$ .

Answer: (a)  $s = -3, -2$

(b)  $\Phi(t) = \begin{bmatrix} 3e^{-2t} - 2e^{-3t} & -6e^{-3t} + 6e^{-2t} \\ e^{-3t} - e^{-2t} & 3e^{-3t} - 2e^{-2t} \end{bmatrix}$

E3.11 Determine a state variable representation for the system described by the transfer function

$$T(s) = \frac{Y(s)}{R(s)} = \frac{4(s+3)}{(s+2)(s+6)}$$

E3.12 Use a state variable model to describe the circuit of Figure E3.12. Obtain the response to an input unit step when the initial current is zero and the initial capacitor voltage is zero.

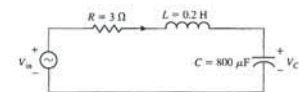


FIGURE E3.12 RLC series circuit.

E3.13 A system is described by the two differential equations

$$\frac{dy}{dt} + y - 2u + aw = 0,$$

and

$$\frac{dw}{dt} - by + 4u = 0,$$

where  $w$  and  $y$  are functions of time, and  $u$  is an input  $u(t)$ . (a) Select a set of state variables. (b) Write the matrix differential equation and specify the elements of the matrices. (c) Find the characteristic roots of the system in terms of the parameters  $a$  and  $b$ .

Answer: (c)  $s = -1/2 \pm \sqrt{1 - 4ab}/2$

E3.14 Develop the state-space representation of a radioactive material of mass  $M$  to which additional radioactive material is added at the rate  $i(t) = K\alpha(t)$ , where  $K$  is a constant. Identify the state variables.

c.  $\Phi(t,0) = \begin{bmatrix} 1 & 5t \\ 1 & 1 \end{bmatrix}$   
 d.  $\Phi(t,0) = \begin{bmatrix} 1 & 5t & t^2 \\ 0 & 1 & t \\ 0 & 0 & 1 \end{bmatrix}$

8. For the initial conditions  $x_1(0) = x_2(0) = 1$ , the response  $x(t)$  for the zero-input response is:
  - a.  $x_1(t) = (1+t)$ ,  $x_2(t) = 1$  for  $t \geq 0$
  - b.  $x_1(t) = (5+t)$ ,  $x_2(t) = t$  for  $t \geq 0$
  - c.  $x_1(t) = (5t+1)$ ,  $x_2(t) = 1$  for  $t \geq 0$
  - d.  $x_1(t) = x_2(t) = 1$  for  $t \geq 0$

9. A single-input, single-output system has the state variable representation

$$\dot{x} = \begin{bmatrix} 0 & 1 \\ -5 & -10 \end{bmatrix} x + \begin{bmatrix} 1 \\ 0 \end{bmatrix} u$$

$$y = [0 \ 10]x$$

The transfer function of the system  $T(s) = Y(s)/U(s)$  is:

- a.  $T(s) = \frac{-50}{s^2 + 5s + 50}$
- b.  $T(s) = \frac{-50}{s^2 + 10s + 5}$
- c.  $T(s) = \frac{-5}{s + 5}$
- d.  $T(s) = \frac{-50}{s^2 + 5s + 5}$

10. The differential equation model for two first-order systems in series is

$$\ddot{x}(t) + 4\dot{x}(t) + 3x(t) = u(t),$$

where  $u(t)$  is the input of the first system and  $x(t)$  is the output of the second system.

The response  $x(t)$  of the system to a unit impulse  $u(t)$  is:

- a.  $x(t) = e^{-t} - 2e^{-2t}$
- b.  $x(t) = \frac{1}{2}e^{-2t} - \frac{1}{3}e^{-3t}$
- c.  $x(t) = \frac{1}{2}e^{-t} - \frac{1}{2}e^{-3t}$
- d.  $x(t) = e^{-t} - e^{-3t}$

11. A first-order dynamic system is represented by the differential equation

$$5\dot{x}(t) + x(t) = u(t).$$

The corresponding transfer function and state-space representation are

- a.  $G(s) = \frac{1}{1+5s}$  and  $\dot{x} = -0.2x + 0.5u$   
 $y = 0.4x$
- b.  $G(s) = \frac{10}{1+5s}$  and  $\dot{x} = -0.2x + u$   
 $y = x$
- c.  $G(s) = \frac{1}{s+5}$  and  $\dot{x} = -5x + u$   
 $y = x$
- d. None of the above

c.  $\dot{x} = \begin{bmatrix} -10 & -20 & -50 \\ 1 & 0 & 0 \\ 0 & 1 & 0 \end{bmatrix} x + \begin{bmatrix} 1 \\ 0 \\ 0 \end{bmatrix} u$   
 $y = [0 \ 5 \ 50]x$   
 d.  $\dot{x} = \begin{bmatrix} -10 & -20 \\ 0 & 1 \end{bmatrix} x + \begin{bmatrix} 1 \\ 0 \end{bmatrix} u$   
 $y = [0 \ 5]x$

In the following Word Match problems, match the term with the definition by writing the correct letter in the space provided.

- |                                |  |       |
|--------------------------------|--|-------|
| a. State vector                | The differential equation for the state vector $\dot{x} = Ax + Bu$ .   | _____ |
| b. State of a system           | The matrix exponential function that describes the unforced response of the system.  | _____ |
| c. Time-varying system         | The mathematical domain that incorporates the time response and the description of a system in terms of time, $t$ .  | _____ |
| d. Transition matrix           | Vector containing all $n$ state variables, $x_1, x_2, \dots, x_n$ .  | _____ |
| e. State variables             | A set of numbers such that the knowledge of these numbers and the input function will, with the equations describing the dynamics, provide the future state of the system. | _____ |
| f. State differential equation | A system for which one or more parameters may vary with time.  | _____ |
| g. Time domain                 | The set of variables that describe the system.   | _____ |

EXERCISES

E3.1 For the circuit shown in Figure E3.1 identify a set of state variables.

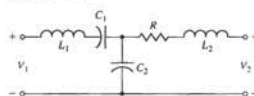


FIGURE E3.1 RLC circuit.

E3.2 A robot-arm drive system for one joint can be represented by the differential equation [8]

$$\frac{dv(t)}{dt} = -k_1v(t) - k_2y(t) + k_3i(t),$$

where  $v(t)$  is velocity,  $x(t)$  is position, and  $i(t)$  is the control-motor current. Put the equations in state variable form and set up the matrix form for  $k_1 = k_2 = 1$ .

E3.3 A system can be represented by the state vector differential equation of Equation (3.16), where

$$A = \begin{bmatrix} 0 & 1 \\ -1 & -2 \end{bmatrix}$$

Find the characteristic roots of the system.

Answer:  $-1, -1$

E3.4 Obtain a state variable matrix for a system with a differential equation

$$\frac{d^2y}{dt^2} + 4\frac{dy}{dt} + 6y = 20u(t).$$

E3.5 A system is represented by a block diagram as shown in Figure E3.5. Write the state equations in the form of Equations (3.16) and (3.17).

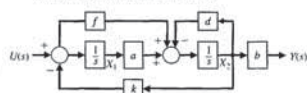


FIGURE E3.5 Block diagram.



Obtain the transfer function  $G(s) = Y(s)/U(s)$  and determine the response of the system to a unit step input.

**E3.22** Consider the system in state variable form

$$\dot{\mathbf{x}} = \mathbf{A}\mathbf{x} + \mathbf{B}u$$

$$y = \mathbf{C}\mathbf{x} + \mathbf{D}u$$

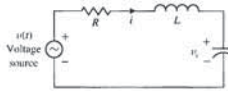
with

$$\mathbf{A} = \begin{bmatrix} 3 & 2 \\ 3 & 4 \end{bmatrix}, \mathbf{B} = \begin{bmatrix} 1 \\ -1 \end{bmatrix}, \mathbf{C} = [1 \ 0], \text{ and } \mathbf{D} = [0].$$

- (a) Compute the transfer function  $G(s) = Y(s)/U(s)$ .  
 (b) Determine the poles and zeros of the system. (c) If possible, represent the system as a first-order system

**PROBLEMS**

**P3.1** An *RLC* circuit is shown in Figure P3.1. (a) Identify a suitable set of state variables. (b) Obtain the set of first-order differential equations in terms of the state variables. (c) Write the state differential equation.



**FIGURE P3.1** RLC circuit.

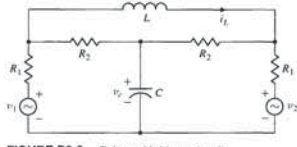
**P3.2** A balanced bridge network is shown in Figure P3.2.

(a) Show that the  $\mathbf{A}$  and  $\mathbf{B}$  matrices for this circuit are

$$\mathbf{A} = \begin{bmatrix} -2/((R_1 + R_2)C) & 0 \\ 0 & -2R_1R_2/((R_1 + R_2)L) \end{bmatrix}$$

$$\mathbf{B} = \frac{1}{(R_1 + R_2)} \begin{bmatrix} 1/C & 1/C \\ R_2/L & -R_1/L \end{bmatrix}$$

- (b) Sketch the block diagram. The state variables are  $(x_1, x_2) = (v_c, i_L)$ .



**FIGURE P3.2** Balanced bridge network.

$$\dot{x} = ax + bu$$

$$y = cx + du$$

where  $a, b, c,$  and  $d$  are scalars such that the transfer function is the same as obtained in (a).

**E3.23** Consider a system modeled via the third-order differential equation

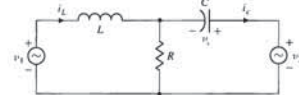
$$\ddot{x}(t) + 3\dot{x}(t) + 3x(t) + x(t) = \ddot{u}(t) + 2\dot{u}(t) + 4u(t) + (t).$$

Develop a state variable representation and obtain a block diagram of the system assuming the output is  $x(t)$  and the input is  $u(t)$ .

**P3.3** An *RLC* network is shown in Figure P3.3. Define the state variables as  $x_1 = i_L$  and  $x_2 = v_C$ . Obtain the state differential equation.

Partial answer:

$$\mathbf{A} = \begin{bmatrix} 0 & 1/L \\ -1/C & -1/(RC) \end{bmatrix}$$



**FIGURE P3.3** RLC circuit.

**P3.4** The transfer function of a system is

$$T(s) = \frac{Y(s)}{R(s)} = \frac{s^2 + 2s + 10}{s^3 + 4s^2 + 6s + 10}$$

Sketch the block diagram and obtain a state variable model.

**P3.5** A closed-loop control system is shown in Figure P3.5. (a) Determine the closed-loop transfer function  $T(s) = Y(s)/R(s)$ . (b) Sketch a block diagram model for the system and determine a state variable model.

**P3.6** Determine the state variable matrix equation for the circuit shown in Figure P3.6. Let  $x_1 = v_1, x_2 = v_2,$  and  $x_3 = i_L$ .

**P3.7** An automatic depth-control system for a robot submarine is shown in Figure P3.7. The depth is measured

$K_1 = 0.5$ . (a) Determine the closed-loop transfer function

$$T(s) = \frac{w(s)}{R(s)}$$

(b) Determine a state variable representation. (c) Determine the characteristic equation obtained from the  $\mathbf{A}$  matrix.

**P3.10** Many control systems must operate in two dimensions, for example, the  $x$ - and  $y$ -axes. A two-axis control system is shown in Figure P3.10, where a set of state variables is identified. The gain of each axis is  $K_1$  and  $K_2$ , respectively. (a) Obtain the state differential equation. (b) Find the characteristic equation from the  $\mathbf{A}$  matrix. (c) Determine the state transition matrix for  $K_1 = 1$  and  $K_2 = 2$ .

**P3.11** A system is described by

$$\dot{\mathbf{x}} = \mathbf{A}\mathbf{x} + \mathbf{B}u$$

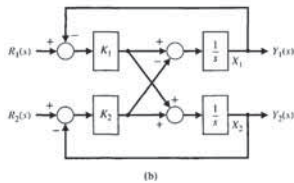
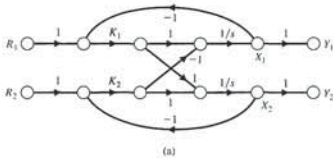
where

$$\mathbf{A} = \begin{bmatrix} 1 & -2 \\ 2 & -3 \end{bmatrix}, \mathbf{B} = \begin{bmatrix} 0 \\ 0 \end{bmatrix}$$

and  $x_1(0) = x_2(0) = 10$ . Determine  $x_1(t)$  and  $x_2(t)$ .

**P3.12** A system is described by its transfer function

$$\frac{Y(s)}{R(s)} = T(s) = \frac{8(s+5)}{s^3 + 12s^2 + 44s + 48}$$



**FIGURE P3.10** Two-axis system. (a) Signal-flow graph. (b) Block diagram model.

- (a) Determine a state variable model.  
 (b) Determine  $\Phi(t)$ , the state transition matrix.

**P3.13** Consider again the *RLC* circuit of Problem P3.1 when  $R = 2.5, L = 1/4,$  and  $C = 1/6$ . (a) Determine whether the system is stable by finding the characteristic equation with the aid of the  $\mathbf{A}$  matrix. (b) Determine the transition matrix of the network. (c) When the initial inductor current is 0.1 amp,  $v_C(0) = 0,$  and  $u(t) = 0,$  determine the response of the system. (d) Repeat part (c) when the initial conditions are zero and  $u(t) = E,$  for  $t > 0,$  where  $E$  is a constant.

**P3.14** Determine a state variable representation for a system with the transfer function

$$\frac{Y(s)}{R(s)} = T(s) = \frac{s + 50}{s^4 + 12s^3 + 10s^2 + 34s + 50}$$

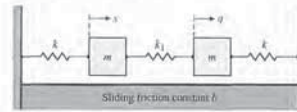
**P3.15** Obtain a block diagram and a state variable representation of this system.

$$\frac{Y(s)}{R(s)} = T(s) = \frac{14(s + 4)}{s^3 + 10s^2 + 31s + 16}$$

**P3.16** The dynamics of a controlled submarine are significantly different from those of an aircraft, missile, or surface ship. This difference results primarily from the moment in the vertical plane due to the buoyancy effect. Therefore, it is interesting to consider the control

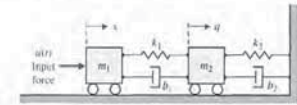
**Exercises**

**E3.15** Consider the case of the two masses connected as shown in Figure E3.15. The sliding friction of each mass has the constant  $b$ . Determine a state variable matrix differential equation.



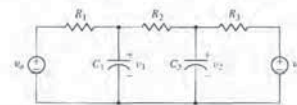
**FIGURE E3.15** Two-mass system.

**E3.16** Two carts with negligible rolling friction are connected as shown in Figure E3.16. An input force is  $u(t)$ . The output is the position of cart 2, that is,  $y(t) = q(t)$ . Determine a state space representation of the system.



**FIGURE E3.16** Two carts with negligible rolling friction.

**E3.17** Determine a state variable differential matrix equation for the circuit shown in Figure E3.17.



**FIGURE E3.17** RC circuit.

**E3.18** Consider a system represented by the following differential equations:

$$Ri_1 + L \frac{di_1}{dt} + v = v_a$$

$$L \frac{di_2}{dt} + v = v_b$$

$$\dot{i}_1 + i_2 = C \frac{dv}{dt}$$

where  $R, L_1, L_2$  and  $C$  are given constants, and  $v_a$  and  $v_b$  are inputs. Let the state variables be defined as  $x_1 = i_1, x_2 = i_2,$  and  $x_3 = v$ . Obtain a state variable representation of the system where the output is  $x_3$ .

**E3.19** A single-input, single-output system has the matrix equations

$$\dot{\mathbf{x}} = \begin{bmatrix} 0 & 1 \\ -3 & -4 \end{bmatrix} \mathbf{x} + \begin{bmatrix} 0 \\ 1 \end{bmatrix} u$$

and

$$y = [10 \ 0] \mathbf{x}.$$

Determine the transfer function  $G(s) = Y(s)/U(s)$ .

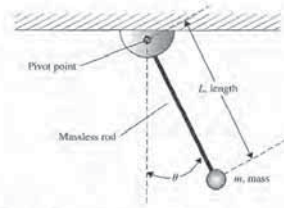
Answer:  $G(s) = \frac{10}{s^2 + 4s + 3}$

**E3.20** For the simple pendulum shown in Figure E3.20, the nonlinear equations of motion are given by

$$\ddot{\theta} + \frac{g}{L} \sin \theta = \frac{k}{m} \dot{\theta} = 0,$$

where  $g$  is gravity,  $L$  is the length of the pendulum,  $m$  is the mass attached at the end of the pendulum (we assume the rod is massless), and  $k$  is the coefficient of friction at the pivot point.

- (a) Linearize the equations of motion about the equilibrium condition  $\theta = 0^\circ$ .  
 (b) Obtain a state variable representation of the system. The system output is the angle  $\theta$ .



**FIGURE E3.20** Simple pendulum.

**E3.21** A single-input, single-output system is described by

$$\dot{\mathbf{x}}(t) = \begin{bmatrix} 0 & 1 \\ -1 & -2 \end{bmatrix} \mathbf{x}(t) + \begin{bmatrix} 1 \\ 0 \end{bmatrix} u(t)$$

$$y(t) = [0 \ 1] \mathbf{x}(t)$$

$K_1 = 0.5$ . (a) Determine the closed-loop transfer function

$$T(s) = \frac{w(s)}{R(s)}$$

(b) Determine a state variable representation. (c) Determine the characteristic equation obtained from the  $\mathbf{A}$  matrix.

**P3.10** Many control systems must operate in two dimensions, for example, the  $x$ - and  $y$ -axes. A two-axis control system is shown in Figure P3.10, where a set of state variables is identified. The gain of each axis is  $K_1$  and  $K_2$ , respectively. (a) Obtain the state differential equation. (b) Find the characteristic equation from the  $\mathbf{A}$  matrix. (c) Determine the state transition matrix for  $K_1 = 1$  and  $K_2 = 2$ .

**P3.11** A system is described by

$$\dot{\mathbf{x}} = \mathbf{A}\mathbf{x} + \mathbf{B}u$$

where

$$\mathbf{A} = \begin{bmatrix} 1 & -2 \\ 2 & -3 \end{bmatrix}, \mathbf{B} = \begin{bmatrix} 0 \\ 0 \end{bmatrix}$$

and  $x_1(0) = x_2(0) = 10$ . Determine  $x_1(t)$  and  $x_2(t)$ .

**P3.12** A system is described by its transfer function

$$\frac{Y(s)}{R(s)} = T(s) = \frac{8(s+5)}{s^3 + 12s^2 + 44s + 48}$$

- (a) Determine a state variable model.  
 (b) Determine  $\Phi(t)$ , the state transition matrix.

**P3.13** Consider again the *RLC* circuit of Problem P3.1 when  $R = 2.5, L = 1/4,$  and  $C = 1/6$ . (a) Determine whether the system is stable by finding the characteristic equation with the aid of the  $\mathbf{A}$  matrix. (b) Determine the transition matrix of the network. (c) When the initial inductor current is 0.1 amp,  $v_C(0) = 0,$  and  $u(t) = 0,$  determine the response of the system. (d) Repeat part (c) when the initial conditions are zero and  $u(t) = E,$  for  $t > 0,$  where  $E$  is a constant.

**P3.14** Determine a state variable representation for a system with the transfer function

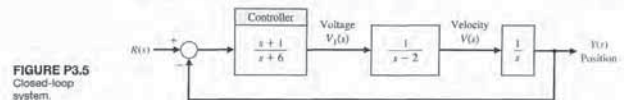
$$\frac{Y(s)}{R(s)} = T(s) = \frac{s + 50}{s^4 + 12s^3 + 10s^2 + 34s + 50}$$

**P3.15** Obtain a block diagram and a state variable representation of this system.

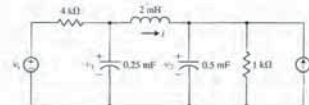
$$\frac{Y(s)}{R(s)} = T(s) = \frac{14(s + 4)}{s^3 + 10s^2 + 31s + 16}$$

**P3.16** The dynamics of a controlled submarine are significantly different from those of an aircraft, missile, or surface ship. This difference results primarily from the moment in the vertical plane due to the buoyancy effect. Therefore, it is interesting to consider the control

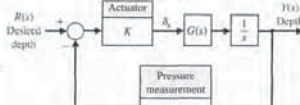
**Problems**



**FIGURE P3.5** Closed-loop system.



**FIGURE P3.6** RLC circuit.



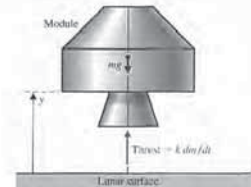
**FIGURE P3.7** Submarine depth control.

by a pressure transducer. The gain of the stern plane actuator is  $K = 1$  when the vertical velocity is 25 m/s. The submarine has the transfer function

$$G(s) = \frac{(s + 1)^2}{s^2 + 1}$$

and the feedback transducer is  $H(s) = 2s + 1$ . Determine a state variable representation for the system.

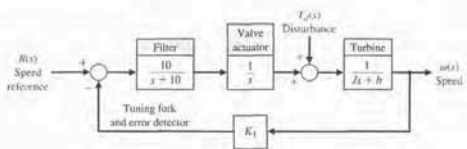
**P3.8** The soft landing of a lunar module descending on the moon can be modeled as shown in Figure P3.8. Define the state variables as  $x_1 = y, x_2 = \dot{y}$ ,  $x_3 = m$  and the control as  $u = dm/dt$ . Assume that  $g$  is the gravity constant on the moon. Find a state variable model for this system. Is this a linear model?



**FIGURE P3.8** Lunar module landing control.

**P3.9** A speed control system using fluid flow components is to be designed. The system is a pure fluid control system because it does not have any moving mechanical parts. The fluid may be a gas or a liquid. A system is desired that maintains the speed within 0.5% of the desired speed by using a tuning fork reference and a valve actuator. Fluid control systems are insensitive and reliable over a wide range of temperature, electromagnetic and nuclear radiation,

acceleration, and vibration. The amplification within the system is achieved by using a fluid jet deflection amplifier. The system can be designed for a 500-kW steam turbine with a speed of 12,000 rpm. The block diagram of the system is shown in Figure P3.9. In dimensionless units, we have  $b = 0.1, J = 1,$  and



**FIGURE P3.9** Steam turbine control.

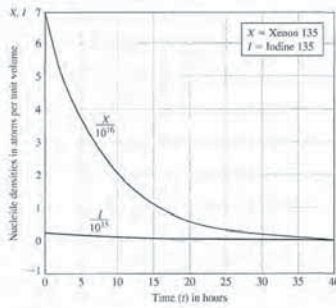


FIGURE P3.20 Nuclear reactor response.

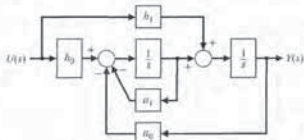


FIGURE P3.21 Model of second-order system. ultimately varying the output flow rate. The system has the transfer function

$$\frac{Q_2(s)}{U(s)} = G(s) = \frac{1}{s^2 + 10s^2 + 31s + 20}$$

for the block diagram shown in Figure P3.23(b). Obtain a block diagram model and a state variable model.

P3.24 It is desirable to use well-designed controllers to maintain building temperature with solar collector space-heating systems. One solar heating system can be described by [10]

$$\frac{dx_1}{dt} = 3x_1 + u_1 + u_2$$

and

$$\frac{dx_2}{dt} = 2x_2 + u_2 + d$$

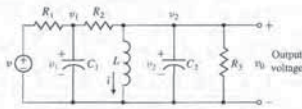


FIGURE P3.22 RLC circuit.

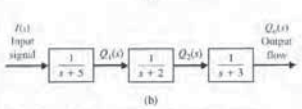
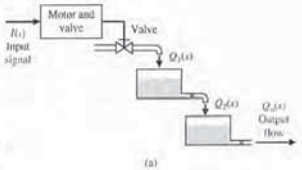


FIGURE P3.23 A two-tank system with the motor current controlling the output flow rate. (a) Physical diagram. (b) Block diagram.

Problems

of the depth of a submarine. The equations describing the dynamics of a submarine can be obtained by using Newton's laws and the angles defined in Figure P3.16. To simplify the equations, we will assume that  $\theta$  is a small angle and the velocity  $v$  is constant and equal to 25 ft/s. The state variables of the submarine, considering only vertical control, are  $x_1 = \theta$ ,  $x_2 = d\theta/dt$ , and  $x_3 = \alpha$ , where  $\alpha$  is the angle of attack. Thus the state vector differential equation for this system, when the submarine has an Albacore type hull, is

$$\dot{\mathbf{x}} = \begin{bmatrix} 0 & 1 & 0 \\ -0.0071 & -0.111 & 0.12 \\ 0 & 0.07 & -0.3 \end{bmatrix} \mathbf{x} + \begin{bmatrix} 0 \\ -0.095 \\ +0.072 \end{bmatrix} u(t)$$

where  $u(t) = \delta_s(t)$ , the deflection of the stern plane. (a) Determine whether the system is stable. (b) Determine the response of the system to a stern plane step command of  $0.285^\circ$  with the initial conditions equal to zero.

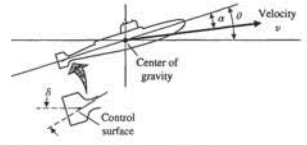


FIGURE P3.16 Submarine depth control.

P3.17 A system is described by the state variable equations

$$\dot{\mathbf{x}} = \begin{bmatrix} 1 & 1 & -1 \\ 4 & 3 & 0 \\ -2 & 1 & 10 \end{bmatrix} \mathbf{x} + \begin{bmatrix} 0 \\ 0 \\ 4 \end{bmatrix} u$$

$$y = [1 \ 0 \ 0]x$$

Determine  $G(s) = Y(s)/U(s)$ .

P3.18 Consider the control of the robot shown in Figure P3.18. The motor turning at the elbow moves the wrist through the forearm, which has some flexibility as shown [16]. The spring has a spring constant  $k$  and friction-damping constant  $b$ . Let the state variables be  $x_1 = \phi_1 - \phi_2$  and  $x_2 = \omega_1/\omega_0$ , where

$$\omega_0 = \frac{k(J_1 + J_2)}{J_1 J_2}$$

Write the state variable equation in matrix form when  $x_1 = \omega_1/\omega_0$ .

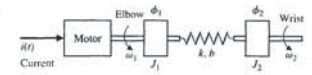


FIGURE P3.18 An industrial robot. (Courtesy of GCA Corporation.)

P3.19 Consider the system described by

$$\dot{\mathbf{x}}(t) = \begin{bmatrix} 0 & 1 \\ -2 & -3 \end{bmatrix} \mathbf{x}(t)$$

where  $\mathbf{x}(t) = [x_1(t) \ x_2(t)]^T$ . (a) Compute the state transition matrix  $\Phi(t, 0)$ . (b) Using the state transition matrix from (a) and for the initial conditions  $x_1(0) = 1$  and  $x_2(0) = -1$ , find the solution  $\mathbf{x}(t)$  for  $t \geq 0$ .

P3.20 A nuclear reactor that has been operating in equilibrium at a high thermal-neutron flux level is suddenly shut down. At shutdown, the density  $X$  of xenon 135 and the density  $I$  of iodine 135 are  $7 \times 10^{15}$  and  $3 \times 10^{15}$  atoms per unit volume, respectively. The half-lives of  $I_{135}$  and  $Xe_{135}$  nuclei are 6.7 and 9.2 hours, respectively. The decay equations are [15, 19]

$$\dot{I} = -\frac{0.693}{6.7}I, \quad \dot{X} = \frac{0.693}{9.2}X - I$$

Determine the concentrations of  $I_{135}$  and  $Xe_{135}$  as functions of time following shutdown by determining (a) the transition matrix and the system response. (b) Verify that the response of the system is that shown in Figure P3.20.

P3.21 Consider the block diagram in Figure P3.21. (a) Verify that the transfer function is

$$G(s) = \frac{Y(s)}{U(s)} = \frac{h_1 s + h_0 + a_1 h_1}{s^2 + a_1 s + a_0}$$

(b) Show that a state variable model is given by

$$\dot{\mathbf{x}} = \begin{bmatrix} 0 & 1 \\ -a_0 & -a_1 \end{bmatrix} \mathbf{x} + \begin{bmatrix} h_1 \\ h_0 \end{bmatrix} u$$

$$y = [1 \ 0]x$$

P3.22 Determine a state variable model for the circuit shown in Figure P3.22. The state variables are  $x_1 = i_1$ ,  $x_2 = v_1$ , and  $x_3 = v_2$ . The output variable is  $v_2(t)$ .

P3.23 The two-tank system shown in Figure P3.23(a) is controlled by a motor adjusting the input valve and

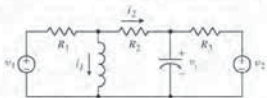


FIGURE P3.30 Two-input RLC circuit.

P3.31 Extenders are robot manipulators that extend (that is, increase) the strength of the human arm in load-maneuvering tasks (Figure P3.31) [19, 22]. The system is represented by the transfer function

$$\frac{Y(s)}{U(s)} = G(s) = \frac{30}{s^2 + 4s + 3}$$

where  $U(s)$  is the force of the human hand applied to the robot manipulator, and  $Y(s)$  is the force of the robot manipulator applied to the load. Determine a state variable model and the state transition matrix for the system.

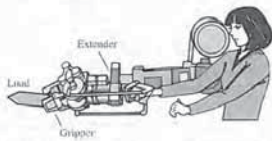


FIGURE P3.31 Extender for increasing the strength of the human arm in load maneuvering tasks.

P3.32 A drug taken orally is ingested at a rate  $r$ . The mass of the drug in the gastrointestinal tract is denoted by  $m_1$  and in the bloodstream by  $m_2$ . The rate of change

of the mass of the drug in the gastrointestinal tract is equal to the rate at which the drug is ingested minus the rate at which the drug enters the bloodstream, a rate that is taken to be proportional to the mass present. The rate of change of the mass in the bloodstream is proportional to the amount coming from the gastrointestinal tract minus the rate at which mass is lost by metabolism, which is proportional to the mass present in the blood. Develop a state space representation of this system.

P3.33 The attitude dynamics of a rocket are represented by

$$\frac{Y(s)}{U(s)} = G(s) = \frac{1}{s^2}$$

and state variable feedback is used where  $x_1 = \gamma(t)$ ,  $x_2 = \dot{\gamma}(t)$ , and  $u = -x_2 - 0.5x_1$ . Determine the roots of the characteristic equation of this system and the response of the system when the initial conditions are  $x_1(0) = 0$  and  $x_2(0) = 1$ . The input  $U(s)$  is the applied torque and  $Y(s)$  is the rocket attitude.

P3.34 A system has the transfer function

$$\frac{Y(s)}{R(s)} = T(s) = \frac{6}{s^3 + 6s^2 + 11s + 6}$$

(a) Construct a state variable representation of the system.  
(b) Determine the element  $\phi_{11}(t)$  of the state transition matrix for this system.

P3.35 Determine a state-space representation for the system shown in Figure P3.35. The motor inductance is negligible, the motor constant is  $K_m = 10$ , the back electromagnet force constant is  $K_b = 0.0706$ , the

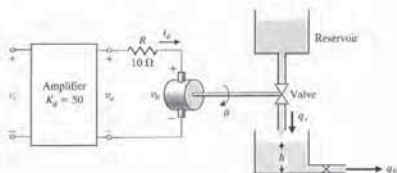


FIGURE P3.35 One-tank system.

Problems

where  $x_1 =$  temperature deviation from desired equilibrium, and  $x_2 =$  temperature of the storage material (such as a water tank). Also,  $u_1$  and  $u_2$  are the respective flow rates of conventional and solar heat, where the transport medium is forced air. A solar disturbance on the storage temperature (such as overcast skies) is represented by  $d$ . Write the matrix equations and solve for the system response when  $u_1 = 0$ ,  $u_2 = 1$ , and  $d = 1$ , with zero initial conditions.

P3.25 A system has the following differential equation:

$$\dot{\mathbf{x}} = \begin{bmatrix} -1 & 0 \\ 2 & -3 \end{bmatrix} \mathbf{x} + \begin{bmatrix} 0 \\ 1 \end{bmatrix} r(t)$$

Determine  $\Phi(t)$  and its transform  $\Phi(s)$  for the system.

P3.26 A system has a block diagram as shown in Figure P3.26. Determine a state variable model and the state transition matrix  $\Phi(s)$ .

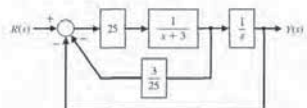


FIGURE P3.26 Feedback system.

P3.27 A gyroscope with a single degree of freedom is shown in Figure P3.27. Gyroscopes sense the angular motion of a system and are used in automatic flight control systems. The gimbal moves about the output axis  $OB$ . The input is measured around the input axis  $OA$ . The equation of motion about the output axis is obtained by equating the rate of change of angular momentum to the sum of torques. Obtain a state-space representation of the gyro system.

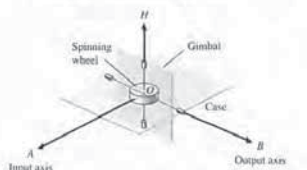


FIGURE P3.27 Gyroscope.

P3.28 A two-mass system is shown in Figure P3.28. The rolling friction constant is  $b$ . Determine a state variable representation when the output variable is  $y_2(t)$ .

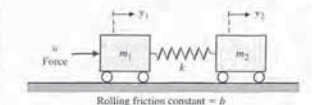


FIGURE P3.28 Two-mass system.

P3.29 There has been considerable engineering effort directed at finding ways to perform manipulative operations in space—for example, assembling a space station and acquiring target satellites. To perform such tasks, space shuttles carry a remote manipulator system (RMS) in the cargo bay [4, 12, 21]. The RMS has proven its effectiveness on recent shuttle missions, but now a new design approach can be considered—a manipulator with inflatable arm segments. Such a design might reduce manipulator weight by a factor of four while producing a manipulator that, prior to inflation, occupies only one-eighth as much space in the cargo bay as the present RMS.

The use of an RMS for constructing a space structure in the shuttle bay is shown in Figure P3.29(a), and a model of the flexible RMS arm is shown in Figure P3.29(b), where  $J$  is the inertia of the drive motor and  $L$  is the distance to the center of gravity of the load component. Derive the state equations for this system.

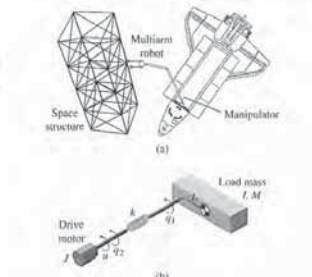


FIGURE P3.29 Remote manipulator system.

P3.30 Obtain the state equations for the two-input and one-output circuit shown in Figure P3.30, where the output is  $i_2$ .



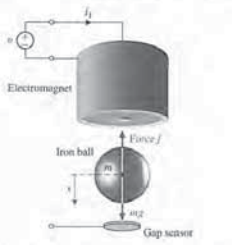


FIGURE AP3.1 Electromagnetic suspension system.

is  $f = k(x_1/x_2)^2$ , where  $k = 2.9 \times 10^{-4} \text{ N m}^2/\text{A}^2$ . Determine the matrix differential equation and the equivalent transfer function  $X(s)/V(s)$ .

AP3.2 Consider the mass  $m$  mounted on a massless cart, as shown in Figure AP3.2. Determine the transfer function  $Y(s)/U(s)$ , and use the transfer function to obtain a state-space representation of the system.

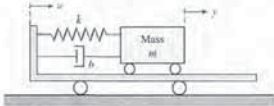


FIGURE AP3.2 Mass on cart.

AP3.3 The control of an autonomous vehicle motion from one point to another point depends on accurate control of the position of the vehicle [16]. The control of the autonomous vehicle position  $Y(s)$  is obtained by the system shown in Figure AP3.3. Obtain a state variable representation of the system.

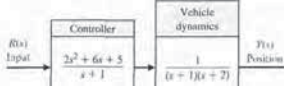


FIGURE AP3.3 Position control.

AP3.4 Front suspensions have become standard equipment on mountain bikes. Replacing the rigid fork that attaches the bicycle's front tire to its frame, such suspensions absorb bump impact energy, shielding both frame and rider from jolts. Commonly used forks, however, use only one spring constant and treat bump impacts at high and low speeds—impacts that vary greatly in severity—essentially the same.

A suspension system with multiple settings that are adjustable while the bike is in motion would be attractive. One air and coil spring with an oil damper is available that permits an adjustment of the damping constant to the terrain as well as to the rider's weight [17]. The suspension system model is shown in Figure AP3.4, where  $b$  is adjustable. Select the appropriate value for  $b$  so that the bike accommodates (a) a large bump at high speeds and (b) a small bump at low speeds. Assume that  $k_2 = 1$  and  $k_1 = 2$ .

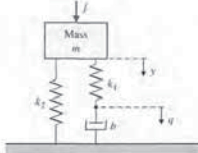


FIGURE AP3.4 Shock absorber.

AP3.5 Figure AP3.5 shows a mass  $M$  suspended from another mass  $m$  by means of a light rod of length  $L$ . Obtain a state variable model using a linear model assuming a small angle for  $\theta$ . Assume the output is the angle,  $\theta$ .

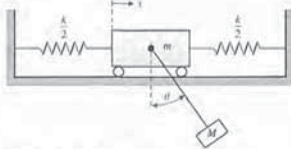


FIGURE AP3.5 Mass suspended from cart.

AP3.6 Consider a crane moving in the  $x$  direction while the mass  $m$  moves in the  $z$  direction, as shown in

DESIGN PROBLEMS

CDP3.1 The traction drive uses the capstan drive system shown in Figure CDP2.1. Neglect the effect of the motor inductance and determine a state variable model for the system. The parameters are given in Table CDP2.1. The friction of the slide is negligible.

DP3.1 A spring-mass-damper system, as shown in Figure 3.3, is used as a shock absorber for a large high-performance motorcycle. The original parameters selected are  $m = 1 \text{ kg}$ ,  $b = 9 \text{ N s/m}$ , and  $k = 20 \text{ N/m}$ . (a) Determine the system matrix, the characteristic roots, and the transition matrix  $\Phi(t)$ . The harsh initial conditions are assumed to be  $y(0) = 1$  and  $dy/dt|_{t=0} = 2$ . (b) Plot the response of  $y(t)$  and  $dy/dt$  for the first two seconds. (c) Redesign the shock absorber by changing the spring constant and the damping constant in order to reduce the effect of a high rate of acceleration force  $d^2y/dt^2$  on the rider. The mass must remain constant at  $1 \text{ kg}$ .

DP3.2 A system has the state variable matrix equation in phase variable form

$$\dot{\mathbf{x}} = \begin{bmatrix} 0 & 1 \\ -a & -b \end{bmatrix} \mathbf{x} + \begin{bmatrix} 0 \\ d \end{bmatrix} u(t)$$

$$y = [1 \ 0] \mathbf{x}$$

It is desired that the canonical diagonal form of the differential equation be

$$\dot{\mathbf{z}} = \begin{bmatrix} -5 & 0 \\ 0 & -2 \end{bmatrix} \mathbf{z} + \begin{bmatrix} 1 \\ 1 \end{bmatrix} u$$

$$y = [-2 \ 2] \mathbf{z}$$

Determine the parameters  $a$ ,  $b$ , and  $d$  to yield the required diagonal matrix differential equation.

DP3.3 An aircraft arresting gear is used on an aircraft carrier as shown in Figure DP3.3. The linear model of each energy absorber has a drag force  $f_D = K_D v$ . It is desired to halt the airplane within 30 m after engaging the arresting cable [13]. The speed of the aircraft on landing is 60 m/s. Select the required constant  $K_D$ , and plot the response of the state variables.

DP3.4 The Mile-High Bungee Jumping Company wants you to design a bungee jumping system (i.e., a cord) so that the jumper cannot hit the ground when his or her mass is less than 100 kg, but greater than 50 kg. Also, the company wants a hang time (the time a jumper is moving up and down) greater than 25 seconds, but less than 40 seconds. Determine the characteristics of the cord. The jumper stands on a platform 50 m above the ground, and the cord will be attached to a fixed beam secured 10 m above the platform. Assume that the jumper is 2 m tall and the cord is attached at the waist (1 m high).

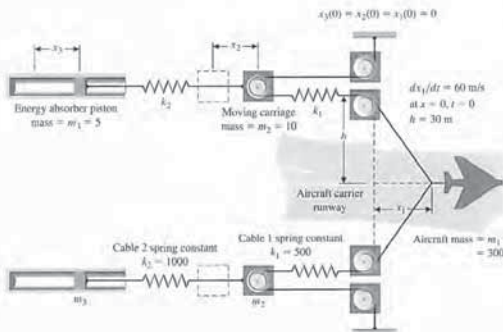


FIGURE DP3.3 Aircraft arresting gear.

motor friction is negligible. The motor and valve inertia is  $J = 0.006$ , and the area of the tank is  $50 \text{ m}^2$ . Note that the motor is controlled by the armature current  $i_a$ . Let  $x_1 = h$ ,  $x_2 = \theta$ , and  $x_3 = dh/dt$ . Assume that  $q_1 = 800$ , where  $\theta$  is the shaft angle. The output flow is  $q_0 = 50h(t)$ .

AP3.6 Consider the two-mass system in Figure P3.36. Find a state variable representation of the system. Assume the output is  $x$ .

AP3.7 Consider the block diagram in Figure P3.37. Using the block diagram as a guide, obtain the state variable model of the system in the form

$$\dot{\mathbf{x}} = \mathbf{A}\mathbf{x} + \mathbf{B}u$$

$$y = \mathbf{C}\mathbf{x} + \mathbf{D}u$$

Using the state variable model as a guide, obtain a third-order differential equation model for the system.

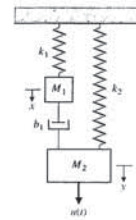


FIGURE P3.36 Two-mass system with two springs and one damper.

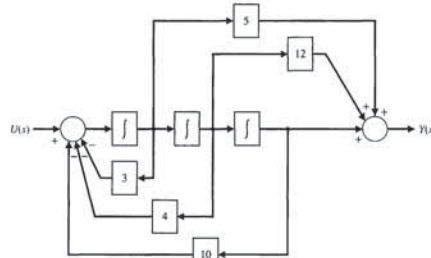


FIGURE P3.37 A block diagram model of a third-order system.

ADVANCED PROBLEMS

AP3.1 Consider the electromagnetic suspension system shown in Figure AP3.1. An electromagnet is located at the upper part of the experimental system. Using the electromagnetic force  $f$ , we want to suspend the iron ball. Note that this simple electromagnetic suspension system is essentially unworkable. Hence feedback control is indispensable. As a gap sensor, a standard induction probe of the type of eddy current is placed below the ball [20].

Assume that the state variables are  $x_1 = x$ ,  $x_2 = dx/dt$ , and  $x_3 = i$ . The electromagnet has an inductance  $L = 0.508 \text{ H}$  and a resistance  $R = 23.2 \Omega$ . Use a Taylor series approximation for the electromagnetic force. The current is  $i = I_0 + i$ , where  $I_0 = 1.06 \text{ A}$  is the operating point and  $i$  is the variable. The mass  $m$  is equal to 1.75 kg. The gap is  $x_r = X_0 + x$ , where  $X_0 = 4.36 \text{ mm}$  is the operating point and  $x$  is the variable. The electromagnetic force

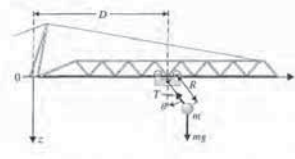


FIGURE AP3.6 A crane moving in the  $x$ -direction while the mass  $m$  moves in the  $z$ -direction.

Figure AP3.6. The trolley motor and the hoist motor are very powerful with respect to the mass of the trolley, the hoist wire, and the load  $m$ . Consider the input control variables as the distances  $D$  and  $R$ . Also assume that  $\theta < 50^\circ$ . Determine a linear model, and describe the state variable differential equation.

AP3.7 Consider the single-input, single-output system described by

$$\dot{\mathbf{x}}(t) = \mathbf{A}\mathbf{x}(t) + \mathbf{B}u(t)$$

$$y(t) = \mathbf{C}\mathbf{x}(t)$$

where

$$\mathbf{A} = \begin{bmatrix} -1 & 1 \\ 0 & 0 \end{bmatrix}, \mathbf{B} = \begin{bmatrix} 0 \\ 1 \end{bmatrix}, \mathbf{C} = [2 \ 1]$$

Assume that the input is a linear combination of the states that is,

$$u(t) = -\mathbf{K}\mathbf{x}(t) + r(t),$$

where  $r(t)$  is the reference input. The matrix  $\mathbf{K} = [K_1 \ K_2]$  is known as the gain matrix. Substituting  $u(t)$  into the state variable equation gives the closed-loop system

$$\dot{\mathbf{x}}(t) = [\mathbf{A} - \mathbf{B}\mathbf{K}]\mathbf{x}(t) + \mathbf{B}r(t)$$

$$y(t) = \mathbf{C}\mathbf{x}(t)$$

The design process involves finding  $\mathbf{K}$  so that the eigenvalues of  $\mathbf{A} - \mathbf{B}\mathbf{K}$  are at desired locations in the left-half plane. Compute the characteristic polynomial associated with the closed-loop system and determine values of  $\mathbf{K}$  so that the closed-loop eigenvalues are in the left-half plane.

AP3.8 A system for dispensing radioactive fluid into capsules is shown in Figure AP3.8(a). The horizontal axis moving the tray of capsules is actuated by a linear motor. The  $x$ -axis control is shown in Figure AP3.8(b).

(a) Obtain a state variable model of the closed-loop system with input  $r(t)$  and output  $y(t)$ . (b) Determine the characteristic roots of the system and compute  $\mathbf{K}$  such that the characteristic values are all co-located at  $s_1 = -2$ ,  $s_2 = -2$ , and  $s_3 = -2$ . (c) Determine analytically the unit step-response of the closed-loop system.

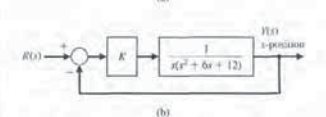
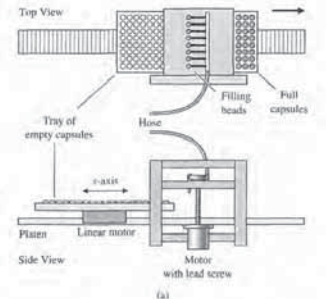


FIGURE AP3.8 Automatic fluid dispenser.

and

$$\dot{\mathbf{x}}_2 = \begin{bmatrix} 0.5000 & 0.5000 & 0.7071 \\ -0.5000 & -0.5000 & 0.7071 \\ -6.3640 & -0.7071 & -8.0000 \end{bmatrix} \mathbf{x}_2 + \begin{bmatrix} 0 \\ 0 \\ 4 \end{bmatrix} u, \quad (2)$$

$$y = [0.7071 \quad -0.7071 \quad 0] \mathbf{x}_2$$

- (a) Using the tf function, determine the transfer function  $Y(s)/U(s)$  for system (1).  
 (b) Repeat part (a) for system (2).  
 (c) Compare the results in parts (a) and (b) and comment.
- CP3.6** Consider the closed-loop control system in Figure CP3.6.
- (a) Determine a state variable representation of the controller.  
 (b) Repeat part (a) for the process.  
 (c) With the controller and process in state variable form, use the series and feedback functions to compute a closed-loop system representation in state variable form and plot the closed-loop system impulse response.

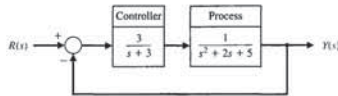


FIGURE CP3.6 A closed-loop feedback control system.

**CP3.7** Consider the following system:

$$\dot{\mathbf{x}} = \begin{bmatrix} 0 & 1 \\ -2 & -3 \end{bmatrix} \mathbf{x} + \begin{bmatrix} 0 \\ 1 \end{bmatrix} u$$

$$y = [1 \quad 0] \mathbf{x}$$

with

$$\mathbf{x}(0) = \begin{bmatrix} 1 \\ 0 \end{bmatrix}$$

Using the tfm function obtain and plot the system response for  $x_1(t)$  and  $x_2(t)$  when  $u(t) = 0$ .

**CP3.8** Consider the state variable model with parameter  $K$  given by

$$\dot{\mathbf{x}} = \begin{bmatrix} 0 & 1 & 0 \\ 0 & 0 & 1 \\ -2 & -K & -2 \end{bmatrix} \mathbf{x} + \begin{bmatrix} 0 \\ 0 \\ 1 \end{bmatrix} u,$$

$$y = [1 \quad 0 \quad 0] \mathbf{x}.$$

Plot the characteristic values of the system as a function of  $K$  in the range  $0 \leq K \leq 100$ . Determine that range of  $K$  for which all the characteristic values lie in the left half-plane.

**ANSWERS TO SKILLS CHECK**

- True or False: (1) True; (2) True; (3) False; (4) False; (5) False.  
 Multiple Choice: (6) a; (7) b; (8) c; (9) b; (10) c; (11) a; (12) a; (13) c; (14) c; (15) c

Word Match (in order, top to bottom): f, d, g, a, b, c, e

**TERMS AND CONCEPTS**

**Canonical form** A fundamental or basic form of the state variable model representation, including phase variable canonical form, input feedforward canonical form, diagonal canonical form, and Jordan canonical form.  
**Diagonal canonical form** A decoupled canonical form displaying the  $n$  distinct system poles on the diagonal of the state variable representation  $A$  matrix.

**Fundamental matrix** See Transition matrix.  
**Input feedforward canonical form** A canonical form described by  $n$  feedback loops involving the  $a_n$  coefficients of the  $n$ th order denominator polynomial of the transfer function and feedforward loops obtained by feeding forward the input signal.

**Computer Problems**

- DP3.5** Consider the single-input, single-output system described by
- $$\dot{\mathbf{x}}(t) = \mathbf{A}\mathbf{x}(t) + \mathbf{B}u(t)$$
- $$y(t) = \mathbf{C}\mathbf{x}(t)$$
- where
- $$\mathbf{A} = \begin{bmatrix} 0 & 1 \\ -2 & 3 \end{bmatrix}, \mathbf{B} = \begin{bmatrix} 0 \\ 1 \end{bmatrix}, \mathbf{C} = [1 \quad 0].$$
- Assume that the input is a linear combination of the states that is,

$u(t) = -\mathbf{K}\mathbf{x}(t) + r(t)$ , where  $r(t)$  is the reference input. Determine  $\mathbf{K} = [K_1 \quad K_2]$  so that the closed-loop system

$$\dot{\mathbf{x}}(t) = [\mathbf{A} - \mathbf{B}\mathbf{K}]\mathbf{x}(t) + \mathbf{B}r(t)$$

$$y(t) = \mathbf{C}\mathbf{x}(t)$$

possesses closed-loop eigenvalues at  $r_1$  and  $r_2$ . Note that if  $r_1 = \sigma + j\omega$  is a complex number, then  $r_2 = \sigma - j\omega$  is its complex conjugate.

**COMPUTER PROBLEMS**

**CP3.1** Determine a state variable representation for the following transfer functions (without feedback) using the SS function:

- (a)  $G(s) = \frac{1}{s+10}$   
 (b)  $G(s) = \frac{s^2 + 5s + 3}{s^2 + 8s + 5}$   
 (c)  $G(s) = \frac{s+1}{s^3 + 3s^2 + 3s + 1}$

**CP3.2** Determine a transfer function representation for the following state variable models using the tf function:

- (a)  $\mathbf{A} = \begin{bmatrix} 0 & 1 \\ 2 & 8 \end{bmatrix}, \mathbf{B} = \begin{bmatrix} 0 \\ 1 \end{bmatrix}, \mathbf{C} = [1 \quad 0]$   
 (b)  $\mathbf{A} = \begin{bmatrix} 1 & 1 & 0 \\ -2 & 0 & 4 \\ 5 & 4 & -7 \end{bmatrix}, \mathbf{B} = \begin{bmatrix} -1 \\ 0 \\ 1 \end{bmatrix}, \mathbf{C} = [0 \quad 1 \quad 0]$   
 (c)  $\mathbf{A} = \begin{bmatrix} 0 & 1 \\ -1 & -2 \end{bmatrix}, \mathbf{B} = \begin{bmatrix} 0 \\ 1 \end{bmatrix}, \mathbf{C} = [-2 \quad 1].$

**CP3.3** Consider the circuit shown in Figure CP3.3. Determine the transfer function  $V_d(s)/V_{in}(s)$ . Assume an ideal op-amp.

- (a) Determine the state variable representation when  $R_1 = 1 \text{ k}\Omega, R_2 = 10 \text{ k}\Omega, C_1 = 0.5 \text{ mF}$ , and  $C_2 = 0.1 \text{ mF}$ .  
 (b) Using the state variable representation from part (a), plot the unit step response with the step function.

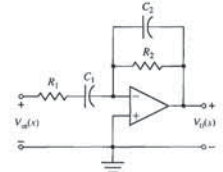


FIGURE CP3.3 An op-amp circuit.

- CP3.4** Consider the system
- $$\dot{\mathbf{x}} = \begin{bmatrix} 0 & 1 & 0 \\ 0 & 0 & 1 \\ -3 & -2 & -5 \end{bmatrix} \mathbf{x} + \begin{bmatrix} 0 \\ 0 \\ 1 \end{bmatrix} u,$$
- $$y = [1 \quad 0 \quad 0] \mathbf{x}$$
- (a) Using the tf function, determine the transfer function  $Y(s)/U(s)$ .  
 (b) Plot the response of the system to the initial condition  $\mathbf{x}(0) = [0 \quad -1 \quad 1]^T$  for  $0 \leq t \leq 10$ .  
 (c) Compute the state transition matrix using the expm function, and determine  $\mathbf{x}(t)$  at  $t = 10$  for the initial condition given in part (b). Compare the result with the system response obtained in part (b).

**CP3.5** Consider the two systems

$$\dot{\mathbf{x}}_1 = \begin{bmatrix} 0 & 1 & 0 \\ 0 & 0 & 1 \\ -4 & -5 & -8 \end{bmatrix} \mathbf{x}_1 + \begin{bmatrix} 0 \\ 0 \\ 4 \end{bmatrix} u,$$

$$y = [1 \quad 0 \quad 0] \mathbf{x}_1 \quad (1)$$

# CHAPTER 4 Feedback Control System Characteristics

4.1 Introduction 235  
 4.2 Error Signal Analysis 237  
 4.3 Sensitivity of Control Systems to Parameter Variations 239  
 4.4 Disturbance Signals in a Feedback Control System 242  
 4.5 Control of the Transient Response 247  
 4.6 Steady-State Error 250  
 4.7 The Cost of Feedback 253  
 4.8 Design Examples 254  
 4.9 Control System Characteristics Using Control Design Software 268  
 4.10 Sequential Design Example: Disk Drive Read System 273  
 4.11 Summary 277

**P R E V I E W**

In this chapter, we explore the role of error signals to characterize feedback control system performance. The areas of interest include the reduction of sensitivity to model uncertainties, disturbance rejection, measurement noise attenuation, steady-state errors and transient response characteristics. The error signal is used to control the process by negative feedback. Generally speaking, the goal is to minimize the error signal. We discuss the sensitivity of a system to parameter changes, since it is desirable to minimize the effects of parameter variations and uncertainties. We also wish to diminish the effect of unwanted disturbances and measurement noise on the ability of the system to track a desired input. We then describe the transient and steady-state performance of a feedback system and show how this performance can be readily improved with feedback. Of course, the benefits of a control system come with an attendant cost. The chapter concludes with a system performance analysis of the Sequential Design Example: Disk Drive Read System.

**DESIRED OUTCOMES**

- Upon completion of Chapter 4, students should:
- Be aware of the central role of error signals in analysis of control systems.
  - Recognize the improvements afforded by feedback control in reducing system sensitivity to parameter changes, disturbance rejection, and measurement noise attenuation.
  - Understand the differences between controlling the transient response and the steady-state response of a system.
  - Have a sense of the benefits and costs of feedback in the control design process.

**Terms and Concepts**

**Jordan canonical form** A block diagonal canonical form for systems that do not possess distinct system poles.  
**Matrix exponential function** An important matrix function, defined as  $e^{At} = \mathbf{I} + \mathbf{A}t + (\mathbf{A}t)^2/2! + \dots + (\mathbf{A}t)^k/k! + \dots$ , that plays a role in the solution of linear constant coefficient differential equations.  
**Output equation** The algebraic equation that relates the state vector  $\mathbf{x}$  and the inputs  $\mathbf{u}$  to the outputs  $\mathbf{y}$  through the relationship  $\mathbf{y} = \mathbf{C}\mathbf{x} + \mathbf{D}\mathbf{u}$ .  
**Phase variable canonical form** A canonical form described by  $n$  feedback loops involving the  $a_n$  coefficients of the  $n$ th order denominator polynomial of the transfer function and  $m$  feedforward loops involving the  $b_m$  coefficients of the  $m$ th order numerator polynomial of the transfer function.  
**Phase variables** The state variables associated with the phase variable canonical form.  
**Physical variables** The state variables representing the physical variables of the system.

**State differential equation** The differential equation for the state vector:  $\dot{\mathbf{x}} = \mathbf{A}\mathbf{x} + \mathbf{B}\mathbf{u}$ .  
**State of a system** A set of numbers such that the knowledge of these numbers and the input function will, with the equations describing the dynamics, provide the future state of the system.  
**State-space representation** A time-domain model comprising the state differential equation  $\dot{\mathbf{x}} = \mathbf{A}\mathbf{x} + \mathbf{B}\mathbf{u}$  and the output equation,  $\mathbf{y} = \mathbf{C}\mathbf{x} + \mathbf{D}\mathbf{u}$ .  
**State variables** The set of variables that describe the system.  
**State vector** The vector containing all  $n$  state variables,  $x_1, x_2, \dots, x_n$ .  
**Time domain** The mathematical domain that incorporates the time response and the description of a system in terms of time  $t$ .  
**Time-varying system** A system for which one or more parameters may vary with time.  
**Transition matrix  $\Phi(t)$**  The matrix exponential function that describes the unforced response of the system.



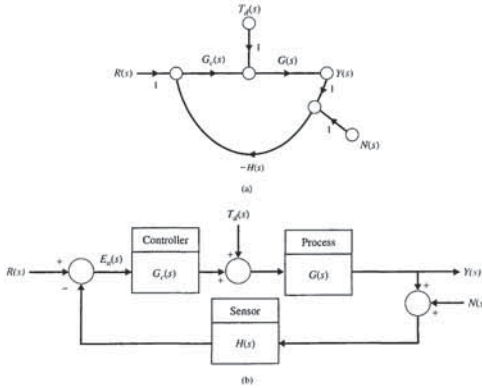
**An open-loop system operates without feedback and directly generates the output in response to an input signal.**

By contrast, a closed-loop, negative feedback control system is shown in Figure 4.3.

**A closed-loop system uses a measurement of the output signal and a comparison with the desired output to generate an error signal that is used by the controller to adjust the actuator.**

The two forms of control systems are shown in both block diagram and signal-flow graph form. Despite the cost and increased system complexity, closed-loop feedback control has the following advantages:

- Decreased sensitivity of the system to variations in the parameters of the process.
- Improved rejection of the disturbances.
- Improved measurement noise attenuation.
- Improved reduction of the steady-state error of the system.
- Easy control and adjustment of the transient response of the system.



**FIGURE 4.3** A closed-loop control system. (a) Signal-flow graph. (b) Block diagram.

4.1 INTRODUCTION

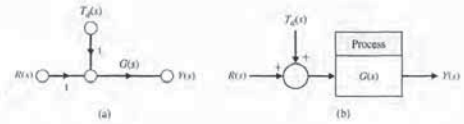
A control system is defined as an interconnection of components forming a system that will provide a desired system response. Because the desired system response is known, a signal proportional to the error between the desired and the actual response is generated. The use of this signal to control the process results in a closed-loop sequence of operations that is called a feedback system. This closed-loop sequence of operations is shown in Figure 4.1. The introduction of feedback to improve the control system is often necessary. It is interesting that this is also the case for systems in nature, such as biological and physiological systems; feedback is inherent in these systems. For example, the human heart rate control system is a feedback control system.

To illustrate the characteristics and advantages of introducing feedback, we will consider a single-loop feedback system. Although many control systems are multi-loop, a single-loop system is illustrative. A thorough comprehension of the benefits of feedback can best be obtained from the single-loop system and then extended to multiloop systems.

A system without feedback, often called an open-loop system, is shown in Figure 4.2. The disturbance,  $T_d(s)$ , directly influences the output,  $Y(s)$ . In the absence of feedback, the control system is highly sensitive to disturbances and to changes in parameters of  $G(s)$ .



**FIGURE 4.1** A closed-loop system.



**FIGURE 4.2** An open-loop system with a disturbance input,  $T_d(s)$ . (a) Signal-flow graph. (b) Block diagram.

Then, in terms of  $F(s)$ , we define the sensitivity function as

$$S(s) = \frac{1}{F(s)} = \frac{1}{1 + L(s)} \tag{4.5}$$

Similarly, in terms of the loop gain, we define the complementary sensitivity function as

$$C(s) = \frac{L(s)}{1 + L(s)} \tag{4.6}$$

In terms of the functions  $S(s)$  and  $C(s)$ , we can write the tracking error as

$$E(s) = S(s)R(s) - S(s)G(s)T_d(s) + C(s)N(s). \tag{4.7}$$

Examining Equation (4.7), we see that (for a given  $G(s)$ ), if we want to minimize the tracking error, we want both  $S(s)$  and  $C(s)$  to be small. Remember that  $S(s)$  and  $C(s)$  are both functions of the controller,  $G_c(s)$ , which the control design engineer must select. However, the following special relationship between  $S(s)$  and  $C(s)$  holds

$$S(s) + C(s) = 1. \tag{4.8}$$

We cannot simultaneously make  $S(s)$  and  $C(s)$  small. Obviously, design compromises must be made.

To analyze the tracking error equation, we need to understand what it means for a transfer function to be “large” or to be “small.” The discussion of magnitude of a transfer function is the subject of Chapters 8 and 9 on frequency response methods. However, for our purposes here, we describe the magnitude of the loop gain  $L(s)$  by considering the magnitude  $|L(j\omega)|$  over the range of frequencies,  $\omega$ , of interest.

Considering the tracking error in Equation (4.4), it is evident that, for a given  $G(s)$ , to reduce the influence of the disturbance,  $T_d(s)$ , on the tracking error,  $E(s)$ , we desire  $L(s)$  to be large over the range of frequencies that characterize the disturbances. That way, the transfer function  $G(s)/(1 + L(s))$  will be small, thereby reducing the influence of  $T_d(s)$ . Since  $L(s) = G_c(s)G(s)$ , this implies that we need to design the controller  $G_c(s)$  to have a large magnitude. Conversely, to attenuate the measurement noise,  $N(s)$ , and reduce the influence on the tracking error, we desire  $L(s)$  to be small over the range of frequencies that characterize the measurement noise. The transfer function  $L(s)/(1 + L(s))$  will be small, thereby reducing the influence of  $N(s)$ . Again, since  $L(s) = G_c(s)G(s)$ , that implies that we need to design the controller  $G_c(s)$  to have a small magnitude. Fortunately, the apparent conflict between wanting to make  $G_c(s)$  large to reject disturbances and the wanting to make  $G_c(s)$  small to attenuate measurement noise can be addressed in the design phase by making the loop gain,  $L(s)$ , large at low frequencies (generally associated with the frequency range of disturbances), and making  $L(s)$  small at high frequencies (generally associated with measurement noise).

More discussion on disturbance rejection and measurement noise attenuation follows in the subsequent sections. Next, we discuss how we can use feedback to reduce the sensitivity of the system to variations and uncertainty in parameters in the process,  $G(s)$ . This is accomplished by analyzing the tracking error in Equation (4.2) when  $T_d(s) = N(s) = 0$ .

In this chapter, we examine how the application of feedback can result in the benefits listed above. Using the notion of a tracking error signal, it will be readily apparent that it is possible to utilize feedback with a controller in the loop to improve system performance.

4.2 ERROR SIGNAL ANALYSIS

The closed-loop feedback control system shown in Figure 4.3 has three inputs— $R(s)$ ,  $T_d(s)$ , and  $N(s)$ —and one output,  $Y(s)$ . The signals  $T_d(s)$  and  $N(s)$  are the disturbance and measurement noise signals, respectively. Define the **tracking error** as

$$E(s) = R(s) - Y(s). \tag{4.1}$$

For ease of discussion, we will consider a unity feedback system, that is,  $H(s) = 1$ , in Figure 4.3. In Section 5.5 of the following chapter, the influence of a nonunity feedback element in the loop is considered.

After some block diagram manipulation, we find that the output is given by

$$Y(s) = \frac{G_c(s)G(s)}{1 + G_c(s)G(s)}R(s) + \frac{G(s)}{1 + G_c(s)G(s)}T_d(s) - \frac{G_c(s)G(s)}{1 + G_c(s)G(s)}N(s). \tag{4.2}$$

Therefore, with  $E(s) = R(s) - Y(s)$ , we have

$$E(s) = \frac{1}{1 + G_c(s)G(s)}R(s) - \frac{G(s)}{1 + G_c(s)G(s)}T_d(s) + \frac{G_c(s)G(s)}{1 + G_c(s)G(s)}N(s). \tag{4.3}$$

Define the function

$$L(s) = G_c(s)G(s).$$

The function,  $L(s)$ , is known as the **loop gain** and plays a fundamental role in control system analysis [12]. In terms of  $L(s)$  the tracking error is given by

$$E(s) = \frac{1}{1 + L(s)}R(s) - \frac{G(s)}{1 + L(s)}T_d(s) + \frac{L(s)}{1 + L(s)}N(s). \tag{4.4}$$

We can define the function

$$F(s) = 1 + L(s).$$

smaller sensitivity,  $S(s)$ . The question arises, how do we define sensitivity? Since our goal is to reduce system sensitivity, it makes sense to formally define the term.

The **system sensitivity** is defined as the ratio of the percentage change in the system transfer function to the percentage change of the process transfer function. The system transfer function is

$$T(s) = \frac{Y(s)}{R(s)} \tag{4.10}$$

and therefore the sensitivity is defined as

$$S = \frac{\Delta T(s)/T(s)}{\Delta G(s)/G(s)} \tag{4.11}$$

In the limit, for small incremental changes, Equation (4.11) becomes

$$S = \frac{\partial T/T}{\partial G/G} = \frac{\partial \ln T}{\partial \ln G} \tag{4.12}$$

**System sensitivity is the ratio of the change in the system transfer function to the change of a process transfer function (or parameter) for a small incremental change.**

The sensitivity of the open-loop system to changes in the plant  $G(s)$  is equal to 1. The sensitivity of the closed-loop is readily obtained by using Equation (4.12). The system transfer function of the closed-loop system is

$$T(s) = \frac{G_c(s)G(s)}{1 + G_c(s)G(s)}$$

Therefore, the sensitivity of the feedback system is

$$S_G^T = \frac{\partial T}{\partial G} \cdot \frac{G}{T} = \frac{G_c}{(1 + G_c G)^2} \cdot \frac{G}{G_c/(1 + G_c G)}$$

or

$$S_G^T = \frac{1}{1 + G_c(s)G(s)} \tag{4.13}$$

We find that the sensitivity of the system may be reduced below that of the open-loop system by increasing  $L(s) = G_c(s)G(s)$  over the frequency range of interest. Note that  $S_G^T$  in Equation (4.12) is exactly the same as the sensitive function  $S(s)$  given in Equation (4.5). In fact, these functions are one and the same.

Often, we seek to determine  $S_a^T$ , where  $a$  is a parameter within the transfer function of a block  $G$ . Using the chain rule, we find that

$$S_a^T = S_G^T S_G^G \tag{4.14}$$

4.3 SENSITIVITY OF CONTROL SYSTEMS TO PARAMETER VARIATIONS

A process, represented by the transfer function  $G(s)$ , whatever its nature, is subject to a changing environment, aging, ignorance of the exact values of the process parameters, and other natural factors that affect a control process. In the open-loop system, all these errors and changes result in a changing and inaccurate output. However, a closed-loop system senses the change in the output due to the process changes and attempts to correct the output. The sensitivity of a control system to parameter variations is of prime importance. A primary advantage of a closed-loop feedback control system is its ability to reduce the system's sensitivity [1-4, 18].

For the closed-loop case, if  $G_c(s)G(s) \gg 1$  for all complex frequencies of interest, we can use Equation (4.2) to obtain (letting  $T_d(s) = 0$  and  $N(s) = 0$ )

$$Y(s) \approx R(s).$$

The output is approximately equal to the input. However, the condition  $G_c(s)G(s) \gg 1$  may cause the system response to be highly oscillatory and even unstable. But that increasing the magnitude of the loop gain reduces the effect of  $G(s)$  on the output is an exceedingly useful result. Therefore, the first advantage of a feedback system is that the effect of the variation of the parameters of the process,  $G(s)$ , is reduced.

Suppose the process (or plant)  $G(s)$  undergoes a change such that the true plant model is  $G(s) + \Delta G(s)$ . The change in the plant may be due to a changing external environment or natural aging, or it may just represent the uncertainty in certain plant parameters. We consider the effect on the tracking error  $E(s)$  due to  $\Delta G(s)$ . Relying on the principle of superposition, we can let  $T_d(s) = N(s) = 0$  and consider only the reference input  $R(s)$ . From Equation (4.3), it follows that

$$E(s) + \Delta E(s) = \frac{1}{1 + G_c(s)(G(s) + \Delta G(s))} R(s).$$

Then the change in the tracking error is

$$\Delta E(s) = \frac{-G_c(s) \Delta G(s)}{(1 + G_c(s)G(s) + G_c(s) \Delta G(s))(1 + G_c(s)G(s))} R(s).$$

Since we usually find that  $G_c(s)G(s) \gg G_c(s) \Delta G(s)$ , we have

$$\Delta E(s) \approx \frac{-G_c(s) \Delta G(s)}{(1 + L(s))^2} R(s).$$

We see that the change in the tracking error is reduced by the factor  $1 + L(s)$ , which is generally greater than 1 over the range of frequencies of interest.

For large  $L(s)$ , we have  $1 + L(s) \approx L(s)$ , and we can approximate the change in the tracking error by

$$\Delta E(s) \approx \frac{1}{L(s)} \frac{\Delta G(s)}{G(s)} R(s). \tag{4.9}$$

Larger magnitude  $L(s)$  translates into smaller changes in the tracking error (that is, reduced sensitivity to changes in  $\Delta G(s)$  in the process). Also, larger  $L(s)$  implies

Very often, the transfer function of the system  $T(s)$  is a fraction of the form [1]

$$T(s, \alpha) = \frac{N(s, \alpha)}{D(s, \alpha)} \tag{4.15}$$

where  $\alpha$  is a parameter that may be subject to variation due to the environment. Then we may obtain the sensitivity to  $\alpha$  by rewriting Equation (4.11) as

$$S_\alpha^T = \frac{\partial \ln T}{\partial \ln \alpha} = \frac{\partial \ln N}{\partial \ln \alpha} - \frac{\partial \ln D}{\partial \ln \alpha} \Big|_{\alpha_0} = S_\alpha^N - S_\alpha^D \tag{4.16}$$

where  $\alpha_0$  is the nominal value of the parameter.

An important advantage of feedback control systems is the ability to reduce the effect of the variation of parameters of a control system by adding a feedback loop. To obtain highly accurate open-loop systems, the components of the open-loop,  $G(s)$ , must be selected carefully in order to meet the exact specifications. However, a closed-loop system allows  $G(s)$  to be less accurately specified, because the sensitivity to changes or errors in  $G(s)$  is reduced by the loop gain  $L(s)$ . This benefit of closed-loop systems is a profound advantage for the electronic amplifiers of the communication industry. A simple example will illustrate the value of feedback for reducing sensitivity.

EXAMPLE 4.1 Feedback amplifier

An amplifier used in many applications has a gain  $-K_a$ , as shown in Figure 4.4(a). The output voltage is

$$v_o = -K_a v_{in} \tag{4.17}$$

We often add feedback using a potentiometer  $R_p$ , as shown in Figure 4.4(b). The transfer function of the amplifier without feedback is

$$T = -K_a \tag{4.18}$$

and the sensitivity to changes in the amplifier gain is

$$S_{K_a}^T = 1. \tag{4.19}$$

The block diagram model of the amplifier with feedback is shown in Figure 4.5, where

$$\beta = \frac{R_2}{R_1} \tag{4.20}$$

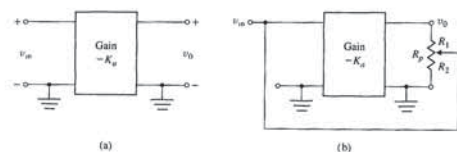


FIGURE 4.4 (a) Open-loop amplifier. (b) Amplifier with feedback.

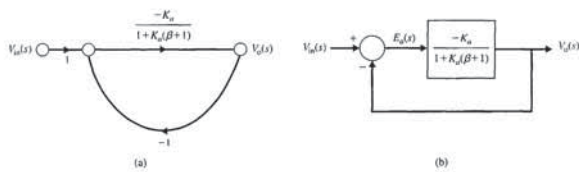


FIGURE 4.5 Block diagram model of feedback amplifier assuming  $R_p \gg R_o$  of the amplifier.

and

$$R_p = R_1 + R_2 \tag{4.21}$$

The closed-loop transfer function of the feedback amplifier is

$$T = \frac{-K_a}{1 + K_a \beta} \tag{4.22}$$

The sensitivity of the closed-loop feedback amplifier is

$$S_{K_a}^T = S_{K_a}^T S_{K_a}^G = \frac{1}{1 + K_a \beta} \tag{4.23}$$

If  $K_a$  is large, the sensitivity is low. For example, if

$$K_a = 10^4$$

and

$$\beta = 0.1, \tag{4.24}$$

we have

$$S_{K_a}^T = \frac{1}{1 + 10^3}, \tag{4.25}$$

or the magnitude is one-thousandth of the magnitude of the open-loop amplifier.

We shall return to the concept of sensitivity in subsequent chapters. These chapters will emphasize the importance of sensitivity in the design and analysis of control systems. ■

4.4 DISTURBANCE SIGNALS IN A FEEDBACK CONTROL SYSTEM

An important effect of feedback in a control system is the control and partial elimination of the effect of disturbance signals. A **disturbance signal** is an unwanted input signal that affects the output signal. Many control systems are subject to extraneous disturbance signals that cause the system to provide an inaccurate output. Electronic amplifiers have inherent noise generated within the integrated circuits or transistors;



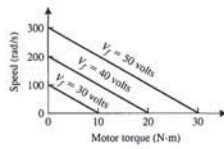


FIGURE 4.8 Motor speed-torque curves.

The change in speed due to the load disturbance is then

$$E(s) = -\omega(s) = \frac{1}{Js + b + K_m K_b / R_a} T_d(s). \quad (4.26)$$

The steady-state error in speed due to the load torque,  $T_d(s) = D/s$ , is found by using the final-value theorem. Therefore, for the open-loop system, we have

$$\begin{aligned} \lim_{t \rightarrow \infty} E(t) &= \lim_{s \rightarrow 0} s E(s) = \lim_{s \rightarrow 0} s \frac{1}{Js + b + K_m K_b / R_a} \left( \frac{D}{s} \right) \\ &= \frac{D}{b + K_m K_b / R_a} = -\omega_0(\infty). \end{aligned} \quad (4.27)$$

The closed-loop speed control system is shown in block diagram form in Figure 4.9. The closed-loop system is shown in signal-flow graph and block diagram form in Figure 4.10, where  $G_1(s) = K_a K_m / R_a$ ,  $G_2(s) = 1/(Js + b)$ , and  $H(s) = K_t + K_b / K_a$ . The error,  $E(s) = -\omega(s)$ , of the closed-loop system of Figure 4.10 is:

$$E(s) = -\omega(s) = \frac{G_2(s)}{1 + G_1(s)G_2(s)H(s)} T_d(s). \quad (4.28)$$

Then, if  $G_1 G_2 H(s)$  is much greater than 1 over the range of  $s$ , we obtain the approximate result

$$E(s) \approx \frac{1}{G_1(s)H(s)} T_d(s). \quad (4.29)$$

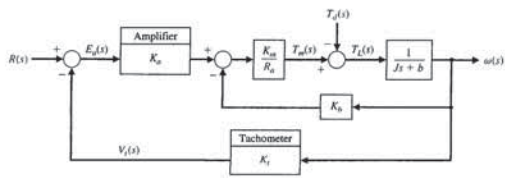


FIGURE 4.9 Closed-loop speed tachometer control system.

radar antennas are subjected to wind gusts; and many systems generate unwanted distortion signals due to nonlinear elements. The benefit of feedback systems is that the effect of distortion, noise, and unwanted disturbances can be effectively reduced.

**Disturbance Rejection**

When  $R(s) = N(s) = 0$ , it follows from Equation (4.4) that

$$E(s) = -S(s)G(s)T_d(s) = \frac{G(s)}{1 + L(s)} T_d(s).$$

For a fixed  $G(s)$  and a given  $T_d(s)$ , as the loop gain  $L(s)$  increases, the effect of  $T_d(s)$  on the tracking error decreases. In other words, the sensitivity function  $S(s)$  is small when the loop gain is large. We say that large loop gain leads to good disturbance rejection. More precisely, for good disturbance rejection, we require a large loop gain over the frequencies of interest associated with the expected disturbance signals.

In practice, the disturbance signals are often low frequency. When that is the case, we say that we want the loop gain to be large at low frequencies. This is equivalent to stating that we want to design the controller  $G_c(s)$  so that the sensitivity function  $S(s)$  is small at low frequencies.

As a specific example of a system with an unwanted disturbance, let us consider again the speed control system for a steel rolling mill. The rolls, which process steel, are subjected to large load changes or disturbances. As a steel bar approaches the rolls (see Figure 4.6), the rolls are empty. However, when the bar engages in the rolls, the load on the rolls increases immediately to a large value. This loading effect can be approximated by a step change of disturbance torque. Alternatively, the response can be seen from the speed-torque curves of a typical motor, as shown in Figure 4.8.

The transfer function model of an armature-controlled DC motor with a load torque disturbance was determined in Example 2.5 and is shown in Figure 4.7, where it is assumed that  $L_a$  is negligible. Let  $R(s) = 0$  and examine  $E(s) = -\omega(s)$ , for a disturbance  $T_d(s)$ .

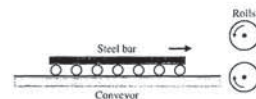


FIGURE 4.6 Steel rolling mill.

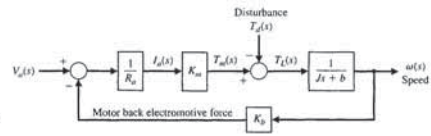


FIGURE 4.7 Open-loop speed control system (without tachometer feedback).

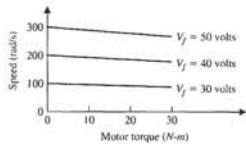


FIGURE 4.11 The speed-torque curves for the closed-loop system.

Figure 4.11. The improvement of the feedback system is evidenced by the almost horizontal curves, which indicate that the speed is almost independent of the load torque.

**Measurement Noise Attenuation**

When  $R(s) = T_d(s) = 0$ , it follows from Equation (4.4) that

$$E(s) = C(s)N(s) = \frac{L(s)}{1 + L(s)} N(s).$$

As the loop gain  $L(s)$  decreases, the effect of  $N(s)$  on the tracking error decreases. In other words, the complementary sensitivity function  $C(s)$  is small when the loop gain  $L(s)$  is small. If we design  $G_c(s)$  such that  $L(s) \ll 1$ , then the noise is attenuated because

$$C(s) \approx L(s).$$

We say that small loop gain leads to good noise attenuation. More precisely, for effective measurement noise attenuation, we need a small loop gain over the frequencies associated with the expected noise signals.

In practice, measurement noise signals are often high frequency. Thus we want the loop gain to be low at high frequencies. This is equivalent to a small complementary sensitivity function at high frequencies. The separation of disturbances (at low frequencies) and measurement noise (at high frequencies) is very fortunate because it gives the control system designer a way to approach the design process: the controller should be high gain at low frequencies and low gain at high frequencies. Remember that by low and high we mean that the loop gain magnitude is low/high at the various high/low frequencies. It is not always the case that the disturbances are low frequency or that the measurement noise is high frequency. For example, an astronaut running on a treadmill on a space station may impart disturbances to the spacecraft at high frequencies. If the frequency separation does not exist, the design process usually becomes more involved (for example, we may have to use notch filters to reject disturbances at known high frequencies). A noise signal that is prevalent in many systems is the noise generated by the measurement sensor. This noise,  $N(s)$ , can be represented as shown in Figure 4.3. The effect of the noise on the output is

$$Y(s) = \frac{-G_c(s)G(s)}{1 + G_c(s)G(s)} N(s). \quad (4.34)$$

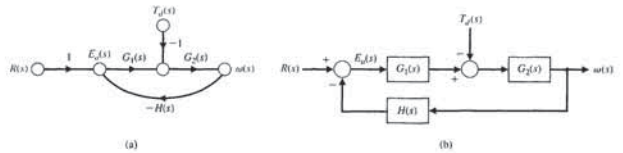


FIGURE 4.10 Closed-loop system. (a) Signal-flow graph model. (b) Block diagram model.

Therefore, if  $G_1(s)H(s)$  is made sufficiently large, the effect of the disturbance can be decreased by closed-loop feedback. Note that

$$G_1(s)H(s) = \frac{K_a K_m}{R_a} \left( K_t + \frac{K_b}{K_a} \right) \approx \frac{K_a K_m K_t}{R_a},$$

since  $K_a \gg K_b$ . Thus, we strive to obtain a large amplifier gain,  $K_a$ , and keep  $R_a < 2 \Omega$ . The error for the system shown in Figure 4.10 is

$$E(s) = R(s) - \omega(s),$$

and  $R(s) = \omega_d(s)$ , the desired speed. For calculation ease, we let  $R(s) = 0$  and examine  $\omega(s)$ .

To determine the output for the speed control system of Figure 4.9, we must consider the load disturbance when the input  $R(s) = 0$ . This is written as

$$\begin{aligned} \omega(s) &= \frac{-1/(Js + b)}{1 + (K_a K_m K_t / R_a)[1/(Js + b)] + (K_m K_b / R_a)[1/(Js + b)]} T_d(s) \\ &= \frac{-1}{Js + b + (K_m / R_a)(K_a K_t + K_b)} T_d(s). \end{aligned} \quad (4.30)$$

The steady-state output is obtained by utilizing the final-value theorem, and we have

$$\lim_{t \rightarrow \infty} \omega(t) = \lim_{s \rightarrow 0} (s\omega(s)) = \frac{-1}{b + (K_m / R_a)(K_a K_t + K_b)} D; \quad (4.31)$$

when the amplifier gain  $K_a$  is sufficiently high, we have

$$\omega(\infty) \approx \frac{-R_a}{K_a K_m K_t} D = \omega_0(\infty). \quad (4.32)$$

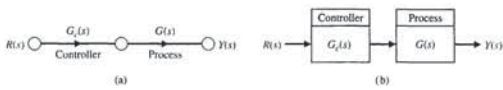
The ratio of closed-loop to open-loop steady-state speed output due to an undesired disturbance is

$$\frac{\omega_0(\infty)}{\omega(\infty)} = \frac{R_a b + K_m K_b}{K_a K_m K_t} \quad (4.33)$$

and is usually less than 0.02.

This advantage of a feedback speed control system can also be illustrated by considering the speed-torque curves for the closed-loop system, which are shown in

**FIGURE 4.12** Cascade controller system (without feedback). (a) Signal-flow graph. (b) Block diagram.



To make this concept more comprehensible, consider a specific control system, which may be operated in an open- or closed-loop manner. A speed control system, as shown in Figure 4.13, is often used in industrial processes to move materials and products. Several important speed control systems are used in steel mills for rolling the steel sheets and moving the steel through the mill [19]. The transfer function of the open-loop system (without feedback) is obtained in Equation (2.70). For  $\omega(s)/V_a(s)$ , we have

$$\frac{\omega(s)}{V_a(s)} = G(s) = \frac{K_1}{\tau_1 s + 1} \quad (4.39)$$

where

$$K_1 = \frac{K_m}{R_a b + K_b K_m} \quad \text{and} \quad \tau_1 = \frac{R_a J}{R_a b + K_b K_m}$$

In the case of a steel mill, the inertia of the rolls is quite large, and a large armature-controlled motor is required. If the steel rolls are subjected to a step command for a speed change of

$$V_a(s) = \frac{k_2 E}{s} \quad (4.40)$$

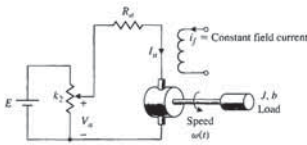
the output response is

$$\omega(s) = G(s)V_a(s) \quad (4.41)$$

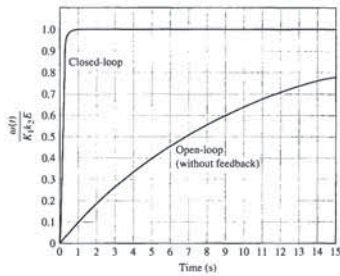
The transient speed change is then

$$\omega(t) = K_1(k_2 E)(1 - e^{-t/\tau_1}) \quad (4.42)$$

If this transient response is too slow, we must choose another motor with a different time constant  $\tau_1$ , if possible. However, because  $\tau_1$  is dominated by the load inertia,  $J$ , it may not be possible to achieve much alteration of the transient response.



**FIGURE 4.13** Open-loop speed control system (without feedback).



**FIGURE 4.15** The response of the open-loop and closed-loop speed control system when  $\tau = 10$  and  $K_a K_f K_1 = 100$ . The time to reach 98% of the final value for the open-loop and closed-loop system is 40 seconds and 0.4 seconds, respectively.

motor and its associated torque signal must be larger for the closed-loop than for the open-loop operation. Therefore, a higher-power motor will be required to avoid saturation of the motor. The responses of the closed-loop system and the open-loop system are shown in Figure 4.15. Note the rapid response of the closed-loop system.

While we are considering this speed control system, it will be worthwhile to determine the sensitivity of the open- and closed-loop systems. As before, the sensitivity of the open-loop system to a variation in the motor constant or the potentiometer constant  $k_2$  is unity. The sensitivity of the closed-loop system to a variation in  $K_m$  is

$$S_{K_m}^{\omega} = S_{G(s)}^{\omega} = \frac{[s + (1/\tau_1)]}{s + (K_a K_f K_1 + 1)/\tau_1}$$

Using the typical values given in the previous paragraph, we have

$$S_{K_m}^{\omega} \approx \frac{(s + 0.10)}{s + 10}$$

We find that the sensitivity is a function of  $s$  and must be evaluated for various values of frequency. This type of frequency analysis is straightforward but will be deferred until a later chapter. However, it is clearly seen that at a specific low frequency—for example,  $s = j\omega = j1$ —the magnitude of the sensitivity is approximately  $|S_{K_m}^{\omega}| \approx 0.1$ .

4.6 STEADY-STATE ERROR

A feedback control system is valuable because it provides the engineer with the ability to adjust the transient response. In addition, as we have seen, the sensitivity of the system and the effect of disturbances can be reduced significantly. However, as a further requirement, we must examine and compare the final steady-state error

which is approximately

$$Y(s) \approx -N(s) \quad (4.35)$$

for large loop gain  $L(s) = G_c(s)G(s)$ . This is consistent with the earlier discussion that smaller loop gain leads to measurement noise attenuation. Clearly, the designer must shape the loop gain appropriately.

The equivalency of sensitivity,  $S_{G(s)}^{\omega}$ , and the response of the closed-loop system tracking error to a reference input can be illustrated by considering Figure 4.3. The sensitivity of the system to  $G(s)$  is

$$S_{G(s)}^{\omega} = \frac{1}{1 + G_c(s)G(s)} = \frac{1}{1 + L(s)} \quad (4.36)$$

The effect of the reference on the tracking error (with  $T_d(s) = 0$  and  $N(s) = 0$ ) is

$$\frac{E(s)}{R(s)} = \frac{1}{1 + G_c(s)G(s)} = \frac{1}{1 + L(s)} \quad (4.37)$$

In both cases, we find that the undesired effects can be alleviated by increasing the loop gain. Feedback in control systems primarily reduces the sensitivity of the system to parameter variations and the effect of disturbance inputs. Note that the measures taken to reduce the effects of parameter variations or disturbances are equivalent, and fortunately, they reduce simultaneously. As a final illustration, consider the effect of the noise on the tracking error:

$$\frac{E(s)}{T_d(s)} = \frac{G_c(s)G(s)}{1 + G_c(s)G(s)} = \frac{L(s)}{1 + L(s)} \quad (4.38)$$

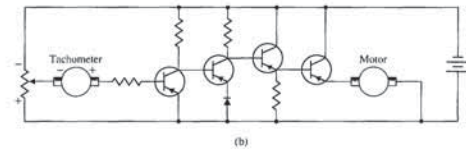
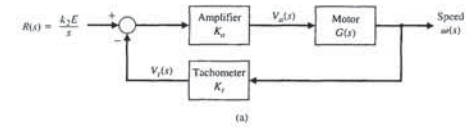
We find that the undesired effects of measurement noise can be alleviated by decreasing the loop gain. Keeping in mind the relationship

$$S(s) + C(s) = 1,$$

the trade-off in the design process is evident.

4.5 CONTROL OF THE TRANSIENT RESPONSE

One of the most important characteristics of control systems is their transient response. The **transient response** is the response of a system as a function of time. Because the purpose of control systems is to provide a desired response, the transient response of control systems often must be adjusted until it is satisfactory. If an open-loop control system does not provide a satisfactory response, then the process,  $G(s)$ , must be replaced with a more suitable process. By contrast, a closed-loop system can often be adjusted to yield the desired response by adjusting the feedback loop parameters. It is often possible to alter the response of an open-loop system by inserting a suitable cascade controller,  $G_c(s)$ , preceding the process,  $G(s)$ , as shown in Figure 4.12. Then it is necessary to design the cascade transfer function,  $G_c(s)G(s)$ , so that the resulting transfer function provides the desired transient response.



**FIGURE 4.14** (a) Closed-loop speed control system. (b) Transistorized closed-loop speed control system.

A closed-loop speed control system is easily obtained by using a tachometer to generate a voltage proportional to the speed, as shown in Figure 4.14(a). This voltage is subtracted from the potentiometer voltage and amplified as shown in Figure 4.14(a). A practical transistor amplifier circuit for accomplishing this feedback in low-power applications is shown in Figure 4.14(b) [1, 5, 7]. The closed-loop transfer function is

$$\begin{aligned} \frac{\omega(s)}{R(s)} &= \frac{K_a G(s)}{1 + K_a K_f G(s)} \\ &= \frac{K_a K_1}{\tau_1 s + 1 + K_a K_f K_1} = \frac{K_a K_1 / \tau_1}{s + (1 + K_a K_f K_1) / \tau_1} \end{aligned} \quad (4.43)$$

The amplifier gain,  $K_a$ , may be adjusted to meet the required transient response specifications. Also, the tachometer gain constant,  $K_f$ , may be varied, if necessary.

The transient response to a step change in the input command is then

$$\omega(t) = \frac{K_a K_1}{1 + K_a K_f K_1} (k_2 E)(1 - e^{-pt}) \quad (4.44)$$

where  $p = (1 + K_a K_f K_1) / \tau_1$ . Because the load inertia is assumed to be very large, we alter the response by increasing  $K_a$ . Thus, we have the approximate response

$$\omega(t) \approx \frac{1}{K_f} (k_2 E) \left[ 1 - \exp\left(-\frac{(K_a K_f K_1)t}{\tau_1}\right) \right] \quad (4.45)$$

For a typical application, the open-loop pole might be  $1/\tau_1 = 0.10$ , whereas the closed-loop pole could be at least  $(K_a K_f K_1) / \tau_1 = 10$ , a factor of one hundred in the improvement of the speed of response. To attain the gain  $K_a K_f K_1$ , the amplifier gain  $K_a$  must be reasonably large, and the armature voltage signal to the





**FIGURE 4.16** The DLR German Aerospace Center is developing an advanced robotic hand. The final goal—fully autonomous operation—has not yet been achieved. Currently, the control is accomplished via a telemanipulation system consisting of a lightweight robot with a four-fingered articulated hand mounted on a mobile platform. The hand operator receives stereo video feedback and force feedback. This information is employed in conjunction with a data glove equipped with force feedback and an input device to control the robot. (Used with permission. Credit: DLR Institute of Robotics and Mechatronics.)

an example. Consider a unity feedback system with a process transfer function

$$G(s) = \frac{K}{\tau s + 1}, \quad (4.51)$$

which could represent a thermal control process, a voltage regulator, or a water-level control process. For a specific setting of the desired input variable, which may be represented by the normalized unit step input function, we have  $R(s) = 1/s$ . Then the steady-state error of the open-loop system is, as in Equation (4.49),

$$e_0(\infty) = 1 - G(0) = 1 - K \quad (4.52)$$

when a consistent set of dimensional units is utilized for  $R(s)$  and  $K$ . The error for the closed-loop system is

$$E_c(s) = R(s) - T(s)R(s)$$

where  $T(s) = G_c(s)G(s)/(1 + G_c(s)G(s))$ . The steady-state error is

$$e_c(\infty) = \lim_{s \rightarrow 0} s[1 - T(s)] \frac{1}{s} = 1 - T(0).$$

When  $G_c(s) = 1/(\tau_1 s + 1)$ , we obtain  $G_c(0) = 1$  and  $G(0) = K$ . Then we have

$$e_c(\infty) = 1 - \frac{K}{1 + K} = \frac{1}{1 + K}. \quad (4.53)$$

For the open-loop system, we would calibrate the system so that  $K = 1$  and the steady-state error is zero. For the closed-loop system, we would set a large gain  $K$ . If  $K = 100$ , the closed-loop system steady-state error is  $e_c(\infty) = 1/101$ .

If the calibration of the gain setting drifts or changes by  $\Delta K/K = 0.1$  (a 10% change), the open-loop steady-state error is  $\Delta e_0(\infty) = 0.1$ . Then the percent change from the calibrated setting is

$$\frac{\Delta e_c(\infty)}{|e_c(\infty)|} = \frac{0.10}{1}. \quad (4.54)$$

for an open-loop and a closed-loop system. The **steady-state error** is the error after the transient response has decayed, leaving only the continuous response.

The error of the open-loop system shown in Figure 4.2 is

$$E_0(s) = R(s) - Y(s) = (1 - G(s))R(s), \quad (4.46)$$

when  $T_d(s) = 0$ . Figure 4.3 shows the closed-loop system. When  $T_d(s) = 0$  and  $N(s) = 0$ , and we let  $H(s) = 1$ , the tracking error is given by (Equation 4.3)

$$E_c(s) = \frac{1}{1 + G_c(s)G(s)}R(s). \quad (4.47)$$

To calculate the steady-state error, we use the final-value theorem

$$\lim_{t \rightarrow \infty} e(t) = \lim_{s \rightarrow 0} sE(s). \quad (4.48)$$

Therefore, using a unit step input as a comparable input, we obtain for the open-loop system

$$e_0(\infty) = \lim_{s \rightarrow 0} s(1 - G(s)) \left( \frac{1}{s} \right) = \lim_{s \rightarrow 0} (1 - G(s)) = 1 - G(0). \quad (4.49)$$

For the closed-loop system we have

$$e_c(\infty) = \lim_{s \rightarrow 0} s \left( \frac{1}{1 + G_c(s)G(s)} \right) \left( \frac{1}{s} \right) = \frac{1}{1 + G_c(0)G(0)}. \quad (4.50)$$

The value of  $G(s)$  when  $s = 0$  is often called the DC gain and is normally greater than one. Therefore, the open-loop system will usually have a steady-state error of significant magnitude. By contrast, the closed-loop system with a reasonably large DC loop gain  $L(0) = G_c(0)G(0)$  will have a small steady-state error. In Chapter 5, we discuss steady-state error in much greater detail.

Upon examination of Equation (4.49), we note that the open-loop control system can possess a zero steady-state error by simply adjusting and calibrating the system's DC gain,  $G(0)$ , so that  $G(0) = 1$ . Therefore, we may logically ask, What is the advantage of the closed-loop system in this case? To answer this question, we return to the concept of the sensitivity of the system to parameter changes. In the open-loop system, we may calibrate the system so that  $G(0) = 1$ , but during the operation of the system, it is inevitable that the parameters of  $G(s)$  will change due to environmental changes and that the DC gain of the system will no longer be equal to 1. Because it is an open-loop system, the steady-state error will not equal zero until the system is maintained and recalibrated. By contrast, the closed-loop feedback system continually monitors the steady-state error and provides an actuating signal to reduce the steady-state error. Because systems are susceptible to parameter drift, environmental effects, and calibration errors, negative feedback provides benefits. An example of an ingenious feedback control system is shown in Figure 4.16.

The advantage of the closed-loop system is that it reduces the steady-state error resulting from parameter changes and calibration errors. This may be illustrated by

$G(s)$  equal to 1, we imply that the output is directly connected to the input. We must recall that a specific output (such as temperature, shaft rotation, or engine speed), is desired, whereas the input can be a potentiometer setting or a voltage. The process  $G(s)$  is necessary to provide the physical process between  $R(s)$  and  $Y(s)$ . Therefore, a transfer function  $G(s) = 1$  is unrealizable, and we must settle for a practical transfer function.

#### 4.8 DESIGN EXAMPLES

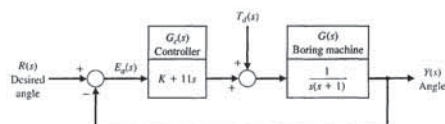
In this section we present three illustrative examples: the English Channel boring machine, the Mars rover, and a blood pressure control problem during anesthesia. The English Channel boring machine example focuses on the closed-loop system response to disturbances. The Mars rover example highlights the advantages of closed-loop feedback control in decreasing system sensitivity to plant changes. The final example on blood pressure control is a more in-depth look at the control design problem. Since patient models in the form of transfer functions are difficult to obtain from basic biological and physical principles, a different approach using measured data is discussed. The positive impact of closed-loop feedback control is illustrated in the context of design.

##### EXAMPLE 4.2 English Channel boring machines

The construction of the tunnel under the English Channel from France to Great Britain began in December 1987. The first connection of the boring tunnels from each country was achieved in November 1990. The tunnel is 23.5 miles long and is bored 200 feet below sea level. The tunnel, completed in 1992 at a total cost of \$14 billion, accommodates 50 train trips daily. This construction is a critical link between Europe and Great Britain, making it possible for a train to travel from London to Paris in three hours.

The machines, operating from both ends of the channel, bored toward the middle. To link up accurately in the middle of the channel, a laser guidance system kept the machines precisely aligned. A model of the boring machine control is shown in Figure 4.17, where  $Y(s)$  is the actual angle of direction of travel of the boring machine and  $R(s)$  is the desired angle. The effect of load on the machine is represented by the disturbance,  $T_d(s)$ .

The design objective is to select the gain  $K$  so that the response to input angle changes is desirable while we maintain minimal error due to the disturbance. The



**FIGURE 4.17** A block diagram model of a boring machine control system.

or 10%. By contrast, the steady-state error of the closed-loop system, with  $\Delta K/K = 0.1$ , is  $e_c(\infty) = 1/91$  if the gain decreases. Thus, the change is

$$\Delta e_c(\infty) = \frac{1}{101} - \frac{1}{91}, \quad (4.55)$$

and the relative change is

$$\frac{\Delta e_c(\infty)}{|e_c(\infty)|} = 0.0011, \quad (4.56)$$

or 0.11%. This is a significant improvement, since the closed-loop relative change is two orders of magnitude lower than that of the open-loop system.

#### 4.7 THE COST OF FEEDBACK

Adding feedback to a control system results in the advantages outlined in the previous sections. Naturally, however, these advantages have an attendant cost. The first cost of feedback is an increased number of **components and complexity** in the system. To add the feedback, it is necessary to consider several feedback components; the measurement component (sensor) is the key one. The sensor is often the most expensive component in a control system. Furthermore, the sensor introduces noise and inaccuracies into the system.

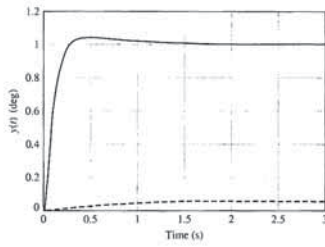
The second cost of feedback is the **loss of gain**. For example, in a single-loop system, the open-loop gain is  $G_c(s)G(s)$  and is reduced to  $G_c(s)G(s)/(1 + G_c(s)G(s))$  in a unity negative feedback system. The closed-loop gain is smaller by a factor of  $1/(1 + G_c(s)G(s))$ , which is exactly the factor that reduces the sensitivity of the system to parameter variations and disturbances. Usually, we have extra open-loop gain available, and we are more than willing to trade it for increased control of the system response.

We should note that it is the gain of the input-output transmittance that is reduced. The control system does retain the substantial power gain of a power amplifier and actuator, which is fully utilized in the closed-loop system.

The final cost of feedback is the introduction of the possibility of **instability**. Whereas the open-loop system is stable, the closed-loop system may not be always stable. The question of the stability of a closed-loop system is deferred until Chapter 6, where it can be treated more completely.

The addition of feedback to dynamic systems causes more challenges for the designer. However, for most cases, the advantages far outweigh the disadvantages, and a feedback system is desirable. Therefore, it is necessary to consider the additional complexity and the problem of stability when designing a control system.

Clearly, we want the output of the system,  $Y(s)$ , to equal the input,  $R(s)$ . However, upon reflection, we might ask, Why not simply set the transfer function  $G(s) = Y(s)/R(s)$  equal to 1? (See Figure 4.2, assuming  $T_d(s) = 0$ .) The answer to this question becomes apparent once we recall that the process (or plant)  $G(s)$  is necessary to provide the desired output; that is, the transfer function  $G(s)$  represents a real process and possesses dynamics that cannot be neglected. If we set



**FIGURE 4.19** The response  $y(t)$  for a unit step input (solid line) and for a unit step disturbance (dashed line) for  $K = 20$ .

together in Figure 4.19. Since the overshoot of the response is small (less than 4%) and the steady state is attained in 2 seconds, we would prefer that  $K = 20$ . The results are summarized in Table 4.1.

The steady-state error of the system to a unit step input  $R(s) = 1/s$  is

$$\lim_{t \rightarrow \infty} e(t) = \lim_{s \rightarrow 0} s \frac{1}{1 + \frac{K + 11s}{s(s + 1)} \left(\frac{1}{s}\right)} = 0. \quad (4.58)$$

The steady-state value of  $y(t)$  when the disturbance is a unit step,  $T_d(s) = 1/s$ , and the desired value is  $r(t) = 0$  is

$$\lim_{t \rightarrow \infty} y(t) = \lim_{s \rightarrow 0} \left[ \frac{1}{s(s + 12) + K} \right] = \frac{1}{K}. \quad (4.59)$$

Thus, the steady-state value is 0.01 and 0.05 for  $K = 100$  and 20, respectively.

Finally, we examine the sensitivity of the system to a change in the process  $G(s)$  using Equation (4.12). Then

$$S_G^T = \frac{s(s + 1)}{s(s + 12) + K}. \quad (4.60)$$

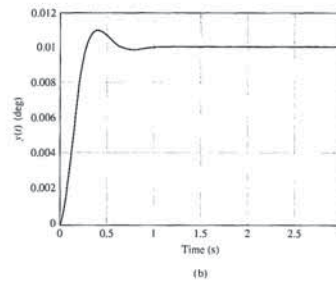
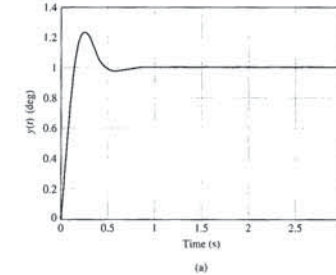
**Table 4.1** Response of the Boring System for Two Gains

Gain $K$	Overshoot of response to $r(t) = \text{step}$	Time for response to $r(t) = \text{step}$ to reach steady state (2% criterion)	Steady-state response $y(t)$ for unit step disturbance with $r(t) = 0$	Steady-state error of response to $r(t) = \text{step}$ with zero disturbance
100	22%	0.7s	0.01	0
20	4%	1.0s	0.05	0

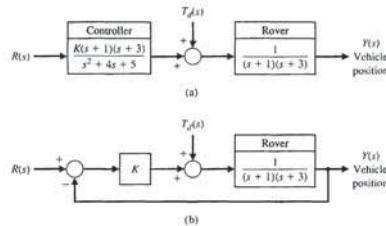
output due to the two inputs is

$$Y(s) = \frac{K + 11s}{s^2 + 12s + K} R(s) + \frac{1}{s^2 + 12s + K} T_d(s). \quad (4.57)$$

Thus, to reduce the effect of the disturbance, we wish to set the gain greater than 10. When we select  $K = 100$  and let the disturbance be zero, we have the step response for a unit step input  $r(t)$ , as shown in Figure 4.18(a). When the input  $r(t) = 0$  and we determine the response to the unit step disturbance, we obtain  $y(t)$  as shown in Figure 4.18(b). The effect of the disturbance is quite small. If we set the gain  $K$  equal to 20, we obtain the responses of  $y(t)$  due to a unit step input  $r(t)$  and disturbance  $T_d(t)$  displayed



**FIGURE 4.18** The response  $y(t)$  to (a) a unit input step  $r(t)$  and (b) a unit disturbance step input with  $T_d(s) = 1/s$  for  $K = 100$ .



**FIGURE 4.21** Control system for the rover. (a) Open-loop (without feedback). (b) Closed-loop with feedback.

and the transfer function for the closed-loop system is

$$T_c(s) = \frac{Y(s)}{R(s)} = \frac{K}{s^2 + 4s + 3 + K}. \quad (4.63)$$

Then, for  $K = 2$ ,

$$T(s) = T_c(s) = \frac{2}{s^2 + 4s + 5}.$$

Hence, we can compare the sensitivity of the open-loop and closed-loop systems for the same transfer function.

The sensitivity for the open-loop system is

$$S_K^T = \frac{dT_c}{dK} \frac{K}{T_c} = 1, \quad (4.64)$$

and the sensitivity for the closed-loop system is

$$S_K^T = \frac{dT_c}{dK} \frac{K}{T_c} = \frac{s^2 + 4s + 3}{s^2 + 4s + 3 + K}. \quad (4.65)$$

To examine the effect of the sensitivity at low frequencies, we let  $s = j\omega$  to obtain

$$S_K^T = \frac{(3 - \omega^2) + j4\omega}{(3 + K - \omega^2) + j4\omega}. \quad (4.66)$$

For  $K = 2$ , the sensitivity at low frequencies,  $\omega < 0.1$ , is  $|S_K^T| = 0.6$ .

A frequency plot of the magnitude of the sensitivity is shown in Figure 4.22. Note that the sensitivity for low frequencies is

$$|S_K^T| < 0.8, \quad \text{for } \omega \leq 1.$$

The effect of the disturbance can be determined by setting  $R(s) = 0$  and letting  $T_d(s) = 1/s$ . Then, for the open-loop system, we have the steady-state value

$$y(\infty) = \lim_{s \rightarrow 0} s \left\{ \frac{1}{(s + 1)(s + 3)} \right\} \frac{1}{s} = \frac{1}{3}. \quad (4.67)$$

For low frequencies ( $|s| < 1$ ), the sensitivity can be approximated by

$$S_G^T \approx \frac{s}{K}. \quad (4.61)$$

where  $K \geq 20$ . Thus, the sensitivity of the system is reduced by increasing the gain,  $K$ . In this case, we choose  $K = 20$  for a reasonable design compromise. ■

**EXAMPLE 4.3 Mars rover vehicle**

The solar-powered Mars rover named *Sojourner* landed on Mars on July 4, 1997, and was deployed on its journey on July 5, 1997. The rover was controlled by operators on Earth using controls on the rover [21, 22]. The Mars rovers, aptly dubbed *Spirit* and *Opportunity*, are known as the twin Mars Exploration Rovers and landed on the planet in 2004. These new rovers differ in size and capability from the *Sojourner* rover. *Sojourner* was about 65 cm (2 ft) long and weighed 10 kg (22 lb), while *Spirit* and *Opportunity* are each 1.6 m (5.2 ft) long and weigh 174 kg (384 lbs). *Sojourner* traveled a total distance of about 100 m during its 12 weeks of activity on Mars. *Spirit* has traveled over 7 km and *Opportunity* has traveled over 19 km. *Opportunity* has traveled over 32 times further than expected for a successful mission. The Mars Exploration Rovers are more autonomous; each carries its own telecommunications equipment, camera, and computers, whereas the *Sojourner* housed most of its equipment on the lander left at the base site. The solar-powered Mars rover *Spirit* is shown in Figure 4.20. The vehicle is controlled from Earth by sending it path commands,  $r(t)$ .

A very simplified model of a rover is depicted in Figure 4.21. The system may be operated without feedback, as shown in Figure 4.21(a), or with feedback, as shown in Figure 4.21(b). The goal is to operate the rover with modest effects from disturbances such as rocks and with low sensitivity to changes in the gain  $K$ .

The transfer function for the open-loop system is

$$T_o(s) = \frac{Y(s)}{R(s)} = \frac{K}{s^2 + 4s + 5}. \quad (4.62)$$



**FIGURE 4.20** Mars Exploration Rovers are significantly more capable than their predecessor, the Mars Pathfinder *Sojourner*. (Courtesy of NASA.)



assistance that the anesthetist can obtain automatically will increase the safety margins by freeing the anesthetist to attend to other functions not easily automated. This is an example of human computer interaction for the overall control of a process. Clearly, patient safety is the ultimate objective. Our control goal then is to develop an automated system to regulate the depth of anesthesia. This function is amenable to automatic control and in fact is in routine use in clinical applications [24, 25].

We consider how to measure the depth of anesthesia. Many anesthetists regard mean arterial pressure (MAP) as the most reliable measure of the depth of anesthesia [26]. The level of the MAP serves as a guide for the delivery of inhaled anesthesia. Based on clinical experience and the procedures followed by the anesthetist, we determine that the variable to be controlled is the mean arterial pressure.

The elements of the control system design process emphasized in this example are illustrated in Figure 4.23. From the control system design perspective, the control goal can be stated in more concrete terms:

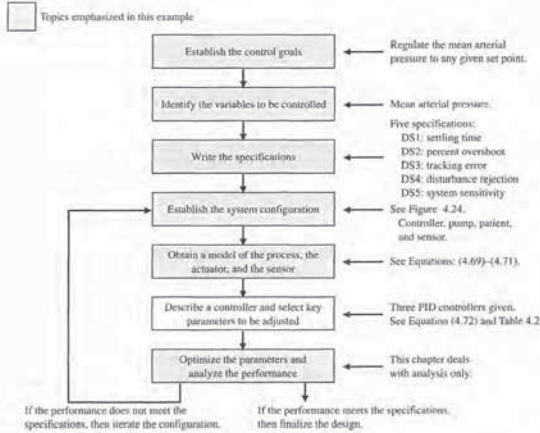


FIGURE 4.23 Elements of the control system design process emphasized in the blood pressure control example.

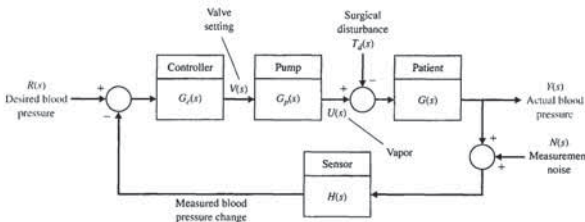


FIGURE 4.24 Blood pressure control system configuration.

vapor is equal to the input valve setting, or

$$\dot{u}(t) = v(t).$$

The transfer function of the pump is thus given by

$$G_p(s) = \frac{U(s)}{V(s)} = \frac{1}{s}. \tag{4.69}$$

This is equivalent to saying that, from an input/output perspective, the pump has the impulse response

$$h(t) = 1 \quad t \geq 0.$$

Developing an accurate model of a patient is much more involved. Because the physiological systems in the patient (especially in a sick patient) are not easily modeled, a modeling procedure based on knowledge of the underlying physical processes is not practical. Even if such a model could be developed, it would, in general, be a nonlinear, time-varying, multi-input, multi-output model. This type of model is not directly applicable here in our linear, time-invariant, single-input, single-output system setting.

On the other hand, if we view the patient as a system and take an input/output perspective, we can use the familiar concept of an impulse response. Then if we restrict ourselves to small changes in blood pressure from a given set-point (such as 100 mmHg), we might make the case that in a small region around the set-point the patient behaves in a linear time-invariant fashion. This approach fits well into our requirement to maintain the blood pressure around a given set-point (or baseline). The impulse response approach to modeling the patient response to anesthesia has been used successfully in the past [27].

Suppose that we take a black-box approach and obtain the impulse response in Figure 4.25 for a hypothetical patient. Notice that the impulse response initially has a time delay. This reflects the fact that it takes a finite amount of time for the patient MAP to respond to the infusion of anesthesia vapor. We ignore the time-delay in

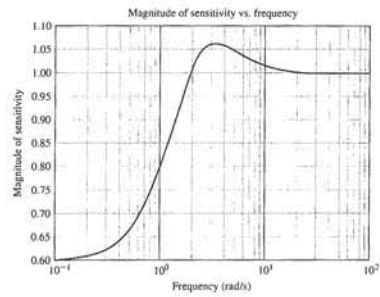


FIGURE 4.22 The magnitude of the sensitivity of the closed-loop system for the Mars rover vehicle.

As shown in Section 4.4, the output of the closed-loop system with a unit step disturbance,  $T_d(s) = 1/s$ , is

$$y(\infty) = \lim_{s \rightarrow 0} s \left\{ \frac{1}{(s^2 + 4s + 3 + K)} \right\} \frac{1}{s} = \frac{1}{3 + K}. \tag{4.68}$$

When  $K = 2$ ,  $y(\infty) = 1/5$ . Because we seek to minimize the effect of the disturbance, it is clear that a larger value of  $K$  would be desirable. An increased value of  $K$ , such as  $K = 50$ , will further reduce the effect of the disturbance as well as reduce the magnitude of the sensitivity (Equation 4.66). However, as we increase  $K$  beyond  $K = 50$ , the transient performance of the system for the ramp input,  $r(t)$ , begins to deteriorate. ■

EXAMPLE 4.4 Blood pressure control during anesthesia

The objectives of anesthesia are to eliminate pain, awareness, and natural reflexes so that surgery can be conducted safely. Before about 150 years ago, alcohol, opium and cannabis were used to achieve these goals, but they proved inadequate [23]. Pain relief was insufficient both in magnitude and duration; too little pain medication and the patient felt great pain, too much medication and the patient died or became comatose. In the 1850s ether was used successfully in the United States in tooth extractions, and shortly thereafter other means of achieving unconsciousness safely were developed, including the use of chloroform and nitrous oxide.

In a modern operating room, the depth of anesthesia is the responsibility of the anesthetist. Many vital parameters, such as blood pressure, heart rate, temperature, blood oxygenation, and exhaled carbon dioxide, are controlled within acceptable bounds by the anesthetist. Of course, to ensure patient safety, adequate anesthesia must be maintained during the entire surgical procedure. Any

Control Goal

Regulate the mean arterial pressure to any desired set-point and maintain the prescribed set-point in the presence of unwanted disturbances.

Associated with the stated control goal, we identify the variable to be controlled:

Variable to Be Controlled

Mean arterial pressure (MAP).

Because it is our desire to develop a system that will be used in clinical applications, it is essential to establish realistic design specifications. In general terms the control system should have minimal complexity while satisfying the control specifications. Minimal complexity translates into increased system reliability and decreased cost.

The closed-loop system should respond rapidly and smoothly to changes in the MAP set-point (made by the anesthetist) without excessive overshoot. The closed-loop system should minimize the effects of unwanted disturbances. There are two important categories of disturbances: surgical disturbances, such as skin incisions and measurement errors, such as calibration errors and random stochastic noise. For example, a skin incision can increase the MAP rapidly by 10 mmHg [26]. Finally, since we want to apply the same control system to many different patients and we cannot (for practical reasons) have a separate model for each patient, we must have a closed-loop system that is insensitive to changes in the process parameters (that is, it meets the specifications for many different people).

Based on clinical experience [24], we can explicitly state the control specifications as follows:

Control Design Specifications

- DS1 Settling time less than 20 minutes for a 10% step change from the MAP set-point.
- DS2 Percent overshoot less than 15% for a 10% step change from the MAP set-point.
- DS3 Zero steady-state tracking error to a step change from the MAP set-point.
- DS4 Zero steady-state error to a step surgical disturbance input (of magnitude  $|d(t)| \leq 50$ ) with a maximum response less than  $\pm 5\%$  of the MAP set-point.
- DS5 Minimum sensitivity to process parameter changes.

We cover the notion of percent overshoot (DS1) and settling time (DS2) more thoroughly in Chapter 5. They fall more naturally in the category of system performance. The remaining three design specifications, DS3–DS5, covering steady-state tracking errors (DS3), disturbance rejection (DS4), and system sensitivity to parameter changes (DS5) are the main topics of this chapter. The last specification, DS5, is somewhat vague; however, this is a characteristic of many real-world specifications. In the system configuration, Figure 4.24, we identify the major system elements as the controller, anesthesia pump/vaporizer, sensor, and patient.

The system input  $R(s)$  is the desired mean arterial pressure change, and the output  $Y(s)$  is the actual pressure change. The difference between the desired and the measured blood pressure change forms a signal used by the controller to determine valve settings to the pump/vaporizer that delivers anesthesia vapor to the patient.

The model of the pump/vaporizer depends directly on the mechanical design. We will assume a simple pump/vaporizer, where the rate of change of the output

$$E(s) = R(s) - Y(s) = \frac{1}{1 + G_c(s)G_p(s)G(s)}R(s),$$

or

$$E(s) = \frac{s^4 + 2ps^3 + p^2s^2}{s^4 + 2ps^3 + (p^2 + K_D)s^2 + K_Ps + K_I}R(s).$$

Using the final-value theorem, we determine that the steady-state tracking error is

$$\lim_{s \rightarrow 0} sE(s) = \lim_{s \rightarrow 0} \frac{R_0(s^4 + 2ps^3 + p^2s^2)}{s^4 + 2ps^3 + (p^2 + K_D)s^2 + K_Ps + K_I} = 0,$$

where  $R(s) = R_0/s$  is a step input of magnitude  $R_0$ . Therefore,

$$\lim_{t \rightarrow \infty} e(t) = 0.$$

With a PID controller, we expect a zero steady-state tracking error (to a step input) for any nonzero values of  $K_P$ ,  $K_D$ , and  $K_I$ . As we will see in Chapter 5, the integral term,  $K_I/s$ , in the PID controller is the reason that the steady-state error to a unit step is zero. Thus design specification DS3 is satisfied.

When considering the effect of a step disturbance input, we let  $R(s) = 0$  and  $N(s) = 0$ . We want the steady-state output  $Y(s)$  to be zero for a step disturbance. The transfer function from the disturbance  $T_d(s)$  to the output  $Y(s)$  is

$$Y(s) = \frac{-G(s)}{1 + G_c(s)G_p(s)G(s)}T_d(s) = \frac{-s^2}{s^4 + 2ps^3 + (p^2 + K_D)s^2 + K_Ps + K_I}T_d(s).$$

When

$$T_d(s) = \frac{D_0}{s},$$

we find that

$$\lim_{s \rightarrow 0} sY(s) = \lim_{s \rightarrow 0} \frac{-D_0s^2}{s^4 + 2ps^3 + (p^2 + K_D)s^2 + K_Ps + K_I} = 0.$$

Therefore,

$$\lim_{t \rightarrow \infty} y(t) = 0.$$

Thus a step disturbance of magnitude  $D_0$  will produce no output in the steady-state, as desired.

The sensitivity of the closed-loop transfer function to changes in  $p$  is given by

$$S_p^T = S_G^T S_p^G.$$

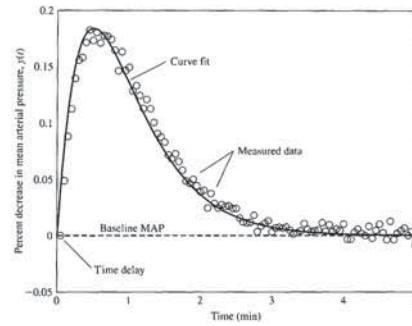


FIGURE 4.25 Mean arterial pressure (MAP) impulse response for a hypothetical patient.

our design and analysis, but we do so with caution. In subsequent chapters we will learn to handle time delays. We keep in mind that the delay does exist and should be considered in the analysis at some point.

A reasonable fit of the data shown in Figure 4.25 is given by

$$y(t) = te^{-pt} \quad t \geq 0,$$

where  $p = 2$  and time  $t$  is measured in minutes. Different patients are associated with different values of the parameter  $p$ . The corresponding transfer function is

$$G(s) = \frac{1}{(s + p)^2}. \tag{4.70}$$

For the sensor we assume a perfect noise-free measurement and

$$H(s) = 1. \tag{4.71}$$

Therefore, we have a unity feedback system.

A good controller for this application is a proportional-integral-derivative (PID) controller:

$$G_c(s) = K_p + sK_D + \frac{K_I}{s} = \frac{K_Ds^2 + K_Ps + K_I}{s}. \tag{4.72}$$

where  $K_p$ ,  $K_D$ , and  $K_I$  are the controller gains to be determined to satisfy all design specifications. The selected key parameters are as follows:

**Select Key Tuning Parameters**

Controller gains  $K_p$ ,  $K_D$ , and  $K_I$ .

We begin the analysis by considering the steady-state errors. The tracking error (shown in Figure 4.24 with  $T_d(s) = 0$  and  $N(s) = 0$ ) is

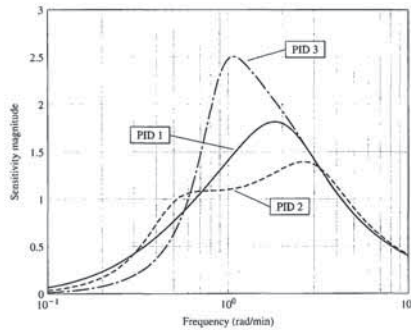


FIGURE 4.26 System sensitivity to variations in the parameter  $p$ .

11.5%, as illustrated in Figure 4.27. The settling time is the time required for the system output to settle within a certain percentage (for example, 2%) of the desired steady-state output amplitude. We cover the notions of overshoot and settling time more thoroughly in Chapter 5. The overshoot and settling times are summarized in Table 4.2.

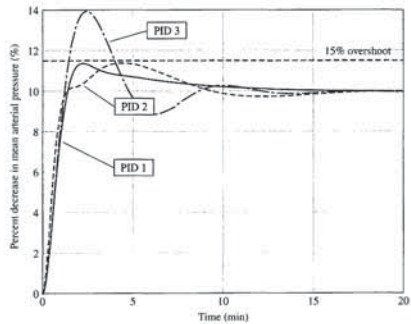


FIGURE 4.27 Mean arterial pressure (MAP) step input response with  $R(s) = 10/s$ .

We compute  $S_p^G$  as follows:

$$S_p^G = \frac{\partial G(s)}{\partial p} \cdot \frac{p}{G(s)} = \frac{-2p}{s + p},$$

and

$$S_G^T = \frac{1}{1 + G_c(s)G_p(s)G(s)} = \frac{s^2(s + p)^2}{s^4 + 2ps^3 + (p^2 + K_D)s^2 + K_Ps + K_I}.$$

Therefore,

$$S_p^T = S_G^T S_p^G = -\frac{2p(s + p)s^2}{s^4 + 2ps^3 + (p^2 + K_D)s^2 + K_Ps + K_I}. \tag{4.73}$$

We must evaluate the sensitivity function  $S_p^T$  at various values of frequency. For low frequencies we can approximate the system sensitivity  $S_p^T$  by

$$S_p^T \approx \frac{2p^2s^2}{K_I}.$$

So at low frequencies and for a given  $p$  we can reduce the system sensitivity to variations in  $p$  by increasing the PID gain,  $K_I$ . Suppose that three PID gain sets have been proposed, as shown in Table 4.2. With  $p = 2$  and the PID gains given as the cases 1–3 in Table 4.2, we can plot the magnitude of the sensitivity  $S_p^T$  as a function of frequency for each PID controller. The result is shown in Figure 4.26. We see that by using the PID 3 controller with the gains  $K_p = 6$ ,  $K_D = 4$ , and  $K_I = 4$ , we have the smallest system sensitivity (at low frequencies) to changes in the process parameter,  $p$ . PID 3 is the controller with the largest gain  $K_I$ . As the frequency increases we see in Figure 4.26 that the sensitivity increases, and that PID 3 has the highest peak sensitivity.

Now we consider the transient response. Suppose we want to reduce the MAP by a 10% step change. The associated input is

$$R(s) = \frac{R_0}{s} = \frac{10}{s}.$$

The step response for each PID controller is shown in Figure 4.27. PID 1 and PID 2 meet the settling time and overshoot specifications; however PID 3 has excessive overshoot. The overshoot is the amount the system output exceeds the desired steady-state response. In this case the desired steady-state response is a 10% decrease in the baseline MAP. When a 15% overshoot is realized, the MAP is decreased by

Table 4.2 PID Controller Gains and System Performance Results

PID	$K_p$	$K_D$	$K_I$	Input response overshoot (%)	Settling time (min)	Disturbance overshoot (%)
1	6	4	1	14.0	10.9	5.25
2	5	7	2	14.2	8.7	4.39
3	6	4	4	39.7	11.1	5.16



4.9 CONTROL SYSTEM CHARACTERISTICS USING CONTROL DESIGN SOFTWARE

In this section, the advantages of feedback will be illustrated with two examples. In the first example, we will introduce feedback control to a speed tachometer system in an effort to reject disturbances. The tachometer speed control system example can be found in Section 4.5. The reduction in system sensitivity to process variations, adjustment of the transient response, and reduction in steady-state error will be demonstrated using the English Channel boring machine example of Section 4.8.

EXAMPLE 4.5 Speed control system

The open-loop block diagram description of the armature-controlled DC motor with a load torque disturbance  $T_d(s)$  is shown in Figure 4.7. The values for the various parameters (taken from Figure 4.7) are given in Table 4.3. We have two inputs to our system,  $V_a(s)$  and  $T_d(s)$ . Relying on the principle of superposition, which applies to our linear system, we consider each input separately. To investigate the effects of disturbances on the system, we let  $V_a(s) = 0$  and consider only the disturbance  $T_d(s)$ . Conversely, to investigate the response of the system to a reference input, we let  $T_d(s) = 0$  and consider only the input  $V_a(s)$ .

The closed-loop speed tachometer control system block diagram is shown in Figure 4.9. The values for  $K_a$  and  $K_f$  are given in Table 4.3.

If our system displays good disturbance rejection, then we expect the disturbance  $T_d(s)$  to have a small effect on the output  $\omega(s)$ . Consider the open-loop system in Figure 4.11 first. We can compute the transfer function from  $T_d(s)$  to  $\omega(s)$  and evaluate the output response to a unit step disturbance (that is,  $T_d(s) = 1/s$ ). The time response to a unit step disturbance is shown in Figure 4.29(a). The script shown in Figure 4.29(b) is used to analyze the open-loop speed tachometer system.

The open-loop transfer function (from Equation (4.26)) is

$$\frac{\omega(s)}{T_d(s)} = \frac{-1}{2s + 1.5} = \text{sys}_o,$$

where  $\text{sys}_o$  represents the open-loop transfer function in the script. Since our desired value of  $\omega(t)$  is zero (remember that  $V_a(s) = 0$ ), the steady-state error is just the final value of  $\omega(t)$ , which we denote by  $\omega_s(t)$  to indicate open-loop. The steady-state error, shown on the plot in Figure 4.29(a), is approximately the value of the speed when  $t = 7$  seconds. We can obtain an approximate value of the steady-state error by looking at the last value in the output vector  $y_o$ , which we computed in the process of generating the plot in Figure 4.29(a). The approximate steady-state value of  $\omega_s$  is

$$\omega_s(\infty) \approx \omega_s(7) = -0.66 \text{ rad/s}.$$

The plot verifies that we have reached steady state.

Table 4.3 Tachometer Control System Parameters

$R_a$	$K_m$	J	b	$K_b$	$K_a$	$K_f$
1 $\Omega$	10 Nm/A	2 kg m <sup>2</sup>	0.5 Nm s	0.1 Vs	54	1 Vs

We conclude the analysis by considering the disturbance response. From previous analysis we know that the transfer function from the disturbance input  $T_d(s)$  to the output  $Y(s)$  is

$$Y(s) = \frac{-G(s)}{1 + G_c(s)G_p(s)G(s)} T_d(s) = \frac{-s^2}{s^4 + 2ps^3 + (p^2 + K_D)s^2 + K_Ps + K_I} T_d(s).$$

To investigate design specification DS4, we compute the disturbance step response with

$$T_d(s) = \frac{D_0}{s} = \frac{50}{s}.$$

This is the maximum magnitude disturbance ( $|T_d(t)| = D_0 = 50$ ). Since any step disturbance of smaller magnitude (that is,  $|T_d(t)| = D_0 < 50$ ) will result in a smaller maximum output response, we need only to consider the maximum magnitude step disturbance input when determining whether design specification DS4 is satisfied.

The unit step disturbance for each PID controller is shown in Figure 4.28. Controller PID 2 meets design specification DS4 with a maximum response less than  $\pm 5\%$  of the MAP set-point, while controllers PID 1 and 3 nearly meet the specification. The peak output values for each controller are summarized in Table 4.2.

In summary, given the three PID controllers, we would select PID 2 as the controller of choice. It meets all the design specifications while providing a reasonable insensitivity to changes in the plant parameter. ■

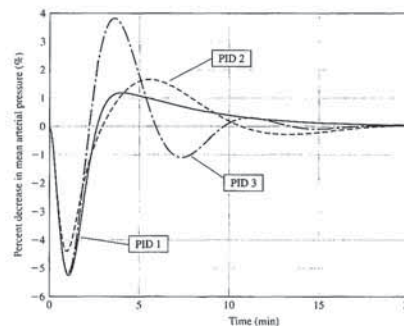
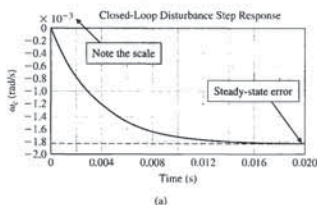


FIGURE 4.28 Mean arterial pressure (MAP) disturbance step response.



```

%Speed Tachometer Example
%
Ra=1; Km=10; J=2; b=0.5; Kb=0.1; Ka=54; Kf=1;
num1=[1]; den1=[J,b]; sys1=tf(num1,den1);
num2=[Ka*Kf]; den2=[1]; sys2=tf(num2,den2);
num3=[Kb]; den3=[1]; sys3=tf(num3,den3);
num4=[Km/Ra]; den4=[1]; sys4=tf(num4,den4);
sysa=parallel(sys2,sys3);
sysb=series(sysa,sys4);
sys_c=feedback(sys1,sysb);
%
% Change sign of transfer function since the
% disturbance has negative sign in the diagram.
sys_c=-sys_c;
%
% Compute response to step disturbance.
[y_c,T]=step(sys_c);
plot(T,y_c)
title('Closed-Loop Disturbance Step Response')
xlabel('Time (s)'); ylabel('omega_c (rad/s)'); grid
%
% Steady-state error -> last value of output y_c.
yc=length(T)
    
```

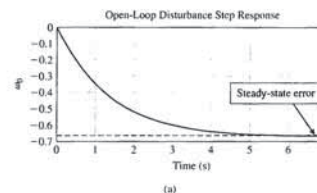
FIGURE 4.30 Analysis of the closed-loop speed control system. (a) Response. (b) m-file script.

We have achieved a remarkable improvement in disturbance rejection. It is clear that the addition of the negative feedback loop reduced the effect of the disturbance on the output. This demonstrates the disturbance rejection property of closed-loop feedback systems. ■

EXAMPLE 4.6 English Channel boring machines

The block diagram description of the English Channel boring machines is shown in Figure 4.17. The transfer function of the output due to the two inputs is (Equation (4.57))

$$Y(s) = \frac{K + 11s}{s^2 + 12s + K} R(s) + \frac{1}{s^2 + 12s + K} T_d(s).$$



```

%Speed Tachometer Example
%
Ra=1; Km=10; J=2; b=0.5; Kb=0.1;
num1=[1]; den1=[J,b]; sys1=tf(num1,den1);
num2=[Km*Kb/Ra]; den2=[1]; sys2=tf(num2,den2);
sys_o=feedback(sys1,sys2);
%
% Change sign of transfer function since the
% disturbance has negative sign in the diagram.
sys_o=-sys_o;
%
% Compute response to step disturbance.
[y_o,T]=step(sys_o);
plot(T,y_o)
title('Open-Loop Disturbance Step Response')
xlabel('Time (s)'); ylabel('omega_o'); grid
%
% Steady-state error -> last value of output y_o.
yo=length(T)
    
```

FIGURE 4.29 Analysis of the open-loop speed control system. (a) Response. (b) m-file script.

In a similar fashion, we begin the closed-loop system analysis by computing the closed-loop transfer function from  $T_d(s)$  to  $\omega(s)$  and then generating the time response of  $\omega(t)$  to a unit step disturbance input. The output response and the script `cltach.m` are shown in Figure 4.30. The closed-loop transfer function from the disturbance input (from Equation (4.30)) is

$$\frac{\omega(s)}{T_d(s)} = \frac{-1}{2s + 541.5} = \text{sys}_c.$$

As before, the steady-state error is just the final value of  $\omega(t)$ , which we denote by  $\omega_s(t)$  to indicate that it is a closed-loop. The steady-state error is shown on the plot in Figure 4.30(a). We can obtain an approximate value of the steady-state error by looking at the last value in the output vector  $y_o$ , which we computed in the process of generating the plot in Figure 4.30(a). The approximate steady-state value of  $\omega_s$  is

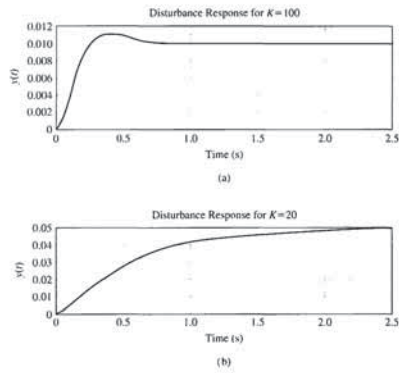
$$\omega_s(\infty) \approx \omega_s(0.02) = -0.002 \text{ rad/s}.$$

We generally expect that  $\omega_s(\infty)/\omega_s(\infty) < 0.02$ . In this example, the ratio of closed-loop to open-loop steady-state speed output due to a unit step disturbance input is

$$\frac{\omega_s(\infty)}{\omega_s(\infty)} = 0.003.$$

can be altered by feedback control gain,  $K$ . Based on our analysis thus far, we would prefer to use  $K = 20$ . Other considerations must be taken into account before we can establish the final design.

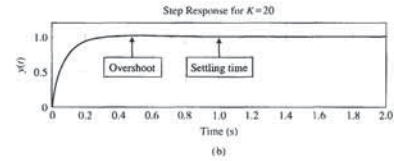
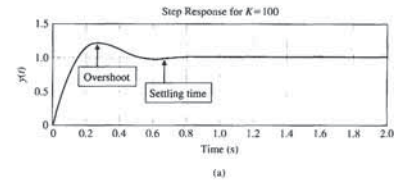
Before making the final choice of  $K$ , it is important to consider the system response to a unit step disturbance, as shown in Figure 4.32. We see that increasing  $K$  reduces the



```
% Response to a Disturbance Td(s)=1/s for K=20 and K=100
%
numg=[1]; deng=[1 1 0];
sysg=tf(numg,deng);
K1=100; K2=20;
num1=[11 K1]; num2=[11 K2]; den=[0 1];
sys1=tf(num1,den); sys2=tf(num2,den);
%
sysa=feedback(sysg,sys1); sysa=minreal(sysa);
sysb=feedback(sysg,sys2); sysb=minreal(sysb);
%
t=[0:0.01:2.5];
[y1,t]=step(sysa,t); [y2,t]=step(sysb,t);
subplot(211),plot(t,y1), title('Disturbance Response for K=100')
xlabel('Time (s)'),ylabel('y(t)'), grid
subplot(212),plot(t,y2), title('Disturbance Response for K=20')
xlabel('Time (s)'),ylabel('y(t)'), grid
```

FIGURE 4.32 The response to a step disturbance when (a)  $K = 100$  and (b)  $K = 20$ . (c) m-file script.

(c)

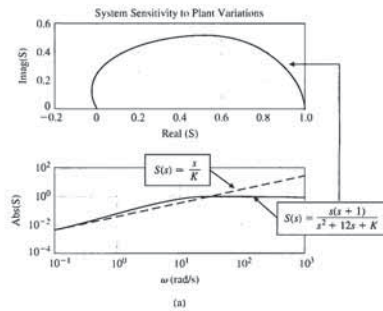


```
% Response to a Unit Step Input R(s)=1/s for K=20 and K=100
%
numg=[1]; deng=[1 1 0]; sysg=tf(numg,deng);
K1=100; K2=20;
num1=[11 K1]; num2=[11 K2]; den=[0 1];
sys1=tf(num1,den); sys2=tf(num2,den);
%
sysa=series(sys1,sysg); sysb=series(sys2,sysg);
sysc=feedback(sysa,1); sysd=feedback(sysb,1);
%
t=[0:0.01:2.0];
[y1,t]=step(sysc,t); [y2,t]=step(sysd,t);
subplot(211),plot(t,y1), title('Step Response for K=100')
xlabel('Time (s)'),ylabel('y(t)'), grid
subplot(212),plot(t,y2), title('Step Response for K=20')
xlabel('Time (s)'),ylabel('y(t)'), grid
```

FIGURE 4.31 The response to a step input when (a)  $K = 100$  and (b)  $K = 20$ . (c) m-file script.

(c)

The effect of the control gain,  $K$ , on the transient response is shown in Figure 4.31 along with the script used to generate the plots. Comparing the two plots in parts (a) and (b), it is apparent that decreasing  $K$  decreases the overshoot. Although it is not as obvious from the plots in Figure 4.31, it is also true that decreasing  $K$  increases the settling time. This can be verified by taking a closer look at the data used to generate the plots. This example demonstrates how the transient response



```
% System Sensitivity Plot
%
K=20; num=[1 1 0]; den=[1 12 K];
w=logspace(-1,5,200); s=j*w;
ns=s^2 + s; d= ns^2 + 12*s + K; S=ns/d;
n2= ns; d2=K; S2=n2/d2;
%
subplot(211), plot(real(S),imag(S))
title('System Sensitivity to Plant Variations')
xlabel('Real(S)'), ylabel('Imag(S)'), grid
subplot(212), loglog(w,abs(S),w,abs(S2))
xlabel('omega(rad/s)'), ylabel('Abs(S)'), grid
```

FIGURE 4.33 (a) System sensitivity to plant variations ( $s = j\omega$ ). (b) m-file script.

(b)

physical shocks, wear or wobble in the spindle bearings, and parameter changes due to component changes. In this section, we will examine the performance of the disk drive system in response to disturbances and changes in system parameters. In addition, we examine the steady-state error of the system for a step command and the transient response as the amplifier gain  $K_a$  is adjusted. Thus, in this section, we are carrying out the last two steps of the design process shown in Figure 1.15.

Let us consider the system shown in Figure 4.34. This closed-loop system uses an amplifier with a variable gain as the controller. Using the parameters specified in Table 2.10, we obtain the transfer functions as shown in Figure 4.35. First, we will determine the steady states for a unit step input,  $R(s) = 1/s$ , when  $T_d(s) = 0$ . When  $H(s) = 1$ , we obtain

$$E(s) = R(s) - Y(s) = \frac{1}{1 + K_a G_1(s) G_2(s)} R(s).$$

Table 4.4 Response of the Boring Machine Control System for  $K = 20$  and  $K = 100$

	$K = 20$	$K = 100$
Step Response		
Overshoot	4%	22%
$T_s$	1.0 s	0.7 s
Disturbance Response		
$\epsilon_{ss}$	5%	1%

steady-state response of  $y(t)$  to the step disturbance. The steady-state value of  $y(t)$  is 0.05 and 0.01 for  $K = 20$  and 100, respectively. The steady-state errors, percent overshoot, and settling times (2% criteria) are summarized in Table 4.4. The steady-state values are predicted from the final-value theorem for a unit disturbance input as follows:

$$\lim_{t \rightarrow \infty} y(t) = \lim_{s \rightarrow 0} s \left\{ \frac{1}{s(s+12) + K} \right\} \frac{1}{s} = \frac{1}{K}.$$

If our only design consideration is disturbance rejection, we would prefer to use  $K = 100$ .

We have just experienced a very common trade-off situation in control system design. In this particular example, increasing  $K$  leads to better disturbance rejection, whereas decreasing  $K$  leads to better performance (that is, less overshoot). The final decision on how to choose  $K$  rests with the designer. Although control design software can certainly assist in the control system design, it cannot replace the engineer's decision-making capability and intuition.

The final step in the analysis is to look at the system sensitivity to changes in the process. The system sensitivity is given by (Equation 4.60),

$$S_G^T = \frac{s(s+1)}{s(s+12) + K}.$$

We can compute the values of  $S_G^T(s)$  for different values of  $s$  and generate a plot of the system sensitivity. For low frequencies, we can approximate the system sensitivity by

$$S_G^T \approx \frac{s}{K}.$$

Increasing the gain  $K$  reduces the system sensitivity. The system sensitivity plots when  $s = j\omega$  are shown in Figure 4.33 for  $K = 20$ .

4.10 SEQUENTIAL DESIGN EXAMPLE: DISK DRIVE READ SYSTEM



The design of a disk drive system is an exercise in compromise and optimization. The disk drive must accurately position the head reader while being able to reduce the effects of parameter changes and external shocks and vibrations. The mechanical arm and flexure will resonate at frequencies that may be caused by excitations such as a shock to a notebook computer. Disturbances to the operation of the disk drive include



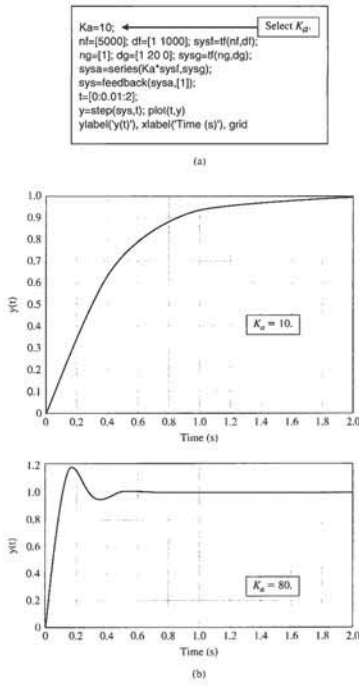


FIGURE 4.36 Closed-loop response. (a) m-file script. (b) Step response for  $K_d = 10$  and  $K_d = 80$ .

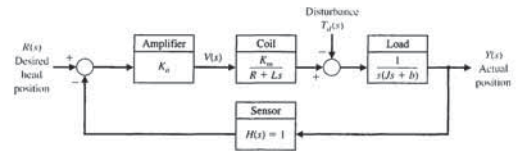


FIGURE 4.34 Control system for disk drive head reader.

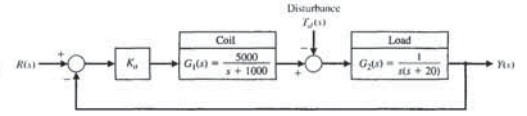


FIGURE 4.35 Disk drive head control system with the typical parameters of Table 2.10.

Therefore,

$$\lim_{t \rightarrow \infty} e(t) = \lim_{s \rightarrow 0} \left[ \frac{1}{1 + K_d G_1(s) G_2(s)} \right] \frac{1}{s} \quad (4.74)$$

Then the steady-state error is  $e(\infty) = 0$  for a step input. This performance is obtained in spite of changes in the system parameters.

Now let us determine the transient performance of the system as  $K_d$  is adjusted. The closed-loop transfer function (with  $T_d(s) = 0$ ) is

$$T(s) = \frac{Y(s)}{R(s)} = \frac{K_d G_1(s) G_2(s)}{1 + K_d G_1(s) G_2(s)} = \frac{5000 K_d}{s^3 + 1020s^2 + 20000s + 5000K_d} \quad (4.75)$$

Using the script shown in Figure 4.36(a), we obtain the response of the system for  $K_d = 10$  and  $K_d = 80$ , shown in Figure 4.36(b). Clearly, the system is faster in responding to the command input when  $K_d = 80$ , but the response is unacceptably oscillatory.

Now let us determine the effect of the disturbance  $T_d(s) = 1/s$  when  $R(s) = 0$ . We wish to decrease the effect of the disturbance to an insignificant level. Using the system of Figure 4.35, we obtain the response  $Y(s)$  for the input  $T_d(s)$  when  $K_d = 80$  as

$$Y(s) = \frac{G_2(s)}{1 + K_d G_1(s) G_2(s)} T_d(s) \quad (4.76)$$

Using the script shown in Figure 4.37(a), we obtain the response of the system when  $K_d = 80$  and  $T_d(s) = 1/s$ , as shown in Figure 4.37(b). In order to further reduce the

The loop gain  $L(s) = G_c(s)G(s)$  plays a fundamental role in control system analysis. Associated with the loop gain we can define the sensitivity and complementary sensitivity functions as

$$S(s) = \frac{1}{1 + L(s)} \quad \text{and} \quad C(s) = \frac{L(s)}{1 + L(s)}$$

respectively. The tracking error is given by

$$E(s) = S(s)R(s) - S(s)G(s)T_d(s) + C(s)N(s)$$

In order to minimize the tracking error,  $E(s)$ , we desire to make  $S(s)$  and  $C(s)$  small. Because the sensitivity and complementary sensitivity functions satisfy the constraint

$$S(s) + C(s) = 1,$$

we are faced with the fundamental trade-off in control system design between rejecting disturbances and reducing sensitivity to plant changes on the one hand, and attenuating measurement noise on the other hand.

The benefits of feedback can be illustrated by considering the system shown in Figure 4.38(a). This system can be considered for several values of gain  $K$ . Table 4.5 summarizes the results of the system operated as an open-loop system (with the feedback path disconnected) and for several values of gain,  $K$ , with the feedback connected. It is clear that the rise time and sensitivity of the system are reduced as

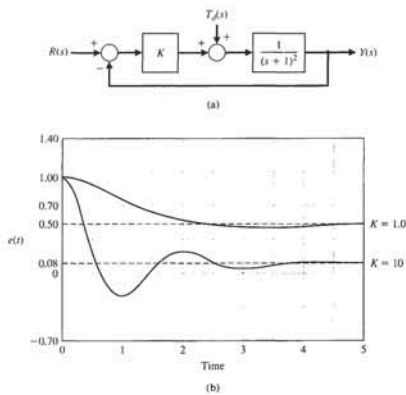


FIGURE 4.38 (a) A single-loop feedback control system. (b) The error response for a unit step disturbance when  $R(s) = 0$ .

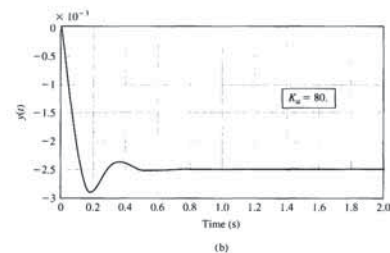
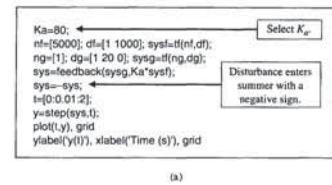


FIGURE 4.37 Disturbance step response. (a) m-file script. (b) Disturbance response for  $K_d = 80$ .

effect of the disturbance, we would need to raise  $K_d$  above 80. However, the response to a step command  $r(t) = 1, t > 0$  is unacceptably oscillatory. In the next chapter, we attempt to determine the best value for  $K_d$ , given our requirement for a quick, yet nonoscillatory response.

4.11 SUMMARY

The fundamental reasons for using feedback, despite its cost and additional complexity, are as follows:

1. Decrease in the sensitivity of the system to variations in the parameters of the process.
2. Improvement in the rejection of the disturbances.
3. Improvement in the attenuation of measurement noise.
4. Improvement in the reduction of the steady-state error of the system.
5. Ease of control and adjustment of the transient response of the system.

5. An advantage of using feedback is a decreased sensitivity of the system to variations in the parameters of the process. *True or False*
6. The loop transfer function of the system in Figure 4.39 is

$$G_c(s)G(s) = \frac{50}{\tau s + 10}$$

The sensitivity of the closed-loop system to small changes in  $\tau$  is:

- a.  $S_c^{\tau}(s) = \frac{\tau}{\tau s + 60}$
- b.  $S_c^{\tau}(s) = \frac{\tau}{\tau s + 10}$
- c.  $S_c^{\tau}(s) = \frac{\tau}{\tau s + 60}$
- d.  $S_c^{\tau}(s) = \frac{\tau s}{\tau s + 10}$

7. Consider the two systems in Figure 4.40.

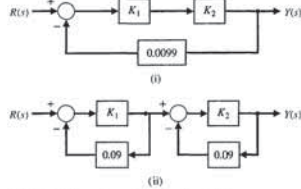


FIGURE 4.40 Two feedback systems with gains  $K_1$  and  $K_2$ .

These systems have the same transfer function when  $K_1 = K_2 = 100$ . Which system is most sensitive to variations in the parameter  $K_1$ ? Compute the sensitivity using the nominal values  $K_1 = K_2 = 100$ .

- a. System (i) is more sensitive and  $S_c^{K_1} = 0.01$
- b. System (ii) is more sensitive and  $S_c^{K_1} = 0.1$
- c. System (ii) is more sensitive and  $S_c^{K_1} = 0.01$
- d. Both systems are equally sensitive to changes in  $K_1$ .

8. Consider the closed-loop transfer function

$$T(s) = \frac{A_1 + kA_2}{A_3 + kA_4}$$

where  $A_1, A_2, A_3,$  and  $A_4$  are constants. Compute the sensitivity of the system to variations in the parameter  $k$ .

- a.  $S_c^k = \frac{k(A_2A_3 - A_1A_4)}{(A_3 + kA_4)(A_1 + kA_2)}$
- b.  $S_c^k = \frac{k(A_2A_3 + A_1A_4)}{(A_3 + kA_4)(A_1 + kA_2)}$

Table 4.5 System Response of the System Shown in Figure 4.38(a)

	Open Loop*			
	$K = 1$	$K = 1$	$K = 8$	$K = 10$
Rise time (s) (10% to 90% of final value)	3.35	1.52	0.45	0.38
Percent overshoot (%)	0	4.31	33	40
Final value of $y(t)$ due to a disturbance, $T_d(s) = 1/s$	1.0	0.50	0.11	0.09
Percent steady-state error for unit step input	0	50%	11%	9%
Percent change in steady-state error due to 10% decrease in $K$	10%	5.3%	1.2%	0.9%

\*Response only when  $K = 1$  exactly.

the gain is increased. Also, the feedback system demonstrates excellent reduction of the steady-state error as the gain is increased. Finally, Figure 4.38(b) shows the response for a unit step disturbance (when  $R(s) = 0$ ) and shows how a larger gain will reduce the effect of the disturbance.

Feedback control systems possess many beneficial characteristics. Thus, it is not surprising that there is a multitude of feedback control systems in industry, government, and nature.



SKILLS CHECK

In this section, we provide three sets of problems to test your knowledge: True or False, Multiple Choice, and Word Match. To obtain direct feedback, check your answers with the answer key provided at the conclusion of the end-of-chapter problems. Use the block diagram in Figure 4.39 as specified in the various problem statements.

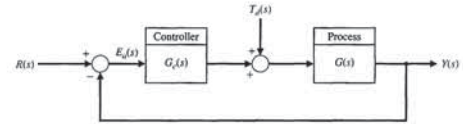


FIGURE 4.39 Block diagram for the Skills Check.

In the following True or False and Multiple Choice problems, circle the correct answer.

- 1. One of the most important characteristics of control systems is their transient response. *True or False*
- 2. The system sensitivity is the ratio of the change in the system transfer function to the change of a process transfer function for a small incremental change. *True or False*
- 3. A primary advantage of an open-loop control system is the ability to reduce the system's sensitivity. *True or False*
- 4. A disturbance is a desired input signal that affects the system output signal. *True or False*

Consider the block diagram in Figure 4.39 for Problems 13–14 with  $G_c(s) = K$  and  $G(s) = \frac{b}{s + 1}$ .

13. The sensitivity  $S_c^b$  is:

- a.  $S_c^b = \frac{1}{s + Kb + 1}$
- b.  $S_c^b = \frac{s + 1}{s + Kb + 1}$
- c.  $S_c^b = \frac{s + 1}{s + Kb + 2}$
- d.  $S_c^b = \frac{s}{s + Kb + 2}$

14. Compute the minimal value of  $K$  so that the steady-state error due to a unit step disturbance is less than 10%.

- a.  $K = 1 - \frac{1}{b}$
- b.  $K = b$
- c.  $K = 10 - \frac{1}{b}$
- d. The steady-state error is  $\infty$  for any  $K$

15. A process is designed to follow a desired path described by

$$r(t) = (5 - t + 0.5t^2)u(t)$$

where  $r(t)$  is the desired response and  $u(t)$  is a unit step function. Consider the unity feedback system in Figure 4.39. Compute the steady-state error ( $E(s) = R(s) - Y(s)$ ) with  $T_d(s) = 0$  when the loop transfer function is

$$L(s) = G_c(s)G(s) = \frac{10(s + 1)}{s^2(s + 5)}$$

- a.  $e_{ss} = \lim_{t \rightarrow \infty} e(t) \rightarrow \infty$
- b.  $e_{ss} = \lim_{t \rightarrow \infty} e(t) = 1$
- c.  $e_{ss} = \lim_{t \rightarrow \infty} e(t) = 0.5$
- d.  $e_{ss} = \lim_{t \rightarrow \infty} e(t) = 0$

In the following Word Match problems, match the term with the definition by writing the correct letter in the space provided.

- a. Instability An unwanted input signal that affects the system output signal. \_\_\_\_\_
- b. Steady-state error The difference between the desired output,  $R(s)$ , and the actual output,  $Y(s)$ . \_\_\_\_\_
- c. System sensitivity A system without feedback that directly generates the output in response to an input signal. \_\_\_\_\_
- d. Components The error when the time period is large and the transient response has decayed leaving the continuous response. \_\_\_\_\_

- c.  $S_c^k = \frac{k(A_1 + kA_2)}{(A_3 + kA_4)}$
- d.  $S_c^k = \frac{k(A_3 + kA_4)}{(A_1 + kA_2)}$

Consider the block diagram in Figure 4.39 for Problems 9–12 where  $G_c(s) = K_1$  and  $G(s) = \frac{K}{s + K_1K_2}$ .

- 9. The closed-loop transfer function is:
  - a.  $T(s) = \frac{KK_1^2}{s + K_1(K + K_2)}$
  - b.  $T(s) = \frac{KK_1}{s + K_1(K + K_2)}$
  - c.  $T(s) = \frac{KK_1}{s - K_1(K + K_2)}$
  - d.  $T(s) = \frac{KK_1}{s^2 + K_1Ks + K_1K_2}$
- 10. The sensitivity  $S_c^{K_1}$  of the closed-loop system to variations in  $K_1$  is:
  - a.  $S_c^{K_1}(s) = \frac{Ks}{(s + K_1(K + K_2))^2}$
  - b.  $S_c^{K_1}(s) = \frac{2s}{s + K_1(K + K_2)}$
  - c.  $S_c^{K_1}(s) = \frac{s}{s + K_1(K + K_2)}$
  - d.  $S_c^{K_1}(s) = \frac{K_1(s + K_1K_2)}{(s + K_1(K + K_2))^2}$
- 11. The sensitivity  $S_c^K$  of the closed-loop system to variations in  $K$  is:
  - a.  $S_c^K(s) = \frac{s + K_1K_2}{s + K_1(K + K_2)}$
  - b.  $S_c^K(s) = \frac{Ks}{(s + K_1(K + K_2))^2}$
  - c.  $S_c^K(s) = \frac{s + KK_1}{s + K_1K_2}$
  - d.  $S_c^K(s) = \frac{K_1(s + K_1K_2)}{(s + K_1(K + K_2))^2}$
- 12. The steady-state tracking error to a unit step input  $R(s) = 1/s$  with  $T_d(s) = 0$  is:
  - a.  $e_{ss} = \frac{K}{K + K_2}$
  - b.  $e_{ss} = \frac{K_1}{K + K_2}$
  - c.  $e_{ss} = \frac{K_2}{K_1(K + K_2)}$
  - d.  $e_{ss} = \frac{K_1}{K + K_2}$



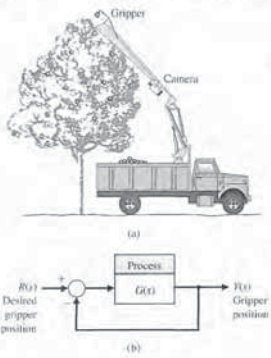


FIGURE E4.3 Robot fruit picker.

step change in the desired input? (b) Calculate the required  $K$  in order to yield a steady-state error of 0.1 mm for a ramp input of 10 cm/s.  
**Answers:** (a)  $e_{ss} = 0$ ;  $K = 100$

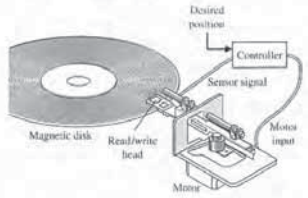


FIGURE E4.4 Disk drive control.

E4.5 A feedback system has the closed-loop transfer function given by

$$T(s) = \frac{s^2 + \beta s + 10}{s^3 + 2ps^2 + 4s + (3-p)}$$

Compute the sensitivity of the closed-loop transfer function to changes in the parameter  $p$ , where  $p > 0$ .

Compute the steady-state error to a unit step input as a function of the parameter  $p$ .

E4.6 A unity feedback system has the loop transfer function

$$L(s) = G_c(s)G(s) = \frac{10K}{s(s+b)}$$

Determine the relationship between the steady-state error to a ramp input and the gain  $K$  and system parameter  $b$ . For what values of  $K$  and  $b$  can we guarantee that the magnitude of the steady-state error to a ramp input is less than 0.1?

E4.7 Most people have experienced an out-of-focus slide projector. A projector with an automatic focus adjusts for variations in slide position and temperature disturbances [1]. Draw the block diagram of an autofocus system, and describe how the system works. An unfocused slide projection is a visual example of steady-state error.

E4.8 Four-wheel drive automobiles are popular in regions where winter road conditions are often slippery due to snow and ice. A four-wheel drive vehicle with antilock brakes uses a sensor to keep each wheel rotating to maintain traction. One system is shown in Figure E4.8. Find the closed-loop response of this system as it attempts to maintain a constant speed of the wheel. Determine the response when  $R(s) = A/s$ .

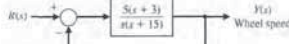


FIGURE E4.8 Four-wheel drive auto.

E4.9 Submersibles with clear plastic hulls have the potential to revolutionize underwater leisure. One small submersible vehicle has a depth-control system as illustrated in Figure E4.9.

- Determine the closed-loop transfer function  $T(s) = Y(s)/R(s)$ .
- Determine the sensitivity  $S_{K_1}^T$  and  $S_{K_2}^T$ .
- Determine the steady-state error due to a disturbance  $T_d(s) = 1/s$ .
- Calculate the response  $y(t)$  for a step input  $R(s) = 1/s$  when  $K = K_2 = 1$  and  $1 < K_1 < 10$ . Select  $K_1$  for the fastest response.

E4.10 Consider the feedback control system shown in Figure E4.10. (a) Determine the steady-state error for a step input in terms of the gain  $K$ . (b) Determine the overshoot for the step response for  $40 \leq K \leq 400$ . (c) Plot the overshoot and the steady-state error versus  $K$ .

E4.11 Consider the closed-loop system in Figure E4.11, where

$$G(s) = \frac{K}{s+10} \quad \text{and} \quad H(s) = \frac{14}{s^2+5s+6}$$

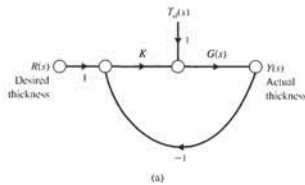


FIGURE E4.13 Control system for a steel rolling mill. (a) Signal flow graph. (b) Block diagram.

E4.14 Consider the unity feedback system shown in Figure E4.14. The system has two parameters, the controller gain  $K$  and the constant  $K_1$  in the process.

- Calculate the sensitivity of the closed-loop transfer function to changes in  $K_1$ .
- How would you select a value for  $K$  to minimize the effects of external disturbances,  $T_d(s)$ ?

E4.15 Reconsider the unity feedback system discussed in E4.14. This time select  $K = 120$  and  $K_1 = 10$ . The closed-loop system is depicted in Figure E4.15.

- Calculate the steady-state error of the closed-loop system due to a unit step input,  $R(s) = 1/s$ , with  $T_d(s) = 0$ . Recall that the tracking error is defined as  $E(s) = R(s) - Y(s)$ .
- Calculate the steady-state response,  $y_{ss} = \lim_{t \rightarrow \infty} y(t)$ , when  $T_d(s) = 1/s$  and  $R(s) = 0$ .

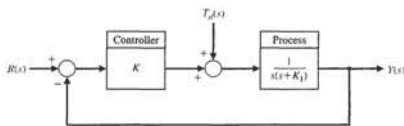


FIGURE E4.14 Closed-loop feedback system with two parameters,  $K$  and  $K_1$ .

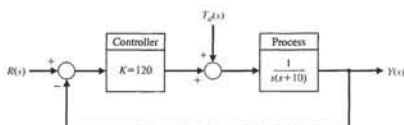


FIGURE E4.15 Closed-loop feedback system with  $K = 120$  and  $K_1 = 10$ .

- e. Disturbance signal: The ratio of the change in the system transfer function to the change of a process transfer function (or parameter) for a small incremental change.
- f. Transient response: The response of a system as a function of time.
- g. Complexity: A system with a measurement of the output signal and a comparison with the desired output to generate an error signal that is applied to the actuator.
- h. Error signal: A measure of the structure, intricateness, or behavior of a system that characterizes the relationships and interactions between various components.
- i. Closed-loop system: The parts, subsystems, or subassemblies that comprise a total system.
- j. Loss of gain: An attribute of a system that describes a tendency of the system to depart from the equilibrium condition when initially displaced.
- k. Open-loop system: A reduction in the amplitude of the ratio of the output signal to the input signal through a system, usually measured in decibels.

EXERCISES

E4.1 A closed-loop system is used to track the sun to obtain maximum power from a photovoltaic array. The tracking system may be represented by Figure 4.3 with  $H(s) = 1$  and

$$G(s) = \frac{100}{\tau s + 1}$$

where  $\tau = 3$  seconds nominally. (a) Calculate the sensitivity of this system for a small change in  $\tau$ . (b) Calculate the time constant of the closed-loop system response.

**Answers:**  $S = -3s/(3s+101)$ ;  $\tau_c = 3/101$  seconds

E4.2 A digital audio system is designed to minimize the effect of disturbances as shown in Figure E4.2. As an approximation, we may represent  $G(s) = K_2$ . (a) Calculate the sensitivity of the system due to  $K_2$ . (b) Calculate the effect of the disturbance noise  $T_d(s)$  on  $V_o(s)$ . (c) What value would you select for  $K_1$  to minimize the effect of the disturbance?

E4.3 A robotic arm and camera could be used to pick fruit, as shown in Figure E4.3(s). The camera is used to close the feedback loop to a microcomputer.

which controls the arm [8, 9]. The transfer function for the process is

$$G(s) = \frac{K}{(s+5)^2}$$

(a) Calculate the expected steady-state error of the gripper for a step command  $A$  as a function of  $K$ . (b) Name a possible disturbance signal for this system.

**Answers:** (a)  $e_{ss} = \frac{A}{1+K/25}$

E4.4 A magnetic disk drive requires a motor to position a read/write head over tracks of data on a spinning disk, as shown in Figure E4.4. The motor and head may be represented by the transfer function

$$G(s) = \frac{10}{s(\tau s + 1)}$$

where  $\tau = 0.001$  second. The controller takes the difference of the actual and desired positions and generates an error. This error is multiplied by an amplifier  $K$ . (a) What is the steady-state position error for a

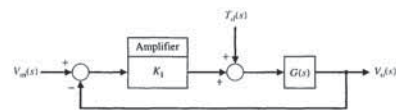


FIGURE E4.2 Digital audio system.

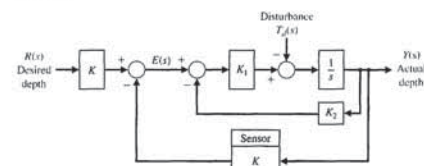


FIGURE E4.9 Depth control system.

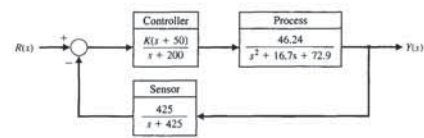


FIGURE E4.10 Feedback control system.

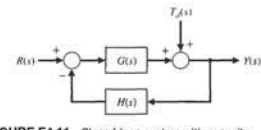


FIGURE E4.11 Closed-loop system with nonunity feedback.

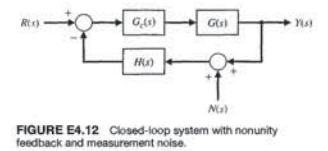


FIGURE E4.12 Closed-loop system with nonunity feedback and measurement noise.

- Compute the transfer function  $T(s) = Y(s)/R(s)$ .
- Define the tracking error to be  $E(s) = R(s) - Y(s)$ . Compute  $E(s)$  and determine the steady-state tracking error due to a unit step input, that is, let  $R(s) = 1/s$ .
- Compute the transfer function  $Y(s)/T_d(s)$  and determine the steady-state error of the output due to a unit step disturbance input, that is, let  $T_d(s) = 1/s$ .
- Compute the sensitivity  $S_{K_1}^T$ .

E4.12 In Figure E4.12, consider the closed-loop system with measurement noise  $N(s)$ , where

$$G(s) = \frac{100}{s+100}, \quad G_c(s) = K_1, \quad \text{and} \quad H(s) = \frac{K_2}{s+5}$$

In the following analysis, the tracking error is defined to be  $E(s) = R(s) - Y(s)$ .

- Compute the transfer function  $T(s) = Y(s)/R(s)$  and determine the steady-state tracking error

to a unit step response, that is, let  $R(s) = 1/s$  and assume that  $N(s) = 0$ .

- Compute the transfer function  $Y(s)/N(s)$  and determine the steady-state tracking error due to a unit step disturbance response, that is, let  $N(s) = 1/s$  and assume that  $R(s) = 0$ . Remember, in this case, the desired output is zero.

(c) If the goal is to track the input while rejecting the measurement noise (in other words, while minimizing the effect of  $N(s)$  on the output), how would you select the parameters  $K_1$  and  $K_2$ ?

E4.13 A closed-loop system is used in a high-speed steel rolling mill to control the accuracy of the steel strip thickness. The transfer function for the process shown in Figure E4.13 can be represented as

$$G(s) = \frac{1}{s(s+20)}$$

Calculate the sensitivity of the closed-loop transfer function to changes in the controller gain  $K$ .

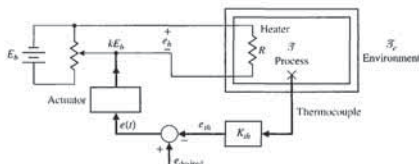


FIGURE P4.3 Temperature control system.

actuator. Then the linearized open-loop response of the system is

$$\bar{T}(s) = \frac{k_1 k_2 E_a}{\tau s + 1} E(s) + \frac{\bar{T}_e(s)}{\tau s + 1}$$

where

- $\tau = MC/(\rho A)$
- $M =$  mass in tank,
- $A =$  surface area of tank,
- $\rho =$  heat transfer constant,
- $C =$  specific heat constant,
- $k_1 =$  a dimensionality constant, and
- $e_{th} =$  output voltage of thermocouple.

Determine and compare the open-loop and closed-loop systems for (a) sensitivity to changes in the constant  $K = k_1 k_2 E_a$ , (b) the ability to reduce the effects of a step disturbance in the environmental temperature  $\Delta \bar{T}_e(s)$ , and (c) the steady-state error of the temperature controller for a step change in the input  $e_{desired}$ .

P4.4 A control system has two forward paths, as shown in Figure P4.4. (a) Determine the overall transfer function  $T(s) = Y(s)/R(s)$ . (b) Calculate the sensitivity,  $S_{L_1}^T$ , using Equation (4.16). (c) Does the sensitivity depend on  $L(s)$  or  $M(s)$ ?

P4.5 Large microwave antennas have become increasingly important for radio astronomy and satellite tracking. A large antenna with a diameter of 60 ft, for example, is subject to large wind gust torques. A proposed antenna is required to have an error of less than  $0.10^\circ$  in a 35 mph wind. Experiments show that this wind force exerts a maximum disturbance at the antenna of 200,000 ft lb at 35 mph, or the equivalent to 10 volts at the input  $T_d(s)$  to the amplidyne. One problem of driving large antennas is the form of the system transfer function that possesses a structural resonance. The antenna servosystem is shown in Figure P4.5. The transfer function of the antenna, drive motor, and amplidyne is approximated by

$$G(s) = \frac{\omega_n^2}{s(s^2 + 2\zeta\omega_n s + \omega_n^2)}$$

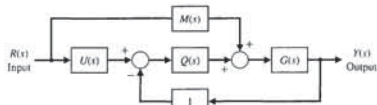


FIGURE P4.4 Two-path system.

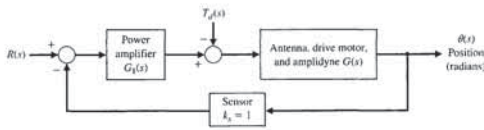


FIGURE P4.5 Antenna control system.

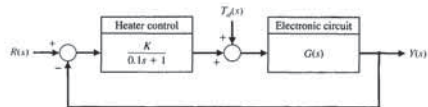


FIGURE P4.8 Temperature control system.

P4.9 A useful unidirectional sensing device is the photoemitter sensor [15]. A light source is sensitive to the emitter current flowing and alters the resistance of the photosensor. Both the light source and the photoconductor are packaged in a single four-terminal device. This device provides a large gain and total isolation. A feedback circuit utilizing this device is shown in Figure P4.9(a), and the nonlinear resistance-current characteristic is shown in Figure P4.9(b) for the Raytheon CK1116. The resistance curve can be represented by the equation

$$\log_{10} R = \frac{0.175}{(i - 0.005)^{1/2}}$$

where  $i$  is the lamp current. The normal operating point is obtained when  $v_o = 35$  V, and  $v_{in} = 2.0$  V.

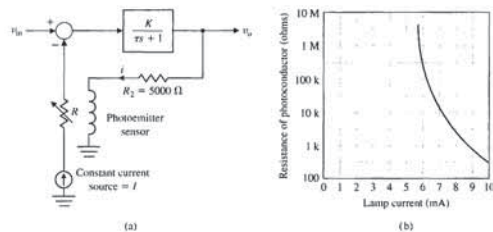


FIGURE P4.9 Photoemitter sensor system.

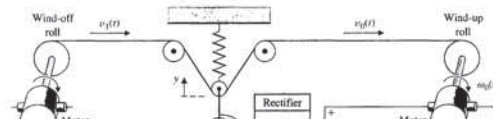


FIGURE P4.10 Paper tension control.

PROBLEMS

P4.1 The open-loop transfer function of a fluid-flow system can be written as

$$G(s) = \frac{\Delta Q_2(s)}{\Delta Q_1(s)} = \frac{1}{\tau s + 1}$$

where  $\tau = RC$ ,  $R$  is a constant equivalent to the resistance offered by the orifice so that  $1/R = 1/2kH_0^{-1/2}$ , and  $C$  is the cross-sectional area of the tank. Since  $\Delta H = R \Delta Q_2$ , we have the following for the transfer function relating the head to the input change:

$$G_1(s) = \frac{\Delta H(s)}{\Delta Q_1(s)} = \frac{R}{RCs + 1}$$

For a closed-loop feedback system, a float-level sensor and valve may be used as shown in Figure P4.1. Assuming the float is a negligible mass, the valve is controlled so that a reduction in the flow rate,  $\Delta Q_1$ , is proportional to an increase in head,  $\Delta H$ , or  $\Delta Q_1 = -K \Delta H$ . Draw a closed-loop flow graph or block diagram. Determine and compare the open-loop and closed-loop systems for (a) sensitivity to changes in the equivalent coefficient  $R$  and the feedback coefficient  $K$ , (b) the ability to reduce the effects of a disturbance in the level  $\Delta H(s)$ , and (c) the steady-state error of the level (head) for a step change of the input  $\Delta Q_1(s)$ .

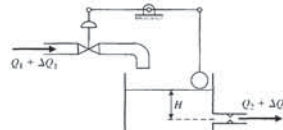


FIGURE P4.1 Tank level control.

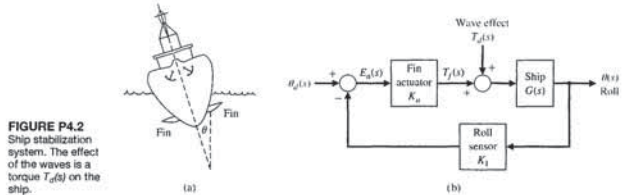


FIGURE P4.2 Ship stabilization system. The effect of the waves is a torque  $T_d(s)$  on the ship.

Problems

where  $\zeta = 0.707$  and  $\omega_n = 15$ . The transfer function of the power amplifier is approximately

$$G_1(s) = \frac{k_p}{\tau s + 1}$$

where  $\tau = 0.15$  second. (a) Determine the sensitivity of the system to a change of the parameter  $k_p$ . (b) The system is subjected to a disturbance  $T_d(s) = 10/s$ . Determine the required magnitude of  $k_p$  in order to maintain the steady-state error of the system less than  $0.10^\circ$  when the input  $R(s)$  is zero. (c) Determine the error of the system when subjected to a disturbance  $T_d(s) = 10/s$  when it is operating as an open-loop system ( $k_1 = 0$ ) with  $R(s) = 0$ .

P4.6 An automatic speed control system will be necessary for passenger cars traveling on the automatic highways of the future. A model of a feedback speed control system for a standard vehicle is shown in Figure P4.6. The load disturbance due to a percent grade  $\Delta T_d(s)$  is also shown. The engine gain  $K_e$  varies within the range of 10 to 1000 for various models of automobiles. The engine time constant  $\tau_e$  is 20 seconds. (a) Determine the sensitivity of the system to changes in the engine gain  $K_e$ . (b) Determine the effect of the load torque on the speed. (c) Determine the constant percent grade  $\Delta T_d(s) = \Delta d/s$  for which the vehicle stalls (velocity  $V(s) = 0$ ) in terms of the gain factors. Note that since the grade is constant, the steady-state solution is sufficient. Assume that

$R(s) = 30/s$  km/hr and that  $K_e K_1 \gg 1$ . When  $K_e K_1 = 2$ , what percent grade  $\Delta d$  would cause the automobile to stall?

P4.7 A robot uses feedback to control the orientation of each joint axis. The load effect varies due to varying load objects and the extended position of the gripper. Thus, the system may be represented by Figure P4.7, where the load torque is  $T_d(s) = D/s$ . Assume  $R(s) = 0$  at the index position. (a) What is the effect of  $T_d(s)$  on  $Y(s)$ ? (b) Determine the sensitivity of the closed loop to  $k_2$ . (c) What is the steady-state error when  $R(s) = 1/s$  and  $T_d(s) = 0$ ?

P4.8 Extreme temperature changes result in many failures of electronic circuits [1]. Temperature control feedback systems reduce the change of temperature by using a heater to overcome outdoor low temperatures. A block diagram of one system is shown in Figure P4.8. The effect of a drop in environmental temperature is a step decrease in  $T_d(s)$ . The actual temperature of the electronic circuit is  $Y(s)$ . The dynamics of the electronic circuit temperature change are represented by the transfer function.

$$G(s) = \frac{180}{s^2 + 20s + 180}$$

(a) Determine the sensitivity of the system to  $K$ . (b) Obtain the effect of the disturbance  $T_d(s)$  on the output  $Y(s)$ .

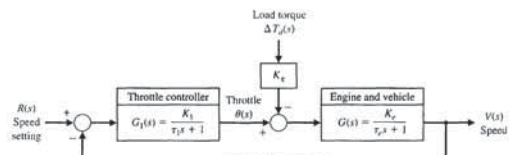


FIGURE P4.6 Automobile speed control.

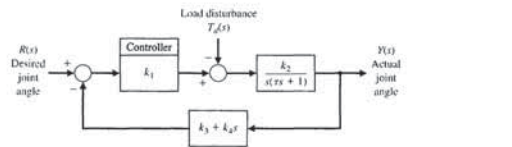


FIGURE P4.7 Robot control system.



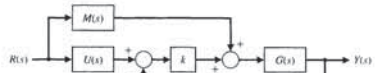


FIGURE P4.13 Closed-loop system.

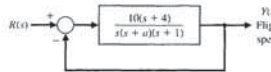


FIGURE P4.14 Hypersonic airplane speed control.

P4.13 One form of a closed-loop transfer function is

$$T(s) = \frac{G_1(s) + kG_2(s)}{G_1(s) + kG_2(s)}$$

(a) Use Equation (4.16) to show that [1]

$$S_1^T = \frac{k(G_2G_1 - G_1G_2)}{(G_1 + kG_2)(G_1 + kG_2)}$$

(b) Determine the sensitivity of the system shown in Figure P4.13, using the equation verified in part (a).

P4.14 A proposed hypersonic plane would climb to 100,000 feet, fly 3800 miles per hour, and cross the Pacific in 2 hours. Control of the aircraft speed could be represented by the model in Figure P4.14. Find the sensitivity of the closed-loop transfer function  $T(s)$  to a small change in the parameter  $a$ .

P4.15 The steering control of a modern ship may be represented by the system shown in Figure P4.15 [16, 20].

(a) Find the steady-state effect of a constant wind force represented by  $T_d(s) = 1/s$  for  $K = 10$  and  $K = 25$ . Assume that the rudder input  $R(s)$  is zero, without any disturbance, and has not been adjusted. (b) Show that the rudder can then be used to bring the ship deviation back to zero.

P4.16 Figure P4.16 shows the model of a two-tank system containing a heated liquid, where  $T_0$  is the temperature of the fluid flowing into the first tank and  $T_2$  is the temperature of the liquid flowing out of the second tank. The system of two tanks has a heater in the first tank with a controllable heat input  $Q$ . The time constants are  $\tau_1 = 10$  s and  $\tau_2 = 50$  s. (a) Determine  $T_2(s)$  in terms of  $T_0(s)$  and  $T_d(s)$ . (b) If  $T_2(s)$ , the desired output temperature, is changed instantaneously from  $T_{2d}(s) = A/s$  to  $T_{2d}(s) = 2A/s$ , where

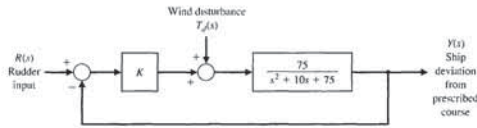


FIGURE P4.15 Ship steering control.

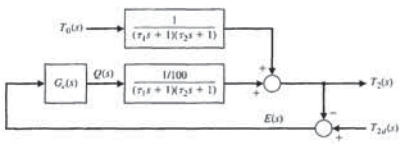


FIGURE P4.16 Two-tank temperature control.

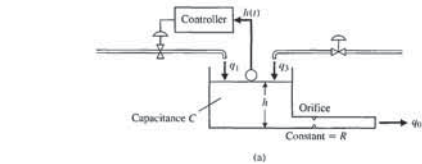


FIGURE AP4.1 A tank level regulator.

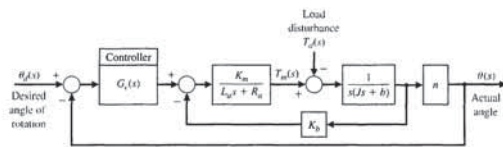


FIGURE AP4.2 Robot joint control.

effect is  $T_d(s) = M/s$ , determine the steady-state error when (a)  $G_c(s) = K$  and (b)  $G_c(s) = K/s$ .

AP4.3 A machine tool is designed to follow a desired path so that

$$r(t) = (1 - t)u(t),$$

where  $u(t)$  is the unit step function. The machine tool control system is shown in Figure AP4.3.

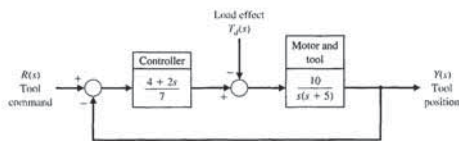


FIGURE AP4.3 Machine tool feedback.

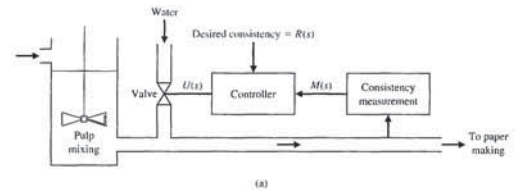


FIGURE P4.11 Paper-making control.

Therefore, the measure of the tension is described by the relation  $2T(s) = k_1 y$ , where  $y$  is the deviation from the equilibrium condition, and  $T(s)$  is the vertical component of the deviation in tension from the equilibrium condition. The time constant of the motor is  $\tau = L_m/R_m$  and the linear velocity of the wind-up roll is twice the angular velocity of the motor, that is,  $\omega(t) = 2\omega_m(t)$ . The equation of the motor is then

$$E_d(s) = \frac{1}{K_m} [\tau s \omega_m(s) + \omega_m(s)] + k_2 \Delta T(s),$$

where  $\Delta T = \tau$  is a tension disturbance. (a) Draw the closed-loop block diagram for the system, including the disturbance  $\Delta T(s)$ . (b) Add the effect of a disturbance in the wind-off roll velocity  $\Delta V_1(s)$  to the block diagram. (c) Determine the sensitivity of the system to the motor constant  $K_m$ . (d) Determine the steady-state error in the tension when a step disturbance in the input velocity,  $\Delta V_1(s) = A/s$ , occurs.

P4.11 One important objective of the paper-making process is to maintain uniform consistency of the stock output as it progresses to drying and rolling. A diagram of the thick stock consistency dilution control system is shown in Figure P4.11(a). The amount of water added determines the consistency. The block diagram of the system is shown in Figure P4.11(b). Let  $H(s) = 1$  and

$$G_1(s) = \frac{K}{8s + 1}, \quad G_2(s) = \frac{1}{3s + 1}$$

Determine (a) the closed-loop transfer function  $T(s) = Y(s)/R(s)$ , (b) the sensitivity  $S_K^T$ , and (c) the steady-state error for a step change in the desired consistency  $R(s) = A/s$ . (d) Calculate the value of  $K$  required for an allowable steady-state error of 2%.

P4.12 Two feedback systems are shown in Figures P4.12(a) and (b). (a) Evaluate the closed-loop transfer functions  $T_1$  and  $T_2$  for each system. (b) Compare the sensitivities of the two systems with respect to the parameter  $K_1$  for the nominal values of  $K_1 = K_2 = 1$ .

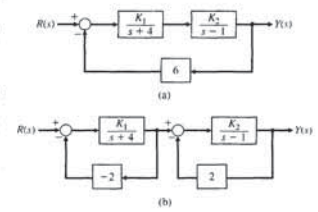


FIGURE P4.12 Two feedback systems.

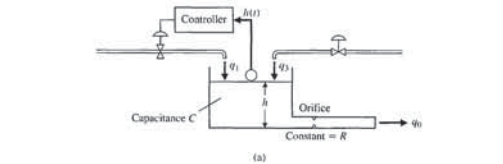


FIGURE AP4.1 A tank level regulator.

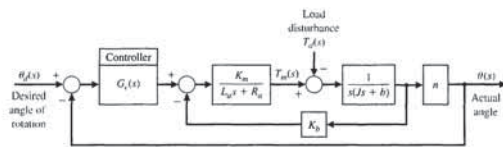


FIGURE AP4.2 Robot joint control.

effect is  $T_d(s) = M/s$ , determine the steady-state error when (a)  $G_c(s) = K$  and (b)  $G_c(s) = K/s$ .

AP4.3 A machine tool is designed to follow a desired path so that

$$r(t) = (1 - t)u(t),$$

where  $u(t)$  is the unit step function. The machine tool control system is shown in Figure AP4.3.

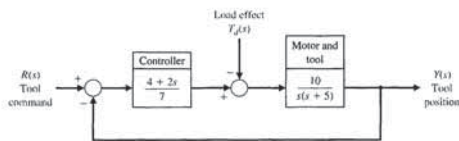


FIGURE AP4.3 Machine tool feedback.

$T_d(s) = A/s$ , determine the transient response of  $T_2(t)$  when  $G_c(s) = K = 500$ . (c) Find the steady-state error  $e_{ss}$  for the system of part (b), where  $E(s) = T_2(s) - T_2^d(s)$ .

P4.17 A robot gripper, shown in part (a) of Figure P4.17, is to be controlled so that it closes to an angle  $\theta$  when the input is  $r(t) = t, t > 0$ . (Assume that  $T_d(s) = 0$ .)

The model of the control system is shown in part (c), where  $K_m = 30$ ,  $R_f = 1$  \Omega,  $K_f = K_t = 1$ ,  $J = 0.1$ , and  $b = 1$ . (a) Determine the response  $\theta(t)$  of the system to a step change in  $\theta_d(t)$  when  $K = 20$ . (b) Assuming  $\theta_d(t) = 0$ , find the effect of a load disturbance  $T_d(s) = A/s$ . (c) Determine the steady-state error  $e_{ss}$  when the input is  $r(t) = t, t > 0$ . (Assume that  $T_d(s) = 0$ .)

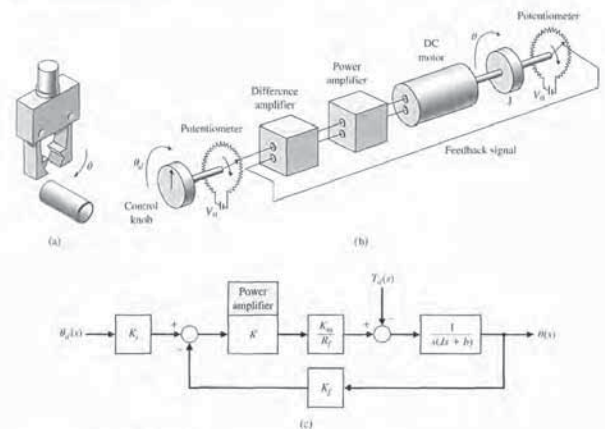


FIGURE P4.17 Robot gripper control.

ADVANCED PROBLEMS

AP4.1 A tank level regulator control is shown in Figure AP4.1(a). It is desired to regulate the level  $h$  in response to a disturbance change  $\theta_1$ . The block diagram shows small variable changes about the equilibrium conditions so that the desired  $\theta_d(t) = 0$ . Determine the equation for the error  $E(s)$ , and determine the steady-state error for a unit step disturbance when (a)  $G(s) = K$  and (b)  $G(s) = K/s$ .

AP4.2 The shoulder joint of a robotic arm uses a DC motor with armature control and a set of gears on the output shaft. The model of the system is shown in Figure AP4.2 with a disturbance torque  $T_d(t)$  which represents the effect of the load. Determine the steady-state error when the desired angle input is a step so that  $\theta_d(t) = A/s$ ,  $G_c(s) = K$ , and the disturbance input is zero. When  $\theta_d(t) = 0$  and the load

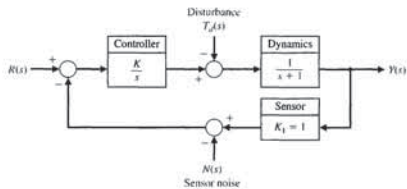


FIGURE AP4.7 Feedback system with noise.

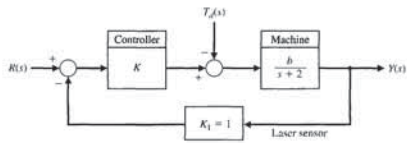


FIGURE AP4.8 Machine-tool control.

DESIGN PROBLEMS

**CDP4.1** A capstan drive for a table slide is described in CDP2.1. The position of the slide  $x$  is measured with a capacitance gauge, as shown in Figure CDP4.1, which is very linear and accurate. Sketch the model of the feedback system and determine the response of the system when the controller is an amplifier and  $H(s) = 1$ . Determine the step response for several selected values of the amplifier gain  $G_c(s) = K_p$ .

**DP4.1** A closed-loop speed control system is subjected to a disturbance due to a load, as shown in Figure DP4.1. The desired speed is  $\omega_d(t) = 100$  rad/s, and the load disturbance is a unit step input  $T_L(s) = 1/s$ . Assume that the speed has attained the no-load speed of 100 rad/s and is in steady state. (a) Determine the steady-state effect of the load disturbance, and (b) plot  $\omega(t)$  for the step disturbance for selected values of gain  $K$ .

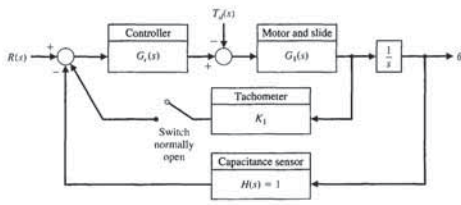


FIGURE CDP4.1 The model of the feedback system with a capacitance measurement sensor. The tachometer may be mounted on the motor (optional), and the switch will normally be open.

Advanced Problems

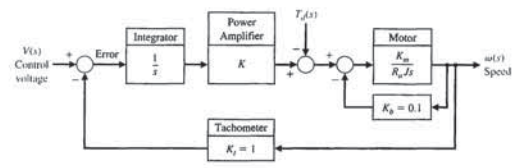


FIGURE AP4.4 DC motor with feedback.

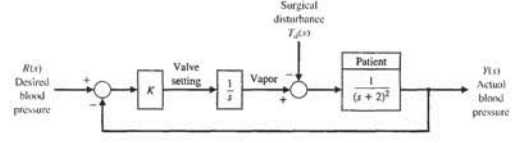


FIGURE AP4.5 Blood pressure control.

**AP4.4** An armature-controlled DC motor with tachometer feedback is shown in Figure AP4.4. Assume that  $K_m = 10$ ,  $J = 1$ , and  $R = 1$ .

- Determine the required gain,  $K$ , to restrict the steady-state error to a ramp input  $v(t) = t$  for  $t > 0$  to 0.1 (assume that  $T_d(s) = 0$ ).
- For the gain selected in part (a), determine and plot the error,  $e(t)$ , due to a ramp disturbance for  $0 \leq t \leq 5$  seconds.

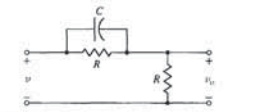


FIGURE AP4.6 A lead network.

**AP4.5** A system that controls the mean arterial pressure during anesthesia has been designed and tested [12]. The level of arterial pressure is postulated to be a proxy for depth of anesthesia during surgery. A block diagram of the system is shown in Figure AP4.5, where the impact of surgery is represented by the disturbance  $T_d(s)$ .

- Determine the steady-state error due to a disturbance  $T_d(s) = 1/s$  (let  $R(s) = 0$ ).
- Determine the steady-state error for a ramp input  $r(t) = t$ ,  $t > 0$  (let  $T_d(s) = 0$ ).
- Select a suitable value of  $K$  less than or equal to 10, and plot the response  $y(t)$  for a unit step disturbance input (assume  $r(t) = 0$ ).

**AP4.6** A useful circuit, called a lead network, which we discuss in Chapter 10, is shown in Figure AP4.6.

- Determine the transfer function  $G(s) = V_o(s)/V(s)$ .
- Determine the sensitivity of  $G(s)$  with respect to the capacitance  $C$ .

(c) Determine and plot the transient response  $v_o(t)$  for a step input  $V(s) = 1/s$ .

**AP4.7** A feedback control system with sensor noise and a disturbance input is shown in Figure AP4.7. The goal is to reduce the effects of the noise and the disturbance. Let  $R(s) = 0$ .

- Determine the effect of the disturbance on  $Y(s)$ .
- Determine the effect of the noise on  $Y(s)$ .
- Select the best value for  $K$  when  $1 \leq K \leq 100$  so that the effect of steady-state error due to the disturbance and the noise is minimized. Assume  $T_d(s) = A/s$ , and  $N(s) = B/s$ .

**AP4.8** The block diagram of a machine-tool control system is shown in Figure AP4.8.

- Determine the transfer function  $T(s) = Y(s)/R(s)$ .
- Determine the sensitivity  $S_y^C$ .
- Select  $K$  when  $1 \leq K \leq 50$  so that the effects of the disturbance and  $S_y^C$  are minimized.

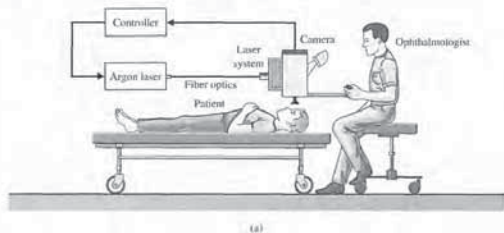


FIGURE DP4.4 Laser eye surgery system.

**DP4.5** An op-amp circuit can be used to generate a short pulse. The circuit shown in Figure DP4.5 can generate the pulse  $v_o(t) = 5e^{-100t}$ ,  $t > 0$ , when the input  $v_i(t)$  is a unit step [6]. Select appropriate values for the resistors and capacitors. Assume an ideal op-amp.

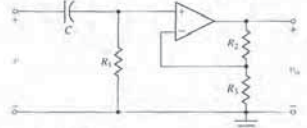


FIGURE DP4.5 Op-amp circuit.

**DP4.6** A hydrobot is under consideration for remote exploration under the ice of Europa, a moon of the giant planet Jupiter. Figure DP4.6(a) shows an artistic version of the mission. The hydrobot is a self-propelled underwater vehicle that would analyze the chemical composition of the water in a search for signs of life. An important aspect of the vehicle is a controlled vertical descent to depth in the presence of underwater currents. A simplified control feedback

system is shown in Figure DP4.6(b). The parameter  $J > 0$  is the pitching moment of inertia. (a) Suppose that  $G_c(s) = K$ . For what range of  $K$  is the system stable? (b) What is the steady-state error to a unit step disturbance when  $G_c(s) = K$ ? (c) Suppose that  $G_c(s) = K_p + K_D s$ . For what range of  $K_p$  and  $K_D$  is the system stable? (d) What is the steady-state error to a unit step disturbance when  $G_c(s) = K_p + K_D s$ ?

**DP4.7** Interest in unmanned underwater vehicles (UUVs) has been increasing recently, with a large number of possible applications being considered. These include intelligence-gathering, mine detection, and surveillance applications. Regardless of the intended mission, a strong need exists for reliable and robust control of the vehicle. The proposed vehicle is shown in Figure DP4.7 (a) [28].

We want to control the vehicle through a range of operating conditions. The vehicle is 30 feet long with a vertical sail near the front. The control inputs are stern plane, rudder, and shaft speed commands. In this case, we wish to control the vehicle roll by using the stern planes. The control system is shown in Figure DP4.7(b), where  $R(s) = 0$ , the desired roll angle, and  $T_d(s) = 1/s$ . Suppose that the controller is

$$G_c(s) = K(s + 2).$$

Design Problems

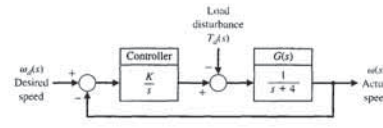


FIGURE DP4.1 Speed control system.

that  $10 \leq K \leq 25$ . Determine a suitable value for the gain  $K$ .

**DP4.2** The control of the roll angle of an airplane is achieved by using the torque developed by the ailerons. A linear model of the roll control system for a small experimental aircraft is shown in Figure DP4.2, where

$$G(s) = \frac{1}{s^2 + 4s + 9}.$$

The goal is to maintain a small roll angle  $\theta$  due to disturbances. Select an appropriate gain  $KK_1$  that will reduce the effect of the disturbance while attaining a desirable transient response to a step disturbance, with  $\theta_r(t) = 0$ . To obtain a desirable transient response, let  $KK_1 < 35$ .

**DP4.3** The speed control system of Figure DP4.1 is altered so that  $G(s) = 1/(s + 5)$  and the feedback is  $K_1$ , as shown in Figure DP4.3.

(a) Determine the range of  $K_1$  allowable so that the steady state is  $e_{ss} \leq 1\%$ .

(b) Determine a suitable value for  $K_1$  and  $K$  so that the magnitude of the steady-state error to a wind disturbance  $T_d(t) = 2t$  mrad/s,  $0 \leq t < 5$  s, is less than 0.1 mrad.

**DP4.4** Lasers have been used in eye surgery for more than 25 years. They can cut tissue or aid in coagulation

[17]. The laser allows the ophthalmologist to apply heat to a location in the eye in a controlled manner. Many procedures use the retina as a laser target. The retina is the thin sensory tissue that rests on the inner surface of the back of the eye and is the actual transducer of the eye, converting light energy into electrical pulses. On occasion, this layer will detach from the wall, resulting in death of the detached area from lack of blood and leading to partial or total blindness in that eye. A laser can be used to "weld" the retina into its proper place on the inner wall.

Automated control of position enables the ophthalmologist to indicate to the controller where lesions should be inserted. The controller then monitors the retina and controls the laser's position so that each lesion is placed at the proper location. A wide-angle video-camera system is required to monitor the movement of the retina, as shown in Figure DP4.4(a). If the eye moves during the irradiation, the laser must be either redirected or turned off. The position-control system is shown in Figure DP4.4(b). Select an appropriate gain for the controller so that the transient response to a step change in  $\theta(t)$  is satisfactory and the effect of the disturbance due to noise in the system is minimized. Also, ensure that the steady-state error for a step input command is zero. To ensure acceptable transient response, require that  $K < 10$ .

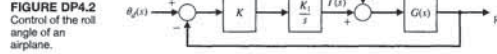


FIGURE DP4.2 Control of the roll angle of an airplane.

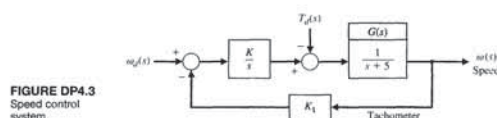


FIGURE DP4.3 Speed control system.



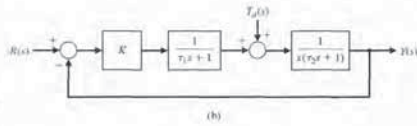
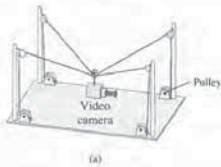


FIGURE DP4.8 Remote-controlled TV camera.

represented by the system in Figure DP4.8(b), where the nominal values are  $\tau_1 = 20$  ms and  $\tau_2 = 2$  ms. (a) Compute the sensitivity  $S_y^k$  and the sensitivity  $S_y^{\tau_1}$ .

(b) Design the controller gain  $K$  such that the steady-state tracking error to a unit step disturbance is less than 0.05.

COMPUTER PROBLEMS

CP4.1 Consider a unity feedback system with

$$G(s) = \frac{12}{s^2 + 2s + 10}$$

Obtain the step response and determine the percent overshoot. What is the steady-state error?

CP4.2 Consider the transfer function (without feedback)

$$G(s) = \frac{4}{s^2 + 2s + 20}$$

When the input is a unit step, the desired steady-state value of the output is one. Using the step function, show that the steady-state error to a unit step input is 0.8.

CP4.3 Consider the closed-loop transfer function

$$T(s) = \frac{5K}{s^2 + 15s + K}$$

Obtain the family of step responses for  $K = 10, 200,$  and  $500$ . Co-plot the responses and develop a table of results that includes the percent overshoot, settling time, and steady-state error.

CP4.4 Consider the feedback system in Figure CP4.4. Suppose that the controller is

$$G_c(s) = K = 10.$$

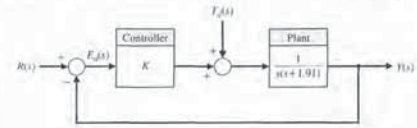


FIGURE CP4.4 Unity feedback system with controller gain  $K$ .

A closed-loop control system for the system is shown in Figure CP4.7(b). Suppose the desired angle  $\theta_d = 0^\circ$ ,  $k = 5$ ,  $b = 0.9$ , and  $J = 1$ .

- (a) Determine the open-loop response  $\theta(t)$  of the system for a unit step disturbance (set  $r(t) = 0$ ).
- (b) With the controller gain  $K_0 = 50$ , determine the closed-loop response,  $\theta(t)$  to a unit step disturbance.
- (c) Plot the open-loop versus the closed-loop response to the disturbance input. Discuss your results and make an argument for using closed-loop feedback control to improve the disturbance rejection properties of the system.

CP4.8 A negative feedback control system is depicted in Figure CP4.8. Suppose that our design objective is to find a controller  $G_c(s)$  of minimal complexity such that our closed-loop system can track a unit step input with a steady-state error of zero.

- (a) As a first try, consider a simple proportional controller  $G_c(s) = K$ , where  $K$  is a fixed gain. Let  $K = 2$ . Plot the unit step response and determine the steady-state error from the plot.
- (b) Now consider a more complex controller  $G_c(s) = K_0 + \frac{K_1}{s}$ , where  $K_0 = 2$  and  $K_1 = 20$ . This controller is known as a proportional, integral (PI) controller. Plot the unit step response, and determine the steady-state error from the plot.
- (c) Compare the results from parts (a) and (b), and discuss the trade-off between controller complexity and steady-state tracking error performance.

CP4.9 Consider the closed-loop system in Figure CP4.9, whose transfer function is

$$G(s) = \frac{10s}{s + 100} \quad \text{and} \quad H(s) = \frac{5}{s + 50}$$

- (a) Obtain the closed-loop transfer function  $T(s) = Y(s)/R(s)$  and the unit step response; that is, let  $R(s) = 1/s$  and assume that  $N(s) = 0$ .

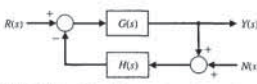


FIGURE CP4.9 Closed-loop system with nonunity feedback and measurement noise.

(b) Obtain the disturbance response when

$$N(s) = \frac{100}{s^2 + 100}$$

is a sinusoidal input of frequency  $\omega = 10$  rad/s. Assume that  $R(s) = 0$ .

- (c) In the steady-state, what is the frequency and peak magnitude of the disturbance response from part (b)?
- CP4.10 Consider the closed-loop system is depicted in Figure CP4.10. The controller gain  $K$  can be modified to meet the design specifications.
- (a) Determine the closed-loop transfer function  $T(s) = Y(s)/R(s)$ .
  - (b) Plot the response of the closed-loop system for  $K = 5, 10,$  and  $50$ .
  - (c) When the controller gain is  $K = 10$ , determine the steady-state value of  $y(t)$  when the disturbance is a unit step, that is, when  $T_d(s) = 1/s$  and  $R(s) = 0$ .

CP4.11 Consider the non-unity feedback system is depicted in Figure CP4.11.

- (a) Determine the closed-loop transfer function  $T(s) = Y(s)/R(s)$ .
- (b) For  $K = 10, 12,$  and  $15$ , plot the unit step responses. Determine the steady-state errors and the settling times from the plots.

For parts (a) and (b), develop an m-file that computes the closed-loop transfer function and generates the plots for varying  $K$ .

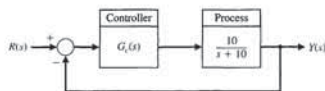


FIGURE CP4.8 A simple single-loop feedback control system.

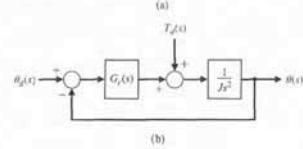


FIGURE DP4.6 (a) Europa exploration under the ice. (Used with permission. Credit: NASA.) (b) Feedback system.

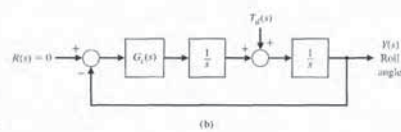
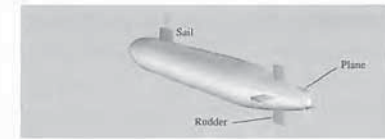


FIGURE DP4.7 Control of an underwater vehicle.

- (a) Design the controller gain  $K$  such that the maximum roll angle due to the unit step disturbance input is less than 0.05. (b) Compute the steady-state roll angle error to the disturbance input and explain the result.

DP4.8 A new suspended, mobile, remote-controlled video camera system to bring three-dimensional mobility to professional football is shown in Figure DP4.8(a) [29]. The camera can be moved over the field, as well as up and down. The motor control on each pulley is

Computer Problems

- (a) Develop an m-file to compute the closed-loop transfer function  $T(s) = Y(s)/R(s)$  and plot the unit step response. (b) In the same m-file, compute the transfer function from the disturbance  $T_d(s)$  to the output  $Y(s)$  and plot the unit step disturbance response. (c) From the plots in (a) and (b) above, estimate the steady-state tracking error to the unit step input and the steady-state tracking error to the unit step disturbance input. (d) From the plots in (a) and (b) above, estimate the maximum tracking error to the unit step input and the maximum tracking error to the unit step disturbance input. At approximately what times do the maximum errors occur?

- CP4.5 Consider the closed-loop control system shown in Figure CP4.5. Develop an m-file script to assist in the search for a value of  $k$  so that the percent overshoot to a unit step input is greater than 1%, but less than 10%. The script should compute the closed-loop transfer function  $T(s) = Y(s)/R(s)$  and generate the step response. Verify graphically that the steady-state error to a unit step input is zero.
- CP4.6 Consider the closed-loop control system shown in Figure CP4.6. The controller gain is  $K = 2$ . The nominal value of the plant parameter is  $a = 1$ . The nominal

value is used for design purposes only since in reality the value is not precisely known. The objective of our analysis is to investigate the sensitivity of the closed-loop system to the parameter  $a$ .

- (a) When  $a = 1$ , show analytically that the steady-state value of  $y(t)$  is equal to 2 when  $r(t)$  is a unit step. Verify that the unit step response is within 2% of the final value after 4 seconds.
- (b) The sensitivity of the system to changes in the parameter  $a$  can be investigated by studying the effects of parameter changes on the transient response. Plot the unit step response for  $a = 0.5, 2,$  and  $5$ . Discuss the results.

CP4.7 Consider the torsional mechanical system in Figure CP4.7(a). The torque due to the twisting of the shaft is  $-b\theta$ ; the damping torque due to the braking device is  $-b\dot{\theta}$ ; the disturbance torque is  $T_d(t)$ ; the input torque is  $r(t)$ ; and the moment of inertia of the mechanical system is  $J$ . The transfer function of the torsional mechanical system is

$$G(s) = \frac{1/J}{s^2 + (b/J)s + k/J}$$

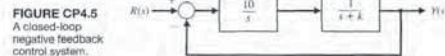


FIGURE CP4.5 A closed-loop negative feedback control system.

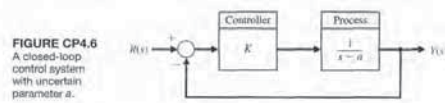


FIGURE CP4.6 A closed-loop control system with uncertain parameter  $a$ .

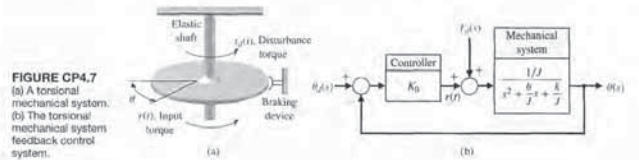


FIGURE CP4.7 (a) A torsional mechanical system. (b) The torsional mechanical system feedback control system.

5.1 Introduction 305  
 5.2 Test Input Signals 305  
 5.3 Performance of Second-Order Systems 308  
 5.4 Effects of a Third Pole and a Zero on the Second-Order System Response 314  
 5.5 The s-Plane Root Location and the Transient Response 320  
 5.6 The Steady-State Error of Feedback Control Systems 322  
 5.7 Performance Indices 330  
 5.8 The Simplification of Linear Systems 339  
 5.9 Design Examples 342  
 5.10 System Performance Using Control Design Software 356  
 5.11 Sequential Design Example: Disk Drive Read System 360  
 5.12 Summary 364

PREVIEW

The ability to adjust the transient and steady-state response of a control system is a beneficial outcome of the design of control systems. In this chapter, we introduce the time-domain performance specifications and we use key input signals to test the response of the control system. The correlation between the system performance and the location of the transfer function poles and zeros is discussed. We will develop relationships between the performance specifications and the natural frequency and damping ratio for second-order systems. Relying on the notion of dominant poles, we can extrapolate the ideas associated with second-order systems to those of higher order. The concept of a performance index will be considered. We will present a set of popular quantitative performance indices that adequately represent the performance of the control system. The chapter concludes with a performance analysis of the Sequential Design Example: Disk Drive Read System.

DESIRED OUTCOMES

Upon completion of Chapter 5, students should:

- Be aware of key test signals used in controls and of the resulting transient response characteristics of second-order systems to test signal inputs.
- Recognize the direct relationship between the pole locations of second-order systems and the transient response.
- Be familiar with the design formulas that relate the second-order pole locations to percent overshoot, settling time, rise time, and time to peak.
- Be aware of the impact of a zero and a third pole on the second-order system response.
- Gain a sense of optimal control as measured with performance indices.

Terms and Concepts

FIGURE CP4.10 Closed-loop feedback system with external disturbances.

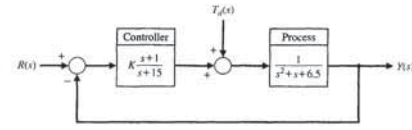
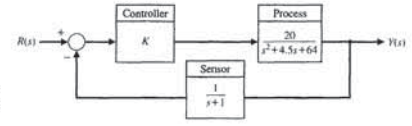


FIGURE CP4.11 Closed-loop system with a sensor in the feedback loop.



ANSWERS TO SKILLS CHECK

True or False: (1) True; (2) True; (3) False; (4) False; (5) True  
 Word Match (in order, top to bottom): e, h, k, b, c, f, i, g, d, a, j  
 Multiple Choice: (6) a; (7) b; (8) a; (9) b; (10) c;  
 (11) a; (12) b; (13) b; (14) c; (15) c

TERMS AND CONCEPTS

- Closed-loop system** A system with a measurement of the output signal and a comparison with the desired output to generate an error signal that is applied to the actuator.
- Complexity** A measure of the structure, intricateness, or behavior of a system that characterizes the relationships and interactions between various components.
- Components** The parts, subsystems, or subassemblies that comprise a total system.
- Disturbance signal** An unwanted input signal that affects the system's output signal.
- Error signal** The difference between the desired output  $R(s)$  and the actual output  $Y(s)$ . Therefore,  $E(s) = R(s) - Y(s)$ .
- Instability** An attribute of a system that describes a tendency of the system to depart from the equilibrium condition when initially displaced.
- Loop gain** The ratio of the feedback signal to the controller actuating signal. For a unity feedback system we have  $L(s) = G_c(s)G(s)$ .
- Loss of gain** A reduction in the amplitude of the ratio of the output signal to the input signal through a system, usually measured in decibels.
- Open-loop system** A system without feedback that directly generates the output in response to an input signal.
- Steady-state error** The error when the time period is large and the transient response has decayed, leaving the continuous response.
- System sensitivity** The ratio of the change in the system transfer function to the change of a process transfer function (or parameter) for a small incremental change.
- Tracking error** See error signal.
- Transient response** The response of a system as a function of time.

Chapter 5 The Performance of Feedback Control Systems

determine initially whether the system is stable; we can achieve this goal by using the techniques of ensuing chapters. If the system is stable, the response to a specific input signal will provide several measures of the performance. However, because the actual input signal of the system is usually unknown, a standard test input signal is normally chosen. This approach is quite useful because there is a reasonable correlation between the response of a system to a standard test input and the system's ability to perform under normal operating conditions. Furthermore, using a standard input allows the designer to compare several competing designs. Many control systems experience input signals that are very similar to the standard test signals.

The standard test input signals commonly used are the step input, the ramp input, and the parabolic input. These inputs are shown in Figure 5.2. The equations representing these test signals are given in Table 5.1, where the Laplace transform can be obtained by using Table 2.3 and a more complete list of Laplace transform pairs can be found at the MCS website. The ramp signal is the integral of the step input, and the parabola is simply the integral of the ramp input. A unit impulse function is also useful for test signal purposes. The unit impulse is based on a rectangular function

$$f_\epsilon(t) = \begin{cases} 1/\epsilon, & -\epsilon/2 \leq t \leq \epsilon/2 \\ 0, & \text{otherwise,} \end{cases}$$

where  $\epsilon > 0$ . As  $\epsilon$  approaches zero, the function  $f_\epsilon(t)$  approaches the unit impulse function  $\delta(t)$ , which has the following properties:

$$\int_{-\infty}^{\infty} \delta(t) dt = 1 \quad \text{and} \quad \int_{-\infty}^{\infty} \delta(t - a)g(t) dt = g(a). \quad (5.1)$$

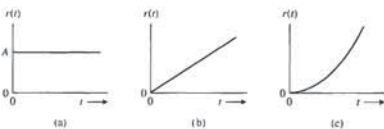


FIGURE 5.2 Test input signals: (a) step, (b) ramp, and (c) parabolic.

Table 5.1 Test Signal Inputs

Test Signal	$r(t)$	$R(s)$
Step	$r(t) = A, t > 0$ $= 0, t < 0$	$R(s) = A/s$
Ramp	$r(t) = At, t > 0$ $= 0, t < 0$	$R(s) = A/s^2$
Parabolic	$r(t) = At^2, t > 0$ $= 0, t < 0$	$R(s) = 2A/s^3$

Section 5.2 Test Input Signals

5.1 INTRODUCTION

The ability to adjust the transient and steady-state performance is a distinct advantage of feedback control systems. To analyze and design a control system, we must define and measure its performance. Based on the desired performance of the control system, the system parameters may be adjusted to provide the desired response. Because control systems are inherently dynamic, their performance is usually specified in terms of both the transient response and the steady-state response. The transient response is the response that disappears with time. The steady-state response is the response that exists for a long time following an input signal initiation.

The design specifications for control systems normally include several time-response indices for a specified input command, as well as a desired steady-state accuracy. In the course of any design, the specifications are often revised to effect a compromise. Therefore, specifications are seldom a rigid set of requirements, but rather a first attempt at listing a desired performance. The effective compromise and adjustment of specifications are graphically illustrated in Figure 5.1. The parameter  $p$  may minimize the performance measure  $M_2$  if we select  $p$  as a very small value. However, this results in large measure  $M_1$ , an undesirable situation. If the performance measures are equally important, the crossover point at  $p_{min}$  provides the best compromise. This type of compromise is normally encountered in control system design. It is clear that if the original specifications called for both  $M_1$  and  $M_2$  to be zero, the specifications could not be simultaneously met; they would then have to be altered to allow for the compromise resulting with  $p_{min}$  [1, 10, 15, 20].

The specifications, which are stated in terms of the measures of performance, indicate the quality of the system to the designer. In other words, the performance measures help to answer the question, How well does the system perform the task for which it was designed?

5.2 TEST INPUT SIGNALS

The time-domain performance specifications are important indices because control systems are inherently time-domain systems. That is, the system transient or time performance is the response of prime interest for control systems. It is necessary to

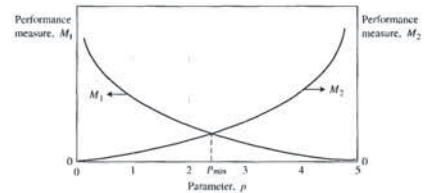


FIGURE 5.1 Two performance measures versus parameter  $p$ .



and the steady-state response is

$$y(\infty) = 0.9.$$

If the error is  $E(s) = R(s) - Y(s)$ , then the steady-state error is

$$e_{ss} = \lim_{s \rightarrow 0} sE(s) = 0.1.$$

5.3 PERFORMANCE OF SECOND-ORDER SYSTEMS

Let us consider a single-loop second-order system and determine its response to a unit step input. A closed-loop feedback control system is shown in Figure 5.4. The closed-loop system is

$$Y(s) = \frac{G(s)}{1 + G(s)}R(s). \tag{5.6}$$

We may rewrite Equation (5.6) as

$$Y(s) = \frac{\omega_n^2}{s^2 + 2\zeta\omega_n s + \omega_n^2}R(s). \tag{5.7}$$

With a unit step input, we obtain

$$Y(s) = \frac{\omega_n^2}{s(s^2 + 2\zeta\omega_n s + \omega_n^2)}. \tag{5.8}$$

for which the transient output, as obtained from the Laplace transform table in Table 2.3, is

$$y(t) = 1 - \frac{1}{\beta} e^{-\zeta\omega_n t} \sin(\omega_n \beta t + \theta), \tag{5.9}$$

where  $\beta = \sqrt{1 - \zeta^2}$ ,  $\theta = \cos^{-1} \zeta$ , and  $0 < \zeta < 1$ . The transient response of this second-order system for various values of the damping ratio  $\zeta$  is shown in Figure 5.5.

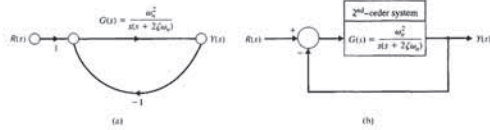


FIGURE 5.4 Second-order closed-loop control system.

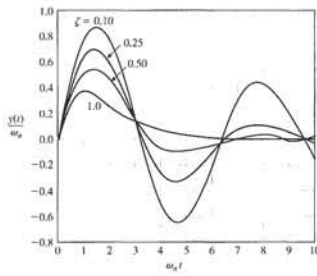


FIGURE 5.6 Response of a second-order system for an impulse function input.

As  $\zeta$  decreases, the closed-loop roots approach the imaginary axis, and the response becomes increasingly oscillatory. The response as a function of  $\zeta$  and time is also shown in Figure 5.5(b) for a step input.

The Laplace transform of the unit impulse is  $R(s) = 1$ , and therefore the output for an impulse is

$$Y(s) = \frac{\omega_n^2}{s^2 + 2\zeta\omega_n s + \omega_n^2}, \tag{5.10}$$

which is  $T(s) = Y(s)/R(s)$ , the transfer function of the closed-loop system. The transient response for an impulse function input is then

$$y(t) = \frac{\omega_n}{\beta} e^{-\zeta\omega_n t} \sin(\omega_n \beta t), \tag{5.11}$$

which is the derivative of the response to a step input. The impulse response of the second-order system is shown in Figure 5.6 for several values of the damping ratio  $\zeta$ . The designer is able to select several alternative performance measures from the transient response of the system for either a step or impulse input.

Standard performance measures are usually defined in terms of the step response of a system as shown in Figure 5.7. The swiftness of the response is measured by the **rise time**  $T_r$  and the **peak time**  $T_p$ . For underdamped systems with an overshoot, the 0–100% rise time is a useful index. If the system is overdamped, then the peak time is not defined, and the 10–90% rise time  $T_r$  is normally used. The similarity with which the actual response matches the step input is measured by the percent overshoot and settling time  $T_s$ . The **percent overshoot** is defined as

$$P.O. = \frac{M_p - f_v}{f_v} \times 100\% \tag{5.12}$$



FIGURE 5.3 Open-loop control system.

The impulse input is useful when we consider the convolution integral for the output  $y(t)$  in terms of an input  $r(t)$ , which is written as

$$y(t) = \int_{-\infty}^t g(t - \tau)r(\tau) d\tau = \mathcal{L}^{-1}\{G(s)R(s)\}. \tag{5.2}$$

This relationship is shown in block diagram form in Figure 5.3. If the input is a unit impulse function, we have

$$y(t) = \int_{-\infty}^t g(t - \tau)\delta(\tau) d\tau. \tag{5.3}$$

The integral has a value only at  $\tau = 0$ ; therefore,

$$y(t) = g(t).$$

the impulse response of the system  $G(s)$ . The impulse response test signal can often be used for a dynamic system by subjecting the system to a large-amplitude, narrow-width pulse of area  $A$ .

The standard test signals are of the general form

$$r(t) = t^n, \tag{5.4}$$

and the Laplace transform is

$$R(s) = \frac{n!}{s^{n+1}}. \tag{5.5}$$

Hence, the response to one test signal may be related to the response of another test signal of the form of Equation (5.4). The step input signal is the easiest to generate and evaluate and is usually chosen for performance tests.

Consider the response of the system shown in Figure 5.3 for a unit step input when

$$G(s) = \frac{9}{s + 10}.$$

Then the output is

$$Y(s) = \frac{9}{s(s + 10)},$$

the response during the transient period is

$$y(t) = 0.9(1 - e^{-10t}).$$

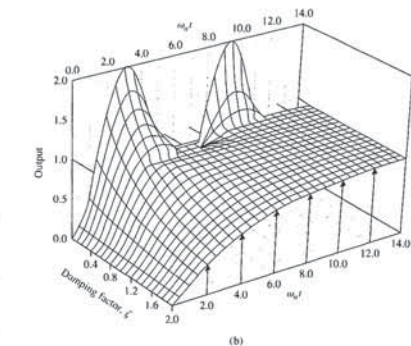
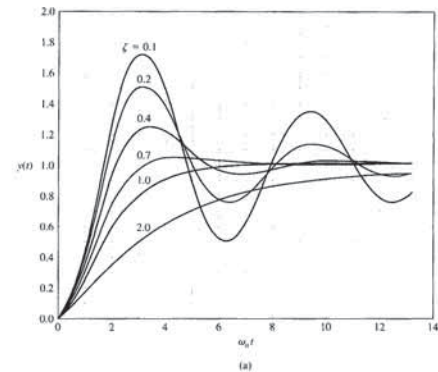


FIGURE 5.5 (a) Transient response of a second-order system (Equation 5.9) for a step input. (b) The transient response of a second-order system (Equation 5.9) for a step input as a function of  $\zeta$  and  $\omega_n t$ . (Courtesy of Professor R. Jacquot, University of Wyoming.)

As nature would have it, these are contradictory requirements; thus, a compromise must be obtained. To obtain an explicit relation for  $M_p$  and  $T_p$  as a function of  $\zeta$ , one can differentiate Equation (5.9) and set it equal to zero. Alternatively, one can utilize the differentiation property of the Laplace transform, which may be written as

$$\mathcal{L}\left\{\frac{dy(t)}{dt}\right\} = sY(s)$$

when the initial value of  $y(t)$  is zero. Therefore, we may acquire the derivative of  $y(t)$  by multiplying Equation (5.8) by  $s$  and thus obtaining the right side of Equation (5.10). Taking the inverse transform of the right side of Equation (5.10), we obtain Equation (5.11), which is equal to zero when  $\omega_n \omega_d t = \pi$ . Thus, we find that the peak time relationship for this second-order system is

$$T_p = \frac{\pi}{\omega_n \sqrt{1 - \zeta^2}} \tag{5.14}$$

and the peak response is

$$M_p = 1 + e^{-\zeta\pi/\sqrt{1-\zeta^2}} \tag{5.15}$$

Therefore, the percent overshoot is

$$P.O. = 100e^{-\zeta\pi/\sqrt{1-\zeta^2}} \tag{5.16}$$

The percent overshoot versus the damping ratio,  $\zeta$ , is shown in Figure 5.8. Also, the normalized peak time,  $\omega_n T_p$ , is shown versus the damping ratio,  $\zeta$ , in Figure 5.8. The percent overshoot versus the damping ratio is listed in Table 5.2 for selected values of

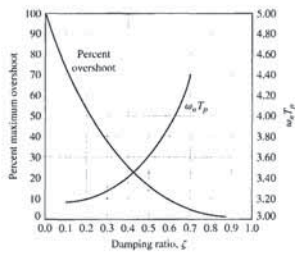


FIGURE 5.8 Percent overshoot and normalized peak time versus damping ratio  $\zeta$  for a second-order system (Equation 5.8).

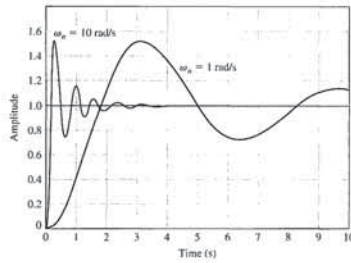


FIGURE 5.10 The step response for  $\zeta = 0.2$  for  $\omega_n = 1$  and  $\omega_n = 10$ .

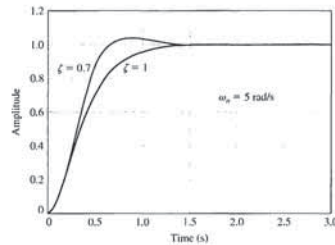


FIGURE 5.11 The step response for  $\omega_n = 5$  with  $\zeta = 0.7$  and  $\zeta = 1$ .

5.4 EFFECTS OF A THIRD POLE AND A ZERO ON THE SECOND-ORDER SYSTEM RESPONSE

The curves presented in Figure 5.8 are exact only for the second-order system of Equation (5.8). However, they provide a remarkably good source of data because many systems possess a dominant pair of roots, and the step response can be estimated by utilizing Figure 5.8. This approach, although an approximation, avoids the evaluation of the inverse Laplace transformation in order to determine the percent overshoot and other performance measures. For example, for a third-order system with a closed-loop transfer function

$$T(s) = \frac{1}{(s^2 + 2\zeta s + 1)(\gamma s + 1)} \tag{5.18}$$

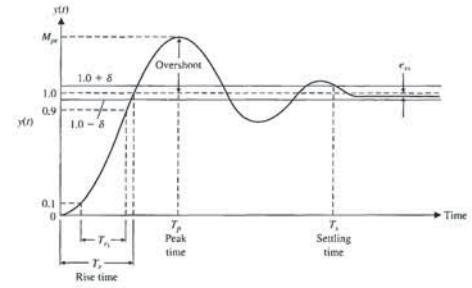


FIGURE 5.7 Step response of a control system (Equation 5.9).

for a unit step input, where  $M_p$  is the peak value of the time response, and  $f_v$  is the final value of the response. Normally,  $f_v$  is the magnitude of the input, but many systems have a final value significantly different from the desired input magnitude. For the system with a unit step represented by Equation (5.8), we have  $f_v = 1$ .

The settling time,  $T_s$ , is defined as the time required for the system to settle within a certain percentage  $\delta$  of the input amplitude. This band of  $\pm\delta$  is shown in Figure 5.7. For the second-order system with closed-loop damping constant  $\zeta\omega_n$  and a response described by Equation (5.9), we seek to determine the time  $T_s$  for which the response remains within 2% of the final value. This occurs approximately when

$$e^{-\zeta\omega_n T_s} < 0.02,$$

or

$$\zeta\omega_n T_s \cong 4.$$

Therefore, we have

$$T_s = 4\tau = \frac{4}{\zeta\omega_n} \tag{5.13}$$

Hence, we will define the settling time as four time constants (that is,  $\tau = 1/\zeta\omega_n$ ) of the dominant roots of the characteristic equation. The steady-state error of the system may be measured on the step response of the system as shown in Figure 5.7.

The transient response of the system may be described in terms of two factors:

1. The swiftness of response, as represented by the rise time and the peak time.
2. The closeness of the response to the desired response, as represented by the overshoot and settling time.

Table 5.2 Percent Peak Overshoot Versus Damping Ratio for a Second-Order System

Damping ratio	0.9	0.8	0.7	0.6	0.5	0.4	0.3
Percent overshoot	0.2	1.5	4.6	9.5	16.3	25.4	37.2

the damping ratio. Again, we are confronted with a necessary compromise between the swiftness of response and the allowable overshoot.

The swiftness of step response can be measured as the time it takes to rise from 10% to 90% of the magnitude of the step input. This is the definition of the rise time,  $T_{r1}$ , shown in Figure 5.7. The normalized rise time,  $\omega_n T_{r1}$ , versus  $\zeta$  ( $0.05 \leq \zeta \leq 0.95$ ) is shown in Figure 5.9. Although it is difficult to obtain exact analytic expressions for  $T_{r1}$ , we can utilize the linear approximation

$$T_{r1} = \frac{2.16\zeta + 0.60}{\omega_n} \tag{5.17}$$

which is accurate for  $0.3 \leq \zeta \leq 0.8$ . This linear approximation is shown in Figure 5.9.

The swiftness of a response to a step input as described by Equation (5.17) is dependent on  $\zeta$  and  $\omega_n$ . For a given  $\zeta$ , the response is faster for larger  $\omega_n$ , as shown in Figure 5.10. Note that the overshoot is independent of  $\omega_n$ .

For a given  $\omega_n$ , the response is faster for lower  $\zeta$ , as shown in Figure 5.11. The swiftness of the response, however, will be limited by the overshoot that can be accepted.

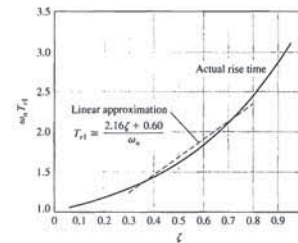


FIGURE 5.9 Normalized rise time,  $T_{r1}$ , versus  $\zeta$  for a second-order system.



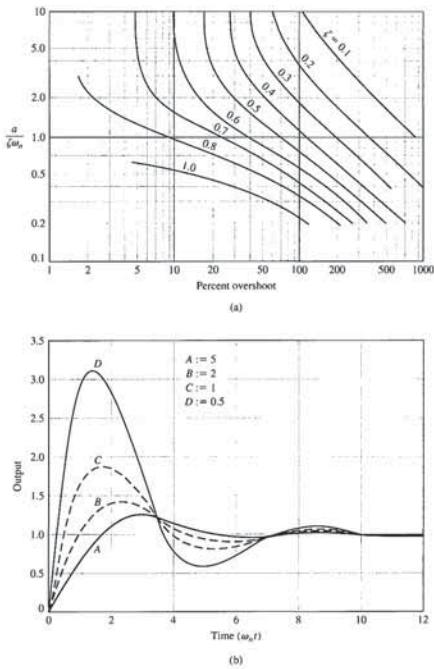


FIGURE 5.13 (a) Percent overshoot as a function of  $\zeta$  and  $\omega_n$  when a second-order transfer function contains a zero. Redrawn with permission from R. N. Clark, *Introduction to Automatic Control Systems* (New York: Wiley, 1962). (b) The response for the second-order transfer function with a zero for four values of the ratio  $a/\zeta\omega_n$ :  $A = 5$ ,  $B = 2$ ,  $C = 1$ , and  $D = 0.5$  when  $\zeta = 0.45$ .

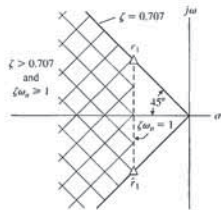


FIGURE 5.15 Specifications and root locations on the  $s$ -plane.

we require that the real part of the complex poles of  $T(s)$  be

$$\zeta\omega_n \geq 1.$$

This region is also shown in Figure 5.15. The region that will satisfy both time-domain requirements is shown cross-hatched on the  $s$ -plane of Figure 5.15.

When the closed-loop roots are  $r_1 = -1 + j1$  and  $\bar{r}_1 = -1 - j1$ , we have  $T_s = 4$  s and an overshoot of 4.3%. Therefore,  $\zeta = 1/\sqrt{2}$  and  $\omega_n = 1/\zeta = \sqrt{2}$ . The closed-loop transfer function is

$$T(s) = \frac{G(s)}{1 + G(s)} = \frac{K}{s^2 + ps + K} = \frac{\omega_n^2}{s^2 + 2\zeta\omega_n s + \omega_n^2}.$$

Hence, we require that  $K = \omega_n^2 = 2$  and  $p = 2\zeta\omega_n = 2$ . A full comprehension of the correlation between the closed-loop root location and the system transient response is important to the system analyst and designer. Therefore, we shall consider the matter more completely in the following sections. ■

**EXAMPLE 5.2 Dominant poles of  $T(s)$**

Consider a system with a closed-loop transfer function

$$\frac{Y(s)}{R(s)} = T(s) = \frac{\frac{\omega_n^2}{a}(s + a)}{(s^2 + 2\zeta\omega_n s + \omega_n^2)(1 + \tau s)}.$$

Both the zero and the real pole may affect the transient response. If  $a \gg \zeta\omega_n$  and  $\tau \ll 1/\zeta\omega_n$ , then the pole and zero will have little effect on the step response.

Assume that we have

$$T(s) = \frac{62.5(s + 2.5)}{(s^2 + 6s + 25)(s + 6.25)}$$

Note that the DC gain is equal to 1 ( $T(0) = 1$ ), and we expect a zero steady-state error for a step input. We have  $\zeta\omega_n = 3$ ,  $\tau = 0.16$ , and  $a = 2.5$ . The poles and the

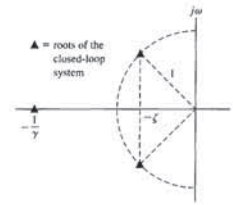


FIGURE 5.12 An  $s$ -plane diagram of a third-order system.

the  $s$ -plane diagram is shown in Figure 5.12. This third-order system is normalized with  $\omega_n = 1$ . It was ascertained experimentally that the performance (as indicated by the percent overshoot,  $P.O.$ , and the settling time,  $T_s$ ), was adequately represented by the second-order system curves when [4]

$$|1/\gamma| \geq 10|\zeta\omega_n|.$$

In other words, the response of a third-order system can be approximated by the **dominant roots** of the second-order system as long as the real part of the dominant roots is less than one tenth of the real part of the third root [15, 20].

Using a computer simulation, we can determine the response of a system to a unit step input when  $\zeta = 0.45$ . When  $\gamma = 2.25$ , we find that the response is overdamped because the real part of the complex poles is  $-0.45$ , whereas the real pole is equal to  $-0.444$ . The settling time (to within 2% of the final value) is found via the simulation to be 9.6 seconds. If  $\gamma = 0.90$  or  $1/\gamma = 1.11$  is compared with  $\zeta\omega_n = 0.45$  of the complex poles, the overshoot is 12% and the settling time is 8.8 seconds. If the complex roots were dominant, we would expect the overshoot to be 20% and the settling time to be  $4/\zeta\omega_n = 8.9$  seconds. The results are summarized in Table 5.3.

The performance measures of Figure 5.8 are correct only for a transfer function without finite zeros. If the transfer function of a system possesses finite zeros and they are located relatively near the dominant complex poles, then the zeros will materially affect the transient response of the system [5].

Table 5.3 Effect of a Third Pole (Equation 5.18) for  $\zeta = 0.45$

$\gamma$	$\frac{1}{\gamma}$	Percent Overshoot	Settling Time
2.25	0.444	0	9.63
1.5	0.666	3.9	6.3
0.9	1.111	12.3	8.81
0.4	2.50	18.6	8.67
0.05	20.0	20.5	8.37
0 $\infty$	20.5	8.24	

\*Note: Settling time is normalized time,  $\omega_n T_s$ , and uses a 2% criterion.

Table 5.4 The Response of a Second-Order System with a Zero and  $\zeta = 0.45$

$a/\zeta\omega_n$	Percent Overshoot	Settling Time	Peak Time
5	23.1	8.0	3.0
2	39.7	7.6	2.2
1	89.9	10.1	1.8
0.5	210.0	10.3	1.5

Note: Time is normalized as  $\omega_n t$ , and settling time is based on a 2% criterion.

The transient response of a system with one zero and two poles may be affected by the location of the zero [5]. The percent overshoot for a step input as a function of  $a/\zeta\omega_n$ , when  $\zeta \leq 1$ , is given in Figure 5.13(a) for the system transfer function

$$T(s) = \frac{(\omega_n^2/a)(s + a)}{s^2 + 2\zeta\omega_n s + \omega_n^2}.$$

The actual transient response for a step input is shown in Figure 5.13(b) for selected values of  $a/\zeta\omega_n$ . The actual response for these selected values is summarized in Table 5.4 when  $\zeta = 0.45$ .

The correlation of the time-domain response of a system with the  $s$ -plane location of the poles of the closed-loop transfer function is very useful for selecting the specifications of a system. To illustrate clearly the utility of the  $s$ -plane, let us consider a simple example.

**EXAMPLE 5.1 Parameter selection**

A single-loop feedback control system is shown in Figure 5.14. We select the gain  $K$  and the parameter  $p$  so that the time-domain specifications will be satisfied. The transient response to a step should be as fast as is attainable while retaining an overshoot of less than 5%. Furthermore, the settling time to within 2% of the final value should be less than 4 seconds. The damping ratio,  $\zeta$ , for an overshoot of 4.3% is 0.707. This damping ratio is shown graphically as a line in Figure 5.15. Because the settling time is

$$T_s = \frac{4}{\zeta\omega_n} \leq 4 \text{ s},$$

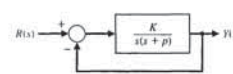


FIGURE 5.14 Single-loop feedback control system.

The time constant for the exponential decay is  $\tau = 1/(\zeta\omega_n)$  in seconds. The number of cycles of the damped sinusoid during one time constant is

$$(\text{cycles/time}) \times \tau = \frac{\omega}{2\pi\zeta\omega_n} = \frac{\omega_n\beta}{2\pi\zeta\omega_n} = \frac{\beta}{2\pi\zeta}$$

Assuming that the response decays in  $n$  visible time constants, we have

$$\text{cycles visible} = \frac{n\beta}{2\pi\zeta} \quad (5.19)$$

For the second-order system, the response remains within 2% of the steady-state value after four time constants ( $4\tau$ ). Hence,  $n = 4$ , and

$$\text{cycles visible} = \frac{4\beta}{2\pi\zeta} = \frac{4(1 - \zeta^2)^{1/2}}{2\pi\zeta} \approx \frac{0.55}{\zeta} \quad (5.20)$$

for  $0.2 \leq \zeta \leq 0.6$ .

As an example, examine the response shown in Figure 5.5(a) for  $\zeta = 0.4$ . Use  $y(t) = 0$  as the first minimum point and count 1.4 cycles visible (until the response settles with 2% of the final value). Then we estimate

$$\zeta = \frac{0.55}{\text{cycles}} = \frac{0.55}{1.4} = 0.39.$$

We can use this approximation for systems with dominant complex poles so that

$$T(s) \approx \frac{\omega_n^2}{s^2 + 2\zeta\omega_n s + \omega_n^2}$$

Then we are able to estimate the damping ratio  $\zeta$  from the actual system response of a physical system.

An alternative method of estimating  $\zeta$  is to determine the percent overshoot for the step response and use Figure 5.8 to estimate  $\zeta$ . For example, we determine an overshoot of 25% for  $\zeta = 0.4$  from the response of Figure 5.5(a). Using Figure 5.8, we estimate that  $\zeta = 0.4$ , as expected.

5.5 THE s-PLANE ROOT LOCATION AND THE TRANSIENT RESPONSE

The transient response of a closed-loop feedback control system can be described in terms of the location of the poles of the transfer function. The closed-loop transfer function is written in general as

$$T(s) = \frac{Y(s)}{R(s)} = \frac{\sum P_i(s) \Delta_i(s)}{\Delta(s)}$$

where  $\Delta(s) = 0$  is the characteristic equation of the system. For the single-loop system of Figure 5.4, the characteristic equation reduces to  $1 + G(s) = 0$ . It is the

represented in terms of the poles and zeros of its transfer function  $T(s)$ . On the other hand, system performance is often analyzed by examining time-domain responses, particularly when dealing with control systems.

The capable system designer will envision the effects on the step and impulse responses of adding, deleting, or moving poles and zeros of  $T(s)$  in the s-plane. Likewise, the designer should visualize the necessary changes for the poles and zeros of  $T(s)$ , in order to effect desired changes in the model's step and impulse responses.

An experienced designer is aware of the effects of zero locations on system response. The poles of  $T(s)$  determine the particular response modes that will be present, and the zeros of  $T(s)$  establish the relative weightings of the individual mode functions. For example, moving a zero closer to a specific pole will reduce the relative contribution of the mode function corresponding to the pole.

A computer program can be developed to allow a user to specify arbitrary sets of poles and zeros for the transfer function of a linear system. Then the computer will evaluate and plot the system's impulse and step responses individually. It will also display them in reduced form along with the pole-zero plot.

Once the program has been run for a set of poles and zeros, the user can modify the locations of one or more of them. Plots may then be presented showing the old and new poles and zeros in the complex plane and the old and new impulse and step responses.

5.6 THE STEADY-STATE ERROR OF FEEDBACK CONTROL SYSTEMS

One of the fundamental reasons for using feedback, despite its cost and increased complexity, is the attendant improvement in the reduction of the steady-state error of the system. As illustrated in Section 4.6, the steady-state error of a stable closed-loop system is usually several orders of magnitude smaller than the error of an open-loop system. The system actuating signal, which is a measure of the system error, is denoted as  $E_s(s)$ . Consider the closed-loop feedback system shown in Figure 5.18. According to the discussions in Chapter 4, we know from Equation (4.3) that with  $N(s) = 0$ ,  $T_f(s) = 0$ , the tracking error is

$$E(s) = \frac{1}{1 + G_c(s)G(s)} R(s).$$

Using the final value theorem and computing the steady-state tracking error yields

$$\lim_{t \rightarrow \infty} e(t) = e_{ss} = \lim_{s \rightarrow 0} s \frac{1}{1 + G_c(s)G(s)} R(s). \quad (5.23)$$

It is useful to determine the steady-state error of the system for the three standard test inputs for the unity feedback system. Later in this section we will consider steady-state tracking errors for non-unity feedback systems.

**Step Input.** The steady-state error for a step input of magnitude  $A$  is therefore

$$e_{ss} = \lim_{s \rightarrow 0} \frac{s(A/s)}{1 + G_c(s)G(s)} = \frac{A}{1 + \lim_{s \rightarrow 0} G_c(s)G(s)}$$

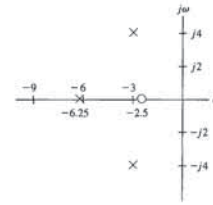


FIGURE 5.16 The poles and zeros on the s-plane for a third-order system.

zero are shown on the s-plane in Figure 5.16. As a first approximation, we neglect the real pole and obtain

$$T(s) \approx \frac{10(s + 2.5)}{s^2 + 6s + 25}$$

We now have  $\zeta = 0.6$  and  $\omega_n = 5$  for dominant poles with one accompanying zero for which  $\eta/(\zeta\omega_n) = 0.833$ . Using Figure 5.13(a), we find that the percent overshoot is 55%. We expect the settling time to within 2% of the final value to be

$$T_s = \frac{4}{\zeta\omega_n} = \frac{4}{0.6(5)} = 1.33 \text{ s.}$$

Using a computer simulation for the actual third-order system, we find that the percent overshoot is equal to 38% and the settling time is 1.6 seconds. Thus, the effect of the third pole of  $T(s)$  is to dampen the overshoot and increase the settling time (hence the real pole cannot be neglected). ■

The damping ratio plays a fundamental role in closed-loop system performance. As seen in the design formulas for settling time, percent overshoot, peak time, and rise time, the damping ratio is a key factor in determining the overall performance. In fact, for second-order systems, the damping ratio is the only factor determining the value of the percent overshoot to a step input. As it turns out, the damping ratio can be estimated from the response of a system to a step input [12]. The step response of a second-order system for a unit step input is given in Equation (5.9), which is

$$y(t) = 1 - \frac{1}{\beta} e^{-\beta t} \sin(\omega_n \beta t + \theta),$$

where  $\beta = \sqrt{1 - \zeta^2}$ , and  $\theta = \cos^{-1} \zeta$ . Hence, the frequency of the damped sinusoidal term for  $\zeta < 1$  is

$$\omega = \omega_n(1 - \zeta^2)^{1/2} = \omega_n \beta,$$

and the number of cycles in 1 second is  $\omega/(2\pi)$ .

Section 5.5 The s-Plane Root Location and the Transient Response

poles and zeros of  $T(s)$  that determine the transient response. However, for a closed-loop system, the poles of  $T(s)$  are the roots of the characteristic equation  $\Delta(s) = 0$  and the poles of  $\sum P_i(s) \Delta_i(s)$ . The output of a system (with gain = 1) without repeated roots and a unit step input can be formulated as a partial fraction expansion as

$$Y(s) = \frac{1}{s} + \sum_{i=1}^M \frac{A_i}{s + \sigma_i} + \sum_{k=1}^N \frac{B_k s + C_k}{s^2 + 2\alpha_k s + (\alpha_k^2 + \omega_k^2)}, \quad (5.21)$$

where the  $A_i$ ,  $B_k$ , and  $C_k$  are constants. The roots of the system must be either  $s = -\sigma_i$  or complex conjugate pairs such as  $s = -\alpha_k \pm j\omega_k$ . Then the inverse transform results in the transient response as the sum of terms

$$y(t) = 1 + \sum_{i=1}^M A_i e^{-\sigma_i t} + \sum_{k=1}^N D_k e^{-\alpha_k t} \sin(\omega_k t + \theta_k), \quad (5.22)$$

where  $D_k$  is a constant and depends on  $B_k$ ,  $C_k$ ,  $\alpha_k$ , and  $\omega_k$ . The transient response is composed of the steady-state output, exponential terms, and damped sinusoidal terms. For the response to be stable—that is, bounded for a step input—the real part of the roots,  $-\sigma_i$  and  $-\alpha_k$ , must be in the left-hand portion of the s-plane. The impulse response for various root locations is shown in Figure 5.17. The information imparted by the location of the roots is graphic indeed, and usually well worth the effort of determining the location of the roots in the s-plane.

It is important for the control system analyst to understand the complete relationship of the complex-frequency representation of a linear system, the poles and zeros of its transfer function, and its time-domain response to step and other inputs. In such areas as signal processing and control, many of the analysis and design calculations are done in the complex-frequency plane, where a system model is

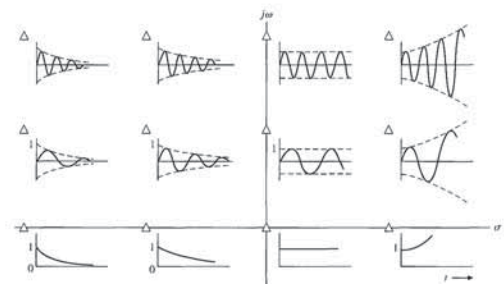


FIGURE 5.17 Impulse response for various root locations in the s-plane. (The conjugate root is not shown.)



The steady-state tracking error for a step input of magnitude  $A$  is thus given by

$$e_{ss} = \frac{A}{1 + K_p} \quad (5.26)$$

Hence, the steady-state error for a unit step input with one integration or more,  $N \geq 1$ , is zero because

$$\begin{aligned} e_{ss} &= \lim_{s \rightarrow 0} \frac{A}{1 + K \prod_{i=1}^N z_i / (s^N \prod_{k=1}^Q p_k)} \\ &= \lim_{s \rightarrow 0} \frac{A s^N}{s^N + K \prod_{i=1}^N z_i / \prod_{k=1}^Q p_k} = 0. \end{aligned} \quad (5.27)$$

**Ramp Input.** The steady-state error for a ramp (velocity) input with a slope  $A$  is

$$e_{ss} = \lim_{s \rightarrow 0} \frac{s(A/s^2)}{1 + G_c(s)G(s)} = \lim_{s \rightarrow 0} \frac{A}{s G_c(s)G(s)} = \lim_{s \rightarrow 0} \frac{A}{s G_c(s)G(s)}. \quad (5.28)$$

Again, the steady-state error depends upon the number of integrations,  $N$ . For a type-zero system,  $N = 0$ , the steady-state error is infinite. For a type-one system,  $N = 1$ , the error is

$$e_{ss} = \lim_{s \rightarrow 0} \frac{A}{s K \prod_{i=1}^M (s + z_i) / [s \prod_{k=1}^Q (s + p_k)]}$$

or

$$e_{ss} = \frac{A}{K \prod_{k=1}^Q p_k / \prod_{i=1}^M p_k} = \frac{A}{K_v} \quad (5.29)$$

where  $K_v$  is designated the **velocity error constant**. The velocity error constant is computed as

$$K_v = \lim_{s \rightarrow 0} s G_c(s)G(s).$$

When the transfer function possesses two or more integrations,  $N \geq 2$ , we obtain a steady-state error of zero. When  $N = 1$ , a steady-state error exists. However, the steady-state velocity of the output is equal to the velocity of input, as we shall see shortly.

**Acceleration Input.** When the system input is  $r(t) = At^2/2$ , the steady-state error is

$$e_{ss} = \lim_{s \rightarrow 0} \frac{s(A/s^3)}{1 + G_c(s)G(s)} = \lim_{s \rightarrow 0} \frac{A}{s^2 G_c(s)G(s)} \quad (5.30)$$

Therefore, the steady-state error of the system for a step input when  $K_2 = 0$  and  $G_c(s) = K_1$  is

$$e_{ss} = \frac{A}{1 + K_p}, \quad (5.33)$$

where  $K_p = KK_1$ . When  $K_2$  is greater than zero, we have a type-1 system,

$$G_c(s) = \frac{K_1 s + K_2}{s},$$

and the steady-state error is zero for a step input.

If the steering command is a ramp input, the steady-state error is

$$e_{ss} = \frac{A}{K_v}, \quad (5.34)$$

where

$$K_v = \lim_{s \rightarrow 0} s G_c(s)G(s) = K_2 K.$$

The transient response of the vehicle to a triangular wave input when  $G_c(s) = (K_1 s + K_2)/s$  is shown in Figure 5.20. The transient response clearly shows the effect of the steady-state error, which may not be objectionable if  $K_v$  is sufficiently large. Note that the output attains the desired velocity as required by the input, but it exhibits a steady-state error. ■

The control system's error constants,  $K_p$ ,  $K_v$ , and  $K_a$ , describe the ability of a system to reduce or eliminate the steady-state error. Therefore, they are utilized as numerical measures of the steady-state performance. The designer determines the error constants for a given system and attempts to determine methods of increasing the error constants while maintaining an acceptable transient response. In the case of the steering control system, we want to increase the gain factor  $KK_2$  in order to increase  $K_v$  and reduce the steady-state error. However, an increase in  $KK_2$  results in an attendant decrease in the system's damping ratio  $\zeta$  and therefore a

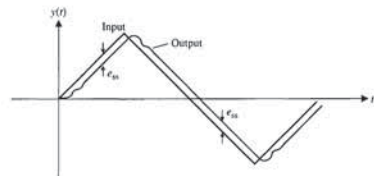


FIGURE 5.20 Triangular wave response.

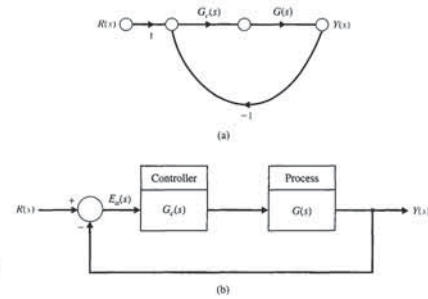


FIGURE 5.18 Closed-loop control system with unity feedback.

It is the form of the loop transfer function  $G_c(s)G(s)$  that determines the steady-state error. The loop transfer function is written in general form as

$$G_c(s)G(s) = \frac{K \prod_{i=1}^M (s + z_i)}{s^N \prod_{k=1}^Q (s + p_k)}, \quad (5.24)$$

where  $\prod$  denotes the product of the factors and  $z_i \neq 0$ ,  $p_k \neq 0$  for any  $1 \leq i \leq M$  and  $1 \leq k \leq Q$ . Therefore, the loop transfer function as  $s$  approaches zero depends on the number of integrations,  $N$ . If  $N$  is greater than zero, then  $\lim_{s \rightarrow 0} G_c(s)G(s)$  approaches infinity, and the steady-state error approaches zero. The number of integrations is often indicated by labeling a system with a **type number** that simply is equal to  $N$ .

Consequently, for a type-zero system,  $N = 0$ , the steady-state error is

$$e_{ss} = \frac{A}{1 + G_c(0)G(0)} = \frac{A}{1 + K \prod_{i=1}^M z_i / \prod_{k=1}^Q p_k}. \quad (5.25)$$

The constant  $G_c(0)G(0)$  is denoted by  $K_p$ , the **position error constant**, and is given by

$$K_p = \lim_{s \rightarrow 0} G_c(s)G(s).$$

Table 5.5 Summary of Steady-State Errors

Number of Integrations in $G_c(s)G(s)$ , Type Number	Input		
	Step, $r(t) = A$ , $R(s) = A/s$	Ramp, $At$ , $A/s^2$	Parabola, $At^2/2$ , $A/s^3$
0	$e_{ss} = \frac{A}{1 + K_p}$	Infinite	Infinite
1	$e_{ss} = 0$	$\frac{A}{K_v}$	Infinite
2	$e_{ss} = 0$	0	$\frac{A}{K_a}$

The steady-state error is infinite for one integration. For two integrations,  $N = 2$ , and we obtain

$$e_{ss} = \frac{A}{K \prod_{i=1}^M z_i / \prod_{k=1}^Q p_k} = \frac{A}{K_a}, \quad (5.31)$$

where  $K_a$  is designated the **acceleration error constant**. The acceleration error constant is

$$K_a = \lim_{s \rightarrow 0} s^2 G_c(s)G(s).$$

When the number of integrations equals or exceeds three, then the steady-state error of the system is zero.

Control systems are often described in terms of their type number and the error constants,  $K_p$ ,  $K_v$ , and  $K_a$ . Definitions for the error constants and the steady-state error for the three inputs are summarized in Table 5.5. The usefulness of the error constants can be illustrated by considering a simple example.

**EXAMPLE 5.3 Mobile robot steering control**

A mobile robot may be designed as an assisting device or servant for a severely disabled person [7]. The steering control system for such a robot can be represented by the block diagram shown in Figure 5.19. The steering controller is

$$G_c(s) = K_1 + K_2/s. \quad (5.32)$$

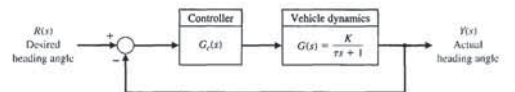


FIGURE 5.19 Block diagram of steering control system for a mobile robot.

since  $Y(s) = T(s)R(s)$ . Note that

$$T(s) = \frac{K_1 G_c(s)G(s)}{1 + H(s)G_c(s)G(s)} = \frac{(\tau s + 1)K_1 G_c(s)G(s)}{\tau s + 1 + K_1 G_c(s)G(s)}$$

and therefore,

$$E(s) = \frac{1 + \tau s(1 - K_1 G_c(s)G(s))}{\tau s + 1 + K_1 G_c(s)G(s)} R(s).$$

Then the steady-state error for a unit step input is

$$e_{ss} = \lim_{s \rightarrow 0} s E(s) = \frac{1}{1 + K_1 \lim_{s \rightarrow 0} G_c(s)G(s)} \quad (5.36)$$

We assume here that

$$\lim_{s \rightarrow 0} s G_c(s)G(s) = 0.$$

**EXAMPLE 5.4 Steady-state error**

Let us determine the appropriate value of  $K_1$  and calculate the steady-state error for a unit step input for the system shown in Figure 5.21 when

$$G_c(s) = 40 \quad \text{and} \quad G(s) = \frac{1}{s + 5}$$

and

$$H(s) = \frac{20}{s + 10}.$$

We can rewrite  $H(s)$  as

$$H(s) = \frac{2}{0.1s + 1}.$$

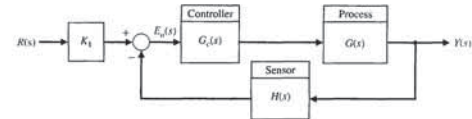
Selecting  $K_1 = K_2 = 2$ , we can use Equation (5.36) to determine

$$e_{ss} = \frac{1}{1 + K_1 \lim_{s \rightarrow 0} G_c(s)G(s)} = \frac{1}{1 + 2(40)(1/5)} = \frac{1}{17}$$

or 5.9% of the magnitude of the step input. ■

**EXAMPLE 5.5 Feedback system**

Let us consider the system of Figure 5.24, where we assume we cannot insert a gain  $K_1$  following  $R(s)$  as we did for the system of Figure 5.21. Then the actual error is given by Equation (5.35), which is



**FIGURE 5.21** A nonunity feedback system.

more oscillatory response to a step input. Thus, we want a compromise that provides the largest  $K_v$  based on the smallest  $\zeta$  allowable.

In the preceding discussions, we assumed that we had a unity feedback system where  $H(s) = 1$ . Now we consider nonunity feedback systems. A general feedback system with nonunity feedback is shown in Figure 5.21. For a system in which the feedback is not unity, the units of the output  $Y(s)$  are usually different from the output of the sensor. For example, a speed control system is shown in Figure 5.22, where  $H(s) = K_2$ . The constants  $K_1$  and  $K_2$  account for the conversion of one set of units to another set of units (here we convert rad/s to volts). We can select  $K_1$ , and thus we set  $K_1 = K_2$  and move the block for  $K_1$  and  $K_2$  past the summing node. Then we obtain the equivalent block diagram shown in Figure 5.23. Thus, we obtain a unity feedback system as desired.

Let us return to the system of Figure 5.21 with  $H(s)$ . In this case, suppose

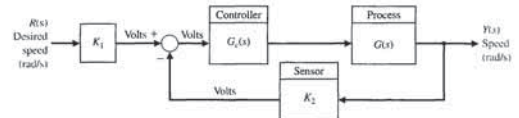
$$H(s) = \frac{K_2}{\tau s + 1}$$

which has a DC gain of

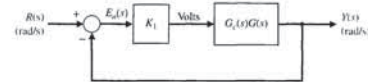
$$\lim_{s \rightarrow 0} H(s) = K_2.$$

The factor  $K_2$  is a conversion-of-units factor. If we set  $K_2 = K_1$ , then the system is transformed to that of Figure 5.23 for the steady-state calculation. To see this, consider error of the system  $E(s)$ , where

$$E(s) = R(s) - Y(s) = [1 - T(s)]R(s), \quad (5.35)$$



**FIGURE 5.22** A speed control system.



**FIGURE 5.23** The speed control system of Figure 5.22 with  $K_1 = K_2$ .

The loop transfer function of the equivalent unity feedback system is  $Z(s)$ . It follows that the error constants for nonunity feedback systems are given as:

$$K_p = \lim_{s \rightarrow 0} Z(s), \quad K_v = \lim_{s \rightarrow 0} sZ(s), \quad \text{and} \quad K_a = \lim_{s \rightarrow 0} s^2 Z(s).$$

Note that when  $H(s) = 1$ , then  $Z(s) = G_c(s)G(s)$  and we maintain the unity feedback error constants. For example, when  $H(s) = 1$ , then  $K_p = \lim_{s \rightarrow 0} Z(s) = \lim_{s \rightarrow 0} G_c(s)G(s)$ , as expected.

5.7 PERFORMANCE INDICES

Increasing emphasis on the mathematical formulation and measurement of control system performance can be found in the recent literature on automatic control. Modern control theory assumes that the systems engineer can specify quantitatively the required system performance. Then a performance index can be calculated or measured and used to evaluate the system's performance. A quantitative measure of the performance of a system is necessary for the operation of modern adaptive control systems, for automatic parameter optimization of a control system, and for the design of optimum systems.

Whether the aim is to improve the design of a system or to design a control system, a performance index must be chosen and measured.

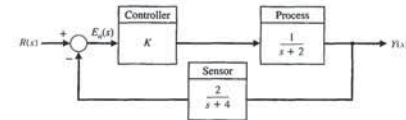
**A performance index is a quantitative measure of the performance of a system and is chosen so that emphasis is given to the important system specifications.**

A system is considered an **optimum control system** when the system parameters are adjusted so that the index reaches an extremum, commonly a minimum value. To be useful, a performance index must be a number that is always positive or zero. Then the best system is defined as the system that minimizes this index.

A suitable performance index is the integral of the square of the error, ISE, which is defined as

$$ISE = \int_0^T e^2(t) dt. \quad (5.37)$$

The upper limit  $T$  is a finite time chosen somewhat arbitrarily so that the integral approaches a steady-state value. It is usually convenient to choose  $T$  as the settling time  $T_s$ . The step response for a specific feedback control system is shown in Figure 5.25(b), and the error in Figure 5.25(c). The error squared is shown in Figure 5.25(d), and the integral of the error squared in Figure 5.25(e). This criterion will discriminate between excessively overdamped and excessively underdamped systems. The minimum value of the integral occurs for a compromise value of the damping. The performance index of Equation (5.37) is easily adapted for practical measurements because a squaring circuit is readily obtained. Furthermore, the squared error is mathematically convenient for analytical and computational purposes.



**FIGURE 5.24** A system with a feedback  $H(s)$ .

$$E(s) = [1 - T(s)]R(s).$$

Let us determine an appropriate gain  $K$  so that the steady-state error to a step input is minimized. The steady-state error is

$$e_{ss} = \lim_{s \rightarrow 0} s[1 - T(s)]\frac{1}{s},$$

where

$$T(s) = \frac{G_c(s)G(s)}{1 + G_c(s)G(s)H(s)} = \frac{K(s + 4)}{(s + 2)(s + 4) + 2K}.$$

Then we have

$$T(0) = \frac{4K}{8 + 2K}.$$

The steady-state error for a unit step input is

$$e_{ss} = 1 - T(0).$$

Thus, to achieve a zero steady-state error, we require that

$$T(0) = \frac{4K}{8 + 2K} = 1,$$

or  $8 + 2K = 4K$ . Thus,  $K = 4$  will yield a zero steady-state error. ■

The determination of the steady-state error is simpler for unity feedback systems. However, it is possible to extend the notion of error constants to nonunity feedback systems by first appropriately rearranging the block diagram to obtain an equivalent unity feedback system. Remember that the underlying system must be stable, otherwise our use of the final value theorem will be compromised. Consider the nonunity feedback system in Figure 5.21 and assume that  $K_1 = 1$ . The closed-loop transfer function is

$$\frac{Y(s)}{R(s)} = T(s) = \frac{G_c(s)G(s)}{1 + H(s)G_c(s)G(s)}.$$

By manipulating the block diagram appropriately we can obtain the equivalent unity feedback system with

$$\frac{Y(s)}{R(s)} = T(s) = \frac{Z(s)}{1 + Z(s)} \quad \text{where} \quad Z(s) = \frac{G_c(s)G(s)}{1 + G_c(s)G(s)(H(s) - 1)}.$$



The performance index ITAE provides the best selectivity of the performance indices; that is, the minimum value of the integral is readily discernible as the system parameters are varied. The general form of the performance integral is

$$I = \int_0^T f(e(t), r(t), y(t), t) dt, \quad (5.41)$$

where  $f$  is a function of the error, input, output, and time. We can obtain numerous indices based on various combinations of the system variables and time. Note that the minimization of IAE or ISE is often of practical significance. For example, the minimization of a performance index can be directly related to the minimization of fuel consumption for aircraft and space vehicles.

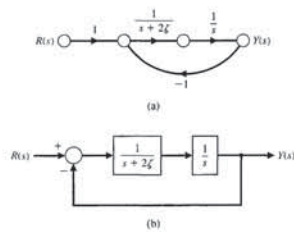
Performance indices are useful for the analysis and design of control systems. Two examples will illustrate the utility of this approach.

**EXAMPLE 5.6 Performance criteria**

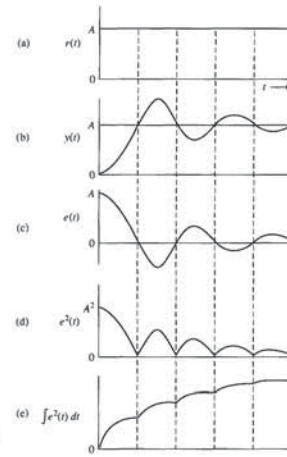
A single-loop feedback control system is shown in Figure 5.26, where the natural frequency is the normalized value,  $\omega_n = 1$ . The closed-loop transfer function is then

$$T(s) = \frac{1}{s^2 + 2\zeta s + 1} \quad (5.42)$$

Three performance indices—ISE, ITAE, and ITSE—calculated for various values of the damping ratio  $\zeta$  and for a step input are shown in Figure 5.27. These curves show the selectivity of the ITAE index in comparison with the ISE index. The value of the damping ratio  $\zeta$  selected on the basis of ITAE is 0.7. For a second-order system, this results in a swift response to a step with a 4.6% overshoot. ■



**FIGURE 5.26** Single-loop feedback control system. (a) Signal-flow graph. (b) Block diagram model.



**FIGURE 5.25** The calculation of the integral squared error.

Another readily instrumented performance criterion is the integral of the absolute magnitude of the error, IAE, which is written as

$$IAE = \int_0^T |e(t)| dt. \quad (5.38)$$

This index is particularly useful for computer simulation studies.

To reduce the contribution of the large initial error to the value of the performance integral, as well as to emphasize errors occurring later in the response, the following index has been proposed [6]:

$$ITAE = \int_0^T t|e(t)| dt. \quad (5.39)$$

This performance index is designated the integral of time multiplied by absolute error, ITAE. Another similar index is the integral of time multiplied by the squared error, or

$$ITSE = \int_0^T te^2(t) dt. \quad (5.40)$$

for the disturbance is obtained by using Mason's signal-flow gain formula as follows:

$$\begin{aligned} \frac{Y(s)}{T_d(s)} &= \frac{P_1(s) \Delta_1(s)}{\Delta(s)} \\ &= \frac{1 \cdot (1 + K_1 K_3 s^{-1})}{1 + K_1 K_3 s^{-1} + K_1 K_2 K_p s^{-2}} \\ &= \frac{s(s + K_1 K_3)}{s^2 + K_1 K_3 s + K_1 K_2 K_p} \end{aligned} \quad (5.43)$$

Typical values for the constants are  $K_1 = 0.5$  and  $K_1 K_2 K_p = 2.5$ . Then the natural frequency of the vehicle is  $f_n = \sqrt{2.5}/(2\pi) = 0.25$  cycles/s. For a unit step disturbance, the minimum ISE can be analytically calculated. The attitude is

$$y(t) = \frac{\sqrt{10}}{\beta} \left[ e^{-0.25K_3 t} \sin\left(\frac{\beta}{2}t + \psi\right) \right], \quad (5.44)$$

where  $\beta = \sqrt{10 - K_3^2}/4$ . Squaring  $y(t)$  and integrating the result, we have

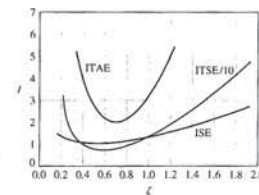
$$\begin{aligned} I &= \int_0^\infty \frac{10}{\beta^2} e^{-0.5K_3 t} \sin^2\left(\frac{\beta}{2}t + \psi\right) dt \\ &= \int_0^\infty \frac{10}{\beta^2} e^{-0.5K_3 t} \left(\frac{1}{2} - \frac{1}{2}\cos(\beta t + 2\psi)\right) dt \\ &= \frac{1}{K_3} + 0.1K_3. \end{aligned} \quad (5.45)$$

Differentiating  $I$  and equating the result to zero, we obtain

$$\frac{dI}{dK_3} = -K_3^{-2} + 0.1 = 0. \quad (5.46)$$

Therefore, the minimum ISE is obtained when  $K_3 = \sqrt{10} = 3.2$ . This value of  $K_3$  corresponds to a damping ratio  $\zeta$  of 0.50. The values of ISE and IAE for this system are plotted in Figure 5.29. The minimum for the IAE performance index is obtained when  $K_3 = 4.2$  and  $\zeta = 0.665$ . While the ISE criterion is not as selective as the IAE criterion, it is clear that it is possible to solve analytically for the minimum value of ISE. The minimum of IAE is obtained by measuring the actual value of IAE for several values of the parameter of interest. ■

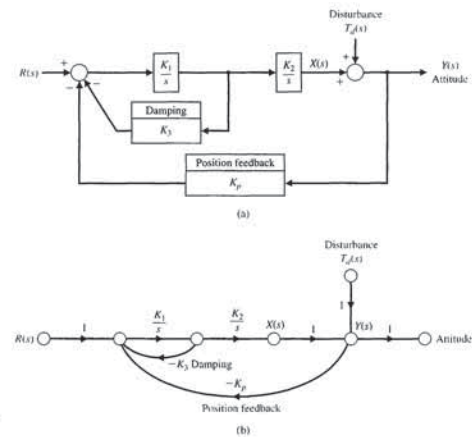
A control system is optimum when the selected performance index is minimized. However, the optimum value of the parameters depends directly on the definition of optimum, that is, the performance index. Therefore, in Examples 5.6



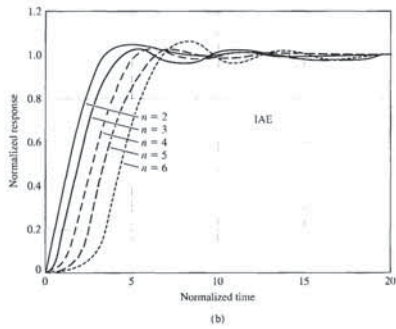
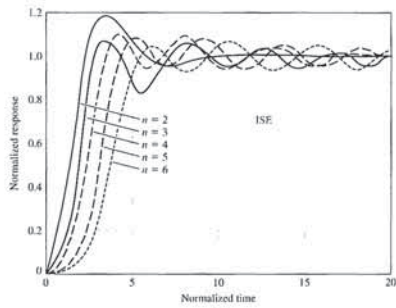
**FIGURE 5.27** Three performance criteria for a second-order system.

**EXAMPLE 5.7 Space telescope control system**

The signal-flow graph and block diagram of a space telescope pointing control system are shown in Figure 5.28 [9]. We desire to select the magnitude of the gain,  $K_3$ , to minimize the effect of the disturbance,  $T_d(s)$ . In this case, the disturbance is equivalent to an initial attitude error. The closed-loop transfer function



**FIGURE 5.28** A space telescope pointing control system. (a) Block diagram. (b) Signal-flow graph.

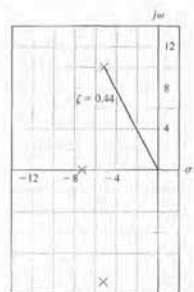
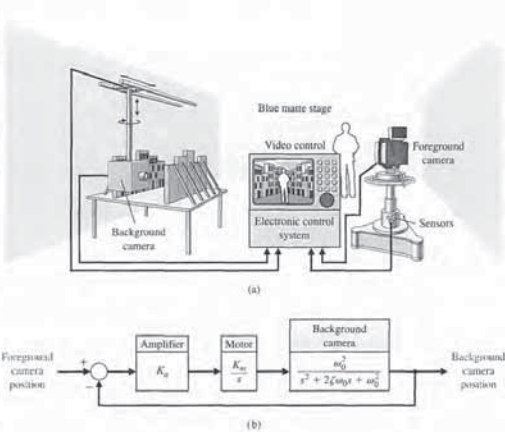


**FIGURE 5.30** Step responses of a normalized transfer function using optimum coefficients for (a) ISE, (b) IAE, and (c) ITAE. The response is for normalized time,  $\omega_n t$ .

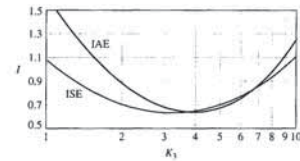
foreground camera to control the movement of the background camera. The block diagram of the background camera system is shown in Figure 5.31(b) for one axis of movement of the background camera. The closed-loop transfer function is

$$T(s) = \frac{K_a K_m \omega_0^2}{s^3 + 2\zeta \omega_0 s^2 + \omega_0^2 s + K_a K_m \omega_0^2} \quad (5.48)$$

**FIGURE 5.31** The foreground camera, which may be either a film or video camera, is trained on the blue cyclorama stage. The electronic servocontrol installation permits the slaving, by means of electronic servodevices, of the two cameras. The background camera reaches into the miniature set with a periscope lens and instantaneously reproduces all movements of the foreground camera in the scale of the miniature. The video control installation allows the composite image to be monitored and recorded live. (Part (a) reprinted with permission from *Electronic Design* 24, 11, May 24, 1978. Copyright © Hayden Publishing Co., Inc., 1978.)



**FIGURE 5.32** The closed-loop roots of a minimum ITAE system.



**FIGURE 5.29** The performance indices of the telescope control system versus  $K_1$ .

and 5.7, we found that the optimum setting varied for different performance indices.

The coefficients that will minimize the ITAE performance criterion for a step input have been determined for the general closed-loop transfer function [6]

$$T(s) = \frac{Y(s)}{R(s)} = \frac{b_0}{s^n + b_{n-1}s^{n-1} + \dots + b_1s + b_0} \quad (5.47)$$

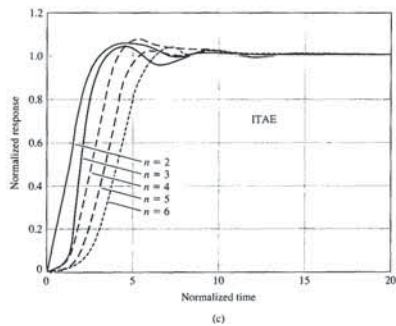
This transfer function has a steady-state error equal to zero for a step input. Note that the transfer function has  $n$  poles and no zeros. The optimum coefficients for the ITAE criterion are given in Table 5.6. The responses using optimum coefficients for a step input are given in Figure 5.30 for ISE, IAE, and ITAE. The responses are provided for normalized time  $\omega_n t$ . Other standard forms based on different performance indices are available and can be useful in aiding the designer to determine the range of coefficients for a specific problem. A final example will illustrate the utility of the standard forms for ITAE.

**EXAMPLE 5.8 Two-camera control**

A very accurate and rapidly responding control system is required for a system that allows live actors to appear as if they are performing inside of complex miniature sets. The two-camera system is shown in Figure 5.31(a), where one camera is trained on the actor and the other on the miniature set. The challenge is to obtain rapid and accurate coordination of the two cameras by using sensor information from the

**Table 5.6 The Optimum Coefficients of  $T(s)$  Based on the ITAE Criterion for a Step Input**

$n$	$2\zeta\omega_n$	$\omega_0^2$	$K_a K_m \omega_0^2$
2	1.4	$\omega_n^2$	$\omega_n^2$
3	1.75	$2.15\omega_n^2$	$\omega_n^2$
4	2.1	$3.4\omega_n^2$	$2.7\omega_n^2$
5	2.8	$5.0\omega_n^2$	$5.5\omega_n^2$
6	3.25	$6.6\omega_n^2$	$8.6\omega_n^2$



**FIGURE 5.30** (Continued)

The standard form for a third-order system given in Table 5.6 requires that

$$2\zeta\omega_0 = 1.75\omega_n, \quad \omega_0^2 = 2.15\omega_n^2, \quad \text{and} \quad K_a K_m \omega_0^2 = \omega_n^2.$$

Examining Figure 5.30(c) for  $n = 3$ , we estimate that the settling time is approximately 8 seconds (normalized time). Therefore, we estimate that

$$\omega_n T_s = 8.$$

Because a rapid response is required, a large  $\omega_n$  will be selected so that the settling time will be less than 1 second. Thus,  $\omega_n$  will be set equal to 10 rad/s. Then, for an ITAE system, it is necessary that the parameters of the camera dynamics be

$$\omega_0 = 14.67 \text{ rad/s}$$

and

$$\zeta = 0.597.$$

The amplifier and motor gain are required to be

$$K_a K_m = \frac{\omega_n^2}{\omega_0^2} = \frac{10^2}{2.15 \times 14.67^2} = 2.15$$

Then the closed-loop transfer function is

$$T(s) = \frac{1000}{s^3 + 17.5s^2 + 215s + 1000} = \frac{1000}{(s + 7.08)(s + 5.21 + j10.68)(s + 5.21 - j10.68)} \quad (5.49)$$



A more sophisticated approach attempts to match the frequency response of the reduced-order transfer function with the original transfer function frequency response as closely as possible. Although frequency response methods are covered in Chapter 8, the associated approximation method strictly relies on algebraic manipulation and is presented here. We will let the high-order system be described by the transfer function

$$G_H(s) = K \frac{a_m s^m + a_{m-1} s^{m-1} + \dots + a_1 s + 1}{b_p s^p + b_{p-1} s^{p-1} + \dots + b_1 s + 1}, \quad (5.51)$$

in which the poles are in the left-hand  $s$ -plane and  $m \leq n$ . The lower-order approximate transfer function is

$$G_L(s) = K \frac{c_p s^p + \dots + c_1 s + 1}{d_p s^p + \dots + d_1 s + 1}, \quad (5.52)$$

where  $p \leq q < n$ . Notice that the gain constant,  $K$ , is the same for the original and approximate system; this ensures the same steady-state response. The method outlined in Example 5.9 is based on selecting  $c_i$  and  $d_i$  in such a way that  $G_L(s)$  has a frequency response (see Chapter 8) very close to that of  $G_H(s)$ . This is equivalent to stating that  $G_H(j\omega)/G_L(j\omega)$  is required to deviate the least amount from unity for various frequencies. The  $c$  and  $d$  coefficients are obtained by using the equations

$$M^{(k)}(s) = \frac{d^k}{ds^k} M(s) \quad (5.53)$$

and

$$\Delta^{(k)}(s) = \frac{d^k}{ds^k} \Delta(s), \quad (5.54)$$

where  $M(s)$  and  $\Delta(s)$  are the numerator and denominator polynomials of  $G_H(s)/G_L(s)$ , respectively. We also define

$$M_{2q} = \sum_{k=0}^{2q} \frac{(-1)^{k+q} M^{(k)}(0) M^{(2q-k)}(0)}{k!(2q-k)!}, \quad q = 0, 1, 2, \dots \quad (5.55)$$

and an analogous equation for  $\Delta_{2q}$ . The solutions for the  $c$  and  $d$  coefficients are obtained by equating

$$M_{2q} = \Delta_{2q} \quad (5.56)$$

for  $q = 1, 2, \dots$  up to the number required to solve for the unknown coefficients. Let us consider an example to clarify the use of these equations.

Equation (5.56) with  $q = 1$  requires that  $M_2 = \Delta_2$ ; therefore,

$$-2d_2 + d_1^2 = \frac{49}{36} \quad (5.64)$$

Completing the process for  $M_4 = \Delta_4$ , we obtain

$$d_2^2 = \frac{7}{18} \quad (5.65)$$

Solving Equations (5.64) and (5.65) yields  $d_1 = 1.615$  and  $d_2 = 0.624$ . (The other sets of solutions are rejected because they lead to unstable poles.) The lower-order system transfer function is

$$G_L(s) = \frac{1}{1 + 1.615s + 0.624s^2} = \frac{1.60}{s^2 + 2.590s + 1.60} \quad (5.66)$$

It is interesting to see that the poles of  $G_H(s)$  are  $s = -1, -2, -3$ , whereas the poles of  $G_L(s)$  are  $s = -1.024$  and  $-1.565$ . Because the lower-order model has two poles, we estimate that we would obtain a slightly overdamped step response with a settling time to within 2% of the final value in approximately 3 seconds. ■

It is sometimes desirable to retain the dominant poles of the original system,  $G_H(s)$ , in the low-order model. This can be accomplished by specifying the denominator of  $G_L(s)$  to be the dominant poles of  $G_H(s)$  and allowing the numerator of  $G_L(s)$  to be subject to approximation.

Another novel and useful method for reducing the order is the Routh approximation method based on the idea of truncating the Routh table used to determine stability. The Routh approximants can be computed by a finite recursive algorithm that is suited for programming on a digital computer [19].

A robot named Domo was developed to investigate robot manipulation in unstructured environments [22–23]. The robot shown in Figure 5.33 has 29 degrees of freedom, making it a very complex system. Domo employs two six-degree-of-freedom arms and hands with compliant and force-sensitive actuators coupled with a behavior-based system architecture to achieve robotic manipulation tasks in human environments. Designing a controller to control the motion of the arm and hands would require significant model reduction and approximation before the methods of design discussed in the subsequent chapters (e.g., root locus design methods) could be successfully applied.

5.9 DESIGN EXAMPLES

In this section we present two illustrative examples. The first example is a simplified view of the Hubble space telescope pointing control problem. The Hubble space telescope problem highlights the process of computing controller gains to achieve desired percent overshoot specifications, as well as meeting steady-state error specifications. The second example considers the control of the bank angle of an airplane. The airplane attitude motion control example represents a more in-depth look

Table 5.7 The Optimum Coefficients of  $T(s)$  Based on the ITAE Criterion for a Ramp Input

$$\begin{aligned} & s^2 + 3.2\omega_n s + \omega_n^2 \\ & s^3 + 1.75\omega_n s^2 + 3.25\omega_n^2 s + \omega_n^3 \\ & s^4 + 2.41\omega_n s^3 + 4.93\omega_n^2 s^2 + 5.14\omega_n s + \omega_n^4 \\ & s^5 + 2.19\omega_n s^4 + 6.50\omega_n^2 s^3 + 6.30\omega_n s^2 + 5.24\omega_n s + \omega_n^5 \end{aligned}$$

The locations of the closed-loop roots dictated by the ITAE system are shown in Figure 5.32. The damping ratio of the complex roots is  $\zeta = 0.44$ . However, the complex roots do not dominate. The actual response to a step input using a computer simulation showed the overshoot to be only 2% and the settling time (to within 2% of the final value) to be equal to 0.75 second.

For a ramp input, the coefficients have been determined that minimize the ITAE criterion for the general closed-loop transfer function [6]

$$T(s) = \frac{b_1 s + b_0}{s^p + b_{p-1} s^{p-1} + \dots + b_1 s + b_0} \quad (5.50)$$

This transfer function has a steady-state error equal to zero for a ramp input. The optimum coefficients for this transfer function are given in Table 5.7. The transfer function, Equation (5.50), implies that the process  $G(s)$  has two or more pure integrations, as required to provide zero steady-state error. ■

5.8 THE SIMPLIFICATION OF LINEAR SYSTEMS

It is quite useful to study complex systems with high-order transfer functions by using lower-order approximate models. For example, a fourth-order system could be approximated by a second-order system leading to a use of the performance indices in Figure 5.8. Several methods are available for reducing the order of a systems transfer function.

One relatively simple way to delete a certain insignificant pole of a transfer function is to note a pole that has a negative real part that is much more negative than the other poles. Thus, that pole is expected to affect the transient response insignificantly.

For example, if we have a system with transfer function

$$G(s) = \frac{K}{s(s+2)(s+30)}$$

we can safely neglect the impact of the pole at  $s = -30$ . However, we must retain the steady-state response of the system, so we reduce the system to

$$G(s) = \frac{(K/30)}{s(s+2)}$$

EXAMPLE 5.9 A simplified model

Consider the third-order system

$$G_H(s) = \frac{6}{s^3 + 6s^2 + 11s + 6} = \frac{1}{1 + \frac{11}{6}s + s^2 + \frac{1}{6}s^3} \quad (5.57)$$

Using the second-order model

$$G_L(s) = \frac{1}{1 + d_1 s + d_2 s^2}, \quad (5.58)$$

we determine that

$$M(s) = 1 + d_1 s + d_2 s^2, \quad \text{and} \quad \Delta(s) = 1 + \frac{11}{6}s + s^2 + \frac{1}{6}s^3.$$

Then we know that

$$M^{(0)}(s) = 1 + d_1 s + d_2 s^2, \quad (5.59)$$

and  $M^{(0)}(0) = 1$ . Similarly, we have

$$M^{(1)} = \frac{d}{ds} (1 + d_1 s + d_2 s^2) = d_1 + 2d_2 s. \quad (5.60)$$

Therefore,  $M^{(1)}(0) = d_1$ . Continuing this process, we find that

$$\begin{aligned} M^{(0)}(0) &= 1 & \Delta^{(0)}(0) &= 1, \\ M^{(1)}(0) &= d_1 & \Delta^{(1)}(0) &= \frac{11}{6}, \\ M^{(2)}(0) &= 2d_2 & \Delta^{(2)}(0) &= 2, \end{aligned} \quad (5.61)$$

and

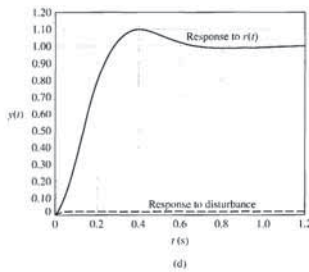
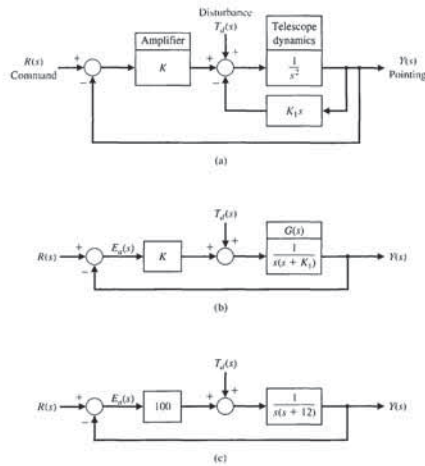
$$M^{(3)}(0) = 0 \quad \Delta^{(3)}(0) = 1.$$

We now equate  $M_{2q} = \Delta_{2q}$  for  $q = 1$  and 2. We find that, for  $q = 1$ ,

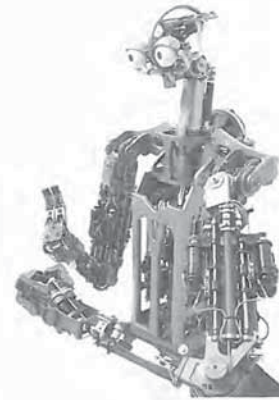
$$\begin{aligned} M_2 &= (-1) \frac{M^{(0)}(0)M^{(2)}(0)}{2} + \frac{M^{(1)}(0)M^{(1)}(0)}{1} + (-1) \frac{M^{(2)}(0)M^{(0)}(0)}{2} \\ &= -d_2 + d_1^2 - d_2 = -2d_2 + d_1^2. \end{aligned} \quad (5.62)$$

Since the equation for  $\Delta_2$  is similar, we have

$$\begin{aligned} \Delta_2 &= (-1) \frac{\Delta^{(0)}(0)\Delta^{(2)}(0)}{2} + \frac{\Delta^{(1)}(0)\Delta^{(1)}(0)}{1} + (-1) \frac{\Delta^{(2)}(0)\Delta^{(0)}(0)}{2} \\ &= -1 + \frac{121}{36} - 1 = \frac{49}{36}. \end{aligned} \quad (5.63)$$



**FIGURE 5.34** (a) The Hubble telescope pointing system, (b) reduced block diagram, (c) system design, and (d) system response to a unit step input command and a unit step disturbance input.



**FIGURE 5.33** An upper-torso humanoid robot named Domo helps researchers investigate robot manipulation in unstructured environments. (Photo courtesy of Aaron Edsinger, MIT Humanoid Robotics Group.)

at the control design problem. Here we consider a complex fourth-order model of the lateral dynamics of the aircraft motion that is approximated by a second-order model using the approximation methods of Section 5.8. The simplified model can be used to gain insight into the controller design and the impact of key controller parameters on the transient performance.

**EXAMPLE 5.10 Hubble space telescope control**

The orbiting Hubble space telescope is the most complex and expensive scientific instrument that has ever been built. Launched to 380 miles above the earth on April 24, 1990, the telescope has pushed technology to new limits. The telescope's 2.4 meter (94.5-inch) mirror has the smoothest surface of any mirror made, and its pointing system can center it on a dime 400 miles away [18]. The telescope had a spherical aberration that was largely corrected during space missions in 1993 and 1997 [21]. Consider the model of the telescope-pointing system shown in Figure 5.34.

Therefore,  $\omega_n = \sqrt{K}$ , and the second term of the denominator of Equation (5.69) requires  $K_1 = 2(0.6)\omega_n$ . Then  $K_1 = 1.2\sqrt{K}$ , so the ratio  $K/K_1$  becomes

$$\frac{K}{K_1} = \frac{K}{1.2\sqrt{K}} = \frac{\sqrt{K}}{1.2}$$

Selecting  $K = 25$ , we have  $K_1 = 6$  and  $K/K_1 = 4.17$ . If we select  $K = 100$ , we have  $K_1 = 12$  and  $K/K_1 = 8.33$ . Realistically, we must limit  $K$  so that the system's operation remains linear. Using  $K = 100$ , we obtain the system shown in Figure 5.34(c). The responses of the system to a unit step input command and a unit step disturbance input are shown in Figure 5.34(d). Note how the effect of the disturbance is relatively insignificant.

Finally, we note that the steady-state error for a ramp input (see Equation 5.70) is

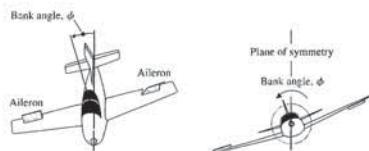
$$e_{ss} = \frac{B}{8.33} = 0.12B.$$

This design, using  $K = 100$ , is an excellent system. ■

**EXAMPLE 5.11 Attitude control of an airplane**

Each time we fly on a commercial airliner, we experience first-hand the benefits of automatic control systems. These systems assist pilots by improving the handling qualities of the aircraft over a wide range of flight conditions and by providing pilot relief (for such emergencies as going to the restroom) during extended flights. The special relationship between flight and controls began in the early work of the Wright brothers. Using wind tunnels, the Wright brothers applied systematic design techniques to make their dream of powered flight a reality. This systematic approach to design contributed to their success.

Another significant aspect of their approach was their emphasis on flight controls: the brothers insisted that their aircraft be pilot-controlled. Observing birds control their rolling motion by twisting their wings, the Wright brothers built aircraft with mechanical mechanisms that twisted their airplane wings. Today we no longer use wing warping as a mechanism for performing a roll maneuver; instead we control rolling motion by using ailerons, as shown in Figure 5.35. The Wright brothers also used elevators (located forward) for longitudinal



**FIGURE 5.35** Control of the bank angle of an airplane using differential deflections of the ailerons.

The goal of the design is to choose  $K_1$  and  $K$  so that (1) the percent overshoot of the output to a step command,  $r(t)$ , is less than or equal to 10%, (2) the steady-state error to a ramp command is minimized, and (3) the effect of a step disturbance is reduced. Since the system has an inner loop, block diagram reduction can be used to obtain the simplified system of Figure 5.34(b).

The output due to the two inputs of the system of Figure 5.34(b) is given by

$$Y(s) = T(s)R(s) + [T(s)/K]T_d(s), \tag{5.67}$$

where

$$T(s) = \frac{KG(s)}{1 + KG(s)} = \frac{L(s)}{1 + L(s)}.$$

The error is

$$E(s) = \frac{1}{1 + L(s)}R(s) - \frac{G(s)}{1 + L(s)}T_d(s). \tag{5.68}$$

First, let us select  $K$  and  $K_1$  to meet the percent overshoot requirement for a step input,  $R(s) = A/s$ . Setting  $T_d(s) = 0$ , we have

$$Y(s) = \frac{KG(s)}{1 + KG(s)}R(s) = \frac{K}{s(s + K_1) + K} \left( \frac{A}{s} \right) = \frac{K}{s^2 + K_1s + K} \left( \frac{A}{s} \right). \tag{5.69}$$

To set the overshoot less than 10%, we select  $\zeta = 0.6$  by examining Figure 5.8 or using Equation (5.16) to determine that the overshoot will be 9.5% for  $\zeta = 0.6$ . We next examine the steady-state error for a ramp,  $r(t) = Bt, t \geq 0$ , using (Equation 5.28):

$$e_{ss} = \lim_{s \rightarrow 0} \left\{ \frac{B}{sKG(s)} \right\} = \frac{B}{K/K_1}. \tag{5.70}$$

The steady-state error due to a unit step disturbance is equal to  $-1/K$ . (The student should show this.) The transient response of the error due to the step disturbance input can be reduced by increasing  $K$  (see Equation 5.68). In summary, we seek a large  $K$  and a large value of  $K/K_1$  to obtain a low steady-state error for the ramp input (see Equation 5.70). However, we also require  $\zeta = 0.6$  to limit the overshoot.

For our design, we need to select  $K$ . With  $\zeta = 0.6$ , the characteristic equation of the system is

$$s^2 + 2\zeta\omega_n s + \omega_n^2 = s^2 + 2(0.6)\omega_n s + K. \tag{5.71}$$



We begin by considering the model of the lateral dynamics of an airplane moving along a steady, wings-level flight path. By lateral dynamics, we mean the attitude motion of the aircraft about the forward velocity. An accurate mathematical model describing the motion (translational and rotational) of an aircraft is a complicated set of highly nonlinear, time-varying, coupled differential equations. A good description of the process of developing such a mathematical model appears in Etkin and Reid [25].

For our purposes a simplified dynamic model is required for the autopilot design process. A simplified model might consist of a transfer function describing the input/output relationship between the aileron deflection and the aircraft bank angle. Obtaining such a transfer function would require many prudent simplifications to the original high-fidelity, nonlinear mathematical model.

Suppose we have a rigid aircraft with a plane of symmetry. The airplane is assumed to be cruising at subsonic or low supersonic ( $Mach < 3$ ) speeds. This allows us to make a flat-earth approximation. We ignore any rotor gyroscopic effects due to spinning masses on the aircraft (such as propellers or turbines). These assumptions allow us to decouple the longitudinal rotational (pitching) motion from the lateral rotational (rolling and yawing) motion.

Of course, we also need to consider a linearization of the nonlinear equations of motion. To accomplish this, we consider only steady-state flight conditions such as

- Steady, wings-level flight
- Steady, level turning flight
- Steady, symmetric pull-up
- Steady roll.

For this example we assume that the airplane is flying at low speed in a steady, wings-level attitude, and we want to design an autopilot to control the rolling motion. We can state the control goal as follows:

**Control Goal**

Regulate the airplane bank angle to zero degrees (steady, wings level) and maintain the wings-level orientation in the presence of unpredictable external disturbances.

We identify the variable to be controlled as

**Variable to Be Controlled**

Airplane bank angle (denoted by  $\phi$ ).

Defining system specifications for aircraft control is complicated, so we do not attempt it here. It is a subject in and of itself, and many engineers have spent significant efforts developing good, practical design specifications. The goal is to design a control system such that the dominant closed-loop system poles have satisfactory natural frequency and damping [24]. We must define satisfactory and choose test input signals on which to base our analysis.

The Cooper-Harper pilot opinion ratings provide a way to correlate the feel of the airplane with control design specifications [26]. These ratings address the handling qualities issues. Many flying qualities requirements are specified by government agencies, such as the United States Air Force [27]. The USAF MIL-F-8785C is a source of time-domain control system design specifications.

control (pitch motion) and rudders for lateral control (yaw motion). Today's aircraft still use both elevators and rudders, although the elevators are generally located on the tail (rearward).

The first controlled, powered, unassisted take-off flight occurred in 1903 with the *Wright Flyer I* (a.k.a. *Kitty Hawk*). The first practical airplane, the *Flyer III*, could fly figure eights and stay aloft for half an hour. Three-axis flight control was a major (and often overlooked) contribution of the Wright brothers. A concise historical perspective is presented in Stevens and Lewis [24]. The continuing desire to fly faster, lighter, and longer fostered further developments in automatic flight control. Today's challenge is to develop a single-stage-to-orbit aircraft/spaceraft that can take off and land on a standard runway.

The main topic of this chapter is control of the automatic rolling motion of an airplane. The elements of the design process emphasized in this chapter are illustrated in Figure 5.36.

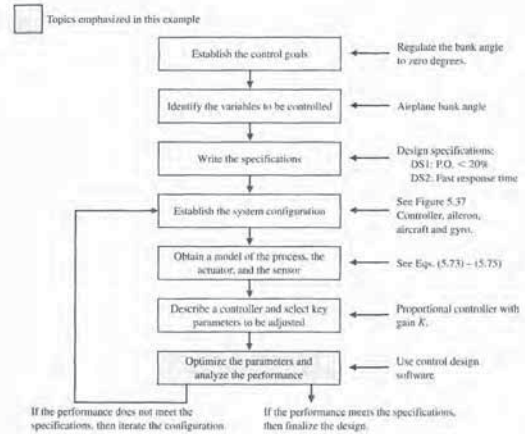


FIGURE 5.36 Elements of the control system design process emphasized in the airplane attitude control example.

we have  $e_0 = 3.57$  and  $d_0 = 0.0128$  [24]. The complex conjugate poles given by the term  $s^2 + f_1s + f_0$  represent the Dutch roll motion.

For low angles of attack (such as with steady, wings-level flight), the Dutch roll mode generally cancels out of the transfer function with the  $s^2 + b_1s + b_0$  term. This is an approximation, but it is consistent with our other simplifying assumptions. Also, we can ignore the spiral mode since it is essentially a yaw motion only weakly coupled to the roll motion. The zero at  $s = c_0$  represents a gravity effect that causes the aircraft to sideslip as it rolls. We assume that this effect is negligible, since it is most pronounced in a slow roll maneuver in which the sideslip is allowed to build up, and we assume that the aircraft sideslip is small or zero. Therefore we can simplify the transfer function in Eq. (5.72) to obtain a single-degree-of-freedom approximation:

$$\frac{\phi(s)}{\delta_a(s)} = \frac{k}{s(s + e_0)} \quad (5.73)$$

For our aircraft we select  $e_0 = 1.4$  and  $k = 11.4$ . The associated time-constant of the roll subsidence is  $\tau = 1/e_0 = 0.7$  s. These values represent a fairly fast rolling motion response.

For the aileron actuator model, we typically use a simple first-order system model,

$$\frac{\delta_a(s)}{e(s)} = \frac{p}{s + p} \quad (5.74)$$

where  $e(s) = \phi_d(s) - \phi(s)$ . In this case we select  $p = 10$ . This corresponds to a time constant of  $\tau = 1/p = 0.1$  s. This is a typical value consistent with a fast response. We need to have an actuator with a fast response so that the dynamics of the actively controlled airplane will be the dominant component of the system response. A slow actuator is akin to a time delay that can cause performance and stability problems.

For a high-fidelity simulation, we would need to develop an accurate model of the gyro dynamics. The gyro, typically an integrating gyro, is usually characterized by a very fast response. To remain consistent with our other simplifying assumptions, we ignore the gyro dynamics in the design process. This means we assume that the sensor measures the bank angle precisely. The gyro model is given by a unity transfer function,

$$K_g = 1. \quad (5.75)$$

Thus our physical system model is given by Equations (5.73), (5.74), and (5.75).

The controller we select for this design is a proportional controller,

$$G_c(s) = K.$$

The system configuration is shown in Figure 5.37. The select key parameter is as follows:

**Select Key Tuning Parameter**

Controller gain  $K$ .

The closed-loop transfer function is

$$T(s) = \frac{\phi(s)}{\phi_d(s)} = \frac{114K}{s^3 + 11.4s^2 + 14s + 114K} \quad (5.76)$$

For example we might design an autopilot control system for an aircraft in steady, wings-level flight to achieve a 20% overshoot to a step input with minimal oscillatory motion and rapid response time (that is, a short time-to-peak). Subsequently we implement the controller in the aircraft control system and conduct flight tests or high-fidelity computer simulations, after which the pilots tell us whether they liked the performance of the aircraft. If the overall performance was not satisfactory, we change the time-domain specification (in this case a percent overshoot specification) and redesign until we achieve a feel and performance that pilots (and ultimately passengers) will accept. Despite the simplicity of this approach and many years of research, precise-control system design specifications that provide acceptable airplane flying characteristics in all cases are still not available [24].

The control design specifications given in this example may seem somewhat contrived. In reality the specifications would be much more involved and, in many ways, less precisely known. But recall in Chapter 1 we discussed the fact that we must begin the design process somewhere. With that approach in mind, we select simple design specifications and begin the iterative design process. The design specifications are

**Control Design Specifications**

- DS1 Percent overshoot less than 20% for a unit step input.
- DS2 Fast response time as measured by time-to-peak.

By making the simplifying assumptions discussed above and linearizing about the steady, wings-level flight condition, we can obtain a transfer function model describing the bank angle output,  $\phi(s)$ , to the aileron deflection input,  $\delta_a(s)$ . The transfer function has the form

$$\frac{\phi(s)}{\delta_a(s)} = \frac{k(s - c_0)(s^2 + b_1s + b_0)}{s(s + d_0)(s + e_0)(s^2 + f_1s + f_0)} \quad (5.72)$$

The lateral (roll/yaw) motion has three main modes: Dutch roll mode, spiral mode, and roll subsidence mode. The Dutch roll mode, which gets its name from its similarities to the motion of an ice speed skater, is characterized by a rolling and yawing motion. The airplane center of mass follows nearly a straightline path, and a rudder impulse can excite this mode. The spiral mode is characterized by a mainly yawing motion with some roll motion. This is a weak mode, but it can cause an airplane to enter a steep spiral dive. The roll subsidence motion is almost a pure roll motion. This is the motion we are concerned with for our autopilot design. The denominator of the transfer function in Equation (5.72) shows two first-order modes (spiral and roll subsidence modes) and a second-order mode (Dutch roll mode).

In general the coefficients  $c_0, b_0, b_1, d_0, e_0, f_0, f_1$  and the gain  $k$  are complicated functions of stability derivatives. The stability derivatives are functions of the flight conditions and the aircraft configuration; they differ for different aircraft types. The coupling between the roll and yaw is included in Equation (5.72).

In the transfer function in Equation (5.72), the pole at  $s = -d_0$  is associated with the spiral mode. The pole at  $s = -e_0$  is associated with the roll subsidence mode. Generally,  $e_0 \gg d_0$ . For an F-16 flying at 500 ft/s in steady, wings-level flight,

we can solve for the unknown parameters of the approximate function. The index  $q$  is incremented until sufficient equations are obtained to solve for the unknown coefficients of the approximate function. In this case,  $q = 1, 2$  since we have two parameters  $d_1$  and  $d_2$  to compute.

We have

$$M(s) = 1 + d_1s + d_2s^2$$

$$M^{(1)}(s) = \frac{dM}{ds} = d_1 + 2d_2s$$

$$M^{(2)}(s) = \frac{d^2M}{ds^2} = 2d_2$$

$$M^{(3)}(s) = M^{(4)}(s) = \dots = 0.$$

Thus evaluating at  $s = 0$  yields

$$M^{(1)}(0) = d_1$$

$$M^{(2)}(0) = 2d_2$$

$$M^{(3)}(0) = M^{(4)}(0) = \dots = 0.$$

Similarly,

$$\Delta(s) = 1 + \frac{14}{114K}s + \frac{11.4}{114K}s^2 + \frac{s^3}{114K}$$

$$\Delta^{(1)}(s) = \frac{d\Delta}{ds} = \frac{14}{114K} + \frac{22.8}{114K}s + \frac{3}{114K}s^2$$

$$\Delta^{(2)}(s) = \frac{d^2\Delta}{ds^2} = \frac{22.8}{114K} + \frac{6}{114K}s$$

$$\Delta^{(3)}(s) = \frac{d^3\Delta}{ds^3} = \frac{6}{114K}$$

$$\Delta^{(4)}(s) = \Delta^{(5)}(s) = \dots = 0.$$

Evaluating at  $s = 0$ , it follows that

$$\Delta^{(1)}(0) = \frac{14}{114K}$$

$$\Delta^{(2)}(0) = \frac{22.8}{114K}$$

$$\Delta^{(3)}(0) = \frac{6}{114K}$$

$$\Delta^{(4)}(0) = \Delta^{(5)}(0) = \dots = 0.$$

Comparing coefficients in Equations (5.82) and (5.83) yields

$$\omega_n^2 = 11.29K \quad \text{and} \quad \zeta^2 = \frac{0.043}{K} - 0.065. \quad (5.84)$$

The design specification that the percent overshoot  $P.O.$  is to be less than 20% implies that we want  $\zeta \geq 0.45$ . This follows from solving Equation (5.16)

$$P.O. = 100e^{-\pi\zeta/\sqrt{1-\zeta^2}}$$

for  $\zeta$ . Setting  $\zeta = 0.45$  in Equation (5.84) and solving for  $K$  yields

$$K = 0.16.$$

With  $K = 0.16$  we compute

$$\omega_n = \sqrt{11.29K} = 1.34.$$

Then we can estimate the time-to-peak  $T_p$  from Equation (5.14) to be

$$T_p = \frac{\pi}{\omega_n\sqrt{1-\zeta^2}} = 2.62s.$$

We might be tempted at this point to select  $\zeta > 0.45$  so that we reduce the percent overshoot even further than 20%. What happens if we decide to try this approach? From Equation (5.84) we see that  $K$  decreases as  $\zeta$  increases. Then, since

$$\omega_n = \sqrt{11.29K},$$

as  $K$  decreases, then  $\omega_n$  also decreases. But the time-to-peak, given by

$$T_p = \frac{\pi}{\omega_n\sqrt{1-\zeta^2}},$$

increases as  $\omega_n$  decreases. Since our goal is to meet the specification of percent overshoot less than 20% while minimizing the time-to-peak, we use the initial selection of  $\zeta = 0.45$  so that we do not increase  $T_p$  unnecessarily.

The second-order system approximation has allowed us to gain insight into the relationship between the parameter  $K$  and the system response, as measured by percent overshoot and time-to-peak. Of course, the gain  $K = 0.16$  is only a starting point in the design because we in fact have a third-order system and must consider the effect of the third pole (which we have ignored so far).

A comparison of the third-order aircraft model in Equation (5.76) with the second-order approximation in Equation (5.82) for a unit step input is shown in Figure 5.38. The step response of the second-order system is a good approximation of the original system step response, so we would expect that the analytic analysis using the simpler second-order system to provide accurate indications of the relationship between  $K$  and the percent overshoot and time-to-peak.

With the second-order approximation, we estimate that with  $K = 0.16$  the percent overshoot  $P.O. = 20\%$  and the time-to-peak  $T_p = 2.62$  seconds. As shown in

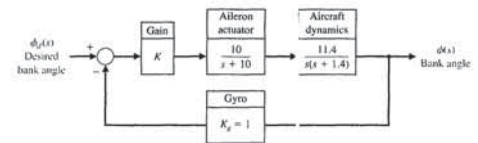


FIGURE 5.37 Bank angle control autopilot.

We want to determine analytically the value of  $K$  that will give us the desired response, namely, a percent overshoot less than 20% and a fast time-to-peak. The analytic analysis would be simpler if our closed-loop system were a second-order system (since we have valuable relationships between settling time, percent overshoot, natural frequency and damping ratio); however we have a third-order system, given by  $T(s)$  in Equation (5.76). We could consider approximating the third-order transfer function by a second-order transfer function—this is sometimes a very good engineering approach to analysis. There are many methods available to obtain approximate transfer functions. Here we use the algebraic method described in Section 5.8 that attempts to match the frequency response of the approximate system as closely as possible to the actual system.

Our transfer function can be rewritten as

$$T(s) = \frac{1}{1 + \frac{14}{114K}s + \frac{11.4}{114K}s^2 + \frac{1}{114K}s^3},$$

by factoring the constant term out of the numerator and denominator. Suppose our approximate transfer function is given by the second-order system

$$G_L(s) = \frac{1}{1 + d_1s + d_2s^2}.$$

The objective is to find appropriate values of  $d_1$  and  $d_2$ . As in Section 5.8, we define  $M(s)$  and  $\Delta(s)$  as the numerator and denominator of  $T(s)/G_L(s)$ . We also define

$$M_{2q} = \sum_{k=0}^{2q} \frac{(-1)^{k+q} M^{(k)}(0) M^{(2q-k)}(0)}{k!(2q-k)!}, \quad q = 1, 2, \dots \quad (5.77)$$

and

$$\Delta_{2q} = \sum_{k=0}^{2q} \frac{(-1)^{k+q} \Delta^{(k)}(0) \Delta^{(2q-k)}(0)}{k!(2q-k)!}, \quad q = 1, 2, \dots \quad (5.78)$$

Then, forming the set of algebraic equations

$$M_{2q} = \Delta_{2q}, \quad q = 1, 2, \dots \quad (5.79)$$

Using Equation (5.77) for  $q = 1$  and  $q = 2$  yields

$$M_2 = -\frac{M(0)M^{(2)}(0)}{2} + \frac{M^{(1)}(0)M^{(1)}(0)}{1} - \frac{M^{(2)}(0)M(0)}{2} = -2d_2 + d_1^2$$

and

$$M_4 = \frac{M(0)M^{(4)}(0)}{0!4!} - \frac{M^{(1)}(0)M^{(3)}(0)}{1!3!} + \frac{M^{(2)}(0)M^{(2)}(0)}{2!2!} - \frac{M^{(3)}(0)M^{(1)}(0)}{3!1!} + \frac{M^{(4)}(0)M(0)}{4!0!} = d_2^2$$

Similarly using Equation (5.78), we find that

$$\Delta_2 = \frac{-22.8}{114K} + \frac{196}{(114K)^2} \quad \text{and} \quad \Delta_4 = \frac{101.96}{(114K)^3}.$$

Thus forming the set of algebraic equations in Equation (5.79),

$$M_2 = \Delta_2 \quad \text{and} \quad M_4 = \Delta_4.$$

we obtain

$$-2d_2 + d_1^2 = \frac{-22.8}{114K} + \frac{196}{(114K)^2} \quad \text{and} \quad d_2^2 = \frac{101.96}{(114K)^3}.$$

Solving for  $d_1$  and  $d_2$  yields

$$d_1 = \frac{\sqrt{196 - 296.96K}}{114K}, \quad (5.80)$$

$$d_2 = \frac{10.097}{114K}, \quad (5.81)$$

where we always choose the positive values of  $d_1$  and  $d_2$  so that  $G_L(s)$  has poles in the left half-plane. Thus (after some manipulation) the approximate transfer function is

$$G_L(s) = \frac{11.29K}{s^2 + \sqrt{1.92 - 2.91K}s + 11.29K}. \quad (5.82)$$

We require that  $K < 0.65$  so that the coefficient of the  $s$  term remains a real number (we do not want to have a transfer function with complex valued parameters). Our desired second-order transfer function can be written as

$$G_L(s) = \frac{\omega_n^2}{s^2 + 2\zeta\omega_n s + \omega_n^2} \quad (5.83)$$



**Table 5.8 Performance Comparison for  $K = 0.10, 0.16, \text{ and } 0.20$ .**

$K$	P.O. (%)	$T_p$ (s)
0.10	9.5	3.74
0.16	20.5	2.73
0.20	26.5	2.38

predicted, as the percent overshoot decreases the time-to-peak increases. The results are summarized in Table 5.8. ■

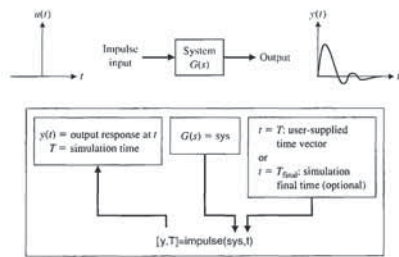
**5.10 SYSTEM PERFORMANCE USING CONTROL DESIGN SOFTWARE**

In this section, we will investigate time-domain performance specifications given in terms of transient response to a given input signal and the resulting steady-state tracking errors. We conclude with a discussion of the simplification of linear systems. The function introduced in this section is `impz`. We will revisit the `lsim` function (introduced in Chapter 3) and see how these functions are used to simulate a linear system.

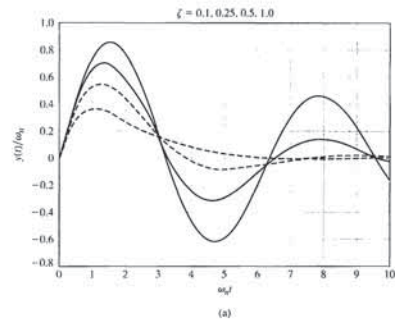
**Time-Domain Specifications.** Time-domain performance specifications are generally given in terms of the transient response of a system to a given input signal. Because the actual input signals are generally unknown, a standard test input signal is used. Consider the second-order system shown in Figure 5.4. The closed-loop output is

$$Y(s) = \frac{\omega_n^2}{s^2 + 2\zeta\omega_n s + \omega_n^2} R(s). \quad (5.85)$$

We have already discussed the use of the `step` function to compute the step response of a system. Now we address another important test signal: the impulse. The impulse response is the time derivative of the step response. We compute the impulse response with the `impz` function shown in Figure 5.40.



**FIGURE 5.40** The impulse function.



```

%Compute impulse response for a second-order system
%Duplicate Figure 5.6
%
t=[0:0.1:10]; num=1;
zeta1=0.1; den1=[1 2*zeta1 1]; sys1=tf(num,den1);
zeta2=0.25; den2=[1 2*zeta2 1]; sys2=tf(num,den2);
zeta3=0.5; den3=[1 2*zeta3 1]; sys3=tf(num,den3);
zeta4=1.0; den4=[1 2*zeta4 1]; sys4=tf(num,den4);
%
[y1,T1]=impz(sys1,1);
[y2,T2]=impz(sys2,1);
[y3,T3]=impz(sys3,1);
[y4,T4]=impz(sys4,1);
%
plot(t,y1,y2,y3,y4)
xlabel('omega_n*t'), ylabel('y(t)/omega_n')
title('zeta = 0.1, 0.25, 0.5, 1.0'), grid
    
```

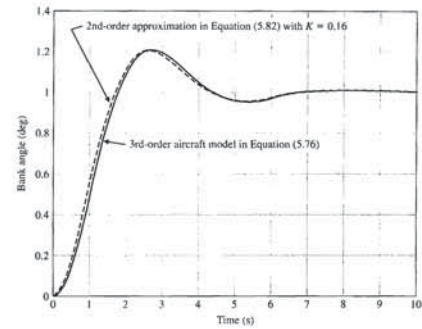
**FIGURE 5.42** (a) Response of a second-order system to an impulse function input. (b) m-file script.

shown in Figure 5.43. We studied the `lsim` function in Chapter 3 for use with state-variable models; however, now we consider the use of `lsim` with transfer function models. An example of the use of `lsim` is given in Example 5.12.

**EXAMPLE 5.12 Mobile robot steering control**

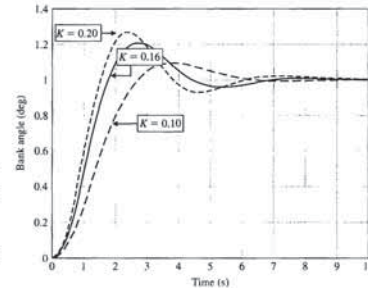
The block diagram for a steering control system for a mobile robot is shown in Figure 5.19. Suppose the transfer function of the steering controller is

$$G_c(s) = K_1 + \frac{K_2}{s}$$

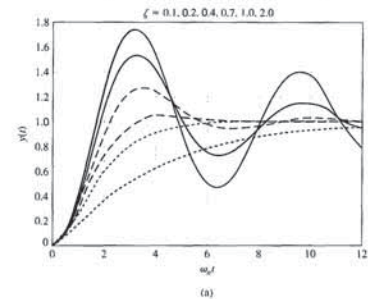


**FIGURE 5.38** Step response comparison of third-order aircraft model versus second-order approximation.

Figure 5.39 the percent overshoot of the original third-order system is  $P.O. = 20.5\%$  and the time-to-peak  $T_p = 2.73$  s. Thus, we see that analytic analysis using the approximate system is an excellent predictor of the actual response. For comparison purposes, we select two variations in the gain and observe the response. For  $K = 0.1$ , the percent overshoot is  $9.5\%$  and the time-to-peak  $T_p = 3.74$  s. For  $K = 0.2$ , the percent overshoot is  $26.5\%$  and the time-to-peak  $T_p = 2.38$  s. So as predicted, as  $K$  decreases the damping ratio increases, leading to a reduction in the percent overshoot. Also as



**FIGURE 5.39** Step response of the 3<sup>rd</sup>-order aircraft model with  $K = 0.10, 0.16, \text{ and } 0.20$  showing that, as predicted, as  $K$  decreases percent overshoot decreases while the time-to-peak increases.



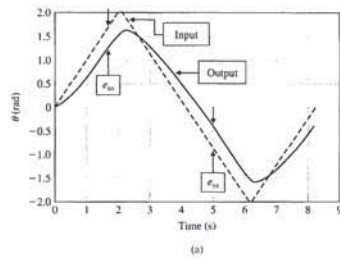
```

%Compute step response for a second-order system
%Duplicate Figure 5.5 (a)
%
t=[0:0.1:12]; num=1;
zeta1=0.1; den1=[1 2*zeta1 1]; sys1=tf(num,den1);
zeta2=0.2; den2=[1 2*zeta2 1]; sys2=tf(num,den2);
zeta3=0.4; den3=[1 2*zeta3 1]; sys3=tf(num,den3);
zeta4=0.7; den4=[1 2*zeta4 1]; sys4=tf(num,den4);
zeta5=1.0; den5=[1 2*zeta5 1]; sys5=tf(num,den5);
zeta6=2.0; den6=[1 2*zeta6 1]; sys6=tf(num,den6);
%
[y1,T1]=step(sys1,1); [y2,T2]=step(sys2,1);
[y3,T3]=step(sys3,1); [y4,T4]=step(sys4,1);
[y5,T5]=step(sys5,1); [y6,T6]=step(sys6,1);
%
plot(T1,y1,T2,y2,T3,y3,T4,y4,T5,y5,T6,y6)
xlabel('omega_n*t'), ylabel('y(t)')
title('zeta = 0.1, 0.2, 0.4, 0.7, 1.0, 2.0'), grid
    
```

**FIGURE 5.41** (a) Response of a second-order system to a step input. (b) m-file script.

We can obtain a plot similar to that of Figure 5.5(a) with the step function, as shown in Figure 5.41. Using the impulse function, we can obtain a plot similar to that of Figure 5.6. The response of a second-order system for an impulse function input is shown in Figure 5.42. In the script, we set  $\omega_n = 1$ , which is equivalent to computing the step response versus  $\omega_n t$ . This gives us a more general plot valid for any  $\omega_n > 0$ .

In many cases, it may be necessary to simulate the system response to an arbitrary but known input. In these cases, we use the `lsim` function. The `lsim` function is



```

%Compute the response of the Mobile Robot Control
%System to a triangular wave input
%
numg=[10 20]; deng=[1 10 0]; sysg=tf(numg,deng);
[sys]=feedback(sysg,1);
t=[0:0.1:8.2];
v1=[0:0.1:2];v2=[2:-0.1:-2];v3=[-2:0.1:0];
u=[v1,v2,v3];
[y,T]=lsim(sys,u,t);
plot(T,y,'b','-');
xlabel('Time (s)'); ylabel('theta (rad)'); grid
    
```

FIGURE 5.44 (a) Transient response of the mobile robot steering control system to a ramp input. (b) m-file script.

A second-order approximation (see Example 5.9) is

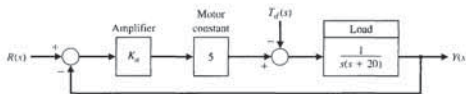
$$G_T(s) = \frac{1.60}{s^2 + 2.590s + 1.60}$$

A comparison of their respective step responses is given in Figure 5.45. ■

5.11 SEQUENTIAL DESIGN EXAMPLE: DISK DRIVE READ SYSTEM



In Section 4.10, we considered the response of the closed-loop reader head control system. Let us further consider the system shown in Figure 4.35. In this section, we further consider the design process. We will specify the desired performance for the system. Then we will attempt to adjust the amplifier gain  $K_a$  in order to obtain the best performance possible.



$$\begin{aligned}
 Y(s) &= \frac{5K_a}{s(s+20) + 5K_a} R(s) \\
 &= \frac{5K_a}{s^2 + 20s + 5K_a} R(s) \\
 &= \frac{\omega_n^2}{s^2 + 2\zeta\omega_n s + \omega_n^2} R(s).
 \end{aligned}
 \tag{5.87}$$

Therefore,  $\omega_n^2 = 5K_a$ , and  $2\zeta\omega_n = 20$ . We then determine the response of the system as shown in Figure 5.47. Table 5.10 shows the performance measures for selected values of  $K_a$ .

```

Ka=30; % Select Ka
t=[0:0.01:1];
nc=[Ka 5];dc=[1]; sysc=tf(nc,dc);
ng=[1];dg=[1 20 0]; sysg=tf(ng,dg);
sys1=series(sysc,sysg);
sys=feedback(sys1,1);
y=step(sys,1);
plot(t,y), grid
xlabel('Time (s)')
ylabel('y(t)')
    
```

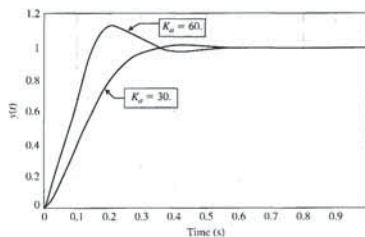


FIGURE 5.47 Response of the system to a unit step input.  $r(t) = 1, t > 0$ . (a) m-file script. (b) Response for  $K_a = 30$  and  $60$ .

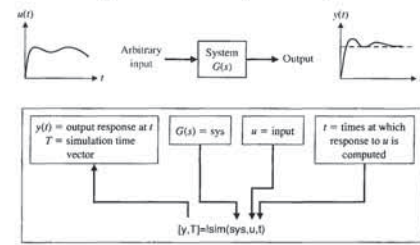


FIGURE 5.43 The lsim function.

When the input is a ramp, the steady-state error is

$$e_{ss} = \frac{A}{K_v} \tag{5.86}$$

where

$$K_v = K_2 K.$$

The effect of the controller constant,  $K_2$ , on the steady-state error is evident from Equation (5.86). Whenever  $K_2$  is large, the steady-state error is small.

We can simulate the closed-loop system response to a ramp input using the lsim function. The controller gains,  $K_1$  and  $K_2$ , and the system gain  $K$  can be represented symbolically in the script so that various values can be selected and simulated. The results are shown in Figure 5.44 for  $K_1 = K = 1, K_2 = 2$ , and  $\tau = 1/10$ . ■

**Simplification of Linear Systems.** It may be possible to develop a lower-order approximate model that closely matches the input-output response of a high-order model. A procedure for approximating transfer functions is given in Section 5.8. We can use computer simulation to compare the approximate model to the actual model, as illustrated in the following example.

EXAMPLE 5.13 A simplified model

Consider the third-order system

$$G_H(s) = \frac{6}{s^3 + 6s^2 + 11s + 6}$$

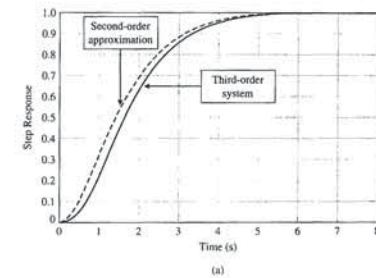


FIGURE 5.45 (a) Step response comparison for an approximate transfer function versus the actual transfer function. (b) m-file script.

```

% Compare step response for second-order approximation
%
num1=[6]; den1=[1 6 11 6]; sys1=tf(num1,den1);
num2=[1.6]; den2=[1 2.594 1.6]; sys2=tf(num2,den2);
t=[0:0.1:8];
[y1,T1]=step(sys1,1);
[y2,T2]=step(sys2,1);
plot(T1,y1,T2,y2,'-'), grid
xlabel('Time (s)'); ylabel('Step Response')
    
```

Table 5.9 Specifications for the Transient Response

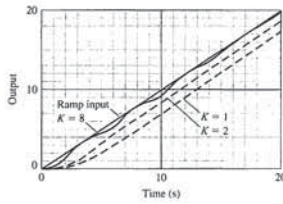
Performance Measure	Desired Value
Percent overshoot	Less than 5%
Settling time	Less than 250 ms
Maximum value of response to a unit step disturbance	Less than $5 \times 10^{-3}$

Our goal is to achieve the fastest response to a step input  $r(t)$  while (1) limiting the overshoot and oscillatory nature of the response and (2) reducing the effect of a disturbance on the output position of the read head. The specifications are summarized in Table 5.9.

Let us consider the second-order model of the motor and arm, which neglects the effect of the coil inductance. We then have the closed-loop system shown in Figure 5.46. Then the output when  $T_r(s) = 0$  is



**FIGURE 5.49**  
The response of a feedback system to a ramp input with  $K = 1, 2,$  and  $8$  when  $G(s) = K/(s + 1)(s + 3)$ . The steady-state error is reduced as  $K$  is increased, but the response becomes oscillatory at  $K = 8$ .



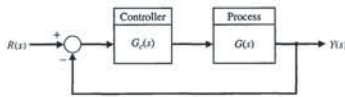
5.12 SUMMARY

In this chapter, we have considered the definition and measurement of the performance of a feedback control system. The concept of a performance measure or index was discussed, and the usefulness of standard test signals was outlined. Then, several performance measures for a standard step input test signal were delineated. For example, the overshoot, peak time, and settling time of the response of the system under test for a step input signal were considered. The fact that the specifications on the desired response are often contradictory was noted, and the concept of a design compromise was proposed. The relationship between the location of the  $s$ -plane root of the system transfer function and the system response was discussed. A most important measure of system performance is the steady-state error for specific test signals. Thus, the relationship of the steady-state error of a system in terms of the system parameters was developed by utilizing the final-value theorem. The capability of a feedback control system is demonstrated in Figure 5.49. Finally, the utility of an integral performance index was outlined, and several design examples that minimized a system's performance index were completed. Thus, we have been concerned with the definition and usefulness of quantitative measures of the performance of feedback control systems.



SKILLS CHECK

In this section, we provide three sets of problems to test your knowledge: True or False, Multiple Choice, and Word Match. To obtain direct feedback, check your answers with the answer key provided at the conclusion of the end-of-chapter problems. Use the block diagram in Figure 5.50 as specified in the various problem statements.



**FIGURE 5.50** Block diagram for the Skills Check.

Using the notion of dominant poles, estimate the expected percent overshoot.

- a.  $P.O. \approx 5\%$
- b.  $P.O. \approx 20\%$
- c.  $P.O. \approx 50\%$
- d. No overshoot expected

11. Consider the unity feedback control system in Figure 5.50 where

$$L(s) = G_c(s)G(s) = \frac{K}{s(s + 5)}$$

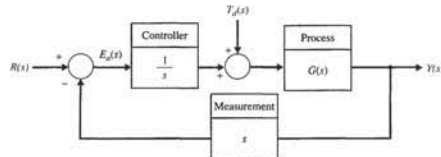
The design specifications are:

- i. Peak time  $T_p \leq 1.0$
- ii. Percent overshoot  $P.O. \leq 10\%$

With  $K$  as the design parameter, it follows that

- a. Both specifications can be satisfied.
- b. Only the first specification  $T_p \leq 1.0$  can be satisfied.
- c. Only the second specification  $P.O. \leq 10\%$  can be satisfied.
- d. Neither specification can be satisfied.

12. Consider the feedback control system in Figure 5.51 where  $G(s) = \frac{K}{s + 10}$ .



**FIGURE 5.51** Feedback system with integral controller and derivative measurement.

The nominal value of  $K = 10$ . Using a 2% criterion, compute the settling time,  $T_s$  for a unit step disturbance,  $T_d(s) = 1/s$ .

- a.  $T_s = 0.02$  s
- b.  $T_s = 0.19$  s
- c.  $T_s = 1.03$  s
- d.  $T_s = 4.83$  s

13. A plant has the transfer function given by

$$G(s) = \frac{1}{(1 + s)(1 + 0.5s)}$$

and is controlled by a proportional controller  $G_c(s) = K$ , as shown in the block diagram in Figure 5.50. The value of  $K$  that yields a steady-state error  $E(s) = Y(s) - R(s)$  with a magnitude equal to 0.01 for a unit step input is:

- a.  $K = 49$
- b.  $K = 99$

**Table 5.10** Response for the Second-Order Model for a Step Input

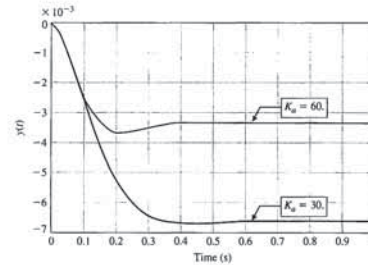
$K_a$	20	30	40	60	80
Percent overshoot	0	1.2%	4.3%	10.8%	16.3%
Settling time (s)	0.55	0.40	0.40	0.40	0.40
Damping ratio	1	0.82	0.707	0.58	0.50
Maximum value of the response $y(t)$ to a unit disturbance	$-10 \times 10^{-3}$	$-6.6 \times 10^{-3}$	$-5.2 \times 10^{-3}$	$-3.7 \times 10^{-3}$	$-2.9 \times 10^{-3}$

When  $K_a$  is increased to 60, the effect of a disturbance is reduced by a factor of 2. We can show this by plotting the output,  $y(t)$ , as a result of a unit step disturbance input, as shown in Figure 5.48. Clearly, if we wish to meet our goals with this system, we need to select a compromise gain. In this case, we select  $K_a = 40$  as the best compromise. However, this compromise does not meet all the specifications. In the next chapter, we consider again the design process and change the configuration of the control system.

```

Ka=30; % Select Ka
t=[0:0.01:1];
nc=[Ka 5];dc=[1]; sysc=tf(nc,dc);
ng=[1];dg=[1 20 0]; sysg=tf(ng,dg);
sys=feedback(sysc,sysg);
sys=sys; % Disturbance enters summer
y=step(sys,t); plot(t,y)
xlabel('Time (s)'); ylabel('y(t)'); grid
    
```

(a)



(b)

**FIGURE 5.48**  
Response of the system to a unit step disturbance,  $T_d(s) = 1/s$ .  
(a) m-file script.  
(b) Response for  $K_a = 30$  and 60.

Skills Check

In the following True or False and Multiple Choice problems, circle the correct answer.

1. In general, a third-order system can be approximated by a second-order system's dominant roots if the real part of the dominant roots is less than 1/10 of the real part of the third root. True or False
2. The number of zeros of the forward path transfer function at the origin is called the type number. True or False
3. The rise time is defined as the time required for the system to settle within a certain percentage of the input amplitude. True or False
4. For a second-order system with no zeros, the percent overshoot to a unit step is a function of the damping ratio only. True or False
5. A type-1 system has a zero steady-state tracking error to a ramp input. True or False

Consider the closed-loop control system in Figure 5.50 for Problems 6 and 7 with

$$L(s) = G_c(s)G(s) = \frac{6}{s(s + 3)}$$

6. The steady-state error to a unit step input  $R(s) = 1/s$  is:
    - a.  $e_{ss} = \lim_{t \rightarrow \infty} e(t) = 1$
    - b.  $e_{ss} = \lim_{t \rightarrow \infty} e(t) = 1/2$
    - c.  $e_{ss} = \lim_{t \rightarrow \infty} e(t) = 1/6$
    - d.  $e_{ss} = \lim_{t \rightarrow \infty} e(t) = \infty$
  7. The percent overshoot of the output to a unit step input is:
    - a.  $P.O. = 9\%$
    - b.  $P.O. = 1\%$
    - c.  $P.O. = 20\%$
    - d. No overshoot
- Consider the block diagram of the control system shown in Figure 5.50 in Problems 8 and 9 with the loop transfer function

$$L(s) = G_c(s)G(s) = \frac{K}{s(s + 10)}$$

8. Find the value of  $K$  so that the system provides an optimum ITAE response.
  - a.  $K = 1.10$
  - b.  $K = 12.56$
  - c.  $K = 51.02$
  - d.  $K = 104.7$
9. Compute the expected percent overshoot to a unit step input.
  - a.  $P.O. = 1.4\%$
  - b.  $P.O. = 4.6\%$
  - c.  $P.O. = 10.8\%$
  - d. No overshoot expected
10. A system has the closed-loop transfer function  $T(s)$  given by

$$T(s) = \frac{Y(s)}{R(s)} = \frac{2500}{(s + 20)(s^2 + 10s + 125)}$$

- n. Design specifications The constituent of the system response that exists a long time following any signal initiation. \_\_\_\_\_
- o. Performance index The constituent of the system response that disappears with time. \_\_\_\_\_
- p. Optimum control system A test input consisting of an impulse of infinite amplitude and zero width, and having an area of unity. \_\_\_\_\_

EXERCISES

**E5.1** A motor control system for a computer disk drive must reduce the effect of disturbances and parameter variations, as well as reduce the steady-state error. We want to have no steady-state error for the head-positioning control system, which is of the form shown in Figure 5.18. (a) What type number is required? (How many integrations?) (b) If the input is a ramp signal, and we want to achieve a zero steady-state error, what type number is required?

**E5.2** The engine, body, and tires of a racing vehicle affect the acceleration and speed attainable [9]. The speed control of the car is represented by the model shown in Figure E5.2. (a) Calculate the steady-state error of the car to a step command in speed. (b) Calculate overshoot of the speed to a step command.  
 Answer: (a)  $e_{ss} = A/11$ ; (b)  $P.O. = 36\%$

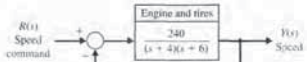


FIGURE E5.2 Racing car speed control.

**E5.3** New passenger rail systems that could profitably compete with air travel are under development. Two of these systems, the French TGV and the Japanese Shinkansen, reach speeds of 160 mph [17]. The Transrapid, a magnetic levitation train, is shown in Figure E5.3(a).

that the system provides an optimum ITAE response. (b) Using Figure 5.8, determine the expected overshoot to a step input of  $f(t)$ .  
 Answer:  $K = 100, 4.6\%$

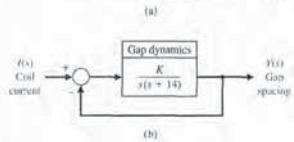
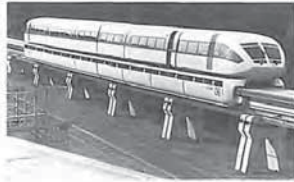


FIGURE E5.3 Levitated train control.

**E5.4** A feedback system with negative unity feedback has a loop transfer function

$$L(s) = G_c(s)G(s) = \frac{2(s + 8)}{s(s + 4)}$$

- (a) Determine the closed-loop transfer function  $T(s) = Y(s)/R(s)$ .
- (b) Find the time response,  $y(t)$ , for a step input  $r(t) = A$  for  $t > 0$ .
- (c) Using Figure 5.13(a), determine the overshoot of the response.
- (d) Using the final-value theorem, determine the steady-state value of  $y(t)$ .

Answer: (b)  $y(t) = 1 - 1.07e^{-3t} \sin(\sqrt{7}t + 1.2)$

FIGURE E5.11 Unity feedback system.

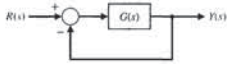
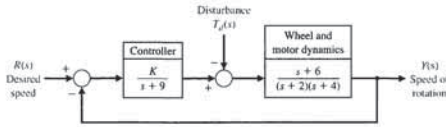


FIGURE E5.12 Speed control of a Ferris wheel.



**E5.12** We are all familiar with the Ferris wheel featured at state fairs and carnivals. George Ferris was born in Galesburg, Illinois, in 1859; he later moved to Nevada and then graduated from Rensselaer Polytechnic Institute in 1881. By 1891, Ferris had considerable experience with iron, steel, and bridge construction. He conceived and constructed his famous wheel for the 1893 Columbian Exposition in Chicago [8]. To avoid upsetting passengers, set a requirement that the steady-state speed must be controlled to within 5% of the desired speed for the system shown in Figure E5.12.

- (a) Determine the required gain  $K$  to achieve the steady-state requirement.
- (b) For the gain of part (a), determine and plot the error  $e(t)$  for a disturbance  $T_p(s) = 1/s$ . Does the speed change more than 5%? (Set  $R(s) = 0$  and recall that  $E(s) = R(s) - T(s)$ .)

**E5.13** For the system with unity feedback shown in Figure E5.11, determine the steady-state error for a step and a ramp input when

$$G(s) = \frac{20}{s^2 + 14s + 50}$$

Answer:  $e_{ss} = 0.71$  for a step and  $e_{ss} = \infty$  for a ramp.

**E5.14** A feedback system is shown in Figure E5.14.

- (a) Determine the steady-state error for a unit step when  $K = 0.4$  and  $G_c(s) = 1$ .

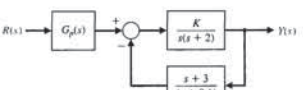


FIGURE E5.14 Feedback system.

- (b) Select an appropriate value for  $G_c(s)$  so that the steady-state error is equal to zero for the unit step input.

**E5.15** A closed-loop control system has a transfer function  $T(s)$  as follows:

$$\frac{Y(s)}{R(s)} = T(s) = \frac{2500}{(s + 50)(s^2 + 10s + 50)}$$

Plot  $y(t)$  for a step input  $R(s)$  when (a) the actual  $T(s)$  is used, and (b) using the relatively dominant complex poles. Compare the results.

**E5.16** A second-order system is

$$\frac{Y(s)}{R(s)} = T(s) = \frac{(10/z)(s + z)}{(s + 1)(s + 8)}$$

Consider the case where  $1 < z < 8$ . Obtain the partial fraction expansion, and plot  $y(t)$  for a step input  $r(t)$  for  $z = 2, 4, \text{ and } 6$ .

**E5.17** A closed-loop control system transfer function  $T(s)$  has two dominant complex conjugate poles. Sketch the region in the left-hand  $s$ -plane where the complex poles should be located to meet the given specifications.

- (a)  $0.6 \leq \zeta \leq 0.8, \omega_n \leq 10$
- (b)  $0.5 \leq \zeta \leq 0.707, \omega_n \geq 10$
- (c)  $\zeta \geq 0.5, 5 \leq \omega_n \leq 10$
- (d)  $\zeta \leq 0.707, 5 \leq \omega_n \leq 10$
- (e)  $\zeta \geq 0.6, \omega_n \leq 6$

**E5.18** A system is shown in Figure E5.18(a). The response to a unit step, when  $K = 1$ , is shown in Figure E5.18(b). Determine the value of  $K$  so that the steady-state error is equal to zero.

Answer:  $K = 1.25$ .

**E5.19** A second-order system has the closed-loop transfer function

$$T(s) = \frac{Y(s)}{R(s)} = \frac{\omega_n^2}{s^2 + 2\zeta\omega_n s + \omega_n^2} = \frac{7}{s^2 + 3.175s + 7}$$

- c.  $K = 169$
- d. None of the above

In Problems 14 and 15, consider the control system in Figure 5.50, where

$$G(s) = \frac{6}{(s + 5)(s + 2)} \text{ and } G_c(s) = \frac{K}{s + 50}$$

**14.** A second-order approximate model of the loop transfer function is:

- a.  $\hat{G}_c(s)\hat{G}(s) = \frac{(3/25)K}{s^2 + 7s + 10}$
- b.  $\hat{G}_c(s)\hat{G}(s) = \frac{(1/25)K}{s^2 + 7s + 10}$
- c.  $\hat{G}_c(s)\hat{G}(s) = \frac{(3/25)K}{s^2 + 7s + 500}$
- d.  $\hat{G}_c(s)\hat{G}(s) = \frac{6K}{s^2 + 7s + 10}$

**15.** Using the second-order system approximation (see Problem 14), estimate the gain  $K$  so that the percent overshoot is approximately  $P.O. \approx 15\%$ .

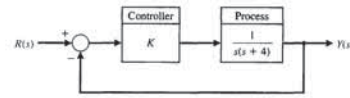
- a.  $K = 10$
- b.  $K = 300$
- c.  $K = 1000$
- d. None of the above

In the following Word Match problems, match the term with the definition by writing the correct letter in the space provided.

- a. Unit impulse The time for a system to respond to a step input and rise to a peak response. \_\_\_\_\_
- b. Rise time The roots of the characteristic equation that cause the dominant transient response of the system. \_\_\_\_\_
- c. Settling time The number  $N$  of poles of the transfer function,  $G(s)$ , at the origin. \_\_\_\_\_
- d. Type number The constant evaluated as  $\lim_{s \rightarrow 0} sG(s)$ . \_\_\_\_\_
- e. Percent overshoot An input signal used as a standard test of a system's ability to respond adequately. \_\_\_\_\_
- f. Position error constant,  $K_p$  The time required for the system output to settle within a certain percentage of the input amplitude. \_\_\_\_\_
- g. Velocity error constant,  $K_v$  A set of prescribed performance criteria. \_\_\_\_\_
- h. Steady-state response A system whose parameters are adjusted so that the performance index reaches an extremum value. \_\_\_\_\_
- i. Peak time A quantitative measure of the performance of a system. \_\_\_\_\_
- j. Dominant roots The time for a system to respond to a step input and attain a response equal to a percentage of the magnitude of the input. \_\_\_\_\_
- k. Test input signal The amount by which the system output response proceeds beyond the desired response. \_\_\_\_\_
- l. Acceleration error constant,  $K_a$  The constant evaluated as  $\lim_{s \rightarrow 0} s^2G(s)$ . \_\_\_\_\_
- m. Transient response The constant evaluated as  $\lim_{t \rightarrow \infty} G(s)$ . \_\_\_\_\_

Exercises

FIGURE E5.5 Feedback system with proportional controller.



**E5.5** Consider the feedback system in Figure E5.5. Find  $K$  such that the closed-loop system minimizes the ITAE performance criterion for a step input.

**E5.6** Consider the block diagram shown in Figure E5.6 [16]. (a) Calculate the steady-state error for a ramp input. (b) Select a value of  $K$  that will result in zero overshoot to a step input. Provide the most rapid response that is attainable.

Plot the poles and zeros of this system and discuss the dominance of the complex poles. What overshoot for a step input do you expect?

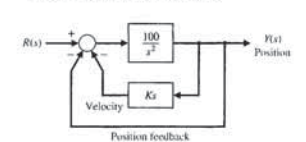


FIGURE E5.6 Block diagram with position and velocity feedback.

**E5.7** Effective control of insulin injections can result in better lives for diabetic persons. Automatically controlled insulin injection by means of a pump and a sensor that measures blood sugar can be very effective. A pump and injection system has a feedback control as shown in Figure E5.7. Calculate the suitable gain  $K$  so that the overshoot of the step response due to the drug injection is approximately 7%.  $R(s)$  is the desired blood-sugar level and  $Y(s)$  is the actual blood-sugar level. (Hint: Use Figure 5.13a.)  
 Answer:  $K = 1.67$

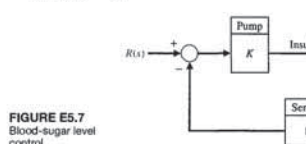


FIGURE E5.7 Blood-sugar level control.

**E5.8** A control system for positioning the head of a floppy disk drive has the closed-loop transfer function

$$T(s) = \frac{11.1(s + 18)}{(s + 20)(s^2 + 4s + 10)}$$

Plot the poles and zeros of this system and discuss the dominance of the complex poles. What overshoot for a step input do you expect?

**E5.9** A unity negative feedback control system has the loop transfer function

$$L(s) = G_c(s)G(s) = \frac{K}{s(s + \sqrt{2}K)}$$

- (a) Determine the percent overshoot and settling time (using a 2% settling criterion) due to a unit step input.
- (b) For what range of  $K$  is the settling time less than 1 second?

**E5.10** A second-order control system has the closed-loop transfer function  $T(s) = Y(s)/R(s)$ . The system specifications for a step input follow:

- (1) Percent overshoot  $P.O. \leq 5\%$ .
- (2) Settling time  $T_s < 4s$ .
- (3) Peak time  $T_p < 1s$ .

Show the permissible area for the poles of  $T(s)$  in order to achieve the desired response. Use a 2% settling criterion to determine settling time.

**E5.11** A system with unity feedback is shown in Figure E5.11. Determine the steady-state error for a step and a ramp input when

$$G(s) = \frac{5(s + 8)}{s(s + 1)(s + 4)(s + 10)}$$



**P5.3** A laser beam can be used to weld, drill, etch, cut, and mark metals, as shown in Figure P5.3(a) [14]. Assume we have a work requirement for an accurate laser to mark a parabolic path with a closed-loop control system, as shown in Figure P5.3(b). Calculate the necessary gain to result in a steady-state error of 5 mm for  $r(t) = t^2$  cm.

**P5.4** The loop transfer function of a unity negative feedback system (see Figure E5.11) is

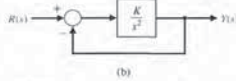
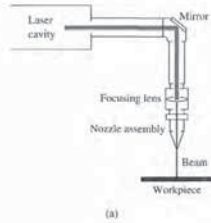
$$L(s) = G_c(s)G(s) = \frac{K}{s(s+2)}$$

A system response to a step input is specified as follows:

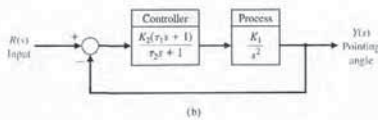
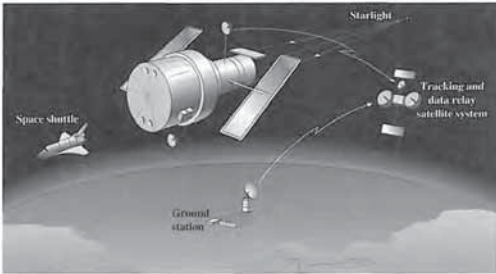
peak time  $T_p = 1.1$  s,  
percent overshoot  $P.O. = 5\%$ .

(a) Determine whether both specifications can be met simultaneously. (b) If the specifications cannot be met simultaneously, determine a compromise value for  $K$  so that the peak time and percent overshoot specifications are relaxed by the same percentage.

**P5.5** A space telescope is to be launched to carry out astronomical experiments [8]. The pointing control system is desired to achieve 0.01 minute of arc and track solar objects with apparent motion up to 0.21 arc minute per second. The system is illustrated in Figure P5.5(a). The control system is shown in



**FIGURE P5.3** Laser beam control.



**FIGURE P5.5** (a) The space telescope. (b) The space telescope pointing control system.

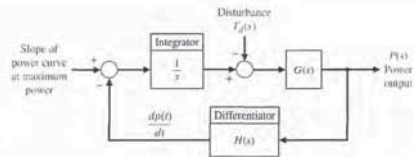
necessary gain  $K_1$  to maintain a steady-state error equal to 1 cm when the input is a ramp  $r(t) = t$  (meters). (b) With this gain  $K_1$ , determine the necessary gain  $K_2$  in order to restrict the percent overshoot to 10%. (c) Determine analytically the gain  $K_1K_2$  in order to minimize the ISE performance index for a step input.

**P5.8** Photovoltaic arrays (solar cells) generate a DC voltage that can be used to drive DC motors or that can be converted to AC power and added to the distribution network. It is desirable to maintain the power out of

the array at its maximum available as the solar incidence changes during the day. One such closed-loop system is shown in Figure P5.8. The transfer function for the process is

$$G(s) = \frac{K}{s + 20}$$

where  $K = 20$ . Find (a) the time constant of the closed-loop system and (b) the settling time to within 2% of the final value of the system to a unit step disturbance.



**FIGURE P5.8** Solar cell control.

**P5.9** The antenna that receives and transmits signals to the *Telstar* communication satellite is the largest horn antenna ever built. The microwave antenna is 177 ft long, weighs 340 tons, and rolls on a circular track. A photo of the antenna is shown in Figure P5.9. The *Telstar* satellite is 34 inches in diameter and moves about 16,000 mph at an altitude of 2500 miles. The

antenna must be positioned accurately to 1/10 of a degree, because the microwave beam is 0.2° wide and highly attenuated by the large distance. If the antenna is following the moving satellite, determine the  $K_c$  necessary for the system.

**P5.10** A speed control system of an armature-controlled DC motor uses the back emf voltage of the motor as a feedback signal. (a) Draw the block diagram of this system (see Equation 2.69). (b) Calculate the steady-state error of this system to a step input command setting the speed to a new level. Assume that  $K_a = T_m = J = b = 1$ , the motor constant is  $K_m = 1$ , and  $K_b = 1$ . (c) Select a feedback gain for the back emf signal to yield a step response with an overshoot of 15%.

**P5.11** A simple unity feedback control system has a process transfer function

$$\frac{Y(s)}{E(s)} = G(s) = \frac{K}{s}$$

The system input is a step function with an amplitude  $A$ . The initial condition of the system at time  $t_0$  is  $y(t_0) = Q$ , where  $y(t)$  is the output of the system. The performance index is defined as

$$I = \int_{t_0}^{\infty} e^2(t) dt$$

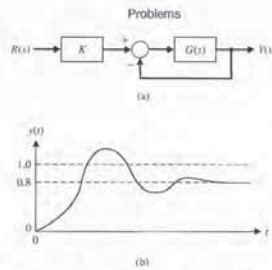


**FIGURE P5.9** A model of the antenna for the *Telstar* System at Andover, Maine. (Photo courtesy of Bell Telephone Laboratories, Inc.)

**E5.20** Consider the closed-loop system in Figure E5.19, where

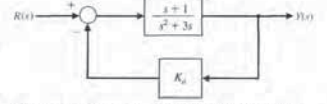
$$G_c(s)G(s) = \frac{s+1}{s^2+0.3s}$$

- (a) Determine the closed-loop transfer function  $T(s) = Y(s)/R(s)$ .
- (b) Determine the steady-state error of the closed-loop system response to a unit ramp input,  $R(s) = 1/s^2$ .
- (c) Select a value for  $K_c$  so that the steady-state error of the system response to a unit step input,  $R(s) = 1/s$ , is zero.



**FIGURE E5.18** Feedback system with prefilter.

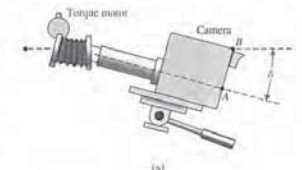
- (a) Determine the percent overshoot  $P.O.$ , the time to peak  $T_p$ , and the settling time  $T_s$  of the unit step response,  $R(s) = 1/s$ . To compute the settling time, use a 2% criterion.
- (b) Obtain the system response to a unit step and verify the results in part (a).



**FIGURE E5.20** Nonunity closed-loop feedback control system with parameter  $K_c$ .

**PROBLEMS**

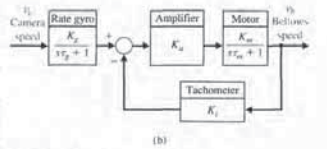
**P5.1** An important problem for television systems is the jumping or wobbling of the picture due to the movement of the camera. This effect occurs when the camera is mounted in a moving truck or airplane. The Dynalens system has been designed to reduce the effect of rapid scanning motion; see Figure P5.1. A maximum scanning motion of  $25^\circ/s$  is expected. Let  $K_a = K_v = 1$  and assume that  $\tau_m$  is negligible. (a) Determine the error of the system  $E(s)$ . (b) Determine the necessary loop gain  $K_cK_mK_t$  when a 1% steady-state error is allowable. (c) The motor time constant is 0.40 s. Determine the necessary loop gain so that the settling time (to within 2% of the final value of  $y_0$ ) is less than or equal to 0.03 s.



**P5.2** A specific closed-loop control system is to be designed for an underdamped response to a step input. The specifications for the system are as follows:

- 10% < percent overshoot < 20%,  
Settling time < 0.6 s.

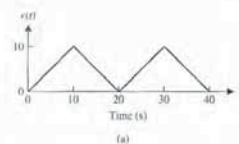
- (a) Identify the desired area for the dominant roots of the system. (b) Determine the smallest value of a third root  $r_3$  if the complex conjugate roots are to represent the dominant response. (c) The closed-loop system transfer function  $T(s)$  is third-order, and the feedback has a unity gain. Determine the forward transfer function  $G(s) = Y(s)/E(s)$  when the settling time to within 2% of the final value is 0.6 s and the percent overshoot is 20%.



**FIGURE P5.1** Camera wobble control.

**Problems**

Figure P5.5(b). Assume that  $\tau_1 = 1$  second and  $\tau_2 = 0$  (an approximation). (a) Determine the gain  $K = K_1K_2$  required so that the response to a step command is as rapid as reasonable with an overshoot of less than 5%. (b) Determine the steady-state error of the system for a step and a ramp input. (c) Determine the value of  $K_1K_2$  for an ITAE optimal system for (1) a step input and (2) a ramp input.



**P5.6** A robot is programmed to have a tool or welding torch follow a prescribed path [7, 11]. Consider a robot tool that is to follow a sawtooth path, as shown in Figure P5.6(a). The transfer function of the plant is

$$G(s) = \frac{75(s+1)}{s(s+5)(s+25)}$$

for the closed-loop system shown in Figure 5.6(b). Calculate the steady-state error.

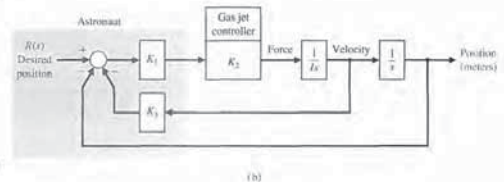
**FIGURE P5.6** Robot path control.

**P5.7** Astronaut Bruce McCandless II took the first untethered walk in space on February 7, 1984, using the gas-jet propulsion device illustrated in Figure P5.7(a).



**FIGURE P5.7**

(a) Astronaut Bruce McCandless II is shown a few meters away from the earth-orbiting space shuttle. He used a nitrogen-propelled hand-controlled device called the manned maneuvering unit. (Courtesy of National Aeronautics and Space Administration.) (b) Block diagram of controller.



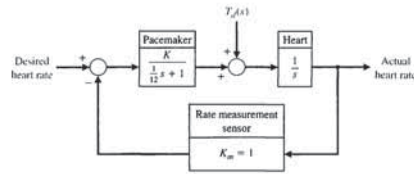


FIGURE P5.17 Heart pacemaker.

**P5.18** Consider the original third-order system given in Example 5.9. Determine a first-order model with one pole unspecified and no zeros that will represent the third-order system.

**P5.19** A closed-loop control system with negative unity feedback has a loop transfer function

$$L(s) = G_c(s)G(s) = \frac{8}{s(s^2 + 6s + 12)}$$

(a) Determine the closed-loop transfer function  $T(s)$ . (b) Determine a second-order approximation for  $T(s)$ . (c) Plot the response of  $T(s)$  and the second-order approximation to a unit step input and compare the results.

**P5.20** A system is shown in Figure P5.20.

(a) Determine the steady-state error for a unit step input in terms of  $K$  and  $K_1$ , where  $E(s) = R(s) - Y(s)$ . (b) Select  $K_1$  so that the steady-state error is zero.

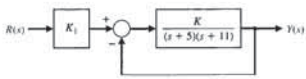


FIGURE P5.20 System with pregain,  $K_1$ .

**P5.21** Consider the closed-loop system in Figure P5.21. Determine values of the parameters  $k$  and  $a$  so that the following specifications are satisfied:

(a) The steady-state error to a unit step input is zero.

(b) The closed-loop system has a percent overshoot of less than 5%.

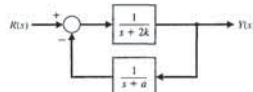


FIGURE P5.21 Closed-loop system with parameters  $k$  and  $a$ .

**P5.22** Consider the closed-loop system in Figure P5.22, where

$$G_c(s)G(s) = \frac{2}{s + 0.2K} \quad \text{and} \quad H(s) = \frac{2}{2s + \tau}$$

(a) If  $\tau = 2.43$ , determine the value of  $K$  such that the steady-state error of the closed-loop system response to a unit step input,  $R(s) = 1/s$ , is zero.

(b) Determine the percent overshoot  $PO$  and the time to peak  $T_p$  of the unit step response when  $K$  is as in part (a).

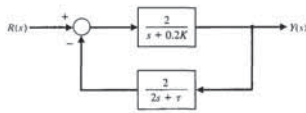


FIGURE P5.22 Nonunity closed-loop feedback control system.

(a) Show that  $J = (A - Q)^2/(2K)$ . (b) Determine the gain  $K$  that will minimize the performance index  $J$ . Is this gain a practical value? (c) Select a practical value of gain and determine the resulting value of the performance index.

**P5.12** Train travel between cities will increase as trains are developed that travel at high speeds, making the travel time from city center to city center equivalent to airline travel time. The Japanese National Railway has a train called the Bullet Express that travels between Tokyo and Osaka on the Tokaido line. This train travels the 320 miles in 3 hours and 10 minutes, an average speed of 101 mph [17]. This speed will be increased as new systems are used, such as magnetically levitated systems to float vehicles above an aluminum guideway. To maintain a desired speed, a speed control system is proposed that yields a zero steady-state error to a ramp input. A third-order system is sufficient. Determine the optimum system transfer function  $T(s)$  for an ITAE performance criterion. Estimate the settling time (with a 2% criterion) and overshoot for a step input when  $\omega_n = 10$ .

**P5.13** We want to approximate a fourth-order system by a lower-order model. The transfer function of the original system is

$$G_H(s) = \frac{s^3 + 7s^2 + 24s + 24}{s^4 + 10s^3 + 35s^2 + 50s + 24} = \frac{s^3 + 7s^2 + 24s + 24}{(s+1)(s+2)(s+3)(s+4)}$$

Show that if we obtain a second-order model by the method of Section 5.8, and we do not specify the poles

and the zero of  $G_L(s)$ , we have

$$G_L(s) = \frac{0.2917s + 1}{0.399s^2 + 1.375s + 1} = \frac{0.731(s + 3.428)}{(s + 1.043)(s + 2.4)}$$

**P5.14** For the original system of Problem P5.13, we want to find the lower-order model when the poles of the second-order model are specified as  $-1$  and  $-2$  and the model has one unspecified zero. Show that this low-order model is

$$G_L(s) = \frac{0.986s + 2}{s^2 + 3s + 2} = \frac{0.986(s + 2.028)}{(s + 1)(s + 2)}$$

**P5.15** Consider a unity feedback system with loop transfer function

$$L(s) = G_c(s)G(s) = \frac{K(s + 1)}{(s + 4)(s^2 + s + 10)}$$

Determine the value of the gain  $K$  such that the percent overshoot to a unit step is minimized.

**P5.16** A magnetic amplifier with a low-output impedance is shown in Figure P5.16 in cascade with a low-pass filter and a preamplifier. The amplifier has a high-input impedance and a gain of 1 and is used for adding the signals as shown. Select a value for the capacitance  $C$  so that the transfer function  $V_o(s)/V_d(s)$  has a damping ratio of  $1/\sqrt{2}$ . The time constant of the magnetic amplifier is equal to 1 second, and the gain is  $K = 10$ . Calculate the settling time (with a 2% criterion) of the resulting system.

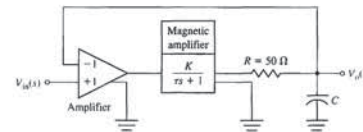


FIGURE P5.16 Feedback amplifier.

**P5.17** Electronic pacemakers for human hearts regulate the speed of the heart pump. A proposed closed-loop system that includes a pacemaker and the measurement of the heart rate is shown in Figure P5.17 [2, 3]. The transfer function of the heart pump and the pacemaker is found to be

$$G(s) = \frac{K}{s(s/12 + 1)}$$

Design the amplifier gain to yield a system with a settling time to a step disturbance of less than 1 second. The overshoot to a step in desired heart rate should be less than 10%. (a) Find a suitable range of  $K$ . (b) If the nominal value of  $K$  is  $K = 10$ , find the sensitivity of the system to small changes in  $K$ . (c) Evaluate the sensitivity of part (b) at  $DC$  (set  $s = 0$ ). (d) Evaluate the magnitude of the sensitivity at the normal heart rate of 60 beats/minute.

**AP5.6** The block diagram model of an armature-current-controlled DC motor is shown in Figure AP5.6.

(a) Determine the steady-state tracking error to a ramp input  $r(t) = t, t \geq 0$ , in terms of  $K, K_a$ , and  $K_m$ .

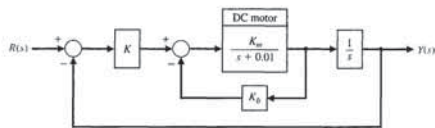


FIGURE AP5.6 DC motor control.

(b) Let  $K_m = 10$  and  $K_a = 0.05$ , and select  $K$  so that steady-state tracking error is equal to 1.

(c) Plot the response to a unit step input and a unit ramp input for 20 seconds. Are the responses acceptable?

**AP5.7** Consider the closed-loop system in Figure AP5.7 with transfer functions

$$G_c(s) = \frac{100}{s + 100} \quad \text{and} \quad G(s) = \frac{K}{s(s + 50)}$$

where

$$1000 \leq K \leq 5000.$$

(a) Assume that the complex poles dominate and estimate the settling time and percent overshoot to a unit step input for  $K = 1000, 2000, 3000, 4000$ , and  $5000$ .

(b) Determine the actual settling time and percent overshoot to a unit step for the values of  $K$  in part (a).

(c) Co-plot the results of (a) and (b) and comment.

**AP5.8** A unity negative feedback system (as shown in Figure E5.11) has the loop transfer function

$$L(s) = G_c(s)G(s) = \frac{K(s + 2)}{s^2 + \frac{1}{2}s + \frac{1}{4}}$$

Determine the gain  $K$  that minimizes the damping ratio  $\zeta$  of the closed-loop system poles. What is the minimum damping ratio?

**AP5.9** The unity negative feedback system in Figure AP5.9 has the process given by

$$G(s) = \frac{1}{s(s + 15)(s + 25)}$$

The controller is a proportional plus integral controller with gains  $K_p$  and  $K_I$ . The objective is to design the controller gains such that the dominant roots have a damping ratio  $\zeta$  equal to 0.707. Determine the resulting peak time and settling time (with a 2% criterion) of the system to a unit step input.

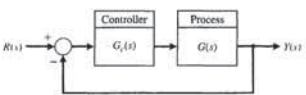
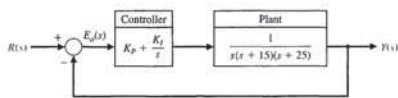


FIGURE AP5.7 Closed-loop system with unity feedback.

**FIGURE AP5.9** Feedback control system with a proportional plus integral controller.



ADVANCED PROBLEMS

**AP5.1** A closed-loop transfer function is

$$T(s) = \frac{Y(s)}{R(s)} = \frac{108(s + 3)}{(s + 9)(s^2 + 8s + 36)}$$

(a) Determine the steady-state error for a unit step input  $R(s) = 1/s$ .

(b) Assume that the complex poles dominate, and determine the overshoot and settling time to within 2% of the final value.

(c) Plot the actual system response, and compare it with the estimates of part (b).

**AP5.2** A closed-loop system is shown in Figure AP5.2. Plot the response to a unit step input for the system for  $\tau_p = 0, 0.05, 0.1$ , and  $0.5$ . Record the percent overshoot, rise time, and settling time (with a 2% criterion) as  $\tau_p$  varies. Describe the effect of varying  $\tau_p$ . Compare the location of the zero  $-1/\tau_p$  with the location of the closed-loop poles.

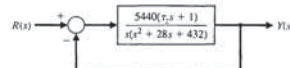


FIGURE AP5.2 System with a variable zero.

**AP5.3** A closed-loop system is shown in Figure AP5.3. Plot the response to a unit step input for the system with  $\tau_p = 0, 0.5, 2$ , and  $5$ . Record the percent overshoot, rise time, and settling time (with a 2% criterion) as  $\tau_p$  varies. Describe the effect of varying  $\tau_p$ . Compare the location of the open-loop pole  $-1/\tau_p$  with the location of the closed-loop poles.

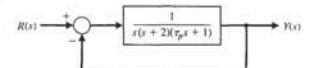


FIGURE AP5.3 System with a variable pole in the process.

**AP5.4** The speed control of a high-speed train is represented by the system shown in Figure AP5.4 [17]. Determine the equation for steady-state error for  $K$  for a unit step input  $r(t)$ . Consider the three values for  $K$  equal to 1, 10, and 100.

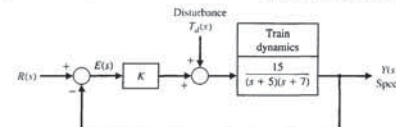


FIGURE AP5.4 Speed control.

**AP5.5** A system with a controller is shown in Figure AP5.5. The zero of the controller may be varied. Let  $\alpha = 0, 10, 100$ .

(a) Determine the steady-state error for a step input  $r(t)$  for  $\alpha = 0$  and  $\alpha \neq 0$ .

(b) Plot the response of the system to a step input disturbance for the three values of  $\alpha$ . Compare the results and select the best value of the three values of  $\alpha$ .

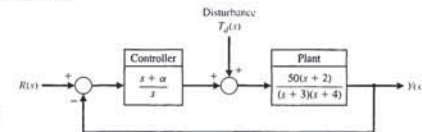
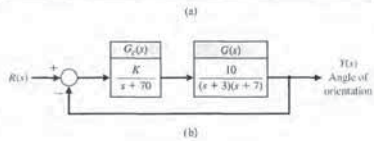


FIGURE AP5.5 System with controller parameter  $\alpha$ .



**DP5.4** The space satellite shown in Figure DP5.4(a) uses a control system to readjust its orientation, as shown in Figure DP5.4(b).



**FIGURE DP5.4** Control of a space satellite.

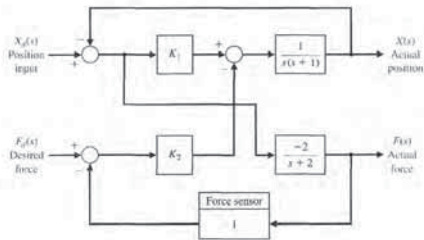
**DP5.5** A deburring robot can be used to smooth off machined parts by following a preplanned path (input command signal). In practice, errors occur due to robot inaccuracy, machining errors, large tolerances, and tool wear. These errors can be eliminated using force feedback to modify the path online [8, 11].

While force control has been able to address the problem of accuracy, it has been more difficult to solve the contact stability problem. In fact, by closing the force loop and introducing a compliant wrist force

sensor (the most common type of force control), one can add to the stability problem.

A model of a robot deburring system is shown in Figure DP5.5. Determine the region of stability for the system for  $K_1$  and  $K_2$ . Assume both adjustable gains are greater than zero.

**DP5.6** The model for a position control system using a DC motor is shown in Figure DP5.6. The goal is to select  $K_1$  and  $K_2$  so that the peak time is  $T_p \approx 0.5$



**FIGURE DP5.5** Deburring robot.

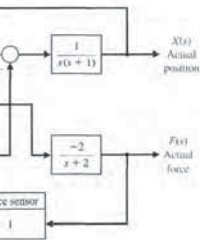


Figure DP5.8(a) [7]. We wish to investigate the system when  $K = 1, 10,$  and  $20$ . The feedback control block diagram is shown in Figure DP5.8(b). (a) For the three values of  $K$ , determine the percent overshoot, the settling time (with a 2% criterion), and the steady-state

error for a unit step input. Record your results in a table. (b) Choose one of the three values of  $K$  that provides acceptable performance. (c) For the value selected in part (b), determine  $y(t)$  for a disturbance  $T_d(s) = 1/s$  when  $R(s) = 0$ .

**COMPUTER PROBLEMS**

**CP5.1** Consider the closed-loop transfer function

$$T(s) = \frac{15}{s^2 + 8s + 15}$$

Obtain the impulse response analytically and compare the result to one obtained using the impulse function.

**CP5.2** A unity negative feedback system has the loop transfer function

$$L(s) = G_c(s)G(s) = \frac{s + 10}{s^2(s + 15)}$$

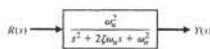
Using *leim*, obtain the response of the closed-loop system to a unit ramp input.

$$R(s) = 1/s^2.$$

Consider the time interval  $0 \leq t \leq 50$ . What is the steady-state error?

**CP5.3** A working knowledge of the relationship between the pole locations of the second-order system shown in Figure CP5.3 and the transient response is important in control design. With that in mind, consider the following four cases:

1.  $\omega_n = 2, \zeta = 0,$
2.  $\omega_n = 2, \zeta = 0.1,$
3.  $\omega_n = 1, \zeta = 0,$
4.  $\omega_n = 1, \zeta = 0.2.$



**FIGURE CP5.3** A simple second-order system.

Using the impulse and subplot functions, create a plot containing four subplots, with each subplot depicting the impulse response of one of the four cases listed. Compare the plot with Figure 5.17 in Section 5.5, and discuss the results.

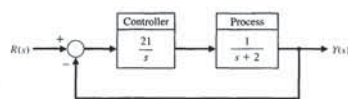
**CP5.4** Consider the control system shown in Figure CP5.4.

- (a) Show analytically that the expected percent overshoot of the closed-loop system response to a unit step input is about 50%.
- (b) Develop an m-file to plot the unit step response of the closed-loop system and estimate the percent overshoot from the plot. Compare the result with part (a).

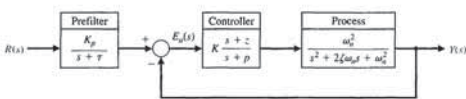
**CP5.5** Consider the feedback system in Figure CP5.5. Develop an m-file to design a controller and prefilter

$$G_c(s) = K \frac{s + z}{s + p} \quad \text{and} \quad G_p(s) = \frac{K_p}{s + \tau}$$

such that the ITAE performance criterion is minimized. For  $\omega_n = 0.45$  and  $\zeta = 0.59$ , plot the unit step response and determine the percent overshoot and settling time.



**FIGURE CP5.4** A negative feedback control system.



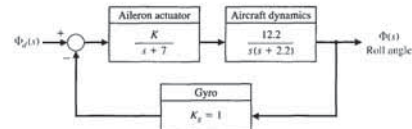
**FIGURE CP5.5** Feedback control system with controller and prefilter.

**DESIGN PROBLEMS**

**CDP5.1** The capstan drive system of the previous problems (see CDP1.1–CDP4.1) has a disturbance due to changes in the part that is being machined as material is removed. The controller is an amplifier  $G_c(s) = K_c$ . Evaluate the effect of a unit step disturbance, and determine the best value of the amplifier gain so that the overshoot to a step command  $r(t) = A, t > 0$  is less than 5%, while reducing the effect of the disturbance as much as possible.

**DP5.1** The roll control autopilot of a jet fighter is shown in Figure DP5.1. The goal is to select a suitable  $K$  so that the response to a unit step command  $\phi_d(t) = A, t \geq 0$ ,

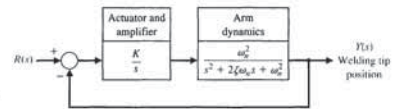
will provide a response  $\phi(t)$  that is a fast response and has an overshoot of less than 20%. (a) Determine the closed-loop transfer function  $\phi(s)/\phi_d(s)$ . (b) Determine the roots of the characteristic equation for  $K = 0.7, 3,$  and  $6$ . (c) Using the concept of dominant roots, find the expected overshoot and peak time for the approximate second-order system. (d) Plot the actual response and compare with the approximate results of part (c). (e) Select the gain  $K$  so that the percentage overshoot is equal to 16%. What is the resulting peak time?



**FIGURE DP5.1** Roll angle control.

**DP5.2** The design of the control for a welding arm with a long reach requires the careful selection of the parameters [13]. The system is shown in Figure DP5.2, where  $\zeta = 0.6$ , and the gain  $K$  and the natural frequency  $\omega_n$  can be selected. (a) Determine  $K$  and  $\omega_n$  so that the response to a unit step input achieves a peak

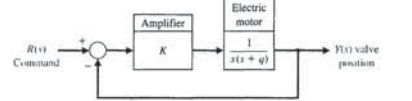
time for the first overshoot (above the desired level of 1) that is less than or equal to 1 second and the overshoot is less than 5%. (Hint: Try  $0.2 < K/\omega_n < 0.4$ .) (b) Plot the response of the system designed in part (a) to a step input.



**FIGURE DP5.2** Welding tip position control.

**DP5.3** Active suspension systems for modern automobiles provide a comfortable firm ride. The design of an active suspension system adjusts the valves of the shock absorber so that the ride fits the conditions. A small electric motor, as shown in Figure DP5.3, changes the valve settings [13]. Select a design value

for  $K$  and the parameter  $q$  in order to satisfy the ITAE performance for a step command  $R(s)$  and a settling time (with a 2% criterion) for the step response of less than or equal to 0.5 second. Upon completion of your design, predict the resulting overshoot for a step input.



**FIGURE DP5.3** Active suspension system.

error for a unit step input. Record your results in a table. (b) Choose one of the three values of  $K$  that provides acceptable performance. (c) For the value selected in part (b), determine  $y(t)$  for a disturbance  $T_d(s) = 1/s$  when  $R(s) = 0$ .

error for a unit step input. Record your results in a table. (b) Choose one of the three values of  $K$  that provides acceptable performance. (c) For the value selected in part (b), determine  $y(t)$  for a disturbance  $T_d(s) = 1/s$  when  $R(s) = 0$ .

**COMPUTER PROBLEMS**

**CP5.1** Consider the closed-loop transfer function

$$T(s) = \frac{15}{s^2 + 8s + 15}$$

Obtain the impulse response analytically and compare the result to one obtained using the impulse function.

**CP5.2** A unity negative feedback system has the loop transfer function

$$L(s) = G_c(s)G(s) = \frac{s + 10}{s^2(s + 15)}$$

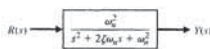
Using *leim*, obtain the response of the closed-loop system to a unit ramp input.

$$R(s) = 1/s^2.$$

Consider the time interval  $0 \leq t \leq 50$ . What is the steady-state error?

**CP5.3** A working knowledge of the relationship between the pole locations of the second-order system shown in Figure CP5.3 and the transient response is important in control design. With that in mind, consider the following four cases:

1.  $\omega_n = 2, \zeta = 0,$
2.  $\omega_n = 2, \zeta = 0.1,$
3.  $\omega_n = 1, \zeta = 0,$
4.  $\omega_n = 1, \zeta = 0.2.$



**FIGURE CP5.3** A simple second-order system.

Using the impulse and subplot functions, create a plot containing four subplots, with each subplot depicting the impulse response of one of the four cases listed. Compare the plot with Figure 5.17 in Section 5.5, and discuss the results.

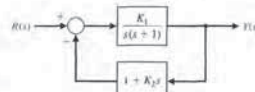
**CP5.4** Consider the control system shown in Figure CP5.4.

- (a) Show analytically that the expected percent overshoot of the closed-loop system response to a unit step input is about 50%.
- (b) Develop an m-file to plot the unit step response of the closed-loop system and estimate the percent overshoot from the plot. Compare the result with part (a).

**CP5.5** Consider the feedback system in Figure CP5.5. Develop an m-file to design a controller and prefilter

$$G_c(s) = K \frac{s + z}{s + p} \quad \text{and} \quad G_p(s) = \frac{K_p}{s + \tau}$$

such that the ITAE performance criterion is minimized. For  $\omega_n = 0.45$  and  $\zeta = 0.59$ , plot the unit step response and determine the percent overshoot and settling time.



**FIGURE DP5.6** Position control robot.

second and the overshoot *P.O.* for a step input is *P.O.*  $\leq 2\%$ .

**DP5.7** A three-dimensional cam for generating a function of two variables is shown in Figure DP5.7(a). Both  $x$  and  $y$  may be controlled using a position control system

[3]. The control of  $x$  may be achieved with a DC motor and position feedback of the form shown in Figure DP5.7(b), with the DC motor and load represented by

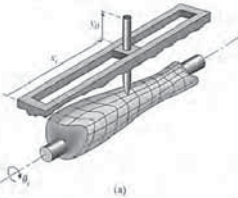
$$G(s) = \frac{K}{s(s + p)(s + 4)}$$

where  $K = 2$  and  $p = 2$ . Design a proportional plus derivative controller

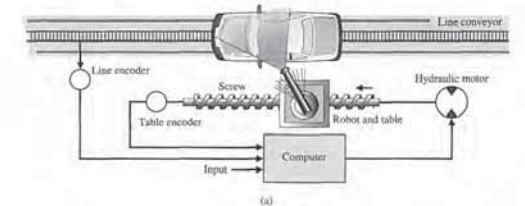
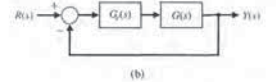
$$G_c(s) = K_p + K_d s$$

to achieve a percent overshoot *P.O.*  $\leq 5\%$  to a unit step input and a settling time  $T_s \leq 2$  seconds.

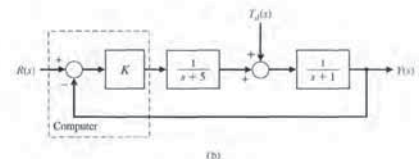
**DP5.8** Computer control of a robot to spray-paint an automobile is accomplished by the system shown in

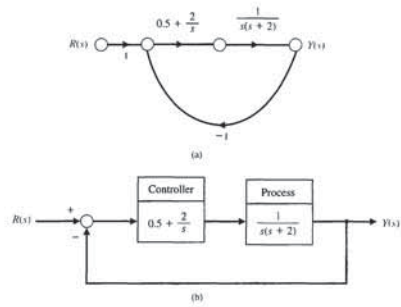


**FIGURE DP5.7** (a) Three-dimensional cam and (b) x-axis control system.



**FIGURE DP5.8** Spray-paint robot.





**FIGURE CP5.11** A single loop unity feedback system. (a) Signal flow graph. (b) Block diagram.

**CP5.12** A closed-loop transfer function is given by

$$T(s) = \frac{Y(s)}{R(s)} = \frac{77(s+2)}{(s+7)(s^2+4s+22)}$$

(a) Obtain the response of the closed-loop transfer function  $T(s) = Y(s)/R(s)$  to a unit step input.

What is the settling time  $T_s$  (use a 2% criterion) and percent overshoot  $PO$ ?

(b) Neglecting the real pole at  $s = -7$ , determine the settling time  $T_s$  and percent overshoot  $PO$ . Compare the results with the actual system response in part (a). What conclusions can be made regarding neglecting the pole?



**ANSWERS TO SKILLS CHECK**

True or False: (1) True; (2) False; (3) False; (4) True; (5) False  
 Multiple Choice: (6) a; (7) a; (8) c; (9) b; (10) b; (11) a; (12) b; (13) b; (14) a; (15) b

Word Match (in order, top to bottom): i, j, d, g, k, c, n, p, o, b, e, l, L, h, m, a

**TERMS AND CONCEPTS**

**Acceleration error constant,  $K_a$**  The constant evaluated as  $\lim_{s \rightarrow 0} [s^2 G_c(s)G(s)]$ . The steady-state error for a parabolic input,  $r(t) = At^2/2$ , is equal to  $A/K_a$ .

**Design specifications** A set of prescribed performance criteria.

**Dominant roots** The roots of the characteristic equation that cause the dominant transient response of the system.

**Optimum control system** A system whose parameters are adjusted so that the performance index reaches an extremum value.

**Peak time** The time for a system to respond to a step input and rise to a peak response.

**Percent overshoot** The amount by which the system output response proceeds beyond the desired response.

**Performance index** A quantitative measure of the performance of a system.

**Position error constant,  $K_p$**  The constant evaluated as  $\lim_{s \rightarrow 0} G_c(s)G(s)$ . The steady-state error for a step input (of magnitude  $A$ ) is equal to  $A/(1 + K_p)$ .

**Rise time** The time for a system to respond to a step input and attain a response equal to a percentage of the

**CP5.6** The loop transfer function of a unity negative feedback system is

$$L(s) = G_c(s)G(s) = \frac{25}{s(s+5)}$$

Develop an m-file to plot the unit step response and determine the values of peak overshoot  $M_p$ , time to peak  $T_p$ , and settling time  $T_s$  (with a 2% criterion).

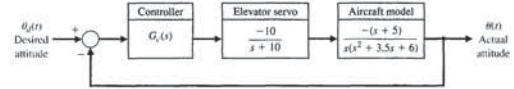
**CP5.7** An autopilot designed to hold an aircraft in straight and level flight is shown in Figure CP5.7.

(a) Suppose the controller is a constant gain controller given by  $G_c(s) = 2$ . Using the *lsim* function, compute and plot the ramp response for  $\theta_d(t) = at$ , where  $a = 0.5^\circ/s$ . Determine the attitude error after 10 seconds.

(b) If we increase the complexity of the controller, we can reduce the steady-state tracking error. With this objective in mind, suppose we replace the constant gain controller with the more sophisticated controller

$$G_c(s) = K_1 + \frac{K_2}{s} = 2 + \frac{1}{s}$$

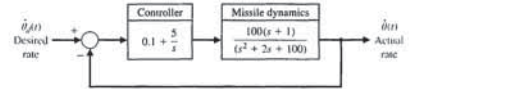
This type of controller is known as a proportional plus integral (PI) controller. Repeat the simulation of part (a) with the PI controller, and compare the steady-state tracking errors of the constant gain controller versus the PI controller.



**FIGURE CP5.7** An aircraft autopilot block diagram.

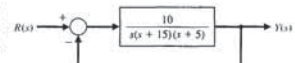
**CP5.8** The block diagram of a rate loop for a missile autopilot is shown in Figure CP5.8. Using the analytic formulas for second-order systems, predict  $M_p$ ,  $T_p$ , and  $T_s$  for the closed-loop system due to a unit step input.

Compare the predicted results with the actual unit step response obtained with the *step* function. Explain any differences.

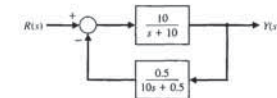


**FIGURE CP5.8** A missile rate loop autopilot.

**CP5.9** Develop an m-file that can be used to analyze the closed-loop system in Figure CP5.9. Drive the system with a step input and display the output on a graph. What is the settling time and the percent overshoot?



**FIGURE CP5.10** Closed-loop system for m-file.



**FIGURE CP5.9** Nonunity feedback system.

**CP5.10** Develop an m-file to simulate the response of the system in Figure CP5.10 to a ramp input  $R(s) = 1/s^2$ . What is the steady-state error? Display the output on an x-y graph.

**CP5.11** Consider the closed-loop system in Figure CP5.11. Develop an m-file to accomplish the following tasks:

(a) Determine the closed-loop transfer function  $T(s) = Y(s)/R(s)$ .

(b) Plot the closed-loop system response to an impulse input  $R(s) = 1$ , a unit step input  $R(s) = 1/s$ , and a unit ramp input  $R(s) = 1/s^2$ . Use the *subplot* function to display the three system responses.

**Terms and Concepts**

**Steady-state error** The difference between the desired value and the actual value of the system output after a long time following any signal initiation.

**Steady-state response** The constituent of the system response that exists a long time following any signal initiation.

**Test input signal** An input signal used as a standard test of a system's ability to respond adequately.

**Setting time** The time required for the system output to settle within a certain percentage of the input amplitude.

**Steady-state response** The constituent of the system response that exists a long time following any signal initiation.

**Transient response** The constituent of the system response that disappears with time.

**Type number** The number  $N$  of poles of the transfer function,  $G_c(s)G(s)$ , at the origin.  $G_c(s)G(s)$  is the loop transfer function.

**Unit impulse** A test input consisting of an impulse of infinite amplitude and zero width, and having an area of unity. The unit impulse is used to determine the impulse response.

**Velocity error constant,  $K_v$**  The constant evaluated as  $\lim_{s \rightarrow 0} [sG_c(s)G(s)]$ . The steady-state error for a ramp input (of slope  $A$ ) for a system is equal to  $A/K_v$ .